Antennas and Wave Propagation

By: Harish, A.R.; Sachidananda, M.

Oxford University Press

ISBN: 978-0-19-568666-1

Preface

Antennas are a key component of all types of wireless communication—be it the television sets in our homes, the FM radios in our automobiles, or the mobile phones which have become an almost integral part of most people's daily lives. All these devices require an antenna to function. In fact, it was an antenna which led Arno Penzias and Robert Wilson to their Nobel Prize winning discovery of cosmic background radiation.

The study of antennas and their field patterns is an important aspect of understanding many applications of wireless transmission technology. Antennas vary widely in their shapes, sizes, and radiation characteristics. Depending on the usage requirements, an antenna can be a single piece of wire, a huge reflective disc, or a complex array of electrical and electronic components. The analysis of antennas is almost invariably concomitant with the study of the basic concepts of the propagation of electromagnetic waves through various propagation media and the discontinuities encountered in the path of propagation.

About the Book

Evolved from the lecture notes of courses taught by the authors at the Indian Institute of Technology Kanpur over several years, *Antennas and Wave Propagation* is primarily meant to fulfil the requirements of a single-semester undergraduate course on antennas and propagation theory.

It is assumed that the reader has already gone through a basic course on electromagnetics and is familiar with Maxwell's equations, plane waves, reflection and refraction phenomena, transmission lines, and waveguides. The book provides a lucid overview of electromagnetic theory and a comprehensive introduction to various types of antennas and their radiation characteristics. Further, a clear-cut presentation of the basic concepts of

wave propagation, including ground wave and ionospheric propagation, goes on to make this text a useful and self-contained reference on antennas and radio wave propagation.

While a rigorous analysis of an antenna is highly mathematical, often a simplified analysis is sufficient for understanding the basic principles of operation of an antenna. Keeping this fact in mind, this book emphasizes the conceptual understanding of the principles of radiation and wave propagation by keeping the mathematical analysis to a minimum.

In most cases, the design of an antenna is system specific. Simplified design procedures, rather than a rigorous mathematical analysis, are useful and practical for designing and building antennas for many communication applications. Hence, several simple antenna design procedures have been included, which give an engineering flavour to the book.

Content and Structure

This book contains eight chapters which provide a comprehensive treatment of antennas and wave propagation.

Chapter 1 is essentially a review of basic electromagnetic theory. It also introduces the vector potential approach to the solution of the wave equation and the concept of the Hertzian dipole.

In Chapter 2, students are introduced to the terminology used for describing the radiation and input characteristics of antennas. The terms used for characterizing an antenna as a receiver are also clearly explained. The calculation of free space communication link budget is illustrated with examples.

The development of antenna theory starts from a study of the radiation from an infinitesimal current element. In Chapter 3, the field computation is extended to antennas carrying linear current distributions, e.g., short dipole, half-wave dipole, monopole, and loop antennas. Detailed procedures for the computation of the performance parameters of these antennas are also given.

A class of antennas which can be looked at as radiation from an aperture is treated in Chapter 4. Various forms of the field equivalence principle and its applications in the computation of the radiation fields of an aperture are explained. Several aperture type antennas, such as a slot, an open-ended waveguide, horn, reflector, etc., are also discussed.

Chapter 5 is devoted to the study of antenna arrays. It starts with the pattern multiplication principle and goes on to explain various pattern properties using a two-element array as an example. Use of polynomial representation of the array factor of a uniformly-spaced linear array and its pole-zero

representation on a circle diagram is explained. The chapter ends with a discussion on the design of binomial and Chebyshev patterns.

A large number of specially designed antennas exist for specific usage requirements. Chapter 6 details a select set of such antennas under the title *Special Antennas*. These antennas cover a wide range of applications in various frequency bands. Some of the antennas discussed are monopole, V antenna, Yagi–Uda array, turnstile antenna, helix, spiral, microstrip patch, etc. The radiation pattern properties and some simple design procedures are explained.

Chapter 7 is focused on the techniques used to measure antenna parameters. Indoor and outdoor measurement ranges which provide free-space-like conditions for the antenna are explained. Schematic block diagrams of the measurement instrumentation are presented. Procedures for the measurement of the gain, directivity, radiation pattern, etc. are also discussed.

Finally, Chapter 8 deals with the issues related to the propagation of radio waves. In this chapter, we study the interaction of the media and the discontinuities with electromagnetic waves. The effect of the earth and the troposphere on the propagation of electromagnetic waves is considered in detail. This is followed by an exposition of the nature of the ionosphere and its effect on sky wave propagation.

Each chapter is divided into sections that are independent. A large number of solved problems are interspersed through the text to enable the student to comprehensively grasp concepts and their applications. Suitable figures and diagrams have been provided for easy understanding of the concepts involved. Relevant numerical problems with answers have been included as end-chapter exercises to test the understanding of the topics introduced in each chapter. Seven different appendices provide easy reference to important formulae that are used throughout the book. These are followed by a list of references for those interested in further reading. A special attempt has been made to include topics that are part of curricula of courses offered by a large cross-section of educational institutes.

Acknowledgements

It is a pleasure to thank our wives Radha and Shalini, and children Bhavana and Bharath for their love, care, and emotional support. We are grateful to them for enduring the countless hours of absence during the preparation of the manuscript. We appreciate the advice and support from friends and colleagues, which helped us in the preparation of the manuscript. We would like to thank IIT Kanpur, and especially the Department of Electrical

Engineering, IIT Kanpur, for providing a conducive environment for writing the book. We are grateful to the Centre for Development of Technical Education, IIT Kanpur, for the financial support. Prof. R. Nityananda, Centre Director, NCRA, TIFR, Pune, has been kind enough to permit us to use a photograph of the GMRT facility. We would like to thank him for his kind gesture. The editorial team at Oxford University Press India has done a commendable job in bringing out this book. We would like to express our gratitude for the excellent editing, graphics, and design of the book. Teaching the antenna theory course has given us an opportunity to interact with many students, which has helped in improving the presentation of the material. We thank all the students who have interacted with us.

Although much care has been taken to ensure an error-free text, some errors may have crept in. Feedback from the readers regarding such errors will be highly appreciated and will go a long way in helping us improve the subsequent editions.

A.R. Harish
M. Sachidananda

Contents

CHAPTER 1

Electromagnetic Radiation

Introduction

Most of us are familiar with cellular phones. In cellular communication systems, there is a two-way wireless transmission between the cellular phone handset and the base station tower. The cell phone converts the audio signals into electrical form using a microphone. This information is imposed on a high frequency carrier signal by the process of modulation. The modulated carrier is radiated into free space as an electromagnetic wave which is picked up by the base station tower. Similarly, the signals transmitted by the tower are received by the handset, thus establishing a two way communication. This is one of the typical examples of a wireless communication system which uses free space as a medium to transfer information from the transmitter to the receiver. A key component of a wireless link is the antenna which efficiently couples electromagnetic energy from the transmitter to free space and from free space to the receiver. An antenna is generally a bidirectional device, i.e., the power through the antenna can flow in both the directions, hence it works as a transmitting as well as a receiving antenna.

Transmission lines are used to transfer electromagnetic energy from one point to another within a circuit and this mode of energy transfer is generally known as *guided wave* propagation. An antenna acts as an interface between the radiated electromagnetic waves and the guided waves. It can be thought of as a mode transformer which transforms a guided-wave field distribution into a radiated-wave field distribution. Since the wave impedances of the guided and the radiated waves may be different, the antenna can also be thought of as an impedance transformer. A proper design of this part is necessary for the efficient coupling of the energy from the circuit to the free space and vice versa.

One of the important properties of an antenna is its ability to transmit power in a preferred direction. The angular distribution of the transmitted

Fig. 1.1 Parabolic dish antenna at the Department of Electrical Engineering, Indian Institute of Technology, Kanpur, India (Courtesy: Dept of EE, IIT Kanpur)

power around the antenna is generally known as the *radiation pattern* (A more precise definition is given in Chapter 2). For example, a cellular phone needs to communicate with a tower which could be in any direction, hence the cellular phone antenna needs to radiate equally in all directions. Similarly, the tower antenna also needs to communicate with cellular phones located all around it, hence its radiation also needs to be independent of the direction.

There are large varieties of communication applications where the directional property is used to an advantage. For example, in point-to-point communication between two towers it is sufficient to radiate (or receive) only in the direction of the other tower. In such cases a highly directional parabolic dish antenna can be used. A 6.3 m diameter parabolic dish antenna used for communication with a geo-stationary satellite is shown in Fig. 1.1. This antenna radiates energy in a very narrow beam pointing towards the satellite.

Radio astronomy is another area where highly directional antennas are used. In radio astronomy the antenna is used for receiving the electromagnetic radiations from outer space. The power density of these signals from outer space is very low, hence it is necessary to collect the energy over a very large area for it to be useful for scientific studies. Therefore, radio astronomy antennas are large in size. In order to increase the collecting aperture,

Fig. 1.2 A panoramic view of the Giant Metrewave Radio Telescope (GMRT), Pune, India, consisting of 30 fully-steerable parabolic dish antennas of 45 m diameter each spread over distances up to 25 km.[1] (Photograph by Mr. Pravin Raybole, Courtesy: GMRT, Pune, http://www.gmrt.ncra.tifr.res.in)

the Giant Metrewave Radio Telescope (GMRT) near Pune in India, has an array of large dish antennas, as shown in Fig. 1.2.

The ability of an antenna to concentrate power in a narrow beam depends on the size of the antenna in terms of wavelength. Electromagnetic waves of wavelengths ranging from a few millimetres to several kilometres are used in various applications requiring efficient antennas working at these wavelengths. These frequencies, ranging from hundreds of giga hertz to a few kilo hertz, form the radio wave spectrum. Figure 1.3 depicts the radio wave spectrum along with band designations and typical applications.

The radiation pattern of an antenna is usually computed assuming the surroundings to be infinite free space in which the power density (power per unit area) decays as inverse square of the distance from the antenna. In practical situations the environment is more complex and the decay is not as simple. If the environment consists of well defined, finite number of scatterers, we can use theories of reflection, refraction, diffraction, etc., to predict the propagation of electromagnetic waves. However, in a complex environment, such as a cell phone operating in an urban area, the field strength is obtained by empirical relations.

The atmosphere plays a significant role in the propagation of electromagnetic waves. The density of the air molecules and, hence, the refractive index of the atmosphere changes with height. An electromagnetic wave passing through media having different refractive indices undergoes refraction. Thus, the path traced by an electromagnetic wave as it propagates through

[1]The GMRT was built and is operated by the National Centre for Radio Astrophysics (NCRA) of the Tata Institute of Fundamental Research (TIFR).

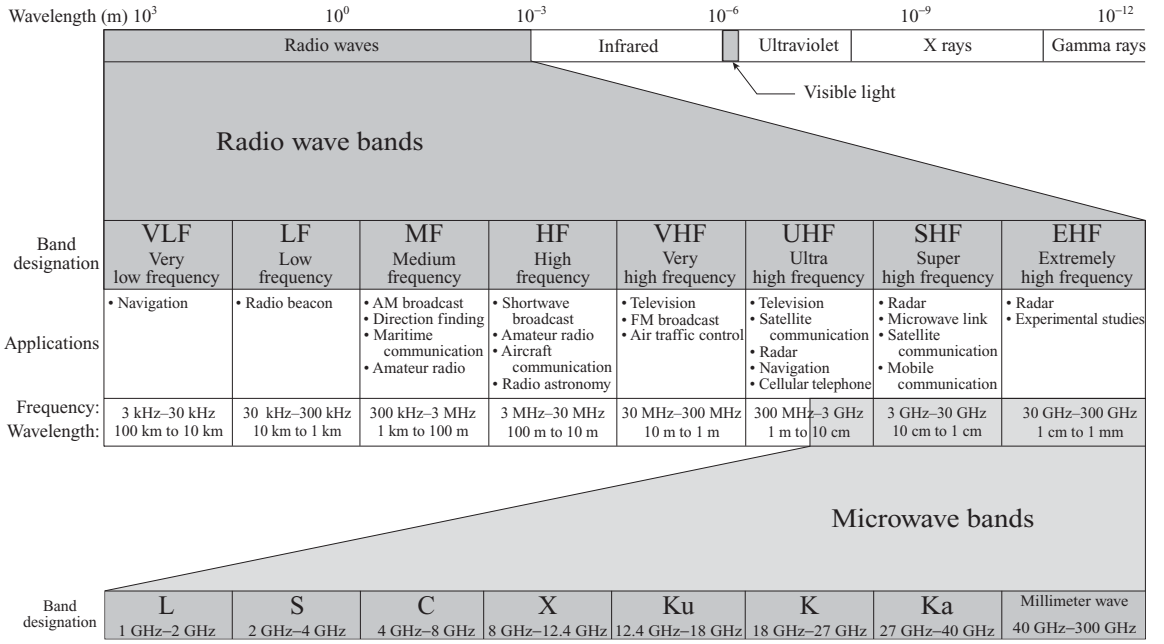

Fig. 1.3 Radio wave spectrum along with the band designations and typical applications.

the atmosphere is not a straight line. The air molecules also get ionized by solar radiation and cosmic rays. The layer of ionized particles in the atmosphere, known as the *ionosphere*, reflects high frequency (3 MHz to 30 MHz) waves. A multi-hop communication link is established by repeated reflections of the electromagnetic waves between the ionosphere and the surface of the earth. This is the mode of propagation of shortwave radio signals over several thousand kilometres.

Both the radiation properties of the antennas and the propagation conditions play a very important role in establishing a successful communication link. This book addresses both these issues in some detail. It is assumed that the students have some basic knowledge of electromagnetic theory. However, in the following section some of the basic concepts of electromagnetic theory used in the analysis of antennas are presented for easy reference as well as for introducing the notation used in the book.

1.1 Review of Electromagnetic Theory

Electromagnetic fields are produced by time-varying charge distributions which can be supported by time-varying current distributions. Consider sinusoidally varying electromagnetic sources. (Sources having arbitrary variation

with respect to time can be represented in terms of sinusoidally varying functions using Fourier analysis.) A sinusoidally varying current $i(t)$ can be expressed as a function of time, t, as

$$i(t) = I_0 \cos(\omega t + \varphi) \tag{1.1}$$

where I_0 is the amplitude (unit: ampere, A), ω is the angular frequency (unit: radian per second, rad/s), and φ is the phase (unit: radian, rad). The angular frequency, ω, is related to the frequency, f (unit: cycle per second or Hz), by the relation $\omega = 2\pi f$. One may also express the current $i(t)$ as a sine function

$$i(t) = I_0 \sin(\omega t + \varphi') \tag{1.2}$$

where $\varphi' = \varphi + \pi/2$. Therefore, we need to identify whether the phase has been defined taking the cosine function or the sine function as a reference. In this text, we have chosen the cosine function as the reference to define the phase of the sinusoidal quantity.

Since $\cos(\omega t + \varphi) = \mathrm{Re}\left\{e^{j(\omega t+\varphi)}\right\}$ where, Re{} represents the real part of the quantity within the curly brackets, the current can now be written as

$$i(t) = I_0 \mathrm{Re}\left\{e^{j(\omega t+\varphi)}\right\} \tag{1.3}$$

$$= \mathrm{Re}\left\{I_0 e^{j\varphi} e^{j\omega t}\right\} \tag{1.4}$$

The quantity $I_0 e^{j\varphi}$ is known as a phasor and contains the amplitude and phase information of $i(t)$ but is independent of time, t.

EXAMPLE 1.1

Express $i(t) = (\cos\omega t + 2\sin\omega t)$ A in phasor form.

Solution: First we must express $\sin\omega t$ in terms of the cosine function using the relation $\cos(\omega t - \pi/2) = \sin\omega t$. Therefore

$$i(t) = \cos\omega t + 2\cos\left(\omega t - \frac{\pi}{2}\right)$$

Using the relation $\cos(\omega t + \varphi) = \mathrm{Re}\left\{e^{j(\omega t+\varphi)}\right\}$

$$i(t) = \mathrm{Re}\left\{e^{j\omega t}\right\} + \mathrm{Re}\left\{2e^{j(\omega t-\pi/2)}\right\}$$

For any two complex quantities Z_1 and Z_2, $\text{Re}\{Z_1 + Z_2\} = \text{Re}\{Z_1\} + \text{Re}\{Z_2\}$ and, hence, the current can be written as

$$\begin{aligned} i(t) &= \text{Re}\{(1 + 2e^{-j\pi/2})e^{j\omega t}\} \\ &= \text{Re}\{(1 - j2)e^{j\omega t}\} \\ &= \text{Re}\{2.24e^{-j1.1071}e^{j\omega t}\} \end{aligned}$$

Therefore, in the phasor notation the current is given by

$$I = 2.24e^{-j1.1071} \text{ A}$$

EXAMPLE 1.2

Express the phasor current $I = (I_1 e^{j\varphi_1} + I_2 e^{j\varphi_2})$ as a function of time.

Solution: The instantaneous current can be expressed as

$$i(t) = \text{Re}\{Ie^{j\omega t}\}$$

Substituting the value of I

$$\begin{aligned} i(t) &= \text{Re}\{I_1 e^{j\varphi_1} e^{j\omega t} + I_2 e^{j\varphi_2} e^{j\omega t}\} \\ &= I_1 \cos(\omega t + \varphi_1) + I_2 \cos(\omega t + \varphi_2) \end{aligned}$$

The field vectors that vary with space, and are sinusoidal functions of time, can also be represented by phasors. For example, an electric field vector $\bar{\mathcal{E}}(x, y, z, t)$, a function of space (x, y, z) having a sinusoidal variation with time, can be written as

$$\bar{\mathcal{E}}(x, y, z, t) = \text{Re}\Big\{\mathbf{E}(x, y, z)e^{j\omega t}\Big\} \tag{1.5}$$

where $\mathbf{E}(x, y, z)$ is a phasor that contains the direction, magnitude, and phase information of the electric field, but is independent of time. In the text that follows, $e^{j\omega t}$ time variation is implied in all the field and source quantities and is not written explicitly. In this text, bold face symbols (e.g., $\mathbf{E}$) are used for vectors, phasors, or matrices, italic characters for scalar quantities (e.g., t), script characters (e.g., $\mathcal{E}$) for instantaneous scalar quantities, and script characters with an over-bar (e.g., $\bar{\mathcal{E}}$) for instantaneous vector quantities.

Using phasor notation, Maxwell's equations can be written for the fields and sources that are sinusoidally varying with time as[1]

$$\nabla \times \mathbf{E} = -j\omega\mu\mathbf{H} \tag{1.6}$$

$$\nabla \times \mathbf{H} = j\omega\epsilon\mathbf{E} + \mathbf{J} \tag{1.7}$$

$$\nabla \cdot \mathbf{D} = \rho \tag{1.8}$$

$$\nabla \cdot \mathbf{B} = 0 \tag{1.9}$$

The symbols used in Eqns (1.6) to (1.9) are explained below:

$\mathbf{E}$: Electric field intensity (unit: volt per metre, V/m)

$\mathbf{H}$: Magnetic field intensity (unit: ampere per metre, A/m)

$\mathbf{D}$: Electric flux density (unit: coulomb per metre, C/m)

$\mathbf{B}$: Magnetic flux density (unit: weber per metre, Wb/m or tesla, T)

$\mathbf{J}$: Current density (unit: ampere per square metre, A/m^2)

ρ : Charge density (unit: coulomb per cubic metre, C/m^3)

The first two curl equations are the mathematical representations of Faraday's and Ampere's laws, respectively. The divergence equation [Eqn (1.8)] represents Gauss's law. Since magnetic monopoles do not exist in nature, we have zero divergence for $\mathbf{B}$ [Eqn (1.9)].

The current density, $\mathbf{J}$, consists of two components. One is due to the impressed or actual sources and the other is the current induced due to the applied electric field, which is equal to $\sigma\mathbf{E}$, where σ is the conductivity of the medium (unit: siemens per metre, S/m). In antenna problems, we are mostly working with fields radiated into free space with $\sigma = 0$. Therefore, in the analyses that follow, unless explicitly specified, $\mathbf{J}$ represents impressed-source current density.

In an isotropic and homogeneous medium, the electric flux density, $\mathbf{D}$, and the electric field intensity, $\mathbf{E}$, are related by

$$\mathbf{D} = \epsilon\mathbf{E} \tag{1.10}$$

where ϵ is the electric permittivity (unit: farad per metre, F/m) of the medium. ϵ_0 is the permittivity of free space ($\epsilon_0 = 8.854 \times 10^{-12}$ F/m) and the ratio, $\epsilon/\epsilon_0 = \epsilon_r$ is known as the relative permittivity of the medium. It is

[1]See Cheng 2002, Hayt et al. 2001, Jordan et al. 2004, and Ramo et al. 2004.

a dimensionless quantity. Similarly, magnetic flux density, $\mathbf{B}$, and magnetic field intensity, $\mathbf{H}$, are related by

$$\mathbf{B} = \mu\mathbf{H} \tag{1.11}$$

where $\mu = \mu_0\mu_r$ is the magnetic permeability (unit: henry per metre, H/m) of the medium. μ_0 is the permeability of free space ($\mu_0 = 4\pi \times 10^{-7}$ H/m) and the ratio, $\mu/\mu_0 = \mu_r$, is known as the relative permeability of the medium. For an isotropic medium ϵ and μ are scalars and for a homogeneous medium they are independent of position.

One of the problems in antenna analysis is that of finding the $\mathbf{E}$ and $\mathbf{H}$ fields in the space surrounding the antenna. An antenna operating in the transmit mode is normally excited at a particular input point in the antenna structure. (The same point is connected to the receiver in the receive mode). Given an antenna structure and an input excitation, the current distribution on the antenna structure is established in such a manner that Maxwell's equations are satisfied everywhere and at all times (along with the boundary conditions which, again, are derived from Maxwell's equations using the behaviour of the fields at material boundaries). The antenna analysis can be split into two parts—(a) determination of the current distribution on the structure due to the excitation and (b) evaluation of the field due to this current distribution in the space surrounding the antenna. The first part generally leads to an integral equation, the treatment of which is beyond the scope of this book. We will be mainly concerned with the second part, i.e., establishing the antenna fields, given the current distribution.

Maxwell's equations [Eqns (1.6)–(1.9)] are time-independent, first order differential equations to be solved simultaneously. It is a common practice to reduce these equations to two second order differential equations called wave equations. For example, in a source-free region ($\rho = 0$ and $\mathbf{J} = 0$) we can take the curl of the first equation [Eqn (1.6)], substitute it in the second equation [Eqn (1.7)] to eliminate $\mathbf{H}$, and get the wave equation, $\nabla^2\mathbf{E} + k^2\mathbf{E} = 0$, satisfied by the $\mathbf{E}$ field. Similarly, we can also derive the wave equation satisfied by the $\mathbf{H}$ field. (Start from the curl of Eqn (1.7) and substitute in Eqn (1.6) to eliminate $\mathbf{E}$). Thus, it is sufficient to solve one equation to find both $\mathbf{E}$ and $\mathbf{H}$ fields, since they satisfy the same wave equation.

To simplify the problem of finding the $\mathbf{E}$ and $\mathbf{H}$ fields due to a current distribution, we can split it into two parts by defining intermediate potential functions which are related to the $\mathbf{E}$ and $\mathbf{H}$ fields. This is known as the vector potential approach and is discussed in the following subsection.

1.1.1 Vector Potential Approach

Given a current distribution on the antenna, the problem is one of determining the **E** and **H** fields due to this current distribution which satisfies all four of Maxwell's equations along with the boundary conditions, if any. In the vector potential approach we carry out the solution to this problem in two steps by defining intermediate potential functions. In the first step, we determine the potential function due to the current distribution and in the second step, the **E** and **H** fields are computed from the potential function. In the analysis that follows, the relationships between the vector potential and the current distribution as well as the **E** and **H** fields are derived. All four of Maxwell's equations are embedded in these relationships.

Let us start with the last of the Maxwell's equations, $\nabla \cdot \mathbf{B} = 0$. Since the curl of a vector field is divergence-free (vector identity: $\nabla \cdot \nabla \times \mathbf{A} = 0$), **B** can be expressed as a curl of an arbitrary vector field, **A**. We call this a magnetic vector potential function because it is related to the magnetic flux density, **B**, via the relationship

$$\mu\mathbf{H} = \mathbf{B} = \nabla \times \mathbf{A} \tag{1.12}$$

or

$$\mathbf{H} = \frac{1}{\mu}\nabla \times \mathbf{A} \tag{1.13}$$

Substituting this into the equation $\nabla \times \mathbf{E} = -j\omega\mu\mathbf{H}$, Maxwell's first equation is also incorporated

$$\nabla \times \mathbf{E} = -j\omega(\mu\mathbf{H}) = -j\omega(\nabla \times \mathbf{A}) \tag{1.14}$$

or

$$\nabla \times (\mathbf{E} + j\omega\mathbf{A}) = 0 \tag{1.15}$$

Since the curl of a gradient function is zero (vector identity: $\nabla \times \nabla V = 0$), the above equation suggests that the quantity in brackets can be replaced by the gradient of a scalar function. Specifically, a scalar potential function V is defined such that

$$(\mathbf{E} + j\omega\mathbf{A}) = -\nabla V \tag{1.16}$$

Using this we relate the **E** field to the potential functions as

$$\mathbf{E} = -(\nabla V + j\omega\mathbf{A}) \tag{1.17}$$

Equations (1.13) and (1.17) relate the **H** and **E** fields to the potential functions **A** and V. Now, to satisfy Maxwell's second equation, $\nabla \times \mathbf{H} = j\omega\epsilon\mathbf{E} + \mathbf{J}$, substitute the expression for the **E** and **H** fields in terms of the potential functions [Eqns (1.13) and (1.17)]

$$\frac{1}{\mu}\nabla \times (\nabla \times \mathbf{A}) = -j\omega\epsilon(\nabla V + j\omega\mathbf{A}) + \mathbf{J} \tag{1.18}$$

which is valid for a homogeneous medium. Expanding the left hand side using the vector identity

$$\nabla \times \nabla \times \mathbf{A} = \nabla(\nabla \cdot \mathbf{A}) - \nabla^2\mathbf{A} \tag{1.19}$$

we have

$$\nabla^2\mathbf{A} + \omega^2\mu\epsilon\mathbf{A} = -\mu\mathbf{J} + \nabla(\nabla \cdot \mathbf{A} + j\omega\mu\epsilon V) \tag{1.20}$$

So far we have satisfied three of Maxwell's four equations. Note that only the curl of **A** is defined so far. Since the curl and divergence are two independent parts of any vector field, we can now define the divergence of **A**. We define $\nabla \cdot \mathbf{A}$ so as to relate **A** and V as well as simplify Eqn (1.20) by eliminating the second term on the right hand side of the equation. We relate **A** and V by the equation

$$\nabla \cdot \mathbf{A} = -j\omega\mu\epsilon V \tag{1.21}$$

This relationship is known as the Lorentz condition. With this the magnetic vector potential, **A**, satisfies the vector wave equation

$$\nabla^2\mathbf{A} + k^2\mathbf{A} = -\mu\mathbf{J} \tag{1.22}$$

where

$$k = \omega\sqrt{\mu\epsilon} \tag{1.23}$$

is the propagation constant (unit: radian per metre, rad/m) in the medium.

Now, to satisfy Maxwell's fourth equation, $\nabla \cdot \mathbf{D} = \rho$, we substitute $\mathbf{E} = -(\nabla V + j\omega\mathbf{A})$ in this equation to get

$$\nabla \cdot (-\nabla V - j\omega\mathbf{A}) = \frac{\rho}{\epsilon} \tag{1.24}$$

or

$$\nabla^2 V + j\omega(\nabla \cdot \mathbf{A}) = -\frac{\rho}{\epsilon} \tag{1.25}$$

Eliminating **A** from this equation using the Lorentz condition [Eqn (1.21)]

$$\nabla^2 V + k^2 V = -\frac{\rho}{\epsilon} \tag{1.26}$$

Thus, both **A** and V must satisfy the wave equation, the source function being the current density for the magnetic vector potential, **A**, and the charge density for the electric scalar potential function V.

1.1.2 Solution of the Wave Equation

Consider a spherically symmetric charge distribution of finite volume, V', centred on the origin. Our goal is to compute the scalar potential $V(x, y, z)$ [or $V(r, \theta, \phi)$[1]] due to this source, which is the solution of the inhomogeneous wave equation as given by Eqn (1.26). Since the charge is spherically symmetric, we will solve the wave equation in the spherical coordinate system. The Laplacian $\nabla^2 V$ in the spherical coordinate system[2] is written as

$$\nabla^2 V = \frac{1}{r^2}\frac{\partial}{\partial r}\left(r^2 \frac{\partial V}{\partial r}\right) + \frac{1}{r^2 \sin\theta}\frac{\partial}{\partial \theta}\left(\sin\theta \frac{\partial V}{\partial \theta}\right) + \frac{1}{r^2 \sin^2\theta}\frac{\partial^2 V}{\partial \phi^2} \tag{1.27}$$

The scalar potential, $V(r, \theta, \phi)$, produced by a spherically symmetric charge distribution is independent of θ and ϕ. Therefore, the wave equation, Eqn (1.26), reduces to

$$\frac{1}{r^2}\frac{\partial}{\partial r}\left(r^2 \frac{\partial V}{\partial r}\right) + k^2 V = -\frac{\rho}{\epsilon} \tag{1.28}$$

The right hand side of this equation is zero everywhere except at the source itself. Therefore, in the source-free region, V satisfies the homogeneous wave equation

$$\frac{1}{r^2}\frac{\partial}{\partial r}\left(r^2 \frac{\partial V}{\partial r}\right) + k^2 V = 0 \tag{1.29}$$

The solutions for V are the scalar spherical waves given by

$$V(r) = V_0^{\pm} \frac{e^{\mp jkr}}{r} \tag{1.30}$$

where V_0^+ is a complex amplitude constant and e^{-jkr}/r is a spherical wave travelling in the $+r$-direction. V_0^- is the complex amplitude of the scalar

[1] (x, y, z): rectangular co-ordinates; (r, θ, ϕ): spherical co-ordinates.

[2] See Appendix E for details on the coordinate systems and vector operations in different coordinate systems.

spherical wave e^{jkr}/r travelling in the $-r$-direction. By substituting this in the wave equation, it can be shown that it satisfies the homogeneous wave equation [Eqn (1.29)].

EXAMPLE 1.3

Show that

$$V(r) = V_0^{\pm} \frac{e^{\mp jkr}}{r}$$

are solutions of

$$\frac{1}{r^2}\frac{\partial}{\partial r}\left(r^2 \frac{\partial V}{\partial r}\right) + k^2 V = 0$$

Solution: Let us consider the wave travelling in the positive r-direction

$$V(r) = V_0^{+} \frac{e^{-jkr}}{r}$$

Substituting into the left hand side (LHS) of the given equation

$$\begin{aligned}
\text{LHS} &= \frac{1}{r^2}\frac{\partial}{\partial r}\left[r^2 \frac{\partial}{\partial r}\left(V_0^{+}\frac{e^{-jkr}}{r}\right)\right] + k^2 V_0^{+}\frac{e^{-jkr}}{r} \\
&= V_0^{+}\frac{1}{r^2}\frac{\partial}{\partial r}\left[r^2\left(-\frac{e^{-jkr}}{r^2} - jk\frac{e^{-jkr}}{r}\right)\right] + k^2 V_0^{+}\frac{e^{-jkr}}{r} \\
&= V_0^{+}\frac{1}{r^2}\frac{\partial}{\partial r}\left(-e^{-jkr} - jkre^{-jkr}\right) + k^2 V_0^{+}\frac{e^{-jkr}}{r} \\
&= V_0^{+}\frac{1}{r^2}\left[jke^{-jkr} - jke^{-jkr} - k^2 re^{-jkr}\right] + k^2 V_0^{+}\frac{e^{-jkr}}{r} \\
&= 0
\end{aligned}$$

Therefore, the positive wave is a solution of the given differential equation.

Now, let us consider the wave that is travelling along the negative r-direction

$$V(r) = V_0^{-}\frac{e^{jkr}}{r}$$

Substituting into the left hand side of the given differential equation

$$\begin{aligned}\text{LHS} &= \frac{1}{r^2}\frac{\partial}{\partial r}\left[r^2\frac{\partial}{\partial r}\left(V_0^-\frac{e^{jkr}}{r}\right)\right] + k^2 V_0^-\frac{e^{jkr}}{r} \\ &= V_0^-\frac{1}{r^2}\frac{\partial}{\partial r}\left[-r^2\frac{1}{r^2}e^{jkr} + jkre^{jkr}\right] + k^2 V_0^-\frac{e^{jkr}}{r} \\ &= V_0^-\frac{1}{r^2}\left[-jke^{jkr} + jke^{jkr} - rk^2e^{jkr}\right] + k^2 V_0^-\frac{e^{jkr}}{r} \\ &= 0\end{aligned}$$

The wave travelling in the $-r$-direction satisfies the differential equation, hence it is also a solution.

These are the two solutions of the wave equation in free space and represent spherical waves propagating away from the origin ($+r$-direction) and converging on to the origin ($-r$-direction). Taking physical considerations into account, the wave converging towards the source is discarded.

The instantaneous value of the scalar potential $\mathcal{V}(r,t)$ for the wave propagating in the $+r$-direction can be written as

$$\mathcal{V}(r,t) = \text{Re}\left\{V_0^+\frac{e^{j(\omega t - kr)}}{r}\right\} \tag{1.31}$$

Since V_0^+ is a complex quantity, it can be expressed as, $V_0^+ = |V_0^+|e^{j\varphi_v}$, where φ_v is the phase angle of V_0^+. The equation for the constant phase spherical wave front is

$$\varphi_v + \omega t - kr = \text{const} \tag{1.32}$$

The velocity of the wave is the rate at which the constant phase front moves with time. Differentiating the expression for the constant phase front surface with respect to time, we get

$$j\omega - jk\frac{dr}{dt} = 0 \tag{1.33}$$

This follows from the fact that V_0^+ and, hence, the phase φ_v, is independent of time, i.e., $d\varphi_v/dt = 0$. Therefore, the velocity (v, unit: metre per second,

m/s) of the wave can be expressed as

$$v = \frac{dr}{dt} = \frac{\omega}{k} \tag{1.34}$$

Substituting the value of the propagation constant from Eqn (1.23), the wave velocity is

$$v = \frac{\omega}{\omega\sqrt{\mu\epsilon}} = \frac{1}{\sqrt{\mu\epsilon}} \tag{1.35}$$

The velocity of the wave in free space is equal to 3×10^8 m/s. The distance between two points that are separated in phase by 2π radians is known as the wavelength (λ, unit: metre, m) of the wave. Consider two points r_1 and r_2 on the wave with corresponding phases

$$\varphi_1 = \varphi_v + \omega t - kr_1$$
$$\varphi_2 = \varphi_v + \omega t - kr_2$$

such that

$$\varphi_2 - \varphi_1 = k(r_1 - r_2) = k\lambda = 2\pi \tag{1.36}$$

Therefore, the wavelength and the propagation constant are related by

$$k = \frac{2\pi}{\lambda} \tag{1.37}$$

The velocity can be written in terms of the frequency and the wavelength of the wave

$$v = \frac{\omega}{k} = \frac{2\pi f}{2\pi/\lambda} = f\lambda \tag{1.38}$$

EXAMPLE 1.4

The electric field of an electromagnetic wave propagating in a homogeneous medium is given by

$$\bar{\mathcal{E}}(x, y, z, t) = \mathbf{a}_\theta \frac{50}{r} \cos(4\pi \times 10^6 t - 0.063r) \text{ V/m}$$

Calculate the frequency, propagation constant, velocity, and the magnetic field intensity of the wave if the relative permeability of the medium is equal to unity.

Solution: The θ-component of the electric field can be expressed as

$$\mathcal{E}_\theta = \mathrm{Re}\left\{\frac{50}{r}e^{j(4\pi\times10^6 t-0.063r)}\right\}$$

Comparing this with Eqn (1.31), $\omega = 4\pi \times 10^6$ rad/s, hence frequency of the wave is $f = \omega/(2\pi) = 2$ MHz, and the propagation constant is $k = 0.063$ rad/m. The velocity of the wave is given by $v = \omega/k = 4\pi \times 10^6/0.063 = 2 \times 10^8$ m/s.

Expressing the electric field as a phasor

$$\mathbf{E} = \mathbf{a}_\theta \frac{50}{r}e^{-j0.063r} \text{ V/m}$$

Substituting this in Maxwell's equation, Eqn (1.6), and expressing the curl in spherical coordinates

$$-j\omega\mu\mathbf{H} = \nabla \times \mathbf{E} = \frac{1}{r^2\sin\theta}\begin{vmatrix} \mathbf{a}_r & r\mathbf{a}_\theta & r\sin\theta\mathbf{a}_\phi \\ \partial/\partial r & \partial/\partial\theta & \partial/\partial\phi \\ 0 & rE_\theta & 0 \end{vmatrix}$$

Expanding the determinant

$$\nabla \times \mathbf{E} = \frac{1}{r^2\sin\theta}\left[-\mathbf{a}_r\frac{\partial(rE_\theta)}{\partial\phi} + \mathbf{a}_\phi r\sin\theta\frac{\partial(rE_\theta)}{\partial r}\right]$$

Since r and E_θ are not functions of ϕ

$$\nabla \times \mathbf{E} = \mathbf{a}_\phi\frac{50}{r}(-j0.063)e^{-j0.063}$$

Therefore, the magnetic field is given by

$$\mathbf{H} = \frac{1}{-j\omega\mu}\nabla \times \mathbf{E} = \mathbf{a}_\phi\frac{0.063}{\omega\mu} \times \frac{50}{r}e^{-0.063r}$$

Substituting the values of $\omega = 4\pi \times 10^6$ rad/s and $\mu = 4\pi \times 10^{-7}$ H/m

$$\mathbf{H} = \mathbf{a}_\phi\frac{0.2}{r}e^{-j0.063r} \text{ A/m}$$

The magnetic field can also be expressed as a function of time.

$$\bar{\mathcal{H}} = \mathbf{a}_\phi \frac{0.2}{r} \cos(4\pi \times 10^6 t - 0.063r) \text{ A/m}$$

Consider a static point charge q kept at a point with position vector $\mathbf{r}'$ as shown in Fig. 1.4. The electric potential, V, at a point $P(r, \theta, \phi)$, with the position vector $\mathbf{r}$, is given by

$$V(r, \theta, \phi) = \frac{q}{4\pi\epsilon R} \tag{1.39}$$

where R is the distance between the charge and the observation point, $R = |\mathbf{R}| = |\mathbf{r} - \mathbf{r}'|$ (see Fig. 1.4). We are using two coordinate notations, the primed coordinates (x', y', z') for the source point and the unprimed coordinates (x, y, z) or (r, θ, ϕ) for the field point.

If there are more than one point charges, the potential is obtained by the superposition principle, i.e., summing the contributions of all the point charges. If the source is specified as a charge density distribution over a volume, the potential at any field point is obtained by integration over the source volume. To do this, we first consider a small volume $\Delta v'$ centered on $\mathbf{r}'$. The charge contained in this volume is $\rho(\mathbf{r}')\Delta v'$, where $\rho(\mathbf{r}')$ is the

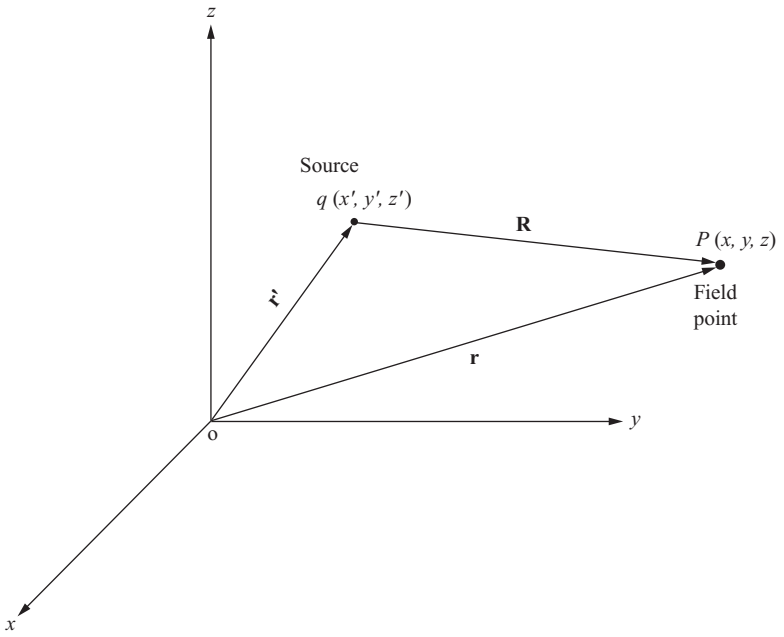

Fig. 1.4 Position vectors of source and field points

volume charge density distribution function. In the limit $\Delta v' \to 0$ we can consider the charge as a point charge and compute the potential at any field point $\mathbf{r}$ due to the charge contained in the volume $\Delta v'$ using the expression given in Eqn (1.39).

$$\Delta V(r, \theta, \phi) = \frac{\rho \Delta v'}{4\pi\epsilon R} \tag{1.40}$$

Let us now consider a time-varying charge $\rho\Delta v'$ with a sinusoidal time variation represented by $e^{j\omega t}$. Heuristically, we can reason out that the effect on the potential due to a change in the charge would travel to the field point with the propagation constant k. Hence for a point charge with an exponential time variation of the form $e^{j\omega t}$, the phase fronts are spherical with the point $\mathbf{r}'$ as the origin. Therefore

$$\Delta V(r, \theta, \phi) = \frac{\rho(x', y', z')\Delta v'}{4\pi\epsilon} \frac{e^{-jkR}}{R} \tag{1.41}$$

The potential at point (r, θ, ϕ) due to a charge distribution $\rho(x', y', z')$ is obtained by integrating Eqn (1.41) over the source distribution

$$V(r, \theta, \phi) = \frac{1}{4\pi\epsilon} \iiint_{V'} \rho(x', y', z') \frac{e^{-jkR}}{R} dv' \tag{1.42}$$

where V' is the volume over which $\rho(x', y', z')$ exists, or the source volume.

The instantaneous value of the scalar potential $\mathcal{V}(r, \theta, \phi, t)$ is obtained by

$$\mathcal{V}(r, \theta, \phi, t) = \mathrm{Re}\Big\{V(r, \theta, \phi) e^{j\omega t}\Big\} = \mathrm{Re}\left\{ \frac{1}{4\pi\epsilon} \iiint_{V'} \rho(x', y', z') \frac{e^{-jkR + j\omega t}}{R} dv' \right\} \tag{1.43}$$

Using the relation $v = \omega/k$, this reduces to

$$\mathcal{V}(r, \theta, \phi, t) = \mathrm{Re}\left\{ \frac{1}{4\pi\epsilon} \iiint_{V'} \rho(x', y', z') \frac{e^{j\omega(t - \frac{R}{v})}}{R} dv' \right\} \tag{1.44}$$

It is clear from this expression that the potential at time t is due to the charge that existed at an earlier time R/v. Or the effect of any change in the source has travelled with a velocity v to the observation point at a distance R from the source. Therefore, V is also known as the retarded scalar potential.

In Section 1.1.1 it is shown that both, electric scalar potential, V and magnetic vector potential, $\mathbf{A}$, satisfy the wave equation with the source terms being ρ/ϵ and $\mu\mathbf{J}$, respectively. Therefore, a similar heuristic argument can be used to derive the relationship between the current density distribution $\mathbf{J}(x', y', z')$ and the vector potential $\mathbf{A}(r, \theta, \phi)$. Starting from the expression for the magnetic vector potential for a static current density we introduce the delay time $-R/v$ to obtain the retarded vector potential expression for the time-varying current density distribution $\mathbf{J}$. The vector potential at any time t is related to the current density distribution at time $(t - R/v)$. Further, the vector $\mathbf{A}$ has the same direction as the current density $\mathbf{J}$. The relationship between the current density $\mathbf{J}(x', y', z')$ and the vector potential $\mathbf{A}(r, \theta, \phi)$ is given by simply multiplying the static relationship with the e^{-jkR} term. Thus, the retarded vector potential is given by

$$\mathbf{A}(r, \theta, \phi) = \frac{\mu}{4\pi} \iiint_{V'} \mathbf{J}(x', y', z') \frac{e^{-jkR}}{R} dv' \tag{1.45}$$

If the current density is confined to a surface with surface density $\mathbf{J}_s$ (in A/m), the volume integral in the vector potential expression reduces to a surface integral

$$\mathbf{A}(r, \theta, \phi) = \frac{\mu}{4\pi} \iint_{S'} \mathbf{J}_s(x', y', z') \frac{e^{-jkR}}{R} ds' \tag{1.46}$$

For a line current $\mathbf{I}$ (in A), the integral reduces to a line integral

$$\mathbf{A}(r, \theta, \phi) = \frac{\mu}{4\pi} \int_{C'} \mathbf{I}(x', y', z') \frac{e^{-jkR}}{R} dl' \tag{1.47}$$

1.1.3 Solution Procedure

The procedure for computing the fields of an antenna requires us to first determine the current distribution on the antenna structure and then compute the vector potential, $\mathbf{A}$, using Eqn (1.45). In a source-free region, $\mathbf{A}$ is related to the $\mathbf{H}$ field via Eqn (1.13)

$$\mathbf{H} = \frac{1}{\mu} \nabla \times \mathbf{A} \tag{1.48}$$

and $\mathbf{H}$ is related to the $\mathbf{E}$ field by (Eqn (1.7) with $\mathbf{J} = 0$ in a source-free region)

$$\mathbf{E} = \frac{1}{j\omega\epsilon}\nabla \times \mathbf{H} \tag{1.49}$$

As mentioned in Section 1.1, the computation of the current distribution on the antenna, starting from the excitation, involves solution of an integral equation and is beyond the scope of this book. Here we assume an approximate current distribution on the antenna structure and proceed with the computation of the radiation characteristics of the antenna.

1.2 Hertzian Dipole

A Hertzian dipole is 'an elementary source consisting of a time-harmonic electric current element of a specified direction and infinitesimal length' (*IEEE Trans. Antennas and Propagation* 1983). Although a single current element cannot be supported in free space, because of the linearity of Maxwell's equations, one can always represent any arbitrary current distribution in terms of the current elements of the type that a Hertzian dipole is made of. If the field of a current element is known, the field due to any current distribution can be computed using a superposition integral or summing the contributions due to all the current elements comprising the current distribution. Thus, the Hertzian dipole is the most basic antenna element and the starting point of antenna analysis.

Consider an infinitesimal time-harmonic current element, $\mathbf{I} = \mathbf{a}_z I_0 dl$, kept at the origin with the current flow directed along the z-direction indicated by the unit vector $\mathbf{a}_z$ (Fig. 1.5). I_0 is the current and dl is the elemental length of the current element. Time variation of the type $e^{j\omega t}$ is implied in saying the current element is time-harmonic. Consider the relationship between the current distribution $\mathbf{I}$ and the vector potential $\mathbf{A}$, as shown in Eqn (1.47) and reproduced here for convenience

$$\mathbf{A}(r, \theta, \phi) = \frac{\mu}{4\pi}\int_{C'} \mathbf{I}(x', y', z')\frac{e^{-jkR}}{R}dl' \tag{1.50}$$

Since we have an infinitesimal current element kept at the origin

$$x' = y' = z' = 0 \tag{1.51}$$

$$R = \sqrt{(x - x')^2 + (y - y')^2 + (z - z')^2} = \sqrt{x^2 + y^2 + z^2} = r \tag{1.52}$$

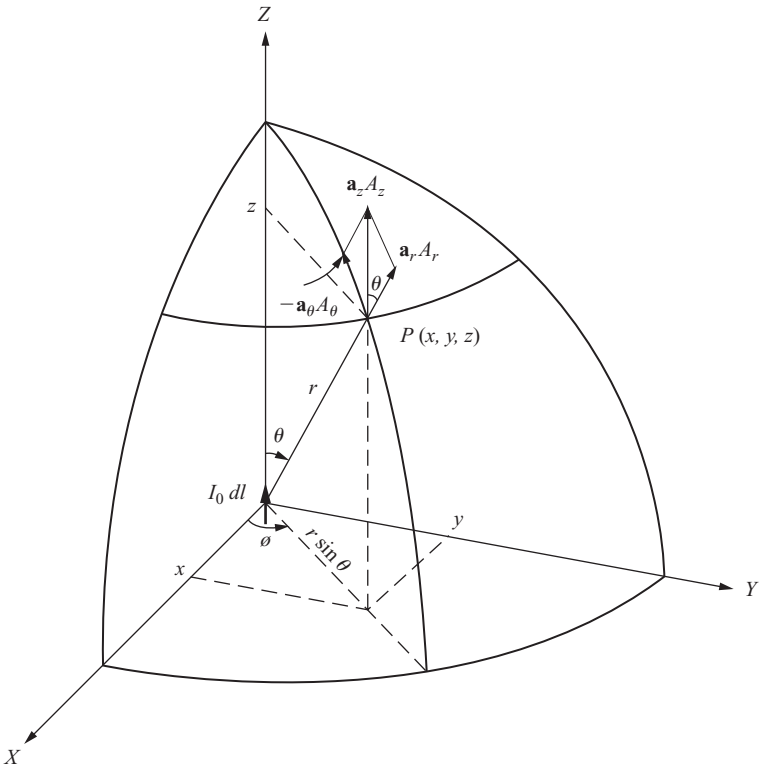

Fig. 1.5 Components of the vector potential on the surface of a sphere of radius r, due to a z-directed current element kept at the origin

Now, the vector potential due to a current element can be written as

$$\mathbf{A}(r,\theta,\phi) = \mathbf{a}_z \frac{\mu}{4\pi} I_0 dl \frac{e^{-jkr}}{r} = \mathbf{a}_z A_z \tag{1.53}$$

Note that the vector potential has the same vector direction as the current element. In this case, the $\mathbf{a}_z$-directed current element produces only the A_z-component of the vector potential.

The **H** and **E** fields of a Hertzian dipole are computed using the relationships given by Eqns (1.48) and (1.49), respectively. The **E** and **H** fields are generally computed in spherical coordinates for the following reasons—(a) the (e^{-jkr}/r) term indicates that the fields consist of outgoing spherical waves which are simple to represent mathematically in spherical coordinates and (b) the spherical coordinate system allows easy visualization of the behaviour of the fields as a function of direction and simplifies the mathematical representation of the radiated fields.

From Fig. 1.5 we can relate the z-component of the vector potential, A_z, to the components in spherical coordinates A_r, A_θ, and A_ϕ as

$$\begin{aligned} A_r &= A_z \cos\theta \\ A_\theta &= -A_z \sin\theta \\ A_\phi &= 0 \end{aligned} \tag{1.54}$$

Taking the curl of $\mathbf{A}$ in spherical coordinates

$$\nabla \times \mathbf{A} = \frac{1}{r^2 \sin\theta} \begin{vmatrix} \mathbf{a}_r & r\mathbf{a}_\theta & r\sin\theta \mathbf{a}_\phi \\ \partial/\partial r & \partial/\partial\theta & \partial/\partial\phi \\ A_r & rA_\theta & r\sin\theta A_\phi \end{vmatrix} \tag{1.55}$$

Substituting the components of $\mathbf{A}$ from Eqn (1.54) into Eqn (1.55), we get

$$\nabla \times \mathbf{A} = \frac{1}{r^2 \sin\theta} \begin{vmatrix} \mathbf{a}_r & r\mathbf{a}_\theta & r\sin\theta \mathbf{a}_\phi \\ \partial/\partial r & \partial/\partial\theta & \partial/\partial\phi \\ A_z\cos\theta & -rA_z\sin\theta & 0 \end{vmatrix} \tag{1.56}$$

Since A_z is a function of r alone, its derivatives with respect to θ and ϕ are zero. Hence, the curl equation reduces to

$$\nabla \times \mathbf{A} = \mathbf{a}_\phi \frac{1}{r}\left[\frac{\partial}{\partial r}(-rA_z \sin\theta) - \frac{\partial}{\partial\theta}(A_z\cos\theta)\right] \tag{1.57}$$

Substituting the expression for A_z and performing the indicated differentiations in Eqn (1.57)

$$\nabla \times \mathbf{A} = \mathbf{a}_\phi \frac{1}{r} A_z \sin\theta\,(jkr + 1) \tag{1.58}$$

Substituting the result in Eqn (1.48) and simplifying, we get the expressions for the components of the $\mathbf{H}$ field of a Hertzian dipole in spherical coordinates as

$$H_r = 0 \tag{1.59}$$

$$H_\theta = 0 \tag{1.60}$$

$$H_\phi = jk\frac{I_0 dl \sin\theta}{4\pi}\frac{e^{-jkr}}{r}\left[1 + \frac{1}{jkr}\right] \tag{1.61}$$

The electric field can be obtained from Maxwell's curl equation. Substituting the expression for $\mathbf{H}$ in Eqn (1.49) we get

$$\mathbf{E} = \frac{1}{j\omega\epsilon}\nabla \times \mathbf{H} = \frac{1}{j\omega\epsilon}\frac{1}{r^2 \sin\theta}\begin{vmatrix} \mathbf{a}_r & r\mathbf{a}_\theta & r\sin\theta\mathbf{a}_\phi \\ \partial/\partial r & \partial/\partial\theta & \partial/\partial\phi \\ 0 & 0 & r\sin\theta H_\phi \end{vmatrix} \tag{1.62}$$

Expanding the determinant the equation reduces to

$$\mathbf{E} = \frac{1}{j\omega\epsilon}\frac{1}{r^2 \sin\theta}\left[\mathbf{a}_r \frac{\partial}{\partial\theta}\left(r\sin\theta H_\phi\right) - r\mathbf{a}_\theta \frac{\partial}{\partial r}\left(r\sin\theta H_\phi\right)\right] \tag{1.63}$$

After performing the indicated derivative operations, Eqn (1.63) can be simplified to give the electric field components of a Hertzian dipole in spherical coordinates as

$$E_r = \eta\frac{I_0 dl\cos\theta}{2\pi r}\frac{e^{-jkr}}{r}\left(1 + \frac{1}{jkr}\right) \tag{1.64}$$

$$E_\theta = j\eta\frac{kI_0 dl\sin\theta}{4\pi}\frac{e^{-jkr}}{r}\left(1 + \frac{1}{jkr} - \frac{1}{(kr)^2}\right) \tag{1.65}$$

$$E_\phi = 0 \tag{1.66}$$

where $\eta = k/(\omega\epsilon)$ is the intrinsic impedance of the medium.

EXAMPLE 1.5

Show that $\eta = k/(\omega\epsilon)$.

Solution: Substituting $k = 2\pi/\lambda$ and $\omega = 2\pi f$ and simplifying

$$\frac{k}{\omega\epsilon} = \frac{2\pi/\lambda}{(2\pi f)\epsilon} = \frac{1}{(\lambda f)\epsilon}$$

The velocity of the wave, v, is related to the frequency, f, and the wavelength, λ, by $v = f\lambda$, and v is related to the permittivity, ϵ, and permeability, μ, of the medium by $v = 1/\sqrt{\mu\epsilon}$. Substituting these in the above equation and simplifying

$$\frac{k}{\omega\epsilon} = \frac{1}{v\epsilon} = \frac{\sqrt{\mu\epsilon}}{\epsilon} = \sqrt{\frac{\mu}{\epsilon}}$$

The impedance of the medium η is related to ϵ and μ by $\eta = \sqrt{\mu/\epsilon}$ and, therefore

$$\frac{k}{\omega\epsilon} = \eta$$

It is interesting to note that a z-directed current element kept at the origin has only the H_ϕ, E_r, and E_θ components and, further, the fields have components that decay as $1/r$, $1/r^2$, and $1/r^3$, away from the current element. Thus, these expressions form a convenient basis for classifying the fields of any antenna depending on the nature of decay away from the antenna.

To understand the nature of the field behaviour as a function of r, Eqns (1.64) and (1.65) can be re-written as

$$E_r = \eta \frac{k^2 I_0 dl \cos\theta}{2\pi} e^{-jkr} \left(\frac{1}{(kr)^2} + \frac{1}{j(kr)^3} \right) \tag{1.67}$$

$$E_\theta = j\eta \frac{k^2 I_0 dl \sin\theta}{4\pi} e^{-jkr} \left(\frac{1}{kr} + \frac{1}{j(kr)^2} - \frac{1}{(kr)^3} \right) \tag{1.68}$$

A plot of $1/(kr)$, $1/(kr)^2$, and $1/(kr)^3$ as functions of (kr) is shown in Fig. 1.6. For large values of r, i.e., $r \gg \lambda$ or $kr \gg 1$, the terms containing $1/(kr)^2$ and $1/(kr)^3$ decay much faster than $1/(kr)$. Therefore, at large

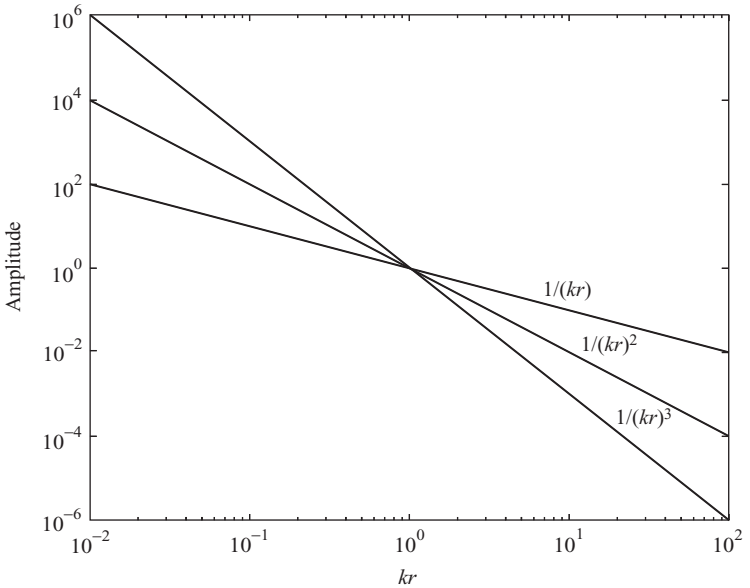

Fig. 1.6 Dependence of $1/(kr)$, $1/(kr)^2$, and $1/(kr)^3$ on (kr)

distances from the Hertzian dipole, only the terms containing $1/r$ are retained in the electric and magnetic field expressions. The electric and the magnetic fields of a z-directed Hertzian dipole for $r \gg \lambda$ are given by

$$E_\theta = j\eta \frac{kI_0 dl \sin\theta}{4\pi} \frac{e^{-jkr}}{r} \tag{1.69}$$

$$H_\phi = j \frac{kI_0 dl \sin\theta}{4\pi} \frac{e^{-jkr}}{r} \tag{1.70}$$

The ratio of E_θ to H_ϕ is equal to the impedance of the medium.

EXAMPLE 1.6

Calculate and compare the r and θ components of the electric field intensities at $x = 100$ m, $y = 100$ m, and $z = 100$ m produced by a Hertzian dipole of length $dl = 1$ m kept at the origin, oriented along the z-axis, excited by a current of $i(t) = 1 \times \cos(10\pi \times 10^6 t)$ A, and radiating into free space.

Solution: The frequency of excitation is $\omega = 10\pi \times 10^6$ rad/s, and therefore $f = 5 \times 10^6$ Hz. The dipole is radiating in free space with parameters $\mu = 4\pi \times 10^{-7}$ H/m and $\epsilon = 8.854 \times 10^{-12}$ F/m. Therefore, the impedance of the medium is

$$\eta = \sqrt{\frac{\mu}{\epsilon}} = \sqrt{\frac{4\pi \times 10^{-7}}{8.854 \times 10^{-12}}} = 376.73\ \Omega$$

and the propagation constant is

$$k = \omega\sqrt{\mu\epsilon} = 10\pi \times 10^6 \sqrt{4\pi \times 10^{-7} \times 8.854 \times 10^{-12}} = 0.1047\ \text{rad/m}$$

The distance r between the field point and the dipole (which is at the origin) is

$$r = \sqrt{x^2 + y^2 + z^2} = \sqrt{100^2 + 100^2 + 100^2} = 173.2\ \text{m}$$

Using the relation $z = r\cos\theta$, we can compute value of θ as

$$\theta = \cos^{-1}\left(\frac{z}{r}\right) = \cos^{-1}\left(\frac{100}{173.2}\right) = 54.73^\circ$$

Substituting these values in Eqn (1.64)

$$\begin{aligned}
E_r &= \eta \frac{I_0 dl \cos\theta}{2\pi r} \frac{e^{-jkr}}{r} \left(1 + \frac{1}{jkr}\right) \\
&= 376.73 \frac{1 \times 1 \times \cos 54.73^\circ}{2\pi \times 173.2} \frac{e^{-j0.1047 \times 173.2}}{173.2} \left(1 + \frac{1}{j0.1047 \times 173.2}\right) \\
&= 1.154 \times 10^{-3}(1 - j0.055)e^{-j18.14} \\
&= 1.154 \times 10^{-3} \times 1.002\angle -3.148^\circ \times 1\angle 40.65^\circ \\
&= 1.156 \times 10^{-3}\angle 37.51^\circ \text{ V/m}
\end{aligned}$$

The θ-component of the electric field is evaluated using Eqn (1.65)

$$\begin{aligned}
E_\theta &= j\eta \frac{kI_0 dl \sin\theta}{4\pi} \frac{e^{-jkr}}{r} \left(1 + \frac{1}{jkr} - \frac{1}{(kr)^2}\right) \\
&= j376.73 \frac{0.1047 \times 1 \times 1 \times \sin 54.73^\circ}{4\pi} \frac{e^{-j18.14}}{173.2} \left(1 + \frac{1}{j18.14} - \frac{1}{18.14^2}\right) \\
&= j0.0148e^{-j18.14}(1 - j0.055 - 3.04 \times 10^{-3}) \\
&= 1\angle 90^\circ \times 0.0148 \times 1\angle 40.65^\circ \times 0.9985\angle -3.158^\circ \\
&= 0.0148\angle 127.49^\circ \text{ V/m}
\end{aligned}$$

The wavelength of the EM wave is 60 m and, therefore, at a distance of 2.88λ the θ-component of the electric field is more than 10 times greater than the r-component.

EXAMPLE 1.7

A vector $\mathbf{A}$ can be represented in rectangular coordinate system as $\mathbf{A} = \mathbf{a}_x A_x + \mathbf{a}_y A_y + \mathbf{a}_z A_z$ and in spherical coordinates as $\mathbf{A} = \mathbf{a}_r A_r + \mathbf{a}_\theta A_\theta + \mathbf{a}_\phi A_\phi$. Express A_x, A_y, and A_z in terms of A_r, A_θ, and A_ϕ and vice versa.

Solution: The position vector of any point $\mathbf{r}$ in the rectangular coordinate system is given by

$$\mathbf{r} = \mathbf{a}_x x + \mathbf{a}_y y + \mathbf{a}_z z$$

From Fig. 1.5

$$x = r \sin\theta \cos\phi$$

$$y = r \sin\theta \sin\phi$$

$$z = r \cos\theta$$

Therefore, the position vector can be written as

$$\mathbf{r} = \mathbf{a}_x r \sin\theta \cos\phi + \mathbf{a}_y r \sin\theta \sin\phi + \mathbf{a}_z r \cos\theta$$

At any point $P(r, \theta, \phi)$, $\mathbf{a}_r$, $\mathbf{a}_\theta$, and $\mathbf{a}_\phi$ denote the unit vectors along the r, θ, and ϕ directions, respectively. The unit vector along the r-direction is given by

$$\mathbf{a}_r = \frac{\mathbf{r}}{|\mathbf{r}|}$$

where $|\mathbf{r}| = \sqrt{(r\sin\theta\cos\phi)^2 + (r\sin\theta\sin\phi)^2 + (r\cos\theta)^2} = r$ and hence

$$\mathbf{a}_r = \mathbf{a}_x \sin\theta\cos\phi + \mathbf{a}_y \sin\theta\sin\phi + \mathbf{a}_z \cos\theta$$

The unit vector $\mathbf{a}_\theta$ is tangential to the θ-direction. The tangent to the θ-direction is given by $\partial\mathbf{r}/\partial\theta$. Therefore, the unit vector along the θ-direction is given by

$$\mathbf{a}_\theta = \frac{\partial\mathbf{r}/\partial\theta}{|\partial\mathbf{r}/\partial\theta|} = \mathbf{a}_x \cos\theta\cos\phi + \mathbf{a}_y \cos\theta\sin\phi - \mathbf{a}_z \sin\theta$$

Similarly, $\mathbf{a}_\phi$ can be written as

$$\mathbf{a}_\phi = \frac{\partial\mathbf{r}/\partial\phi}{|\partial\mathbf{r}/\partial\phi|} = -\mathbf{a}_x \sin\phi + \mathbf{a}_y \cos\phi$$

This transformation from rectangular to spherical coordinates can be expressed in a matrix form as

$$\begin{pmatrix} \mathbf{a}_r \\ \mathbf{a}_\theta \\ \mathbf{a}_\phi \end{pmatrix} = \begin{pmatrix} \sin\theta\cos\phi & \sin\theta\sin\phi & \cos\theta \\ \cos\theta\cos\phi & \cos\theta\sin\phi & -\sin\theta \\ -\sin\phi & \cos\phi & 0 \end{pmatrix} \begin{pmatrix} \mathbf{a}_x \\ \mathbf{a}_y \\ \mathbf{a}_z \end{pmatrix}$$

Equating the rectangular and spherical coordinate representations of $\mathbf{A}$

$$\mathbf{A} = \mathbf{a}_x + \mathbf{a}_y + \mathbf{a}_z = \mathbf{a}_r A_r + \mathbf{a}_\theta A_\theta + \mathbf{a}_\phi A_\phi$$

Substituting the expressions for $\mathbf{a}_r$, $\mathbf{a}_\theta$, and $\mathbf{a}_\phi$ in terms of $\mathbf{a}_x$, $\mathbf{a}_y$, and $\mathbf{a}_z$

$$\begin{aligned} \mathbf{a}_x + \mathbf{a}_y + \mathbf{a}_z = {} & (\mathbf{a}_x \sin\theta\cos\phi + \mathbf{a}_y \sin\theta\sin\phi + \mathbf{a}_z \cos\theta) A_r \\ & + (\mathbf{a}_x \cos\theta\cos\phi + \mathbf{a}_y \cos\theta\sin\phi - \mathbf{a}_z \sin\theta) A_\theta \\ & + (-\mathbf{a}_x \sin\phi + \mathbf{a}_y \cos\phi) A_\phi \end{aligned}$$

This can be rearranged as

$$\begin{aligned}\mathbf{a}_x A_x + \mathbf{a}_y A_y + \mathbf{a}_z A_z = {} & \mathbf{a}_x(\sin\theta\cos\phi A_r + \cos\theta\cos\phi A_\theta - \sin\phi A_\phi) \\ & + \mathbf{a}_y(\sin\theta\sin\phi A_r + \cos\theta\sin\phi A_\theta + \cos\phi A_\phi) \\ & + \mathbf{a}_z(\cos\theta A_r - \sin\theta A_\theta)\end{aligned}$$

Equating the coefficients of $\mathbf{a}_x$, $\mathbf{a}_y$, and $\mathbf{a}_z$ on both sides, we get a relationship between (A_r, A_θ, A_ϕ) and (A_x, A_y, A_z). This can be represented in matrix form as

$$\begin{pmatrix} A_x \\ A_y \\ A_z \end{pmatrix} = \begin{pmatrix} \sin\theta\cos\phi & \cos\theta\cos\phi & -\sin\phi \\ \sin\theta\sin\phi & \cos\theta\sin\phi & \cos\phi \\ \cos\theta & -\sin\theta & 0 \end{pmatrix} \begin{pmatrix} A_r \\ A_\theta \\ A_\phi \end{pmatrix}$$

The 3×3 matrix is known as the transformation matrix. Let us use the symbol $\mathbf{X}$ to represent the transformation matrix.

The components of $\mathbf{A}$ in spherical coordinates can be written in terms of its components in rectangular coordinates by pre-multiplying both the sides of the above equation by the inverse of the transformation matrix.

$$\begin{aligned}\begin{pmatrix} A_r \\ A_\theta \\ A_\phi \end{pmatrix} &= \begin{pmatrix} \sin\theta\cos\phi & \cos\theta\cos\phi & -\sin\phi \\ \sin\theta\sin\phi & \cos\theta\sin\phi & \cos\phi \\ \cos\theta & -\sin\theta & 0 \end{pmatrix}^{-1} \begin{pmatrix} A_x \\ A_y \\ A_z \end{pmatrix} \\ &= \mathbf{X}^{-1} \begin{pmatrix} A_x \\ A_y \\ A_z \end{pmatrix}\end{aligned} \tag{1.7.1}$$

The inverse of the transformation matrix is given by

$$\mathbf{X}^{-1} = \frac{1}{\Delta} \begin{pmatrix} \begin{vmatrix} \cos\theta\sin\phi & \cos\phi \\ -\sin\theta & 0 \end{vmatrix} & -\begin{vmatrix} \sin\theta\sin\phi & \cos\phi \\ \cos\theta & 0 \end{vmatrix} & \begin{vmatrix} \sin\theta\sin\phi & \cos\theta\sin\phi \\ \cos\theta & -\sin\theta \end{vmatrix} \\ -\begin{vmatrix} \cos\theta\cos\phi & -\sin\phi \\ -\sin\theta & 0 \end{vmatrix} & \begin{vmatrix} \sin\theta\cos\phi & -\sin\phi \\ \cos\theta & 0 \end{vmatrix} & -\begin{vmatrix} \sin\theta\cos\phi & \cos\theta\cos\phi \\ \cos\theta & -\sin\theta \end{vmatrix} \\ \begin{vmatrix} \cos\theta\cos\phi & -\sin\phi \\ \cos\theta\sin\phi & \cos\phi \end{vmatrix} & -\begin{vmatrix} \sin\theta\cos\phi & -\sin\phi \\ \sin\theta\sin\phi & \cos\phi \end{vmatrix} & \begin{vmatrix} \sin\theta\cos\phi & \cos\theta\cos\phi \\ \sin\theta\sin\phi & \cos\theta\sin\phi \end{vmatrix} \end{pmatrix}^{\mathrm{T}}$$

where Δ is the determinant of the transformation matrix and is equal to unity. On simplifying

$$\mathbf{X}^{-1} = \begin{pmatrix} \sin\theta\cos\phi & \cos\theta\cos\phi & -\sin\phi \\ \sin\theta\sin\phi & \cos\theta\sin\phi & \cos\phi \\ \cos\theta & -\sin\theta & 0 \end{pmatrix}^{\mathrm{T}}$$

On taking the transpose of the matrix and substituting in Eqn (1.7.1)

$$\begin{pmatrix} A_r \\ A_\theta \\ A_\phi \end{pmatrix} = \begin{pmatrix} \sin\theta\cos\phi & \sin\theta\sin\phi & \cos\theta \\ \cos\theta\cos\phi & \cos\theta\sin\phi & -\sin\theta \\ -\sin\phi & \cos\phi & 0 \end{pmatrix} \begin{pmatrix} A_x \\ A_y \\ A_z \end{pmatrix}$$

The transformation matrix has the unitary property, i.e., $\mathbf{X}^{-1} = \mathbf{X}^{\mathrm{T}}$. Using this property we can transform the unit vectors in spherical coordinates into unit vectors in rectangular coodrinates as

$$\begin{pmatrix} \mathbf{a}_x \\ \mathbf{a}_y \\ \mathbf{a}_z \end{pmatrix} = \begin{pmatrix} \sin\theta\cos\phi & \cos\theta\cos\phi & -\sin\phi \\ \sin\theta\sin\phi & \cos\theta\sin\phi & \cos\phi \\ \cos\theta & -\sin\theta & 0 \end{pmatrix} \begin{pmatrix} \mathbf{a}_r \\ \mathbf{a}_\theta \\ \mathbf{a}_\phi \end{pmatrix}$$

EXAMPLE 1.8

Derive the expressions for the fields of a current element $I_0 dl$ kept at the origin, oriented along the x-axis, and radiating into free space.

Solution: Since the current element is oriented along the x-direction, the magnetic vector potential has only the x-component. Following the procedure given in Section 1.2, we can write the magnetic vector potential as

$$\mathbf{A} = \mathbf{a}_x \frac{\mu_0}{4\pi} I_0 dl \frac{e^{-jkr}}{r}$$

The unit vector $\mathbf{a}_x$ can be written in terms of the unit vectors of the spherical coordinates (see Example 1.7)

$$\mathbf{A} = \frac{\mu_0}{4\pi} I_0 dl \frac{e^{-jkr}}{r} (\mathbf{a}_r \sin\theta\cos\phi + \mathbf{a}_\theta \cos\theta\cos\phi - \mathbf{a}_\phi \sin\phi)$$

The magnetic field is given by

$$\mathbf{H} = \frac{1}{\mu}\nabla \times \mathbf{A} = \frac{1}{\mu r^2 \sin\theta} \begin{vmatrix} \mathbf{a}_r & r\mathbf{a}_\theta & r\sin\theta\mathbf{a}_\phi \\ \partial/\partial r & \partial/\partial\theta & \partial/\partial\phi \\ A_r & rA_\theta & r\sin\theta A_\phi \end{vmatrix}$$

Expanding the determinant

$$\mathbf{H} = \frac{1}{r^2 \sin\theta}\frac{I_0 dl}{4\pi}\left\{\mathbf{a}_r\left[\frac{\partial}{\partial\theta}\left(-r\sin\theta\sin\phi\frac{e^{-jkr}}{r}\right) - \frac{\partial}{\partial\phi}\left(r\cos\theta\cos\phi\frac{e^{-jkr}}{r}\right)\right]\right.$$
$$- \mathbf{a}_\theta r\left[\frac{\partial}{\partial r}\left(-r\sin\theta\sin\phi\frac{e^{-jkr}}{r}\right) - \frac{\partial}{\partial\phi}\left(\sin\theta\cos\phi\frac{e^{-jkr}}{r}\right)\right]$$
$$\left. + \mathbf{a}_\phi r\sin\theta\left[\frac{\partial}{\partial r}\left(r\cos\theta\cos\phi\frac{e^{-jkr}}{r}\right) - \frac{\partial}{\partial\theta}\left(\sin\theta\cos\phi\frac{e^{-jkr}}{r}\right)\right]\right\}$$

Performing the indicated differentiations and simplifying

$$H_\theta = -j\frac{kI_0 dl}{4\pi}\sin\phi\frac{e^{-jkr}}{r}\left(1 + \frac{1}{jkr}\right)$$
$$H_\phi = -j\frac{kI_0 dl}{4\pi}\cos\theta\cos\phi\frac{e^{-jkr}}{r}\left(1 + \frac{1}{jkr}\right)$$

The electric field can be calculated from Maxwell's equation $j\omega\epsilon\mathbf{E} = \nabla \times \mathbf{H}$

$$\mathbf{E} = \frac{1}{j\omega\epsilon}\frac{1}{r^2\sin\theta}\begin{vmatrix} \mathbf{a}_r & r\mathbf{a}_\theta & r\sin\theta\mathbf{a}_\phi \\ \partial/\partial r & \partial/\partial\theta & \partial/\partial\phi \\ 0 & rH_\theta & r\sin\theta H_\phi \end{vmatrix}$$

On expanding the determinant, performing the indicated differentiations, and simplifying

$$E_r = \eta\frac{I_0 dl}{2\pi r}\sin\theta\cos\phi\frac{e^{-jkr}}{r}\left(1 + \frac{1}{jkr}\right)$$
$$E_\theta = -j\eta\frac{kI_0 dl}{4\pi}\cos\theta\cos\phi\frac{e^{-jkr}}{r}\left(1 + \frac{1}{jkr} - \frac{1}{(kr)^2}\right)$$
$$E_\phi = j\eta\frac{kI_0 dl}{4\pi}\sin\phi\frac{e^{-jkr}}{r}\left(1 + \frac{1}{jkr} - \frac{1}{(kr)^2}\right)$$

So far we have learnt how to compute the fields due to a current distribution using the vector potential approach. Every antenna can be looked at as a current distribution producing electric and magnetic fields in the surrounding space and, therefore, we have learnt the basics of computing the fields of an antenna. In the following chapter we will learn about properties of antennas and introduce the various terms associated with antennas.

Exercises

1.1 Prove that the spherical coordinate system is orthogonal.

1.2 Show that for any twice differentiable scalar function, ϕ, $\nabla \times \nabla\phi = 0$.

1.3 Show that for any twice differentiable vector function $\mathbf{A}$, $\nabla \cdot \nabla \times \mathbf{A} = 0$.

1.4 Prove the vector identity $\nabla \times \nabla \times \mathbf{A} = \nabla(\nabla \cdot \mathbf{A}) - \nabla^2\mathbf{A}$.

1.5 In a source-free region show that the $\mathbf{E}$ and $\mathbf{H}$ fields satisfy $\nabla^2\mathbf{E} + k^2\mathbf{E} = 0$ and $\nabla^2\mathbf{H} + k^2\mathbf{H} = 0$, respectively.

1.6 Show that $V(r) = V_0 e^{-jkr}/r$, where V_0 is a complex constant and k is a real number, represents a wave travelling in the positive r-direction.

1.7 Plot the equiphase surfaces of the electric field of an EM wave given by (a) $\mathbf{E} = \mathbf{a}_\phi E_0 e^{-jkr}/r$ and (b) $\mathbf{E} = \mathbf{a}_y E_0 e^{-jkx}$, where E_0 is a complex constant.

1.8 Derive Eqns (1.59)–(1.61) from Eqn (1.57).

1.9 Derive Eqns (1.64)–(1.66) from Eqn (1.63).

1.10 For the Hertzian dipole considered in Section 1.2, compute the electric and magnetic fields in the rectangular coordinate system directly by taking the curl of $\mathbf{a}_z A_z$. Now convert the fields into spherical coordinates and compare them with the results given in Eqns (1.59)–(1.61) and Eqns (1.64)–(1.66).

1.11 Show that $\omega\mu = k\eta$, where the symbols have their usual meaning.

1.12 Show that at large distances from a radiating Hertzian dipole ($r \gg \lambda$), the electric and magnetic fields satisfy Maxwell's equations.

1.13 A z-directed Hertzian dipole placed at the origin has length $dl = 1$ m and is excited by a sinusoidal current of amplitude $I_0 = 10$ A and frequency 1 MHz. If the dipole is radiating into free space, calculate the distance in the x-y plane from the antenna beyond which the magnitude of the electric field strength is less than 1×10^{-3} V/m.

Answer: 6279 m

1.14 Derive an expression for the fields of a Hertzian dipole of length dl carrying a current of I_0 which is located at the origin of the coordinate system and oriented along the y-axis.

1.15 Find the strength of the z-component of the electric field at $(0, 100\text{ m}, 0)$ produced by a z-directed Hertzian dipole of length $dl = 0.5$ m, placed at the origin, carrying a current of $i(t) = 2\cos(6\pi \times 10^6 t)$ A, and radiating into free space. If the dipole is oriented along the x-axis, what will be strength of the x-component of the electric field at the same point?

Answer: $E_z = 0.01856\angle -99.3^\circ$ V/m; $E_x = 0.01856\angle -99.3^\circ$ V/m

CHAPTER 2

Antenna Characteristics

Introduction

An antenna acts as an interface between a guided wave and a free-space wave. One of the most important characteristics of an antenna is its directional property, i.e., its ability to concentrate radiated power in a certain direction or receive power from a preferred direction. The directional property of an antenna is characterized in terms of a pattern which applies to the antenna as a transmitter or as a receiver. For an efficient interface between the free-space wave and the guided wave in the feed transmission line, the input impedance of the antenna must be matched to the characteristic impedance of the transmission line. Thus, the antenna characteristics can be classified into two main categories—(a) radiation characteristics, which are used to describe the way the antenna radiates or receives energy from space and (b) input characteristics, which are used to specify the performance of the antenna looking into its terminals. Radiation characteristics include the radiation pattern, gain, directivity, effective aperture, polarization, etc. and the input characteristics are specified in terms of the input impedance, bandwidth, reflection coefficient, voltage standing wave ratio, etc.

In this chapter, antenna characteristics are explained using an infinitesimal current element radiator, that was introduced in the previous chapter, as one of the examples. The reciprocity theorem is used to show the equivalence between the transmit and receive characteristics of an antenna. Finally, these characteristics are used in the derivation of the link budget of a wireless system and in explaining some of the antenna related issues involved in wireless system design.

2.1 Radiation Pattern

Consider the fields of an infinitesimal Hertzian electric dipole of length dl kept at the origin of the coordinate system. Let I_0 be the z-directed current in the Hertzian dipole radiating into free space. In spherical coordinates, the expressions for the **E** and **H** fields are given by Eqns (1.59)–(1.61) and Eqns (1.64)–(1.66), respectively and are reproduced here for convenience

$$E_r = \eta \frac{I_0 dl \cos\theta}{2\pi} e^{-jkr} \left(\frac{1}{r^2} + \frac{1}{jkr^3} \right) \tag{2.1}$$

$$E_\theta = j\eta \frac{k I_0 dl \sin\theta}{4\pi} e^{-jkr} \left(\frac{1}{r} + \frac{1}{jkr^2} - \frac{1}{k^2 r^3} \right) \tag{2.2}$$

$$E_\phi = 0 \tag{2.3}$$

$$H_r = 0 \tag{2.4}$$

$$H_\theta = 0 \tag{2.5}$$

$$H_\phi = jk \frac{I_0 dl \sin\theta}{4\pi} e^{-jkr} \left[\frac{1}{r} + \frac{1}{jkr^2} \right] \tag{2.6}$$

where the impedance of the medium, η, is given by

$$\eta = \frac{k}{\omega\epsilon} = \sqrt{\frac{\mu}{\epsilon}} \ \ \Omega \tag{2.7}$$

In Eqn (2.7) μ and ϵ are the permeability and permittivity of the medium, respectively. For free space, $\eta = \sqrt{\mu_0/\epsilon_0} = 376.73$ Ω. This is generally approximated to 377 Ω or 120π Ω.

The above field expressions are valid everywhere except on the dipole itself. Since the $1/r^2$ and $1/r^3$ terms decay much faster than the $1/r$ term, at large distances from the dipole ($r \gg \lambda$) we can neglect these terms and simplify the field expression by taking only the $1/r$ terms. This simplified expression is known as the far-field expression. Further, the Poynting vector corresponding to the $1/r^2$ and $1/r^3$ terms is reactive and that due to the $1/r$ term is real. Therefore, the $1/r$ terms are taken as the radiated fields. The region far away from the antenna is known as *far-field* or *Fraunhofer* region. (The region close to the antenna is known *Fresnel* or *radiating near-field* region.) In the far-field region, only E_θ and H_ϕ exist and form a spherical wavefront emanating from the antenna. Thus, the far-field expressions for

E and **H** reduce to

$$\mathbf{E} = \mathbf{a}_\theta E_\theta = \mathbf{a}_\theta j\eta \frac{kI_0 dl \sin\theta}{4\pi} \frac{e^{-jkr}}{r} \tag{2.8}$$

$$\mathbf{H} = \mathbf{a}_\phi H_\phi = \mathbf{a}_\phi j \frac{kI_0 dl \sin\theta}{4\pi} \frac{e^{-jkr}}{r} \tag{2.9}$$

In the far-field, E_θ and H_ϕ are perpendicular to each other and transverse to the direction of propagation. The ratio of the two field components is the same as the intrinsic impedance, η, of the medium

$$\frac{E_\theta}{H_\phi} = \eta \tag{2.10}$$

Thus, the radiated EM wave satisfies all the properties of a transverse electromagnetic (TEM) wave.

The time-averaged power density vector of the wave is given by

$$\mathbf{S} = \frac{1}{2}\text{Re}(\mathbf{E} \times \mathbf{H}^*) = \mathbf{a}_r \frac{1}{2} E_\theta H_\phi^* = \mathbf{a}_r \frac{1}{2\eta} |E_\theta|^2 \quad \text{W/m}^2 \tag{2.11}$$

where $\mathbf{H}^*$ indicates the complex conjugate of **H**. Substituting the value of E_θ from Eqn (2.8), the time-averaged power density or the Poynting vector for a Hertzian dipole reduces to

$$\mathbf{S}(r, \theta, \phi) = \mathbf{a}_r \frac{1}{2}\eta \left| \frac{kI_0 dl}{4\pi} \right|^2 \frac{\sin^2\theta}{r^2} \tag{2.12}$$

This shows that in the far-field of the antenna, the power flows radially outward from the antenna, but the power density is not the same in all directions.

EXAMPLE 2.1

A Hertzian dipole of length $dl = 0.5$ m is radiating into free space. If the dipole current is 4 A and the frequency is 10 MHz, calculate the highest power density at a distance of 2 km from the antenna.

Solution: Since the antenna is radiating into free space, we can choose the coordinate system such that the dipole is oriented along the z-axis. The power density is given by Eqn (2.12) and has a maximum along $\theta = \pi/2$.

Therefore, the maximum power density of a Hertzian dipole is given by

$$S = \frac{1}{2}\eta \left| \frac{kI_0 dl}{4\pi} \right|^2 \frac{1}{r^2} \quad \text{W/m}^2$$

The propagation constant, k, is given by

$$k = \omega\sqrt{\mu\epsilon} = \frac{\omega}{c} = \frac{2\pi \times 10 \times 10^6}{3 \times 10^8} = \frac{2\pi}{30} \quad \text{rad/m}$$

Substituting the values of $I_0 = 4$, $dl = 0.5$, k, and $r = 2000$

$$S = \frac{1}{2} \times 120\pi \left| \frac{2\pi}{30} \times \frac{4 \times 0.5}{4\pi} \right|^2 \frac{1}{2000^2} = 5.24 \times 10^{-8} \quad \text{W/m}^2$$

Consider an antenna kept at the origin of a spherical coordinate system and let $S(r, \theta, \phi)$ be the average radial power density at a distance r from the antenna along the direction (θ, ϕ). Let dA be an elemental area on the surface of the sphere of radius r that subtends a solid angle $d\Omega$ at the centre of the sphere (which is also the origin of the coordinate system). The elemental area dA is given by

$$dA = r^2 d\Omega \quad \text{m}^2 \tag{2.13}$$

In spherical coordinates $dA = r^2 \sin\theta d\theta d\phi$ and hence the elemental solid angle $d\Omega$ (unit: steradian, sr) is given by

$$d\Omega = \sin\theta d\theta d\phi \quad \text{sr} \tag{2.14}$$

EXAMPLE 2.2

Show that there are 4π steradians in a sphere.

Solution: The total solid angle in a sphere is

$$\Omega = \int_{\theta=0}^{\pi} \int_{\phi=0}^{\pi} d\Omega$$

Substituting the expression for $d\Omega$ from Eqn (2.24)

$$\Omega = \int_{\theta=0}^{\pi} \int_{\phi=0}^{\pi} \sin\theta d\theta d\phi$$

Integrating with respect to ϕ and then with respect to θ

$$\Omega = 2\pi \int_{\theta=0}^{\pi} \sin\theta d\theta = 2\pi[-\cos\theta]_0^{\pi} = 4\pi \ \text{ sr}$$

The power crossing the area dA is given by $S(r,\theta,\phi)dA$ and the power crossing per unit solid angle is defined as the *radiation intensity*, $U(\theta,\phi)$, and is given by

$$U(\theta,\phi) = \frac{S(r,\theta,\phi)dA}{d\Omega} = r^2 S(r,\theta,\phi) \ \text{ W/sr} \tag{2.15}$$

The power pattern or the radiation intensity, $U(\theta,\phi)$, of an antenna is the angular distribution of the power per unit solid angle. This can be obtained by multiplying the Poynting vector by r^2. Thus, the radiation intensity pattern of a Hertzian dipole is

$$r^2 S(r,\theta,\phi) = U(\theta,\phi) = \frac{1}{2}\eta \left|\frac{kI_0 dl}{4\pi}\right|^2 \sin^2\theta \ \text{ W/m}^2 \tag{2.16}$$

The normalized power pattern, P_n, is obtained by normalizing the radiation intensity, U, or the time-averaged Poynting vector, S, with respect to their maximum values.

$$P_n(\theta,\phi) = \frac{U(\theta,\phi)}{U_{\max}} = \frac{S(r,\theta,\phi)}{S_{\max}(r)} \tag{2.17}$$

The normalized power is a dimensionless quantity and it is expressed in decibels as

$$P_{n\text{dB}}(\theta,\phi) = 10\log_{10}[P_n(\theta,\phi)] \tag{2.18}$$

For a Hertzian dipole it is given by

$$P_{n\text{dB}}(\theta,\phi) = 10\log_{10}(\sin^2\theta) \tag{2.19}$$

A plot of the far-field electric or magnetic field intensity as a function of the direction at a constant distance from the antenna is known as the electric field pattern or the magnetic field pattern, respectively. Dividing the field quantities by their respective maximum values we get the normalized field patterns. For a Hertzian dipole, the normalized field pattern is given by

$$E_{\theta n}(\theta,\phi) = \frac{E_\theta(r,\theta,\phi)}{E_{\theta\max}(r)} = \sin\theta = H_{\phi n}(\theta,\phi) \tag{2.20}$$

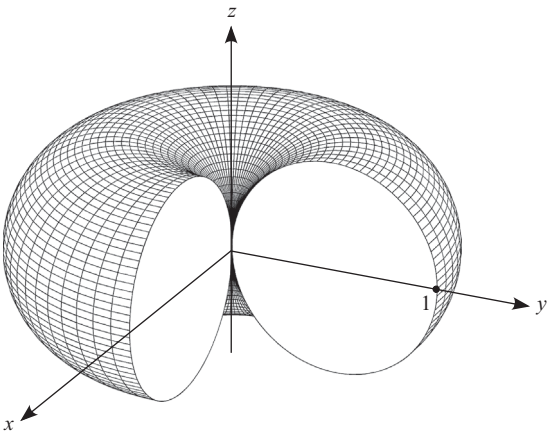

Fig. 2.1 Normalized E_θ field pattern of a Hertzian dipole

A three-dimensional (3D) plot of the normalized electric field (maximum amplitude equal to unity) is shown in Fig. 2.1. The field intensity along a direction (θ, ϕ) is given by the length of the position vector to a point on the surface of the 3D shape in the direction (θ, ϕ).

The *radiation pattern* or *antenna pattern* is defined as 'the spatial distribution of a quantity that characterizes the electromagnetic field generated by an antenna' (IEEE Std 145 1990). The quantity referred to in this definition could be the field amplitude, power, radiation intensity, antenna polarization, relative phase, etc. When the term 'radiation pattern' is used without specifying the quantity, the radiation intensity or the field amplitude is implied.

It is generally convenient to present the pattern in two-dimensional (2D) plots by considering two orthogonal principal plane cuts of the 3D pattern. Principal plane implies that the cut is through the pattern maximum. For a linearly polarized antenna (see Section 2.4 for the definition), the pattern cuts in the principal planes parallel to the **E** and **H** field vectors are chosen. These patterns are called the **E**-plane and the **H**-plane patterns, respectively. For a Hertzian dipole, the x-z and x-y plane cuts of the pattern shown in Fig. 2.1 are the **E**-plane and the **H**-plane patterns and are shown in Fig. 2.2. The **E**-plane pattern resembles the shape of a figure-of-eight and the **H**-plane pattern is a circle.

It is also possible to define the 2D cuts in the spherical coordinate system. For example, the $\theta = 90^\circ$ cut is the same as the x-y cut. However, one half of the x-z cut is denoted by the $\phi = 0^\circ$ cut and the other half by the $\phi = 180^\circ$ cut.

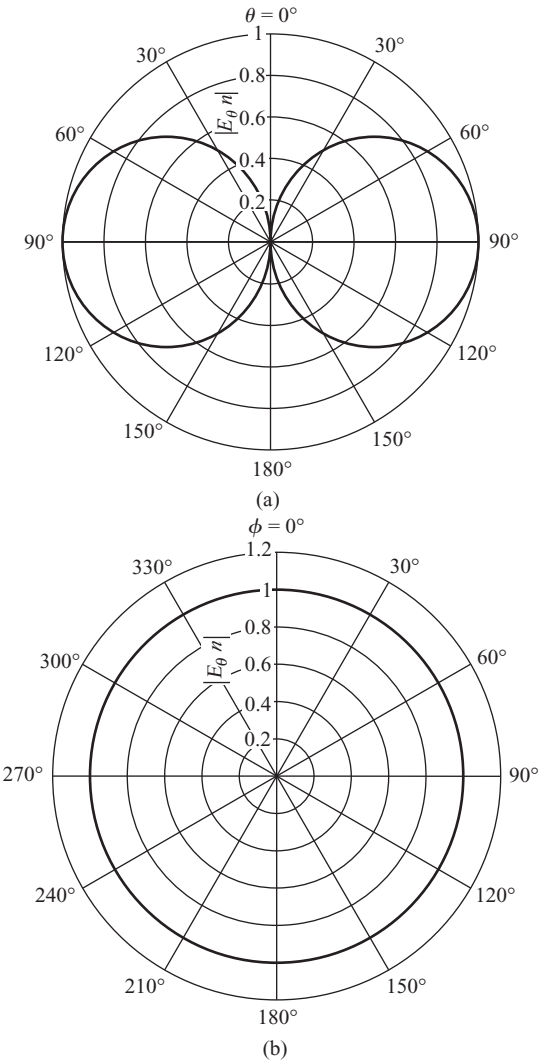

Fig. 2.2 Normalized E_θ field pattern of a Hertzian dipole: (a) **E**-plane pattern (x-z plane); (b) **H**-plane pattern (x-y plane)

A 3D plot of the normalized power pattern expressed in decibels [Eqn (2.19)] is shown in Fig. 2.3(a) and the **E**-plane pattern is shown in Fig. 2.3(b). The pattern has a maximum along $\theta = 90°$ which is also known as the broadside direction of the dipole. The plot indicates the relative level of the radiation intensity with respect to the maximum. For example, along $\theta = 30°$ the radiation intensity is 6 dB below the maximum. The pattern has nulls along $\theta = 0°$ and 180°, which are the directions along the axis of the dipole.

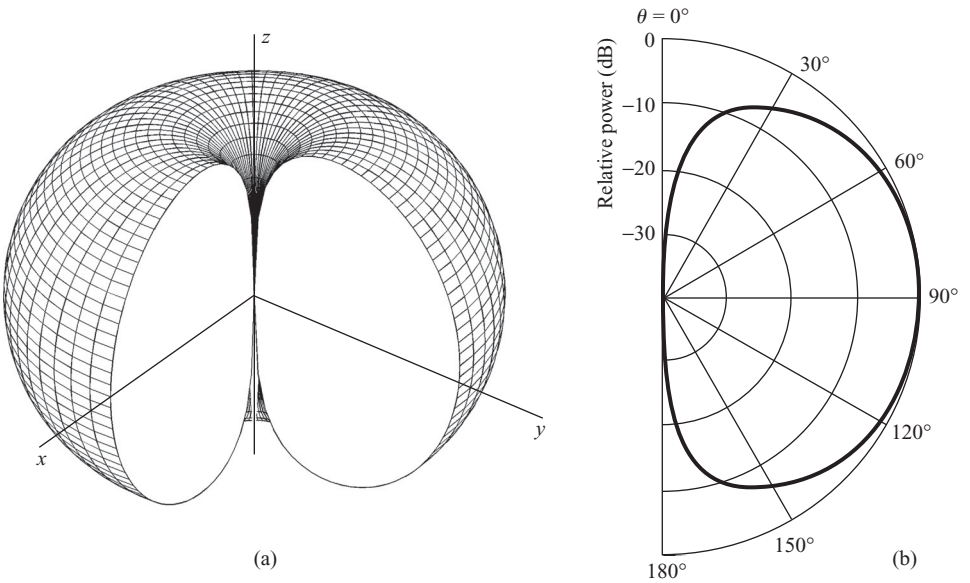

Fig. 2.3 Normalized power pattern of a Hertzian dipole (a) 3D view; (b) **E**-plane pattern ($\phi = 0^\circ$ plane) in dB units

The radiation pattern of an antenna can also have several other features. Consider a three-dimensional normalized power pattern of an antenna as shown in Fig. 2.4. The direction of the radiation maximum is along $(\theta, \phi) = (90^\circ, 90^\circ)$. The pattern indicates regions of higher radiation surrounded by regions of lower radiation. These are known as lobes. The lobe along the direction of maximum radiation is known as main lobe or major lobe and all other lobes are called side lobes. The main lobe is also sometimes referred to as the main beam. The nulls in the pattern indicate that along these directions the radiation is zero. The radiation lobe that makes an angle of about 180° with the main lobe is known as the back lobe (Fig. 2.5).

The two-dimensional cut of a three-dimensional radiation pattern can also be plotted on a rectangular graph with the normalized power (in dB) along the vertical axis and the angle (θ) along the horizontal axis (Fig. 2.6). This representation is very useful for extracting quantitative information about the pattern. For example, we can infer that the first side lobe adjacent to the main lobe is 18 dB below the main lobe.

The angular width of the main beam between its half-power points is known as the half-power beamwidth or the 3 dB beamwidth. For patterns which are very broad, sometimes a 10 dB beamwidth is specified instead of a 3 dB beamwidth. The 10 dB beamwidth is the angle between the two directions on either side of the main lobe peak along which the power density

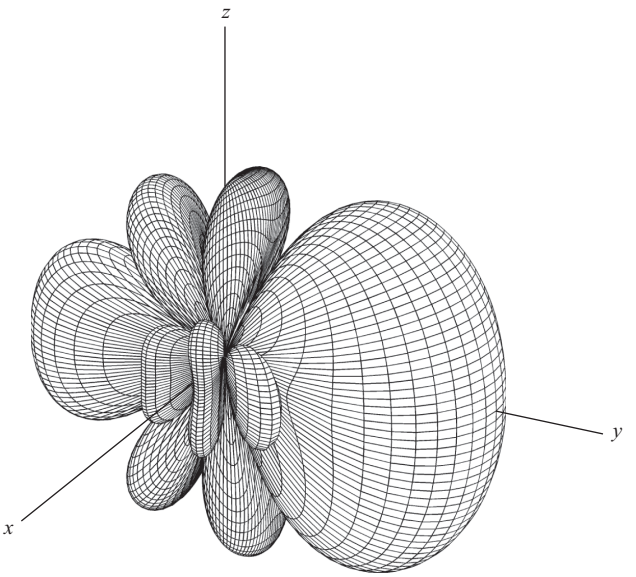

Fig. 2.4 Normalized power pattern of an antenna

is 10 dB below the maximum value. For the pattern shown in Fig. 2.6 the half-power beamwidth is 30° and the 10 dB beamwidth is 50°.

The normalized pattern function, $P_n(\theta, \phi)$, specifies the angular distribution of the total radiated power. For example, consider an antenna that radiates equally in all directions, i.e., the radiation pattern of the antenna is

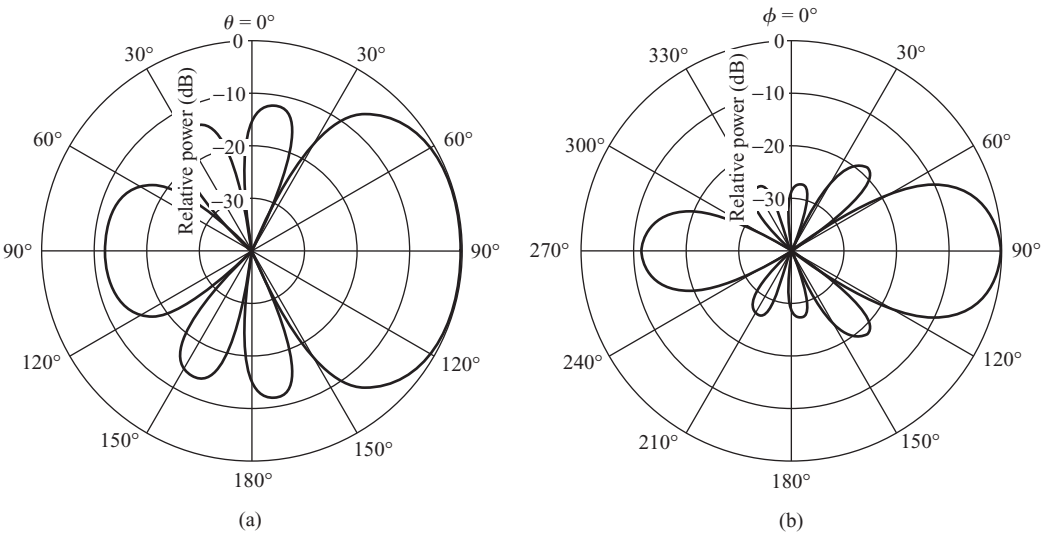

Fig. 2.5 Polar plot of the y-z and x-y cuts of the pattern shown in Fig. 2.4

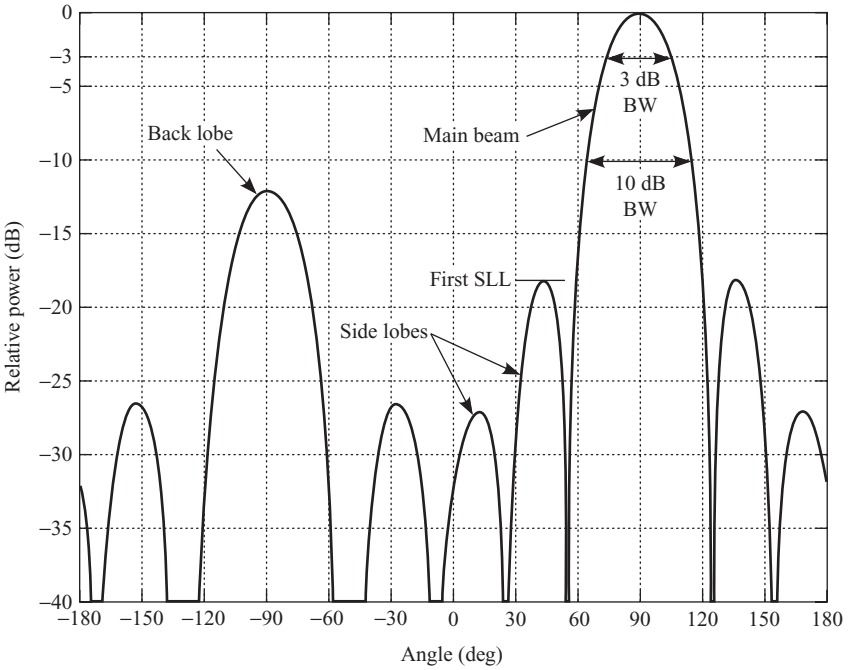

Fig. 2.6 Rectangular plot of the x-y plane cut of the pattern shown in Fig. 2.4

a sphere. Such an antenna is known as an isotropic antenna and the corresponding radiation pattern is known as an isotropic pattern. The radiation pattern of an isotropic antenna is non-directional. The Hertzian dipole, on the other hand, has a non-directional pattern in one plane (x-y plane for a z-oriented dipole), but in any plane orthogonal to it, the pattern is directional. Such a pattern is known as an *omni-directional* pattern. Several terms, such as, the pencil beam, fan beam, shaped beam, etc., are used in describing an antenna pattern based on the shape of the radiation pattern. A pencil beam antenna has maximum radiation in one direction and the beamwidths in the two orthogonal cuts of the pattern are small. If the beamwidth is broad in one cut and narrow in an orthogonal cut, the antenna pattern is called a fan-beam pattern.

EXAMPLE 2.3

The electric field of an antenna is given by

$$\mathbf{E} = \mathbf{a}_\theta \frac{\sin(4\pi \cos\theta)}{4\pi \cos\theta}$$

Calculate **(a)** the direction of the maximum, **(b)** the 3 dB beamwidth, **(c)** the direction and level of the first side lobe, and **(d)** the number of nulls in the pattern. Plot the power pattern on a rectangular graph.

Solution: The electric field has the form $\sin x/x$, which has a maximum amplitude of 1 at $x = 0$, has an amplitude of 0.707 (which corresponds to the 3 dB point) at $x = 1.39$, second peak of -0.217 at $x = 4.49$, and nulls at $x = n\pi; n = 1, 2, \ldots$, where $x = 4\pi \cos\theta$. (See Appendix G for a description of the $\sin x/x$ function).

(a) The maximum of the pattern occurs along $4\pi \cos\theta_{\max} = 0$, which gives a value of $\theta_{\max} = 90^\circ$.

(b) Let θ_1 be the direction along which the power is half of the maximum power. Since the $\sin x/x$ function has a value of 0.707 at $x = 1.39$, we have $1.39 = 4\pi \cos\theta_1$ and, hence, $\theta_1 = \cos^{-1}[1.39/(4\pi)] = 83.65^\circ$. Similarly, on the other side of the maximum, the direction θ_2 along which the electric field is equal to 0.707 of the maximum is $4\pi \cos\theta_2 = -1.39$, which gives, $\theta_2 = 96.35^\circ$. The half-power beamwidth is $\Theta_{\text{HP}} = \theta_2 - \theta_1 = 12.7^\circ$.

(c) The direction of the first side lobe, θ_s, on either side of the main lobe is given by $\pm 4.49 = 4\pi \cos\theta_s$ or $\theta_s = 69.07^\circ$ and 110.93°. The level of the first side lobe peak is $20 \log_{10}(0.217) = -13.3$ dB.

(d) The nth null of the pattern occurs at $x = n\pi$. The direction of the nth null, θ_n is given by $4\pi \cos\theta_n = n\pi$ or $\cos\theta_n = n/4$. This has real solutions only for $n/4 \leq 1$. Therefore, the pattern has 4 nulls between $\theta = 0^\circ$ and $\theta = 90^\circ$ and 4 more nulls between $\theta = 90^\circ$ and $\theta = 180^\circ$ (see Fig. 2.7).

EXAMPLE 2.4

Calculate the beamwidths in the x-y and y-z planes of an antenna the power pattern of which is given by

$$U(\theta, \phi) = \begin{cases} \sin^2\theta \sin\phi & 0 \leq \theta \leq \pi; \quad 0 \leq \phi \leq \pi \\ 0 & 0 \leq \theta \leq \pi; \ \pi \leq \phi \leq 2\pi \end{cases}$$

Solution: In the x-y plane, $\theta = \pi/2$ and the power pattern is given by

$$U\left(\frac{\pi}{2}, \phi\right) = \sin\phi$$

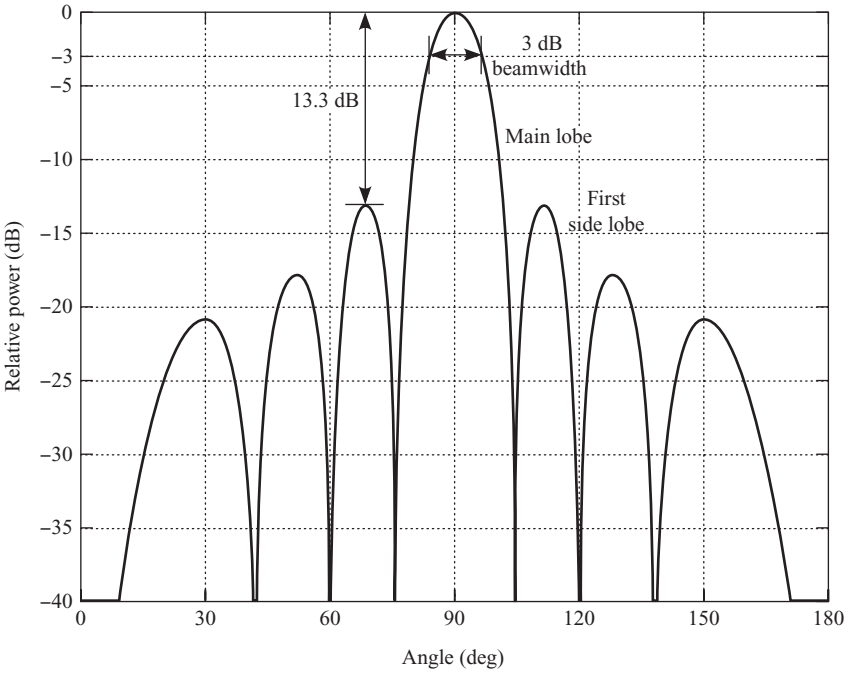

Fig. 2.7 Radiation pattern of the antenna of Example 2.3; $P_{n\text{dB}}(\theta, \phi) = 20 \log_{10} [\sin(4\pi \cos\theta)/(4\pi \cos\theta)]$

The angles along which the power is half the maximum value (3 dB below the maximum) is given by the solutions of

$$\sin\phi = 0.5$$

which is satisfied for $\phi = 30°$ and $\phi = 150°$. Therefore, the 3 dB beamwidth in the x-y plane is $150° - 30° = 120°$.

In the y-z plane ($\phi = \pi/2$), the power pattern is given by

$$U\left(\theta, \frac{\pi}{2}\right) = \sin^2\theta$$

and the 3 dB points occur along θ satisfying the condition

$$\sin^2\theta = 0.5$$

which gives the values of θ as 45° and 135°. Therefore, the beamwidth in the y-z plane is 90°.

EXAMPLE 2.5

Derive an expression for the time-averaged power density vector of the electromagnetic wave radiated by a Hertzian dipole of length dl, kept at the origin, oriented along the x-axis, and excited by a current of amplitude I_0.

Solution: The far-fields of a Hertzian dipole oriented along the x-direction are (see Example 1.8)

$$H_\theta = -j\frac{kI_0 dl}{4\pi}\sin\phi\frac{e^{-jkr}}{r}$$
$$H_\phi = -j\frac{kI_0 dl}{4\pi}\cos\theta\cos\phi\frac{e^{-jkr}}{r}$$
$$E_\theta = -j\eta\frac{kI_0 dl}{4\pi}\cos\theta\cos\phi\frac{e^{-jkr}}{r}$$
$$E_\phi = j\eta\frac{kI_0 dl}{4\pi}\sin\phi\frac{e^{-jkr}}{r}$$

The time-averaged power density is given by

$$\mathbf{S} = \frac{1}{2}\mathrm{Re}\{\mathbf{E}\times\mathbf{H}^*\}$$

Expressing the field vectors in terms of their components

$$\mathbf{S} = \frac{1}{2}\mathrm{Re}\{(\mathbf{a}_\theta E_\theta + \mathbf{a}_\phi E_\phi)\times(\mathbf{a}_\theta H_\theta + \mathbf{a}_\phi H_\phi)^*\}$$

Expanding the cross product using the identities $\mathbf{a}_\theta\times\mathbf{a}_\theta = 0$, $\mathbf{a}_\phi\times\mathbf{a}_\phi = 0$, $\mathbf{a}_\theta\times\mathbf{a}_\phi = \mathbf{a}_r$, and $\mathbf{a}_\phi\times\mathbf{a}_\theta = -\mathbf{a}_r$

$$\mathbf{S} = \frac{1}{2}\mathrm{Re}\{\mathbf{a}_r E_\theta H_\phi^* - \mathbf{a}_r E_\phi H_\theta^*\}$$

Substituting the field expressions and simplifying

$$\mathbf{S} = \mathbf{a}_r\frac{1}{2}\eta\left(\frac{k|I_0|\,dl}{4\pi r}\right)^2\left[\cos^2\theta\cos^2\phi + \sin^2\phi\right]$$

A 3D plot of the radiation intensity as a function of θ and ϕ is shown in Fig. 2.8. The radiation pattern is identical to that of a z-directed dipole but rotated by 90°.

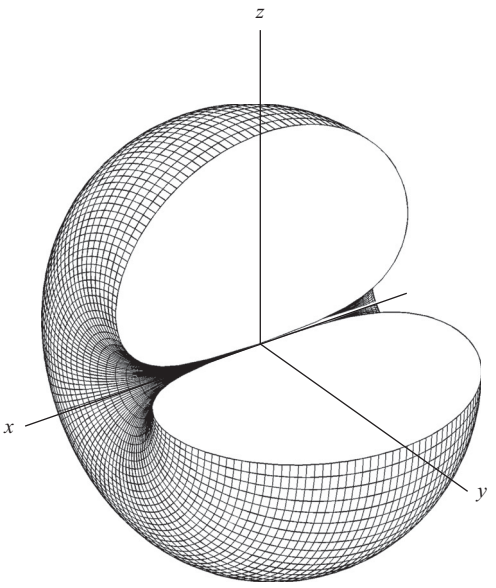

Fig. 2.8 Normalized power pattern of an x-directed Hertzian dipole

2.2 Beam Solid Angle, Directivity, and Gain

The total power radiated by an antenna is obtained by integrating the Poynting vector over the entire area of the sphere of radius r.

$$P_{\text{rad}} = \oint_{\Omega} \mathbf{S}_{\text{rad}}(r, \theta, \phi) \cdot \mathbf{a}_r \, dA \quad \text{W} \tag{2.21}$$

where $\mathbf{S}(r, \theta, \phi)$ is the Poynting vector on the sphere and dA is the elemental area. In spherical coordinates the elemental area is given by

$$dA = r^2 \sin\theta d\theta d\phi \tag{2.22}$$

Using Eqn (2.15), the total radiated power can also be written in terms of the radiation intensity as

$$P_{\text{rad}} = \oint_{\Omega} U(\theta, \phi) d\Omega \quad \text{W} \tag{2.23}$$

where the elemental solid angle, $d\Omega$, is given by

$$d\Omega = \sin\theta d\theta d\phi \tag{2.24}$$

Using Eqn (2.17), $U(\theta, \phi) = U_{\max} P_n(\theta, \phi)$, the total radiated power is

$$P_{\text{rad}} = U_{\max} \oint_{\Omega} P_n(\theta, \phi) d\Omega \quad \text{W} \tag{2.25}$$

Defining the beam solid angle, Ω_A, as

$$\Omega_A = \oint_{\Omega} P_n(\theta, \phi) d\Omega \quad \text{sr} \tag{2.26}$$

the radiated power can be expressed in terms of the beam solid angle and the maximum radiation intensity as

$$P_{\text{rad}} = \Omega_A U_{\max} \quad \text{W} \tag{2.27}$$

This equation suggests that if all the power is radiated uniformly within a solid angle Ω_A, it would have an intensity equal to $U_{\max}$. For a pencil beam pattern, the beam solid angle is approximately equal to the product of half-power beamwidths in the two principal planes

$$\Omega_A = \Theta_{1\text{HP}} \Theta_{2\text{HP}} \quad \text{sr} \tag{2.28}$$

where, $\Theta_{1\text{HP}}$ (rad) and $\Theta_{2\text{HP}}$ (rad) are the half power beamwidths in the two principal planes.

Since there are 4π steradians over a sphere, the average radiation intensity is

$$U_{\text{avg}} = \frac{P_{\text{rad}}}{4\pi} \quad \text{W/sr} \tag{2.29}$$

The directivity of an antenna in a given direction, $D(\theta, \phi)$, is defined as the ratio of the radiation intensity in that direction to the average radiation intensity

$$D(\theta, \phi) = \frac{U(\theta, \phi)}{U_{\text{avg}}} = 4\pi \frac{U(\theta, \phi)}{P_{\text{rad}}} \tag{2.30}$$

If the directivity of an antenna is specified without the associated direction, then the maximum value of D is assumed, i.e.

$$D = 4\pi \frac{U_{\max}}{P_{\text{rad}}} = \frac{4\pi}{\Omega_A} \tag{2.31}$$

where, the second expression is obtained by using Eqn (2.27), which relates the radiated power to the beam solid angle. For a pencil-beam pattern, the maximum directivity can also be expressed in terms of the half-power beamwidths in the two principal planes

$$D = \frac{4\pi}{\Theta_{1\mathrm{HP}}\Theta_{2\mathrm{HP}}} \tag{2.32}$$

For an isotropic antenna, the radiation intensity, U_0, is independent of the direction and the total radiated power is

$$P_{\mathrm{rad}} = \oint_{\Omega} U_0 d\Omega = 4\pi U_0 \quad \mathrm{W} \tag{2.33}$$

Thus, the radiation intensity of an isotropic antenna is given by

$$U_0 = \frac{P_{\mathrm{rad}}}{4\pi} \tag{2.34}$$

This is the same as the U_{avg} of Eqn (2.29) and hence the directivity can also be looked upon as the ratio of radiation intensity in a given direction to that produced by an isotropic antenna, both radiating the same amount of power.

The directivity of an isotropic antenna is unity. The directivity of an antenna indicates how well it radiates in a particular direction in comparison with an isotropic antenna radiating the same amount of power.

The directivity is also expressed in decibels as

$$D_{\mathrm{dB}} = 10\log_{10} D \quad \mathrm{dB} \tag{2.35}$$

Sometimes, the reference to an isotropic antenna is explicitly indicated by the unit dBi instead of dB. Similarly, the power in decibel units referenced to 1 mW and 1 W are expressed in dBm and dBW units, respectively. The power is expressed in dBm units using

$$P_{\mathrm{dBm}} = 10\log_{10}\left(\frac{P}{1\times 10^{-3}}\right) \quad \mathrm{dBm} \tag{2.36}$$

where P is in watts. The same can be expressed in dBW units as

$$P_{\mathrm{dBW}} = 10\log_{10}\left(\frac{P}{1}\right) \quad \mathrm{dBW} \tag{2.37}$$

The total power radiated by a Hertzian dipole is given by

$$P_{\mathrm{rad}} = \oint_{\Omega} U(\theta,\phi) d\Omega = \oint_{\Omega} U(\theta,\phi)\sin\theta d\theta d\phi \tag{2.38}$$

Substituting $U(\theta, \phi)$ from Eqn (2.16) and performing the integration over the sphere, the total radiated power is

$$P_{\text{rad}} = \eta \frac{\pi}{3} \left(I_0 \frac{dl}{\lambda} \right)^2 \quad \text{W} \tag{2.39}$$

The directivity of a Hertzian dipole is calculated by dividing the radiation intensity, $U(\theta, \phi)$, by the average radiation intensity ($U_{\text{avg}} = P_{\text{rad}}/4\pi$), which gives

$$D(\theta, \phi) = 1.5 \sin^2 \theta \tag{2.40}$$

The maximum value of the directivity of a Hertzian dipole is 1.5 (or 1.76 dBi) and occurs along $\theta = 90°$.

Any physical antenna has losses associated with it. Depending on the antenna structure, both ohmic and dielectric losses can be present in the antenna. Let P_{loss} be the power dissipated in the antenna due to the losses in the structure and $P_{\text{in}} = P_{\text{rad}} + P_{\text{loss}}$ be the power input to the antenna. Radiation efficiency, κ, of an antenna is the ratio of the total power radiated to the net power input to the antenna

$$\kappa = \frac{P_{\text{rad}}}{P_{\text{in}}} \tag{2.41}$$

From the definition of the directivity, it is clear that directivity is a parameter dependent on the shape of the radiation pattern alone. To account for the losses in the antenna, we multiply the directivity by the efficiency and define this as the gain of the antenna.

$$G(\theta, \phi) = \kappa D(\theta, \phi) = 4\pi \frac{U(\theta, \phi)}{P_{\text{in}}} \tag{2.42}$$

Generally, when a single value is specified as the gain (or directivity) of an antenna, it is understood that it is the gain (or directivity) along the main beam peak or the maximum value. These are denoted by G and D without the argument (θ, ϕ).

EXAMPLE 2.6

Calculate the radiation efficiency of an antenna if the input power is 100 W and the power dissipated in it is 1 W.

Solution: The input power, $P_{\text{in}} = 100$ W, and the power radiated is $P_{\text{rad}} = 100 - 1 = 99$ W. Substituting these values in Eqn (2.41), the radiation efficiency is $\kappa = P_{\text{rad}}/P_{\text{in}} = 99/100 = 0.99$.

EXAMPLE 2.7

Calculate the maximum power density at a distance of 1000 m from a Hertzian dipole radiating 10 W of power. Assume that the dipole has no losses. What are the electric and magnetic field intensities at the given point? If the same power were to be radiated by an isotropic antenna, what will be the power density and the field intensities? How much power should the isotropic antenna radiate so that the field intensities of the isotropic antenna and the Hertzian dipole (along the maximum) are the same?

Solution: The maximum directivity of an antenna is given by Eqn (2.30)

$$D = 4\pi \frac{U_{\max}}{P_{\text{rad}}} = 4\pi \frac{S_{\max} r^2}{P_{\text{rad}}}$$

where, $P_{\text{rad}} = 10$ W is the total radiated power, $r = 1000$ m is the distance from the antenna to the field point, and $S_{\max}$ is the maximum radiated power density. Since the maximum directivity of a Hertzian dipole is 1.5, the maximum power density is

$$S_{\max} = \frac{1.5 P_{\text{rad}}}{4\pi r^2} = \frac{1.5 \times 10}{4\pi 1000^2} = 1.1937 \times 10^{-6} \text{ W/m}^2$$

In the far-field region, the electric field intensity $|E|$ and the power density are related by, $S = |E|^2/\eta$, where $\eta = 120\pi\ \Omega$, is the free-space impedance, thus the maximum electric field intensity is $|E_{\max}| = \sqrt{S_{\max}\eta} = 0.0212$ V/m. The magnetic field intensity is given by, $|H| = |E|/\eta = 5.627 \times 10^{-5}$ A/m.

If $P_{\text{rad}i}$ is the power radiated and $S_{\max i}$ is the radiation power density of an isotropic antenna, then

$$S_{\max i} = \frac{P_{\text{rad}i}}{4\pi r^2} \text{ W/m}^2$$

For the maximum fields of the Hertzian dipole and the isotropic antenna to be identical, the radiated power density of the two antennas should be equal, i.e., $S_{\max i} = 1.1937 \times 10^{-6}$ W/m^2, which gives, $P_{\text{rad}i} = 4\pi r^2 S_{\max i} = 4\pi \times 1000^2 \times 1.1937 \times 10^{-6} = 15$ W.

EXAMPLE 2.8

Calculate the directivity of an antenna the power pattern of which is given by

$$U(\theta, \phi) = \begin{cases} \sin\theta \sin\phi & 0 \le \theta \le \pi;\ \ 0 \le \phi \le \pi \\ 0 & 0 \le \theta \le \pi;\ \pi \le \phi \le 2\pi \end{cases}$$

Solution: The total power radiated by the antenna is given by (Eqn (2.23))

$$P_{\text{rad}} = \oint_{\Omega} U(\theta, \phi) d\Omega \ \ \text{W}$$

where $d\Omega = \sin\theta d\theta d\phi$. Substituting the value of the radiation intensity

$$\begin{aligned} P_{\text{rad}} &= \int_{\theta=0}^{\pi} \int_{\phi=0}^{\pi} \sin\theta \sin\phi \sin\theta d\theta d\phi + \int_{\theta=0}^{\pi} \int_{\phi=\pi}^{2\pi} 0 d\Omega \\ &= \int_{\theta=0}^{\pi} \int_{\phi=0}^{\pi} \sin^2\theta \sin\phi d\theta d\phi \\ &= \int_{\theta=0}^{\pi} \int_{\phi=0}^{\pi} \frac{1}{2}(1 - \cos 2\theta) \sin\phi d\theta d\phi \\ &= \frac{1}{2}\left(\theta - \frac{1}{2}\sin 2\theta\right)|_{\theta=0}^{\pi}(-\cos\phi)|_{\phi=0}^{\pi} \\ &= \pi \ \ \text{W} \end{aligned}$$

The directivity is given by

$$D(\theta, \phi) = \frac{4\pi U(\theta, \phi)}{P_{\text{rad}}} = \frac{4\pi \sin\theta \sin\phi}{\pi} = 4\sin\theta\sin\phi$$

The maximum value of the directivity is 4 ($D_{\text{dB}} = 10\log_{10}(4) = 6.02$ dB) and occurs along the y-axis, i.e., $(\theta = \pi/2, \phi = \pi/2)$.

2.3 Input Impedance

The function of an antenna in a system is to radiate power into space or receive the electromagnetic energy from space. The antenna is generally connected to a transmitter or to a receiver via a transmission line or a waveguide with some characteristic impedance. The antenna acts as a transformer between free space and the transmission line. In this section we shall treat the antenna as a transmitting antenna. The antenna as a receiver is treated separately later in this chapter. In a practical antenna connected to a transmitter via a transmission line, the applied radio frequency voltage establishes a current distribution on the antenna structure. This, in turn, radiates power into free space. A small part of the input power is dissipated due to ohmic/dielectric losses in the antenna. Further, the applied voltage also establishes a reactive field in the vicinity of the antenna. One can think of the antenna as an equivalent complex impedance, Z_a, which draws exactly the same amount of complex power from the transmission line as

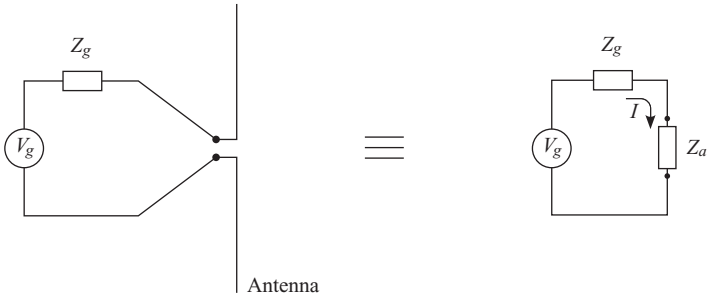

Fig. 2.9 An antenna connected to a source and its equivalent circuit

the antenna. This is known as the antenna input impedance. The real part accounts for the radiated power and the power dissipated in the antenna. The reactive part accounts for the reactive power stored in the near-field of the antenna. Note that there is no physical resistance or reactance at the antenna input terminals and that the antenna impedance, Z_a, is the ratio of the input voltage to the input current at the antenna terminals.

Consider an antenna in the transmit mode, having an input impedance of $Z_a = R_a + jX_a$, where R_a and X_a are the resistive and reactive parts respectively, connected directly to a source having an equivalent Thevenin's voltage, V_g, and an internal impedance $Z_g = R_g + jX_g$, as shown in Fig. 2.9.

The maximum power transfer takes place when the antenna is conjugate-matched to the source, i.e.,

$$R_a = R_g \qquad X_a = -X_g \tag{2.43}$$

Under the complex conjugate-match condition, the antenna input current is

$$I = \frac{V_g}{2R_g} = \frac{V_g}{2R_a} \tag{2.44}$$

and the real power supplied by the source is

$$P_g = \frac{1}{2}\mathrm{Re}\{\, V_g I^*\} = \frac{|\, V_g|^2}{4R_a} \tag{2.45}$$

Half the power supplied by the source is lost in the source resistance, R_g, and the other half gets dissipated in the antenna resistance, R_a. Power input to the antenna is

$$P_{\text{in}} = \frac{1}{2}|I|^2 R_a = \frac{|V_g|^2}{8R_a} \tag{2.46}$$

The antenna resistance, R_a, is comprised of two components, namely, the radiation resistance, R_{rad}, and the loss resistance, R_{loss}

$$R_a = R_{\text{rad}} + R_{\text{loss}} \tag{2.47}$$

The total power dissipated in the antenna resistance, R_a, can be split into two parts

$$P_{\text{rad}} = \frac{1}{2}|I|^2 R_{\text{rad}} \tag{2.48}$$

$$P_{\text{loss}} = \frac{1}{2}|I|^2 R_{\text{loss}} \tag{2.49}$$

where P_{rad} is the power dissipated in R_{rad} which is actually the radiated power. P_{loss} represents the ohmic losses in the antennas. For a matched antenna these are given by

$$P_{\text{rad}} = \frac{|V_g|^2}{8R_a^2} R_{\text{rad}} \tag{2.50}$$

$$P_{\text{loss}} = \frac{|V_g|^2}{8R_a^2} R_{\text{loss}} \tag{2.51}$$

Substituting Eqn (2.46) and Eqn (2.48) into Eqn (2.41), the radiation efficiency can be expressed in terms of the radiation and the loss resistance as

$$\kappa = \frac{P_{\text{rad}}}{P_{\text{in}}} = \frac{R_{\text{rad}}}{R_{\text{rad}} + R_{\text{loss}}} \tag{2.52}$$

For example, the radiation resistance of a Hertzian dipole carrying a current I_0 can be computed by substituting the expression for the total power radiated into Eqn (2.48) [see Eqn (2.39)]

$$P_{\text{rad}} = \eta \frac{\pi}{3} \left(|I_0| \frac{dl}{\lambda} \right)^2 = \frac{1}{2}|I_0|^2 R_{\text{rad}} \tag{2.53}$$

Thus the radiation resistance of a Hertzian dipole can be written as

$$R_{\text{rad}} = \frac{2}{3}\pi\eta \left(\frac{dl}{\lambda} \right)^2 \tag{2.54}$$

EXAMPLE 2.9

A voltage source of amplitude $V_g = (50 + j40)$ V and a source impedance $Z_g = 50\ \Omega$ is connected to an antenna having a radiation resistance $R_{\text{rad}} = 70\ \Omega$, loss resistance $R_{\text{loss}} = 1\ \Omega$, and a reactance $jX = j25\ \Omega$. Calculate the radiation efficiency of the antenna, the real power delivered by the source,

the real power input to the antenna, power radiated by the antenna, and the power dissipated in the antenna.

Solution: Radiation efficiency is given by Eqn (2.52)

$$\kappa = \frac{R_{\text{rad}}}{R_a} = \frac{R_{\text{rad}}}{R_{\text{rad}} + R_{\text{loss}}} = \frac{70}{70+1} = 0.986$$

The radiation efficiency percentage is 98.6%.

The current through the circuit is

$$I = \frac{V_g}{R_g + R_{\text{rad}} + R_{\text{loss}} + jX} = \frac{50 + j40}{50 + 70 + 1 + j25} = \frac{64.03\angle 38.66^\circ}{123.56\angle 11.67^\circ}$$
$$= 0.518\angle 26.99^\circ \text{ A}$$

The real power P_g delivered by the source is

$$P_g = \frac{1}{2}\text{Re}\{V_g I^*\} = \frac{1}{2}\text{Re}\{64.03\angle 38.66^\circ \times 0.518\angle -26.99^\circ\} = 16.24 \text{ W}$$

The real power input to the antenna is given by

$$P_{\text{in}} = \frac{1}{2}|I|^2(R_{\text{rad}} + R_{\text{loss}}) = \frac{1}{2} \times 0.518^2 \times (70+1) = 9.53 \text{ W}$$

The power radiated by the antenna is

$$P_{\text{rad}} = \frac{1}{2}|I|^2 R_{\text{rad}} = \frac{1}{2} \times 0.518^2 \times 70 = 9.39 \text{ W}$$

The power dissipated in the antenna is

$$P_{\text{loss}} = \frac{1}{2}|I|^2 R_{\text{loss}} = \frac{1}{2} \times 0.518^2 \times 1 = 0.134 \text{ W}$$

EXAMPLE 2.10

Calculate the radiation resistance and the efficiency of a Hertzian dipole of length $dl = 0.05\lambda$, having a loss resistance of 1 Ω, a reactance of $-j100$ Ω, and radiating into free space. If the dipole is connected to a 100 V (peak voltage) source having a source impedance of 50 Ω, calculate the real power radiated by the antenna and the power generated by the source.

Solution: The radiation resistance of a Hertzian dipole is given by Eqn (2.54)

$$R_{\text{rad}} = \frac{2}{3}\pi\eta\left(\frac{dl}{\lambda}\right)^2 = \frac{2}{3}\pi \times 120\pi \times \left(\frac{0.05\lambda}{\lambda}\right)^2 = 1.97\ \Omega$$

Using Eqn (2.52)

$$\kappa = \frac{R_{\text{rad}}}{R_{\text{rad}} + R_{\text{loss}}} = \frac{1.97}{1.97 + 1} = 0.66$$

Therefore, the efficiency of the antenna is 66%. The real power radiated by the antenna is given by Eqn (2.48)

$$\begin{aligned} P_{\text{rad}} &= \frac{1}{2}|I|^2 R_{\text{rad}} = \frac{1}{2}\left|\frac{100}{(50 + 1.97 + 1) - j100}\right|^2 \times 1.97 \\ &= \frac{1}{2}\left|\frac{100}{113.16}\right|^2 \times 1.97 = 0.77\ \text{W} \end{aligned}$$

The real power generated by the source is

$$P_g = \frac{1}{2}\text{Re}\{\, V_g I^*\} = \frac{1}{2}\text{Re}\left\{ V\left(\frac{V}{Z}\right)^*\right\} = \frac{1}{2}\text{Re}\left\{\frac{100^2}{52.97 + j100}\right\} = 20.68\ \text{W}$$

The total power input to the antenna is $(P_{\text{rad}}/\kappa) = 1.17$ W and the power dissipated in the antenna loss resistance is 0.4 W. Therefore, 19.51 W is dissipated in the source resistance, R_g.

2.4 Polarization

The polarization of an antenna is the polarization of the wave radiated by the antenna in the far-field. In the far-field region of the antenna, the radiated field essentially has a spherical wavefront with **E** and **H** fields transverse to the radial direction, which is the direction of propagation. As the radius of curvature tends to infinity, the wavefront can be considered as a plane wave locally and the polarization of this plane wave is the polarization of the antenna. Generally the polarization of the antenna is direction-dependent, thus, one could define a polarization pattern, i.e., polarization as a function of (θ, ϕ). However, while specifying the polarization of an antenna, it is a generally accepted convention to specify the polarization of the wave along the main beam direction.

Polarization of a plane wave describes the shape, orientation, and sense of rotation of the tip of the electric field vector as a function of time, looking in the direction of propagation. Consider a general situation in which the radiated electric field has both θ and ϕ components

$$\mathbf{E} = \mathbf{a}_\theta E_\theta + \mathbf{a}_\phi E_\phi \tag{2.55}$$

where, E_θ and E_ϕ are functions of r, θ, and ϕ and can be complex. The instantaneous values of the electric field can be written as

$$\bar{\mathcal{E}}(r,\theta,\phi,t) = \mathbf{a}_\theta \mathrm{Re}(E_\theta e^{j\omega t}) + \mathbf{a}_\phi \mathrm{Re}(E_\phi e^{j\omega t}) \tag{2.56}$$

Let $E_\theta = Ae^{j\alpha}$ and $E_\phi = Be^{j\beta}$, where A and B are the magnitudes and α and β are the phase angles of E_θ and E_ϕ, respectively. Substituting the above in Eqn (2.56) and simplifying

$$\bar{\mathcal{E}}(r,\theta,\phi,t) = \mathbf{a}_\theta A\cos(\omega t+\alpha) + \mathbf{a}_\phi B\cos(\omega t+\beta) \tag{2.57}$$

Depending on the values of A, B, α, and β in Eqn (2.57), the tip of the $\bar{\mathcal{E}}$ field vector can trace a straight line, a circle, or an ellipse. These three cases are termed as linear, circular, and elliptical polarizations and are explained in the following subsections.

2.4.1 Linear Polarization

Consider a field with $B = 0$ in Eqn (2.57). Such an electric field has only a θ-component. Then, the tip of the electric field traces a straight line along the $\mathbf{a}_\theta$-direction. On the other hand, if $A = 0$ and $B \neq 0$, the antenna is still linearly polarized but the orientation of the electric field is along $\mathbf{a}_\phi$. If A and B are not equal to zero and the θ and ϕ components of the electric field are in phase, i.e., if $\alpha = \beta$, the wave is still linearly polarized but the resultant vector is tilted with respect to $\mathbf{a}_\theta$ and the angle of the tilt depends on the A/B ratio. The plane of polarization makes an angle $\tan^{-1}(B/A)$ to the $\mathbf{a}_\theta$-direction.

Let us consider a Hertzian dipole oriented along the z-direction and excited by a current $I_0 = |I_0|e^{j\alpha}$. The electric field in the far-field region, given by Eqn (2.8), has only a θ-component and can be written as

$$\mathbf{E} = \mathbf{a}_\theta j\eta \frac{k|I_0|e^{j\alpha}dl\sin\theta}{4\pi}\frac{e^{-jkr}}{r} = \mathbf{a}_\theta jE_0\sin\theta\frac{e^{-j(kr-\alpha)}}{r} \tag{2.58}$$

where $E_0 = (\eta k |I_0| dl/4\pi)$ is a real quantity. The instantaneous value of the electric field intensity is given by

$$\bar{\mathcal{E}}(r, \theta, \phi, t) = \mathbf{a}_\theta \mathrm{Re}\left\{ jE_0 \sin\theta \frac{e^{-j(kr-\alpha)}}{r} e^{j\omega t} \right\} \tag{2.59}$$

which can be simplified to

$$\bar{\mathcal{E}}(r, \theta, \phi, t) = -\mathbf{a}_\theta \frac{E_0}{r} \sin\theta \sin(\omega t - kr + \alpha) \tag{2.60}$$

Without any loss of generality, it is possible to choose a point r_1 in the far-field of the antenna such that $kr_1 - \alpha$ is equal to an integral multiple of 2π and at this point, the electric field is given by

$$\bar{\mathcal{E}}(r_1, \theta, \phi, t) = -\mathbf{a}_\theta \frac{E_0}{r_1} \sin\theta \sin(\omega t) \tag{2.61}$$

The electric field vector is plotted in Fig. 2.10 for different values of time. As the time progresses, the tip of the electric field vector traces a straight

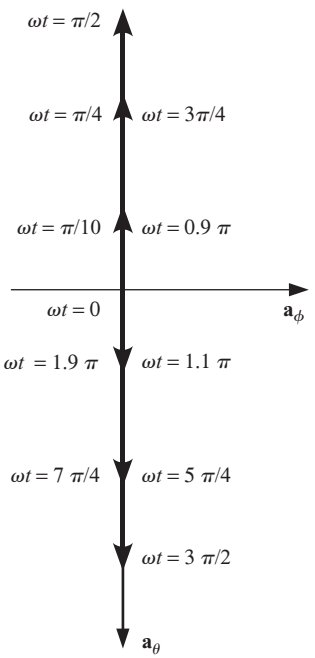

Fig. 2.10 Electric field vector due to a z-directed current element as a function of time

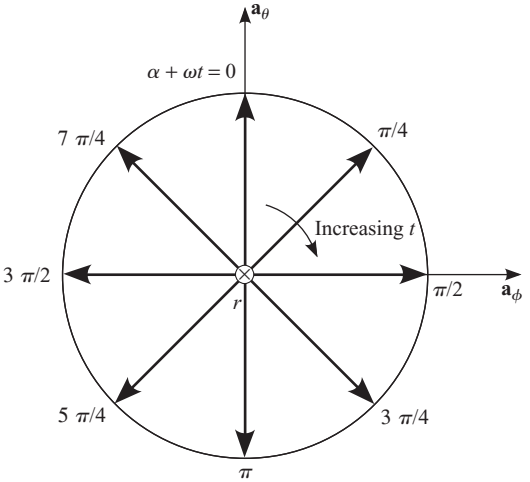

Fig. 2.11 Electric field vector of a right circularly polarized antenna

line along the $\mathbf{a}_\theta$-direction. Thus, the Hertzian dipole is a linearly polarized antenna.

2.4.2 Circular Polarization

If $A = B$ and $\beta = (\alpha - \pi/2)$ in Eqn (2.57), the electric field vector is given by

$$\bar{\mathcal{E}}(r, \theta, \phi, t) = A[\mathbf{a}_\theta \cos(\omega t + \alpha) + \mathbf{a}_\phi \sin(\omega t + \alpha)] \tag{2.62}$$

As a function of time, the electric field vector traces a circle as shown in Fig. 2.11. The direction of rotation of the tip of the electric field vector is clockwise, looking in the direction of wave propagation, which is the positive r-direction. This can also be represented by a right-handed screw that moves along the direction of propagation if rotated clockwise. Such a wave is called a right circularly polarized (RCP) wave and the antenna is known as an RCP antenna. For $A = B$ and $\beta = (\alpha + \pi/2)$ in Eqn (2.57), the electric field vector will still trace a circle but will rotate anticlockwise. Such a wave is called a left circularly polarized (LCP) wave and the antenna producing it would be an LCP antenna.

EXAMPLE 2.11

What is the polarization of a wave propagating in the r-direction if its electric field vector at any fixed point in space is given by **(a)** $\mathbf{E}_a = (\mathbf{a}_\theta + \mathbf{a}_\phi j)$ and **(b)** $\mathbf{E}_b = (\mathbf{a}_\theta j + \mathbf{a}_\phi)$?

Solution:

(a) Expressing the electric field intensity as an instantaneous quantity

$$\bar{\mathcal{E}}_a(t) = \text{Re}\{(\mathbf{a}_\theta + \mathbf{a}_\phi j)e^{j\omega t}\} = \text{Re}\{\mathbf{a}_\theta e^{j\omega t} + \mathbf{a}_\phi e^{j\omega t + \frac{\pi}{2}}\}$$

Taking the real part

$$\bar{\mathcal{E}}_a(t) = \mathbf{a}_\theta \cos(\omega t) - \mathbf{a}_\phi \sin(\omega t)$$

As t increases, the tip of the electric field vector rotates in the anticlockwise direction with constant amplitude. Therefore, this represents a left circularly polarized wave.

(b) Following a similar approach we can write

$$\bar{\mathcal{E}}_b(t) = \text{Re}\{(\mathbf{a}_\theta j + \mathbf{a}_\phi)e^{j\omega t}\}$$

which can be simplified to

$$\bar{\mathcal{E}}_b(t) = -\mathbf{a}_\theta \sin(\omega t) + \mathbf{a}_\phi \cos(\omega t)$$

This represents a right circularly polarized wave.

EXAMPLE 2.12

What is the polarization of a wave radiated along the y-axis, by a z-directed Hertzian dipole? Show that it can be decomposed into left and right circularly polarized waves.

Solution: In the far-field region of a z-directed Hertzian dipole the electric field intensity along the y-axis is given by Eqn (2.8) with $\theta = 90^\circ$

$$\mathbf{E} = \mathbf{a}_\theta j E_0$$

where $E_0 = j\eta k I_0 dl e^{-jkr}/(4\pi r)$. Since it has only a θ-component, it represents a linearly polarized wave. Expressing $\mathbf{a}_\theta$ as

$$\mathbf{a}_\theta = \frac{1}{2}[(\mathbf{a}_\theta + \mathbf{a}_\phi j) + (\mathbf{a}_\theta - \mathbf{a}_\phi j)]$$

we can write the electric field intensity as

$$\mathbf{E} = E_0 \frac{1}{2}[(\mathbf{a}_\theta + \mathbf{a}_\phi j) + (\mathbf{a}_\theta - \mathbf{a}_\phi j)]$$

The first term on the right hand side represents a LCP wave and the second term represents a RCP wave.

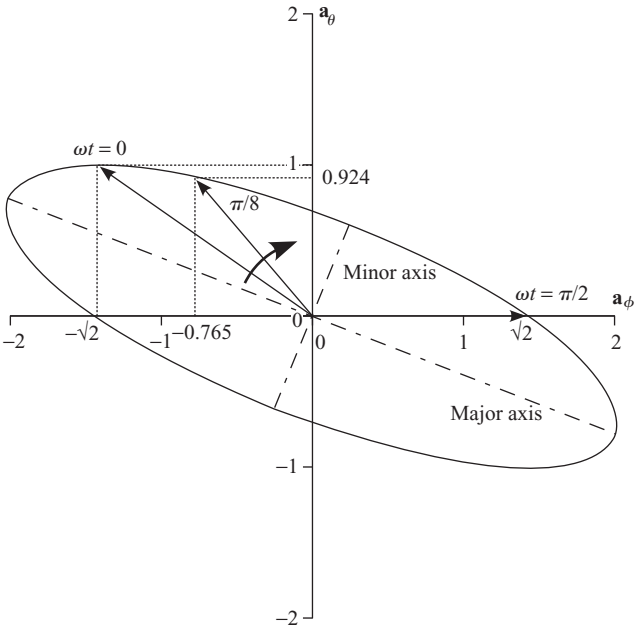

Fig. 2.12 Electric field vector of an elliptically polarized antenna

2.4.3 Elliptical Polarization

In general, for $A \neq B \neq 0$ and $\alpha \neq \beta$, Eqn (2.57) represents an elliptically polarized wave. At any point in space, the tip of the electric field of an elliptically polarized wave traces an ellipse as a function of time (Fig. 2.12). The ratio of lengths of the major and minor axes of the ellipse is known as the *axial ratio* (AR).

$$\text{AR} = \frac{\text{Length of the major axis}}{\text{Length of the minor axis}} \tag{2.63}$$

The orientation of the major axis with respect to the $\mathbf{a}_\theta$-axis is known as the tilt angle. Linear and circular polarizations are the two special cases of elliptical polarization with $\text{AR} = \infty$ and $\text{AR} = 1$, respectively.

EXAMPLE 2.13

The instantaneous electric field vector of a wave, propagating along the positive r-direction, at a fixed point in space, is given by

$$\bar{\mathcal{E}}(t) = \mathbf{a}_\theta \cos(\omega t) - \mathbf{a}_\phi 2 \cos\left(\omega t + \frac{\pi}{4}\right) \quad \text{V/m}$$

Plot this vector as a function of time and describe the polarization of the wave.

Solution: The electric field vectors at various instants of time are given by

$$\begin{aligned}
\omega t = 0; &\quad \bar{\mathcal{E}} = \mathbf{a}_\theta - \mathbf{a}_\phi\sqrt{2} && \text{V/m}\\
\omega t = \frac{\pi}{8}; &\quad \bar{\mathcal{E}} = \mathbf{a}_\theta 0.924 - \mathbf{a}_\phi 0.765 && \text{V/m}\\
\omega t = \frac{\pi}{4}; &\quad \bar{\mathcal{E}} = \mathbf{a}_\theta \frac{1}{\sqrt{2}} && \text{V/m}\\
\omega t = \frac{\pi}{2}; &\quad \bar{\mathcal{E}} = \mathbf{a}_\phi\sqrt{2} && \text{V/m}\\
\omega t = \frac{3\pi}{4}; &\quad \bar{\mathcal{E}} = -\mathbf{a}_\theta \frac{1}{\sqrt{2}} + \mathbf{a}_\phi 2 && \text{V/m}\\
\omega t = \pi; &\quad \bar{\mathcal{E}} = -\mathbf{a}_\theta + \mathbf{a}_\phi\sqrt{2} && \text{V/m}\\
\omega t = \frac{5\pi}{4}; &\quad \bar{\mathcal{E}} = -\mathbf{a}_\theta \frac{1}{\sqrt{2}} && \text{V/m}\\
\omega t = \frac{6\pi}{4}; &\quad \bar{\mathcal{E}} = -\mathbf{a}_\phi\sqrt{2} && \text{V/m}\\
\omega t = \frac{7\pi}{4}; &\quad \bar{\mathcal{E}} = \mathbf{a}_\theta \frac{1}{\sqrt{2}} - \mathbf{a}_\phi 2 && \text{V/m}
\end{aligned}$$

A plot of these vectors is shown in Fig. 2.12. The tip of the electric field vector rotates in the clockwise direction as time increases and traces an ellipse. Hence the wave is right elliptically polarized.

2.5 Bandwidth

The performance parameters of an antenna, such as, the input reflection coefficient, the pattern gain, etc., are functions of frequency. The range of frequencies over which the performance of an antenna is within some specified limits is known as the bandwidth (BW) of the antenna. It is called the input bandwidth if the performance parameter corresponds to the input characteristics. If the performance parameter refers to the pattern characteristics, it is called the pattern bandwidth. For example, over a frequency band covering f_L to f_U ($f_U > f_L$), if the antenna gain is within the specified limits, the bandwidth of the antenna expressed as a percentage of the centre frequency, f_0, is

$$BW = \frac{f_U - f_L}{f_0} \times 100\ \% \tag{2.64}$$

where $f_0 = (f_U + f_L)/2$. Some times the bandwidth is also expressed as a ratio of the two frequencies as

$$BW = \frac{f_U}{f_L} \tag{2.65}$$

The second definition is used for antennas having a very large bandwidth, known as broadband antennas.

2.6 Receiving Antenna

So far the focus was on the antenna in the transmit mode. An antenna is also used to receive energy incident on it. In the receive mode the incident electromagnetic wave induces a current distribution on the antenna similar to the one that is established in the transmit mode. This current distribution drives some power into the load connected to the antenna terminals. Some power is also dissipated in the antenna loss resistance and some is re-radiated or scattered into free space. The scattered power has the same angular distribution as the radiation pattern of the antenna. This power can also be looked at as the power dissipated in the radiation resistance of the antenna. In this section, by invoking the reciprocity theorem, we show that the pattern characteristics of an antenna are the same in the transmit and the receive modes. The parameters which are used to specifically quantify the performance of a receive antenna are also explained.

2.6.1 Reciprocity

The reciprocity theorem states that in a linear time-invariant system, the ratio of the response measured at a point, to an excitation at some other point, is unchanged if the measurement and the excitation points are interchanged. Consider a two-port network with the excitation and the measurement terminals as ports 1 and 2 respectively (Fig. 2.13). The voltage and currents of a linear two-port network are related by the linear equations

$$V_1 = Z_{11}I_1 + Z_{12}I_2 \tag{2.66}$$

$$V_2 = Z_{21}I_1 + Z_{22}I_2 \tag{2.67}$$

where, (V_1, I_1) and (V_2, I_2) are the terminal voltage and current at ports 1 and 2 respectively and $Z_{11} \ldots Z_{22}$ are the Z parameters of the network. If we apply a voltage V_1 to port 1 and measure the short-circuit current, I_2, at port 2, the ratio V_1/I_2 can be calculated from the above equations by

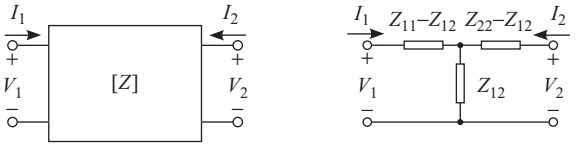

Fig. 2.13 A two-port network and its T-equivalent representation

setting $V_2 = 0$

$$\frac{V_1}{I_2} = \frac{Z_{12}Z_{21} - Z_{11}Z_{22}}{Z_{21}} \tag{2.68}$$

Now, interchanging the excitation and measurement points, we apply a voltage, V_2, to port 2 and measure short-circuit current, I_1, at port 1. Determining the ratio V_2/I_1 with $V_1 = 0$, we get

$$\frac{V_2}{I_1} = \frac{Z_{12}Z_{21} - Z_{11}Z_{22}}{Z_{12}} \tag{2.69}$$

From the reciprocity theorem, these two ratios are equal and hence $Z_{12} = Z_{21}$. If the applied voltages in both the cases are identical, i.e., $V_2 = V_1$, from Eqns (2.68) and (2.69) we get $I_2 = I_1$. Note that in both the cases above, there is no power dissipated in the source or the load because both source and load impedances are zero. The reciprocity theorem can also be applied when the excitation is by a current source and the measurement is the open-circuit voltage. Again note that no power is dissipated in the load or the source because both impedances are infinite. A reciprocal two-port network can be represented in a T-equivalent form as shown in Fig. 2.13 which maintains the same terminal V and I relationships. This is a convenient representation for computing the input and output impedances of a terminated two-port network.

Consider the T-equivalent representation of a two-port network with a source, V_s, and load, Z_L, connected to ports 1 and 2 respectively, as shown in Fig. 2.14. Let Z_S be the source impedance. Now, define a new two-port network with Z_L and Z_S included in the network and select terminals A-B as port $1'$ and C-D as port $2'$. Now the terminal voltage and current are (V_s, I_1) and $(0, I_2)$ at ports $1'$ and $2'$, respectively. Note that the port $2'$ is shorted and the current I_{sc} is the short-circuit current. The power dissipated in the load Z_L is $P_L = (1/2)I_{sc}^2 Z_L$. If the same source V_s is connected to port $2'$ and short-circuit current at port $1'$ is measured, from the reciprocity theorem, we will get the same current, I_{sc}. The power dissipated in the source impedance, Z_S, is $P_S = (1/2)I_{sc}^2 Z_S$. These two powers, P_L and P_S, are equal, if $Z_L = Z_S$.

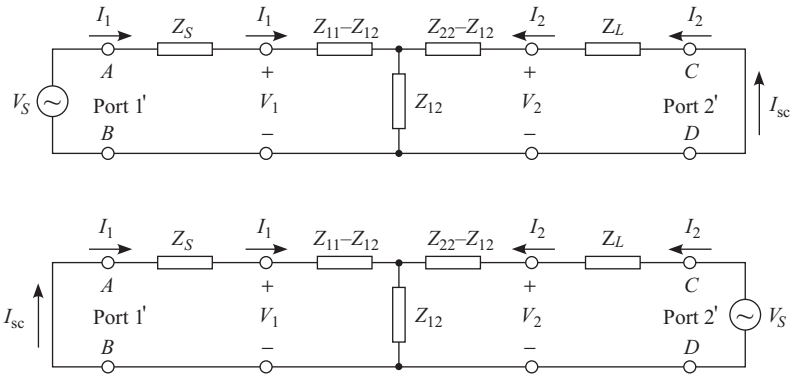

Fig. 2.14 A two-port network with a source and a load

A useful result concerns the power-transfer ratio when the two ports are conjugate-matched. Consider the two-port network shown in Fig. 2.15(a). Let Z_a and Z_b be the impedances looking into the ports 1 and 2, respectively. Using the two-port equations and the conjugate match criteria $Z_S = Z_a^*$ and $Z_L = Z_b^*$, we have

$$Z_a = Z_{11} - \frac{Z_{12}^2}{Z_b^* + Z_{22}} = R_a + jX_a \tag{2.70}$$

and

$$Z_b = Z_{22} - \frac{Z_{12}^2}{Z_a^* + Z_{11}} = R_b + jX_b \tag{2.71}$$

Consider the situation shown in Fig. 2.15(a), where the voltage source is connected to port 1. The power dissipated in the source impedance connected to port 1 is

$$P_1 = \frac{1}{2}\frac{|V|^2}{4R_a} \tag{2.72}$$

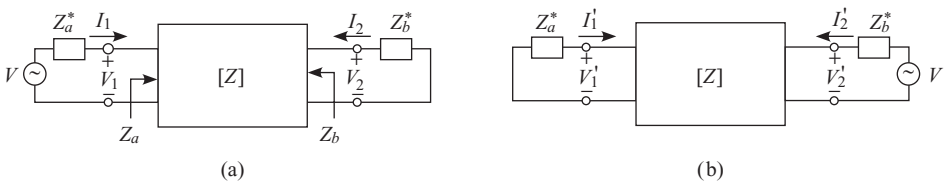

Fig. 2.15 A two-port network with conjugate match at both the ports

where, R_a is the real part of the source impedance Z_a^* and V is the source voltage. If I_2 is the load current in Z_b^*, the power delivered to the load is

$$P_2 = \frac{1}{2}|I_2|^2 R_b \tag{2.73}$$

The power-transfer ratio can be expressed as

$$\frac{P_2}{P_1} = \frac{|I_2|^2 4R_a R_b}{|V|^2} \tag{2.74}$$

Now, move the voltage source to the output side as shown in Fig. 2.15(b). The impedances remain in the original positions. Let the terminal voltage and current be (V_1', I_1') and (V_2', I_2') for ports 1 and 2, respectively. The power-transfer ratio from port 2 to port 1 is

$$\frac{P_1'}{P_2'} = \frac{|I_1'|^2 4R_a R_b}{|V|^2} \tag{2.75}$$

From the reciprocity theorem, $I_1' = I_2$, hence the power-transfer ratios are also equal. Thus, for a reciprocal two-port network with matched ports, the power-transfer ratio is independent of the direction of the power flow.

Now consider a situation where the load and the source impedances are real and unequal, but not matched to the ports. Let R_S and R_L be the source and the load resistances, respectively. The maximum power available from a source of voltage, V, when terminated in a load equal to R_S is

$$P_1 = \frac{|V|^2}{8R_S} \tag{2.76}$$

The power dissipated in the load R_L in $P_2 = |I|^2 R_L/2$. The ratio of P_2 to P_1 is

$$\frac{P_2}{P_1} = \frac{\frac{1}{2}|I|^2 R_L}{\frac{|V|^2}{8R_S}} = \left|\frac{I}{V}\right|^2 4R_L R_S \tag{2.77}$$

where, V is the source voltage at port 1 and I is the load current at port 2. If we interchange the position of the source and the current measurement points with R_S and R_L remaining at ports 1 and 2, respectively, the

power-transfer ratio is

$$\frac{P_1'}{P_2'} = \frac{\frac{1}{2}|I|^2 R_S}{\frac{|V|^2}{8R_L}} = \left|\frac{I}{V}\right|^2 4R_L R_S \tag{2.78}$$

Comparing Eqns (2.77) and (2.78), we can conclude that if the source and load impedances are real (which is usually the case with the source and the detector used in a measurement setup), the power-transfer ratio is independent of the direction of the power flow.

EXAMPLE 2.14

If the Z matrix of a two-port network is given by

$$[Z] = \begin{bmatrix} 10 & 5 \\ 5 & 20 \end{bmatrix} \ \Omega$$

calculate the input impedance at port 1 with port 2 terminated in **(a)** an open circuit and **(b)** a short circuit.

Solution: Input impedance at port 1 is given by

$$Z_{\text{in}} = \frac{V_1}{I_1}$$

With port 2 open-circuited $I_2 = 0$ and, hence, Eqn (2.66) reduces to

$$V_1 = Z_{11} I_1$$

Therefore, the input impedance at port 1 with port 2 open is

$$Z_{\text{oc1}} = \frac{V_1}{I_1} = Z_{11} = 10\ \Omega$$

With port 2 terminated in a short circuit $V_2 = 0$, thus Eqns (2.66) and (2.67) reduce to

$$V_1 = Z_{11} I_1 + Z_{12} I_2$$
$$0 = Z_{21} I_1 + Z_{22} I_2$$

An expression for I_2 in terms of I_1 can be obtained from the second equation as

$$I_2 = -\frac{Z_{21}}{Z_{22}} I_1$$

and substituting this into the first equation

$$V_1 = Z_{11} I_1 - \frac{Z_{12} Z_{21}}{Z_{22}} I_1$$

Therefore, the input impedance is given by

$$Z_{\text{sc1}} = \frac{V_1}{I_1} = Z_{11} - \frac{Z_{12} Z_{21}}{Z_{22}} = 10 - \frac{5 \times 5}{20} = \frac{35}{4} \ \ \Omega$$

EXAMPLE 2.15

Calculate the Z parameters of a two-port network if

(a) the measured parameters, with $V_1 = 1$ V and port 2 open, are $V_2 = 1$ mV and $I_1 = 0.02$ A and

(b) the measured parameters, with $V_2 = 1$ V and port 1 open, are $V_1 = 0.5$ mV and $I_2 = 0.01$ A.

Solution: With port 2 open, $I_2 = 0$ and, hence, from Eqn (2.66)

$$Z_{11} = \left.\frac{V_1}{I_1}\right|_{I_2=0} = \frac{1}{0.02} = 50 \ \Omega$$

Similarly, from Eqn (2.67)

$$Z_{21} = \left.\frac{V_2}{I_1}\right|_{I_2=0} = \frac{1 \times 10^{-3}}{0.02} = 0.05 \ \Omega$$

With the input at port 2 and port 1 open

$$Z_{12} = \left.\frac{V_1}{I_2}\right|_{I_1=0} = \frac{0.5 \times 10^{-3}}{0.01} = 0.05 \ \Omega$$

and from Eqn (2.67)

$$Z_{22} = \left.\frac{V_2}{I_2}\right|_{I_2=0} = \frac{1}{0.01} = 100 \ \Omega$$

2.6.2 Equivalence of Radiation and Receive Patterns

The radiation pattern (power pattern) of an antenna is the distribution of the radiated power in the far-field region as a function of the angle. This can be determined by measuring the power density distribution as a function of the angle at a constant distance from the antenna and normalizing it with respect to the peak measured-power-density. Similarly, when an antenna is used as a receiver, the power delivered into a matched load is a function of the direction of the incident plane wave with a constant power density and a given polarization. This is known as the receive pattern of the antenna. The receive pattern is generally normalized with respect to the maximum received power. From the reciprocity theorem, we can establish that these two patterns are the same.

Consider a two-dipole situation as shown in Fig. 2.16. Select a sufficiently large distance, R, between the antennas so that the antennas are in the far-field of each other. We connect a transmitter to antenna 1 and a receiver to antenna 2 to measure the received power. It is also assumed that the transmitter source impedance and the receiver input impedance are matched to the respective antennas. Typically all RF systems are matched to the transmission line impedances, either $50\,\Omega$ or $75\,\Omega$. The two antenna terminals can be treated as ports of a two-port network, with the entire free space being inside the two-port network. Now, from the reciprocity theorem, we know that for a given transmitter voltage, the received power is invariant with respect to a change of ports. Thus, we can interchange the transmitter and receiver positions, without affecting the received power reading.

With the transmitter connected to antenna 1, the power received by antenna 2 is proportional to the power density at its location. Hence the plot of

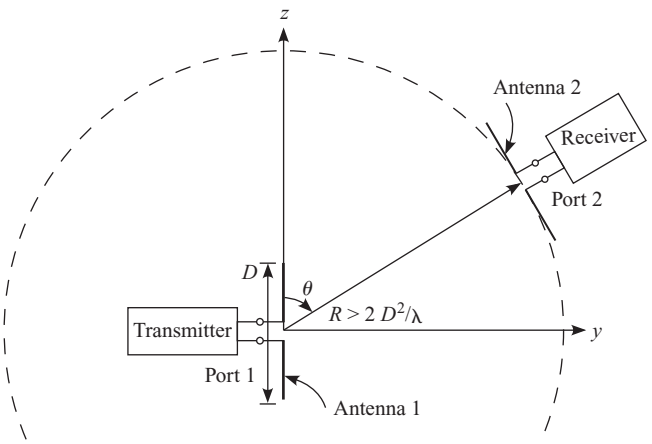

Fig. 2.16 Measurement of radiation pattern

the power received as a function of θ gives the radiation pattern of antenna 1, provided the orientation of antenna 2 with respect to the radial vector from antenna 1 is kept constant.

Now, if we interchange the positions of the transmitter and the receiver, antenna 2 produces a plane wave of constant power density at the location of antenna 1, incident from angle θ, with the $\mathbf{E}$ field oriented along the $\mathbf{a}_\theta$-direction. By definition, a plot of the received power at antenna 1 as antenna 2 is moved around at a constant R, keeping the orientation of antenna 2 along $\mathbf{a}_\theta$, we get the receive pattern of antenna 1. Since, the received power is independent of the position of the transmitter and the receiver, both plots will be the same. Hence, we conclude that the transmit and receive patterns are same for an antenna.

In a practical antenna pattern measurement system, both the antenna locations are generally fixed at a convenient distance. To measure the pattern of antenna 1, instead of moving antenna 2, antenna 1 is rotated about an axis to obtain the same effect as moving antenna 2 around. By selecting the rotation axis, different pattern cuts can be plotted. Since the transmit and receive patterns are identical, it is common practice to connect the receiver to antenna 1 and the transmitter to antenna 2.

2.6.3 Equivalence of Impedances

Consider a transmit–receive system using two antennas separated by a distance R. The terminals of the two antennas can be treated as the ports of a two-port network with the entire free space being inside the two-port network. A two-port network can be characterized by its Z matrix. Let the transmitter be connected to antenna 1 and the receiver to antenna 2. In the transmit mode, the input impedance of antenna 1 is the V/I ratio at its terminals

$$Z_{\text{in}} = Z_{11} - \frac{Z_{12}Z_{21}}{Z_R + Z_{22}} \tag{2.79}$$

where Z_R is the receiver impedance. The input impedance depends on the entire structure seen by the terminals, which includes the two antennas, the entire free space, and the load connected to antenna 2.

In the receive mode, antenna 1 driving a receiver can be modelled as a Thevenin's equivalent source. The Thevenin's equivalent source impedance is the antenna impedance. This impedance can be measured by connecting a transmitter with a source impedance, Z_R (must be same as the receiver impedance), to antenna 2. The ratio of the open-circuit voltage and the

short-circuit current, measured at the antenna 1 terminals, gives Thevenin's equivalent impedance. For a two-port network, this is the same as the input impedance given by Eqn (2.79).

The impedance of an antenna radiating into infinite free space is known as the self-impedance. As the distance between the two antennas tends to infinity, Z_{12} and Z_{21} tend to zero. Therefore, as the antenna separation tends to infinity, $(R \to \infty)$, the second term in Eqn (2.79) tends to zero and Z_{11} tends to self-impedance of the antenna. Although we cannot measure the impedance of the antenna as a receive antenna if we remove the second antenna to infinity, we can infer from the previous result that as a receiver, the antenna's impedance also tends towards the self-impedance for large values of R.

2.6.4 Effective Aperture

The effective aperture (also known as the effective area) of an antenna is the area over which the antenna collects energy from the incident wave and delivers it to the receiver load. If the power density in the wave incident from the (θ, ϕ) direction is S at the antenna and $P_r(\theta, \phi)$ is the power delivered to the load connected to the antenna, then the effective aperture, A_e, is defined as

$$A_e(\theta, \phi) = \frac{P_r(\theta, \phi)}{S} \quad \text{m}^2 \tag{2.80}$$

Referring to the equivalent circuit of the receiving antenna and the load shown in Fig. 2.17, the power delivered to the load, Z_L, connected to the antenna terminals is

$$P_r = \frac{1}{2}|I_R|^2 R_L \tag{2.81}$$

where, R_L is the real part of the load impedance, $Z_L = R_L + jX_L$. Let $Z_a = R_a + jX_a$ be the antenna impedance and V_a be Thevenin's equivalent source corresponding to the incident plane wave. The real part of the antenna impedance can be further divided into two parts, i.e., $R_a = R_{\text{rad}} + R_{\text{loss}}$, where R_{rad} is the radiation resistance and R_{loss} is the loss resistance corresponding to the power lost in the ohmic and dielectric losses in the antenna.

If the antenna is conjugate-matched to the load so that maximum power can be transferred to the load, we have $Z_L = Z_a^*$ or $R_L = R_a$ and $X_L = -X_a$. It is seen from the equivalent circuit that the power collected from the plane wave is dissipated in the three resistances, the receiver load, R_L, the radiation resistance, R_{rad}, and the loss resistance, R_{loss}. For a

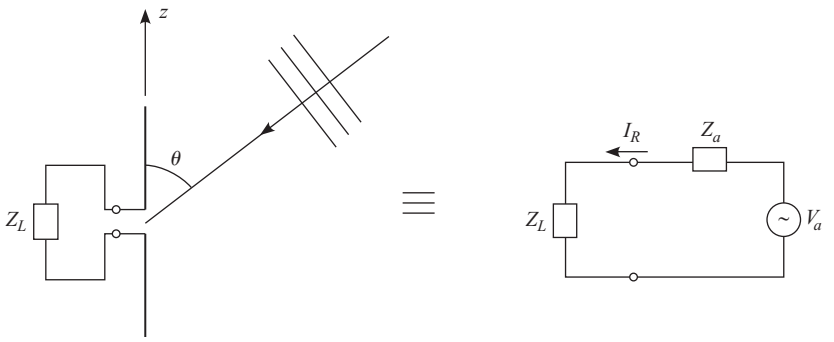

Fig. 2.17 Receiving antenna and its equivalent circuit

conjugate-match, the current through all three resistances is

$$I = \frac{V_a}{R_L + R_{\text{rad}} + R_{\text{loss}}} = \frac{V_a}{2R_L} \tag{2.82}$$

and the three powers are computed using the formulae

$$P_r = \frac{1}{2}|I|^2 R_L = \frac{1}{2}\frac{|V_a|^2}{(2R_L)^2}R_L = \frac{|V_a|^2}{8R_L} \tag{2.83}$$

$$P_{\text{scat}} = \frac{1}{2}|I|^2 R_{\text{rad}} = \frac{|V_a|^2 R_{\text{rad}}}{8R_L^2} \tag{2.84}$$

$$P_{\text{loss}} = \frac{1}{2}|I|^2 R_{\text{loss}} = \frac{|V_a|^2 R_{\text{loss}}}{8R_L^2} \tag{2.85}$$

where P_r is the power delivered to the receiver load, P_{loss} is the power dissipated in the antenna, and P_{scat} is the power scattered, since there is no physical resistance corresponding to the radiation resistance. The total power collected by the antenna is the sum of the three powers

$$P_c = P_r + P_{\text{scat}} + P_{\text{loss}} \tag{2.86}$$

If the power density in the incident wave is S, then the effective collecting aperture, A_c, of the antenna is the equivalent area from which the power is collected

$$A_c(\theta, \phi) = \frac{P_c(\theta, \phi)}{S} \quad \text{m}^2 \tag{2.87}$$

This area is split into three parts—A_e: the effective aperture corresponding to the power delivered to the receiver load, A_{loss}: the loss aperture corresponding to the power loss in the antenna, and A_s: the scattering aperture corresponding to the power re-radiated or scattered by the antenna. These are given by

$$A_e(\theta,\phi) = \frac{P_r(\theta,\phi)}{S} = \frac{|V_a(\theta,\phi)|^2}{8R_L S} \quad \text{m}^2 \tag{2.88}$$

$$A_{\text{loss}}(\theta,\phi) = \frac{P_{\text{loss}}(\theta,\phi)}{S} = \frac{|V_a(\theta,\phi)|^2 R_{\text{loss}}}{8R_L^2 S} \quad \text{m}^2 \tag{2.89}$$

$$A_s(\theta,\phi) = \frac{P_{\text{scat}}(\theta,\phi)}{S} = \frac{|V_a(\theta,\phi)|^2 R_{\text{rad}}}{8R_L^2 S} \quad \text{m}^2 \tag{2.90}$$

All these are functions of the incident direction (θ,ϕ).

Consider an antenna radiating into free space. Let P_{t1} be the total power input to the antenna. If all the power is radiated using an isotropic radiator, the power density at a distance R from the antenna is

$$S_0 = \frac{P_{t1}}{4\pi R^2} \quad \text{W/m}^2 \tag{2.91}$$

If the gain of the antenna is $G_1(\theta,\phi)$, the power density will be larger by that amount in the (θ,ϕ) direction, i.e.

$$S = \frac{P_{t1} G_1(\theta,\phi)}{4\pi R^2} \tag{2.92}$$

Let us label the transmitting antenna as antenna 1.

Now consider a receiving antenna (labelled as antenna 2), kept at a distance R from the transmitting antenna. Let the effective receiving aperture of this antenna be A_{e2}. Thus, the power delivered to the matched load connected to the receiving antenna is

$$P_{r2} = \frac{P_{t1} G_1 A_{e2}}{4\pi R^2} \tag{2.93}$$

or the power-transfer ratio is

$$\frac{P_{r2}}{P_{t1}} = \frac{G_1 A_{e2}}{4\pi R^2} \tag{2.94}$$

The input impedance of the receiver is the load to the receiving antenna. Therefore, the power delivered to the matched load is the power measured by the receiver. We assume that the transmitting antenna is also matched to the source.

If we interchange the positions of the transmitter and the receiver and maintain the conjugate-match at both the antenna ports, the power-transfer ratio will be

$$\frac{P_{r1}}{P_{t2}} = \frac{G_2 A_{e1}}{4\pi R^2} \tag{2.95}$$

where G_2 is the gain of antenna 2 and A_{e1} is the effective aperture of antenna 1. Since the ports are assumed to be matched, the power-transfer ratios are the same from the third result of the reciprocity theorem. Hence we can write

$$\frac{G_1 A_{e2}}{4\pi R^2} = \frac{G_2 A_{e1}}{4\pi R^2} \tag{2.96}$$

or

$$\frac{G_1}{A_{e1}} = \frac{G_2}{A_{e2}} \tag{2.97}$$

Since the antennas are arbitrarily excited, this result shows that the gain-to-effective aperture ratio is a constant for any antenna.

Now, to find the constant we need to relate the fields to the antenna parameters in the transmit and receive modes. Since the above result is independent of the antenna, we select the simplest of the antennas, the Hertzian dipole, to obtain the constant. For simplicity, we also assume that the radiation efficiency of the Hertzian dipole is unity, thus, the directivity and gain are equal, i.e., $D(\theta, \phi) = G(\theta, \phi)$.

From the previous analysis [Eqn (2.54)], the radiation resistance of the Hertzian dipole is

$$R_{\text{rad}} = \frac{2}{3}\pi\eta \left(\frac{dl}{\lambda}\right)^2 = \frac{\pi\eta}{D}\left(\frac{dl}{\lambda}\right)^2 \tag{2.98}$$

$D = 3/2$ of a Hertzian dipole is used to get the last part of Eqn (2.98). If E is the electric field strength, the power density at the antenna is

$$S = \frac{1}{2}\frac{E^2}{\eta} \tag{2.99}$$

The open-circuit voltage induced in the dipole, which is also Thevenin's equivalent voltage shown in the circuit, is

$$V_a = Edl \tag{2.100}$$

assuming E and dl are oriented in the same direction (Fig. 2.17). Power delivered to a matched load R_{rad} is

$$P_r = \frac{|V_a|^2}{8R_{\text{rad}}} \tag{2.101}$$

Dividing the power in the matched load by the power density, we get the effective aperture area of the Hertzian dipole as

$$A_e = \frac{|V_a|^2}{8R_{\text{rad}}} \frac{2\eta}{|E|^2} \tag{2.102}$$

Substituting the expressions for V_a and R_{rad} and simplifying, we get

$$\frac{D}{A_e} = \frac{4\pi}{\lambda^2} \tag{2.103}$$

If the radiation efficiency is not unity, we may replace D by G and write

$$\frac{G}{A_e} = \frac{4\pi}{\lambda^2} \tag{2.104}$$

Thus, the ratio of the gain and the effective aperture is equal to $4\pi/\lambda^2$ for any antenna.

EXAMPLE 2.16

For a Hertzian dipole with radiation efficiency less than 1, show that the gain and the effective aperture are related by

$$\frac{G}{A_e} = \frac{4\pi}{\lambda^2}$$

Solution: Consider a Hertzian dipole which is terminated in a matched load $Z_L = R_L + jX_L$ and receiving electromagnetic energy. Let $R_a = R_{\text{rad}} + R_{\text{loss}}$ be the antenna resistance and, under matched condition, $R_L = R_a$. If V_a is the open-circuit voltage, the power delivered to the matched load is

$$P_r = \frac{|V_a|^2}{8R_L} = \frac{|V_a|^2}{8R_a}$$

Substituting $R_a = R_{\text{rad}} + R_{\text{loss}}$ into Eqn (2.52) and rearranging

$$R_a = \frac{R_{\text{rad}}}{\kappa}$$

Therefore, the power delivered to the load is

$$P_r = \frac{|V_a|^2 \kappa}{8R_{\text{rad}}}$$

If E is the electric field strength of the incident wave, the average power density associated with the wave is given by

$$S = \frac{1}{2}\frac{|E|^2}{\eta}$$

Substituting the expressions for P_r and S into Eqn (2.80)

$$A_e = \frac{P_r}{S} = \frac{|V_a|^2 \kappa}{8R_{\text{rad}}}\frac{2\eta}{|E|^2}$$

The open-circuit voltage developed at the terminals of the dipole due to a polarization-matched wave is

$$V_a = Edl$$

Substituting this into the expression for effective area

$$A_e = \frac{|E|^2 (dl)^2 \kappa}{8R_{\text{rad}}}\frac{2\eta}{|E|^2} = \frac{\eta (dl)^2 \kappa}{4R_{\text{rad}}}$$

Since $G = \kappa D$, the radiation resistance of a Hertzian dipole, given by Eqn (2.98), can be written as

$$R_{\text{rad}} = \frac{\pi\eta\kappa}{G}\left(\frac{dl}{\lambda}\right)^2$$

Substituting this into the expression for A_e

$$A_e = \frac{\eta (dl)^2 \kappa}{4}\frac{G}{\pi\eta\kappa}\left(\frac{\lambda}{dl}\right)^2$$

Simplifying we get

$$A_e = \frac{G\lambda^2}{4\pi}$$

and the result follows.

2.6.5 Vector Effective Length

Let I_{in} be the input current at the terminals of a transmit antenna producing an electric field, $\mathbf{E}_a$, in the far-field region. The vector effective length, $\mathbf{l}_{\text{eff}}$,

is related to $\mathbf{E}_a$ by the relation

$$\mathbf{E}_a = \mathbf{a}_\theta E_\theta + \mathbf{a}_\phi E_\phi = j\eta \frac{kI_{\text{in}}}{4\pi} \frac{e^{-jkr}}{r} \mathbf{l}_{\text{eff}} \tag{2.105}$$

The vector effective length can be written in terms of its components l_θ and l_ϕ along the θ and ϕ directions, respectively, as

$$\mathbf{l}_{\text{eff}} = \mathbf{a}_\theta l_\theta + \mathbf{a}_\phi l_\phi \tag{2.106}$$

In general, l_θ and l_ϕ can be complex quantities. For an ideal current element of length dl carrying a current of I_0, the electric field in the far-field region is given by Eqn (2.8)

$$\mathbf{E} = \mathbf{a}_\theta j\eta \frac{kI_0 dl \sin\theta}{4\pi} \frac{e^{-jkr}}{r} \tag{2.107}$$

and comparing this with Eqn (2.105) the vector effective length is

$$\mathbf{l}_{\text{eff}} = \mathbf{a}_\theta dl \sin\theta \tag{2.108}$$

The vector effective length of a Hertzian dipole is maximum along the direction orthogonal to its axis and zero along its axis.

In the receiving mode, the output voltage developed at the terminals of an antenna due to an incident electromagnetic wave having an electric field $\mathbf{E}^i$ is given by

$$V_a = \mathbf{E}^i \cdot \mathbf{l}^*_{\text{eff}} \tag{2.109}$$

The polarization information of the wave is contained in $\mathbf{E}^i$ and that of the antenna in $\mathbf{l}_{\text{eff}}$. Since $\mathbf{l}_{\text{eff}}$ refers to the antenna in the transmit mode, for the antenna in the receive mode $\mathbf{l}^*_{\text{eff}}$ is used in the definition of V_a, which reverses the direction of rotation of the field vector.

Consider a RCP wave propagating in the positive z-direction. The locus of the tip of the electric field is shown in Fig. 2.18(a). Let us suppose that an RCP antenna is used to receive this wave. The vector effective length of the RCP antenna [$\mathbf{l}_{\text{eff}} = (\mathbf{a}_x - j\mathbf{a}_y)l_0$] represents the polarization in the transmit mode and the locus of the tip of the electric field is shown in Fig. 2.18(b). Although both $\mathbf{E}$ and $(\mathbf{a}_x - j\mathbf{a}_y)$ are rotating in the clockwise direction in the respective coordinate systems, when viewed from a common coordinate system, their directions of rotation are opposite to each other. Let us observe the rotation of $\mathbf{l}^*_{\text{eff}} = (\mathbf{a}_x + j\mathbf{a}_y)l_0$, which is shown in Fig. 2.18(c).

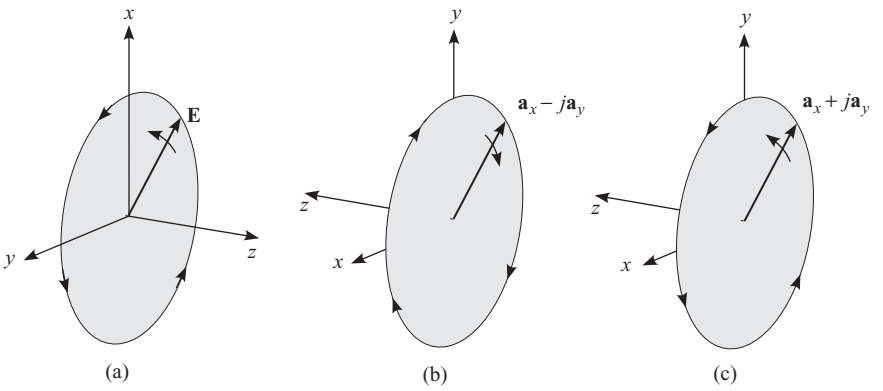

Fig. 2.18 Loci of the tip of the electric field vector of (a) a right circularly polarized wave, (b) an antenna with $\mathbf{l}_{\text{eff}} = (\mathbf{a}_x - j\mathbf{a}_y)l_0$, and (c) an antenna with $\mathbf{l}_{\text{eff}} = (\mathbf{a}_x + j\mathbf{a}_y)l_0$

This represents a wave with its electric field vector rotating in the direction opposite to that of $\mathbf{l}_{\text{eff}}$ or in the same direction as the incident electric field. Therefore, taking the complex conjugate of the vector effective length, we have been able to reverse the direction of rotation of the field vector.

The received power is proportional to the square of the terminal voltage

$$P_r \propto \left|\mathbf{E}^i \cdot \mathbf{l}^*_{\text{eff}}\right|^2 \tag{2.110}$$

If χ is the angle between the vectors $\mathbf{E}^i$ and $\mathbf{l}^*_{\text{eff}}$, Eqn (2.110) can be written as

$$P_r \propto \left(|\mathbf{E}^i||\mathbf{l}^*_{\text{eff}}| \cos\chi\right)^2 \tag{2.111}$$

Under the polarization-matched condition, $\chi = 0$ and the power received will be maximum. Therefore

$$P_{r\max} \propto \left|\mathbf{E}^i\right|^2 |\mathbf{l}^*_{\text{eff}}|^2 \tag{2.112}$$

The polarization efficiency is given by

$$\kappa_p = \frac{\left|\mathbf{E}^i \cdot \mathbf{l}^*_{\text{eff}}\right|^2}{\left|\mathbf{E}^i\right|^2 \left|\mathbf{l}^*_{\text{eff}}\right|^2} = \left|\hat{e}^i \cdot \hat{l}^*_{\text{eff}}\right|^2 \tag{2.113}$$

where

$\hat{e}^i$: unit vector along the incident electric field $\mathbf{E}^i$

$\hat{l}^*_{\text{eff}}$: unit vector along the vector effective length $\mathbf{l}^*_{\text{eff}}$

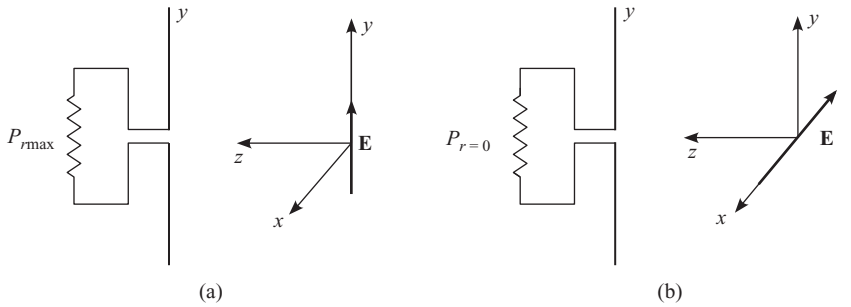

Fig. 2.19 Linearly polarized antenna illuminated by (a) a co-polar and (b) a cross-polar plane wave

The receive antenna is said to be polarization-matched to the incoming wave if the state of polarization of the antenna is the same as that of the incoming wave. This is also known as the co-polar condition. Mathematically, the co-polar condition implies

$$\left|\hat{e}^i \cdot \hat{l}^*_{\text{eff}}\right| = 1 \tag{2.114}$$

On the other hand if $|\hat{e}^i \cdot \hat{l}^*_{\text{eff}}| = 0$, the receiving antenna is cross-polarized or polarized orthogonal to the incoming wave (see Fig. 2.19).

A y-directed dipole radiates a y-directed electric field along the z-axis and similarly, an x-directed dipole produces an x-directed electric field along the z-axis. Consider two crossed dipoles, one along the x-direction and another along the y-direction, excited in phase quadrature. Assume that the characteristic impedances of the transmission lines are matched to the antenna input impedances. The quadrature phasing can be achieved by having the feed transmission line lengths differ by $\lambda/4$ as shown in Fig. 2.20(a). The radiated electric field is given by the sum of the electric fields of the two dipoles

$$\mathbf{E} = (\mathbf{a}_x - j\mathbf{a}_y)E_0 \tag{2.115}$$

The $-j$ factor with the y-component is due to the 90° phase lag introduced by the quarter-wavelength-long transmission line. The unit vector along the vector effective length of this antenna is

$$\hat{l}_{\text{eff}} = \frac{1}{\sqrt{2}}(\mathbf{a}_x - j\mathbf{a}_y) \tag{2.116}$$

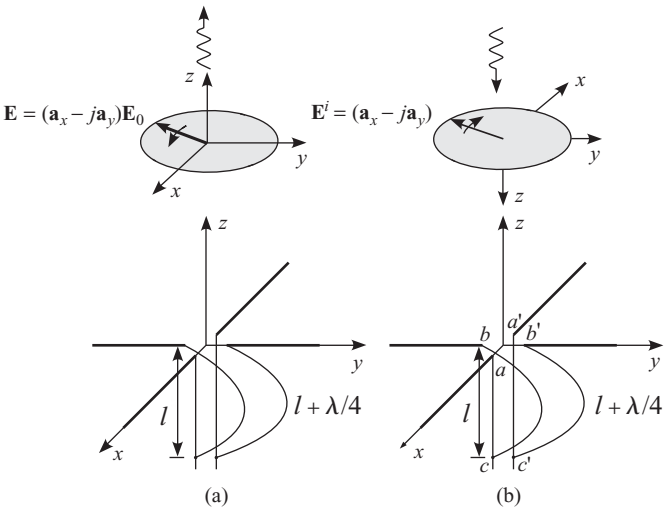

Fig. 2.20 A circularly polarized antenna constructed with a pair of dipoles (a) transmitting RCP wave and (b) receiving RCP wave

Let this antenna be used to receive an RCP plane wave with the incident electric field given by

$$\mathbf{E}^i = E_0(\mathbf{a}_x - j\mathbf{a}_y) \tag{2.117}$$

The incident field in relation to the receiving antenna is shown in Fig. 2.20(b). The x-directed component of the electric field induces a voltage of $V_{aa'} = V_r\angle 180^\circ$ at the terminals a-a' of the dipole. The amplitude of the voltage V_r is a function of the amplitude of the incident wave and the length of the dipole. The 180° phase in the voltage appears because the x-directions of the two coordinate systems are opposite to each other. The voltage due to the y-component of the electric field at the terminals b-b' of the y-directed dipole is $V_{bb'} = V_r\angle -90^\circ$, where the -90° phase is due to the $-j\mathbf{a}_y$ component of the incident field. This voltage gets further delayed by another 90° when it passes through the $\lambda/4$ transmission line connected to the y-directed dipole. Therefore, at the common terminals the two voltages add in phase.

If the incident field is left circularly polarized, the voltage at the common terminal due to the x-directed electric field will still be $V_r\angle 180^\circ$, however, the voltage due to the y-directed dipole would be $V_r\angle 0^\circ$. Therefore, the output at the terminals of a right circularly polarized antenna would be zero for an LCP wave. Thus, an antenna transmits and receives like polarized waves.

EXAMPLE 2.17

What is the vector effective length of an x-directed Hertzian dipole? If this antenna is used to receive a wave with a magnetic field intensity

$$\mathbf{H} = (\mathbf{a}_\theta - j\mathbf{a}_\phi)$$

at the antenna, what is the open-circuit voltage developed at the terminals of the antenna?

Solution: The electric field of an x-directed dipole in its far-field region is given by (see Example 1.8)

$$\mathbf{E} = j\eta \frac{kI_0}{4\pi} \frac{e^{-jkr}}{r} (-\mathbf{a}_\theta \cos\theta \cos\phi + \mathbf{a}_\phi \sin\phi)$$

The vector effective length is related to the far-field electric field by Eqn (2.105) and comparing the previous equation with this

$$\mathbf{l}_{\text{eff}} = -\mathbf{a}_\theta dl \cos\theta \cos\phi + \mathbf{a}_\phi dl \sin\phi$$

The components of the electric and magnetic fields are related to each other by

$$\frac{E_\theta}{H_\phi} = -\frac{E_\phi}{H_\theta} = \eta$$

where η is the intrinsic impedance of the medium. The electric field components are given by

$$E_\theta = \eta H_\phi = \eta(-j)$$

and

$$E_\phi = -\eta H_\theta = -\eta$$

Therefore, the electric field is

$$\mathbf{E} = (-\mathbf{a}_\theta j\eta - \mathbf{a}_\phi \eta)$$

The open-circuit voltage at the terminals of the antenna is given by

$$\begin{aligned} V_a &= \mathbf{E} \cdot \mathbf{l}_{\text{eff}}^* \\ &= (-\mathbf{a}_\theta j\eta - \mathbf{a}_\phi \eta) \cdot (-\mathbf{a}_\theta dl \cos\theta \cos\phi + \mathbf{a}_\phi dl \sin\phi) \\ &= (j\eta dl \cos\theta \cos\phi - \eta dl \sin\phi) \end{aligned}$$

EXAMPLE 2.18

An antenna has $\hat{l}_{\text{eff}} = \mathbf{a}_\theta$. Calculate the polarization efficiency of the antenna if the unit vector in the direction of the incident electric field is **(a)** $\hat{e}^i = \mathbf{a}_\theta$, **(b)** $\hat{e}^i = \mathbf{a}_\phi$, **(c)** $\hat{e}^i = (\mathbf{a}_\theta + \mathbf{a}_\phi)/\sqrt{2}$, and **(d)** $\hat{e}^i = (\mathbf{a}_\theta - j\mathbf{a}_\phi)/\sqrt{2}$.

Solution:

(a) $\kappa_p = \left|\hat{e}^i \cdot \hat{l}_{\text{eff}}\right|^2 = |\mathbf{a}_\theta \cdot \mathbf{a}_\theta|^2 = 1$

This represents an antenna receiving a co-polarized wave.

(b) $\kappa_p = |\mathbf{a}_\theta \cdot \mathbf{a}_\phi|^2 = 0$

The wave is cross-polarized with respect to the antenna.

(c) $\kappa_p = |(\mathbf{a}_\theta \cdot \mathbf{a}_\theta + \mathbf{a}_\theta \cdot \mathbf{a}_\phi)/\sqrt{2}|^2 = \dfrac{1}{2}$

This is a situation where the linearly polarized antenna is not completely aligned with the polarization of the incoming wave.

(d) $\kappa_p = |(\mathbf{a}_\theta \cdot \mathbf{a}_\theta + j\mathbf{a}_\theta \cdot \mathbf{a}_\phi)/\sqrt{2}|^2 = \dfrac{1}{2}$

Only half the power in the incident wave is received if a circularly polarized wave is received using a linearly polarized antenna.

EXAMPLE 2.19

A right circularly polarized antenna has $\hat{l}_{\text{eff}} = (\mathbf{a}_\theta - j\mathbf{a}_\phi)/\sqrt{2}$. Calculate the polarization efficiency of the antenna if the incident electric field is **(a)** right circularly polarized, **(b)** left circularly polarized, and **(c)** linearly polarized in the $\mathbf{a}_\theta$-direction.

Solution:

(a) For a right circular polarized wave, $\hat{e}^i = (\mathbf{a}_\theta - j\mathbf{a}_\phi)/\sqrt{2}$ and, using Eqn (2.113), the polarization efficiency is

$$\kappa_p = \left|\frac{1}{\sqrt{2}}(\mathbf{a}_\theta - j\mathbf{a}_\phi) \cdot \frac{1}{\sqrt{2}}(\mathbf{a}_\theta + j\mathbf{a}_\phi)\right|^2 = \frac{1}{4}(1+1)^2 = 1$$

(b) For a left circular polarized wave, $\hat{e}^i = (\mathbf{a}_\theta + j\mathbf{a}_\phi)/\sqrt{2}$ and hence

$$\kappa_p = \left|\frac{1}{\sqrt{2}}(\mathbf{a}_\theta + j\mathbf{a}_\phi) \cdot \frac{1}{\sqrt{2}}(\mathbf{a}_\theta + j\mathbf{a}_\phi)\right|^2 = \frac{1}{4}(1-1)^2 = 0$$

(c) For a linear polarized wave, $\hat{e}^i = \mathbf{a}_\theta$, thus

$$\kappa_p = \left|\mathbf{a}_\theta \cdot \frac{1}{\sqrt{2}}(\mathbf{a}_\theta + j\mathbf{a}_\phi)\right|^2 = \frac{1}{2}$$

2.6.6 Antenna Temperature

Consider an antenna receiving electromagnetic energy from sources in the sky. The source could be a natural object, such as a planet (Jupiter), a star (the Sun), a quasar, or just background radiation. The power density due to a source at the receiving antenna per unit bandwidth per unit solid angle is known as the brightness of the source and the unit for brightness is W m^{-2} sr^{-2} Hz^{-1}. Any source having a brightness Ψ can be modelled as a blackbody at an equivalent temperature T_b K which also has the same brightness. T_b is known as the brightness temperature of the source. The brightness of a blackbody is given by Planck's radiation law. An approximation to Planck's law, valid in the radio frequency band, is known as the Rayleigh–Jeans radiation law. According to this law, the brightness of a blackbody radiator at a physical temperature, T, is given by

$$\Psi = \frac{2kT}{\lambda^2} \quad \text{W m}^{-2}\ \text{sr}^{-2}\ \text{Hz}^{-1} \tag{2.118}$$

where λ is the wavelength, k is the Boltzmann constant ($k = 1.38 \times 10^{-23}$ J/K), and T is the temperature in kelvin.[1]

An antenna receives electromagnetic energy from several sources in the sky. The brightness and, hence, the brightness temperature of a region in the sky are functions of the direction as seen from the receive antenna. The brightness of the sky in a particular direction (θ, ϕ) is given by

$$\Psi(\theta, \phi) = \frac{2kT_b(\theta, \phi)}{\lambda^2} \tag{2.119}$$

where $T_b(\theta, \phi)$ is the brightness temperature. The power density at the antenna incident from a solid angle, $d\Omega$, and in a bandwidth $d\nu$ is $\Psi(\theta, \phi)d\Omega d\nu$. A lossless antenna receives this noise energy from all directions weighted by its radiation pattern. The energy from different directions is usually incoherent and is noise-like. Therefore, the noise power received by an antenna in an elemental bandwidth, $d\nu$, from an elemental solid angle, $d\Omega$, in a given direction, (θ, ϕ), is

$$dP_{rn} = \Psi(\theta, \phi)A_e P_n(\theta, \phi)d\Omega d\nu \tag{2.120}$$

where $P_n(\theta, \phi)$ is the normalized power pattern and A_e is the maximum effective area of the antenna. Integrating over the entire sphere, Ω, and the frequency band of interest, we get the total noise power as

$$P_{rn} = \frac{1}{2}\int_{\nu}\oint_{\Omega} \Psi(\theta, \phi)A_e P_n(\theta, \phi)d\Omega d\nu \tag{2.121}$$

[1] Celsius to kelvin conversion: K = 273 + °C

The factor (1/2) is due to the unpolarized nature of the thermal radiation received using a polarized antenna. Assuming the frequency dependence of the brightness distribution to be constant over the antenna bandwidth, B, the integration over ν can be replaced by B. Thus

$$P_{rn} = \frac{1}{2} B A_e \oint_{\Omega} \Psi(\theta, \phi) P_n(\theta, \phi) d\Omega \tag{2.122}$$

A resistor is a thermal noise source. The thermal noise voltage (root mean squared value) generated by a resistor, R, kept at a temperature, T, is given by (Pozar 2005)

$$V_n = \sqrt{4kTBR} \quad \text{V} \tag{2.123}$$

where B is the bandwidth in hertz. The power delivered by this noise resistor into a matched load (equal to $R\ \Omega$) is

$$P = kTB \quad \text{W} \tag{2.124}$$

This power is independent of the resistor value, as long as the load is matched to the resistor.

Now, the noise power received by the antenna, given by Eqn (2.122), can be equated to the noise power generated by a matched resistor (the value of which is equal to R_{rad} of the antenna) kept at an equivalent temperature, T_a. Thus

$$P_{rn} = \frac{1}{2} B A_e \oint_{\Omega} \Psi(\theta, \phi) P_n(\theta, \phi) d\Omega = kT_a B \tag{2.125}$$

T_a is known as the *antenna temperature*. Substituting the value of $\Psi(\theta, \phi)$ from Eqn (2.119) and using the relationship $\Omega_A = \lambda^2 / A_e$ [see Eqns (2.31) and (2.103)], we can express T_a as

$$T_a = \frac{1}{\Omega_A} \oint_{\Omega} T_b(\theta, \phi) P_n(\theta, \phi) d\Omega \tag{2.126}$$

If $T_b(\theta, \phi) = T_{b0}$, a constant, we get $T_a = T_{b0}$, since $\oint_{\Omega} P_n(\theta, \phi) d\Omega = \Omega_A$. For a high-gain pencil-beam antenna with low side lobe level, we can approximate Ω_A to an integral only over the main beam and, hence, it is sufficient for $T_b(\theta, \phi)$ to be a constant over the main beam solid angle for the antenna temperature to be equal to the brightness temperature, T_{b0}.

The ground has a brightness temperature of 300 K. The brightness temperature of the sky depends on both the frequency and the direction in which one is looking at the sky. For example, at 4 GHz, the sky has an equivalent brightness temperature of 2.7 K when looking towards the zenith and

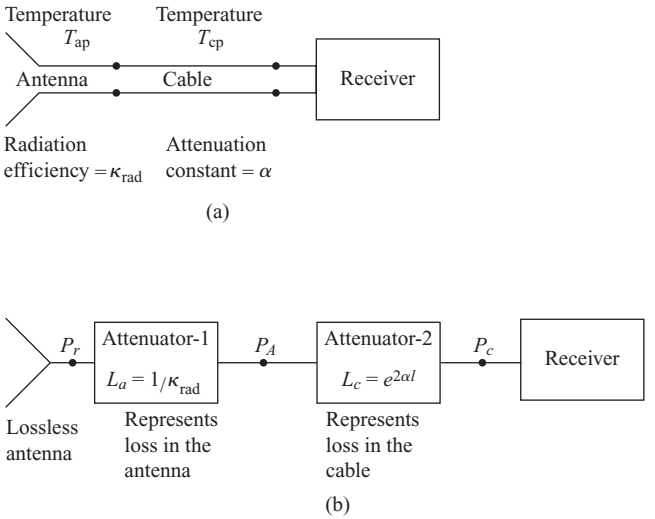

Fig. 2.21 A receiver system showing (a) a receiver connected to an antenna through a cable and (b) its block schematic diagram

100 to 150 K when looking towards the horizon. When looking towards the horizon, the absorption of electromagnetic waves in the atmosphere increases the atmospheric losses and, hence, the brightness temperature is higher. The brightness temperature of the sky at 60 GHz approaches 290 K due to the resonance absorption of molecular oxygen (O_2).

Let us now consider an antenna connected to a receiver through a cable as shown in Fig. 2.21(a). Let the antenna be kept at a physical temperature T_{ap} and the cable be at a physical temperature T_{cp}. Let κ_{rad} be the radiation efficiency of the antenna, l be the length of the cable, and α be the attenuation constant of the cable. Let us also assume that the input impedance of the antenna and the terminal impedance of the receiver are equal to the characteristic impedance of the cable, so that the system is matched. For noise calculation the system can be modelled as a lossless antenna ($\kappa_{\text{rad}} = 1$) followed by an attenuator having a power loss ratio $L_a = 1/\kappa_{\text{rad}}$ (power loss ratio of an attenuator is the input to output power ratio, $L = P_{\text{in}}/P_{\text{out}}$, and is greater than 1). The cable is modelled as an attenuator with a loss ratio $L_c = e^{2\alpha l}$. The equivalent block schematic diagram of the system is shown in Fig. 2.21(b).

The noise power received by the lossless antenna is given by

$$P_{rn} = kT_aB \quad \text{W} \tag{2.127}$$

where T_a is the antenna temperature. If N_i is the noise power input to a noiseless attenuator of attenuation L_a, the output noise power would be $N_0 = N_i/L_a$. An attenuator adds its own noise to the output, which can be modelled as an equivalent input noise power, N_{add}, attenuated by a noiseless attenuator. Thus, the noise power added by the attenuator would be N_{add}/L_a. N_{add} is called the noise added by attenuator 1, referenced to the input of the attenuator. The noise power, P_A, at the output of attenuator 1 is equal to

$$P_A = \frac{P_r}{L_a} + \frac{N_{\text{add}}}{L_a} \tag{2.128}$$

In this book, the noise added by a two-port network is always referenced to the input of the network. The noise added by the network can also be represented in terms of an equivalent noise temperature, T_{e1}, of the network, given by $T_{e1} = N_{\text{add}}/(kB)$. Once again, T_{e1} is the noise equivalent temperature of attenuator 1, referenced to its input terminals, given by $(L_a - 1)T_{\text{ap}}$ (Example 2.20). Hence, the noise added by the attenuator is $N_{\text{add}} = kT_{e1}B = k(L_a - 1)T_{\text{ap}}B$. Substituting this in Eqn (2.128)

$$P_A = \frac{P_r}{L_a} + \frac{L_a - 1}{L_a} kT_{\text{ap}}B \tag{2.129}$$

For attenuator 2 (cable), the input power, P_A, and the output power, P_c, are related by an expression similar to Eqn (2.129), in which we replace L_a by L_c and T_{ap} by T_{cp}. Thus

$$P_c = \frac{P_A}{L_c} + \frac{L_c - 1}{L_c} kT_{\text{cp}}B \tag{2.130}$$

Substituting $L_a = 1/\kappa_{\text{rad}}$, $L_c = e^{2\alpha l}$, $P_{rn} = kT_aB$, and P_A from Eqn (2.129) and simplifying

$$P_c = kB\left\{T_a\kappa_{\text{rad}}e^{-2\alpha l} + (1 - \kappa_{\text{rad}})e^{-2\alpha l}T_{\text{ap}} + (1 - e^{-2\alpha l})T_{\text{cp}}\right\} \tag{2.131}$$

This is the total noise power received from the antenna system into the receiver.

EXAMPLE 2.20

Determine the noise equivalent temperature of a lossy transmission line of length l m, with an attenuation constant of α Np/m, and characteristic impedance $Z_0 = R$, terminated in matched loads at both ends.

Solution: Let $L = e^{2\alpha l}$ be the power-loss ratio of the transmission line. Connect a resistor of resistance R to the input terminals of the transmission line. Let the input resistor be kept at the same temperature, T, as that of the line. Therefore, the entire system is in thermal equilibrium. This can be treated as a resistor of resistance R kept at the temperature T and hence the noise power into a matched load connected to the output terminals of the line is $N_0 = kTB$.

The noise output, N_0, can also be calculated by dividing the total input noise by the loss ratio, L, of the transmission line. The total input noise is given by the sum of the noise input, ($N_i = kTB$ from the resistor at the input) and the noise added, N_{add}, by the transmission line. The noise added by the line is referenced to the input terminals of the line. Therefore, $N_0 = kTB = (N_i + N_{\text{add}})/L = (kTB + N_{\text{add}})/L$. The noise added by the line can be written as $N_{\text{add}} = (L-1)kTB$.

The noise equivalent temperature of the lossy transmission line referenced to its input is $T_e = N_{\text{add}}/(kB) = (L-1)T$.

EXAMPLE 2.21

What is the noise equivalent temperature of a noisy amplifier having power gain G and bandwidth B, if the output noise generated by the amplifier is N_0?

Solution: Terminate both the input and the output of the amplifier in noiseless, matched resistors. If the source resistor is at a temperature of 0 K, the noise input to the amplifier is $N_i = 0$. The noise power at the output of the amplifier, N_0, is the noise generated by the amplifier. We can now obtain the same output noise power from a noiseless amplifier by a matched resistor at the input kept at an equivalent temperature T_e. The noise input to the amplifier is $N_i = kT_eB$ and the noise output is $N_0 = GN_i$. Combining the two equations, the noise equivalent temperature of the amplifier, referenced to its input is given by $T_e = N_0/(GkB)$.

EXAMPLE 2.22

Calculate the noise equivalent temperature of a cascaded system of three gain blocks having gains G_1, G_2, and G_3, and noise equivalent temperatures (referenced to their respective inputs) T_{e1}, T_{e2}, and T_{e3}, respectively. Assume that all the blocks are matched and the system bandwidth is B.

Solution: Let us suppose that the input noise power to the system is $N_i = kT_iB$. The input noise temperature, T_{e1}, of the first amplifier refers to the input noise power of $kT_{e1}B$. Therefore, the total equivalent noise power is $(kT_iB + kT_{e1}B)$. Thus, the noise power at the output of the first stage is

$$N_1 = G_1N_i + G_1kT_{e1}B$$

Similarly, the noise power output of the second stage is

$$N_2 = G_2N_1 + G_2kT_{e2}B$$

Substituting the value of N_1

$$N_2 = G_1G_2k(T_i + T_{e1})B + G_2kT_{e2}B$$

Similarly, the noise power at the output of the third stage is

$$N_0 = G_1G_2G_3k(T_i + T_{e1})B + G_2G_3kT_{e2}B + G_3kT_{e3}B$$

If T_e is the noise equivalent of the entire system, the noise power output is also given by

$$N_0 = G_1G_2G_3k(T_i + T_e)B$$

Equating the last two equations and simplifying, the overall noise equivalent temperature of the system is obtained as

$$T_e = T_{e1} + \frac{T_{e2}}{G_1} + \frac{T_{e3}}{G_1G_2}$$

2.7 Wireless Systems and Friis Transmission Formula

A wireless system consists of a transmitter connected to an antenna radiating electromagnetic energy into free space and at the other end of the system, another antenna picks up the electromagnetic energy, and delivers it to the receiving system. The received power depends on the transmitted power, gains of the transmit and receive antennas, wavelength of the

electromagnetic wave in free space, and the distance between the transmit and the receive antennas. This relationship is known as Friis transmission formula. The Friis formula is extended to take into account the impedance and the polarization mismatch in the system. The effect of the environment on the propagation of the electromagnetic waves is considered in Chapter 8.

Consider an antenna having a gain, G_t, transmitting power P_t into free space. A receive antenna having a gain, G_r, kept at a distance, R, is used to receive the electromagnetic waves. Let λ be the free-space wavelength. The power density at a distance R from the transmitting antenna along the main beam direction is given by [from Eqn (2.92) with $P_{t1} = P_t$ and $G_1 = G_t$]

$$S = \frac{P_t G_t}{4\pi R^2} \tag{2.132}$$

If A_{er} is the effective area of the receiving antenna, the power received by it is

$$P_r = SA_{er} = \frac{P_t G_t A_{er}}{4\pi R^2} \tag{2.133}$$

The gain and the effective area of an antenna are related to each other by Eqn (2.104), which is rewritten as

$$A_{er} = G_r \frac{\lambda^2}{4\pi} \tag{2.134}$$

Substituting Eqn (2.134) into Eqn (2.133)

$$P_r = P_t G_t G_r \left(\frac{\lambda}{4\pi R}\right)^2 \text{ W} \tag{2.135}$$

Equation (2.135) is known as Friis transmission formula which can be expressed in decibel form as

$$P_{r\text{dBm}} = P_{t\text{dBm}} + G_{t\text{dB}} + G_{r\text{dB}} + 20\log_{10}\left(\frac{\lambda}{4\pi R}\right) \text{ dBm} \tag{2.136}$$

In a wireless system, in order to compute the radiated power in a given direction, it is required to specify both the transmit power as well as the antenna gain. In the main beam of the antenna, the product $P_t G_t$ can be thought of as the power radiated by an isotropic antenna with an input

power of $P_t G_t$. Therefore, this product is referred to as *equivalent isotropic radiated power* or EIRP. Specifying EIRP for a system, instead of P_t and G_t, allows the system designer the flexibility to choose an antenna and a corresponding transmitter power. For a receive antenna, given the distance between the two antennas and the wavelength, the received power can only be increased by increasing the EIRP.

So far we have assumed that the transmit antenna is matched to the transmitter and the receive antenna is matched to the receiver. Generally, the transmitter output impedance and the receiver input impedance are made real and matched to the characteristic impedance of the transmission line. Let P_t be the power supplied by the transmitter into a matched load. If the transmitter is not matched, there will be power loss due to reflection. If Γ_t is the reflection coefficient at the transmit end and P_t is the power supplied by the transmitter, the power reflected back from the antenna due to the mismatch is $|\Gamma_t|^2 P_t$. Therefore, the power delivered to the transmit antenna is $(1 - |\Gamma_t|^2)P_t$. Depending on the radiation efficiency of the antenna, a portion of this power is radiated into free space. Similarly, if P_r is the power delivered to a matched load by the receive antenna and Γ_r is the reflection coefficient at the receive end, power delivered to the mismatched load of the receiver will be $(1 - |\Gamma_r|^2)P_r$. Thus, the Friis formula given by Eqn (2.135) is multiplied by the impedance mismatch factor

$$(1 - |\Gamma_t|^2)(1 - |\Gamma_r|^2) \tag{2.137}$$

which takes into account the losses due to the reflections at both the transmit and receive ends.

Further, the Friis formula is multiplied by the polarization efficiency given by [see Eqn (2.113)]

$$\left| \hat{e}^i \cdot \hat{l}^*_{\text{eff}\,r} \right|^2 \tag{2.138}$$

to take into account the polarization mismatch effect. In this expression $\hat{e}^i$ is the unit vector along the radiated electric field of the transmit antenna and, hence, is equal to the unit vector along the vector effective length of the transmit antenna, i.e., $\hat{e}^i = \hat{l}_{\text{eff}\,t}$. In Eqn (2.138) $\hat{l}^*_{\text{eff}\,r}$ is the complex conjugate of the unit vector along the vector effective length of the receive antenna.

Thus, incorporating all the losses in the system, the Friis formula can be written as

$$P_r = P_t G_t G_r \left(\frac{\lambda}{4\pi R}\right)^2 (1 - |\Gamma_t|^2)(1 - |\Gamma_r|^2) \left|\hat{l}_{\text{eff}\,t} \cdot \hat{l}^*_{\text{eff}\,r}\right|^2 \tag{2.139}$$

EXAMPLE 2.23

A 50 W transmitter at 900 MHz is radiating into free space using a linearly polarized 12 dBi omnidirectional antenna.

(a) Calculate the power density and the electric field intensity at a distance of 10 km from the antenna along the direction of the main beam.

(b) If a 1 cm long Hertzian dipole is used to receive the signal, what is the open-circuit voltage developed at its terminals? Assume that the dipole is polarization-matched and its pattern maximum is pointing towards the transmitter.

(c) If the Hertzian dipole has 100% efficiency, what is the power delivered into a matched load connected to its terminals?

(d) Verify that the Friis transmission formula also gives the same value as calculated in part **(c)**.

Solution:

(a) Expressing the gain of the transmit antenna as a ratio

$$G_t = 10^{\frac{G_{t\text{dB}}}{10}} = 10^{1.2} = 15.85$$

The power density at a distance R from an antenna having a gain of G_t and transmitting a power of P_t is

$$S = \frac{P_t G_t}{4\pi R^2}$$

Substituting $P_t = 50$ W, $G_t = 15.85$, and $R = 10000$ m

$$S = \frac{50 \times 15.85}{4\pi \times 10000^2} = 6.3065 \times 10^{-7} \text{ W/m}^2$$

Since the antenna is linearly polarized, without loss of generality we can choose $\mathbf{E} = \mathbf{a}_\theta E_\theta$ and hence $\mathbf{H} = \mathbf{a}_\phi E_\theta/\eta$. (We know that $E_\theta/H_\phi = \eta$.) Therefore, the average power density is

$$\mathbf{S} = \frac{1}{2}\text{Re}\{\mathbf{E} \times \mathbf{H}^*\} = \mathbf{a}_r \frac{1}{2}\text{Re}\left\{E_\theta \frac{E^*_\theta}{\eta}\right\} = \mathbf{a}_r \frac{1}{2}\frac{|E_\theta|^2}{\eta} = \mathbf{a}_r S$$

For free space $\eta = 120\pi\ \Omega$ and hence

$$|E_\theta| = \sqrt{2S\eta} = \sqrt{2 \times 6.3065 \times 10^{-7} \times 120\pi} = 2.1798 \times 10^{-2}\ \text{V/m}$$

(b) The open-circuit voltage developed at the terminals of the dipole is

$$V_a = \mathbf{E} \cdot \mathbf{l}_{\text{eff}}^* = E_\theta dl = 2.1798 \times 10^{-2} \times 0.01 = 2.1798 \times 10^{-4}\ \text{V}$$

The radiation resistance of the Hertzian dipole is given by Eqn (2.54)

$$R_{\text{rad}} = \frac{2}{3}\pi\eta\left(\frac{dl}{\lambda}\right)^2$$

The wavelength at $f = 900$ MHz is

$$\lambda = \frac{c}{f} = \frac{3 \times 10^8}{900 \times 10^6} = \frac{1}{3}\ \text{m}$$

Substituting the values of $\eta = 120\pi\ \Omega$, $dl = 0.01$ m, and $\lambda = (1/3)$ m into the equation for R_{rad}

$$R_{\text{rad}} = \frac{2}{3}\pi \times 120\pi\left(\frac{0.01}{1/3}\right)^2 = 0.7106\ \Omega$$

(c) The power delivered into a matched load is

$$\begin{aligned} P_r &= \frac{1}{2}|I|^2 R_{\text{rad}} = \frac{1}{2}\left|\frac{V_a}{2R_{\text{rad}}}\right|^2 R_{\text{rad}} = \frac{1}{8}\frac{V_a^2}{R_{\text{rad}}} \\ &= \frac{1}{8}\frac{(2.1798 \times 10^{-4})^2}{0.7106} = 8.36 \times 10^{-9}\ \text{W} \end{aligned}$$

(d) Substituting $P_t = 50$ W, $G_t = 15.85$, $G_r = 1.5$ (gain of a lossless Hertzian dipole), and $\lambda = (1/3)$ m in the Friis transmission formula

$$\begin{aligned} P_r &= P_t G_t G_r\left(\frac{\lambda}{4\pi R}\right)^2 = 50 \times 15.85 \times 1.5 \times \left(\frac{1/3}{4\pi \times 10 \times 10^3}\right)^2 \\ &= 8.36 \times 10^{-9}\ \text{W} \end{aligned}$$

Exercises

2.1 Using Maxwell's equations derive an expression for the magnetic field in the far-field region of an antenna if the electric field intensity is given by $\mathbf{E} = (\mathbf{a}_\theta E_0 \cos\theta \sin\phi + \mathbf{a}_\phi E_0 \cos\phi)\, e^{-jkr}/r$ (V/m) and hence verify that

$$\frac{E_\theta}{H_\phi} = -\frac{E_\phi}{H_\theta} = \eta$$

2.2 If the instantaneous Poynting vector is defined by $\bar{\mathcal{S}} = \bar{\mathcal{E}} \times \bar{\mathcal{H}}$, show that the time average power density, $\mathbf{S}$, is given by $\mathbf{S} = (1/2)\mathrm{Re}\{\mathbf{E} \times \mathbf{H}^*\}$.

2.3 Show that in spherical coordinates the elemental area, $dA = r^2 \sin\theta d\theta d\phi$.

2.4 Derive an expression for the average power density vector associated with the electromagnetic wave radiated by a Hertzian dipole of length dl, kept at the origin, oriented along the y-direction, and excited by a current $i(t)$. If the length of the dipole is 1 m and $i(t) = 10\sin(2\pi \times 10^6 t - \pi/4)$ A, calculate the time average power densities at $(r, \theta, \phi) = (4000\ m, \pi/2, 0)$ and (4000 m, $\pi/2$, $\pi/2$).

Answer: 3.25 nW/m^2, 0 W/m^2

2.5 The electric field vector in the far-field region of an antenna is given by

$$\mathbf{E} = (-\mathbf{a}_\theta \cos\theta \cos\phi + \mathbf{a}_\phi \sin\phi)\, E_0 e^{-jkr}/r \text{ V/m}$$

where E_0 is a constant. Plot the power pattern as a function of θ in the $\phi = 0°$ and $\phi = 90°$ planes.

2.6 Calculate the 3 dB beamwidth of an antenna in the $\theta = \pi/2$ plane if the radiated electric field given by

(a) $\mathbf{E} = (\mathbf{a}_\theta E_0 \cos\theta \cos\phi - \mathbf{a}_\phi E_0 \sin\phi) e^{-jkr}/r$ (V/m)

(b) $\mathbf{E} = (\mathbf{a}_\theta E_0 \cos\theta \sin\phi + \mathbf{a}_\phi E_0 \cos\phi) e^{-jkr}/r$ (V/m)

Answer: (a) 90°, (b) 90°

2.7 Calculate the direction of the maximum and the 3 dB beamwidth of an antenna whose radiated electric field in the region $z \geq 0$ is given by

(a) $\mathbf{E} = \mathbf{a}_\theta E_0 \cos\theta e^{-jkr}/r$ (V/m)

(b) $\mathbf{E} = \mathbf{a}_\theta E_0 \cos^2\theta e^{-jkr}/r$ (V/m)

(c) $\mathbf{E} = \mathbf{a}_\theta E_0 \cos^3\theta e^{-jkr}/r$ (V/m)

Answer: (a) 0°, 90° (b) 0°, 65.54° (c) 0°, 54.04°

2.8 Derive an expression for the time-averaged power density associated with the wave radiated by an antenna if the radiated the electric field intensity is given by

$$\mathbf{E} = \mathbf{a}_\theta(\cos\theta - 1)e^{-jkr}/r \text{ V/m}$$

2.9 The radiation intensity of an antenna is given by $U(\theta, \phi) = \sin^n\theta$, where n is an integer. Calculate the direction of the maximum. If $n = 3$, what is the 3 dB beamwidth of the antenna?

Answer: 74.94°

2.10 Show that the total radiated power of a Hertzian dipole of length dl excited by a current I_0 is given by

$$P_{\text{rad}} = \eta\frac{\pi}{3}\left(I_0\frac{dl}{\lambda}\right)^2$$

If the dipole is oriented along the z-direction, show that the directivity is given by

$$D(\theta, \phi) = 1.5\sin^2\theta$$

2.11 Calculate the radiated and the dissipated power by an antenna if the input power is 1.5 kW and its radiation efficiency is 95%.

Answer: 1425 W, 75 W

2.12 What is the effect of doubling the current into a Hertzian dipole on (a) the total

radiated power, (b) the radiation intensity, and (c) the directivity?

2.13 Derive an expression for the directivity of an antenna if the radiated electric field is

(a) $\mathbf{E} = (\mathbf{a}_\theta E_0 \cos\theta \cos\phi - \mathbf{a}_\phi E_0 \sin\phi) e^{-jkr}/r$ (V/m)

(b) $\mathbf{E} = (\mathbf{a}_\theta E_0 \cos\theta \sin\phi + \mathbf{a}_\phi E_0 \cos\phi) e^{-jkr}/r$ (V/m)

What is the maximum value of the directivity in each of the two cases?

Answer: (a) 1.5, (b) 1.5

2.14 Calculate the maximum power density at a distance of 5000 m from an antenna if its directivity is 3.5 dBi, the efficiency is 80%, and the input power is 10 kW.

Answer: 57 μW/m^2

2.15 Calculate the total radiated powers and the maximum directivities of antennas whose radiation intensities are: (a) $U(\theta, \phi) = \cos^2\theta$, (b) $U(\theta, \phi) = \cos^3\theta$, and (c) $U(\theta, \phi) = \cos^4\theta$ in the region $z \geq 0$, and zero elsewhere. Compare the directivity values with those computed using Eqn (2.32).

Answer: (a) 6, 5.09, (b) 8, 7.3 (c) 10, 9.7

2.16 Calculate the radiation efficiency of an antenna if the input power is 2 kW, maximum directivity is 22 dB, and the radiated power density at a distance of 10 km in the direction of the maximum directivity is 0.2 mW/m^2.

Answer: 79.3%

2.17 The radiation intensity of an antenna is given by

$$U(\theta, \phi) = U_0[1 - \sin(2\theta)]$$

where U_0 is a constant. Calculate (a) the direction of maximum, (b) the value of U_0 such that the total radiated power is 1 W, and (c) an expression for the directivity and its maximum value.

Answer: (a) 135° (b) $\frac{1}{4\pi}$ (c) 2

2.18 Show that for a narrow beam pattern with low side lobe level, the maximum directivity is given by

$$D = \frac{41253}{\Theta^\circ_{1\text{HP}}\Theta^\circ_{2\text{HP}}}$$

where $\Theta^\circ_{1\text{HP}}$ and $\Theta^\circ_{2\text{HP}}$ are the 3 dB beamwidths in degrees in the two principal planes.

2.19 An antenna has a radiation resistance of 1.97 Ω, a loss resistance of 1 Ω, and an input reactance of $-j100$ Ω. The antenna is conjugate matched to a 100 V (peak to peak) source having an internal impedance of $(50 + j0)$ Ω by first connecting a series reactance and then an impedance transformer. Calculate (a) the value of the matching reactance and the turns ratio of the matching transformer, (b) the power supplied by the source, (c) the real power input into the antenna, and (d) the power radiated by the antenna.

Answer: (a) $+j100\Omega$, 4.1:1 (b) 6.25 W (c) 6.25 W (d) 4.15 W

2.20 What is the maximum power radiated by an antenna having an efficiency of 80%, if it is fed by a source with an internal impedance of 50 Ω and can deliver a maximum power of 100 W into a 100 Ω load?

Answer: 180 W

2.21 What is the polarization of the wave propagating in the r-direction if the electric field vector at any fixed point in space is given by (a) $\mathbf{E}_a = (\mathbf{a}_\theta - \mathbf{a}_\phi j)$, and (b) $\mathbf{E}_b = (\mathbf{a}_\theta j - \mathbf{a}_\phi)$?

2.22 Determine the polarization of an antenna if the electric field radiated by it is given by

$$\mathbf{E} = -jE_0(\cos\phi - j\sin\phi)(\mathbf{a}\theta - j\mathbf{a}_\phi) e^{-jkr}/r$$

2.23 What is the polarization of a Hertzian dipole oriented along (a) the x-axis and (b) the y-axis?

2.24 What is the angle made with the θ-direction by the instantaneous electric field vector $\bar{\mathcal{E}}(t) = (\mathbf{a}_\theta 3 + \mathbf{a}_\phi 5)\cos(\omega t)$ of a wave propagating in the r-direction?

Answer: 59.04°

2.25 Describe the polarization of the wave propagating in free space along the positive r-direction whose instantaneous field vector at a fixed point in space is given by

(a) $\bar{\mathcal{E}}(t) = \mathbf{a}_\theta 4\cos(\omega t) + \mathbf{a}_\phi 3\sin(\omega t)$

(b) $\bar{\mathcal{H}}(t) = \mathbf{a}_\theta 4\cos(\omega t) + \mathbf{a}_\phi 3\sin(\omega t)$

(c) $\bar{\mathcal{E}}(t) = \mathbf{a}_\theta 4\cos(\omega t) - \mathbf{a}_\phi 2\sin\left(\omega t + \dfrac{\pi}{3}\right)$

2.26 Show that a reciprocal 2-port network can be represented by the T-equivalent shown in Fig. 2.13.

2.27 Prove the reciprocity theorem for a 2-port network represented in terms of Z parameters using an ideal current source as the excitation and the open-circuit voltage as the response.

2.28 For the terminated 2-port network shown in Fig. 2.15, show that the impedances Z_a and Z_b are given by Eqns (2.70) and (2.71), respectively.

2.29 The measured input impedance at part 1 of a reciprocal two-part network with part 2 open-circuited is $Z_{\text{oc1}} = (30 + j15)\ \Omega$ and with part 2 short-circuited, it is $Z_{\text{sc1}} = (25.62 + j14.375)\ \Omega$. Similarly, the measured impedance at part 2 with part 1 open is $Z_{\text{oc2}} = (20 + j20)\ \Omega$. Calculate the Z matrix elements.

Answer: $Z_{11} = (30 + j15)\,\Omega$
$Z_{12} = (10 + j5)\,\Omega \quad Z_{21} = (10 + j5)\,\Omega$
$Z_{22} = (20 + j20)\,\Omega$

2.30 Show that the Thevenin's equivalent impedance of an antenna in the receive mode is given by Eqn (2.79).

2.31 Derive an expression for the vector effective length of a y-directed Hertzian dipole. What are its values along the axis and normal to the axis of the dipole?

2.32 An antenna with a vector effective length of

$$\mathbf{l}_{\text{eff}} = -\mathbf{a}_\theta \cos\theta\cos\phi + \mathbf{a}_\phi \sin\phi$$

is used for receiving an electromagnetic wave of a magnetic field intensity

$$\mathbf{H} = (\mathbf{a}_\theta + j\mathbf{a}_\phi)$$

What is its polarization efficiency?

Answer: 0.5

2.33 Show that for a linearly polarized antenna the effective area and the effective length are related by

$$A_e = \frac{30\pi}{R_{\text{rad}}} l_{\text{eff}}^2$$

2.34 Show that the gain, G, the effective length, l_{eff}, and the radiation resistance, R_{rad}, of a linearly polarized antenna are related by

$$G = \pi \frac{\eta}{R_{\text{rad}}} \left(\frac{l_{\text{eff}}}{\lambda}\right)^2$$

where $\eta = 120\pi\ \ \Omega$ is the free-space impedance.

2.35 What is the polarization efficiency of an x-directed Hertzian dipole kept at the origin used for receiving (a) a θ-polarized and (b) a ϕ-polarized electromagnetic wave incident from $(\theta, \phi) = (\pi/2, \pi/2)$?

2.36 Show that an antenna having a vector effective length, $\mathbf{l}_{\text{eff}} = (\mathbf{a}_x - j\mathbf{a}_y)l_0$, transmits a right circularly polarized wave.

2.37 If the equivalent thermal noise voltage across a resistance, $R_a\ \Omega$, kept at a temperature of T_a K within a given bandwidth, B Hz is given by

$$V_n = \sqrt{4kT_aB}\ \text{V}$$

what is the noise power delivered by this resistor into a matched load?

2.38 Calculate the noise power delivered to a matched load by a 50 Ω resistor kept at

27°C in a bandwidth of 1 kHz. Determine the noise power if the resistor as well as the load are changed to 100 Ω.

Answer: −143.8 dBm, −143.8 dBm

2.39 A noise source is delivering −104 dBm power into a matched load. Calculate the noise equivalent temperature if the system bandwidth is 10 MHz.

Answer: 288.5 K

2.40 An amplifier having a bandwidth of 1 MHz and a gain of 20 dB delivers a noise power output of −98.6 dBm into a matched load with its input terminated in a noiseless matched resistor. What will be the noise power at the output of the amplifier into a matched load if the input is connected directly to the terminals of a low side lobe narrow beam antenna with its main beam pointed towards a region of the sky having a brightness temperature of (a) 10 K and (b) 300 K? Assume that the receiver and the antenna are matched.

Answer: (a) −98.2 dBm (b) −92.6 dBm

2.41 An antenna with a gain of 12 dB and an effective aperture of 3 m^2 is used to receive electromagnetic energy propagating in free space. If the received power into a matched load is 0.1 nW, what is the power density of the wave at the antenna? If this antenna is replaced by another matched antenna having a gain of 20 dB, calculate the received power and express it in watts.

Answer: 33.3 pW/m^2, 631 pW

2.42 The output power of a 900 MHz mobile phone base station transmitter is 100 W. It is connected to an antenna having a gain of 15 dBi by a cable that has a loss of 3 dB. Calculate the power delivered to the receiver kept at a distance of 25 km. Gain of the receiver antenna is −1 dB. Assume that the system is impedance as well as polarization matched.

Answer: −58.5 dBm

2.43 An antenna having a gain of 15 dBi is used to receive a 2.4 GHz signal propagating in free space. If the power density of the wave is 25 μW/m^2, calculate the power received into a matched load of 50 Ω connected to this antenna. Express the power in dBm. Calculate the magnitude of the voltage developed across the load. If the load is disconnected, what will be the magnitude of the open-circuit voltage at the antenna terminals?

Answer: −30 dBm, 9.91 mV, 19.82 mV

2.44 What is the minimum transmit power required to establish a point-to-point communication link at 2.4 GHz between two points 20 km apart, using two 20 dB gain antennas so that the minimum power into a matched receiver is −70 dBm? Assume that the antennas are lossless and matched. Answer: 40.4 mW

2.45 The minimum transmitter power required to establish a communication link with a receiver at a distance of 0.5 m is 20 mW. Calculate the required transmitter power if the range is increased to 1 km.

Answer: 80 kW

2.46 A communication link between a transmitter and a receiver can be established either using a cable or using two antennas and free space propagation. The cable has an attenuation of 1 dB per metre. Each of the antennas used in the free-space link has a gain of 10 dBi. The frequency of operation is 2.4 GHz and the transmitter power is 100 mW. Calculate the distance at which both these approaches would deliver the same power into a matched receiver. Which method would give a longer range if the minimum power required into the receiver for a successful link is −70 dBm? What are the ranges?

Answer: 54.8 m, 90 m, 3.15 km

CHAPTER 3

Wire Antennas

Introduction

In this chapter, we study the radiation characteristics of wire antennas. These antennas are made of thin, conducting, straight or curved wire segments or hollow tubes and are very easy to construct. The dipole and the monopole are examples of straight wire antennas; the loop antenna is an example of a curved wire antenna.

One of the assumptions made for this class of antennas is that the radius of the wire is very small compared to the operating wavelength. As a consequence, we can assume that the current has only one component along the wire. The variation of the current along the wire depends on the length and shape of the wire. The assumed current distribution on the wire enables us to compute the electric and magnetic fields in the far-field region of the antenna using the magnetic vector potential. With the knowledge of the fields, we can compute the antenna characteristics such as directivity, radiation resistance, etc.

3.1 Short Dipole

Consider a short wire dipole of length l ($l < 0.1\lambda$) and radius a ($a \ll \lambda$), symmetrically placed about the origin and oriented along the z-axis as shown in Fig. 3.1. Measurements show that the current on a short wire dipole with feed point as shown in the figure has a triangular distribution with a maximum at the centre and linearly tapering off to zero at the ends (Fig. 3.2). Mathematically, the current on the dipole in the region $0 \leq z' \leq l/2$ can be represented by a straight line having a slope of $-(2/l)I_0$ and an intercept of I_0 at $z' = 0$. Similarly, over the region $-l/2 \leq z' \leq 0$, the current distribution can be represented by a line having a slope of $(2/l)I_0$ and an intercept of I_0 at $z' = 0$.

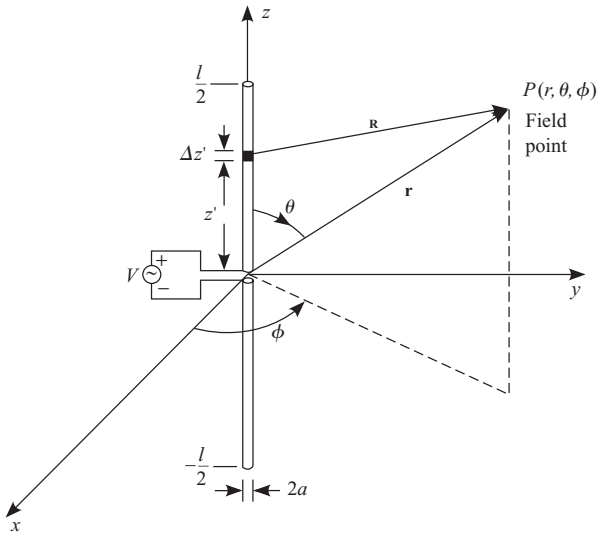

Fig. 3.1 Geometry of a thin wire dipole

Thus, the current on the dipole can be represented by the following expression

$$I_z(z') = \begin{cases} \left(1 - \dfrac{2}{l}z'\right) I_0 \;\; 0 \le z' \le \dfrac{l}{2} \\ \left(1 + \dfrac{2}{l}z'\right) I_0 \;\; -\dfrac{l}{2} \le z' \le 0 \end{cases} \tag{3.1}$$

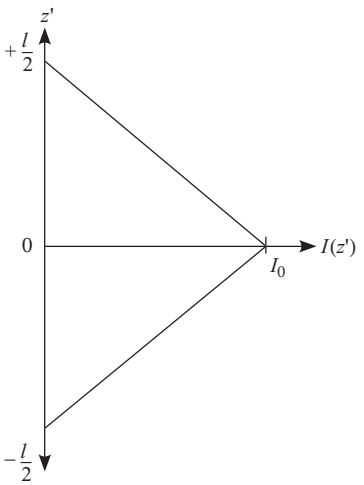

Fig. 3.2 Current distribution on a short wire dipole excited at the centre

Since the current is z-directed, the magnetic vector potential, $\mathbf{A}$, has only a z-component given by

$$\mathbf{A}(x,y,z) = \mathbf{a}_z \frac{\mu}{4\pi} \int_{-l/2}^{l/2} I_z(z') \frac{e^{-jkR}}{R} dz' \tag{3.2}$$

where R is the distance from the source point $(x'=0,\ y'=0,\ z')$ on the dipole to the field point (x,y,z) and is given by

$$R = \sqrt{x^2 + y^2 + (z-z')^2} \tag{3.3}$$

Expressing the field point (x,y,z) in spherical coordinates using the following transformation equations

$$x^2 + y^2 + z^2 = r^2 \tag{3.4}$$

$$z = r\cos\theta \tag{3.5}$$

R can be written as

$$R = \sqrt{r^2 - 2rz'\cos\theta + z'^2} = r\left(1 + \left[-\frac{2z'}{r}\cos\theta + \left(\frac{z'}{r}\right)^2\right]\right)^{\frac{1}{2}} \tag{3.6}$$

For $r \gg z'$, the square root term in Eqn (3.6) has the form $\sqrt{1+x}$ with $|x| < 1$. Therefore, it can be expanded using the binomial series to obtain

$$\begin{aligned} R &= r\left\{1 + \frac{1}{2}\left[-2\frac{z'}{r}\cos\theta + \left(\frac{z'}{r}\right)^2\right] - \frac{1}{8}\left[-2\frac{z'}{r}\cos\theta + \left(\frac{z'}{r}\right)^2\right]^2 + \cdots\right\} \\ &= r - z'\cos\theta + \left(\frac{z'}{r}\right)\left(\frac{z'}{2}\sin^2\theta\right) + \left(\frac{z'}{r}\right)^2\left(\frac{z'}{2}\cos\theta\sin^2\theta\right) + \cdots \end{aligned} \tag{3.7}$$

If the field point is far away from the antenna ($r \gg z'$), the terms involving z'/r and higher powers of z'/r in Eqn (3.7) can be neglected to get an approximate value for R as

$$R \simeq r - z'\cos\theta \tag{3.8}$$

The maximum value of the most significant of the neglected terms in Eqn (3.7) occurs when $\theta = \pi/2$ and is

$$\left(\frac{z'^2}{2r}\sin^2\theta\right)_{\max} = \frac{z'^2}{2r} \tag{3.9}$$

Therefore, if we use Eqn (3.8) instead of Eqn (3.3), the maximum phase error due to the most significant of the neglected terms would be

$$\Delta_{\text{phase}}^{\max} = k\left(\frac{z'^2}{2r}\right) \tag{3.10}$$

If the maximum acceptable error in the phase is $\pi/8$, we get

$$k\left(\frac{z'^2}{2r}\right) \leq \frac{\pi}{8} \tag{3.11}$$

Inserting the maximum value of $z' = l/2$

$$\frac{2\pi}{\lambda}\left(\frac{l^2}{8r}\right) \leq \frac{\pi}{8} \tag{3.12}$$

results in the following condition for r

$$r \geq \frac{2l^2}{\lambda} \tag{3.13}$$

In the expression for the magnetic vector potential, $\mathbf{A}$ [Eqn (3.2)], the distance R between the source and the field point appears both in the amplitude and the phase of the integrand. While evaluating the expression in the far-field of an antenna, we can use the approximation given in Eqn (3.8) for the phase term

$$e^{-jkR} \simeq e^{-jk(r - z'\cos\theta)} \tag{3.14}$$

This approximation results in a maximum phase error of $\pi/8$ rad (or 22.5°). Since both r and R are very large compared to the wavelength, the following approximation is used for the amplitude term

$$R \simeq r \tag{3.15}$$

which results in a very small error in the amplitude. Equations (3.8) and (3.15) together are known as the far-field approximation for R. While evaluating the magnetic vector potential in the far-field region, the term e^{-jkR}/R in the integrand is approximated by

$$\frac{e^{-jkR}}{R} \simeq \frac{e^{-jkr}}{r} e^{jkz'\cos\theta} \tag{3.16}$$

Geometrically, the far-field approximation implies that the vectors $\mathbf{R}$ and $\mathbf{r}$ are parallel to each other and a path difference of $z'\cos\theta$ exists between the two (Fig. 3.3). The following example illustrates the errors introduced in the amplitude and phase due to the far-field approximations.

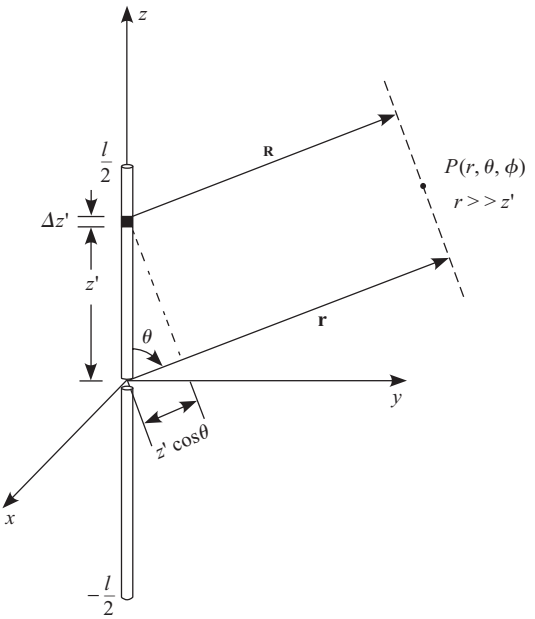

Fig. 3.3 The far-field approximation

EXAMPLE 3.1

Compute the error introduced in the amplitude and phase of e^{-jkR}/R, if the far-field approximation is used in the computation of the magnetic vector potential at a distance of 50λ for a dipole of length 2λ.

Solution: Let us compute the distances for $\theta = \pi/2$, $z' = 1\lambda$, and $r = 50\lambda$. Substituting the values of θ, z', and r in Eqn (3.6) we get

$$R = \sqrt{r^2 + z'^2} = \lambda\sqrt{50^2 + 1^2} = 50.01\lambda$$

and from Eqns (3.8) and (3.15)

$$R \simeq R_a = r = 50\lambda \quad \text{for amplitude}$$
$$R \simeq R_p = r - z'\cos(\pi/2) = 50\lambda \quad \text{for phase}$$

The fractional error in the amplitude, Δ_{amp}, is given by

$$\Delta_{\text{amp}} = \frac{\left|\dfrac{1}{R_a} - \dfrac{1}{R}\right|}{\dfrac{1}{R}}$$
$$= \left|\frac{R}{R_a} - 1\right| = 2 \times 10^{-4}$$

which is very small. The error in phase, Δ_{phase}, is given by

$$\Delta_{\text{phase}} = k(R_p - R) = \frac{2\pi}{\lambda}(50 - 50.01)\lambda = -0.0628 \text{ rad}$$

When $\theta = 0$, Eqn (3.6) reduces to $R = r - z' = 49\lambda$, from Eqn (3.15) we have $R_a = r = 50\lambda$ and from Eqn (3.8) $R_p = r - z' = 49\lambda$. Therefore, the errors in the amplitude and phase are

$$\Delta_{\text{amp}} = \left|\frac{49}{50} - 1\right| = 0.02$$
$$\Delta_{\text{phase}} = 0$$

Now we will evaluate the magnetic vector potential by substituting the current distribution on the dipole given by Eqn (3.1) into Eqn (3.2)

$$\mathbf{A}(x,y,z) = \mathbf{a}_z \frac{\mu}{4\pi}\left[\int_{-l/2}^{0}\left(1 + \frac{2}{l}z'\right) I_0 \frac{e^{-jkR}}{R} dz' + \int_{0}^{l/2}\left(1 - \frac{2}{l}z'\right) I_0 \frac{e^{-jkR}}{R} dz'\right] \tag{3.17}$$

Introducing the far-field approximations $R \simeq r - z'\cos\theta$ for the phase and $R \simeq r$ for the amplitude

$$\mathbf{A}(x,y,z) = \mathbf{a}_z \frac{\mu}{4\pi}\frac{e^{-jkr}}{r} I_0 \left[\int_{-l/2}^{0}\left(1 + \frac{2}{l}z'\right) e^{jkz'\cos\theta} dz' + \int_{0}^{l/2}\left(1 - \frac{2}{l}z'\right) e^{jkz'\cos\theta} dz'\right] \tag{3.18}$$

By evaluating the integrals in Eqn (3.18) and simplifying (see Example 3.2), we can show that for $kl/4 \ll 1$

$$\mathbf{A}(x,y,z) \simeq \mathbf{a}_z \frac{\mu}{4\pi} I_0 \frac{e^{-jkr}}{r}\frac{l}{2} \tag{3.19}$$

EXAMPLE 3.2

Show that the integral within the square brackets in Eqn (3.18) is approximately equal to $l/2$ for $kl/4 \ll 1$.

Solution: Let us denote the term in the square brackets by

$$I = \left[\int_{-l/2}^{0} \left(1 + \frac{2}{l} z'\right) e^{jkz' \cos\theta} dz' + \int_{0}^{l/2} \left(1 - \frac{2}{l} z'\right) e^{jkz' \cos\theta} dz' \right]$$

Substituting $z' = -z''$ in the first integral, and interchanging the limits

$$I = \int_{0}^{l/2} \left(1 - \frac{2}{l} z''\right) e^{-jkz'' \cos\theta} dz'' + \int_{0}^{l/2} \left(1 - \frac{2}{l} z'\right) e^{jkz' \cos\theta} dz'$$

Since both the integrals have the limits 0 to $l/2$, we can write

$$I = \int_{0}^{l/2} \left(1 - \frac{2}{l} z'\right) (e^{jkz' \cos\theta} + e^{-jkz' \cos\theta}) dz'$$

Now we can simplify the integrand by using the identity $e^{jx} + e^{-jx} = 2\cos x$, to get

$$I = \int_{0}^{l/2} \left(1 - \frac{2}{l} z'\right) 2\cos(kz' \cos\theta) dz'$$

Performing the integration

$$I = 2 \left[\frac{\sin(kz' \cos\theta)}{k \cos\theta} \right]_{0}^{l/2} - \frac{4}{l} \left[z' \frac{\sin(kz' \cos\theta)}{k \cos\theta} + \frac{\cos(kz' \cos\theta)}{(k \cos\theta)^2} \right]_{0}^{l/2}$$

Substituting the limits and simplifying, we get

$$I = \frac{4}{l(k \cos\theta)^2} \left[1 - \cos\left(\frac{kl}{2} \cos\theta\right) \right]$$

Using the identity $\cos(2\theta) = 1 - 2\sin^2\theta$, the above expression can be written as

$$I = \frac{4}{l(k \cos\theta)^2} 2 \sin^2\left(\frac{kl}{4} \cos\theta\right)$$

For $kl/4 \ll 1$

$$\sin^2\left(\frac{kl}{4} \cos\theta\right) \simeq \left(\frac{kl}{4} \cos\theta\right)^2$$

and hence the integral reduces to

$$I \simeq \frac{l}{2}$$

Following the procedure described in Section 1.2, we first express the components of the magnetic vector potential in spherical coordinates as

$$A_r = A_z \cos\theta = \frac{\mu}{4\pi} I_0 \frac{e^{-jkr}}{r} \frac{l}{2} \cos\theta \tag{3.20}$$

$$A_\theta = -A_z \sin\theta = \frac{\mu}{4\pi} I_0 \frac{e^{-jkr}}{r} \frac{l}{2} \sin\theta \tag{3.21}$$

The next step is to find the magnetic field using

$$\mathbf{H} = \frac{1}{\mu} \nabla \times \mathbf{A} \tag{3.22}$$

Expanding the curl equation in the spherical coordinate system with the knowledge that the field quantities are ϕ-symmetric and, hence, the result of differentiation with respect to ϕ is zero (see Example 3.3)

$$\mathbf{H} = \mathbf{a}_\phi H_\phi = \mathbf{a}_\phi \frac{1}{r\mu} \left(\frac{\partial (r A_\theta)}{\partial r} - \frac{\partial A_r}{\partial \theta} \right) \tag{3.23}$$

Substituting the values of A_r and A_θ from Eqn (3.20) and Eqn (3.21) into Eqn (3.23) and performing the differentiation

$$H_r = 0 \tag{3.24}$$

$$H_\theta = 0 \tag{3.25}$$

$$H_\phi = j \frac{k I_0 l}{8\pi} \frac{e^{-jkr}}{r} \left(1 + \frac{1}{jkr} \right) \sin\theta \tag{3.26}$$

In the far-field region of the antenna, we can neglect the term containing $1/r^2$ and, hence, the ϕ-component of the magnetic field reduces to

$$H_\phi = j \frac{k I_0 l}{8\pi} \frac{e^{-jkr}}{r} \sin\theta \tag{3.27}$$

The electric field can be computed by substituting the value of the magnetic field into the Maxwell's curl equation for a source-free region

$$\mathbf{E} = \frac{1}{j\omega\epsilon} \nabla \times \mathbf{H} \tag{3.28}$$

Performing the differentiation and neglecting the term containing $1/r^2$ we get the electric field as

$$\mathbf{E} = \mathbf{a}_\theta j\eta \frac{k I_0 l}{8\pi} \frac{e^{-jkr}}{r} \sin\theta \tag{3.29}$$

In the far-field of the dipole the electric and magnetic field intensities are transverse to each other as well as to the direction of propagation. E_θ, H_ϕ,

and the direction of propagation, $\mathbf{a}_r$, form a right handed system. The ratio of E_θ/H_ϕ is equal to the impedance of the medium, η. The expressions for the electric and magnetic field intensities are related to the magnetic vector potential by the following equations

$$\mathbf{E} = -j\omega\mathbf{A}_t \tag{3.30}$$

$$\mathbf{H} = -\frac{j\omega}{\eta}\mathbf{a}_r \times \mathbf{A}_t \tag{3.31}$$

where $\mathbf{A}_t$ represents the transverse component of the magnetic vector potential given by

$$\mathbf{A}_t = \mathbf{a}_\theta A_\theta + \mathbf{a}_\phi A_\phi \tag{3.32}$$

These equations are valid only in the far-field of an antenna.

EXAMPLE 3.3

Given that $\mathbf{A} = \mathbf{a}_r A_r + \mathbf{a}_\theta A_\theta$ is independent of ϕ, show that

$$\mathbf{H} = \mathbf{a}_\phi \frac{1}{r\mu}\left(\frac{\partial(rA_\theta)}{\partial r} - \frac{\partial A_r}{\partial \theta}\right)$$

Solution: From Eqn (3.22)

$$\mathbf{H} = \frac{1}{\mu}\nabla \times \mathbf{A}$$

The curl operation in spherical coordinates can be written as

$$\nabla \times \mathbf{A} = \frac{1}{r^2 \sin\theta}\begin{vmatrix} \mathbf{a}_r & r\mathbf{a}_\theta & r\sin\theta\mathbf{a}_\phi \\ \partial/\partial r & \partial/\partial\theta & \partial/\partial\phi \\ A_r & rA_\theta & r\sin\theta A_\phi \end{vmatrix}$$

Since $A_\phi = 0$

$$\nabla \times \mathbf{A} = \frac{1}{r^2\sin\theta}\left[\mathbf{a}_r\left(-\frac{\partial(rA_\theta)}{\partial\phi}\right) - \mathbf{a}_\theta r\left(-\frac{\partial A_r}{\partial\phi}\right) + \mathbf{a}_\phi r\sin\theta\left(\frac{\partial(rA_\theta)}{\partial r} - \frac{\partial A_r}{\partial\theta}\right)\right]$$

Given that A_r and A_θ are independent of ϕ, the partial derivatives with respect to ϕ are zero. Thus $\nabla \times \mathbf{A}$ reduces to

$$\nabla \times \mathbf{A} = \frac{1}{r}\left[\mathbf{a}_\phi\left(\frac{\partial(rA_\theta)}{\partial r} - \frac{\partial A_r}{\partial \theta}\right)\right]$$

Substituting this expression in Eqn (3.22), gives us the required result.

3.1.1 Radiation Resistance and Directivity

Since for a dipole oriented along the z-direction, only E_θ and H_ϕ exist in the far-field region, the average power density, $\mathbf{S}$, is given by

$$\begin{aligned}\mathbf{S} &= \frac{1}{2}\mathrm{Re}(\mathbf{a}_\theta E_\theta \times \mathbf{a}_\phi H_\phi^*) \\ &= \mathbf{a}_r \frac{1}{2}\mathrm{Re}(E_\theta H_\phi^*)\end{aligned} \tag{3.33}$$

Using the relationship $E_\theta/H_\phi = \eta$ and Eqn (3.29) for E_θ, the power density at a distance r is given by

$$\mathbf{S} = \mathbf{a}_r \frac{1}{2}\mathrm{Re}\left(E_\theta \frac{E_\theta^*}{\eta}\right) = \mathbf{a}_r \frac{1}{2\eta}|E_\theta|^2 = \mathbf{a}_r \frac{\eta}{2}\left|\frac{kI_0 l}{8\pi}\right|^2 \frac{\sin^2\theta}{r^2} \tag{3.34}$$

Total power radiated, P_{rad}, is obtained by integrating the power density over a sphere of radius r

$$P_{\mathrm{rad}} = \int_0^{2\pi}\int_0^{\pi} \mathbf{S}\cdot\mathbf{a}_r r^2 \sin\theta d\theta d\phi \tag{3.35}$$

$$= \frac{\eta}{2}\left|\frac{kI_0 l}{8\pi}\right|^2 \int_0^{2\pi}\int_0^{\pi} \sin^3\theta d\theta d\phi = \eta\frac{\pi}{12}|I_0|^2\left(\frac{l}{\lambda}\right)^2 \tag{3.36}$$

To obtain the radiation resistance, the total radiated power is equated to the power absorbed by an equivalent resistance carrying the same input current, I_0.

$$P_{\mathrm{rad}} = \frac{1}{2}|I_0|^2 R_{\mathrm{rad}} \tag{3.37}$$

Equating Eqn (3.36) and Eqn (3.37) and substituting the value of η for free space, we get the expression for the radiation resistance of a short dipole as

$$R_{\mathrm{rad}} = 20\pi^2\left(\frac{l}{\lambda}\right)^2 \ \Omega \tag{3.38}$$

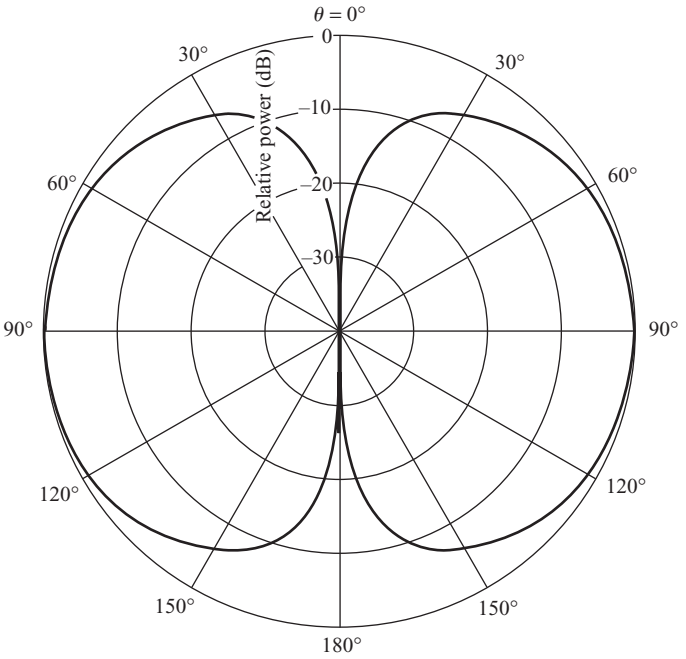

Fig. 3.4 The x-z plane cut of the radiation pattern of a z-directed short dipole

In order to compute the directivity, we first compute the radiation intensity

$$U(\theta, \phi) = r^2 S = \frac{\eta}{2} \left| \frac{kI_0 l}{8\pi} \right|^2 \sin^2 \theta \tag{3.39}$$

where S is the radial component of $\mathbf{S}$. The directivity is given by

$$D(\theta, \phi) = 4\pi \frac{U(\theta, \phi)}{P_{\text{rad}}} \tag{3.40}$$

Substituting the value of P_{rad} and $U(\theta, \phi)$ into Eqn (3.40), we get the directivity of a short dipole as

$$D = 1.5 \sin^2 \theta \tag{3.41}$$

It may be noted that the directivity is same as that of a Hertzian dipole.

The normalized radiation intensity expressed in decibels is given by

$$U_{\text{dB}}(\theta, \phi) = 10 \log_{10}(\sin^2 \theta) \text{ dB} \tag{3.42}$$

and is shown in Fig. 3.4. The radiation pattern has a null along the axis of the dipole and a maximum in the $\theta = 90°$ plane. The radiation pattern

is independent of ϕ. The 3D pattern is obtained by rotating the right half of the pattern about the axis of the dipole. Such a pattern is called an *omni-directional pattern*. An omni-directional pattern has a non-directional pattern in one plane, and a directional pattern in any plane orthogonal to it.

EXAMPLE 3.4

A short dipole with a triangular current distribution radiates P_{rad} watts into free space. Show that the magnitude of the maximum electric field at a distance r is given by

$$E_\theta = \frac{\sqrt{90P_{\text{rad}}}}{r} \text{ V/m}$$

Solution: The maximum value of the electric field given by Eqn (3.29) occurs along $\theta = 90^\circ$ and is given by

$$|E_\theta| = \eta \frac{k|I_0|l}{8\pi} \frac{1}{r}$$

The radiated power can be expressed as [Eqn (3.36)]

$$P_{\text{rad}} = \eta \frac{\pi}{12} |I_0|^2 \left(\frac{l}{\lambda}\right)^2$$

from which we can write $|I_0|$ in terms of P_{rad} as

$$|I_0| = \frac{\lambda}{l} \sqrt{\frac{12P_{\text{rad}}}{\eta\pi}}$$

Substituting the value of $|I_0|$ into $|E_\theta|$

$$|E_\theta| = \eta \frac{kl}{8\pi} \frac{1}{r} \frac{\lambda}{l} \sqrt{\frac{12P_{\text{rad}}}{\eta\pi}}$$

and simplifying, we get

$$E_\theta = \frac{\sqrt{90P_{\text{rad}}}}{r} \text{ V/m}$$

EXAMPLE 3.5

A short dipole of length 0.1λ is kept symmetrically about the origin, oriented along the z-direction and radiating 1 kW power into free space. Calculate the power density at $r = 1$ km along $\theta = 45^\circ$ and $\phi = 90^\circ$.

Solution: The radiation resistance of a short dipole is

$$R_{\text{rad}} = 20\pi^2 \left(\frac{l}{\lambda}\right)^2 = 20\pi^2 0.1^2 = 1.974\ \Omega$$

From the relationship

$$P_{\text{rad}} = \frac{1}{2} I_0^2 R_{\text{rad}}$$

we get the input current as

$$I_0 = \sqrt{\frac{2 \times 1000}{1.974}} = 31.83\ \text{A}$$

Using the equation

$$S = \frac{\eta}{2} \left| \frac{kI_0 l}{8\pi} \right|^2 \frac{\sin^2 \theta}{r^2}$$

the power density at 1 km distance is calculated as

$$S = \frac{120\pi}{2} \left| \frac{2\pi \times 31.83 \times 0.1}{8\pi} \right|^2 \frac{\sin^2(\pi/4)}{1000^2} = 5.9683 \times 10^{-5}\ \text{W/m}^2$$

An alternate approach: Power density, S (in W/m^2) at (r, θ, ϕ) from the antenna with a directivity of $D_t(\theta, \phi)$ and radiated power P_{rad} (in W) is given by

$$S(r, \theta, \phi) = \frac{P_{\text{rad}}}{4\pi r^2} D_t(\theta, \phi)$$

The directivity along (θ, ϕ) is

$$D_t(\theta, \phi) = 1.5 \sin^2 \theta = 1.5 \sin^2(\pi/4) = 0.75$$

Substituting the values $P_{\text{rad}} = 1000$ W, $r = 1000$ m, and $D_t = 0.75$ into the expression for the radiated power density

$$S = \frac{1000}{4\pi \times 1000^2} 0.75 = 5.9683 \times 10^{-5}\ \text{W/m}^2$$

3.2 Half-wave Dipole

The current distribution on a thin (radius, $a \ll \lambda$) wire dipole depends on its length. For a very short dipole ($l < 0.1\lambda$) it is appropriate to assume that the current distribution is triangular. As the length of the dipole approaches a significant fraction of the wavelength, it is found that the current distribution

is closer to a sinusoidal distribution than a triangular distribution. For a centre-fed dipole of length l, symmetrically placed about the origin with its axis along the z-axis (Fig. 3.1), the current on the dipole has only a z-component and is given by

$$\begin{aligned}\mathbf{I}(z') &= \mathbf{a}_z I_z(z') \\ &= \begin{cases} \mathbf{a}_z I_0 \sin\left[k\left(\frac{l}{2} - z'\right)\right], & 0 \le z' \le l/2 \\ \mathbf{a}_z I_0 \sin\left[k\left(\frac{l}{2} + z'\right)\right], & -l/2 \le z' \le 0 \end{cases}\end{aligned} \tag{3.43}$$

where I_0 is the amplitude of the current distribution and k is a constant (equal to the free space propagation constant). The technique to compute the radiation characteristics of a dipole is very similar to that presented in the previous section for a short dipole. First, compute the magnetic vector potential in the far-field region of the antenna and then determine the **E** and **H** fields from it. Since the current has only a z-component, **A** also has only the A_z-component.

$$A_z = \frac{\mu}{4\pi}\frac{e^{-jkr}}{r}\int_{-l/2}^{l/2} I_z(z') e^{jkz'\cos\theta} dz' \tag{3.44}$$

Substituting the value of I_z from Eqn (3.43) into Eqn (3.44)

$$\begin{aligned}A_z = \frac{\mu}{4\pi} I_0 \frac{e^{-jkr}}{r}\Bigg\{&\int_{-l/2}^{0} \sin\left[k\left(\frac{l}{2} + z'\right)\right] e^{jkz'\cos\theta}\, dz' \\ &+ \int_{0}^{l/2} \sin\left[k\left(\frac{l}{2} - z'\right)\right] e^{jkz'\cos\theta} dz'\Bigg\}\end{aligned} \tag{3.45}$$

Integrating this with respect to z' and substituting appropriate limits, the vector potential expression is reduced to

$$A_z = \mu\frac{I_0}{2\pi}\frac{e^{-jkr}}{r}\frac{\left[\cos\left(\frac{kl}{2}\cos\theta\right) - \cos\left(\frac{kl}{2}\right)\right]}{k\sin^2\theta} \tag{3.46}$$

Decomposing A_z into components along the r and θ directions, we have

$$A_r = A_z\cos\theta \tag{3.47}$$

$$A_\theta = -A_z\sin\theta \tag{3.48}$$

In the far-field region of the z-oriented dipole, the component of the magnetic vector potential transverse to the direction of propagation is A_θ, and is given by

$$\mathbf{A}_t = \mathbf{a}_\theta A_\theta \tag{3.49}$$

The electric and magnetic field intensities can be computed using Eqns (3.30) and (3.31)

$$\begin{aligned}
\mathbf{E} &= -j\omega \mathbf{A}_t \\
&= -j\omega \mathbf{a}_\theta A_\theta \\
&= \mathbf{a}_\theta j\eta \frac{I_0}{2\pi} \frac{e^{-jkr}}{r} \frac{\left[\cos\left(\frac{kl}{2}\cos\theta\right) - \cos\left(\frac{kl}{2}\right)\right]}{\sin\theta}
\end{aligned} \tag{3.50}$$

$$\begin{aligned}
\mathbf{H} &= -\frac{j\omega}{\eta} \mathbf{a}_r \times \mathbf{A}_t \\
&= -\frac{j\omega}{\eta} \mathbf{a}_\phi A_\theta \\
&= \mathbf{a}_\phi j \frac{I_0}{2\pi} \frac{e^{-jkr}}{r} \frac{\left[\cos\left(\frac{kl}{2}\cos\theta\right) - \cos\left(\frac{kl}{2}\right)\right]}{\sin\theta}
\end{aligned} \tag{3.51}$$

The relationship $\eta = \omega\mu/k$ has been used in the derivation of the electric field intensity.

The radiation intensity is given by

$$U(\theta) = r^2 \frac{1}{2\eta} |E_\theta|^2 = \frac{\eta}{2} \left|\frac{I_0}{2\pi}\right|^2 \frac{\left[\cos\left(\frac{kl}{2}\cos\theta\right) - \cos\left(\frac{kl}{2}\right)\right]^2}{\sin^2\theta} \tag{3.52}$$

Figures 3.5 and 3.6 show the current distributions and the radiation patterns of thin wire dipoles of different lengths. As the dipole length increases from 0.5λ to 1.2λ, the main beam becomes narrower. The 10 dB beamwidth for a 0.5λ long dipole is 134.4°; it reduces to 85.7° for a λ long dipole and goes down to 60.2° for $l = 1.2\lambda$. As the length further increases to 1.4λ the main beam narrows to 39.6°, however, the side lobe level starts approaching 0 dB. Beyond this length, the main beam splits (Fig. 3.6) and the maximum of the pattern is no longer along $\theta = 90°$.

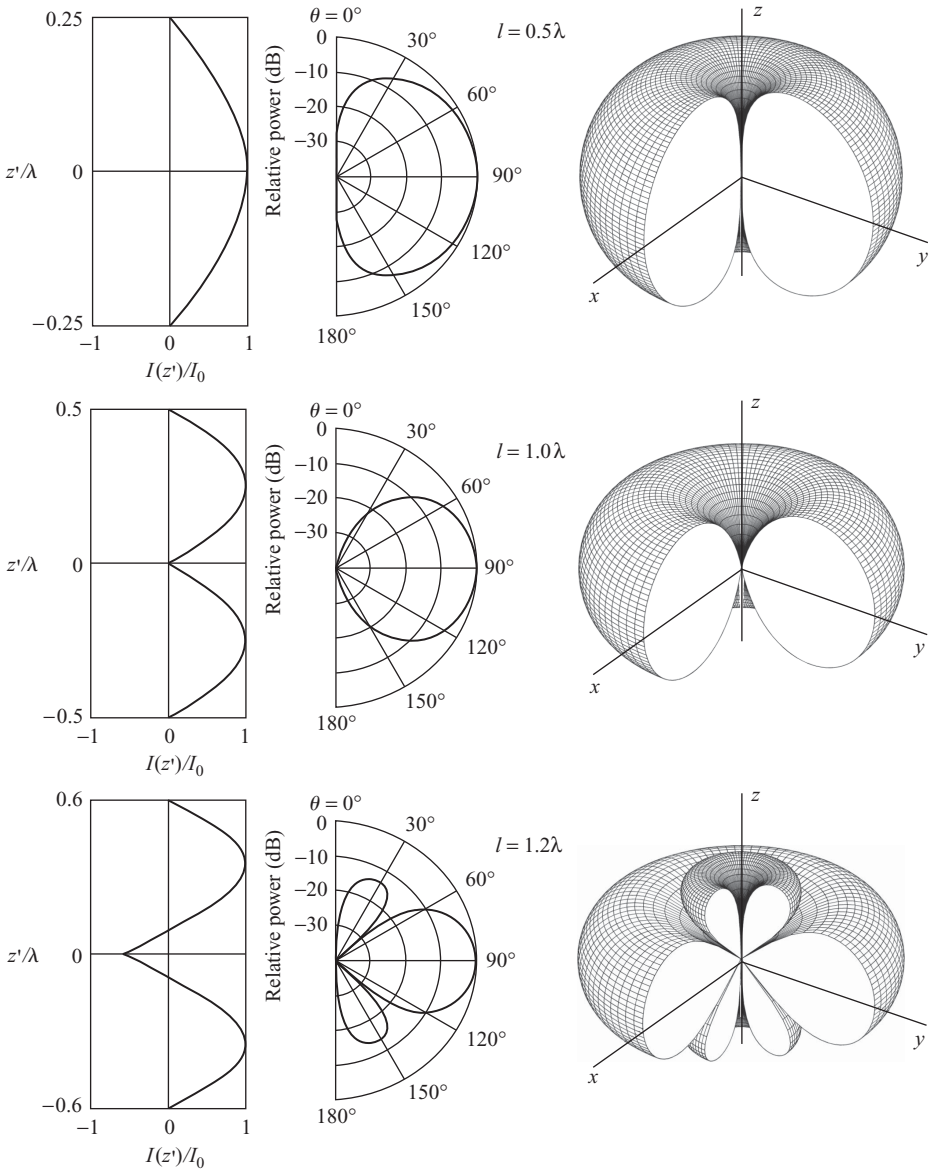

Fig. 3.5 Current distributions and radiation patterns of dipoles of different lengths ($l = 0.5\lambda, 1.0\lambda$, and 1.2λ)

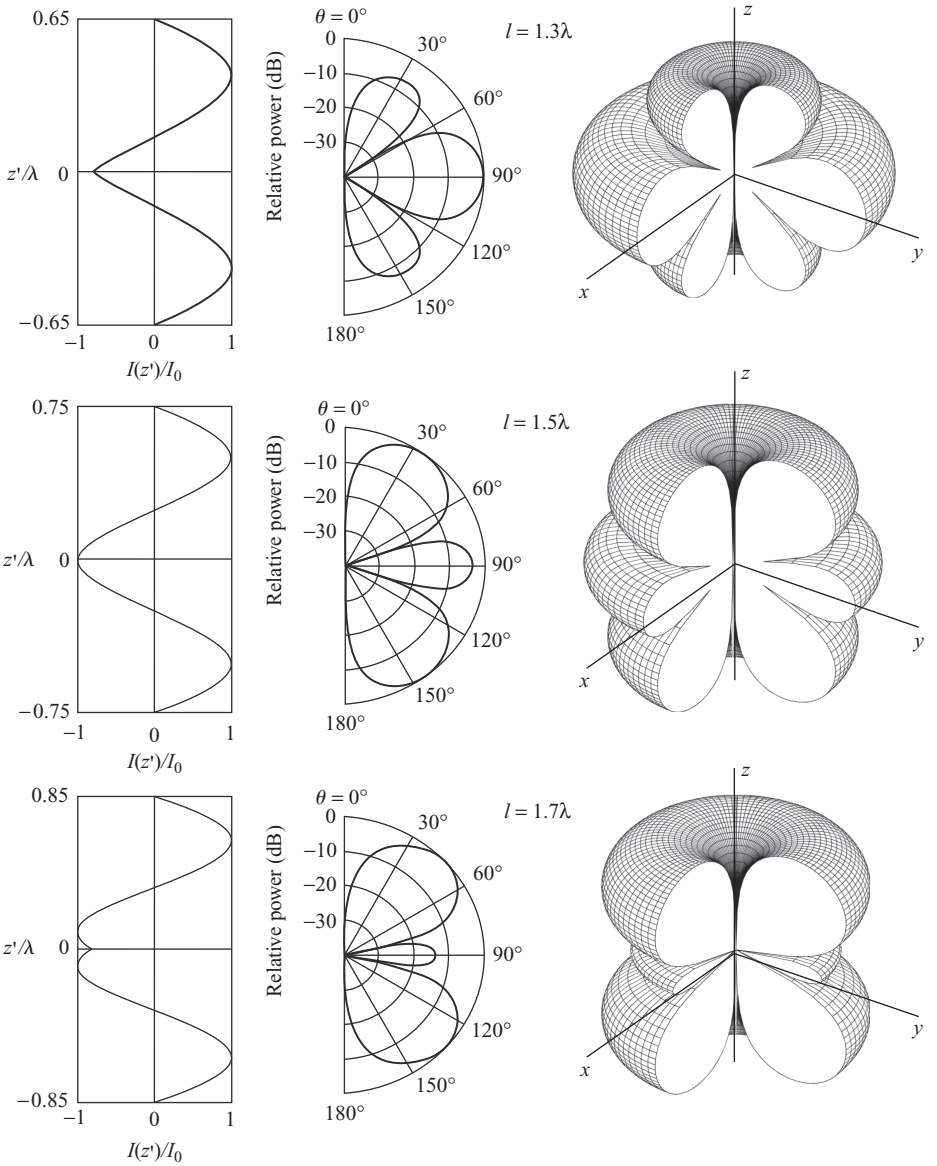

Fig. 3.6 Current distributions and radiation patterns of dipoles of different lengths ($l = 1.3\lambda, 1.5\lambda$, and 1.7λ)

EXAMPLE 3.6

Calculate the length of the dipole with a sinusoidal current distribution to obtain a 60° beamwidth between the first nulls.

Solution: The specified radiation pattern has a maximum along $\theta = \pi/2$, and the beamwidth between the first nulls is $\pi/3$. Therefore, the pattern nulls are at $\theta = \pi/2 \pm 0.5 \times \pi/3 = \pi/3$ and $2\pi/3$. Substituting $\theta = \pi/3$ in Eqn (3.50) and equating it to zero

$$\left[\cos\left\{\frac{kl}{2}\cos\left(\frac{\pi}{3}\right)\right\} - \cos\left(\frac{kl}{2}\right)\right]\frac{1}{\sin(\pi/3)} = 0$$

This can be simplified to

$$\cos\frac{kl}{4} - \cos\frac{kl}{2} = 0$$

This equation is satisfied for $kl/2 = 4\pi/3$, from which we get $l = 1.333\lambda$.

EXAMPLE 3.7

A 6 cm long z-directed dipole carries a current of 1 A at 2.4 GHz. Calculate the electric and magnetic field strengths at a distance of 50 cm along $\theta = 60°$.

Solution: The wavelength at 2.4 GHz is

$$\lambda = \frac{c}{f} = \frac{3 \times 10^8}{2.4 \times 10^9} = 0.125 \text{ m}$$

Therefore, for the given antenna

$$\frac{l}{\lambda} = \frac{6 \times 10^{-2}}{0.125} = 0.48$$

For this length we can assume a sinusoidal current distribution on the dipole. Since $r = 0.5$ m and $2l^2/\lambda = 0.0576$ m, the field point is in the far-field of the antenna. Therefore, we can use Eqn (3.50) to compute the electric field

$$E_\theta = j\eta\frac{I_0}{2\pi}\frac{e^{-jkr}}{r}\left[\cos\left(\frac{kl}{2}\cos\theta\right) - \cos\left(\frac{kl}{2}\right)\right]\frac{1}{\sin\theta}$$

$$kr = \frac{2\pi}{\lambda}r = \frac{2\pi}{0.125}0.5 = 8\pi$$

$$\frac{kl}{2} = \frac{2\pi}{2\lambda}l = \frac{\pi}{0.125}0.06 = 0.48\pi$$

Substituting in Eqn (3.50)

$$E_\theta = j120\pi\frac{1}{2\pi}\frac{e^{-j8\pi}}{0.5}\left[\cos\left(0.48\pi\cos\left(\frac{\pi}{3}\right)\right) - \cos(0.48\pi)\right]\frac{1}{\sin(\pi/3)}$$

On simplifying

$$E_\theta = j92.3e^{-j8\pi} = j92.3 \text{ V/m}$$

The magnetic field in the far-field region is related to the electric field by the following relation

$$\mathbf{H} = \frac{1}{\eta}\mathbf{a}_r \times \mathbf{E} = \mathbf{a}_\phi \frac{1}{\eta} E_\theta$$

Therefore

$$H_\phi = \frac{E_\theta}{\eta} = j\frac{92.3}{120\pi} = j0.2448 \text{ A/m}$$

The computation of the directivity of a dipole of arbitrary length involves integration of Eqn (3.52) over the entire sphere. The analytical computation of the integral is reasonably complicated. Interested readers can refer to Balanis 2002. In this section, we compute the directivity of a half-wave dipole for which the integrand can be simplified. The electric and magnetic field intensities for a half-wave dipole are obtained by substituting $kl/2 = \pi/2$ into Eqns (3.51) and (3.50)

$$H_\phi = j\frac{I_0}{2\pi}\frac{e^{-jkr}}{r}\frac{\cos\left(\frac{\pi}{2}\cos\theta\right)}{\sin\theta} \tag{3.53}$$

$$E_\theta = j\eta\frac{I_0}{2\pi}\frac{e^{-jkr}}{r}\frac{\cos\left(\frac{\pi}{2}\cos\theta\right)}{\sin\theta} \tag{3.54}$$

Using these field expressions the average radiated power density reduces to

$$S(\theta,\phi) = \frac{1}{2\eta}|E_\theta|^2 = \frac{\eta}{2}\left|\frac{I_0}{2\pi}\right|^2 \frac{1}{r^2}\frac{\cos^2\left(\frac{\pi}{2}\cos\theta\right)}{\sin^2\theta} \tag{3.55}$$

The total radiated power is obtained by integrating the power density over the entire sphere of radius r. Integrating Eqn (3.55) over the sphere

$$P_{\text{rad}} = \int_{\phi=0}^{2\pi}\int_{\theta=0}^{\pi} S(\theta,\phi)r^2\sin\theta d\theta d\phi \tag{3.56}$$

$$= \int_{\phi=0}^{2\pi}\int_{\theta=0}^{\pi} \frac{\eta}{2}\left|\frac{I_0}{2\pi}\right|^2 \frac{\cos^2\left(\frac{\pi}{2}\cos\theta\right)}{\sin^2\theta}\sin\theta d\theta d\phi \tag{3.57}$$

$$= 2\pi\frac{\eta}{2}\left|\frac{I_0}{2\pi}\right|^2 \int_{\theta=0}^{\pi} \frac{\cos^2\left(\frac{\pi}{2}\cos\theta\right)}{\sin^2\theta}\sin\theta d\theta \tag{3.58}$$

where, the factor 2π is obtained by integrating over ϕ. On performing the integration over θ (see example 3.4) we get

$$P_{\text{rad}} = \eta\pi\left|\frac{I_0}{2\pi}\right|^2 1.2179 = 36.54\left|I_0^2\right| \tag{3.59}$$

The radiation resistance is computed by equating the average radiated power to the power dissipated in an equivalent resistance carrying the same input current

$$P_{\text{rad}} = 36.54\left|I_0^2\right| = \frac{1}{2}\left|I_0^2\right| R_{\text{rad}} \tag{3.60}$$

Thus, we obtain the radiation resistance for a half-wave dipole as

$$R_{\text{rad}} = 73.08\ \Omega \tag{3.61}$$

Using Eqn (3.55), the radiation intensity can be written as

$$U(\theta,\phi) = r^2 S(\theta,\phi) = \frac{\eta}{2}\left|\frac{I_0}{2\pi}\right|^2 \frac{\cos^2\left(\frac{\pi}{2}\cos\theta\right)}{\sin^2\theta} \tag{3.62}$$

Substituting Eqn (3.62) and Eqn (3.59) into Eqn (3.40), the directivity is

$$\begin{aligned} D(\theta,\phi) &= 4\pi\frac{U(\theta,\phi)}{P_{\text{rad}}} = 4\pi\frac{\eta}{2}\left|\frac{I_0}{2\pi}\right|^2 \frac{\cos^2\left(\frac{\pi}{2}\cos\theta\right)}{\sin^2\theta}\frac{1}{\left|I_0^2\right| 36.54} \\ &= 1.642\frac{\cos^2\left(\frac{\pi}{2}\cos\theta\right)}{\sin^2\theta} \end{aligned} \tag{3.63}$$

The maximum value of the directivity occurs along $\theta = \pi/2$, and is equal to 1.642. Directivity expressed in decibels is

$$D_{\text{dB}} = 10\log_{10}(1.642) = 2.15\ \text{dB} \tag{3.64}$$

EXAMPLE 3.8

Show that

$$\int_{\theta=0}^{\pi} \frac{\cos^2\left(\frac{\pi}{2}\cos\theta\right)}{\sin\theta} d\theta = 1.2179$$

Solution: Let

$$I = \int_{\theta=0}^{\pi} \frac{\cos^2\left(\frac{\pi}{2}\cos\theta\right)}{\sin\theta} d\theta$$
$$= \frac{1}{2}\int_{\theta=0}^{\pi} \frac{1+\cos(\pi\cos\theta)}{\sin\theta} d\theta$$

Substituting $u = \cos\theta$ and $du = -\sin\theta d\theta$, and interchanging the limits of integration

$$I = \frac{1}{2}\int_{-1}^{1} \frac{1+\cos(\pi u)}{1-u^2} du$$

Using the relation

$$\frac{1}{1-u^2} = \frac{1}{2}\left(\frac{1}{1+u} + \frac{1}{1-u}\right)$$

we can write

$$I = \frac{1}{4}\left(\int_{-1}^{1} \frac{1+\cos(\pi u)}{1-u} du + \int_{-1}^{1} \frac{1+\cos(\pi u)}{1+u} du\right)$$

Substituting $u = -t$ in the first integral and interchanging the limits

$$\int_{-1}^{1} \frac{1+\cos(\pi u)}{1-u} du = \int_{-1}^{1} \frac{1+\cos(\pi t)}{1+t} dt$$

Therefore, we can now write

$$I = \frac{1}{2}\int_{-1}^{1} \frac{1+\cos(\pi u)}{1+u} du$$

We make another substitution, $\pi u = y - \pi$, to get

$$I = \frac{1}{2}\int_{0}^{2\pi} \frac{1-\cos y}{y} dy$$

The relation $\cos(y-\pi) = -\cos y$ has been used to arrive at the above expression. The Taylor series expansion of $\cos y$ is

$$\cos y = 1 - \frac{y^2}{2!} + \frac{y^4}{4!} - \frac{y^6}{6!} + \cdots$$

This can be used to rewrite the integral as

$$I = \frac{1}{2}\int_0^{2\pi}\left(\frac{y}{2!} - \frac{y^3}{4!} + \frac{y^5}{6!} - \frac{y^7}{8!} + \cdots\right)dy$$

On performing termwise integration and substituting the limits, we get

$$I = \frac{1}{2}(9.8696 - 16.235 + 14.2428 - 7.5306 + 2.6426 - 0.6586 + 0.1225 - 0.01763 + \cdots) = 1.2179$$

3.3 Monopole

Dipole antennas for HF and VHF applications tend to be several metres long. Constructing a dipole to radiate vertically polarized (electric field orientation is perpendicular to the surface of the earth) electromagnetic waves poses some real challenges due to the size of the antenna and the presence of the earth itself. From the image theory (see Section 4.2.4), we know that the fields due to a vertical electric current element kept above an infinitely large perfect electrical conductor (also known as the ground plane) are the same as the fields radiated by the element and its image (without the ground plane). Therefore, it is possible to virtually create a half-wave dipole by placing a quarter wavelength long wire (called a monopole) vertically above an infinitely large ground plane.

Consider a monopole of length $l/2$, fed at its base and kept above the ground plane as shown in Fig. 3.7. By image theory, this structure is equivalent to a dipole of length l radiating into free space. Therefore, the electric and magnetic fields in the far-field region are given by Eqns (3.51) and (3.50). If the monopole is quarter wavelength long, the field expressions reduce to

$$H_\phi = j\frac{I_0}{2\pi}\frac{e^{-jkr}}{r}\frac{\cos\left(\frac{\pi}{2}\cos\theta\right)}{\sin\theta} \tag{3.65}$$

$$E_\theta = j\eta\frac{I_0}{2\pi}\frac{e^{-jkr}}{r}\frac{\cos\left(\frac{\pi}{2}\cos\theta\right)}{\sin\theta} \tag{3.66}$$

The original problem has an infinitely large ground plane and there are no fields below the ground plane. Therefore, Eqns (3.65) and (3.66) are to be evaluated only in the upper hemisphere, i.e., for $0 \le \theta \le \pi/2$ and for $0 \le \phi \le 2\pi$. The total radiated power is obtained by integrating the

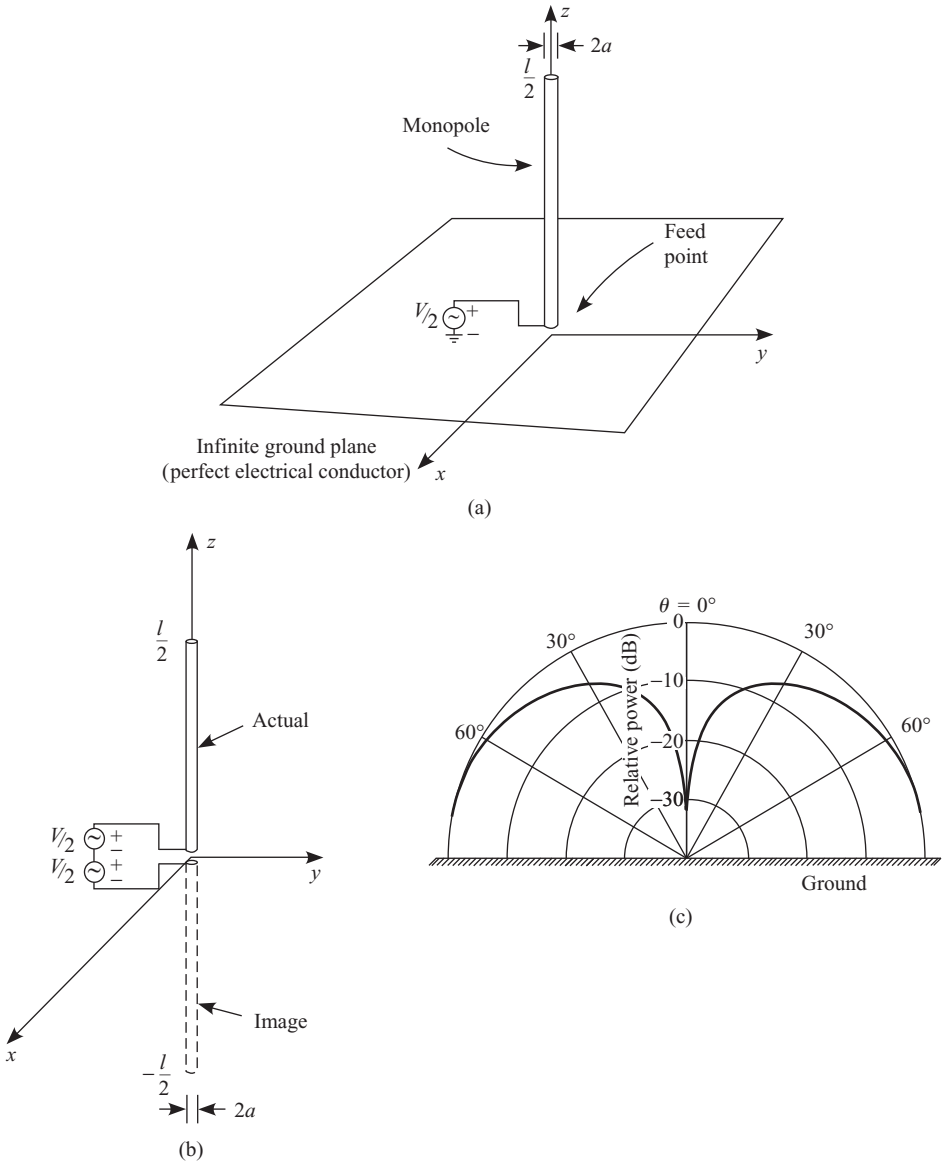

Fig. 3.7 (a) Geometry of a monopole above an infinite perfect electrical conductor, (b) its dipole equivalent, and (c) the radiation pattern for $l = \lambda/2$

radiation intensity over the upper hemisphere

$$P_{\text{rad}} = \int_{\phi=0}^{2\pi} \int_{\theta=0}^{\pi/2} U(\theta, \phi) \sin\theta d\theta d\phi \tag{3.67}$$

$$= \int_{\phi=0}^{2\pi} \int_{\theta=0}^{\pi/2} \frac{\eta}{2} \left| \frac{I_0}{2\pi} \right|^2 \frac{\cos^2\left(\frac{\pi}{2}\cos\theta\right)}{\sin^2\theta} \sin\theta d\theta d\phi \tag{3.68}$$

$$= 2\pi\frac{\eta}{2}\left|\frac{I_0}{2\pi}\right|^2 \int_{\theta=0}^{\pi/2} \frac{\cos^2\left(\frac{\pi}{2}\cos\theta\right)}{\sin^2\theta}\sin\theta d\theta \tag{3.69}$$

On performing the integration over θ, the total radiated power is

$$P_{\text{rad}} = \frac{1}{2}|I_0|^2\, 36.54 \tag{3.70}$$

Equating this to the power dissipated in an equivalent resistor the radiation resistance of a monopole is

$$R_{\text{rad}} = 36.54\ \Omega \tag{3.71}$$

The radiation resistance of a quarter wavelength long monopole place above a ground plane is half that of a half-wave dipole radiating in free space.

The radiation intensity has a maximum value along $\theta = \pi/2$, and is given by

$$U_{\max} = \frac{\eta}{2}\left|\frac{I_0}{2\pi}\right|^2 \tag{3.72}$$

The maximum directivity is calculated by dividing $U_{\max}$ by the average radiation intensity

$$D = 4\pi\frac{U_{\max}}{P_{\text{rad}}} = 3.284 \tag{3.73}$$

Thus, the directivity of a quarter wave monopole above a ground plane is equal to twice that of a half-wave dipole radiating in free space. The maximum directivity occurs along the ground plane and the radiation is vertically polarized.

3.4 Small Loop Antenna

Let us now study another type of antenna called a loop antenna constructed using thin wires. The loop antenna can take different shapes such as a circle, a square, a triangle, etc. The radiation characteristics of a loop antenna depend on the size and shape of the antenna. The circular loop antenna is one of the easiest to construct as well as to analyse.

Consider a single turn circular loop antenna of radius a, symmetrically placed about the origin on the x-y plane, carrying a current $\mathbf{I}_e(x', y', z')$ as shown in Fig. 3.8. The wire diameter is assumed to be very small and, hence, we assume the current $\mathbf{I}_e(x', y', z')$ to be along the wire. The magnetic vector

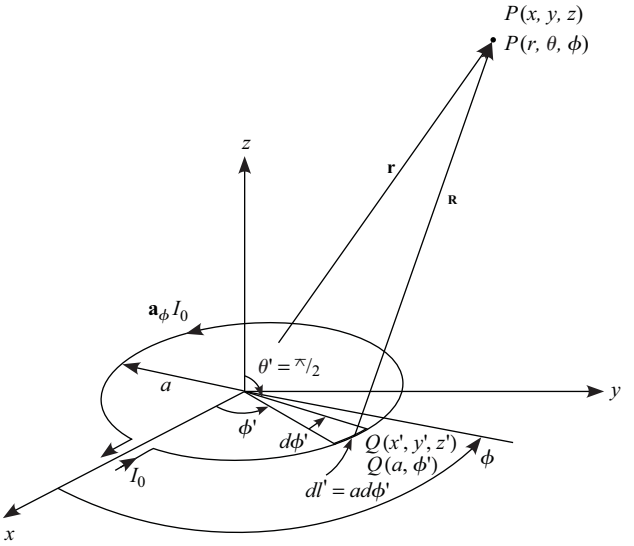

Fig. 3.8 Geometry of a small loop antenna

potential is an integral over the current distribution given by

$$\mathbf{A} = \frac{\mu}{4\pi}\int_c \mathbf{I}_e(x', y', z')\frac{e^{-jkR}}{R}dl' \tag{3.74}$$

where the path of integration is along the loop. The distance, R, from the source point (x', y', z') to the field point (x, y, z), is given by

$$R = \sqrt{(x - x')^2 + (y - y')^2 + (z - z')^2} \tag{3.75}$$

Because of the circular shape of the curve, it is convenient to represent the source point in cylindrical coordinates and, as usual, we use spherical coordinates for the field point. To convert the field point (x, y, z) to (r, θ, ϕ) coordinates, we use the transformation equations

$$x = r\sin\theta\cos\phi \tag{3.76}$$

$$y = r\sin\theta\sin\phi \tag{3.77}$$

$$z = r\cos\theta \tag{3.78}$$

which when substituted into Eqn (3.75) yield

$$R = \sqrt{(r^2 - 2r(x'\sin\theta\cos\phi + y'\sin\theta\sin\phi + z'\cos\theta) + x'^2 + y'^2 + z'^2)} \tag{3.79}$$

If the observation point is far away from the antenna, we may expand the above expression using the binomial series and neglect the terms involving

$1/r$ and its higher powers. With this simplification, R is approximated as

$$R \simeq r - (x' \sin\theta \cos\phi + y' \sin\theta \sin\phi + z' \cos\theta) \tag{3.80}$$

To convert the source point coordinates (x', y', z') to cylindrical coordinates, we can use the transformation equations

$$x' = a \cos\phi' \tag{3.81}$$

$$y' = a \sin\phi' \tag{3.82}$$

$$z' = 0 \tag{3.83}$$

Substituting the above into Eqn (3.80) and simplifying we get the approximate expression for R as

$$R \simeq r - a \sin\theta \cos(\phi - \phi') \tag{3.84}$$

This approximate expression for R is used in the phase term of the vector potential. For the amplitude, the R in the denominator of Eqn (3.74) is replaced by r. The elemental length dl' along the loop in cylindrical coordinates is given by

$$dl' = a d\phi' \tag{3.85}$$

For a loop with a circumference which is small compared to the wavelength, we can assume the current to be constant over the loop and, hence, the current element, $\mathbf{I}_e dl' = \mathbf{a}_\phi I_0 a d\phi'$, can be expressed in rectangular coordinates as

$$\mathbf{I}_e dl' = (-\mathbf{a}_x I_0 \sin\phi' + \mathbf{a}_y I_0 \cos\phi') a d\phi' \tag{3.86}$$

where I_0 is the amplitude of the current.

Substituting this expression for the current and the far-field approximation for R in the vector potential equation [Eqn (3.74)], we get

$$\mathbf{A} = \frac{\mu}{4\pi} I_0 \frac{e^{-jkr}}{r} \int_C \left(-\mathbf{a}_x \sin\phi' + \mathbf{a}_y \cos\phi'\right) e^{jka \sin\theta \cos(\phi - \phi')} a d\phi' \tag{3.87}$$

Now, to convert this expression into spherical coordinates, the unit vectors $\mathbf{a}_x$ and $\mathbf{a}_y$ are written in terms of spherical coordinates. In spherical coordinates the unit vectors $\mathbf{a}_x$ and $\mathbf{a}_y$ are given by

$$\mathbf{a}_x = \mathbf{a}_r \sin\theta \cos\phi + \mathbf{a}_\theta \cos\theta \cos\phi - \mathbf{a}_\phi \sin\phi \tag{3.88}$$

$$\mathbf{a}_y = \mathbf{a}_r \sin\theta \sin\phi + \mathbf{a}_\theta \cos\theta \sin\phi + \mathbf{a}_\phi \cos\phi \tag{3.89}$$

Substituting these into Eqn (3.87) and simplifying we get three individual components of the vector potential in the spherical coordinate system as

$$A_r = \frac{\mu}{4\pi} I_0 \frac{e^{-jkr}}{r} \sin\theta \int_{\phi'=0}^{2\pi} \sin(\phi - \phi') e^{jka\sin\theta\cos(\phi-\phi')} a d\phi' \quad (3.90)$$

$$A_\theta = \frac{\mu}{4\pi} I_0 \frac{e^{-jkr}}{r} \cos\theta \int_{\phi'=0}^{2\pi} \sin(\phi - \phi') e^{jka\sin\theta\cos(\phi-\phi')} a d\phi' \quad (3.91)$$

$$A_\phi = \frac{\mu}{4\pi} I_0 \frac{e^{-jkr}}{r} \int_{\phi'=0}^{2\pi} \cos(\phi - \phi') e^{jka\sin\theta\cos(\phi-\phi')} a d\phi' \quad (3.92)$$

Since the current is ϕ-symmetric, the vector potential is also ϕ-symmetric. Therefore, it is sufficient to evaluate the above integrals at any one value of ϕ. Without loss of generality, we choose $\phi = 0$.

Let us first consider the evaluation of A_ϕ. Splitting the limits of integration into two parts

$$A_\phi = \frac{\mu}{4\pi} I_0 a \frac{e^{-jkr}}{r} \left\{ \int_{\phi'=0}^{\pi} \cos(\phi') e^{jka\sin\theta\cos\phi'} d\phi' + \int_{\phi'=\pi}^{2\pi} \cos(\phi') e^{jka\sin\theta\cos\phi'} d\phi' \right\} \quad (3.93)$$

Substituting $\phi' = \phi'' + \pi$ in the second integral and using the expansion $e^{j\phi} = \cos\phi + j\sin\phi$, A_ϕ can be simplified to

$$A_\phi = \frac{\mu}{4\pi} I_0 a \frac{e^{-jkr}}{r} 2j \int_{\phi'=0}^{\pi} \cos(\phi') \sin(ka\sin\theta\cos\phi') d\phi' \quad (3.94)$$

Since the circumference of the loop is small compared to the wavelength, $ka \ll 1$ and we can further approximate $\sin(ka\sin\theta\cos\phi') \simeq ka\sin\theta\cos\phi'$. Thus we have

$$A_\phi \simeq \frac{\mu}{4} I_0 jka^2 \sin\theta \frac{e^{-jkr}}{r} \quad (3.95)$$

Using the even and odd properties of the integrands in Eqns 3.90 and 3.91, we can show that $A_r = 0$ and $A_\theta = 0$ (see Example 3.9). Since the vector potential $\mathbf{A}$ has only the $\mathbf{a}_\phi$ component, in the far-field region the $\mathbf{E}$ and $\mathbf{H}$ fields computed using the relationships given by Eqns (3.30) and (3.31) result in E_ϕ and H_θ components alone. These are given by

$$E_\phi = \eta \frac{a^2k^2}{4} I_0 \frac{e^{-jkr}}{r} \sin\theta \quad (3.96)$$

$$H_\theta = -\frac{a^2k^2}{4} I_0 \frac{e^{-jkr}}{r} \sin\theta \quad (3.97)$$

The radiation pattern has a null along the axis of the loop ($\theta = 0^\circ$) and the maximum is in the $\theta = 90^\circ$ plane. The fields have the same power pattern as that of a Hertzian dipole (see Fig. 2.3).

EXAMPLE 3.9

Show that A_r given by Eqn (3.90) is equal to zero.

Solution: Since the current is ϕ independent, we can evaluate the integral in Eqn (3.90) at $\phi = 0$. The integral is given by

$$I = \int_{\phi'=0}^{2\pi} \sin(-\phi') e^{jka\sin\theta\cos(-\phi')} d\phi'$$

Substituting $\phi' = \psi - \pi$

$$I = \int_{\psi=-\pi}^{\pi} \sin(\pi - \psi) e^{jka\sin\theta\cos(\pi-\psi)} d\psi$$

and simplifying the integrand

$$I = \int_{\psi=-\pi}^{\pi} \sin(\psi) e^{-jka\sin\theta\cos(\psi)} d\psi$$

Expanding the exponential term using Euler's formula (Kreyszig 1999)

$$I = \int_{\psi=-\pi}^{\pi} \sin(\psi)\cos[ka\sin\theta\cos(\psi)]d\psi - j\int_{\psi=-\pi}^{\pi} \sin(\psi)\sin[ka\sin\theta\cos(\psi)]d\psi$$

$\cos\psi$ is an even function of ψ and, therefore, $\cos(ka\sin\theta\cos\psi)$ is also an even function of ψ. Since $\sin\psi$ is an odd function, the integrand in the first integral is an odd function of ψ. Similarly, $\sin(ka\sin\theta\cos\phi)$ is also an even function. Therefore, the integrand of the second integral is also an odd function of ψ. Using the property of definite integrals

$$\int_{-a}^{a} f(x)dx = 0 \qquad \text{if } f(x) \text{ is an odd function of } x$$

we get

$$I = 0$$

which implies that $A_r = 0$.

Using the procedure outlined in Section 3.1 we can now compute the radiation characteristics of a small loop antenna. For the sake of continuity, we may repeat some of the steps in this section. First, let us compute the time-averaged power density given by

$$\mathbf{S} = \frac{1}{2}\text{Re}(\mathbf{E} \times \mathbf{H}^*) = \frac{1}{2\eta}\mathbf{a}_r|\text{E}_\phi|^2 \tag{3.98}$$

Substituting the value of E_ϕ from Eqn (3.96), this reduces to

$$\mathbf{S} = \mathbf{a}_r S = \mathbf{a}_r \frac{\eta}{2}\left(\frac{a^2k^2|I_0|}{4r}\right)^2 \sin^2\theta \tag{3.99}$$

Thus, the radiation intensity is

$$U(\theta,\phi) = r^2S = \frac{\eta}{2}\left(\frac{a^2k^2|I_0|}{4}\right)^2 \sin^2\theta \text{ W/sr} \tag{3.100}$$

The total radiated power, P_{rad} is obtained by integrating the radiation intensity over 4π solid angle of the sphere

$$P_{\text{rad}} = \int_{\phi=0}^{2\pi}\int_{\theta=0}^{\pi} U(\theta,\phi)\sin\theta d\theta d\phi \tag{3.101}$$

Substituting the value of U from Eqn (3.100) and performing the integration (see Example 3.10), we obtain

$$P_{\text{rad}} = 10\pi^2a^4k^4|I_0|^2 \text{ W} \tag{3.102}$$

Equating this power to the power dissipated in an equivalent resistance carrying the same current

$$10\pi^2a^4k^4|I_0|^2 = \frac{1}{2}|I_0|^2R_{\text{rad}} \tag{3.103}$$

we get the radiation resistance of a loop antenna as

$$R_{\text{rad}} = 20\pi^2k^4a^4 \tag{3.104}$$

Let $L_A = \pi a^2$ be the area of the loop and $L_C = 2\pi a$ be the circumference of the loop. We can show that the radiation resistance can be written as

$$R_{\text{rad}} = 20\pi^2\left(\frac{L_C}{\lambda}\right)^4 = 31171\frac{L_A^2}{\lambda^4} = 320\pi^6\left(\frac{a}{\lambda}\right)^4 \tag{3.105}$$

The radiation resistance of a small loop is generally very small and is difficult to match to the source. The radiation resistance can be increased by having more turns in the loop. For example, the radiation resistance of a single turn loop of radius 0.05λ is 1.92 Ω. If the loop is made of N turns and is carrying the same input current, I_0, the loop current would be NI_0. Hence the field strength of the multi-turn loop would be N times that of a single turn loop. Replacing I_0 by NI_0 in the left hand side of Eqn (3.103), while keeping the same I_0 on the right hand side, we get R_{rad}, N^2 times that of a single turn loop

$$R_{\text{rad}} = 20\pi^2 N^2 \left(\frac{L_C}{\lambda}\right)^4 = 31171 N^2 \frac{L_A^2}{\lambda^4} = 320\pi^6 N^2 \left(\frac{a}{\lambda}\right)^4 \tag{3.106}$$

If the antenna considered in Example above has 10 turns, the radiation resistance becomes 192 Ω. If the loss resistance of a single turn loop is R_{loss}, for an N-turn loop the loss resistance increases only by a factor of N. Therefore, the multi-turn loop has a higher radiation efficiency compared to a single turn loop.

EXAMPLE 3.10

Prove the relation given by Eqn (3.102).

Solution: Substituting the expression for U from Eqn (3.100) into Eqn (3.101)

$$P_{\text{rad}} = \int_{\phi=0}^{2\pi} \int_{\theta=0}^{\pi} \frac{\eta}{2} \left(\frac{a^2 k^2 |I_0|}{4}\right)^2 \sin^2\theta \ \sin\theta d\theta d\phi$$

Integrating over ϕ

$$P_{\text{rad}} = 2\pi \frac{\eta}{2} \left(\frac{a^2 k^2 |I_0|}{4}\right)^2 \int_{\theta=0}^{\pi} \sin^3\theta d\theta$$

$$P_{\text{rad}} = 2\pi \frac{\eta}{2} \left(\frac{a^2 k^2 |I_0|}{4}\right)^2 \int_{\theta=0}^{\pi} \frac{1}{4}(3\sin\theta - \sin 3\theta) d\theta$$

$$P_{\text{rad}} = 2\pi \frac{\eta}{2} \left(\frac{a^2 k^2 |I_0|}{4}\right)^2 \frac{1}{4} \left[-3\cos\theta + \frac{1}{3}\cos 3\theta\right]_0^{\pi}$$

Substituting the limits and simplifying

$$P_{\text{rad}} = 2\pi \frac{120\pi}{2} \frac{a^4 k^4 |I_0|^2}{16} \frac{1}{4} \frac{16}{3} = 10\pi^2 a^4 k^4 |I_0|^2$$

EXAMPLE 3.11

What is the total power radiated by a small circular loop of radius 0.5 m carrying a current of 10 A at 15 MHz? If the loop is symmetrically placed at the origin and in the x-y plane, calculate the magnitude of the electric field intensity in the x-y plane at a distance of 10 km.

Solution: The wavelength of the 15 MHz electromagnetic wave propagating in free space is

$$\lambda = \frac{c}{f} = \frac{3 \times 10^8}{15 \times 10^6} = 20 \text{ m}$$

The propagation constant is

$$k = \frac{2\pi}{\lambda} = \frac{2\pi}{20} \text{ rad/m}$$

Substituting $a = 0.5$ m, $I_0 = 10$ A, and $k = \pi/10$ rad/m into Eqn (3.102)

$$P_{\text{rad}} = 10\pi^2 a^4 k^4 |I_0|^2 = 10\pi^2 0.5^4 \left(\frac{\pi}{10}\right)^4 |10|^2 = 6.01 \text{ W}$$

From Eqn (3.96)

$$\begin{aligned} |E_\phi|_{\theta=90^\circ} &= \frac{\eta a^2 k^2 I_0}{4r} \\ &= \frac{376.73 \times 0.5^2 \times \left(\frac{\pi}{10}\right)^2 \times 10}{4 \times 10 \times 10^3} \\ &= 2.32 \text{ mV/m} \end{aligned}$$

EXAMPLE 3.12

A large circular loop having a circumference of 1λ is placed in the x-y plane symmetrically about the origin. Derive an expression for the electric field of the wave radiated along the z-direction. Show that the wave is circularly polarized if the current on the loop is a travelling wave given by

$$I = I_0 e^{j(\omega t - ka\phi')}$$

where ω is the angular frequency, k is the propagation constant of the current and is equal to the propagation constant in free space, a is the radius of the loop, and ϕ' is the angle measured from the x-axis.

Solution: For a loop of circumference λ, $[a = \lambda/(2\pi)]$

$$ka = \frac{2\pi}{\lambda}\frac{\lambda}{2\pi} = 1$$

Therefore, the current in the loop reduces to

$$I = I_0 e^{-j\phi'} e^{j\omega t}$$

The current phasor can be represented as a vector in the Cartesian coordinate system [see Eqn (3.86)]

$$\mathbf{I}_e = -\mathbf{a}_x I \sin\phi' + \mathbf{a}_y I \cos\phi'$$

Expressing $\mathbf{a}_x$ and $\mathbf{a}_y$ in spherical coordinates and simplifying

$$\mathbf{I}_e = I_0 e^{-j\phi'} [\mathbf{a}_r \sin\theta \sin(\phi - \phi') + \mathbf{a}_\theta \cos\theta \sin(\phi - \phi') + \mathbf{a}_\phi \cos(\phi - \phi')]$$

In the far-field region only the transverse components of $\mathbf{E}$ and $\mathbf{H}$ exist, therefore, it is sufficient to compute A_θ and A_ϕ components of the vector potential [see Eqns (3.30) and (3.31)]. Substituting the expression for the current distribution, $ka = 1$, and the far-field approximations to R into Eqn (3.74) for the vector potential, we can write the transverse components of $\mathbf{A}$ as

$$A_\theta = \frac{\mu}{4\pi} I_0 \frac{e^{-jkr}}{r} \cos\theta \int_{\phi'=0}^{2\pi} \sin(\phi - \phi') e^{j \sin\theta \cos(\phi - \phi')} e^{-j\phi'} a d\phi'$$

$$A_\phi = \frac{\mu}{4\pi} I_0 \frac{e^{-jkr}}{r} \int_{\phi'=0}^{2\pi} \cos(\phi - \phi') e^{j \sin\theta \cos(\phi - \phi')} e^{-j\phi'} a d\phi'$$

For the fields along the z-axis we can further simplify these expressions by substituting $\theta = 0$.

$$A_\theta = \frac{\mu}{4\pi} I_0 \frac{e^{-jkr}}{r} \int_{\phi'=0}^{2\pi} \sin(\phi - \phi') e^{-j\phi'} a d\phi'$$

$$A_\phi = \frac{\mu}{4\pi} I_0 \frac{e^{-jkr}}{r} \int_{\phi'=0}^{2\pi} \cos(\phi - \phi') e^{-j\phi'} a d\phi'$$

Substituting $(\phi' - \phi) = t$, we have $d\phi' = dt$ and the limits of integration $-\phi$ to $2\pi - \phi$. Hence we can write

$$A_\theta = -\frac{\mu}{4\pi} I_0 a \frac{e^{-jkr}}{r} e^{-j\phi} \int_{t=-\phi}^{2\pi-\phi} \sin(t) e^{-jt} dt$$

$$A_\phi = \frac{\mu}{4\pi} I_0 a \frac{e^{-jkr}}{r} e^{-j\phi} \int_{t=-\phi}^{2\pi-\phi} \cos(t) e^{-jt} dt$$

Consider the integral

$$X = \int_{t=-\phi}^{2\pi-\phi} \sin(t) e^{-jt} dt$$

Using the identity

$$\sin t = \frac{e^{jt} - e^{-jt}}{2j}$$

the above integral can be written as

$$X = \frac{1}{2j} \int_{t=-\phi}^{2\pi-\phi} [e^{jt} - e^{-jt}] e^{-jt} dt = \frac{1}{2j} \int_{t=-\phi}^{2\pi-\phi} [1 - e^{-j2t}] dt$$

Performing the indicated integration, substituting the limits and simplifying

$$X = \frac{1}{2j} \left[t + \frac{e^{-j2t}}{2j} \right]_{t=-\phi}^{2\pi-\phi} = -j\pi$$

Similarly, we can show that

$$Y = \int_{t=-\phi}^{2\pi-\phi} \cos(t) e^{-jt} dt = \pi$$

Therefore, the components of the vector potential reduce to

$$A_\theta = -\frac{\mu}{4\pi} I_0 a \frac{e^{-jkr}}{r} e^{-j\phi} (-j\pi)$$

$$A_\phi = \frac{\mu}{4\pi} I_0 a \frac{e^{-jkr}}{r} e^{-j\phi} \pi$$

In the far-field region the electric field vectors can be computed from the magnetic vector potential using Eqn (3.30)

$$\mathbf{E} = -j\omega \mathbf{A}_t = -j\omega (\mathbf{a}_\theta A_\theta + \mathbf{a}_\phi A_\phi)$$

and the components of the electric field are given by

$$E_\theta = -j\omega A_\theta = \frac{\omega\mu}{4} I_0 a \frac{e^{-jkr}}{r} e^{-j\phi}$$

$$E_\phi = -j\omega A_\phi = -j \frac{\omega\mu}{4} I_0 a \frac{e^{-jkr}}{r} e^{-j\phi}$$

Therefore, the electric field can be written as

$$\mathbf{E} = \frac{\omega\mu}{4} I_0 a \frac{e^{-jkr}}{r} e^{-j\phi} (\mathbf{a}_\theta - j\mathbf{a}_\phi)$$

This represents a right circularly polarized wave.

Exercises

3.1 Let $A_r(r,\theta,\phi)$, $A_\theta(r,\theta,\phi)$, and A_ϕ (r,θ,ϕ) be the components of a magnetic vector potential, $\mathbf{A}$. In the far-field region these can be expressed as

$$A_r(r,\theta,\phi) = A_{r0}(\theta,\phi)e^{-jkr}/r$$
$$A_\theta(r,\theta,\phi) = A_{\theta 0}(\theta,\phi)e^{-jkr}/r$$
$$A_\phi(r,\theta,\phi) = A_{\phi 0}(\theta,\phi)e^{-jkr}/r$$

where $A_{r0}(\theta,\phi)$, $A_{\theta 0}(\theta,\phi)$, and $A_{\phi 0}(\theta,\phi)$ are independent of r. Substituting this into $\mathbf{B} = \nabla \times \mathbf{A}$ and taking only the radiated field components show that

$$\mathbf{H} = j\frac{k}{\mu}[\mathbf{a}_\theta A_\phi(r,\theta,\phi) - \mathbf{a}_\phi A_\theta(r,\theta,\phi)]$$

Further, show that this can be expressed as

$$\mathbf{H} = -j\frac{\omega}{\eta}\mathbf{a}_r \times \mathbf{A}_t$$

where $\mathbf{A}_t = [\mathbf{a}_\theta A_\theta(r,\theta,\phi) + \mathbf{a}_\phi A_\phi(r,\theta,\phi)]$. Using this result and

$$\mathbf{E} = \frac{1}{j\omega\epsilon}\nabla \times \mathbf{H}$$

show that

$$\mathbf{E} = -j\omega\mathbf{A}_t$$

3.2 Derive an expression for the vector effective length of a z-oriented short dipole antenna of length l, located at the origin. Assume a triangular current distribution on the dipole.

3.3 Calculate the radiation resistance of a short dipole (with a triangular current distribution) of length 0.3 m operating at 100 MHz. If the total resistance of the antenna is 2.2 Ω, calculate the maximum effective area and the radiation efficiency of the dipole. Calculate the open circuit voltage induced at the terminals of the dipole if it is oriented along the z-direction and the incident electric field at the dipole is $\mathbf{E}^i = (\mathbf{a}_x 4 + \mathbf{a}_y 3 + \mathbf{a}_z 5)$ V/m.

Answer: 1.97 Ω, 0.9597 m^2, 89.5%

3.4 Derive expressions for the radiated electric and magnetic fields of a thin dipole that supports a triangular current distribution, located at (x', y', z') and oriented along the (a) x-direction, (b) y-direction, and (c) z-direction.

3.5 Repeat Problem 3.4 replacing the triangular current distribution by a sinusoidal current distribution.

3.6 On performing the integration, show that Eqn (3.45) reduces to Eqn (3.46).

3.7 Calculate the radiation efficiency of a half-wave dipole if the loss resistance is 1 Ω. What is its maximum effective aperture if the frequency of operation is 145 MHz?

Answer: 98.65%, 0.552 m^2

3.8 Two half-wave dipoles operating at 2.4 GHz are used to establish a wireless communication link. The antennas are matched to the transmitter and the receiver, respectively. The maximum transmit power is 100 mW and for reliable communication the received power has to be at least −80 dBm. Calculate the maximum possible distance over which reliable communication can be established using this system.

Answer: 1.63 km

3.9 If one of the dipoles in Problem 3.8 is replaced by a circularly polarized antenna having the same gain as that of the half-wave dipole, calculate the distance over which the communication link can be established.

Answer: 1.15 km

3.10 Calculate the maximum value of the electric field intensity at a distance of 1 km from a semi-circular loop of radius 10 cm placed in front of an infinitely large, perfect electrical conductor as shown in Fig. 3.9. The loop carries a constant current of 4 A at 100 MHz.

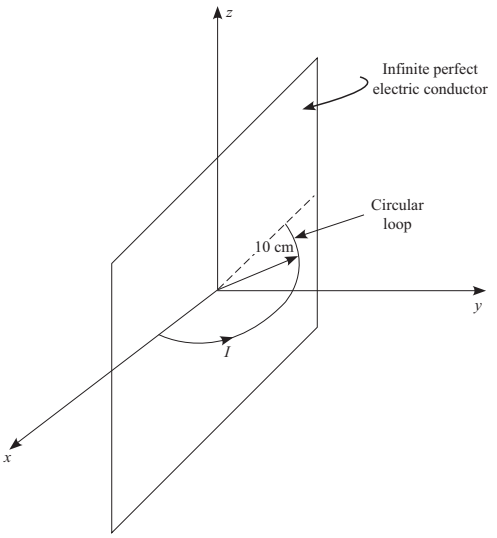

Fig. 3.9 Geometry of a semi-circular loop in front of an infinitely large, perfect electrical conductor

Answer: 16.5 mV/m

3.11 If $R_{\text{rad},1}$ and $R_{\text{loss},1}$ are the radiation and loss resistance of a one-turn small loop, derive an expression for the radiation efficiency of an N-turn loop of identical radius and, hence, show that an N-turn loop is more efficient.

3.12 Calculate the radiation resistance of a 20-turn, 1 m diameter loop antenna operating at 10 MHz. If the loss resistance of a one-turn loop is 1 Ω, calculate the radiation efficiency. Assume a constant current in the loop.

Answer: 32.16%

CHAPTER 4

Aperture Antennas

Introduction

The term aperture refers to an opening in an otherwise closed surface. As applied to antennas, aperture antennas represent a class of antennas that are generally analysed considering the antenna as an opening in a surface. Typical antennas that fall in this category are the slot, horn, reflector, and lens antennas. Some of these antennas are not easily amenable to rigorous electromagnetic field analysis. However, using the aperture theory, reasonably accurate radiation patterns can be computed without having to resort to solution of integral equations. The central idea used in the analysis of aperture type antennas is the conversion of the original antenna geometry into an equivalent geometry which can be looked at as radiation through an aperture in a closed surface. The equivalence is established by the use of an important principle known as the *field equivalence principle*. Along with this principle, the duality and image principles are also useful in the aperture-type antenna analysis. All these can be considered as forms of equivalence principles. The field equivalence principle makes use of the uniqueness theorem which states that for a given set of sources and boundary conditions in a lossy isotropic medium, the solution to Maxwell's equations is unique. This, when extended to a source-free lossless volume, reduces to the following—the electromagnetic fields in a lossless source-free volume are completely determined by the tangential components of the **E** or **H** fields on the surface enclosing the volume. Since the volume is considered to be source-free, the tangential fields on the surface as well as the fields inside the volume are produced by sources external to the volume. In this chapter we shall discuss the uniqueness theorem and the field equivalence principle in some detail before we embark upon the application of these principles to aperture type antennas. As we have seen in the vector potential approach presented in Chapter 1, the fields of an antenna are

expressed in terms of the vector potential which, in turn, is an integral over the current distribution on the antenna surface. The major difficulty in computing the fields of an aperture type antenna is the integration over a complex surface of the antenna. It is somewhat simplified by converting the antenna into an aperture problem, using the field equivalence principle. The aperture geometry is conveniently chosen as some regular surface so that the integration can be carried out with much less effort. All that is needed is the knowledge of the tangential **E** or **H** fields in the aperture to compute the far-fields of the antenna. Obviously, some approximation is involved in determining the tangential fields in the aperture, but in general, the computed far-fields are fairly accurate for all practical purposes, if sufficient care is taken in arriving at this approximation. After these preliminary theoretical aspects we shall discuss some of the most commonly used aperture antennas such as the slot and horn antennas and some typical reflector antennas.

4.1 Magnetic Current and its Fields

In Chapter 1 we discussed the computation of the fields produced by electric current distribution via the vector potential approach. Although we could compute the **E** and **H** fields directly, the vector potential is a convenient intermediate parameter for field computation. The vector potential, **A**, is known as the magnetic-type vector potential because the **H** field is directly related to the curl of **A**. We shall not repeat this analysis here, but give only the final expression for **A** in terms of the current density, **J**. The reader may refer to Chapter 1 for details of the derivation of **A**. If the sources are radiating in free space, we have

$$\mathbf{A}(r,\theta,\phi) = \frac{\mu}{4\pi}\iiint_{V'} \mathbf{J}(x',y',z')\frac{e^{-jkR}}{R}dv' \tag{4.1}$$

$$\mathbf{E} = -j\omega\mathbf{A} - \nabla V = -j\omega\mathbf{A} - \frac{j}{\omega\mu\epsilon}\nabla(\nabla\cdot\mathbf{A}) \tag{4.2}$$

$$\mathbf{H} = \frac{1}{\mu}\nabla\times\mathbf{A} \tag{4.3}$$

In the analysis of aperture antennas using the field equivalence principle, we use the concept of magnetic current density, **M** (unit: volt per square metre, $\mathrm{V/m^2}$). Just as electric current is a flow of electric charges, we postulate magnetic charges, and the flow of magnetic charges is treated as the magnetic current. With the introduction of the magnetic charge density,

ρ_m (unit: weber per cubic metre, $\mathrm{Wb/m^3}$), Maxwell's equations become symmetric:

$$\nabla \times \mathbf{H} = \mathbf{J} + j\omega\epsilon\mathbf{E} \tag{4.4}$$

$$\nabla \times \mathbf{E} = -\mathbf{M} - j\omega\mu\mathbf{H} \tag{4.5}$$

$$\nabla \cdot \mathbf{D} = \rho \tag{4.6}$$

$$\nabla \cdot \mathbf{B} = \rho_m \tag{4.7}$$

$$\nabla \cdot \mathbf{J} = -j\omega\rho \tag{4.8}$$

$$\nabla \cdot \mathbf{M} = -j\omega\rho_m \tag{4.9}$$

The magnetic charges postulated above do not exist in nature, but they are a useful mathematical construct to simplify the computation of fields. In the above equations if ρ_m and $\mathbf{M}$ are set to zero, we get back the equations in the standard form. To evaluate the fields produced by the magnetic current distribution, $\mathbf{M}$, we follow a procedure similar to that for the electric current distribution. We define the $\mathbf{E}$ field as the curl of an electric vector potential $\mathbf{F}$, such that $\mathbf{E} = -(1/\epsilon)\nabla \times \mathbf{F}$, and proceed in a similar way as with $\mathbf{A}$. The expression for $\mathbf{F}$ in terms of the magnetic current density, $\mathbf{M}$, in free space, is derived as

$$\mathbf{F} = \frac{\epsilon}{4\pi} \iiint_{V'} \mathbf{M}(x', y', z') \frac{e^{-jkR}}{R} dv' \tag{4.10}$$

where V' is the volume containing the source current, $\mathbf{M}$.

The $\mathbf{E}$ and $\mathbf{H}$ fields are related to the vector potential by the following equations (see Example 4.1)

$$\mathbf{E} = -\frac{1}{\epsilon}\nabla \times \mathbf{F} \tag{4.11}$$

$$\mathbf{H} = -j\omega\mathbf{F} - \frac{j}{\omega\mu\epsilon}\nabla(\nabla \cdot \mathbf{F}) \tag{4.12}$$

Thus, when both $\mathbf{J}$ and $\mathbf{M}$ are present, the fields are obtained by adding Eqns (4.2) and (4.11) for the $\mathbf{E}$ field and equations Eqns (4.3) and (4.12) for the $\mathbf{H}$ field

$$\mathbf{E} = -\frac{1}{\epsilon}\nabla \times \mathbf{F} - j\omega\mathbf{A} - \frac{j}{\omega\mu\epsilon}\nabla(\nabla \cdot \mathbf{A}) \tag{4.13}$$

$$\mathbf{H} = \frac{1}{\mu}\nabla \times \mathbf{A} - j\omega\mathbf{F} - \frac{j}{\omega\mu\epsilon}\nabla(\nabla \cdot \mathbf{F}) \tag{4.14}$$

It can be shown that in the far-field region the fields are given by (see exercise problem 4.3)

$$E_\theta \simeq -j\omega(A_\theta + \eta F_\phi) \tag{4.15}$$

$$E_\phi \simeq -j\omega(A_\phi - \eta F_\theta) \tag{4.16}$$

$$H_\theta \simeq -\frac{E_\phi}{\eta} \tag{4.17}$$

$$H_\phi \simeq -\frac{E_\theta}{\eta} \tag{4.18}$$

EXAMPLE 4.1

In a homogeneous and isotropic medium consisting only of magnetic current, $\mathbf{M}$, and magnetic charge, ρ_m, we can define the electric vector potential by

$$\mathbf{E} = -\frac{1}{\epsilon}\nabla \times \mathbf{F}$$

Show that the electric vector potential satisfies the wave equation

$$\nabla^2\mathbf{F} + k^2\mathbf{F} = -\epsilon\mathbf{M}$$

and the magnetic field is given by

$$\mathbf{H} = -j\omega\mathbf{F} - \frac{j}{\omega\mu\epsilon}\nabla(\nabla \cdot \mathbf{F})$$

Solution: With $\mathbf{J} = 0$ and $\rho = 0$, Maxwell's equations are

$$\nabla \times \mathbf{H} = j\omega\epsilon\mathbf{E}$$

$$\nabla \times \mathbf{E} = -\mathbf{M} - j\omega\mu\mathbf{H}$$

$$\nabla \cdot \mathbf{D} = 0$$

$$\nabla \cdot \mathbf{B} = \rho_m$$

Substituting $\mathbf{E} = -(1/\epsilon)\nabla \times \mathbf{F}$ into $\nabla \times \mathbf{H} = j\omega\epsilon\mathbf{E}$ and rearranging

$$\nabla \times (\mathbf{H} + j\omega\mathbf{F}) = 0$$

Since the curl of the gradient of a scalar function is always zero, we can express the terms within brackets by the gradient of a scalar function

$$\mathbf{H} + j\omega\mathbf{F} = -\nabla V_m$$

where V_m is known as the magnetic scalar potential. This equation can be rewritten as

$$\mathbf{H} = -j\omega\mathbf{F} - \nabla V_m$$

Substituting the expressions for $\mathbf{E}$ and $\mathbf{H}$ into the second curl equation

$$\nabla \times \left(-\frac{1}{\epsilon}\nabla \times \mathbf{F}\right) = -\mathbf{M} - j\omega\mu(-j\omega\mathbf{F} - \nabla V_m)$$

This can be written as

$$\nabla \times \nabla \times \mathbf{F} = \nabla(\nabla \cdot \mathbf{F}) - \nabla^2\mathbf{F} = \epsilon\mathbf{M} + \omega^2\mu\epsilon\mathbf{F} - j\omega\mu\epsilon\nabla V_m$$

Since $\nabla \cdot \mathbf{F}$ is not defined yet, by choosing $\nabla \cdot \mathbf{F} = -j\omega\mu\epsilon V_m$ (Lorentz condition), the above expression simplifies to

$$\nabla^2\mathbf{F} + k^2\mathbf{F} = -\epsilon\mathbf{M}$$

where $k^2 = \omega^2\mu\epsilon$. Substituting the expression for V_m into $\mathbf{H} = -j\omega\mathbf{F} - \nabla V_m$, we get

$$\mathbf{H} = -j\omega\mathbf{F} - \frac{j}{\omega\mu\epsilon}\nabla(\nabla \cdot \mathbf{F})$$

4.2 Some Theorems and Principles

As mentioned in the introduction, there are several principles used in simplifying the analysis of aperture-type antennas. Some of these are—the image principle, the field equivalence principle, and the duality principle. A plane of symmetry is another concept that is useful in simplifying a field computation problem. The symmetry can be even or odd in nature. On the surface of a perfect electric conductor ($\sigma = \infty$), the tangential electric field is zero. Only the normal component of the electric field can exist on this surface. This is generally called an electric wall boundary or **E**-wall. We can also encounter a similar field condition, viz., $\mathbf{E}_t = 0$, without a physical boundary being present. In such cases, the tangential electric field has an odd symmetry about the plane and even symmetry is exhibited by the normal component. This is also called an **E**-wall. The dual of this is the concept of a magnetic wall or **H**-wall. The **H**-wall boundary, or simply **H**-wall, is the plane on which the tangential magnetic field is zero. Again, in the absence of a physical boundary, the normal and tangential components of the magnetic field, respectively, exhibit even and odd symmetries about the **H**-wall.

4.2.1 Uniqueness Theorem

The uniqueness theorem can be stated in several different forms but it essentially states that *for a given set of sources and boundary conditions in a lossy medium, the solution to Maxwell's equations is unique.* Consider a source-free volume V in an isotropic homogeneous medium bounded by a surface S, and let $(\mathbf{E}_1, \mathbf{H}_1)$ be the fields inside it produced by a set of sources external to the volume. Now, let $(\mathbf{E}_2, \mathbf{H}_2)$ be another possible set of fields in the volume V. It can be shown (Balanis 1989, Harrington 1961) that if either the tangential $\mathbf{E}$ or the tangential $\mathbf{H}$ is the same on the surface S for the two sets of solutions, the fields are identical everywhere in the volume. This is known as the uniqueness theorem.

It is important to note that it is sufficient to equate either the tangential $\mathbf{E}$ or the tangential $\mathbf{H}$ on S for the solution to be unique. In other words, in a source-free region the fields are completely determined by the tangential $\mathbf{E}$ or the tangential $\mathbf{H}$ on the bounding surface. Although the uniqueness theorem is derived for a dissipative medium, one can prove the theorem for a lossless medium by a limiting process as loss tends to zero.

4.2.2 Field Equivalence Principle

Consider a set of current sources in a homogeneous isotropic medium producing electromagnetic fields $\mathbf{E}$ and $\mathbf{H}$ everywhere. Enclose all the sources by a closed surface S, separating the entire space into two parts, volume V_1 containing the sources and the volume V_2 being source-free. Let the surface S be chosen such that it is also source-free. Let $\mathbf{n}$ be a unit normal to the surface drawn from V_1 into V_2 (Fig. 4.1).

According to the field equivalence principle, the fields in V_2 due to the sources in volume V_1 can also be generated by an equivalent set of virtual sources on surface S, given by $\mathbf{J}_s = \mathbf{n} \times \mathbf{H}$ and $\mathbf{M}_s = \mathbf{E} \times \mathbf{n}$, where $\mathbf{E}$ and $\mathbf{H}$ are the fields on the surface S produced by the original set of sources in

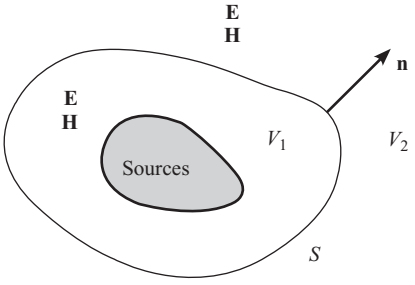

Fig. 4.1 Fields and sources

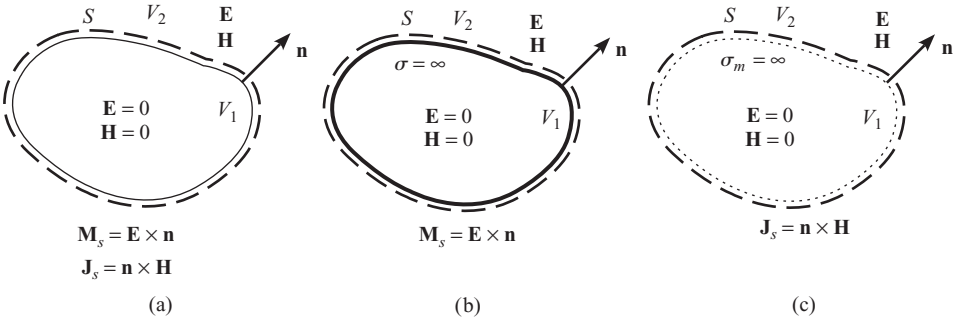

Fig. 4.2 Three forms of the field equivalence principle: (a) surface current densities $\mathbf{J}_s$ and $\mathbf{M}_s$ on the surface S, (b) surface current density $\mathbf{M}_s$ alone on the surface S, which is a conducting surface, and (c) surface current density $\mathbf{J}_s$ alone on the surface S, which is a magnetic conductor surface

volume V_1. Further the set of virtual sources produce null fields everywhere in V_1. Here $\mathbf{M}_s$ represents the magnetic surface current density and $\mathbf{J}_s$ the electric surface current density. The proof of this principle makes use of the uniqueness theorem discussed in Section 4.3.1. Consider a situation where the fields in volume V_2 of Fig. 4.1 are the same as before, $(\mathbf{E}, \mathbf{H})$, but we delete all the sources in V_1 and assume the fields to be identically zero everywhere in V_1 as shown in Fig. 4.1. At the boundary surface, S, the fields are discontinuous and, hence, cannot be supported unless we introduce sources on the discontinuity surface. Specifically, we introduce surface current sheets on S, such that $\mathbf{n} \times \mathbf{H} = \mathbf{J}_s$ and $\mathbf{E} \times \mathbf{n} = \mathbf{M}_s$, so that the boundary conditions are satisfied. Since the tangential $\mathbf{E}$ and $\mathbf{H}$ satisfy the boundary conditions, it is a solution of Maxwell's equations, and from the uniqueness theorem, it is the only solution. Thus, the original sources in V_1 and the new set of surface current sources produce the same fields $(\mathbf{E}, \mathbf{H})$ in the volume V_2. Therefore, these are equivalent problems as far as the fields in the volume V_2 are concerned. The field equivalence principle is generally presented in three different forms. We can choose an appropriate form (whichever leads to the simplest formulation) depending on the antenna problem. The three forms of the field equivalence theorem are depicted in Fig. 4.2.

The first one [Fig. 4.2(a)] is the most general form, in which the surface current sources, $\mathbf{J}_s$ and $\mathbf{M}_s$, radiate in free space. We can use this equivalent provided we can find the tangential $\mathbf{E}$ and $\mathbf{H}$ fields on the surface S. Most often, either $\mathbf{E}$ or $\mathbf{H}$ is available with reasonable accuracy on S. In such cases, and for certain choice of surface S, we can use the other two forms. If the tangential $\mathbf{E}$ is known on S, we use the second form and if tangential $\mathbf{H}$ is known on S, the third form is used. All three forms are equivalent as far

as the fields in the region V_2 are concerned. However, the computation of fields of the second and the third forms is not as simple as in the first form. The field computation must take into account the electric conductor surface boundary and the magnetic conductor surface boundary in the second and third forms, respectively. The free space vector potential formula is not applicable because of the presence of the boundary. To prove the second form of the field equivalence principle shown in Fig. 4.2(b), let us assume that the fields in V_2 are the same as before and that the volume V_1 is filled with a perfect conducting material, which makes $\mathbf{E} = 0$ and $\mathbf{H} = 0$ in V_1. The conducting material forces the tangential $\mathbf{E}$ on S to zero, therefore, to keep the fields in V_2 the same as before we introduce a magnetic surface current density $\mathbf{M}_s = \mathbf{E} \times \mathbf{n}$ just outside the surface S in V_2. This will restore the tangential $\mathbf{E}$ to the same value as before. Since tangential $\mathbf{E}$ is the same on S, the fields in V_2 are unique according to the uniqueness theorem. A similar proof can be given for the third form of the field equivalence principle shown in Fig. 4.2(c). The field equivalence principle suggests that the fields in V_2 can be computed using the original sources in V_1 or the equivalent surface current sources on S. Since surface S can be chosen conveniently as some regular surface to facilitate easy integration, we use the equivalent sources approach in aperture-type antennas. This approach can be looked upon as a two-stage solution to the original antenna problem; first find the tangential $\mathbf{E}$ and $\mathbf{H}$ fields on an imaginary surface S enclosing the antenna and then use the equivalent source formulation to compute the far-fields of the antenna in terms of these equivalent sources. There still remains the problem of finding the tangential $\mathbf{E}$ and $\mathbf{H}$ fields of the original sources on the surface S. This part generally uses some form of approximation, because a rigorous solution is as difficult as the original problem. The second part uses the vector potential approach to compute the fields. The magnetic vector potential approach for computing the fields of an electric current distribution in free space is delineated in Chapter 1 and that due to a magnetic current is given in Section 4.1.

4.2.3 Duality Principle

Duality is a consequence of the symmetry in Maxwell's equations obtained with the introduction of the magnetic charge density, ρ_m, and magnetic current density, $\mathbf{M}$. This is a very useful principle in obtaining the solution of a dual problem from the original solution, without having to solve it again.

Consider the two problems—(a) the $\mathbf{E}$ and $\mathbf{H}$ fields are produced by an electric current and charge distribution $\mathbf{J}$ and ρ, and (b) the $\mathbf{E}$ and $\mathbf{H}$ fields

are produced by a magnetic current and charge distribution $\mathbf{M}$ and ρ_m. The two sets of equations for these problems are

$$\begin{aligned} &\nabla \times \mathbf{H} = \mathbf{J} + j\omega\epsilon\mathbf{E} && -\nabla \times \mathbf{E} = \mathbf{M} + j\omega\mu\mathbf{H} \\ &-\nabla \times \mathbf{E} = j\omega\mu\mathbf{H} && \nabla \times \mathbf{H} = j\omega\epsilon\mathbf{E} \\ &\nabla \cdot \mathbf{D} = \rho && \nabla \cdot \mathbf{B} = \rho_m \\ &\nabla \cdot \mathbf{B} = 0 && \nabla \cdot \mathbf{D} = 0 \end{aligned} \tag{4.19}$$

Comparing these two sets, it is obvious that the mathematical forms are identical except for a change in the symbols. Specifically, if we change the quantities $\mathbf{J}$ by $\mathbf{M}$, $\mathbf{E}$ by $\mathbf{H}$, $\mathbf{H}$ by $-\mathbf{E}$, μ by ϵ, and ρ by ρ_m, in the first set of equations, we get the second set. Therefore, if we solve one set of equations, the solution for the other set can be obtained by simply interchanging the symbols as indicated. These two problems are called the duals of each other.

The following set lists the various parameters and their corresponding dual parameters.

$\mathbf{J}$	$\mathbf{M}$
$\mathbf{E}$	$\mathbf{H}$
$\mathbf{H}$	$-\mathbf{E}$
$\mathbf{A}$	$\mathbf{F}$
ρ	ρ_m
$\sigma + j\omega\epsilon$	$\sigma_m + j\omega\mu$
η	$\frac{1}{\eta}$
$\mathbf{E}$-wall	$\mathbf{H}$-wall
$\mathbf{H}$-wall	$\mathbf{E}$-wall

(4.20)

where ρ_m is the magnetic conductivity, k is the propagation constant, and η is the intrinsic impedance of the medium.

4.2.4 Method of Images

The method of images is another technique for converting a problem into an equivalent problem that is much easier to solve than the original problem. We demonstrate this principle by considering an example of a small electric current element above an infinite, perfectly conducting plane as shown in Fig. 4.3. The treatment of a small current element radiating in free space is given in Chapter 1. Now, the presence of the conducting plane forces the tangential $\mathbf{E}$ field on the conducting surface to zero. This is as

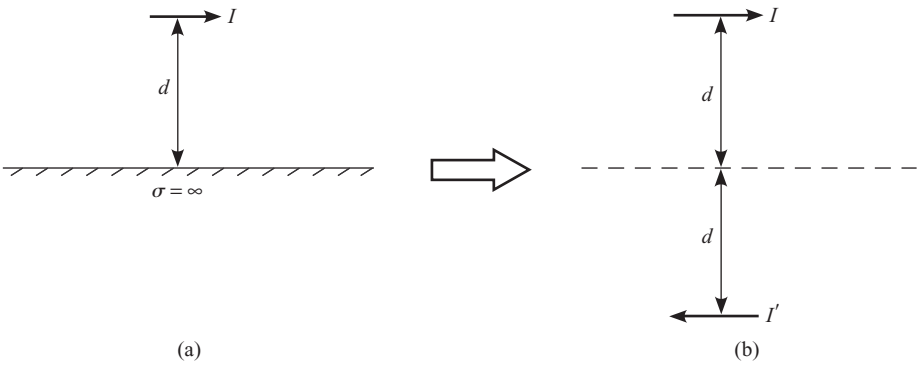

Fig. 4.3 (a) A current element above an infinite conducting plane, and (b) its image theory equivalent

if the **E** field of the current element induces a current distribution on the conducting surface such that the field of the induced current distribution is exactly opposite to the original incident field (from Lenz's law), forcing the resultant tangential **E** field to zero on the conductor. This current distribution, in turn, produces fields everywhere above the conducting surface. Therefore, the field at any point above the conducting surface is a sum of the incident field due to the current element and the scattered field due to the induced current distribution on the conducting surface. To evaluate the fields of a current element kept above an infinite conducting surface, we first need to determine the induced current distribution on the conducting surface and then evaluate the vector potential due to the current element as well as that due to the induced current distribution. The **E** and **H** fields can then be computed using Eqns (4.2) and (4.3). The field computation can be simplified by the applying the image principle.

The idea of the image principle is that we remove the conducting boundary and introduce an image current which, together with the original current source, produces exactly the same fields as those which existed on the conducting surface (i.e., $\mathbf{E}_t = 0$). Consider a current element I', of same magnitude as I, but flowing in the opposite direction and kept at a distance d from the boundary surface, as shown in Fig. 4.3(b). The currents I and I' together produce zero tangential **E** field on the boundary surface. Since the original boundary condition of zero tangential **E** field is satisfied, the uniqueness theorem ensures that the field in the upper half is the same as in the original problem. The second problem of two current elements without the conducting plane is much easier to solve than the first one because we can apply the free-space vector potential expressions [Eqn (4.1)].

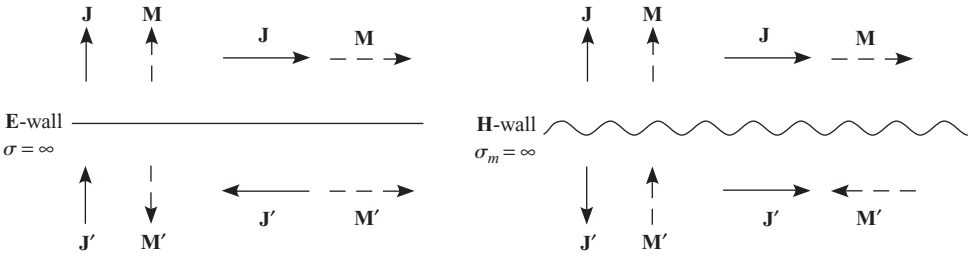

Fig. 4.4 Depiction of the image principle (the primed symbols indicate images)

The image principle can be applied to electric and magnetic current distributions and infinite perfect electric or magnetic reflecting planes. Any current distribution can be decomposed into two components—parallel and perpendicular to the reflecting surface. The four different cases of electric and magnetic current components and their images in **E**-wall and **H**-wall boundaries are depicted in Fig. 4.4. Using these four cases, the image of any current distribution in infinite planes can be generated. The image theory can also be applied to other regular reflecting surfaces, such as cylindrical or spherical surfaces, but the construction of the image becomes more involved. The principle for constructing the image remains the same, i.e., the image and the original source together should produce the same fields as existing on the boundary, so that the boundary can be deleted without affecting the fields in the region of interest.

4.3 Sheet Current Distribution in Free Space

In Section 4.2 we reduced an aperture problem to a magnetic current sheet radiating in free space. Not all problems can be reduced to this form. In general, we may have both $\mathbf{J}_s$ and $\mathbf{M}_s$ on a finite size aperture surface radiating in free space. We may need both the vector potentials $\mathbf{A}$ and $\mathbf{F}$ to compute the fields. Although the equivalent field formulation is exact even for the near-fields, most often, only the far-fields are required in antenna problems. In this section we derive expressions for the far-fields making the usual far-field approximation discussed in Chapter 3.

Consider an aperture, S_a, of size $a \times b$ in the $z = 0$ plane. For simplicity, assume that the aperture fields $\mathbf{E}_a$ and $\mathbf{H}_a$ are constant over the aperture and further, $\mathbf{E}_a = \mathbf{a}_y E_0$, and $\mathbf{H}_a = -\mathbf{a}_x H_0$, where E_0 and H_0 are constants. We also make an assumption that the $\mathbf{E}_a$ and $\mathbf{H}_a$ fields are related via the free space impedance formula, $|\mathbf{E}_a|/|\mathbf{H}_a| = \eta$, the intrinsic impedance of the medium. Thus, $\mathbf{H}_a = -\mathbf{a}_x H_0 = -\mathbf{a}_x E_0/\eta$. Applying the field equivalence

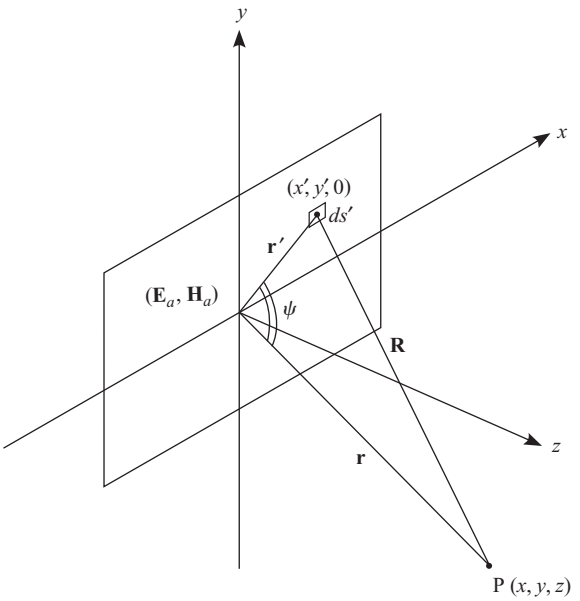

Fig. 4.5 Geometry of a rectangular aperture

principle, the fields in the $z > 0$ space can be computed from the equivalent current sheets $\mathbf{J}_s = \mathbf{a}_z \times (-\mathbf{a}_x H_0) = -\mathbf{a}_y H_0$, and $\mathbf{M}_s = -(\mathbf{a}_z \times \mathbf{a}_y E_0) = \mathbf{a}_x E_0$ in the aperture, radiating into free space. For convenience of integration we use rectangular coordinates (x', y') for the source point and spherical coordinates (r, θ, ϕ) for the field point. The geometry of the problem is shown in Fig. 4.5. Using the far-field approximations [see Eqns (3.8) and (3.15)]

$$R \simeq r - r' \cos\psi \quad \text{in the phase term} \tag{4.21}$$

$$R \simeq r \quad \text{for the amplitude part} \tag{4.22}$$

where the angle ψ is the angle between the vectors $\mathbf{r}$ and $\mathbf{R}$. Substituting these in Eqns (4.1) and (4.10) the vector potentials $\mathbf{A}$ and $\mathbf{F}$ can be reduced to

$$\mathbf{A} = \mu \frac{e^{-jkr}}{4\pi r} \iint_{S_a} \mathbf{J}_s(x', y') e^{jkr' \cos\psi} ds' \tag{4.23}$$

$$\mathbf{F} = \epsilon \frac{e^{-jkr}}{4\pi r} \iint_{S_a} \mathbf{M}_s(x', y') e^{jkr' \cos\psi} ds' \tag{4.24}$$

Using the spherical co-ordinates, the term in the exponent is written as

$$\begin{aligned} r' \cos\psi &= \mathbf{r}' \cdot \mathbf{a}_r \\ &= (\mathbf{a}_x x' + \mathbf{a}_y y') \cdot (\mathbf{a}_x \sin\theta\cos\phi + \mathbf{a}_y \sin\theta \sin\phi) \\ &= x' \sin\theta\cos\phi + y' \sin\theta\sin\phi \end{aligned} \tag{4.25}$$

Substituting $ds' = dx'dy'$, $\mathbf{J}_s = -\mathbf{a}_y H_0$ and $\mathbf{M}_s = \mathbf{a}_x E_0$, we see that $\mathbf{A}$ has only a y-component and $\mathbf{F}$ has only an x-component, given by

$$\begin{aligned} A_y &= -\mu H_0 \frac{e^{-jkr}}{4\pi r} \iint_{S_a} e^{jk(x' \sin\theta\cos\phi + y' \sin\theta\sin\phi)} dx'dy' \\ &= -\mu H_0 GI \end{aligned} \tag{4.26}$$

$$\begin{aligned} F_x &= \epsilon E_0 \frac{e^{-jkr}}{4\pi r} \iint_{S_a} e^{jk(x' \sin\theta\cos\phi + y' \sin\theta\sin\phi)} dx'dy' \\ &= \epsilon E_0 GI \end{aligned} \tag{4.27}$$

where, I represents the integral over the aperture surface S_a and

$$G = e^{-jkr}/(4\pi r)$$

is the scalar spherical wave function. The vector potentials have the same direction as the corresponding current elements. Since we have assumed J_y and M_x alone on the aperture for this particular problem, the vector potentials have only A_y and F_x components.

Now, we evaluate the integral I using the result

$$\int_{-T/2}^{T/2} e^{j\alpha z} dz = T \frac{\sin(\alpha T/2)}{\alpha T/2} \tag{4.28}$$

as

$$I = \int_a \int_b e^{jk(x' \sin\theta\cos\phi + y' \sin\theta\sin\phi)} dx'dy' \tag{4.29}$$

$$= ab \frac{\sin X}{X} \frac{\sin Y}{Y} \tag{4.30}$$

where $X = (ka/2)\sin\theta\cos\phi$, and $Y = (kb/2)\sin\theta\sin\phi$. The rectangular coordinate representation of the vector potentials $\mathbf{A}$ and $\mathbf{F}$ at any far-field point $P(r, \theta, \phi)$ is split into components along the $\mathbf{a}_r$, $\mathbf{a}_\theta$, and $\mathbf{a}_\phi$ directions

using the rectangular to spherical coordinate transformation

$$\begin{bmatrix} A_r \\ A_\theta \\ A_\phi \end{bmatrix} = \begin{bmatrix} \sin\theta\cos\phi & \sin\theta\sin\phi & \cos\theta \\ \cos\theta\cos\phi & \cos\theta\sin\phi & -\sin\theta \\ -\sin\phi & \cos\phi & 0 \end{bmatrix} \begin{bmatrix} A_x \\ A_y \\ A_z \end{bmatrix} \tag{4.31}$$

In the far-field region the radial component is generally negligible and only the θ and ϕ components are of interest, hence we neglect the radial component.

Using the transformation Eqn (4.31) we get the A_θ, A_ϕ, F_θ, and F_ϕ components as

$$A_\theta = A_y \cos\theta \sin\phi \tag{4.32}$$

$$A_\phi = A_y \cos\phi \tag{4.33}$$

$$F_\theta = F_x \cos\theta \cos\phi \tag{4.34}$$

$$F_\phi = -F_x \sin\phi \tag{4.35}$$

Making use of Eqns (4.15) to (4.18) the θ and ϕ components of the **E** and **H** fields in the far-field region can be written as

$$E_\theta = -j\omega(A_\theta + \eta F_\phi) = -j\omega(A_y \cos\theta \sin\phi - \eta F_x \sin\phi) \tag{4.36}$$

$$E_\phi = -j\omega(A_\phi - \eta F_\theta) = -j\omega(A_y \cos\phi - \eta F_x \cos\theta \cos\phi) \tag{4.37}$$

$$H_\theta = -j\omega\left(F_\theta - \frac{1}{\eta}A_\phi\right) = -\frac{E_\phi}{\eta} \tag{4.38}$$

$$H_\phi = -j\omega\left(F_\phi + \frac{1}{\eta}A_\theta\right) = \frac{E_\theta}{\eta} \tag{4.39}$$

where η is the intrinsic impedance of the medium ($\eta = \sqrt{\mu/\epsilon}$). It is noted that the **E** and **H** fields are related by $|\mathbf{E}/\mathbf{H}| = \eta$ in the far-field and hence only the **E** field expressions are given below. Substituting the expressions, $A_y = -\mu H_0 GI = -\mu(E_0/\eta)GI$ and $F_x = \epsilon E_0 GI$, we get

$$E_\theta = jkGabE_0(1 + \cos\theta)\sin\phi \frac{\sin X}{X}\frac{\sin Y}{Y} \tag{4.40}$$

$$E_\phi = jkGabE_0(1 + \cos\theta)\cos\phi \frac{\sin X}{X}\frac{\sin Y}{Y} \tag{4.41}$$

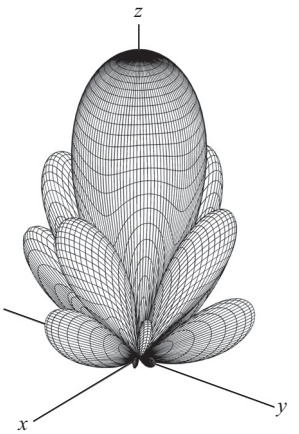

Fig. 4.6 3D depiction of the normalized radiation pattern of a $3\lambda \times 3\lambda$ aperture in the x-y plane with uniform aperture fields

In the far-field region, the radiation intensity is r^2 times the time-averaged power density

$$U(\theta, \phi) = \frac{r^2}{2\eta}(|E_\theta|^2 + |E_\phi|^2) \tag{4.42}$$

Substituting the expressions for E_θ and E_ϕ and simplifying

$$U(\theta, \phi) = \frac{k^2}{2\eta(4\pi)^2}(ab)^2|E_0|^2(1+\cos\theta)^2\left(\frac{\sin X}{X}\right)^2\left(\frac{\sin Y}{Y}\right)^2 \tag{4.43}$$

The normalized radiation pattern of a typical aperture is shown in Fig. 4.6.

4.3.1 Pattern Properties

Let us now determine some of the properties of the radiation pattern of the sheet currents radiating into free space. From Eqns (4.40) and (4.41) we can infer that in the $\phi = 0$ plane, $E_\theta = 0$ and $Y = 0$ and in the $\phi = 90^\circ$ plane, $E_\phi = 0$ and $X = 0$. Thus, we can simplify the expression for the radiation intensity in the two principal planes to

$$U(\theta, 0) = \frac{k^2}{2\eta(4\pi)^2}(ab)^2|E_0|^2(1+\cos\theta)^2\left(\frac{\sin X}{X}\right)^2 \tag{4.44}$$

$$U\left(\theta, \frac{\pi}{2}\right) = \frac{k^2}{2\eta(4\pi)^2}(ab)^2|E_0|^2(1+\cos\theta)^2\left(\frac{\sin Y}{Y}\right)^2 \tag{4.45}$$

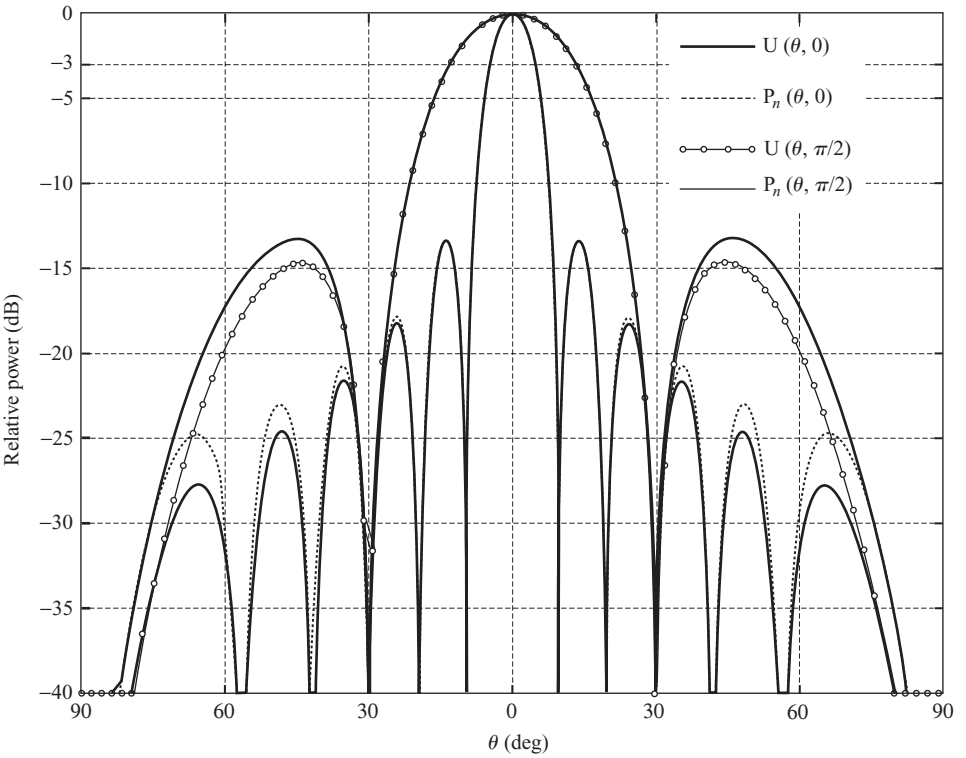

Fig. 4.7 Radiation pattern in the $\phi = 0$ and $\phi = \pi/2$ planes of a $6\lambda \times 2\lambda$ aperture in the x-y plane with uniform aperture fields

Figure 4.7 shows a plot of the normalized radiation patterns in the x-z and y-z planes for $a = 6\lambda$ and $b = 2\lambda$. It is interesting to note that in the x-z plane, the pattern is controlled by the aperture dimension in the x-direction and in the y-z plane, the y-dimension controls it.

For large apertures, i.e., $a \gg \lambda$ and $b \gg \lambda$, the $(1 + \cos\theta)^2$ term is a slowly varying function of θ as compared to the $[(\sin X)/X]^2$ and $[(\sin Y)/Y]^2$ factors. Hence, we can ignore the $(1 + \cos\theta)^2$ factor and write the normalized pattern functions in the x-z plane as

$$P_n(\theta, 0) = \left| \frac{\sin X}{X} \right|^2 \tag{4.46}$$

and in the y-z plane as

$$P_n\left(\theta, \frac{\pi}{2}\right) = \left| \frac{\sin Y}{Y} \right|^2 \tag{4.47}$$

The normalized pattern functions are also plotted in Fig. 4.7. Ignoring the the slow varying $(1+\cos\theta)^2$ factor results in a change in the side lobe level, but has very little effect on the null positions and the half-power beamwidth. The pattern function is mainly controlled by the dimensions of the aperture; x-dimension controlling the pattern $P_n(\theta, 0)$ and y-dimension controlling the pattern $P_n(\theta, \pi/2)$. From the tables of $\sin X/X$ function (see Appendix G) we can determine the pattern nulls, half power points, and side lobe levels. The nulls occur at integral multiples of π, $X = \pm n\pi$; $n = 1, 2, 3, \ldots, \infty$. The actual angle along which the null occurs depends on the aperture dimensions, a and b, in the $\phi = 0$ and $\pi/2$ planes, respectively.

The half-power point of the main beam occurs for $X = 1.391$, which gives

$$\frac{ka}{2}\sin\theta = 1.391 \tag{4.48}$$

or

$$\theta_h = \sin^{-1}\left(\frac{1.391\lambda}{\pi a}\right) \tag{4.49}$$

for the $\phi = 0$ cut and

$$\theta_v = \sin^{-1}\left(\frac{1.391\lambda}{\pi b}\right) \tag{4.50}$$

for the $\phi = \pi/2$ cut. Thus the half-power beamwidth (HPBW) is

$$\text{HPBW}|_{\phi=0} = 2\sin^{-1}\left(\frac{1.391\lambda}{\pi a}\right) \tag{4.51}$$

$$\text{HPBW}|_{\phi=\pi/2} = 2\sin^{-1}\left(\frac{1.391\lambda}{\pi b}\right) \tag{4.52}$$

The first side lobe peak is at -13.26 dB, and the second one is at -17.83 dB. The side lobe level decreases progressively as we move away from the main beam. The nulls occur at angles ($X = \pm n\pi$)

$$\theta_n = \pm\sin^{-1}\left(\frac{n\lambda}{a}\right) \tag{4.53}$$

Using the definition given in Chapter 2, we can write the maximum directivity, $D_{\max}$, as

$$D_{\max} = \frac{4\pi U(\theta_0, \phi_0)}{\oint_\Omega U(\theta, \phi)d\Omega} \tag{4.54}$$

where $U(\theta, \phi)$ is the radiation intensity along (θ, ϕ), Ω represents the integration over the 4π solid angle of the sphere, and (θ_0, ϕ_0) is the direction of the maximum which is $(0, 0)$ for the uniform distribution. It is difficult to evaluate the integral in the denominator which gives the total radiated power. Hence, we use an alternative way of computing the total radiated power. We know that all the radiated power is passing through the aperture and the fields in the aperture $(\mathbf{E}_a, \mathbf{H}_a)$ are known. The power radiated is obtained by integrating the Poynting vector over the aperture. Thus, the power radiated is given by

$$\oint_{\Omega} U(\theta, \phi) d\Omega = \iint_{S_a} (\mathbf{E}_a \times \mathbf{H}_a^*) \cdot d\mathbf{s} \tag{4.55}$$

Assuming $\mathbf{E}_a = \mathbf{a}_y E_0$ and $\mathbf{H}_a = -\mathbf{a}_x E_0/\eta$, the power radiated through the aperture is

$$\iint_{S_a} (\mathbf{E}_a \times \mathbf{H}_a^*) \cdot d\mathbf{s} = \frac{|E_0|^2}{2\eta} \iint_{S_a} da = ab\frac{|E_0|^2}{2\eta} \tag{4.56}$$

Examining the expression for radiation intensity [Eqn (4.42)], we find that the maximum occurs for $X = 0$ and $Y = 0$, which corresponds to $\theta = 0$

$$U_{\max} = \frac{r^2}{2\eta}(|2kGabE_0|^2) \tag{4.57}$$

$$= \frac{1}{2\eta}\left(2\frac{2\pi}{\lambda}\frac{ab|E_0|}{4\pi}\right)^2 \tag{4.58}$$

$$= \frac{1}{2\eta}\left(\frac{ab}{\lambda}\right)^2 |E_0|^2 \tag{4.59}$$

Thus, the directivity expression reduces to

$$D_{\max} = \frac{4\pi\left(\frac{ab}{\lambda}\right)^2 \frac{|E_0|^2}{2\eta}}{ab\frac{|E_0|^2}{2\eta}}$$

$$= 4\pi\frac{ab}{\lambda^2} \tag{4.60}$$

This means that the ratio of the directivity to the aperture area is a constant, $(4\pi/\lambda^2)$, independent of the antenna; a result derived in Chapter 2. If the distribution is not uniform we can define an equivalent uniform aperture

area as the maximum effective aperture area and write

$$D_{\max} = \left(\frac{4\pi}{\lambda^2}\right) A_e \tag{4.61}$$

where A_e is the effective aperture area. For a uniform distribution the effective area is the same as the actual area of the aperture.

EXAMPLE 4.2

Calculate the 3 dB beamwidth of the x-z plane radiation pattern of an aperture ($a = \lambda$) with uniform current distribution **(a)** using the approximate expression given by Eqn (4.51) and **(b)** by solving $P_n(\theta, 0) = 1/2$, where $P_n(\theta, \phi)$ is the normalized pattern function. What is the percentage error in the calculated beamwidth value using the approximation?

Solution:

(a) Using the approximation given by Eqn (4.51)

$$\text{HPBW}|_{\phi=0} = 2\sin^{-1}\left(\frac{1.391\lambda}{\pi\lambda}\right) = 52.56^\circ$$

(b) The normalized pattern is given by

$$P_n(\theta, \phi) = \frac{U(\theta, \phi)}{U_{\max}}$$

where $U(\theta, \phi)$ in $\phi = 0$ plane is given by Eqn (4.44) and is reproduced here.

$$U(\theta, 0) = \frac{k^2}{2\eta(4\pi)^2}(ab)^2|E_0|^2(1 + \cos\theta)^2\left(\frac{\sin X}{X}\right)^2$$

The maximum value of the radiation intensity is given by

$$U_{\max} = \frac{k^2}{32\eta\pi^2}(ab)^2|E_0|^2(2)^2$$

In the $\phi = 0$ plane, the normalized pattern becomes

$$P_n(\theta, 0) = \frac{(1 + \cos\theta)^2}{4}\left(\frac{\sin X}{X}\right)^2$$

Equating it to 1/2, and rearranging we get the following equation for θ_h along which the power is half of the maximum.

$$f(\theta_h) = (1 + \cos\theta_h)\sin(\pi \sin\theta_h) - \sqrt{2}\pi \sin\theta_h = 0$$

Differentiating with respect to θ_h

$$f'(\theta_h) = -\sin\theta_h \sin(\pi \sin\theta_h) + (1 + \cos\theta_h)\cos(\pi \sin\theta_h)\pi \cos\theta_h \\ -\sqrt{2}\pi \cos\theta_h$$

Using the Newton–Raphson method, we can find the solution iteratively using

$$\theta_{h,(n+1)} = \theta_{h,n} - \frac{f(\theta_{h,n})}{f'(\theta_{h,n})}$$

where $\theta_{h,n}$ is the solution of the nth iteration and $\theta_{h,(n+1)}$ is the solution of the $(n+1)$th iteration.

We can start the iteration from the approximate value of θ_h computed using Eqn (4.49).

$$\theta_{h,0} = \sin^{-1}\left(\frac{1.391\lambda}{\pi\lambda}\right) = 0.4587$$

$f(0.4587) = -0.1012$ and $f'(0.4587) = -3.4641$ can be computed and substituted in the iterative expression

$$f(\theta_{h,1}) = 0.4587 - \frac{-0.1012}{-3.4641} = 0.4294$$

Repeating the process, $f(0.4294) = -6.0549 \times 10^{-3}$, $f'(0.4294) = -3.0245$, and

$$f(\theta_{h,2}) = 0.4294 - \frac{-6.0549 \times 10^{-3}}{-3.0245} = 0.4274$$

Therefore, the 3 dB beamwidth is $2 \times 0.4274 \times 180/\pi = 48.98°$ and the error is $(52.56 - 48.98) \times 100/48.98 = 7.3\%$.

4.3.2 Radiation Pattern as a Fourier Transform of the Current Distribution

Since we have assumed that the current distribution is present only in the aperture and is zero elsewhere in the x-y plane, we can change the limits of integration in Eqn (4.29) to $-\infty$ to $+\infty$, without affecting the integrals, and look at the integral as a 2D Fourier transform of the distribution function. Thus, apart from a direction-dependent multiplying factor, the far-field radiation pattern of an aperture is mainly given by the 2D Fourier transform of the distribution function. This is an important observation useful in the design of the aperture antennas.

If we consider a separable type non-uniform current distribution over a rectangular aperture, the field pattern function can be written as a product of the Fourier transforms of the corresponding distribution functions in the x and y directions. A separable distribution is written as

$$M_x(x', y') = f(x')g(y') \tag{4.62}$$

For simplicity, we assume an x-directed magnetic current sheet over a rectangular aperture. Thus the field pattern function (apart from a constant) is

$$\mathcal{F}(k_x, k_y) = \iint_{S_a} f(x')g(y')e^{jk_x x' + k_y y'}\, dx'dy' \tag{4.63}$$

where we have used $k_x = k\sin\theta\cos\phi$ and $k_y = k\sin\theta\sin\phi$ as the angular or the transform domain variables. Because of the assumed separability of the current distribution, we can write this as

$$\begin{aligned}\mathcal{F}(k_x, k_y) &= \int_{-a/2}^{a/2} f(x')e^{jk_x x'}\, dx' \int_{-b/2}^{b/2} g(y')e^{jk_y y'}\, dy' \\ &= \mathcal{F}_x(k_x)\mathcal{F}_y(k_y)\end{aligned} \tag{4.64}$$

Therefore, the pattern can be written as a product of the patterns of the two 1D distributions in the x and y directions. It is important to note that while not all distributions are separable [i.e., can be written as in Eqn (4.62)], most often we come across separable distributions whose patterns are easier to visualize as a product of two patterns of 1D distributions. The slot and open-ended waveguide radiators discussed in the following sections have separable distributions. It may be noted that if an aperture distribution is not separable, it can always be represented as a sum of several separable

distributions. The final pattern also can be looked at as a sum of the products of several patterns of the constituent 1D distributions.

Consider an example of a separable distribution with a cosine distribution in the x-direction and uniform distribution in the y-direction on an aperture of dimensions a and b (with amplitude E_0 set to unity), i.e., $\mathbf{E} = \mathbf{a}_y \cos(\pi x/a)$ or $\mathbf{a}_x M_x = -\mathbf{n} \times \mathbf{E} = \mathbf{a}_x \cos(\pi x/a)$. The two 1D field patterns are obtained as the transforms of the current distributions

$$\begin{aligned} \mathcal{F}_x(k_x) &= \int_{-a/2}^{a/2} \cos\left(\frac{\pi x'}{a}\right) e^{jk_x x'} dx' \\ &= \frac{-\frac{a\pi}{2}\cos\left(\frac{k_x a}{2}\right)}{\left[\left(\frac{k_x a}{2}\right)^2 - \left(\frac{\pi}{2}\right)^2\right]} \end{aligned} \tag{4.65}$$

$$\begin{aligned} \mathcal{F}_y(k_y) &= \int_{-b/2}^{b/2} e^{jk_y y'} dy' \\ &= b\frac{\sin\left(\frac{k_y b}{2}\right)}{\left(\frac{k_y b}{2}\right)} \end{aligned} \tag{4.66}$$

Following the procedure explained in Section 4.3, it can be shown that the electric field components in the far-field region are given by

$$E_\theta = jk(1+\cos\theta)\sin\phi \frac{e^{-jkr}}{4\pi r}\mathcal{F}_x(k_x)\mathcal{F}_y(k_y) \tag{4.67}$$

$$E_\phi = jk(1+\cos\theta)\cos\phi \frac{e^{-jkr}}{4\pi r}\mathcal{F}_x(k_x)\mathcal{F}_y(k_y) \tag{4.68}$$

and the radiation intensity becomes

$$\begin{aligned} U(\theta,\phi) &= \frac{r^2}{2\eta}(|E_\theta|^2 + |E_\phi|^2) \\ &= \frac{1}{2\eta}\frac{k^2(1+\cos\theta)^2}{(4\pi)^2}|\mathcal{F}_x(k_x)|^2|\mathcal{F}_y(k_y)|^2 \\ &= \frac{1}{2\eta}\frac{k^2(1+\cos\theta)^2}{(4\pi)^2}\left|\frac{-\frac{a\pi}{2}\cos\left(\frac{k_x a}{2}\right)}{\left[\left(\frac{k_x a}{2}\right)^2 - \left(\frac{\pi}{2}\right)^2\right]}\right|^2 \left|b\frac{\sin\left(\frac{k_y b}{2}\right)}{\left(\frac{k_y b}{2}\right)}\right|^2 \end{aligned} \tag{4.69}$$

The normalized power pattern can be written as

$$P_n(\theta,\phi) = \frac{U(\theta,\phi)}{U_{\max}} = \frac{1}{4}(1+\cos\theta)^2 P_x(k_x) P_y(k_y) \tag{4.70}$$

where $U_{\max}$ is the maximum value of $U(\theta,\phi)$ which occurs for $\theta = 0$ and

$$P_x(k_x) = \left| \frac{-\left(\frac{\pi}{2}\right)^2 \cos\left(\frac{k_x a}{2}\right)}{\left(\frac{k_x a}{2}\right)^2 - \left(\frac{\pi}{2}\right)^2} \right|^2 \tag{4.71}$$

$$P_y(k_y) = \left| \frac{\sin\left(\frac{k_y b}{2}\right)}{\frac{k_y b}{2}} \right|^2 \tag{4.72}$$

The total pattern is a product of the two 1D patterns [Eqns (4.71) and (4.72)]. Since $k_x = k\sin\theta\cos\phi$ and $k_y = k\sin\theta\sin\phi$, the pattern $P_y(k_y) = 1$ for $\phi = 0$, and $P_x(k_x) = 1$ for $\phi = \pi/2$. Thus, $P_x(k_x)$ and $P_y(k_y)$ are the $\phi = 0$ and $\phi = \pi/2$ cuts of the complete pattern of the 2D distribution. Figure 4.8 shows the patterns P_x and P_y as functions of θ for a square aperture ($a = b = 5\lambda$). It is seen from the plots that a tapered distribution (distribution is tapered along x) produces lower side lobes than a uniform distribution, but with a wider main beam.

Beamwidth between the first nulls of P_x can be computed by equating P_x to zero, i.e., $P_x[(ka/2)\sin\theta] = 0$ or $\{\cos[(ka/2)\sin(\theta)]/[(ka/2)^2\sin(\theta) - (\pi/2)^2]\} = 0$ which gives $\theta = \sin^{-1}[3\lambda/(2a)]$. Note that $k_x a/2 = \pi/2$ or $\theta = \sin^{-1}[\lambda/(2a)]$ is not a zero, because the denominator of $P_x(k_x)$ also goes to zero. Hence, we can write the beamwidth between the first nulls (BWFN) as

$$\text{BWFN}|_{\phi=0} = 2\sin^{-1}\left(\frac{3\lambda}{2a}\right) \tag{4.73}$$

in the x-z plane and

$$\text{BWFN}|_{\phi=\pi/2} = 2\sin^{-1}\left(\frac{\lambda}{b}\right) \tag{4.74}$$

in the y-z plane. The half-power beamwidth is the angle between the two directions on either side of the main beam peak along which the power

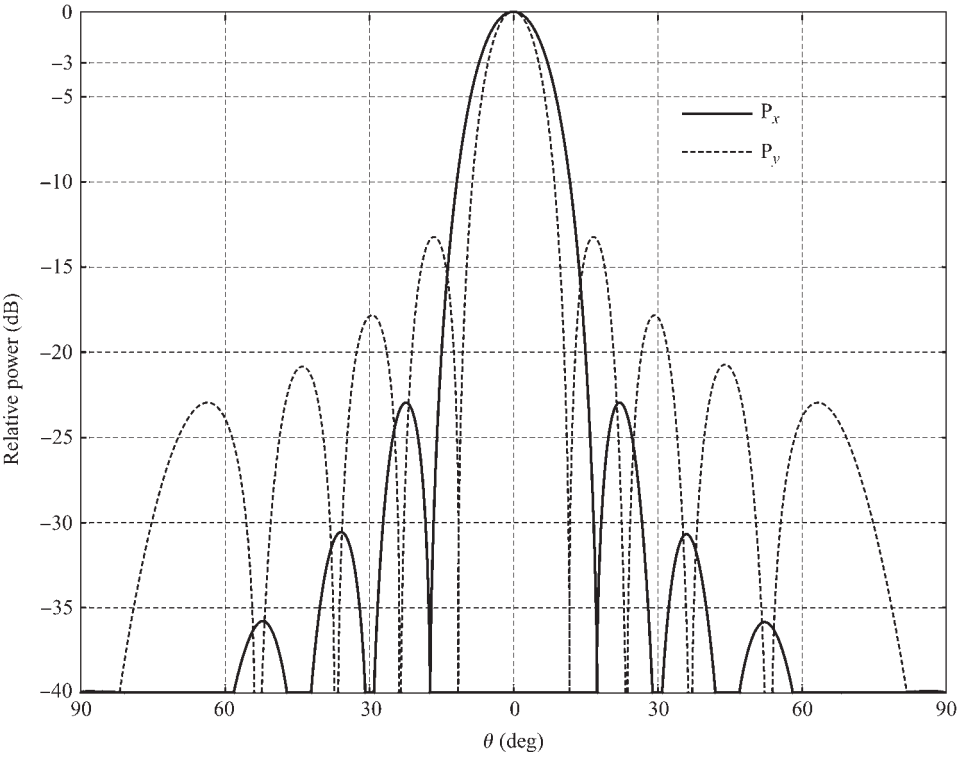

Fig. 4.8 Normalized patterns P_x and P_y of Eqns (4.71) and (4.72) with $a = b = 5\lambda$

radiated is half of that along the peak. Thus, equating $P_x(\theta) = P_x(0)/2$ and $P_y(\theta) = P_y(0)/2$ leads to the following equations

$$\frac{-\cos\left(\frac{ka}{2}\sin\theta\right)}{\left[\left(\frac{ka}{2}\sin\theta\right)^2 - \left(\frac{\pi}{2}\right)^2\right]} = \frac{2\sqrt{2}}{\pi^2} \tag{4.75}$$

for the $\phi = 0$ plane and

$$\frac{\sin\left(\frac{kb}{2}\sin\theta\right)}{\frac{kb}{2}\sin\theta} = \frac{1}{\sqrt{2}} \tag{4.76}$$

for the $\phi = \pi/2$ plane.

The half-power beamwidths in the two planes can be reduced to the formulae

$$\text{HPBW}|_{\phi=0} = 2\sin^{-1}\left(\frac{0.5945\lambda}{a}\right) \tag{4.77}$$

$$\text{HPBW}|_{\phi=\pi/2} = 2\sin^{-1}\left(\frac{0.4428\lambda}{b}\right) \tag{4.78}$$

for $a > 0.5945\lambda$ and $b > 0.4428\lambda$. It can be seen from Fig. 4.8 that the side lobe level of the pattern in the $\phi = \pi/2$ plane has the side lobe level of a $\sin X/X$ pattern discussed earlier in Fig. 4.7. The side lobe level of the $\phi = 0$ plane is much lower, while the main beam is wider than that of the uniform distribution. Using Eqn (4.69) the maximum radiation intensity along the z-axis can be written as

$$\begin{aligned} U_{\max} &= \frac{1}{2\eta}\left|\frac{-abk}{4}\frac{\cos\left(\frac{k_x a}{2}\right)}{\left(\frac{k_x a}{2}\right)^2 - \left(\frac{\pi}{2}\right)^2}\right|^2_{\theta=0} \\ &= \frac{1}{2\eta}\left\{\frac{2ab}{\pi\lambda}\right\}^2 \end{aligned} \tag{4.79}$$

with $X = k_x a/2 = 0$ at $\theta = 0$. The total radiated power can be calculated by integrating the Poynting vector over the aperture

$$\begin{aligned} P_{\text{rad}} &= \frac{1}{2\eta}\iint_S |E_a|^2 ds = \frac{1}{2\eta}\iint_S |\cos\left(\frac{\pi x}{a}\right)|^2 ds \\ &= \frac{ab}{4\eta} \end{aligned} \tag{4.80}$$

Using the definition of the directivity, $D_{\max} = 4\pi U_{\max}/P_r$, the directivity is

$$\begin{aligned} D_{\max} &= 4\pi\frac{\frac{1}{2\eta}\left\{\frac{2ab}{\pi\lambda}\right\}^2}{\frac{ab}{4\eta}} \\ &= \left(\frac{4\pi ab}{\lambda^2}\right)\left(\frac{8}{\pi^2}\right) \end{aligned} \tag{4.81}$$

Comparing this with the expression for a uniform distribution, the cosine distribution in one of the directions has reduced the gain by a factor

$(8/\pi^2) = 0.81$. We can consider $0.81ab$ as the effective aperture area, A_e, in the directivity expression, Eqn (4.61). In general any tapered distribution reduces the effective aperture and, hence, the directivity. The maximum directivity occurs for the uniform distribution. As seen from Fig. 4.8, the side lobe level reduces for a tapered distribution. It is a general observation that with increasing edge taper (i.e., the amplitude is higher at the center and steadily decreases as we move towards the edge) the side lobe level decreases. It can also be inferred that as we reduce the side lobe level by tapering the distribution, the beamwidth increases as the power from the side lobes is shifted to the main beam.

4.4 Expressions for a General Current Distribution

In the above analysis we have assumed that the current components J_y and M_x alone are present in the aperture. In general we may have all three components of the currents and we need to add the contributions of all the components to get the **E** and **H** fields. Given below are some general expressions for the far-fields when all the current components are present.

In general, if the current distribution $\mathbf{J}_s$ has all three components, J_x, J_y, and J_z, (M_x, M_y, and M_z for $\mathbf{M}_s$) giving rise to the corresponding vector potentials components, A_x, A_y, and A_z (F_x, F_y, and F_z for **F**). Inserting $\mathbf{J}_s = (\mathbf{a}_x J_x + \mathbf{a}_y J_y + \mathbf{a}_z J_z)$ in Eqn (4.23) and $\mathbf{M}_s = (\mathbf{a}_x M_x + \mathbf{a}_y M_y + \mathbf{a}_z M_z)$ in Eqn (4.24) we get

$$\mathbf{A} = \mu G \iint_S \{\mathbf{a}_x J_x + \mathbf{a}_y J_y + \mathbf{a}_z J_z\} e^{jkr' \cos\psi} ds' \tag{4.82}$$

$$\mathbf{F} = \epsilon G \iint_S \{\mathbf{a}_x M_x + \mathbf{a}_y M_y + \mathbf{a}_z M_z\} e^{jkr' \cos\psi} ds' \tag{4.83}$$

where

$$\begin{aligned} r' \cos\psi &= \mathbf{r}' \cdot \mathbf{a}_r \\ &= (\mathbf{a}_x x' + \mathbf{a}_y y' + \mathbf{a}_z z') \cdot (\mathbf{a}_x \sin\theta\cos\phi + \mathbf{a}_y \sin\theta\sin\phi + \mathbf{a}_z \cos\theta) \\ &= x' \sin\theta\cos\phi + y' \sin\theta\sin\phi + z' \cos\theta \end{aligned} \tag{4.84}$$

The vector potentials can be looked at as the 3D spatial Fourier transforms of the current distributions multiplied by a spherical wave function. In the far-field region only the θ and ϕ components of the **E** field are of interest

and these are approximated as

$$E_\theta = -j\omega(A_\theta + \eta F_\phi) \tag{4.85}$$

$$E_\phi = j\omega(A_\phi - \eta F_\theta) \tag{4.86}$$

The θ and ϕ components of $\mathbf{A}$ and $\mathbf{F}$ are obtained by the rectangular to spherical coordinate transformation [Eqn (4.31)]. Thus, for any arbitrary current distribution, the θ and ϕ components of $\mathbf{A}$ and $\mathbf{F}$ can be evaluated from the following integrals

$$A_\theta = \mu G \iint_S (J_x \cos\theta \cos\phi + J_y \cos\theta \sin\phi - J_z \sin\theta) e^{jkr' \cos\psi} ds' \tag{4.87}$$

$$A_\phi = \mu G \iint_S (-J_x \sin\phi + J_y \cos\phi) e^{jkr' \cos\psi} ds' \tag{4.88}$$

$$F_\theta = \epsilon G \iint_S (M_x \cos\theta \cos\phi + M_y \cos\theta \sin\phi - M_z \sin\theta) e^{jkr' \cos\psi} ds' \tag{4.89}$$

$$F_\phi = \epsilon G \iint_S (-M_x \sin\phi + M_y \cos\phi) e^{jkr' \cos\psi} ds' \tag{4.90}$$

The Poynting vector gives the power flow in the far-field region. Since we have only θ and ϕ components in the far-field, the time-averaged power flow can be computed from

$$\mathbf{S} = \frac{1}{2}\mathrm{Re}\{(\mathbf{a}_\theta E_\theta + \mathbf{a}_\phi E_\phi) \times (\mathbf{a}_\theta H_\theta + \mathbf{a}_\phi H_\phi)^*\} \tag{4.91}$$

$$= \mathbf{a}_r \frac{1}{2\eta}(|E_\theta|^2 + |E_\phi|^2) \tag{4.92}$$

4.5 Aperture in a Conducting Screen

Before we consider the treatment of aperture type antennas, let us first look at an ideal aperture problem—an opening in an infinite conducting plane. In general, the aperture or the opening can be of any shape but it is convenient to select regular shapes for apertures, such as the rectangular or circular shapes. Let the x-y plane be a perfect conducting plane with a rectangular opening of dimension $a \times b$, a along the x-direction and b along the y-direction, illuminated by a plane wave travelling in the z-direction, incident from the $z < 0$ side. To further simplify the analysis let the plane wave be linearly polarized in the y-direction. Thus, the incident field has only E_y and H_x components as shown in Fig. 4.9. The EM energy will propagate

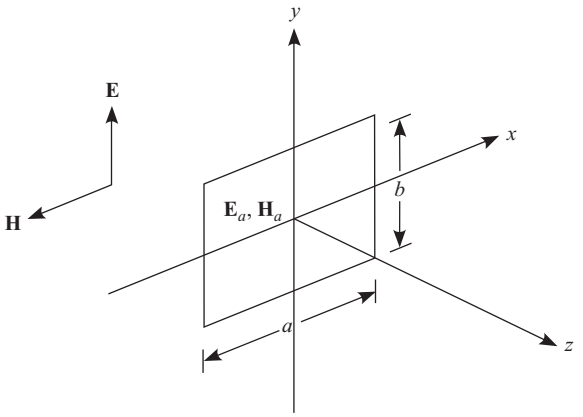

Fig. 4.9 Geometry of a rectangular aperture in an infinite conducting plane

through the aperture and set up **E** and **H** fields in the $z > 0$ region such that Maxwell's equations are satisfied on the conducting surface and everywhere else. The tangential **E** field is zero on the x-y plane except in the aperture. There will be a surface current density $\mathbf{J}_s$ on the conductor. An approximate field distribution is as shown in Fig. 4.10(a).

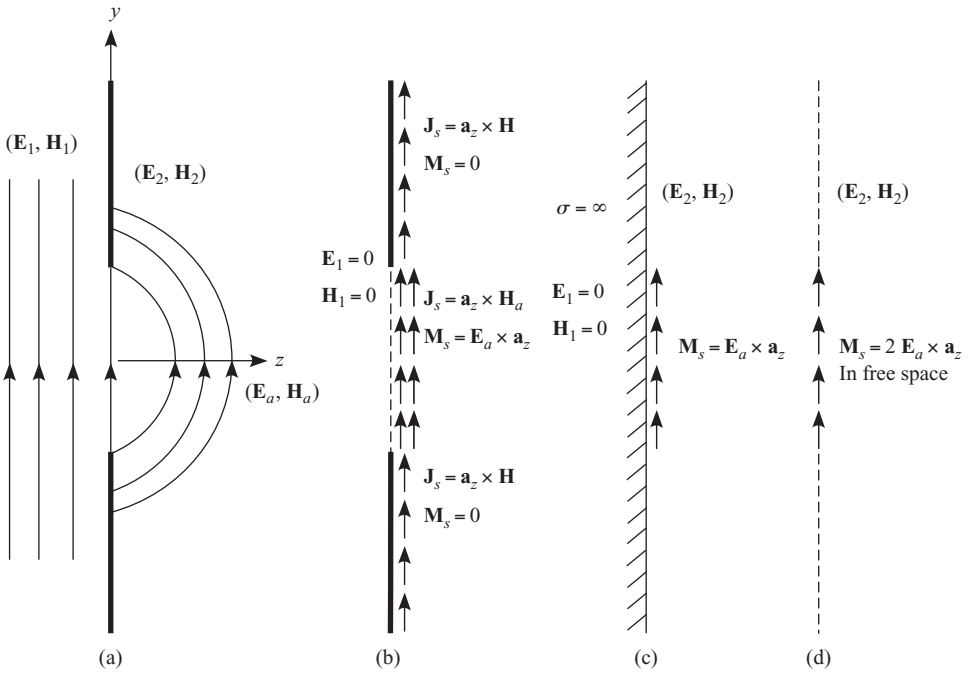

Fig. 4.10 Application of the field equivalence principle to an aperture in a conducting plane

Now, if we consider the $z > 0$ space enclosed by the x-y plane, the uniqueness theorem ensures that the fields everywhere in the $z > 0$ space are determined entirely by the tangential $\mathbf{E}$ or $\mathbf{H}$ on the bounding surface and the current distribution, $\mathbf{J}_s$, on the conducting surface visible from the $z > 0$ side. Figure 4.10(a) is the original problem shown edgewise and Fig. 4.10(b) is the equivalent problem after applying the field equivalence principle (first form). In the equivalent problem, the fields in the $z > 0$ space are completely determined by the equivalent current sheets $\mathbf{J}_s = \mathbf{a}_z \times \mathbf{H}_a$ and $\mathbf{M}_s = \mathbf{E}_a \times \mathbf{a}_z$ in the aperture and actual currents flowing on the rest of the conducting surface (here $\mathbf{E}_a$ and $\mathbf{H}_a$ are the fields in the aperture and $\mathbf{a}_z$ is the unit normal). The magnetic current on the conducting surface is zero because the tangential $\mathbf{E}$ is zero [Fig. 4.10(b)]. Thus, by applying the field equivalence principle we convert the original problem into a new problem in which the above indicated sheet current sources radiate in free space, producing the same fields in the $z > 0$ space and zero fields in the $z < 0$ region. We can evaluate the vector potentials $\mathbf{A}$ and $\mathbf{F}$ and then the $\mathbf{E}$ and $\mathbf{H}$ fields in the $z > 0$ region [Eqns (4.1)–(4.3) and (4.10)–(4.12)]. This, however, is possible only if we know the current distributions. Solving for the current distributions is as difficult as the original problem, especially for $\mathbf{J}_s$ on the conducting part of the surface. To overcome this difficulty we use the second form of the field equivalence principle and make the $z < 0$ region a perfect conductor. This closes the aperture surface making the entire x-y plane a perfect conductor. To sustain the field $\mathbf{E}_a$ in the aperture we introduce a magnetic current sheet $\mathbf{M}_s = \mathbf{E}_a \times \mathbf{a}_z$ just outside the aperture in the $z > 0$ side. The image of $\mathbf{J}_s$ in a conductor is odd and, hence, the source and the image add up to zero everywhere on the surface. Thus, the fields in the $z > 0$ space are completely determined by the magnetic current sheet $\mathbf{M}_s$ in front of a perfect conducting plane. To solve this problem we use the image theory. The image of a magnetic current in a perfect conductor is in the same direction as the original current and as the distance between the current sheet and the conductor tends to zero, the source and its image add to produce a current sheet $2\mathbf{M}_s$ radiating in free space [Fig. 4.10(c) and 4.10(d)]. The original problem is reduced to a magnetic current sheet, $\mathbf{M}_s = 2(\mathbf{E}_a \times \mathbf{a}_z)$, over the aperture surface radiating in free space. Now, we can use the free space integral expression for the electric vector potential $\mathbf{F}$ [Eqn (4.10)]. Of course we need to know $\mathbf{E}_a$ in the aperture.

Thus, the radiation from an aperture in an infinite conducting plane can be reduced to a magnetic current sheet, $\mathbf{M}_s = 2\mathbf{E} \times \mathbf{n}$ radiating in free space. The slot antenna, open-ended waveguide with a large flange, etc. fall in this category. For these types of antennas Eqns (4.41) and (4.40) are simplified

by deleting the contribution of A and multiplying the result by a factor of 2. The modified equations are

$$E_\phi = jkG2abE_0 \cos\theta \frac{\sin X}{X}; \quad \phi = 0 \text{ plane} \tag{4.93}$$

$$E_\theta = jkG2abE_0 \frac{\sin Y}{Y}; \quad \phi = \pi/2 \text{ plane} \tag{4.94}$$

4.6 Slot Antenna

The geometry of a rectangular slot in an infinite ground plane is similar to that shown in Fig. 4.9 except that the y-dimension of the slot, b, is small compared to the wavelength and the x-dimension, a, is of the order of half a wavelength. In order to use the equivalence theorem, we need to approximate the **E** field in the aperture. Since b is small compared to the wavelength, the slot can be considered to be a slot transmission line section shorted at both ends. The slot can be excited by a voltage source connected across the slot at the center point, at $x = 0$. The **E** field setup in the slot can be assumed to have only a y-component, E_y, with a constant distribution in the y-direction and a sinusoidal distribution in the x-direction with zero field at the shorted ends. It can be expressed as

$$\mathbf{E} = \mathbf{a}_y E_0 \cos\left(\frac{\pi x'}{a}\right); \quad \begin{matrix} -\dfrac{a}{2} \le x' \le \dfrac{a}{2} \\ -\dfrac{b}{2} \le y' \le \dfrac{b}{2} \end{matrix} \tag{4.95}$$

Hence, the magnetic sheet current of the equivalent formulation is given by

$$\mathbf{M}_s = 2\mathbf{E} \times \mathbf{a}_z = \mathbf{a}_x 2E_0 \cos\left(\frac{\pi x'}{a}\right) \tag{4.96}$$

or

$$M_x = 2E_0 \cos\left(\frac{\pi x'}{a}\right) \tag{4.97}$$

Inserting this in the electric vector potential expression [Eqns (4.89) and (4.90)] we get

$$\begin{aligned} F_\theta &= \epsilon G(\cos\theta\cos\phi) \iint_S M_x e^{jkr'\cos\psi} ds' \\ &= \epsilon G(\cos\theta\cos\phi) \iint_S 2E_0 \cos\left(\frac{\pi x'}{a}\right) e^{jkr'\cos\psi} ds' \end{aligned} \tag{4.98}$$

$$F_\phi = -\epsilon G \sin\phi \iint_S M_x e^{jkr' \cos\psi} ds'$$
$$= -\epsilon G \sin\phi \iint_S 2E_0 \cos\left(\frac{\pi x'}{a}\right) e^{jkr' \cos\psi} ds' \tag{4.99}$$

Carrying out the indicated integration in Eqns (4.98) and (4.99)

$$\iint_S \cos\left(\frac{\pi x'}{a}\right) e^{jkr' \cos\psi} ds'$$
$$= \iint_S \cos\left(\frac{\pi x'}{a}\right) e^{jk(x' \sin\theta \cos\phi + y' \sin\theta \sin\phi)} dx' dy'$$
$$= \int_{x'} \cos\left(\frac{\pi x'}{a}\right) e^{jk(x' \sin\theta \cos\phi)} dx' \int_{y'} e^{jky' \sin\theta \sin\phi} dy'$$
$$= -\frac{a\pi}{2} \frac{\cos X}{\left[X^2 - \left(\frac{\pi}{2}\right)^2\right]} b \frac{\sin Y}{Y} \tag{4.100}$$

where X and Y are defined by Eqn (4.30). Substituting the expressions for F_θ and F_ϕ in equations for the $\mathbf{E}$ field [Eqns (4.85) and (4.86)] we get

$$E_\theta = -\frac{\pi}{2} C \sin\phi \frac{\cos X}{\left[X^2 - \left(\frac{\pi}{2}\right)^2\right]} \frac{\sin Y}{Y} \tag{4.101}$$

$$E_\phi = -\frac{\pi}{2} C \cos\theta \cos\phi \frac{\cos X}{\left[X^2 - \left(\frac{\pi}{2}\right)^2\right]} \frac{\sin Y}{Y} \tag{4.102}$$

where $C = jabkE_0 e^{-jkr}/(2\pi r)$. H_θ and H_ϕ are obtained using Eqns (4.38) and (4.39), respectively.

Since the slot antenna is excited at the center and is open on both sides of the conducting plane, the radiation occurs equally on both sides of the conducting plane. Hence, the radiation pattern computed for the $z > 0$ space using the equivalent formulation is applicable to the $z < 0$ space also. Therefore, the pattern is symmetric about the $z = 0$ plane.

4.7 Open-ended Waveguide Radiator

An open-ended rectangular waveguide of inner dimensions $a \times b$ with a large conducting flange attached to the opening can be analysed in a similar way as a slot radiator. The main difference being that the radiation is in the

$z > 0$ region only. The field distribution in the rectangular aperture can be approximated to the field distribution of the dominant TE_{10} mode field. The waveguide opening radiates a part of the power incident from the $z < 0$ side in the TE_{10} mode and the rest is reflected back. Assuming the waveguide dimensions are selected such that only the TE_{10} mode propagates, we can assume the aperture fields to be a combination of the incident and reflected TE_{10} mode fields. The expression for the **E** field is the same as that given in Eqn (4.95), except for an additional factor $(1 + \Gamma)$, where Γ is the voltage reflection coefficient. Evaluation of the reflection coefficient is required only to compute the input characteristics of the antenna. For computing the radiation pattern, the distribution function, as given by Eqn (4.95), is sufficient. Applying the field equivalence principle and carrying out the analysis as in the previous section on slot antenna, we get the same expressions because the distribution is the same as that in a slot. Although this type of radiator is simple, the input reflection coefficient makes it unsuitable for practical use unless some matching elements are included in the antenna. Typical methods of matching an open-ended waveguide radiator to the input waveguide is to incorporate matching pins or cuts in the waveguide wall close to the open end of the waveguide. In a practical open-ended waveguide radiator there are currents flowing on the outer wall of the waveguide at the opening which perturbs the pattern. The assumed current distribution over the aperture is valid only if the open-ended waveguide is considered along with a large ground plane attached so that the tangential **E** field on the infinite plane is zero as assumed in the field equivalence formulation.

4.8 Horn Antenna

A horn antenna is a useful and simple radiator excited by a wave guide. Horn antenna is one of the most popular antennas used as a focal point feed in many reflector antennas discussed later in this chapter. Horn antenna is a natural extension of a wave guide. There are a variety of horn antennas such as the pyramidal horn, **E**-plane and **H**-plane sectoral horns, conical horn, corrugated horn, etc. Some of these are depicted in Fig. 4.11. Horn antennas are generally excited by a wave guide, although coaxial inputs can be provided with an additional wave guide-to-coaxial transition.

The two key criteria to be satisfied for an antenna to be useful are the input match and the required radiation pattern characteristics. The radiation characteristics are dependent on the current distribution on the antenna surface or the aperture and the input match, on how the transition from

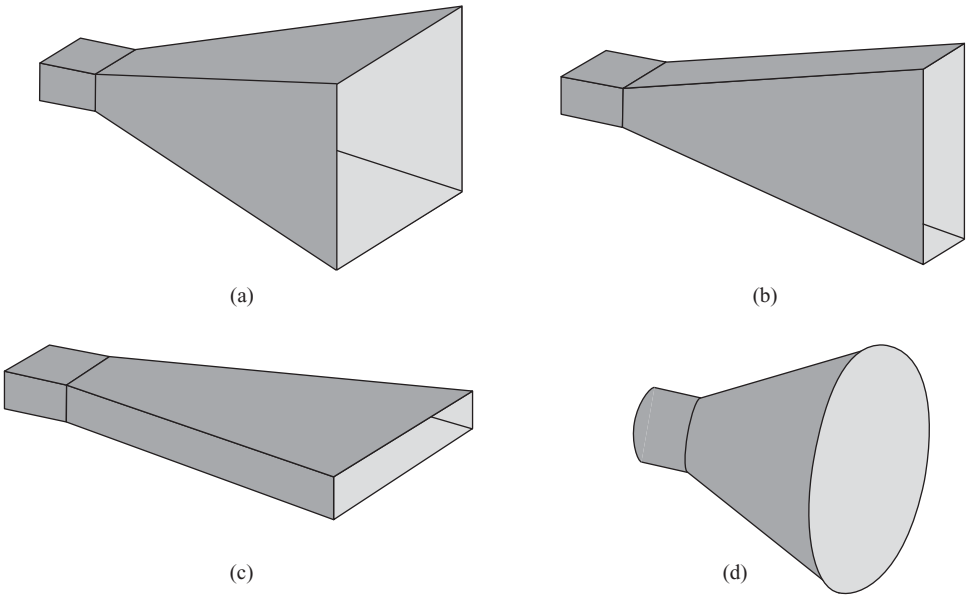

Fig. 4.11 Typical horn antennas—(a) pyramidal horn, (b) **E**-plane horn, (c) **H**-plane horn, and (d) conical horn

the input wave guide to the aperture is constructed. It is a well known fact in transmission line theory that if the cross-section of the transmission line is changed slowly, the reflection coefficient produced by the discontinuity can be made small over a wide band of frequencies. An additional advantage is that it is possible to approximate the field distribution at any cross-section in the wave guide by knowing the field distribution in the wave guide at the input. For example, a pyramidal horn [see Fig. 4.11(a)] is obtained by slowly expanding the rectangular wave guide cross-section to the aperture size. When the aperture size is large compared to the wavelength the wave impedance approaches the free space impedance, asymptotically. Thus, a pyramidal horn provides a slow transition from the wave guide impedance to the free space impedance, provided that the length of the transition is large compared to the wavelength. Given an aperture size and the wave guide size, the apex angle of the pyramid determines the length of the horn. For a good input match the apex angle must be small (large length). The aperture size and the field distribution (or the equivalent current distribution over the aperture) determine the pattern characteristics.

The pyramidal horn is one of the most important horn antennas. A detailed description of this antenna is given in Section 4.9.

4.9 Pyramidal Horn Antenna

The pyramidal horn antenna is one of the most often used horn antennas. The antenna is used as a primary feed for reflector antennas as well as standard gain reference antennas in antenna measurements. The pyramidal horn is obtained by flaring all four sides of a rectangular wave guide to form a pyramid-shaped horn with a rectangular aperture. The cross-sectional drawings of a typical pyramidal horn antenna are shown in Fig. 4.12.

In order to apply the field equivalence principle and obtain the far fields, we first need to approximate the field distribution over the aperture. For small flare angles, we assume the aperture fields to have a similar shape as that of the TE_{10} mode distribution in the exciting wave guide but with a phase variation over the aperture in both x and y directions. To determine the phase variation over the aperture we make several assumptions—(a) it is assumed that the wavefront is cylindrical with its phase center at the intersection line of the two flared sides as shown in Fig. 4.12, (b) the propagation constant within the horn section is assumed to be the same as the free space propagation constant, and (c) it is assumed that there are no higher order modes generated at the discontinuities at the wave guide to horn junction as well as at the horn aperture. All these assumptions are approximately correct for small flare angles but the deviations may be significant for large flare angles. In the x-z and y-z planes the phase centers are not necessarily at the same position. The radius of curvature of the phase front in the x-z plane is given by $r_{ox} = a/\{2\tan(\Psi_h/2)\}$ and in the y-z plane it is given by $r_{oy} = b/\{2\tan(\Psi_e/2)\}$, where Ψ_h and Ψ_e are the flare angles in the H and E planes, respectively. The phase of the field at $(x', 0)$ with respect to the centre of the aperture is given by the product of the path length difference and the propagation constant, k

$$\delta(x') = k\Big\{\sqrt{r_{ox}^2 + x'^2} - r_{ox}\Big\} \tag{4.103}$$

in the x-z plane and

$$\delta(y') = k\Big\{\sqrt{r_{oy}^2 + y'^2} - r_{oy}\Big\} \tag{4.104}$$

in the y-z plane. Combining these two, the phase variation over the aperture can be written as

$$\delta(x', y') = k\Big\{\sqrt{r_{ox}^2 + x'^2} - r_{ox} + \sqrt{r_{oy}^2 + y'^2} - r_{oy}\Big\} \tag{4.105}$$

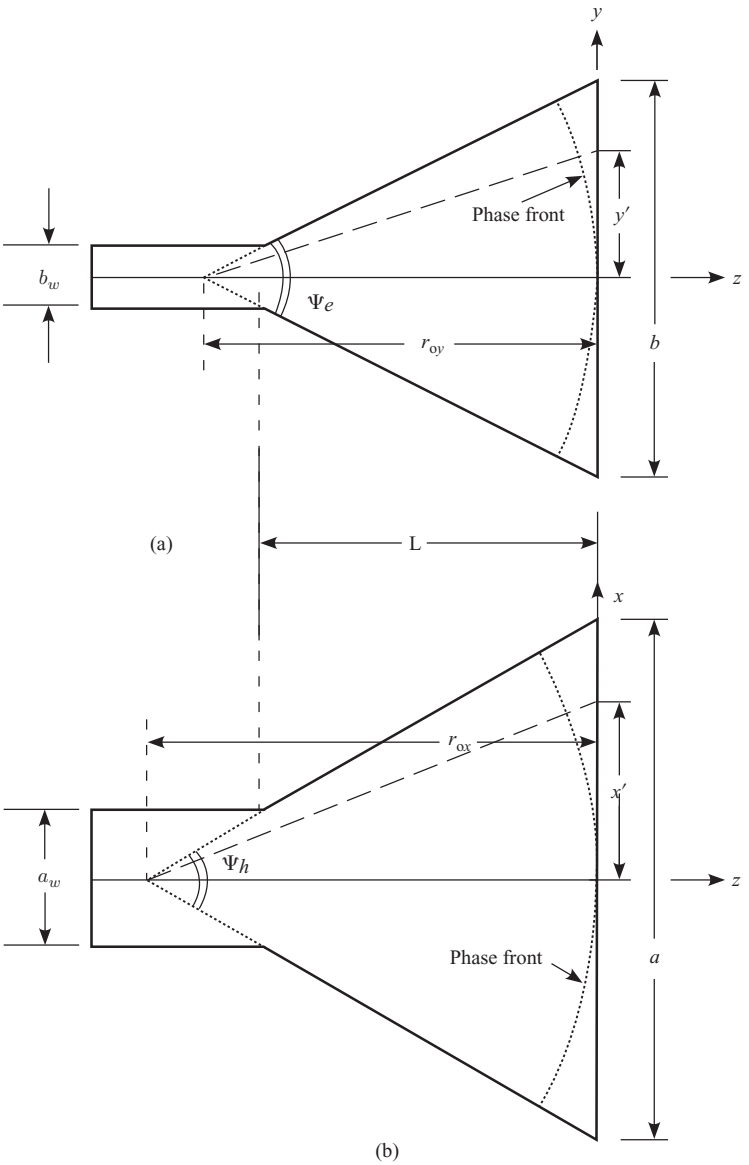

Fig. 4.12 Geometry of the pyramidal horn antenna (a) **E**-plane section (b) **H**-plane section.

For small flare angles, it is common practice to approximate the phase variation to a quadratic form and write the aperture tangential **E** and **H** fields as

$$E_y = E_0 \cos\left(\frac{\pi x'}{a}\right) e^{-jk[\frac{x'^2}{2r_{ox}} + \frac{y'^2}{2r_{oy}}]} \tag{4.106}$$

$$H_x = -\frac{E_0}{\eta} \cos\left(\frac{\pi x'}{a}\right) e^{-jk[\frac{x'^2}{2r_{ox}} + \frac{y'^2}{2r_{oy}}]} \tag{4.107}$$

Applying the field equivalence principle we convert these into equivalent magnetic and electric current sheets in the aperture, $M_x = -E_y$ and $J_y = H_x$, and the far-fields can be computed using the vector potential approach.

Because of the non-uniform phase over the aperture, the far-field computation is fairly complex and, hence, will not be discussed here. The far-field expressions of a pyramidal horn are somewhat similar to those of an open-ended waveguide with the a and b replaced by the horn aperture dimensions. Because of the non-uniform phase over the aperture, there is some degradation in the directivity, and some changes in the shape of the pattern. Specifically, the pattern nulls start filling up as the flare angle increases (or the phase variation increases).

For a given set of waveguide dimensions and the length of the horn, L, as we increase the flare angle, the aperture dimension as well as the phase error increases. These two have opposing effects on the directivity. The net effect is that, for a given length of the horn, there is an optimum flare angle for which maximum gain occurs. The optimum flare angle is different in the **E** and **H** planes because the amplitude distributions are different. In the **H**-plane the optimum flare angle is obtained when the maximum phase error (at the edge of the aperture in the **H**-plane) is equal to $3\pi/4$ and in the **E**-plane it occurs when the maximum phase error is $\pi/2$. The directivity loss factors for these phase errors are 0.8 and 0.77, respectively. Thus, if the horn is designed with optimum phase errors in both planes, we have a directivity expression given by

$$D = 0.8 \times 0.77 \times \frac{8}{\pi^2}\frac{4\pi ab}{\lambda^2} \simeq 0.5 \times \frac{4\pi ab}{\lambda^2} \tag{4.108}$$

The factor $(8/\pi^2)$ occurs due to the cosine amplitude distribution in the x-direction and the remaining factor $(4\pi ab/\lambda^2)$ is the directivity of a uniform distribution over the aperture of dimensions $a \times b$.

In practice, for a given set of wave guide dimensions, it may not be possible to satisfy optimum flare angle condition in both planes simultaneously. But one can choose one of the flare angles to be optimum and the other will generally be slightly less than the optimum. Generally, the losses in the horn are negligible, and hence we can assume the gain of the horn to be the same as the directivity. In a pyramidal horn design, typically the aperture dimensions are chosen to give a desired gain as per Eqn (4.108), and the length of the horn is minimized using the optimum flare angle criterion. Based on the maximum phase error for optimum directivity, we

can work out the optimum flare angles in the E and H planes as

$$\Psi_h = 2\tan^{-1}\left\{\left(\frac{3\lambda}{4r_{ox}}\right)^{1/2}\right\} \tag{4.109}$$

$$\Psi_e = 2\tan^{-1}\left\{\left(\frac{\lambda}{2r_{oy}}\right)^{1/2}\right\} \tag{4.110}$$

For the horn to be realizable, the horn length, L, must satisfy the following equations

$$L = \frac{a - a_w}{2\tan\Psi_h} \tag{4.111}$$

$$L = \frac{b - b_w}{2\tan\Psi_e} \tag{4.112}$$

where $a_w \times b_w$ are the wave guide dimensions and $a \times b$ are the aperture dimensions. These two equations may not be satisfied simultaneously but we select the longer of the two lengths and modify the flare angle in the other equation to satisfy both equations. We select the larger of the two lengths so that the flare angle is optimum in one plane and the phase error in the other plane is less than the optimum. Of course, we can select horn length much longer than the minimum length, in which case the directivity loss factor is less and we get a little more gain than predicted by Eqn (4.108). For a given horn aperture area, ab, the gain varies from $0.81\{4\pi ab/\lambda^2\}$ to $0.5\{4\pi ab/\lambda^2\}$; the factor 0.81 is for zero phase error ($L \to \infty$) and the factor 0.5 is for optimum length.

4.10 Reflector Antenna

In the analysis of aperture antennas it is observed that the far-field intensity pattern of an aperture antenna is essentially given by the 2D Fourier transform of the aperture distribution function, except for a broad weighting function $(1 + \cos\theta)$. The weighting function can be ignored for most narrow beam patterns. Hence for pattern computation, it is sufficient to know the field intensity distribution function over the aperture. The 3 dB beamwidth of a radiation pattern in a given plane is determined primarily by the antenna dimension in that plane; larger the dimension, smaller is the beamwidth. There is also a relationship between the aperture area and the directivity of the antenna, $D = (4\pi A_e/\lambda^2)$, where A_e is the effective area of the antenna. It is also observed that for a given

aperture size, the maximum directivity occurs for a uniform (in amplitude and phase) current distribution over the aperture. There are primarily two ways of achieving a large aperture for the antenna. In the transmit mode, we need to generate a nearly in-phase current distribution over a large area of the aperture and in the receive mode, the power from an incident plane wave from a specific direction should be collected over the same aperture area and added in-phase. From the reciprocity theorem, we know that the transmit and receive properties of an antenna are the same and hence, we can look at the antenna as a transmitter or a receiver. The two primary ways of achieving large aperture antennas are (a) using a large reflector and (b) using an array of small aperture antennas to cover the area. In this section we will discuss the first option. The second option of is discussed in Chapter 5.

As already discussed, the directivity of an antenna is directly related to the aperture size in terms of wavelength and the current distribution over the aperture. Thus, in order to get high directivity, it is not sufficient to make the antenna large but we also need to maintain a current distribution with near uniform phase over the aperture. One of the simplest ways of realizing a large aperture is to use a reflector along with a primary feed antenna of much smaller size. There is a large variety of reflector antennas. Some of the most common ones are flat-plate reflectors, corner reflectors, paraboloidal reflectors, Cassegrain reflector, offset-fed paraboloid, shaped-beam reflector, etc. In this section we will discuss some of these antenna configurations in detail.

There are two approaches to the computation of the fields of a reflector antenna—(a) the current distribution method and (b) the equivalent aperture method. In the current distribution method, we first compute the current distribution on the reflector surface from the incident **H** field and then, using the vector potential approach, compute the far-fields as an integral over the reflector surface. Although this method is more accurate, the evaluation of the integral over the parabolic surface is generally quite difficult and time consuming. In the equivalent aperture approach, the fields on an imaginary flat aperture surface in front of the reflector are approximated using geometric optics (GO) and converted to equivalent magnetic and electric current sheets and then the vector potential approach is used to find the far-fields. The integration is somewhat simpler because the surface is taken to be flat (the surface of the reflector projected onto a flat surface). The pattern computed with this method gives accurately the main lobe and the first few side lobes. This accuracy is generally sufficient for most applications. The far side lobes are not accurately predicted by this

method because it does not take into account the diffraction effects at the edges of the reflector, where the GO criteria is not satisfied. The accuracy of field computation can be improved by a method known as the geometric theory of diffraction (GTD), wherein the diffraction effect is added to the GO solution. However, in this book we shall limit our discussion to the GO solution, which is sufficient for most applications except the ones with very stringent pattern specifications. The GO solution is an approximation to the EM field solution as the wavelength tends to zero. This zero wavelength approximation is used in optics, where the dimensions of the lens and reflectors are large compared to optical wavelengths hence the name GO. The GO approximation can also be used at microwave frequencies provided that the radii of curvature of the wavefront and the reflecting surface are large compared to the wavelength and the currents at the edges are small. These are generally satisfied for most regions of large reflectors except at the edges.

The main principles in GO used are the ray concept and the inverse square law. In an isotropic homogeneous medium the EM waves propagate in straight lines and the power density falls off as inverse square of the distance as it propagates. The other principle used is Snell's law of reflection as derived for a plane wave incident on an infinite reflecting surface, which states that the angle of incidence and reflection are equal. If the radius of curvature of the reflecting surface as well as that of the wavefront is large compared to the operating wavelength, the reflector can be considered flat locally at every point and Snell's law of reflection can be applied. One point that is implicit in reflector analysis is the assumption that the reflector is made of a perfect electric conductor. In the following treatment of reflector antennas we shall make use of these principles.

4.10.1 Flat-plate Reflector

One of the first requirements in a directional antenna is to prevent radiation in the direction opposite to the main beam, which is normally termed as *back radiation*. This is easily accomplished by having a large, conducting flat-plate reflector behind the antenna. We know that if the reflector plane is infinite in extent, then the analysis is simple using the image principle, i.e., we can simply replace the reflector by another identical image antenna at an appropriate location and compute the fields. However, the reflector, in general, is finite in a practical antenna. If the reflector is sufficiently large, we can still use the image principle as a first approximation to the fields of the antenna. For more accurate fields we need to take care of the diffraction from

the edges of the reflector which produces back radiation. Using the image theory, the antenna with a reflector is equivalent to a two-element array with an out-of-phase excitation and a spacing equal to twice the distance between the reflector and the antenna. The reflector produces an increase in the directivity of the antenna depending on the spacing of the reflector from the antenna.

As an example, consider a half-wave dipole with a reflector backing at a distance d, as shown in Fig. 4.13. Assuming the reflector to be large, we apply the image principle and convert the problem to a two-dipole problem without the reflector. This problem is much easier to analyse as compared to the original problem. The two-dipole equivalent is also shown in Fig. 4.13.

The electric field in the far-field region of a z-directed thin dipole of length l, located at (x_0, y_0, z_0) and carrying a sinusoidal current of amplitude I_0, is given by (see Example 4.3)

$$\mathbf{E} = \mathbf{a}_\theta j\eta \frac{I_0}{2\pi} \frac{e^{-jkr}}{r} \frac{\cos\left(\frac{kl}{2}\cos\theta\right) - \cos\left(\frac{kl}{2}\right)}{\sin^2\theta} e^{jk(x_0 \sin\theta\cos\phi + y_0 \sin\theta\sin\phi + z_0\cos\theta)} \tag{4.113}$$

If the dipole is situated at $(0, d, 0)$, the electric field reduces to

$$\mathbf{E}_d = \mathbf{a}_\theta j\eta \frac{I_0}{2\pi} \frac{e^{-jkr}}{r} \frac{\cos\left(\frac{kl}{2}\cos\theta\right) - \cos\left(\frac{kl}{2}\right)}{\sin^2\theta} e^{jkd\sin\theta\sin\phi} \tag{4.114}$$

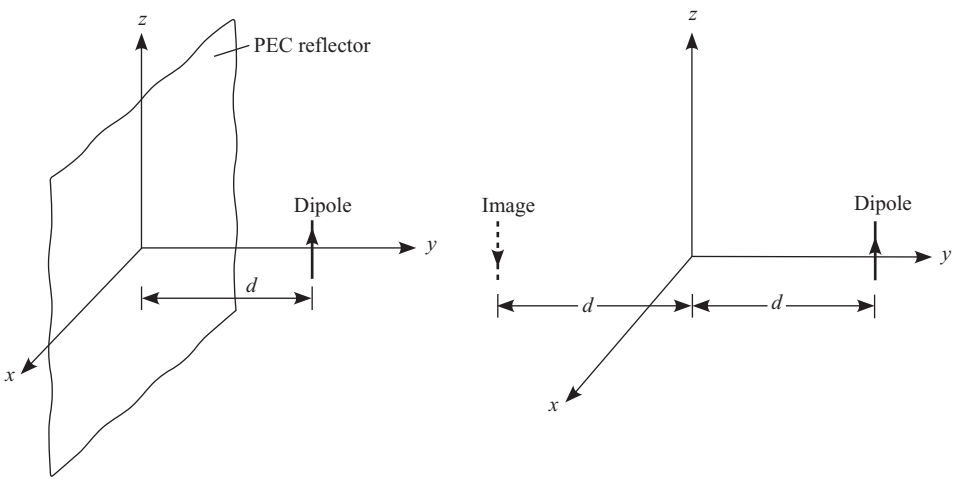

Fig. 4.13 Half-wave dipole in front of a flat-plate reflector and its equivalent

The image dipole is situated at $(0, -d, 0)$ and is carrying a sinuoidal current of amplitude $-I_0$. Therefore, the electric field due to the image dipole is

$$\mathbf{E}_i = \mathbf{a}_\theta j\eta \frac{-I_0}{2\pi} \frac{e^{-jkr}}{r} \frac{\cos\left(\frac{kl}{2}\cos\theta\right) - \cos\left(\frac{kl}{2}\right)}{\sin^2\theta} e^{-jkd\sin\theta\sin\phi} \tag{4.115}$$

The total field in the $y \geq 0$ region is given by the sum of the fields due to the actual dipole and its image

$$\mathbf{E} = \mathbf{a}_\theta j\eta \frac{I_0}{2\pi} \frac{e^{-jkr}}{r} \frac{\cos\left(\frac{kl}{2}\cos\theta\right) - \cos\left(\frac{kl}{2}\right)}{\sin^2\theta} (e^{jkd\sin\theta\sin\phi} - e^{-jkd\sin\theta\sin\phi})$$

$$= -\mathbf{a}_\theta \eta \frac{I_0}{\pi} \frac{e^{-jkr}}{r} \frac{\cos\left(\frac{kl}{2}\cos\theta\right) - \cos\left(\frac{kl}{2}\right)}{\sin^2\theta} \sin\{jkd\sin\theta\sin\phi\} \tag{4.116}$$

A plot of the pattern is shown in Fig. 4.14 for $d = \lambda/4$

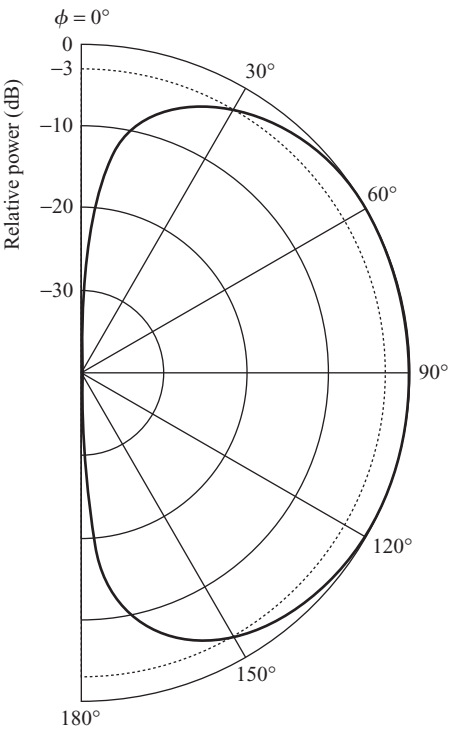

Fig. 4.14 x-y plane pattern of the half-wave dipole with a reflector shown in Fig. 4.13

In general, the finite reflector produces some back radiation due to the diffraction at the edges of the reflector, which has been ignored in this analysis.

EXAMPLE 4.3

A z-directed thin dipole located at (x_0, y_0, z_0) is carrying a current

$$I_z(z') = \begin{cases} I_0 \sin\left[k\left(\dfrac{l}{2} - z' + z_0\right)\right], & z_0 \le z' \le z_0 + l/2 \\ I_0 \sin\left[k\left(\dfrac{l}{2} + z' - z_0\right)\right], & z_0 - l/2 \le z' \le z_0 \end{cases}$$

Show that the electric field in the far-field region is given by

$$\mathbf{E} = \mathbf{a}_\theta j\eta \frac{I_0}{2\pi} \frac{e^{-jkr}}{r} \frac{\cos\left(\dfrac{kl}{2}\cos\theta\right) - \cos\left(\dfrac{kl}{2}\right)}{\sin^2\theta} e^{jk(x_0 \sin\theta\cos\phi + y_0 \sin\theta\sin\phi + z_0\cos\theta)}$$

Solution: The far-field approximation for R is $R \simeq r$ for the amplitude

$$\begin{aligned} R &\simeq r - \mathbf{r}' \cdot \mathbf{a}_r \\ &= r - (x' \sin\theta\cos\phi + y' \sin\theta\sin\phi + z'\cos\theta) \end{aligned}$$

and for the phase
At the centre of the dipole, $x' = x_0$ and $y' = y_0$ and hence

$$R = r - (x_0 \sin\theta\cos\phi + y_0 \sin\theta\sin\phi + z'\cos\theta)$$

The magnetic vector potential is given by

$$\begin{aligned} A_z &= \frac{\mu}{4\pi} \int_{z'=z_0-\frac{l}{2}}^{z_0+\frac{l}{2}} I_z(z') \frac{e^{-jkr}}{r} e^{jk(x_0 \sin\theta\cos\phi + y_0 \sin\theta\sin\phi)} e^{jkz'\cos\theta} dz' \\ &= \frac{\mu}{4\pi} I_0 \frac{e^{-jkr}}{r} e^{jk(x_0 \sin\theta\cos\phi + y_0 \sin\theta\sin\phi)} \\ &\quad \left[\int_{z'=z_0-\frac{l}{2}}^{z_0} \sin\left\{k\left(\frac{l}{2} + z' - z_0\right)\right\} e^{jkz'\cos\theta} dz' \right. \\ &\quad \left. + \int_{z'=z_0}^{z_0+\frac{l}{2}} \sin\left\{k\left(\frac{l}{2} - z' + z_0\right)\right\} e^{jkz'\cos\theta} dz' \right] \end{aligned}$$

Substituting $z' - z_0 = u$, we have

$$A_z = \frac{\mu}{4\pi} I_0 \frac{e^{-jkr}}{r} e^{jk(x_0 \sin\theta\cos\phi + y_0 \sin\theta\sin\phi + z_0\cos\theta)} \left[\int_{u=-\frac{l}{2}}^{0} \sin\left\{k\left(\frac{l}{2}+u\right)\right\} e^{jku\cos\theta} du + \int_{u=0}^{\frac{l}{2}} \sin\left\{k\left(\frac{l}{2}-u\right)\right\} e^{jku\cos\theta} du \right]$$

Integrating with respect to u and substituting the limits

$$A_z = \frac{\mu}{2\pi} I_0 \frac{e^{-jkr}}{r} e^{jk(x_0 \sin\theta\cos\phi + y_0 \sin\theta\sin\phi + z_0\cos\theta)} \frac{\cos\left(\frac{kl}{2}\cos\theta\right) - \cos\left(\frac{kl}{2}\right)}{k\sin^2\theta}$$

The electric field in the far-field region is given by

$$\begin{aligned} \mathbf{E} &= -\mathbf{a}_\theta j\omega A_\theta \\ &= \mathbf{a}_\theta j\omega A_z \sin\theta \end{aligned}$$

Substituting the expression for A_z and using the result $\omega\mu/k = \eta$, we get

$$\mathbf{E} = \mathbf{a}_\theta j\eta \frac{I_0}{2\pi} \frac{e^{-jkr}}{r} \frac{\cos\left(\frac{kl}{2}\cos\theta\right) - \cos\left(\frac{kl}{2}\right)}{\sin^2\theta} e^{jk(x_0 \sin\theta\cos\phi + y_0 \sin\theta\sin\phi + z_0\cos\theta)}$$

EXAMPLE 4.4

Derive an expression for the half-power beamwidth of the x-y plane pattern of a $\lambda/2$ dipole placed in front of a flat reflector as shown in Fig. 4.13. What is the half-power beamwidth if $d = \lambda/4$?

Solution: The electric field in the x-y plane is given by Eqn (4.116) with $\theta = \pi/2$.

$$\mathbf{E}(\pi/2, \phi) = -\mathbf{a}_\theta \eta \frac{I_0}{\pi} \frac{e^{-jkr}}{r} \left[1 - \cos\left(\frac{kl}{2}\right)\right] \sin(jkd\sin\phi)$$

The normalized pattern is given by

$$P_n(\phi) = \sin^2(kd\sin\phi)$$

If ϕ_h is the direction along which the power is half of the maximum, then

$$\sin^2(kd\sin\phi_h) = 0.5$$

Substituting $k = 2\pi/\lambda$, we get

$$\sin(\phi_h) = \frac{\lambda}{8d}$$

There are two solutions for this equation.

$$\phi_{h1} = \sin^{-1}\left(\frac{\lambda}{8d}\right)$$

$$\phi_{h2} = \pi - \sin^{-1}\left(\frac{\lambda}{8d}\right)$$

The half-power beamwidth is given by

$$\text{HPBW} = \phi_{h2} - \phi_{h1} = \pi - 2\sin^{-1}\left(\frac{\lambda}{8d}\right)$$

For $d = \lambda/4$

$$\text{HPBW} = \pi - 2\sin^{-1}\left(\frac{1}{2}\right) = 120^\circ$$

4.10.2 Corner Reflector

The corner reflector is an improvement over the flat-plate reflector and gives a higher directivity. A corner reflector is made up of two flat-plate reflectors joined together to form a corner. The corner reflector is generally used in conjunction with a dipole or dipole array kept parallel to the corner line. For a given included corner angle, there is an optimum dipole position for which the directivity is maximum. Corner reflectors are also used in the passive mode as efficient radar targets. A $\pi/2$ corner reflector has a unique property that a wave incident from any direction is reflected back in the same direction, thus providing a very effective back scatter cross-section for the radar. For the same reason, whenever the radar cross-section is to be minimized, as with aircrafts and ships, all corners are made smooth and rounded to minimize the back scatter.

The fields of a corner reflector excited by a current element or a distribution can be easily analysed using the image theory if the subtended angle $\alpha = \pi/n$, where n is an integer and the reflector is infinite. For finite size corner reflectors the image principle can still be applied to get approximate fields.

For simplicity of analysis, consider a $\pi/2$ corner reflector excited by a point source as shown in Fig. 4.15(a). For pattern computation we apply the image theory and convert the problem to a four-dipole array as shown in Fig. 4.15(c). Considering the corner line as the z-axis, the three images needed to produce fields that satisfy the conducting boundary conditions at the reflector plates are (a) two negative images of the point sources at $(0, d)$ and $(0, -d)$ and (b) one positive image at $(-d, 0)$, in the x-y plane. Here, d is the distance to the point source from the corner line. The equivalent antenna has four point sources with excitation currents as indicated and the reflector is removed [Fig. 4.15(c)]. Note that the four-source array also satisfies the conducting boundary conditions all along the extended reflector shown by dashed lines. Only the fields in the sector $-\pi/4 \leq \phi \leq \pi/4$ are the fields of the original problem. In the rest of the region the fields are zero. The field pattern can be written using superposition, as a sum of the fields due to each of the four sources. The patterns of four point sources are spheres with centers at the four locations. Summing the contributions

$$\begin{aligned} P(\theta, \phi) &= \left| e^{jkd \sin\theta \cos\phi} + e^{-jkd \sin\theta \cos\phi} - e^{jkd \sin\theta \sin\phi} - e^{-jkd \sin\theta \sin\phi} \right|^2 \\ &= 2 \left| \cos(kd \sin\theta \cos\phi) - \cos(kd \sin\theta \sin\phi) \right|^2 \end{aligned} \tag{4.117}$$

This expression is to be evaluated only in the sector $-\pi/4 \leq \phi \leq \pi/4$. If we replace the point source by a dipole oriented parallel to the corner line, we

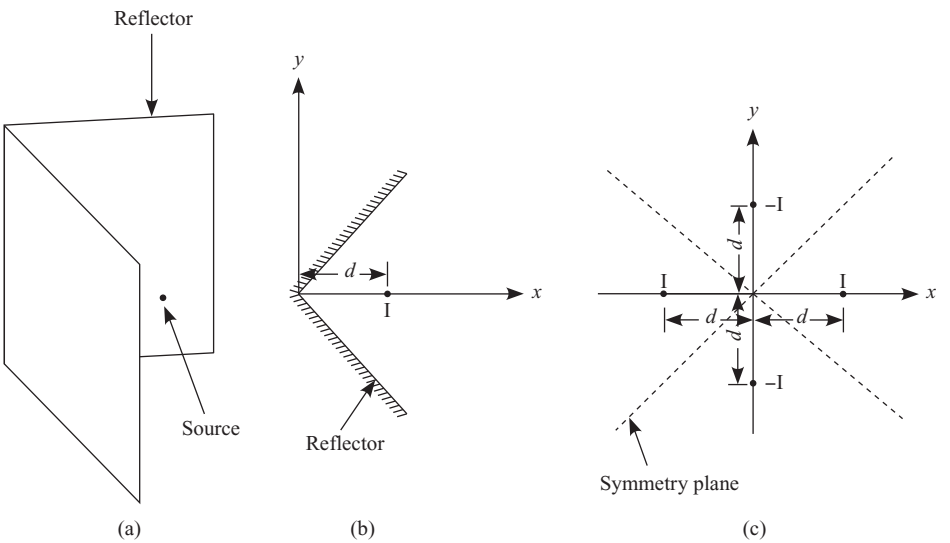

Fig. 4.15 (a) $\pi/2$ corner reflector with point source excitation, (b) plan view of the reflector and source, (c) its equivalent four-point source array

get an additional factor $\sin^2\theta$ in the pattern. The dipole pattern being a broad pattern, the final pattern is mainly controlled by the spacing, d. For $d < 0.7\lambda$, we get a single lobe in the sector $-\pi/4 \leq \phi \leq \pi/4$ with a maximum along $\phi = 0$, but for larger spacing there could be multiple lobes. A typical pattern for $d = 0.7\lambda$ is shown in Fig. 4.16.

For corner angles $\alpha = \pi/n$ (n is an integer), we can still use the image principle to reduce the problem to an array problem. For example, for $n = 3$ the corner angle is $\pi/3$ and we can force a periodic conducting boundary condition on planes $\phi = \pm\pi/6$, $\pm 3\pi/6$, and $\pm 5\pi/6$, by introducing 5 images at $\phi = \pm\pi/3$, $\pm 2\pi/3$, and π. The images at $\phi = \pm\pi/3$ and π are negative and the ones at $\pm 2\pi/3$ are positive. The radial distance of all the images is the same as the original dipole. The field solution is evaluated only in the $\phi = \pm\pi/6$ sector.

EXAMPLE 4.5

Calculate the spacing between the source and the corner of the reflector shown in Fig. 4.15 so that the radiation pattern has a null along the x-direction.

Solution: From Eqn (4.117), the condition for null along $(\theta, \phi) = (\pi/2, 0)$ is

$$|\cos(kd\sin\theta\cos\phi) - \cos(kd\sin\theta\sin\phi)|_{\substack{\theta=\frac{\pi}{2} \\ \phi=0}} = 0$$

which results in

$$\cos(kd) - 1 = 0$$

This corresponds to $kd = 2\pi$ or $d = \lambda$.

4.10.3 Common Curved Reflector Shapes

In this section we shall first discuss common reflector shapes and their properties and then go on to the discussion of some of the important reflector antennas.

Parabolic Cylinder A parabolic cylinder is a reflector shape whose cross-section in the x-y plane is a parabola and this cross-section is independent of z. This has an important property of converting a cylindrical wavefront into a plane wavefront after reflection. To simplify the understanding of this geometry and how it transforms the wavefronts, take an infinite cylindrical surface excited by a line source the cross-section of which is shown in

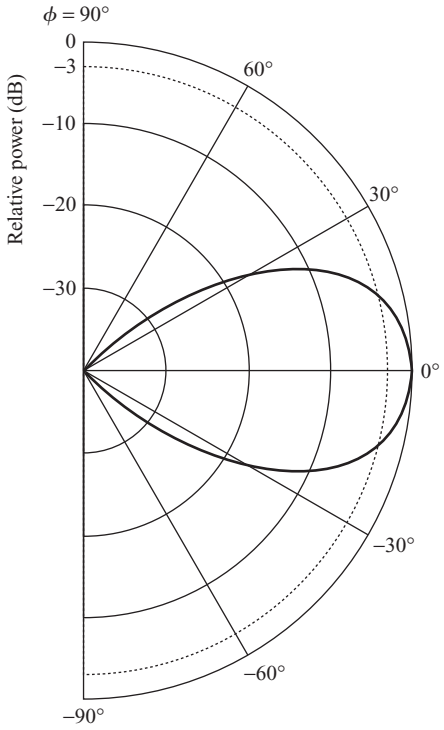

Fig. 4.16 Radiation pattern in the x-y plane of the corner reflector antenna shown in Fig. 4.15(b) for $d = 0.7\lambda$

Fig. 4.17. Referring to this figure, the line current source at point F radiates in all directions.

One such ray, FP, is shown as incident at a point $P(x, y)$ on the reflector, producing a reflected ray, PA. For generating an equi-phase front on the surface $x = x_0$, the total path length between the source point F and the point A on the aperture surface must be the same for each ray. Further the reflected rays must be parallel to the x-axis and the Snell's law must be satisfied at the reflection point, P. First, let us assume that the reflected rays are parallel to the x-axis and derive the expression for the reflector surface which makes the path length same for each ray. Let the point on the reflector be $P(x, y)$ and the line source coordinates be $(f, 0)$. A ray along the $-x$-direction will be reflected back to point B on the aperture surface. Equating the two path lengths we get

$$FO + OB = FP + PA \tag{4.118}$$

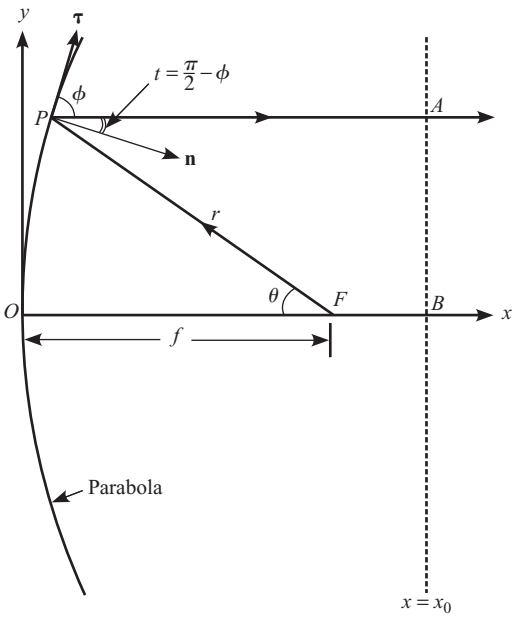

Fig. 4.17 Parabolic cylinder reflector excited by a line source at F

or in terms of the coordinates

$$f + x_0 = \{(f - x)^2 + y^2\}^{1/2} + (x_0 - x) \tag{4.119}$$

This can be simplified to

$$y^2 = 4fx \tag{4.120}$$

which is an equation to a parabola with f as the focal length. By differentiating it with respect to x, we get the slope of the tangent to the parabola at $P(x, y)$ as

$$\tan\phi = \frac{dy}{dx} = \frac{2f}{y} \tag{4.121}$$

Now, the angle $(\pi/2 - \phi) = t$ is the angle between the normal to parabola at $P(x, y)$ and the x-axis. Hence, by substituting $\phi = \pi/2 - t$ in Eqn (4.121), we can write $\tan(t) = y/(2f)$. If the ray FP makes an angle θ to the $-x$-axis, we can write

$$\tan\theta = \frac{y}{f - x} \tag{4.122}$$

$$= \frac{y}{f - \dfrac{y^2}{4f}} \tag{4.123}$$

$$= 2\frac{\dfrac{y}{2f}}{1 - \left(\dfrac{y}{2f}\right)^2} \tag{4.124}$$

$$= 2\frac{\tan t}{1 - \tan^2 t} \tag{4.125}$$

$$= \tan(2t) \tag{4.126}$$

or $\theta = 2t$, which shows that the normal makes an angle $-\theta/2$ with the x-axis. Hence, Snell's law is satisfied at the point of reflection on the parabolic cylinder surface.

Paraboloid A paraboloidal surface is generated by rotating the parabola about its axis. Consider a surface produced by rotating the parabola in Fig. 4.17 about the x-axis and excited by a point source kept at F with coordinates $(f, 0, 0)$. The point source radiates a spherical wavefront. From the symmetry of the spherical wavefront as well as the reflecting surface about the x-axis, it is easy to visualize that the spherical wavefront is converted to a plane wavefront after reflection. In order to produce a plane wavefront after reflection we again have to satisfy an equation similar to Eqn (4.119) but in 3D space. The point P can be any point on the surface and let (x, y, z) be the coordinates of the point P on the paraboloid. In 3D space we can write

$$f + x_0 = r + (x_0 - x) \tag{4.127}$$

where r is the distance between $P(x, y, z)$ and $F(f, 0, 0)$, given by

$$r = \{(f - x)^2 + y^2 + z^2\}^{1/2} \tag{4.128}$$

Substituting Eqn (4.128) into Eqn (4.127), squaring both sides, and simplifying, we get

$$y^2 + z^2 = 4fx \tag{4.129}$$

which is an equation to a paraboloid. From Fig. 4.17 we can write

$$x = f - r\cos\theta \tag{4.130}$$

Substituting this into Eqn (4.127) and rearraning we get the equation for the paraboloid in polar form as

$$r = \frac{2f}{1+\cos\theta} = f\sec^2\left(\frac{\theta}{2}\right) \tag{4.131}$$

With a similar analysis as in the case of the parabolic cylinder geometry, we can show that Snell's law is satisfied at the point of reflection on the paraboloid.

A paraboloidal reflector converts a spherical wavefront into a plane wavefront in the aperture plane. The aperture plane is normally taken as a plane passing through the focal point, $x = f$ plane, or any plane parallel to it.

Hyperboloid Another useful reflecting surface is a hyperboloidal surface that can convert a spherical wavefront into another spherical wavefront emanating from a virtual focal point. Here we use the convex surface of the hyperboloid, unlike the concave surface as in the paraboloid. A hyperboloid is a surface generated by rotating a hyperbola about its axis.

Consider the geometry shown in Fig. 4.18. A point source placed at point S on the x-axis radiates a spherical wavefront and is reflected by the convex surface of the reflector. A typical ray from the source point is incident on the reflector at point P and is reflected along PB. We extend the line PB backwards to intersect the x-axis at point F. Let B and A be points on a spherical wavefront (shown by dotted lines in Fig. 4.18) emanating from the point F. Select a point O exactly mid-way between points S and F as the origin of the coordinate system shown in Fig. 4.18, so that $SO = OF$. Now, for determining the shape of the reflector required to make the reflected wavefront have a phase center at F, the following conditions must be satisfied.

$$SP + PB = SC + CA = SO + OC + CA \tag{4.132}$$

From the geometry we have

$$PB = FB - FP \tag{4.133}$$

and

$$FB = FA \tag{4.134}$$

Substituting Eqns (4.133), (4.134), and $SO = OF$ into Eqn (4.132) and simplifying we get

$$SP - PF = 2OC \tag{4.135}$$

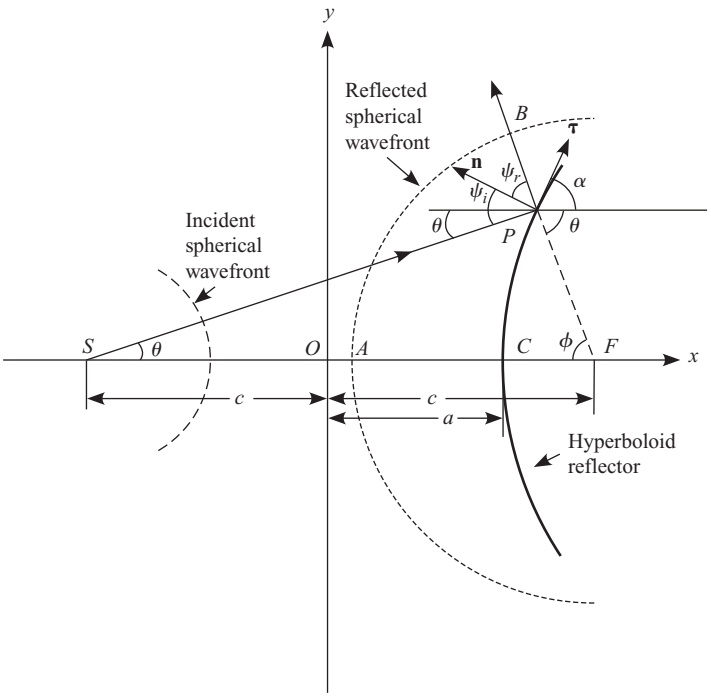

Fig. 4.18 Hyperboloidal reflector geometry with point source at S

which is an equation to a hyperbola. The hyperboloid is generated by rotating the hyperbolic shape in the x-y plane about the x-axis. Substituting the coordinates of the points from Fig. 4.18, $S(-c, 0, 0)$, $C(a, 0, 0)$, $F(c, 0, 0)$, and $P(x, y, z)$, we get

$$[(c+x)^2 + y^2 + z^2]^{1/2} - [(c-x)^2 + y^2 + z^2]^{1/2} = 2a \tag{4.136}$$

Carrying out some algebraic manipulation (see Exercise 4.14) we can reduce this to the standard form for a hyperboloid

$$\frac{x^2}{a^2} - \frac{y^2 + z^2}{c^2 - a^2} = 1 \tag{4.137}$$

It can be shown that Snell's law of reflection is satisfied at the reflection point (see Example 4.6). The two points S and F are the two focal points of the hyperbola. It is seen that a spherical wave emanating from point S appears as a spherical wave emanating from the virtual point F. It is also possible to use the concave surface of the reflector, i.e., if the point

source is kept at point F the reflected wavefront would appear to emanate from the other focal point S. There are some antenna configurations which use this result but most commonly known antennas use the convex surface as the reflecting surface. Although there are many more curved reflector surfaces such as spherical, ellipsoidal, etc., their use is limited to some special applications only. One of the important properties of reflectors is that they are frequency independent. The frequency limitation of the antenna is generally because of the feed. The reflector itself does not limit the bandwidth.

EXAMPLE 4.6

Prove that Snell's law is satisfied at P in Fig. 4.18.

Solution: For convenience, let us prove the result for $z = 0$. Differentiating Eqn (4.137) with respect to y, and rearranging

$$\frac{dy}{dx} = \tan\alpha = \frac{x}{y}\frac{c^2 - a^2}{a^2}$$

where α is the angle between the tangent to the hyperbola at P and the x-axis.

From Fig. 4.18, the angle of reflection is

$$\begin{aligned}\psi_r &= (\alpha + 90^\circ) - (180^\circ - \phi) \\ &= \alpha + \phi - 90^\circ\end{aligned}$$

Therefore

$$\tan\psi_r = \tan(\alpha + \phi - 90^\circ) = \frac{\tan\alpha\tan\phi - 1}{\tan\alpha + \tan\phi}$$

Substituting the expressions for $\tan\alpha$ and $\tan\phi = y/(c - x)$

$$\tan\psi_r = \frac{\left(\dfrac{x}{y}\dfrac{c^2 - a^2}{a^2}\right)\left(\dfrac{y}{c - x}\right) - 1}{\left(\dfrac{x}{y}\dfrac{c^2 - a^2}{a^2}\right) + \left(\dfrac{y}{c - x}\right)}$$

Simplifying

$$\tan\psi_r = \frac{yc(xc - a^2)}{x(c-a)(c^2-a^2) + a^2y^2}$$

From the equation to the hyperbola, we have $a^2y^2 = [x^2(c^2 - a^2) - a^2(c^2 - a^2)]$. Substituting, we get

$$\tan\psi_r = \frac{yc}{c^2 - a^2}$$

Similarly, we can write the angle of incidence as

$$\begin{aligned}\psi_i &= (180^\circ + \theta) - (\alpha + 90^\circ) \\ &= \theta - \alpha + 90^\circ\end{aligned}$$

and

$$\tan\psi_i = \frac{\tan\alpha\tan\theta + 1}{\tan\alpha - \tan\theta}$$

Substituting $\tan\theta = y/(c + x)$ and following a procedure similar to the one used for ψ_r, we can show that

$$\tan\psi_i = \frac{yc}{c^2 - a^2}$$

This proves that Snell's law is satisfied at P.

Parabolic Cylinder Antenna The parabolic cylinder reflector is the easiest to construct. A parabolic cylinder reflector can be made by taking a flat rectangular conducting sheet and bending it in a parabolic shape in one of the planes as shown in Fig. 4.19. Because of the cylindrical geometry, the excitation must be obtained using a line source kept parallel to the axis of the cylinder. Typically we can use a dipole or a linear array of dipoles or slots as the feed. A dipole feed is shown in Fig. 4.19. The reflector cross-section is a parabola in the $z =$ constant plane as shown. For simplicity of analysis, let us consider the cylinder to be infinite in the z-direction, and the excitation is by an infinite line source kept along the z-axis. This simplifies the problem to a 2D problem in the x-y plane. The cross-section of the antenna in the x-y plane is shown in Fig. 4.17.

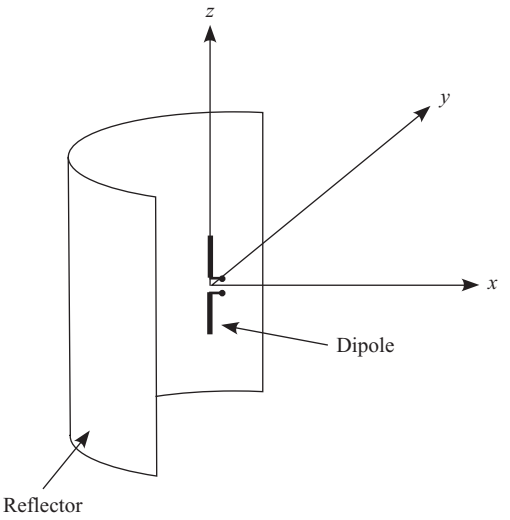

Fig. 4.19 Parabolic cylinder fed by a dipole

A parabolic cylinder converts a cylindrical wavefront to a plane wavefront. The amplitude distribution is determined by the angular radiation pattern of the line source. In a practical antenna, the line source is selected to radiate only towards the reflector, i.e., it is designed to have the main lobe in the sector covering the reflector and very small radiation outside it. The pattern beamwidth in the x-y plane is determined by the aperture dimension in the y-direction and the length of the cylinder determines the beamwidth in the x-z plane. In order to get a narrow beamwidth in the x-z plane the cylinder length as well as the line source need to be long. The design of long feed array offsets the simplicity of reflector fabrication. To limit the primary feed radiation pattern only to the sector covering the reflector requires a more complex feed design than a simple dipole. One of the disadvantages of this configuration is the large aperture blockage. From Fig. 4.17 it can be seen that a ray along the $-x$-direction after reflection travels right back to the feed point. To restrict the feed pattern to the angular sector covering the reflector, the feed antenna must have a certain width. Thus, the reflected rays within this width are blocked by the feed. This is known as aperture blockage. Aperture blockage reduces the directivity as well as increases the side lobe level. The complexity of the feed array design is also a disadvantage of the parabolic cylinder antenna. The field computation of a finite length cylinder excited by a finite length line source is a little involved and will not be attempted here.

Prime Focus-fed Paraboloidal Reflector A prime focus-fed paraboloidal reflector antenna is one of the most often used configurations because of its simplicity and advantages. A paraboloidal reflector converts a spherical

wavefront into a plane wavefront in the aperture plane. The aperture plane is normally taken as a plane passing through the focal point, $x = f$ plane, or any plane parallel to it. In a practical antenna, we need to restrict the radiation from the point source to a sector covering only the reflector, say $0 \leq \theta \leq \theta_m$, where θ_m is the maximum angle subtended by the reflector at the focal point. It is also necessary to produce a spherical wavefront with its center coinciding with the focal point of the paraboloid. This is generally achieved by another antenna such as a horn with a pattern specially designed to produce the desired illumination of the reflector. The primary feed, as it is called, is so located that its phase center coincides with the focal point. The phase center is defined as a virtual point from which the spherical wavefront appears to emanate.

The pattern of the horn feed is designed to produce the desired illumination amplitude distribution on the aperture after reflection. Although accurate field computation makes use of the current distribution method mentioned in the introduction, for most applications the equivalent aperture method is sufficient. The aperture distribution can be obtained from the knowledge of the feed horn pattern using the ray bundle concept.

Consider the geometry of a paraboloidal reflector shown in Fig. 4.20. The primary feed produces a spherical wavefront which, after reflection, is transformed to a plane wavefront (shown by dashed lines in Fig. 4.20) on the aperture plane. Let the intensity pattern of the feed horn be $g(\theta, \phi)$. The total power radiated in an elemental solid angle $d\theta d\phi$ after reflection illuminates the projected elemental area on the aperture $\rho\, d\rho\, d\phi$. Hence, we can equate these two

$$g(\theta, \phi) \sin\theta d\theta d\phi = p(\rho, \phi)\rho\, d\rho\, d\phi \tag{4.138}$$

where $p(\rho, \phi)$ is the aperture power density distribution and ρ is the radial coordinate of any point on the aperture. From the geometry of the paraboloid we also have

$$r \sin(\theta) = \rho \tag{4.139}$$

and the equation to the paraboloid is

$$r = \frac{2f}{1 + \cos\theta} = f \sec^2\left(\frac{\theta}{2}\right) \tag{4.140}$$

Combining, we have

$$\rho = \frac{2f \sin\theta}{1 + \cos\theta} \tag{4.141}$$

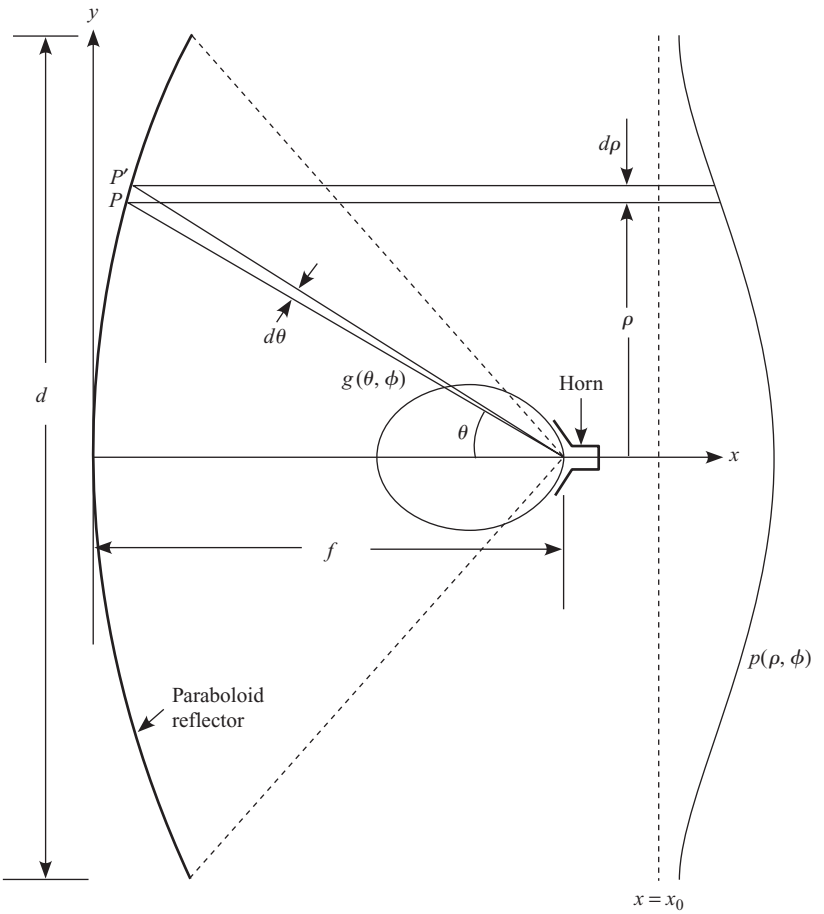

Fig. 4.20 Geometry of a prime focus-fed parabolid reflector

and differentiating with respect to θ

$$\frac{d\rho}{d\theta} = \frac{2f}{1+\cos\theta} \tag{4.142}$$

Substituting Eqn (4.142) in Eqn (4.138) we get

$$p(\rho,\phi) = g(\theta,\phi)\frac{(1+\cos\theta)^2}{4f^2} \tag{4.143}$$

Thus, it is easy to transform the primary horn pattern into the aperture distribution using Eqn (4.143). A 2D Fourier transform of the distribution gives us the field intensity pattern (square of the field intensity pattern is the power pattern). Because of the cylindrical coordinates assumed for the

circular aperture, we need to use the 2D Fourier transform in the polar form to compute the pattern (Balanis 2002).

There is a term called illumination taper efficiency, κ_t, often used in the context of reflector antennas. This is a measure of how well we are able to produce a uniform distribution on the aperture. We know that the directivity is maximum if the aperture distribution is uniform and it is equal to $(\pi d/\lambda)^2$ for a circular of diameter d. With a conventional horn antenna as a primary feed, the illumination at the edge tapers off compared to that at the center of the paraboloid. It is evident from Eqn (4.143) that it is difficult to obtain a uniform illumination because of the $(1 + \cos\theta)^2/4f^2$ term. If the aperture distribution is not uniform, we define the illumination taper efficiency as the ratio of the integral of the normalized aperture distribution to the aperture area.

Further, if the primary reflector forms a maximum subtended angle θ_m at the focus, the power radiated by the primary horn is not fully utilized in illuminating the reflector. The primary horn radiation outside the sector $\theta > \theta_m$ is not intercepted by the reflector. This loss of power, apart from producing some radiation on the back side of the reflector, also affects the overall gain of the antenna. This is called spill over loss. The ratio of the power intercepted by the reflector and the total power radiated by the feed horn is normally called the spill over efficiency, κ_s. In addition to reducing the gain of the antenna, the spill over loss also increases the noise temperature of the antenna if the spill over part of the primary horn pattern is pointed towards the earth. This is typically troublesome in radio astronomy or space communication link applications. In these applications the antenna is generally pointed towards the sky and the primary feed is pointing towards the earth. The earth being at 300 K, the noise received via the part of the primary feed pattern not intercepted by the reflector, increases the effective noise temperature of the antenna.

As shown in Fig. 4.20, the ray reflected from the vertex region of the paraboloid is blocked by the primary horn itself and does not reach the aperture plane. This is known as aperture blockage. The power reflected back into the primary horn appears as an input reflection coefficient or mismatch at the input. This can be taken care of by a matching element in the design of the horn. Sometimes it is taken care of by what is known as vertex plate matching. Because of the aperture blockage, the aperture distribution has a zero intensity region approximately equal to the projected area of the feed horn on to the aperture plane. There is a further loss of directivity and an increase in the side lobe level due to the aperture blockage. This is one of the drawbacks of the front fed paraboloid. In evaluating the pattern integral,

the blockage is normally taken care of by making the aperture distribution $p(\rho, \phi)$ zero in the region $0 < \rho < \rho_b$, where ρ_b is the radius of the blocked area (assumed to be circular).

It is generally observed that the illumination at the edges contributes more to the side lobes and hence, to reduce the side lobe level, it is necessary to keep the edge illumination low. Consequently, since there is a limited control on the radiation pattern shapes that can be obtained using a small aperture horn antenna, the illumination taper efficiency also reduces in the process of reducing the side lobes. Thus the overall efficiency is lower for a low side lobe antenna, while higher efficiency can be obtained if higher side lobes can be tolerated. Again, a trade-off is required because, to make the distribution near uniform, it becomes necessary to have a broader beamwidth for the horn so that the part of the pattern within the maximum angular sector θ_m subtended by the reflector is nearly flat. A broader primary horn pattern results in a smaller horn which is beneficial in reducing the aperture blockage. But the broader pattern increases the spill over loss. Thus, a compromise is generally required in the design of the feed horn.

Another important parameter that is often mentioned in the context of paraboloidal reflectors is the focal length to diameter ratio, typically called the f/d ratio. The importance of this parameter is in reducing the cross-polar radiation from the reflector. This is not apparent from the equivalent aperture analysis explained earlier. To understand the cross-polar performance of the antenna, we need to look at the induced currents on the reflector. The more accurate current distribution method mentioned in the introduction to this section is needed to predict the cross-polar performance of the reflector. However, here we will try to explain the effect in qualitative terms. If the antenna is designed for radiating an RCP wave, the LCP radiation is called the cross-polar radiation. The designed polarization is generally called the co-polar radiation. If the co-polar pattern is linearly polarized in the y-direction, then the x-polarized pattern is the cross-polar pattern. The cross-polar pattern is generally the unwanted part and in an ideal antenna we should have zero cross-polar radiation. However, in practical antennas, zero cross-polar radiation is not easy to achieve; it can only be minimized.

If the pattern of the primary horn is linearly polarized in the y-direction, the induced currents on the paraboloidal surface are primarily y-directed but will have a small orthogonal component because of the curvature of the surface. This component produces a cross-polar radiation. One way to minimize the cross-polar radiation is to have a large f/d ratio so that the curvature of the paraboloid is small. At microwave frequencies, generally

a small f/d ratio is preferred to keep the antenna depth small. The other alternative is to design a feed which reduces the cross-polar currents on the reflector and, hence, the cross-polar radiation. This leads to a more complex feed design such as the multi-mode and the corrugated horn structures. In applications requiring a large f/d ratio for the reflector, the depth of the front-fed reflector antenna becomes too large and the support structure also becomes bulky. Further, a long transmission line is required to connect a receiver or transmitter to the horn, which may lead to transmission losses and hence, worsen the noise performance of the system. In some applications a low noise amplifier is mounted along with the horn to minimize the overall noise figure of the system. These are some of the disadvantages of the front-fed reflector antenna. The Cassegrain configuration discussed in the next sub section overcomes some of these problems.

The power radiated in the cross-polar pattern of the antenna is essentially a loss for the system and can be considered as a reduction in the gain of the antenna. Thus, we can define a polarization efficiency factor, κ_x, to account for this loss. Two other factors that contribute to the reduction in the gain of a reflector antenna are the phase errors over the aperture and the surface irregularities of the reflector surface. As we have seen in the study of horn antennas, a pyramidal horn may not have a precise point phase center, or, in other words, the phase front of the radiated field may not be exactly spherical. The deviation from the spherical wavefront can cause non-uniform phase variations over the aperture after reflection from the paraboloid. An efficiency factor, κ_p, is used to account for the directivity loss due to the non-uniformity of the phase over the aperture. Further, there is always an accuracy with which a paraboloidal shape can be fabricated in practice. Another efficiency factor, κ_r, is used to account for the loss in gain due to the deviations in the reflector surface from the exact paraboloidal shape. This is generally termed as the random error efficiency. The overall aperture efficiency is a product of all these efficiencies. In general, depending on the illumination chosen, a practical prime focus-fed reflector antenna can have overall aperture efficiency from 60 to 85 percent.

A large aperture antenna design involves much more than just the design of the feed horn and the reflector surface geometry. A significant amount of the effort goes in the structural design of the antenna, the scanning mechanism, and the control system, etc., as these type of antennas are generally used in applications where the main beam direction needs to be adjusted or scanned. In some of the large paraboloidal antennas used at lower microwave frequency bands, the reflectors are made of wire grid rather than continuous metal plates. At longer wavelengths, a wire grid of sufficiently close wire

spacing (close in terms of wavelength) is as good as a continuous surface. The advantage of the wire grid structure is a lower weight as well as a lesser wind loading on the reflector. The wind loading is an important factor in outdoor antennas without any protective cover over it. An example of such an antenna, used in a large radio telescope antenna array at GMRT, Pune, is shown in Fig 1.2.

Cassegrain Reflector Configuration This is a dual reflector configuration using a hyperboloidal surface as a secondary reflector (or sub-reflector) and a paraboloid as a primary reflector as shown in Fig. 4.21. We have already seen how a hyperboloid converts a spherical wavefront emanating from one focal point into another spherical wavefront emanating from the virtual focal point. This principle is used to convert the primary wavefront from the horn antenna into a secondary spherical wavefront which is used to illuminate the primary paraboloidal reflector. The main advantage is that the primary feed horn and the associated receiver or transmitter can be located conveniently behind the main reflector. The necessity of running long transmission lines or wave guides is also eliminated. Further, the horn and the primary reflector are facing the same direction. Thus, if the antenna main beam is pointing towards the sky, the noise temperature of the sky being much lower than that of the earth, the noise picked up from the spill over lobes of the primary horn is also minimized. Since the horn feed is kept behind the main reflector (or projecting through a hole in the reflector), one can afford to have a much larger aperture for the horn, hence, a narrower beamwidth for the primary horn pattern. This also reduces the sub-reflector size. The virtual focus can be placed close to the sub-reflector so that the main reflector can have a small focal length and a large subtended angle at its focus. The Cassegrain configuration is equivalent to a prime focus-fed paraboloid shown by dashed lines in Fig. 4.21. This is an imaginary paraboloid of the same diameter as the main reflector fed by the same feed horn with the same subtended angle as the sub-reflector. As can be seen from Fig. 4.21, the angle, θ_m, subtended by the sub-reflector at its focal point S can be made much smaller than ϕ_m, the angle subtended by the main reflector at its focal point F by proper design of the sub-reflector and the horn. This makes the actual focal length, f_a of the main reflector much smaller than the equivalent focal length, f_e, of the equivalent prime focus fed paraboloid. Thus, the curvature of the equivalent paraboloid can be made much smaller than the actual reflector, since the effective focal length, f_e is larger. This results in reduced cross-polar radiation. Another advantage of the Cassegrain system is that the large equivalent focal length leads to an antenna system

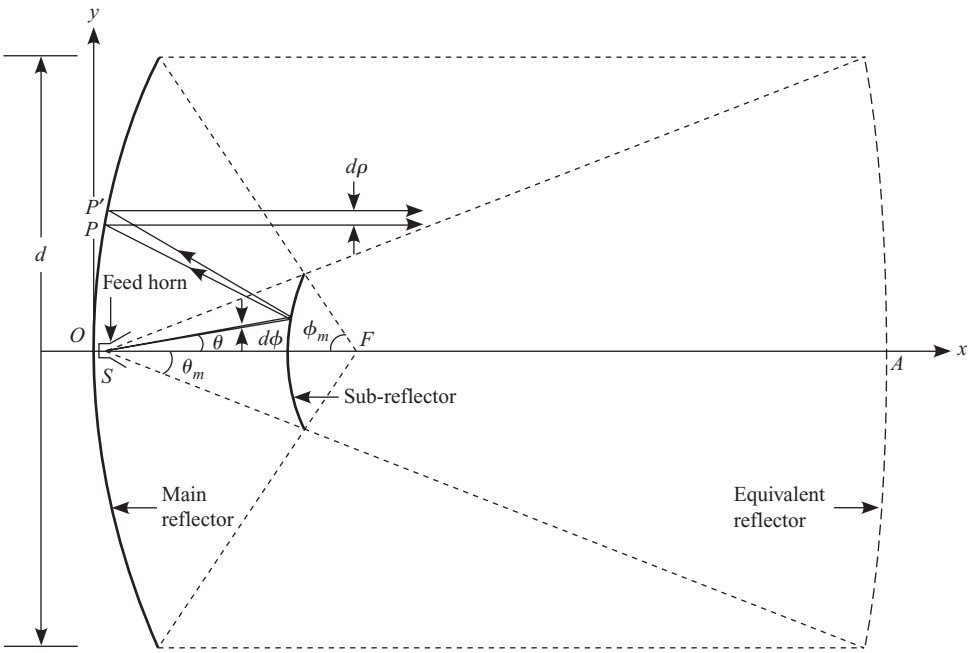

Fig. 4.21 Cassegrain reflector configuration ($OF = f_a$ and $SA = f_e$)

that tolerates much larger errors in the positioning of the primary feed horn without degrading the pattern, as compared to short focal length antenna. The main disadvantage of this configuration is the large aperture blockage by the sub-reflector, hence, the Cassegrain configuration is used only for very large aperture antennas having gain greater than 40 dB. A typical Cassegrain antenna used in satellite communication applications is shown in Fig. 1.1.

Lens Antennas Another class of antennas built using GO concepts are the lens antennas. In optics it is common to use glass lenses to focus the light or collimate the light rays as it is called. The convex lens is a typical example. The lenses work on the principle of refraction at a dielectric–air interface. By an appropriate choice of the refracting surface a spherical wavefront emanating from a point can be transformed into a plane wavefront or collimated as termed in optics. A typical convex lens is shown in Fig. 4.22. A light ray from a point source at F is refracted at two surfaces to emerge parallel to the axis on the other side. Similarly rays parallel to the axis of the lens incident from the right converge at the focal point F. The focal length is determined by the curvature of the lens surface.

The concept of the lens can also be used at microwave frequencies to make antennas. We are familiar with Snell's law of refraction. At a

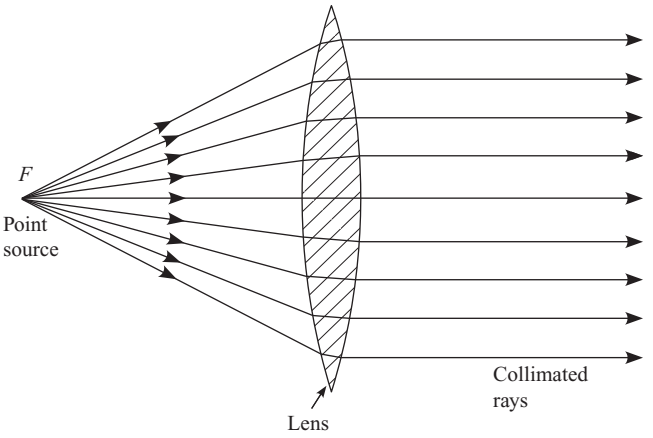

Fig. 4.22 A convex lens used in optics

dielectric–dielectric interface the Snell's law of refraction is given by

$$\frac{\sin\theta_t}{\sin\theta_i} = \sqrt{\frac{\epsilon_{r1}}{\epsilon_{r2}}} \tag{4.144}$$

where θ_i is the angle of incidence and θ_t is the angle of refraction or transmission, both measured with respect to the normal to the interface, and ϵ_{r1} and ϵ_{r2} are the relative dielectric constants of regions 1 and 2, respectively. The radiation is incident on the side of region 1.

For simplicity consider a single refracting surface lens shown in Fig. 4.23. In order that a spherical wavefront emanating from point F emerge as a plane wave on the other side of the lens antenna, the following conditions must be satisfied:

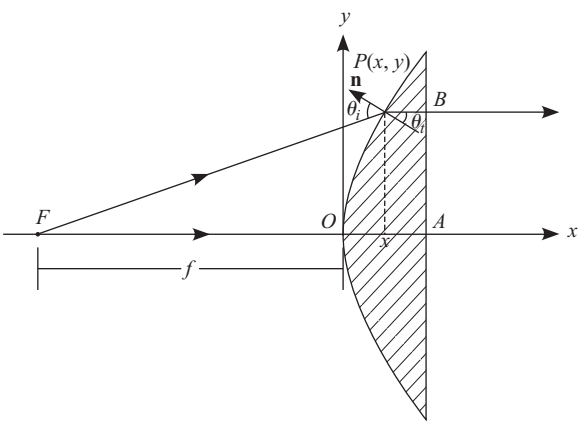

Fig. 4.23 Geometry of a single surface convex lens antenna

(a) The rays must emerge parallel to the axis after refraction at the first curved interface. The normal incidence on the second surface does not produce any refraction.
(b) The phase shift along the ray path $FP + PB$ must be same as that along $FO + OA$.
(c) Snell's law of refraction must be satisfied at the dielectric–air interface.

Assuming the dimensions of the lens and the radius of curvature to be large as compared to the operating wavelength, we can assume the propagation constant within the lens medium to be $k\sqrt{\epsilon_r}$, where ϵ_r is the dielectric constant of the lens material. The equation to the curved surface can be derived by equating the electrical path lengths along the rays indicated in Fig. 4.23.

$$kf + k\sqrt{\epsilon_r}x = k\sqrt{(f+x)^2 + y^2} \tag{4.145}$$

which can be rearranged to give

$$x^2(\epsilon_r - 1) + 2fx(\sqrt{\epsilon_r} - 1) - y^2 = 0 \tag{4.146}$$

This is an equation to a hyperbola. A rotation of the hyperbola about the x-axis gives the hyperboloidal surface for the lens antenna. An important advantage of the lens antenna is the absence of blockage. However, a lens is generally heavy and bulky. One of the methods used to reduce the bulk of the antenna is called zoning. The zoning of a lens antenna is illustrated in Fig. 4.24(a).

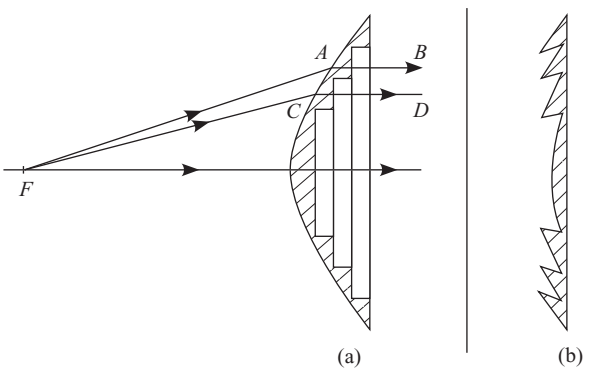

Fig. 4.24 Two methods of zoning in dielectric lens antennas—(a) zoning the non-refracting surface (b) zoning the refracting surface

The lens is divided into several circular zones and the dielectric material is removed from each zone such that the electrical path length between adjacent zones differs by an integer multiple of a wavelength. For example, the phase shift along the ray FAB and along FCD will differ by $2n\pi$ radians so that the phase front is not disturbed. However, this produces ring-like regions with the perturbed phase front falling in the transition region between zones. This is equivalent to an aperture blockage. An alternative way of zoning of a dielectric lens antenna is shown in Fig. 4.24(b). In this the dielectric material is removed from the refracting surface, resulting in a thinner lens antenna. The zoning concept remains the same.

Another problem with lens antennas is the reflection at the dielectric–air interface. From the study of the plane wave incident on a dielectric–air interface we know that the reflection coefficient at the surface for normal incidence is $\Gamma = (1 - \sqrt{\epsilon_r})/(1 + \sqrt{\epsilon_r})$, where ϵ_r is the relative dielectric constant of the lens medium. Because of this reflection a matching quarter wave transformer layer becomes necessary which limits the bandwidth of the lens antenna to the bandwidth of the matching layer.

The use of dielectric lens antennas at microwave frequencies is limited because of the drawbacks mentioned earlier and also due to the availability of better options such as reflector antennas. They are used in the higher end of the microwave spectrum and millimeter wave frequencies. The overall sizes of the antenna are smaller at these wavelengths and the advantages of lens antennas outweigh the disadvantages.

Another type of lens antenna occasionally used at microwave frequencies is the metal-plate lens antenna. This antenna is constructed using parallel metal plates spaced suitably to support the TE mode of propagation. The phase velocity of the TE mode in a parallel-plate waveguide is greater than the free-space phase velocity, c (Jordan and Balmain 1990). The phase velocity in a medium with a dielectric constant ϵ_r is $c/\sqrt{\epsilon_r}$. Since the phase velocity in the parallel plate waveguide is higher than the free-space velocity, the parallel plate medium can be considered to have an equivalent dielectric constant less than unity. A lens made of such a medium must have a concave refracting surface. This configuration retains most of the advantages of a lens antenna while reducing the weight of the antenna. The concept of zoning is also used in these antennas to reduce the depth of the lens.

Exercises

4.1 Show that the fields that exist outside the surface S shown in Fig. 4.2(c) and those shown in Fig. 4.1 are identical.

4.2 Show that the actual currents and their images illustrated in Fig. 4.4 satisfy the respective boundary conditions on the reflecting surface.

4.3 Using the representations

$$\mathbf{A}(r,\theta,\phi) = \{\mathbf{a}_r A_{r0}(\theta,\phi) + \mathbf{a}_\theta A_{\theta 0}(\theta,\phi) + \mathbf{a}_\phi A_{\phi 0}(\theta,\phi)\}(e^{-jkr}/r)$$

and

$$\mathbf{F}(r,\theta,\phi) = \{\mathbf{a}_r F_{r0}(\theta,\phi) + \mathbf{a}_\theta F_{\theta 0}(\theta,\phi) + \mathbf{a}_\phi F_{\phi 0}(\theta,\phi)\}(e^{-jkr}/r)$$

which are valid in the far-field region, derive Eqns (4.15) to (4.18) from Eqns (4.13) and (4.14).

4.4 Prove the result given in Eqn (4.28).

4.5 Show that

$$\mathcal{F}_x(k_x) = \int_{-a/2}^{a/2} \cos\left(\frac{\pi x'}{a}\right) e^{jk_x x'}\, dx'$$

$$= \frac{-\dfrac{a\pi}{2}\cos\left(\dfrac{k_x a}{2}\right)}{\left[\left(\dfrac{k_x a}{2}\right)^2 - \left(\dfrac{\pi}{2}\right)^2\right]}$$

4.6 An aperture in the x-y plane extends over $-a/2 \le x' \le a/2$ and $-b/2 \le y' \le b/2$. If the aperture fields are

$$\mathbf{E} = \mathbf{a}_y \cos\left(\frac{\pi x'}{a}\right)$$

$$\mathbf{H} = -\mathbf{a}_x \frac{1}{\eta}\cos\left(\frac{\pi x'}{a}\right)$$

show that the electric field components in the far-field region are given by

$$E_\theta = jk(1+\cos\theta)\sin\phi\frac{e^{-jkr}}{4\pi r} \times \mathcal{F}_x(k_x)\mathcal{F}_y(k_y)$$

$$E_\phi = jk(1+\cos\theta)\cos\phi\frac{e^{-jkr}}{4\pi r} \times \mathcal{F}_x(k_x)\mathcal{F}_y(k_y)$$

where $\mathcal{F}_x(k_x)$ and $\mathcal{F}_y(k_y)$ are the Fourier transforms of the current distributions in the x and y directions, respectivley. Determine $\mathcal{F}_x(k_x)$ and $\mathcal{F}_y(k_y)$.

4.7 In Problem 4.6, if the aperture fields are replaced by

$$\mathbf{E} = \mathbf{a}_y \sin\left(\frac{\pi x'}{a}\right)$$

$$\mathbf{H} = -\mathbf{a}_x \frac{1}{\eta}\sin\left(\frac{\pi x'}{a}\right)$$

derive expressions for the electric field components in the far-field region.

4.8 Verify the formulae for the half-power beamwidths given by Eqns (4.77) and (4.78) for a rectangular aperture with cosine distribution.

4.9 For given wave guide dimensions $(a' \times b')$, determine the a/b ratio to match the flare angles nearly to optimum, keeping the ab area same. $a \times b$ are the aperture dimensions.

4.10 Design a pyramidal optimum length horn for a gain of 16 dB at 3 cm wavelength with input guide of dimensions 22.86 mm × 10.16 mm and $a/b = 1.3$.

4.11 Reduce $\delta(x', y')$ given in Eqn (4.105) to a quadratic form (as in the exponent of Eqn (4.106) using the binomial expansion and ignoring the second and higher order terms.

4.12 Derive Eqns (4.109) and (4.110).

4.13 Compute the half-power beamwidth of the radiation pattern of an isotropic source placed in front of a $90°$ corner reflector at a distance of 0.7λ from the corner as shown in Fig. 4.15(a).

Answer: $27.4°$

4.14 Transfering the second term on the left hand side of Eqn (4.136) to the right hand side, squaring it, isolating the term within the square root, and once again squaring it, show that the equation reduces to Eqn (4.137).

CHAPTER 5

Antenna Arrays

Introduction

The radiation characteristics of an antenna depend on the current distribution. To an extent it is possible to control the current distribution by adjusting the geometry of the structure. For example, in a dipole antenna supporting a sinusoidal current distribution, the radiation pattern can be made more directional by increasing the length of the dipole. The amount of flexibility in adjusting the current distribution and hence the radiation pattern is limited. The restrictions arise because the current distribution has to satisfy certain conditions in order to exist on a structure. For example, when a voltage is applied to the terminals of a dipole, the current distribution on the dipole is set up by the forward and reflected waves such that the continuity condition and Maxwell's equations are satisfied everywhere. This leads to a sinusoidal distribution with a propagation constant k with zero current at the ends of the dipole. It is obvious from the analysis of the dipoles larger than λ that the current distribution is not only sinusoidal but also changes phase every $\lambda/2$ distance. Thus, to produce a stronger field along the broadside direction, we need to maintain an in-phase current distribution over a long length of the wire, which cannot be achieved by simply increasing the length of the dipole.

It is possible to change the nature of the distribution by modifying the structure (see Section 6.2). However, it is not easy to introduce arbitrary step changes in the current distribution. A step change can be introduced by incorporating a charge storage device (a capacitor) such that the current continuity condition is not violated.

Let us consider a method of maintaining the phase of the current source over a length which is several wavelengths long. Let this long line current distribution be produced by having several $\lambda/2$ dipoles arranged end-to-end and excited by in-phase currents. In fact, we can also excite each dipole

with a different amplitude and phase because they are independent. This arrangement of antennas is called a linear array. Each antenna is called an element of the array.

We can also arrange the antenna elements in 2D or a 3D space to form arrays. It is also possible to construct an array antenna using different types of elements. The pattern of the array is a superposition of the fields of the individual elements. However, introducing some order helps in simplifying the analysis. In general, array antennas are made of identical elements and arranged in some regular grid in a 2D plane or along a line. Further, the orientation of each element is also kept the same so that the array pattern expression is simplified.

In this book, we will be focussing on the linear array of antennas. In the next section, we show that for an array of equi-oriented identical elements, it is possible to compute the total pattern as a product of the radiation pattern of the element kept at the origin and an *array factor*.

5.1 Linear Array and Pattern Multiplication

Consider an infinitesimal dipole of length dl kept at a point $(0,0,z_1')$ in free space (Fig. 5.1). Let the z-directed current in the dipole be I_1. The fields produced by the dipole are computed using the vector potential approach.

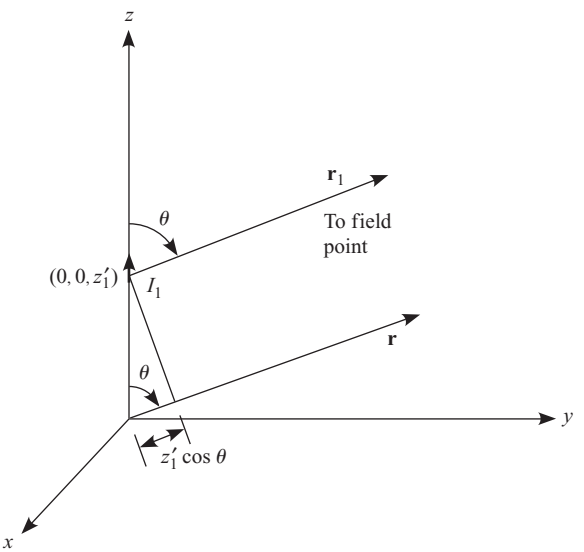

Fig. 5.1 Geometry of a z-directed, infinitesimal dipole radiating into free space

Since the dipole current is z-directed, the vector potential also has only a z-component which is given by

$$A_z = \frac{\mu}{4\pi} I_1 dl \frac{e^{-jkr_1}}{r_1} \tag{5.1}$$

where r_1 is the distance from the center of the current element to the field point (x, y, z). When the field point is at a large distance, we can approximate r_1 to

$$r_1 \simeq r \quad \text{for amplitude} \tag{5.2}$$

$$r_1 \simeq r - z_1' \cos\theta \quad \text{for phase} \tag{5.3}$$

Using the vector potential approach with these far-field approximations we get the electric field radiated by the dipole as

$$E_{\theta_1} = j\eta \frac{kI_1 dl}{4\pi} \sin\theta \frac{e^{-jkr}}{r} e^{jkz_1' \cos\theta} \tag{5.4}$$

Let us now consider N such infinitesimal, z-directed current elements kept along the z-axis at points $z_1', z_2', \ldots, z_N'$. Let the currents in these dipoles be $I_1,\ I_2,\ \cdots\ I_N$, respectively (Fig. 5.2). It is implied that all the currents have the same frequency. Using superposition, the field at any point can be

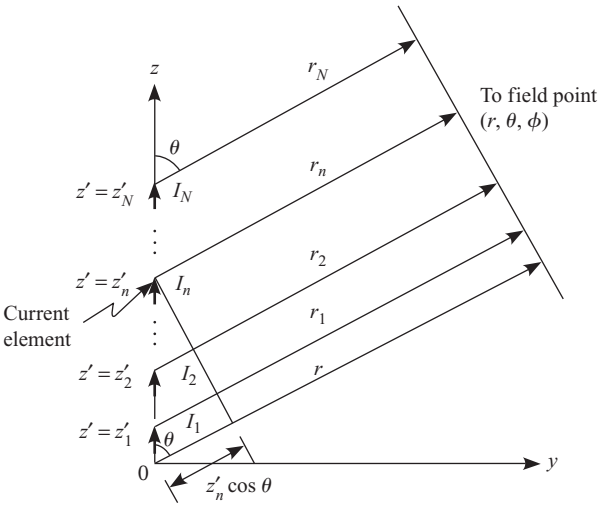

Fig. 5.2 Array of N z-directed, infinitesimal dipoles radiating into free space

written as a sum of the fields due to each of the elements.

$$E_\theta = E_{\theta_1} + E_{\theta_2} + E_{\theta_3} + \cdots + E_{\theta_N} \tag{5.5}$$

$$= j\eta k \frac{dl}{4\pi} \sin\theta \left[I_1 \frac{e^{-jkr_1}}{r_1} + I_2 \frac{e^{-jkr_2}}{r_2} + \cdots + I_N \frac{e^{-jkr_N}}{r_N} \right] \tag{5.6}$$

where, $r_1, r_2, \ldots, r_N$ are respectively the distances from the dipoles 1, 2, ..., N to the field point. In the far-field region of these dipoles, the distance from the nth dipole to the field point, r_n, is approximated to

$$r_n \simeq r; \quad n = 1, 2, 3, \ldots, N \text{ for amplitude} \tag{5.7}$$

$$r_n \simeq r - z'_n \cos\theta; \quad n = 1, 2, 3, \ldots, N \text{ for phase} \tag{5.8}$$

where z'_n is the location of the nth dipole. The r_1, r_2, $\cdots$ r_N in the denominator (amplitude) of Eqn (5.6) are replaced by r and in the exponent (phase term) they are replaced by Eqn (5.8). Now, we can take the (e^{-jkr}/r) term out of the bracket and write the total electric field as

$$E_\theta = \underbrace{j\eta \frac{kdl}{4\pi} \frac{e^{-jkr}}{r} \sin\theta}_{\text{Element pattern}} \underbrace{\sum_{n=1}^{N} I_n e^{jkz'_n \cos\theta}}_{\text{Array factor}} \tag{5.9}$$

The term outside the summation corresponds to the electric field produced by an infinitesimal dipole excited by a unit current kept at the origin and is known as the element pattern. The remaining portion of the equation is called the *array factor*. Thus the radiation pattern of an array of equi-oriented identical antenna elements is given by the product of the element pattern and the array factor. This is known as the *pattern multiplication theorem*.

$$\text{array pattern} = \text{element pattern} \times \text{array factor} \tag{5.10}$$

It can be shown that the pattern multiplication theorem is applicable to any array of identical, equi-oriented antenna elements. The elements can be arranged to form a linear, 2D or 3D array. The type, size, and position of the elements can be arbitrary, but all the elements must be identical and equi-oriented. The term equi-oriented emphasizes that only translation is allowed but not rotation. It is assumed that there is no interaction between the elements, which may result in altering the individual radiation patterns.

In the study of an array of identical antenna elements, it is sufficient to compute the array factor because the element pattern is generally a very broad pattern and the overall pattern is mainly controlled by the array factor. The array factor (AF) is given by

$$\text{AF} = \sum_{n=1}^{N} I_n e^{jkz'_n \cos\theta} \tag{5.11}$$

The array factor depends on the excitation currents (both amplitude and phase) and positions of the elements. Therefore, it is possible to achieve a wide variety of patterns having interesting characteristics by adjusting the excitation amplitudes, phases, and the element positions. In the next section, we will consider a two-element array and demonstrate the possibility of generating different radiation characteristics.

5.2 Two-element Array

Consider two infinitesimal z-directed current elements placed symmetrically about the origin along the z-axis (Fig. 5.3). Let dipole 1 be kept at $z'_1 = -d/2$ and carry a current $I_1 = I_0 e^{-j\alpha/2}$ and dipole 2 be at $z'_2 = d/2$ with a current $I_2 = I_0 e^{j\alpha/2}$. α is known as the relative phase shift. For positive values of α, the current in dipole 2 leads the current in dipole 1. The electric field of the two-element array can be computed using Eqn (5.6) with $N = 2$, which is

$$E_\theta = j\eta \frac{kdl}{4\pi} \frac{e^{-jkr}}{r} \sin\theta \left[I_0 e^{-j\frac{\alpha}{2}} e^{-jk\frac{d}{2}\cos\theta} + I_0 e^{j\frac{\alpha}{2}} e^{jk\frac{d}{2}\cos\theta} \right] \tag{5.12}$$

$$= \underbrace{j\eta \frac{kdl}{4\pi} \frac{e^{-jkr}}{r} \sin\theta}_{\text{Element pattern}} \underbrace{\left[2I_0 \cos\left(\frac{kd}{2}\cos\theta + \frac{\alpha}{2} \right) \right]}_{\text{Array factor}} \tag{5.13}$$

Consider a situation where the two currents are in phase with each other, (i.e. $\alpha = 0$). The array factor of the two-element array reduces to

$$\text{AF} = 2I_0 \cos\left(\frac{kd}{2}\cos\theta \right) \tag{5.14}$$

The array factors of a two-element array for different element spacings from 0.25λ to 2λ are shown in Fig. 5.4. As the element spacing increases from 0.25λ to 0.5λ, the main beam gets narrower. At $d = 0.5\lambda$, two nulls (along $\theta = 0^\circ$ and 180°) appear in the pattern. Further increase in the spacing

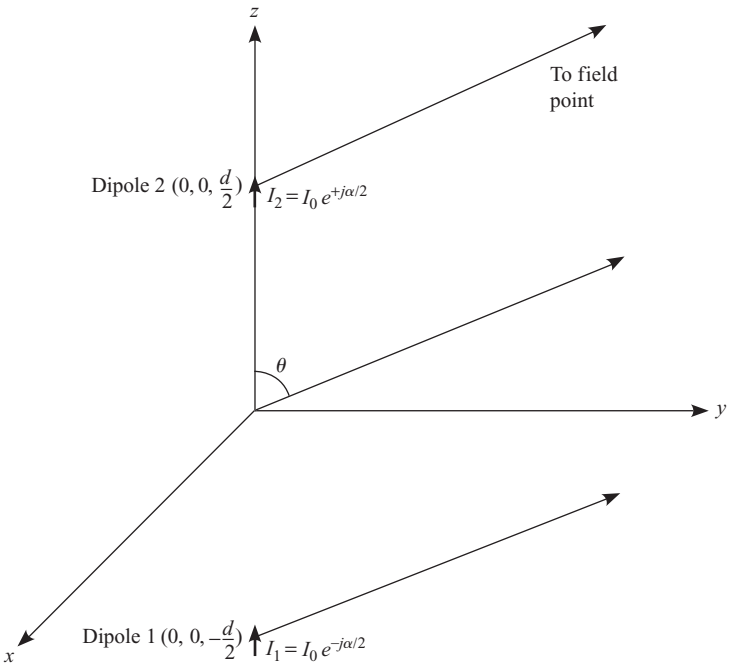

Fig. 5.3 Geometry of two z-directed, infinitesimal dipoles radiating into free space

results in the appearance of multiple lobes in the pattern. At $d = \lambda$, the pattern has three lobes, all of them having the same maximum level. Further increase in the element spacing results in a similar behaviour of narrowing of the main beam and appearance of more lobes. The pattern is independent of ϕ. Therefore, the 3D pattern will be rotationally symmetric about the array axis (Fig. 5.5).

We will now derive the expressions for the directions of the maxima and nulls of the array factor. The maxima of the array factor occur when the argument of the cosine function is equal to an integer multiple of π

$$\frac{kd}{2}\cos\theta|_{\theta=\theta_m} = \pm m\pi;\ m = 0, 1, 2, \ldots \tag{5.15}$$

where, θ_m are the directions of the maxima and can be written as

$$\theta_m = \cos^{-1}\left(\pm\frac{m\lambda}{d}\right);\ m = 0, 1, 2, \ldots \tag{5.16}$$

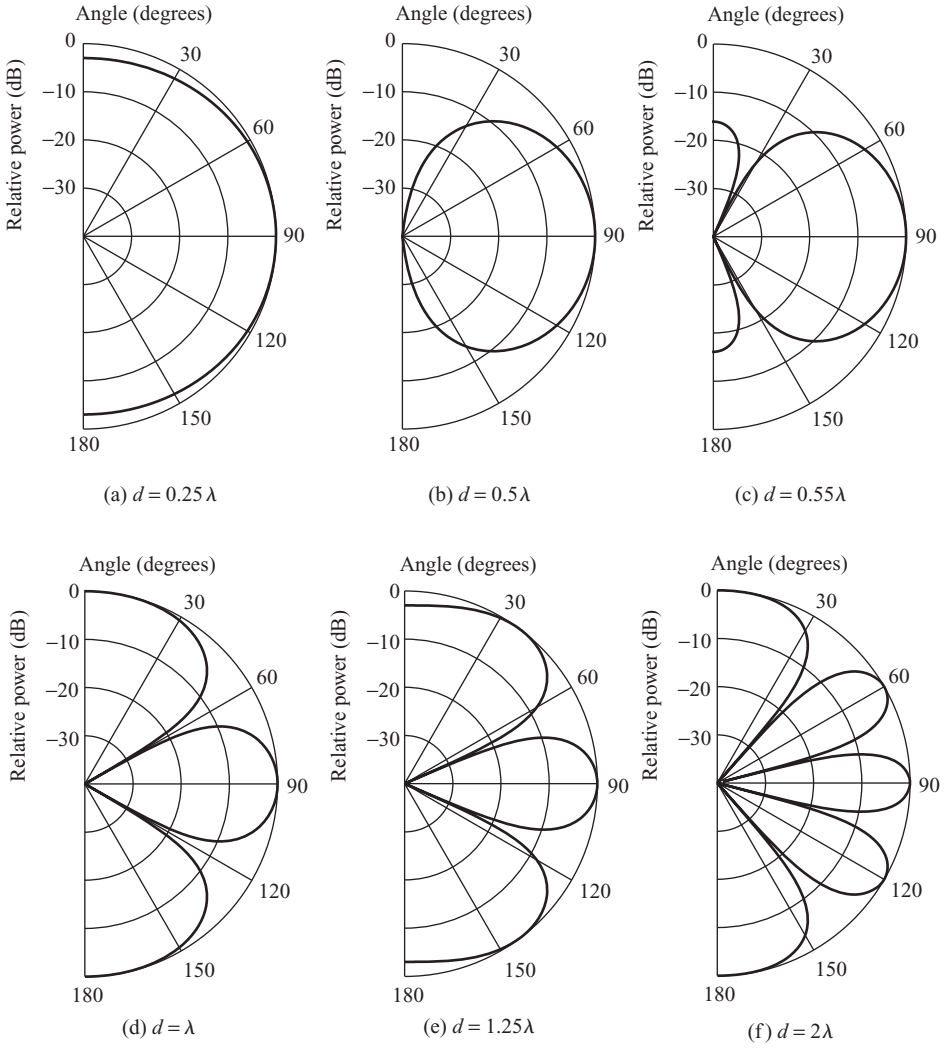

Fig. 5.4 Array factors of a two-element array with $\alpha = 0$ for some selected element spacings

For maxima to occur along the real angles, the argument of the cosine inverse function must be between -1 and $+1$

$$|\frac{m\lambda}{d}| \leq 1 \text{ or } m \leq \frac{d}{\lambda} \tag{5.17}$$

This implies that there is always a maximum corresponding to $m = 0$ which is directed along $\theta = \cos^{-1}(0) = 90°$. The number of maxima in the array factor depends on the spacing between the two elements. If the spacing

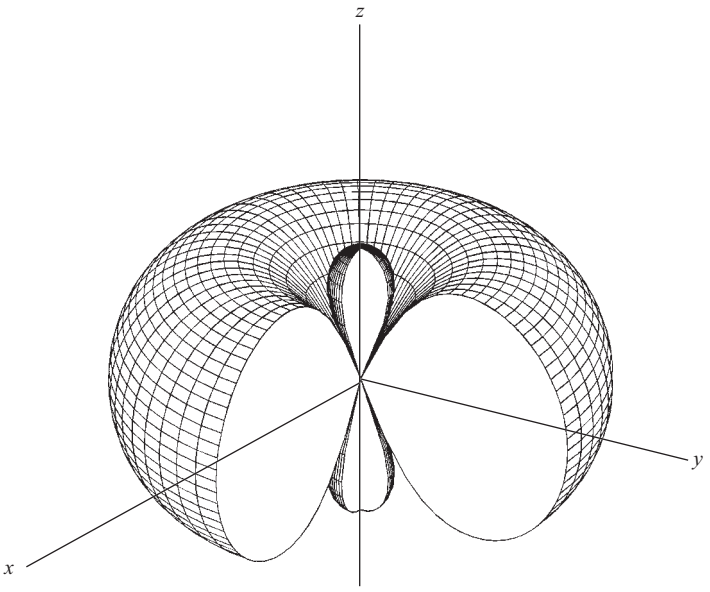

Fig. 5.5 A 3D depiction of the array factor of a two-element array with $\alpha = 0$ and $d = 0.55\lambda$. The array axis is along the z-direction

is less than a wavelength, there is only one maximum in the array factor [see Figs 5.4(a), (b), and (c)]. For spacings $p\lambda \leq d < (p+1)\lambda,\ p = 0, 1, 2, \ldots$, the array factor will have $(2p+1)$ maxima. For example, if the spacing is 2λ, the array factor has 5 maxima [see Fig. 5.4(f)]. The array factor always has a maximum along the $\theta = 90^\circ$ direction or the broadside direction, hence the array is known as *a broadside array.*

The nulls, θ_n, of the array factor satisfy the condition

$$\cos\left[\frac{1}{2}(kd\cos\theta_n)\right] = 0 \tag{5.18}$$

Therefore, the directions of the nulls are given by

$$\theta_n = \cos^{-1}\left[\pm\frac{(2n-1)\pi}{kd}\right];\ n = 1, 2, \ldots \tag{5.19}$$

For the nulls to occur along the real angles, we must have

$$\left|\pm\frac{(2n-1)\pi}{kd}\right| \leq 1;\ n = 1, 2, \ldots \tag{5.20}$$

which gives the condition

$$n \leq \left(\frac{d}{\lambda} + \frac{1}{2}\right) \tag{5.21}$$

For a null to appear in the pattern, the spacing between the elements must be at least equal to $\lambda/2$, and corresponding nulls appear along $\theta = 0$ and π. For spacings $(p\lambda + \lambda/2) \leq d < ((p+1)\lambda + \lambda/2), p = 1, 2, \ldots$, there are $2(p+1)$ nulls in the pattern. For example, if $d = 2\lambda$ the pattern has 4 nulls.

The element pattern of an infinitesimal dipole is shown in Fig. 5.6(a), and the array factor of a two-element array with an inter-element spacing of $\lambda/2$ is shown in Fig. 5.6(b). The array pattern, which is a product of the element pattern and the array factor is shown in Fig. 5.6(c). In this example the array pattern has a narrower beam compared to the array factor.

Consider a two-element array with an inter-element spacing of λ. For this array, the array factor has maxima along $\theta = 0, \pi/2$, and π [Fig. 5.6(e)]. Since the element pattern has nulls along $\theta = 0$ and π [Fig. 5.6(d)], the array pattern has only one maximum along $\theta = \pi/2$ and side lobes along $\theta = 36.65°$ and $\theta = 143.35°$ [Fig. 5.6(f)].

Excitation with a non-zero phase shift Consider two infinitesimal dipoles as shown in Fig. 5.3, carrying currents $I_1 = I_0 e^{-jkd/2}$ and $I_2 = I_0 e^{jkd/2}$, i.e., the current in dipole 2 is leading that in dipole 1 by a phase shift kd. The array factor is obtained from Eqn (5.13) with $\alpha = kd$ as

$$\text{AF} = 2I_0 \cos\left\{\frac{kd}{2}(1 + \cos\theta)\right\} \tag{5.22}$$

The array factor has a maximum when the argument of the cosine function is equal to an integral multiple of π

$$\frac{kd}{2}(1 + \cos\theta_m) = \pm m\pi;\ m = 0, 1, 2, \ldots \tag{5.23}$$

Therefore, the directions along which maxima occur are

$$\theta_m = \cos^{-1}\left(\frac{\pm 2m\pi - kd}{kd}\right);\ m = 0, 1, 2, \ldots \tag{5.24}$$

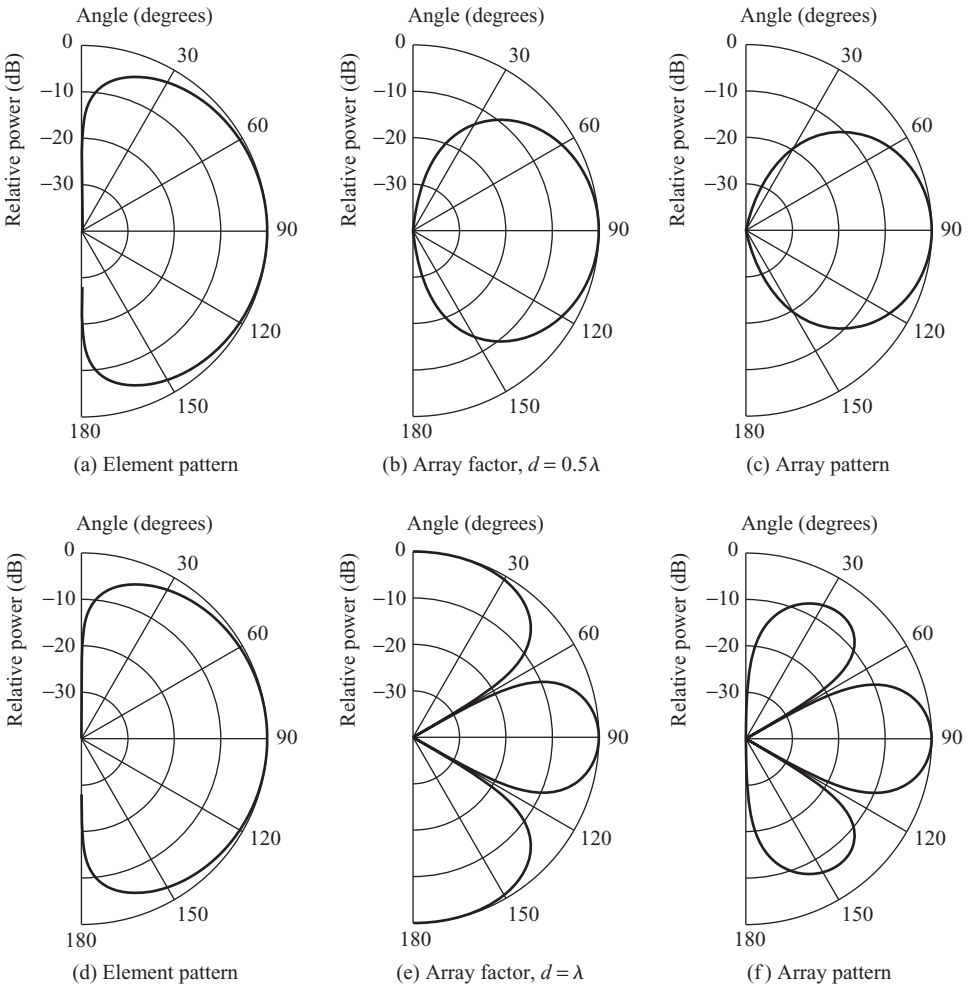

Fig. 5.6 Array patterns of a two-element array with $\alpha = 0$

For the maxima to occur along real angles, the argument of the cosine inverse function should be within ± 1. This gives the condition

$$-1 \leq \frac{\pm 2m\pi - kd}{kd} \leq 1 \tag{5.25}$$

which leads to

$$0 \leq m \leq \frac{2d}{\lambda} \tag{5.26}$$

The array factor has at least one maximum corresponding to $m = 0$ for any spacing d, and the maximum occurs along $\theta_m = \pi$ [Fig. 5.7(a)]. If the spacing is equal to $\lambda/2$, the array factor has two maxima corresponding to $m = 0$ and $m = 1$ occuring along $\theta = 0$ and $\theta = \pi$ [Fig. 5.7(c)]. As the spacing is further increased, the second maximum at $\theta = 0$ starts moving towards $\theta = 180^\circ$ and the third maximum appears in the array factor when $d = 3\lambda/2$. In general, for spacing between $p\lambda/2$ and $(p+1)\lambda/2$, $p = 0, 1, 2, \ldots$, the pattern has $(p+1)$ maxima.

Consider a situation where the current in the dipole 1 leads the current in the dipole 2, i.e., $I_1 = I_0 e^{jkd/2}$ and $I_2 = I_0 e^{-jkd/2}$. For this case, the directions of the maxima are given by

$$\theta_m = \cos^{-1}\left(\frac{\pm 2m\pi + kd}{kd}\right);\ m = 0, 1, 2, \ldots \tag{5.27}$$

The array factor always has a maximum along

$$\theta = \cos^{-1}(1) = 0 \tag{5.28}$$

which corresponds to $m = 0$.

Thus, for a two-element array with a phase shift of $\alpha = \pm kd$ in the excitation, the array factor always has a maximum along $\theta = 180^\circ$ or $\theta = 0^\circ$, which are along the axis of the array. Therefore, this array is known as an *endfire array.*

Further, it is possible to show that the element spacing, d, has to satisfy the condition

$$\frac{d}{\lambda} \geq \frac{2n-1}{4};\ n = 1, 2, \ldots \tag{5.29}$$

for the nulls to appear in the array factor [see Example 5.3]. Therefore, the pattern has nulls only if the spacing $d \geq \lambda/4$ (corresponding to $n = 1$).

EXAMPLE 5.1

Show that the directions of maxima of the array factor of a two-element array shown in Fig. 5.3, with excitations $I_1 = e^{jkd/2}$ and $I_2 = e^{-jkd/2}$, are given by

$$\theta_m = \cos^{-1}\left(\frac{\pm 2m\pi + kd}{kd}\right);\ m = 0, 1, 2, \ldots$$

and the array factor has at least one maximum along $\theta = 0$.

Solution: The array factor of the two-element array shown in the figure with excitations I_1 and I_2 is given by

$$\text{AF} = I_1 e^{-jk\frac{d}{2}\cos\theta} + I_2 e^{jk\frac{d}{2}\cos\theta}$$

Substituting $I_1 = e^{jkd/2}$ and $I_2 = e^{-jkd/2}$, we get

$$\begin{aligned}\text{AF} &= e^{jk\frac{d}{2}(1-\cos\theta)} + e^{-jk\frac{d}{2}(1-\cos\theta)} \\ &= 2\cos\left\{\frac{kd}{2}(1-\cos\theta)\right\}\end{aligned}$$

The array factor reaches a maximum when the argument of the cosine function is equal to an integer multiple of π

$$\frac{kd}{2}(1-\cos\theta_m) = \pm m\pi$$

Therefore the directions of the maxima are

$$\theta_m = \cos^{-1}\left(\frac{\pm 2m\pi + kd}{kd}\right) \quad m = 0, 1, 2, \ldots$$

For $m = 0$

$$\theta_0 = \cos^{-1}(1) = 0$$

Thus, there is always one maximum along $\theta = 0$.

EXAMPLE 5.2

Calculate the directions of the maxima and the nulls of the array factor of an array of two infinitesimal dipoles oriented along the z-direction, kept at $z_1 = -0.125\lambda$ and $z_2 = 0.125\lambda$, and carrying currents $I_1 = e^{-j\pi/4}$ and $I_2 = e^{j\pi/4}$, respectively.

Solution: The array factor of an array of two infinitesimal dipoles oriented along the z-direction, kept at z_1 and z_2 and carrying currents I_1 and I_2 respectively, is given by

$$\text{AF} = I_1 e^{jkz_1\cos\theta} + I_2 e^{jkz_2\cos\theta}$$

Substituting $z_1 = -\lambda/8$, $z_2 = \lambda/8$, $I_1 = e^{-j\pi/4}$ and $I_2 = e^{j\pi/4}$, the array factor can be simplified to

$$\begin{aligned}\text{AF} &= e^{-j\pi/4}e^{-jk\frac{\lambda}{8}\cos\theta} + e^{j\pi/4}e^{jk\frac{\lambda}{8}\cos\theta} \\ &= e^{-j\frac{\pi}{4}(1+\cos\theta)} + e^{j\frac{\pi}{4}(1+\cos\theta)} \\ &= 2\cos\left(\frac{\pi}{4} + \frac{\pi}{4}\cos\theta\right)\end{aligned}$$

The maxima of the array factor occur when

$$\frac{\pi}{4} + \frac{\pi}{4}\cos\theta_m = \pm m\pi \quad m = 0, 1, 2, \ldots$$

which can be rearranged to get an expression for the direction of the maxima θ_m as

$$\theta_m = \cos^{-1}(\pm 4m - 1)$$

This has only one solution corresponding to $m = 0$ and the direction of the maximum is $\theta_m = \pi$.

The nulls of the array factor are along θ_n, which is obtained by solving

$$\frac{\pi}{4} + \frac{\pi}{4}\cos\theta_n = \pm(2n+1)\frac{\pi}{2} \; n = 0, 1, 2, \ldots$$

which gives

$$\theta_n = \cos^{-1}(\pm(2n+1)2 - 1)$$

This also has only one solution corresponding to $n = 0$, which gives the direction of the null as $\theta_n = \cos^{-1}(1) = 0$.

The array factor is shown in Fig. 5.7(b).

EXAMPLE 5.3

Show that for a 2-element array with $\alpha = kd$ the condition for the nulls to appear in the array factor is

$$\frac{d}{\lambda} \geq \frac{2n-1}{4} \; n = 1, 2, \ldots$$

Solution: Null in the pattern along θ_n satisfies the condition

$$\cos\left(\frac{1}{2}\left[kd\cos\theta_n + kd\right]\right) = 0$$

This condition is satisfied if

$$\frac{1}{2}\left[kd\cos\theta + kd\right] = \pm(2n-1)\frac{\pi}{2};\ n = 1, 2, \ldots$$

which results in the following expression for θ_n

$$\theta_n = \cos^{-1}\left[\pm\frac{(2n-1)\lambda}{2d} - 1\right]$$

For the nulls to occur along real angles

$$-1 \leq \left[\pm\frac{(2n-1)\lambda}{2d} - 1\right] \leq 1$$

which gives

$$(2n-1)\frac{\lambda}{d} \leq 4$$

or

$$\frac{d}{\lambda} \geq \frac{2n-1}{4}$$

The array factors of a two-element array with both the elements having equal amplitudes of excitation and a phase shift of kd are shown in Fig. 5.7 for various inter-element spacings. From Figs 5.7(a) and 5.7(b), we can conclude that with $d = 0.22\lambda$ the array factor has no nulls and with $d = 0.25\lambda$ one null in the direction of $\theta = 0^\circ$ appears in the array factor. As the spacing increases beyond 0.25λ, the null moves away from 0° and finally, when $d = \lambda/2$, the array factor has a null along $\theta = 90^\circ$ and a second maxima appears along $\theta = 0^\circ$ [Fig. 5.7(c)]. Further increase in the spacing ($d = 0.75\lambda$) results in the appearance of second null along $\theta = 0^\circ$ [Fig. 5.7(e)], and so on.

Array patterns of a two-element endfire array for two different values of element spacing ($d = \lambda/4$ and $\lambda/2$) are shown Fig. 5.8. For example, with $d = \lambda/4$, the null of the array factor coincides with the peak of the element pattern and vice versa. Hence the array pattern, which is a product of these two, will have nulls along both these directions. The maximum of the antenna pattern is along $\theta = 111.5^\circ$ and does not coincide with either that

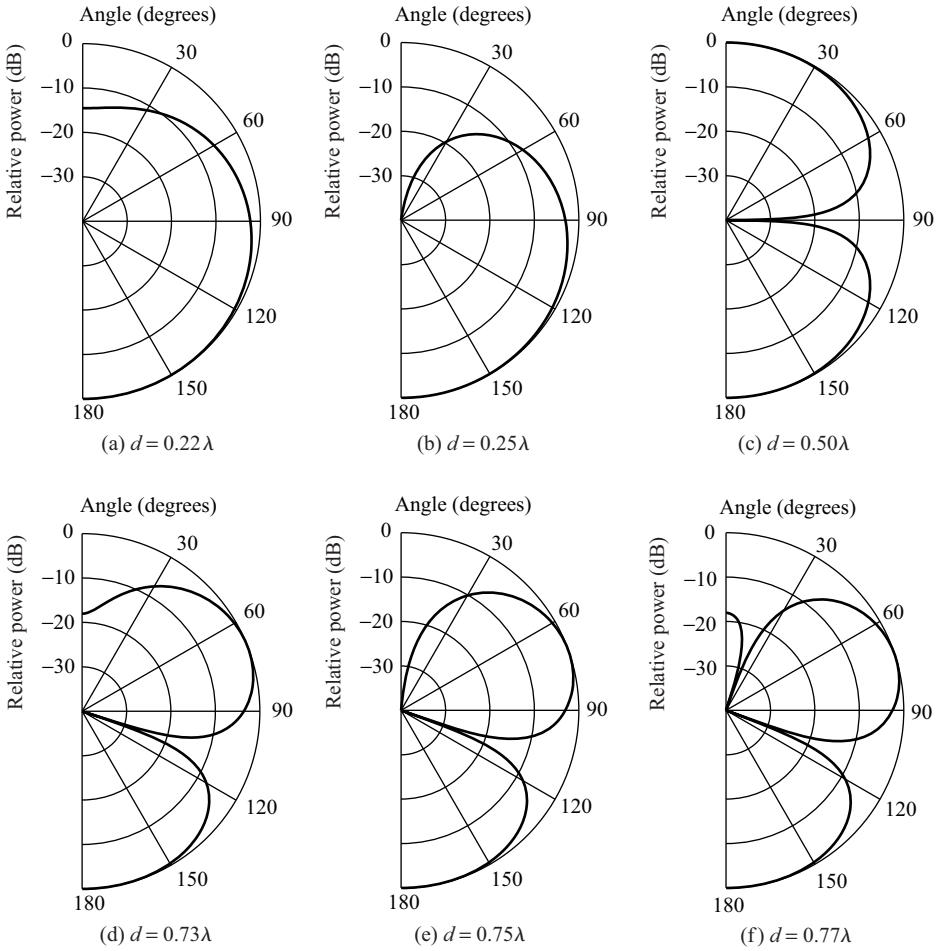

Fig. 5.7 Array factors of two-element arrays (for different spacings) with $\alpha = kd$

of the array factor or that of the element pattern. Similarly, with $d = \lambda/2$, the array pattern has nulls along $\theta = 0^\circ$ and 180° and maxima along 51° and 129°.

In order to realize an array pattern that has a maximum along the endfire direction, we need to choose the elements which also have a maximum in the same direction. Consider a two-element array made of infinitesimal dipoles oriented along the y-direction, kept at $z_1 = -0.125\lambda$ and $z_2 = 0.125\lambda$, and carrying currents of $I_1 = I_0 e^{-j\pi/4}$ and $I_2 = I_0 e^{j\pi/4}$. The spacing and the phases of the excitation currents are chosen such that the phase shift $\alpha = kd = \pi/2$. The element pattern in the $\phi = 90^\circ$ plane for a y-directed

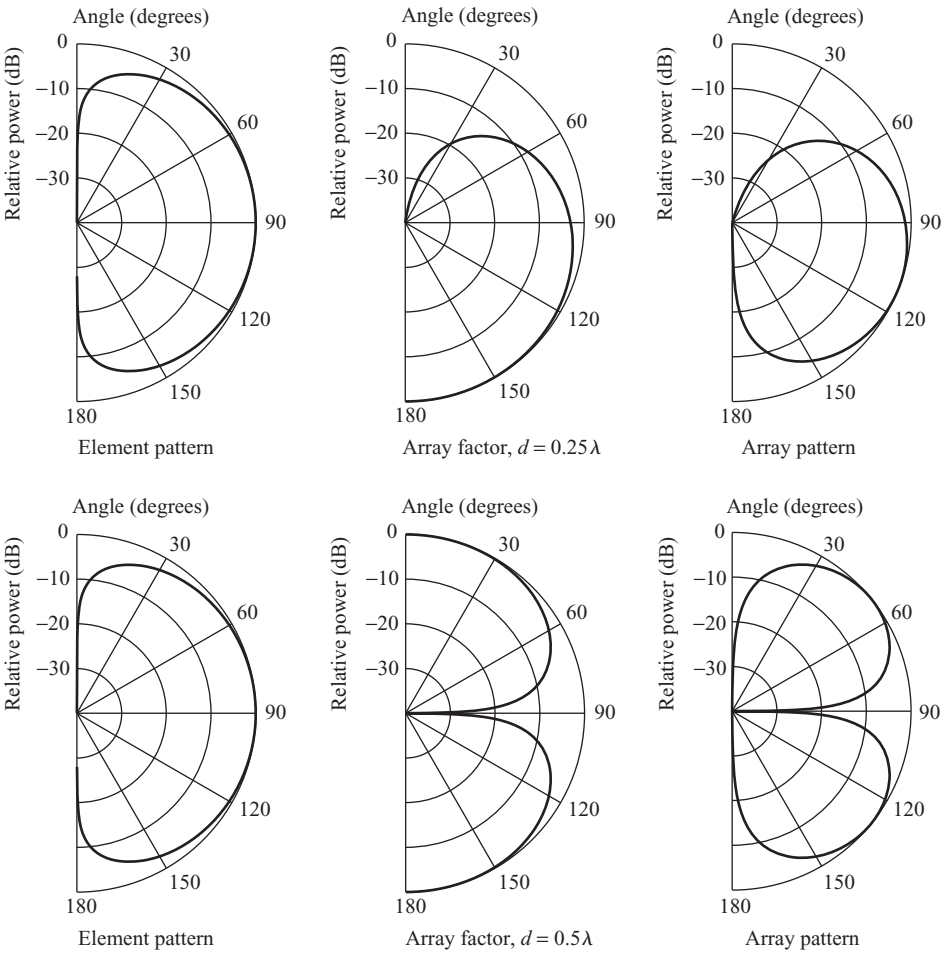

Fig. 5.8 Array patterns of two-element arrays with currents having a relative phase shift $\alpha = kd$

infinitesimal dipole is shown in Fig. 5.9(a) and the array factor in Fig. 5.9(b). The maxima of the element pattern and the array factor are along $\theta = 180^\circ$ and hence the array pattern also has a maximum along the endfire direction ($\theta = 180^\circ$) as shown in Fig. 5.9(c). In this situation, the beamwidth of the array pattern is slightly narrower than the array factor due to the element pattern.

The 3D element pattern of a y-directed infinitesimal dipole is shown in Fig. 5.10(a). It is clear from Fig. 5.10(a) that the element pattern does not show a rotational symmetry about the z-axis. Although the array factor is

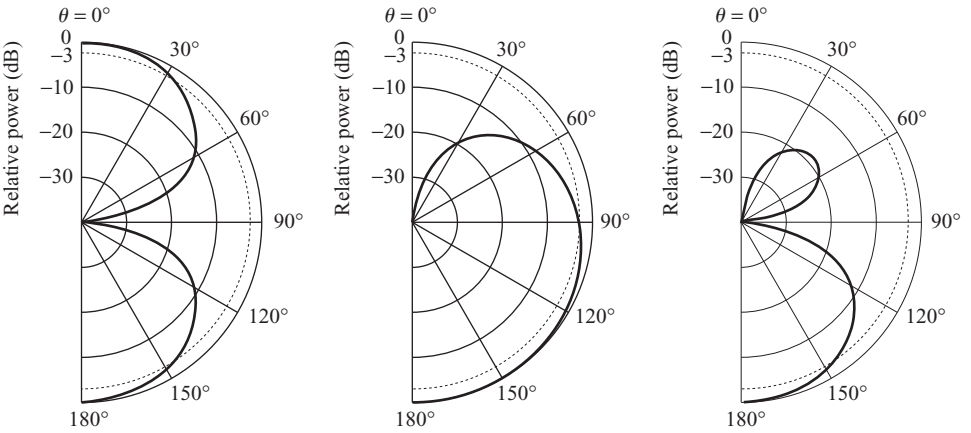

(a) Element pattern (b) Array factor, $d = 0.25\lambda$ (c) Array pattern

Fig. 5.9 Endfire array of two y-directed dipoles with maximum along $\theta = 180°$ (The array axis is the z-axis and all patterns correspond to the $\phi = 90°$ cut)

ϕ-symmetric [Fig. 5.10(b)], the array pattern does not show a rotational symmetry as a function of ϕ [Fig. 5.10(c)].

With these examples, it is clear that in order to achieve a desired antenna array pattern, it is important to choose both the element pattern as well as the array factor appropriately. In the next sections, we will focus on the analysis and design of array factors only. It is assumed that an appropriate element pattern is chosen such that the antenna array has the desired overall radiation pattern.

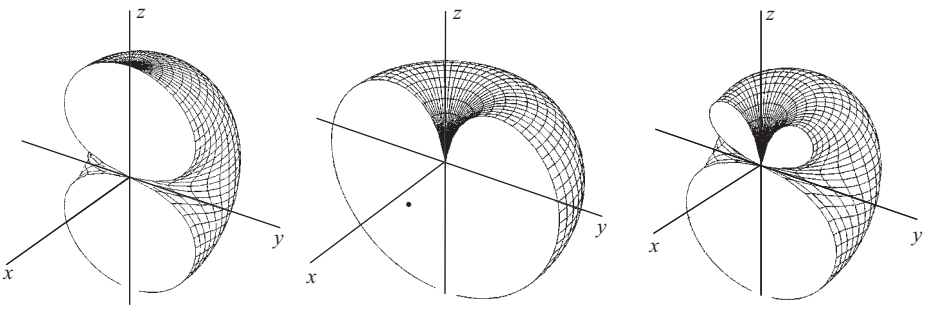

(a) Element pattern of a y-directed infinitesimal dipole (b) Array factor of a 2-element array; $d = \lambda/4$, $\alpha = \pi/2$ (c) Array pattern: product of the element pattern and the array factor

Fig. 5.10 3D patterns of a two-element endfire array with a maximum along $\theta = 180°$

5.3 Uniform Array

Consider an array of N point sources placed along the z-axis with the first element at the origin. Let the distance between any two consecutive elements be equal to d. The excitation currents of all the elements have equal magnitude and a progressive phase shift of α, i.e., the current in the nth element leads the current in the $(n-1)$th element by α. If the current in the first element, $I_1 = I_0$, the current in the nth element can be written as $I_n = I_0 e^{j(n-1)\alpha}$. Such an array is called a uniform array.

The array factor of an N-element linear array along the z-axis is given by Eqn (5.11), and is reproduced here

$$\text{AF} = \sum_{n=1}^{N} I_n e^{jkz'_n \cos\theta} \tag{5.30}$$

where I_n is the current in the nth element and $z'_n = (n-1)d$ is the location of the nth element (Fig. 5.11). Substituting the expressions for I_n and z'_n into the array factor and dividing by I_1 (I_1 is the reference), we get

$$\text{AF} = \sum_{n=1}^{N} e^{j(n-1)\alpha} e^{jk(n-1)d\cos\theta} \tag{5.31}$$

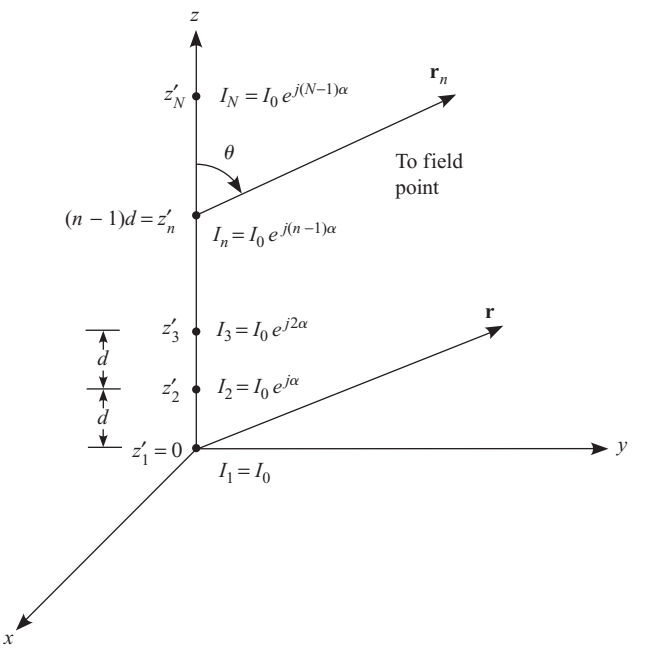

Fig. 5.11 Geometry of a uniform array of point sources radiating into free space

which can be written as

$$\text{AF} = \sum_{n=1}^{N} e^{j(n-1)\psi} \tag{5.32}$$

where $\psi = (kd\cos\theta + \alpha)$. Thus the array factor is a summation of N phasors which forms a geometric series.

$$\text{AF} = 1 + e^{j\psi} + e^{j2\psi} + e^{j3\psi} + \cdots + e^{j(N-1)\psi} \tag{5.33}$$

The magnitude of the array factor depends on the value of ψ. For example, for a 3-element array, computation of the array factor for an arbitrary ψ, $\psi = 0$, and $\psi = 120°$, is shown in Fig. 5.12. With $\psi = 0$, the array factor has a maximum and is zero for $\psi = 120°$. For a given spacing and progressive phase shift, the magnitude of the array factor changes with the angle θ.

Sum of the series representing the array factor can be obtained as follows. Multiply both sides of the array factor [Eqn (5.33)] by $e^{j\psi}$

$$\text{AF}e^{j\psi} = e^{j\psi} + e^{j2\psi} + e^{j3\psi} + \cdots + e^{j(N)\psi} \tag{5.34}$$

Subtracting Eqn (5.33) from Eqn (5.34)

$$\text{AF}(e^{j\psi} - 1) = (e^{jN\psi} - 1) \tag{5.35}$$

This can be rewritten as

$$\text{AF} = \frac{e^{jN\psi} - 1}{e^{j\psi} - 1} \tag{5.36}$$

Taking out $e^{jN\psi/2}$ from the numerator and $e^{j\psi/2}$ from the denominator

$$\text{AF} = e^{j(N-1)\psi/2}\frac{e^{jN\psi/2} - e^{-jN\psi/2}}{e^{j\psi/2} - e^{-j\psi/2}} = e^{j(N-1)\psi/2}\frac{\sin\dfrac{N\psi}{2}}{\sin\dfrac{\psi}{2}} \tag{5.37}$$

The magnitude of the array factor is given by,

$$|\text{AF}| = \left|\frac{\sin\dfrac{N\psi}{2}}{\sin\dfrac{\psi}{2}}\right| \tag{5.38}$$

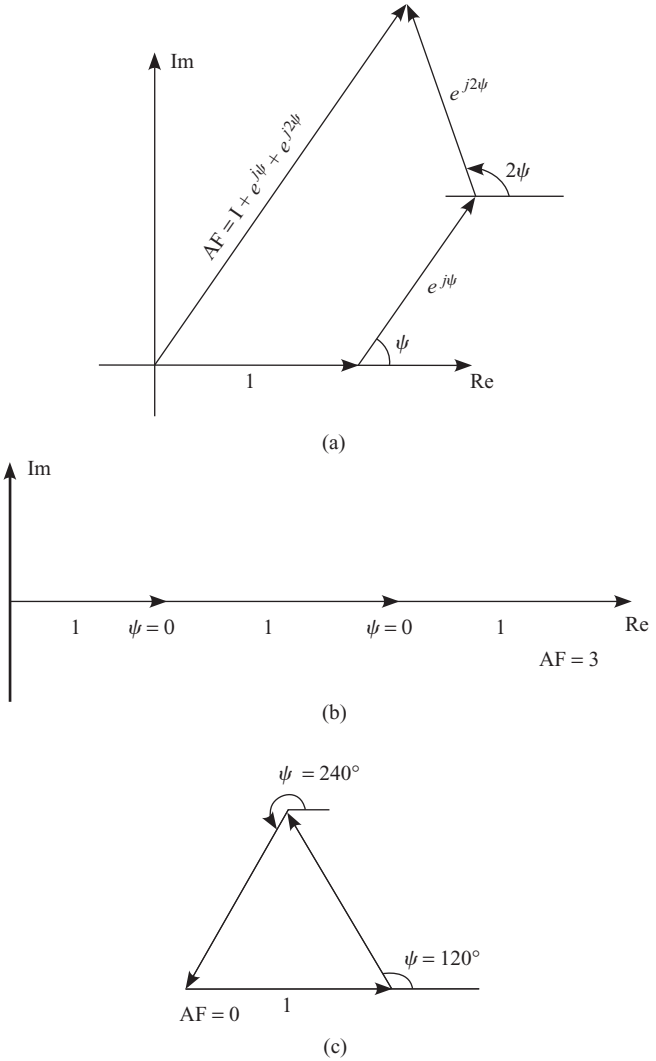

Fig. 5.12 Array factor of a 3-element array for (a) arbitrary ψ, (b) $\psi = 0$, and (c) $\psi = 120°$

as $|e^{j(N-1)\psi/2}| = 1$. For $\psi = 0$, the array factor has a 0/0 form. Therefore, applying L'Hospital's rule

$$|\text{AF}| = \left| \frac{\frac{N}{2}\cos\frac{N\psi}{2}}{\frac{1}{2}\cos\frac{\psi}{2}} \right|_{\psi=0} = N \tag{5.39}$$

Therefore, the normalized array factor is

$$|\mathrm{AF}_n| = \left| \frac{\sin \dfrac{N\psi}{2}}{N \sin \dfrac{\psi}{2}} \right| \tag{5.40}$$

The array factor has a principal maximum if both the numerator and the denominator simultaneously go to zero, which occurs under the following condition

$$\frac{\psi}{2}|_{\psi=\psi_m} = \pm m\pi;\ m = 0, 1, 2, \ldots \tag{5.41}$$

The principal maxima of the array factor occur for

$$\psi_m = \pm 2m\pi;\ m = 0, 1, 2, 3, \ldots \tag{5.42}$$

The array factor has periodic maxima at intervals of 2π (Fig. 5.13). The lobe containing the principal maximum corresponding to $m = 0$ is the main lobe and all other lobes containing principal maxima are called the grating lobes.

Between the two principal maxima, the array factor can have several nulls. The nulls of the array factor occur if the numerator alone goes to zero

$$\frac{N\psi}{2}|_{\psi=\psi_z} = \pm p\pi;\ p = 1, 2, \ldots \text{ with } p \neq 0, N, 2N, 3N, \ldots \tag{5.43}$$

At $p = 0, N, 2N, 3N, \ldots$ the array factor has maxima as both the numerator and the denominator go to zero, and hence are excluded. Therefore, the zeros are given by

$$\psi_z = \left(\frac{\pm 2p\pi}{N} \right) p = 1, 2, \ldots \text{ and } p \neq 0, N, 2N, \ldots \tag{5.44}$$

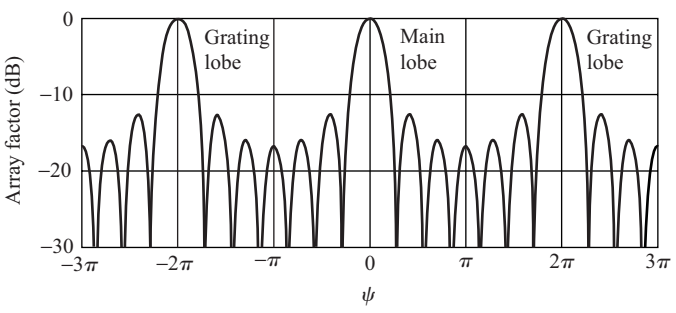

Fig. 5.13 Array factor of a 7-element array

There are $(N-1)$ zeros between two adjacent principal lobes. For example, between the main lobe occurring at $\psi = 0$ and the first grating lobe occurring at $\psi = 2\pi$, there are $(N-1)$ zeros occurring at $l(2\pi/N); l = 1, 2, \ldots (N-1)$. Between any two zeros, the array factor has a minor peak, called a side lobe. The locations of the side lobe peaks on the ψ-axis are obtained by solving the following transcendental equation (see Example 5.4)

$$N \tan\left(\frac{\psi}{2}\right) = \tan\left(\frac{N\psi}{2}\right) \tag{5.45}$$

EXAMPLE 5.4

Show that the peaks of the array factor of an N-element uniform array are given by the solution of the equation

$$N \tan\left(\frac{\psi}{2}\right) = \tan\left(\frac{N\psi}{2}\right)$$

Solution: The array factor of an N-element uniform array is given by Eqn. (5.40) as

$$|\mathrm{AF}(\psi)| = \left| \frac{\sin \dfrac{N\psi}{2}}{N \sin \dfrac{\psi}{2}} \right|$$

Equating the derivative of $\mathrm{AF}(\psi)$ with respect to ψ to zero we get

$$\frac{d(\mathrm{AF}(\psi))}{d\psi} = \frac{N \sin\left(\frac{\psi}{2}\right)\frac{N}{2}\cos\left(\frac{N\psi}{2}\right) - \sin\left(\frac{N\psi}{2}\right)\frac{N}{2}\cos\left(\frac{\psi}{2}\right)}{N^2 \sin^2 \frac{\psi}{2}} = 0$$

Upon rearranging, it reduces to

$$N \sin\left(\frac{\psi}{2}\right)\cos\left(\frac{N\psi}{2}\right) = \sin\left(\frac{N\psi}{2}\right)\cos\left(\frac{\psi}{2}\right)$$

Dividing both the sides by $\cos(N\psi/2)\cos(\psi/2)$ we get the desired result.

The peak of the first side lobe adjacent to the main lobe occurs approximately midway between the two zeros $(2\pi/N)$ and $(4\pi/N)$, i.e. at $\psi \simeq (3\pi/N)$ and the amplitude of the normalized array factor can be

computed by substituting this value of ψ in Eqn (5.40)

$$|\mathrm{AF}_n| \simeq \left| \frac{\sin\left(\frac{N}{2}\frac{3\pi}{N}\right)}{N\sin\left(\frac{1}{2}\frac{3\pi}{N}\right)} \right| = \left| \frac{1}{N\sin\left(\frac{3\pi}{2N}\right)} \right| \tag{5.46}$$

For large N, $\sin(3\pi/(2N)) \simeq 3\pi/(2N)$ and the peak value of the first side lobe reduces to

$$|\mathrm{AF}_n| = \frac{2}{3\pi} \tag{5.47}$$

which can be expressed in decibels as

$$|\mathrm{AF}_n| = 20\log\left(\frac{2}{3\pi}\right) = -13.46 \quad \mathrm{dB} \tag{5.48}$$

The first side lobe level of a uniform array containing large number of elements is 13.46 dB below the main lobe level. All other side lobes are lower than this.

One of the objectives of the array design (also known as the *array synthesis*) is to adjust amplitudes and phases of the excitation, such that the side lobes can be set to the desired levels. This will be explored in Section 5.4.

EXAMPLE 5.5

For a uniform 7-element array with $\alpha = 0$, calculate the exact location of the peak of the first side lobe by solving the transcendental equation [Eqn (5.45)], and calculate its level (in dB) with respect to the main lobe peak.

Solution: The transcendental equation [Eqn (5.45)] to be solved to compute the location of the peaks of the array factor is

$$N\tan\left(\frac{\psi}{2}\right) = \tan\left(\frac{N\psi}{2}\right)$$

For $N = 7$ and $\alpha = 0$ this reduces to

$$7\tan\left(\frac{\psi}{2}\right) = \tan\left(\frac{7\psi}{2}\right)$$

This equation is satisfied for $\psi = 0$, which represents the main lobe and for all other non-zero integer multiples of 2π, the solution corresponds to the grating lobe. Let us plot both the right and left hand sides of this equation

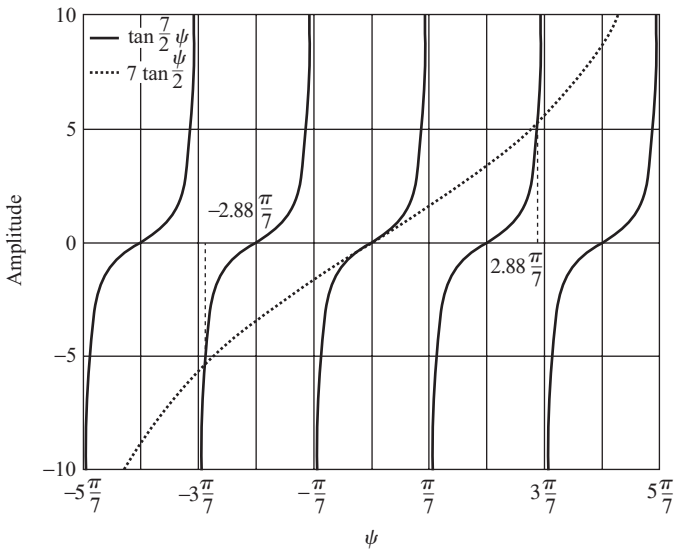

Fig. 5.14 Graphical solution of Eqn (5.45)

as a function of ψ (Fig. 5.14). The points of intersection of the two curves are the solutions to the equation. The solution $\psi \simeq 2.88\pi/7$, corresponds to the peak of the first side lobe.

The side lobe level can be computed by substituting the value of $\psi = 2.88\pi/7$ in Eqn (5.40)

$$|\mathrm{AF}_n| = \left| \frac{\sin\left(\frac{7}{2}2.88\frac{\pi}{7}\right)}{7\sin\left(\frac{1}{2}2.88\frac{\pi}{7}\right)} \right| = 0.233$$

This can be expressed in decibel units as

$$|\mathrm{AF}_n| = 20\log(0.233) = -12.65 \quad \mathrm{dB}$$

The level of the first side lobe approaches -13.46 dB for large values of N.

Visible region The variable ψ is related to the angle θ by $\psi = kd\cos\theta + \alpha$. As θ varies from 0° through 90° to 180°, ψ takes on values from $kd + \alpha$ through α to $-kd + \alpha$. Therefore, $kd + \alpha \geq \psi \geq -kd + \alpha$ is called the visible region (VR) in antenna array theory. For a given number of elements in an array, the array factor expression in terms of ψ remains the same, but as the element spacing increases, the number of lobes in the visible region increases. The array factor for a 7-element uniform array is shown in Fig. 5.15. The visible regions corresponding to $d = 0.5\lambda$ and λ are also shown in the same

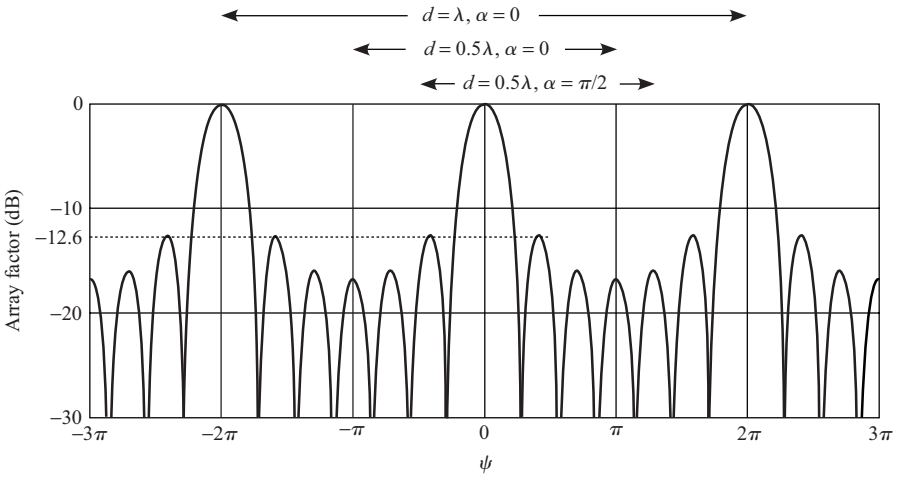

Fig. 5.15 Array factor of a 7-element uniform array

figure for $\alpha = 0$. For $d = \lambda/2$, which corresponds to $kd = \pi$, the visible region extends from $\psi = -\pi$ to $\psi = \pi$, the array factor has one main lobe at $\psi = 0$, and there are three side lobes on either side of the main lobe in the visible region. For $d = \lambda$, the visible region extends from $\psi = -2\pi$ to 2π and the array factor has one main lobe along $\psi = 0$ and two grating lobes, one along $\psi = -2\pi$, and another along $\psi = 2\pi$. With $d = 0.5\lambda$ and $\alpha = \pi/2$ the visible region extends from $\psi = -\pi/2$ to $\psi = 3\pi/2$ and the maximum is along $\psi = 0$ which corresponds to $\theta = \cos^{-1}\{-\alpha/(kd)\} = \cos^{-1}(1/2) = 60^\circ$.

The normalized array factor of a 7-element broadside uniform array is obtained by substituting $N = 7$ in Eqn (5.40)

$$\mathrm{AF}_n = \frac{\sin\frac{7}{2}\psi}{7\sin\frac{\psi}{2}} \tag{5.49}$$

In order to compute the 3 dB beamwidth of the main beam, we first compute the angles corresponding to the 3 dB points by equating the normalized array factor to $1/\sqrt{2}$.

$$\frac{\sin\frac{7}{2}\psi}{7\sin\frac{\psi}{2}} = \frac{1}{\sqrt{2}} \tag{5.50}$$

Solving for ψ iteratively we get $\psi = \pm 0.401$. Since $\psi = kd\cos\theta + \alpha$, and $\alpha = 0$, the corresponding values of θ are

$$\theta_1 = \cos^{-1}\left(\frac{0.401}{kd}\right) = \cos^{-1}\left(\frac{0.0638}{d/\lambda}\right) \tag{5.51}$$

and

$$\theta_2 = \cos^{-1}\left(\frac{-0.401}{kd}\right) = \cos^{-1}\left(-\frac{0.0638}{d/\lambda}\right) \tag{5.52}$$

The 3 dB beamwidth is given by

$$\text{BW}_{3\text{dB}} = \theta_2 - \theta_1 \tag{5.53}$$

For $d = \lambda/2$, the 3 dB beamwidth is 14.7°. As d increases to λ, the main beam gets narrower, and the beamwidth becomes 7.3°, but the first grating lobe appears in the visible region (Fig. 5.16). With $d = \lambda/2$ and $\alpha = \pi/2$ the 3 dB points are still along $\psi_1 = 0.401$ and $\psi_2 = -0.401$ and the 3 dB points in θ are

$$\theta_1 = \cos^{-1}\left(\frac{\psi_1 - \alpha}{kd}\right) = \cos^{-1}\left(\frac{0.401 - (\pi/2)}{(2\pi/\lambda)(\lambda/2)}\right) = 111.86^\circ \tag{5.54}$$

$$\theta_2 = \cos^{-1}\left(\frac{\psi_2 - \alpha}{kd}\right) = \cos^{-1}\left(\frac{-0.401 - (\pi/2)}{(2\pi/\lambda)(\lambda/2)}\right) = 128.88^\circ \tag{5.55}$$

The 3 dB beamwidth is $128.88 - 111.86 = 17.02^\circ$.

$\psi = 0$ corresponds to the main beam peak which occurs along $\theta = \cos^{-1}(\frac{-\alpha}{kd}) = \cos^{-1}(\frac{-1}{2}) = 120^\circ$.

5.3.1 Polynomial Representation

The array factor of a uniform array of N-elements kept along the z-axis with an inter-element spacing of d is given by [Eqn (5.32)]

$$\text{AF} = \sum_{n=1}^{N} e^{j(n-1)\psi} \tag{5.56}$$

where $\psi = (kd\cos\theta + \alpha)$, and α is the progressive phase shift. Let

$$z = e^{j\psi} \tag{5.57}$$

so that the array factor can be expressed in terms of z as

$$\text{AF} = \sum_{n=1}^{N} z^{(n-1)} = 1 + z + z^2 + z^3 + \cdots + z^{N-1} \tag{5.58}$$

This is a polynomial of degree $(N-1)$ and, therefore, has $(N-1)$ roots (or zeros) which correspond to the nulls of the array factor. The nulls of the

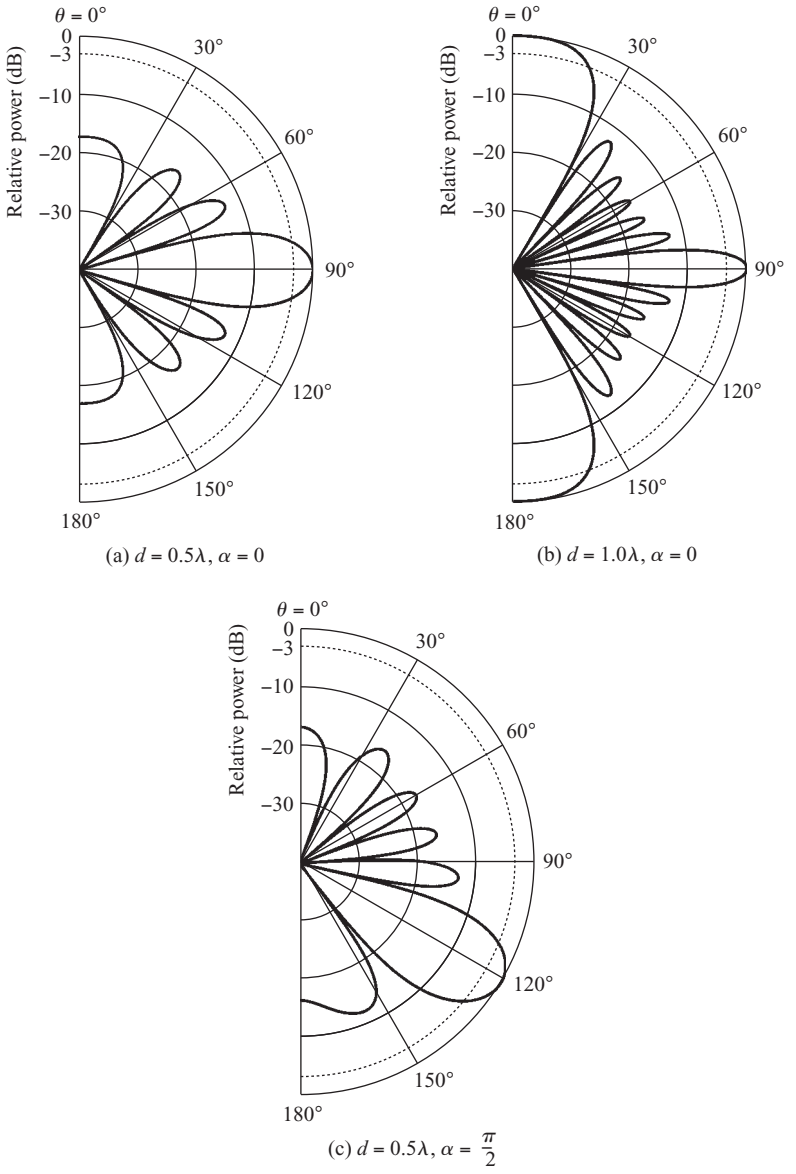

Fig. 5.16 Array factor of a 7-element uniform array

array factor can easily be computed by writing the array factor in the form given by Eqn (5.36)

$$\text{AF} = \frac{e^{jN\psi} - 1}{e^{j\psi} - 1} = \frac{z^N - 1}{z - 1} \tag{5.59}$$

Equating the numerator of the array factor to zero

$$z^N - 1 = 0 \tag{5.60}$$

and solving for z, we get the roots as

$$z = e^{-j\frac{2\pi}{N}},\ e^{-j2\frac{2\pi}{N}},\ e^{-j3\frac{2\pi}{N}},\ \cdots e^{-j(N-1)\frac{2\pi}{N}},\ 1 \tag{5.61}$$

These are the N roots of 1 in the complex plane. Since the magnitudes of the roots are all equal to unity, all the roots lie on the unit circle and are equally spaced. That is, they divide the circle into N equal parts. The last root in the above list, i.e., $z = 1$, corresponds to the maximum of the array factor ($\lim_{z\to 1} \mathrm{AF} = N$). Therefore, except $z = 1$, all other Nth roots of unity correspond to the nulls of the array factor.

Thus, the array factor can be written in the factored form as

$$\mathrm{AF} = (z - z_1)(z - z_2)\cdots(z - z_{N-1}) \tag{5.62}$$

where z_1, z_2, ... are the roots given by Eqn (5.61). The last factor $(z - z_N)$ cancels out with the denominator. z_N corresponds to the peak of the pattern. Thus, for any given z (or direction ψ) the array factor is a product of vectors $(z - z_1)$, $(z - z_2)$, etc.

Consider an equi-spaced, six-element array with uniform excitation. The nulls of the array factor are at

$$z = e^{-j\frac{2\pi}{6}},\ e^{-j2\frac{2\pi}{6}},\ e^{-j3\frac{2\pi}{6}},\ e^{-j4\frac{2\pi}{6}},\ e^{-j5\frac{2\pi}{6}} \tag{5.63}$$

and these are plotted on the unit circle in Fig. 5.17 as hollow circles. The maximum of the array factor, which occurs at $z = 1$, corresponds to $\psi = 0$. This is shown as a filled circle in Fig. 5.17. As angle θ varies from 0° through 90° to 180°, $\psi = kd\cos\theta + \alpha$ varies from $(kd + \alpha)$ through α to $(-kd + \alpha)$. This represents the visible region. As z traverses a zero in the visible region, it produces a null in the array factor. The pattern maximum or the main beam is at $z = 1$. The direction, θ_0, of the maximum, is obtained from

$$\psi = (kd\cos\theta + \alpha)|_{\theta=\theta_0} = 0 \tag{5.64}$$

which gives the direction of the maximum as

$$\theta_0 = \cos^{-1}\left(-\frac{\alpha}{kd}\right) \tag{5.65}$$

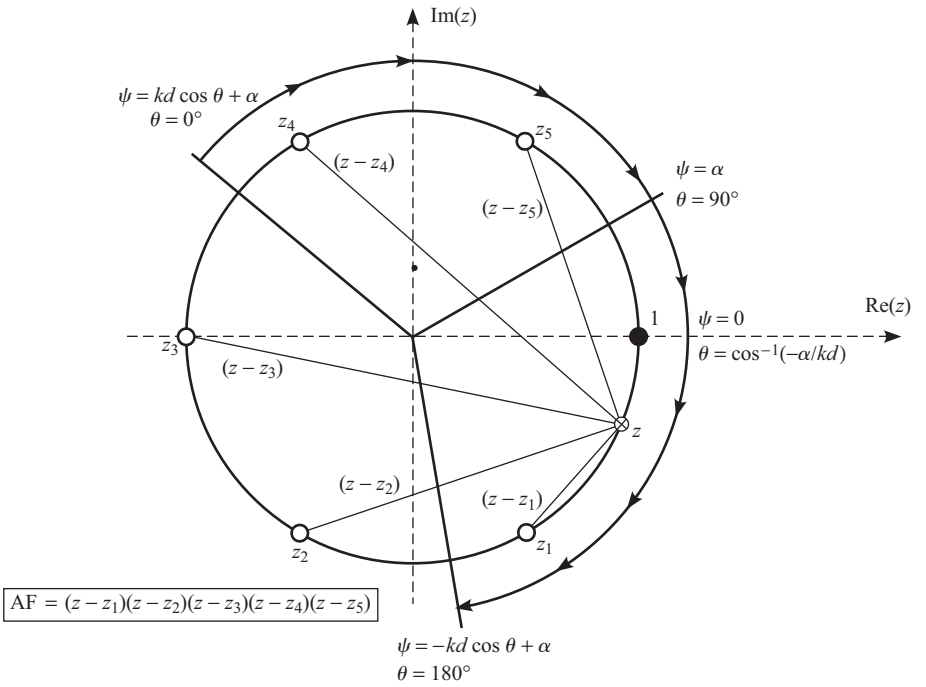

Fig. 5.17 Unit circle representation of a six-element uniform array

For a uniform array with $d = \lambda/3$, consider three specific values for α—(a) $\alpha = 0$, for which the maximum occurs along $\theta = 90°$. This array is known as a broadside array. The visible region extends from $\psi = kd = 120°$ to $\psi = -kd = -120°$ and is symmetric about $\psi = 0$ [Fig. 5.18(a)], (b) $\alpha = kd$, which corresponds to an endfire array with the pattern maximum occurring along $\theta = 180°$. The visible region for this case extends from $\psi = 2kd = 240°$ to $\psi = 0$ [Fig. 5.18(b)], and (c) $\alpha = -kd$, which corresponds to an endfire array with the maximum occurring along $\theta = 0°$. The visible region for this case extends from $\psi = 0$ to $\psi = -2kd = -240°$ [Fig. 5.18(c)].

As θ goes from 0° to 180°, ψ spans over a range of $2kd$. If $d = \lambda/2$, it corresponds to ψ traversing over one complete circle from $\alpha + \pi$ through α to $\alpha - \pi$ [Fig. 5.19(a)]. The pattern has one maximum and all the nulls are crossed at least once. Hence the array factor has at least $(N - 1)$ nulls in the visible region. If α is equal to an integer multiple of $2\pi/N$, one zero is touched twice and, hence, the array factor has N nulls in the visible region [Fig. 5.19(b)].

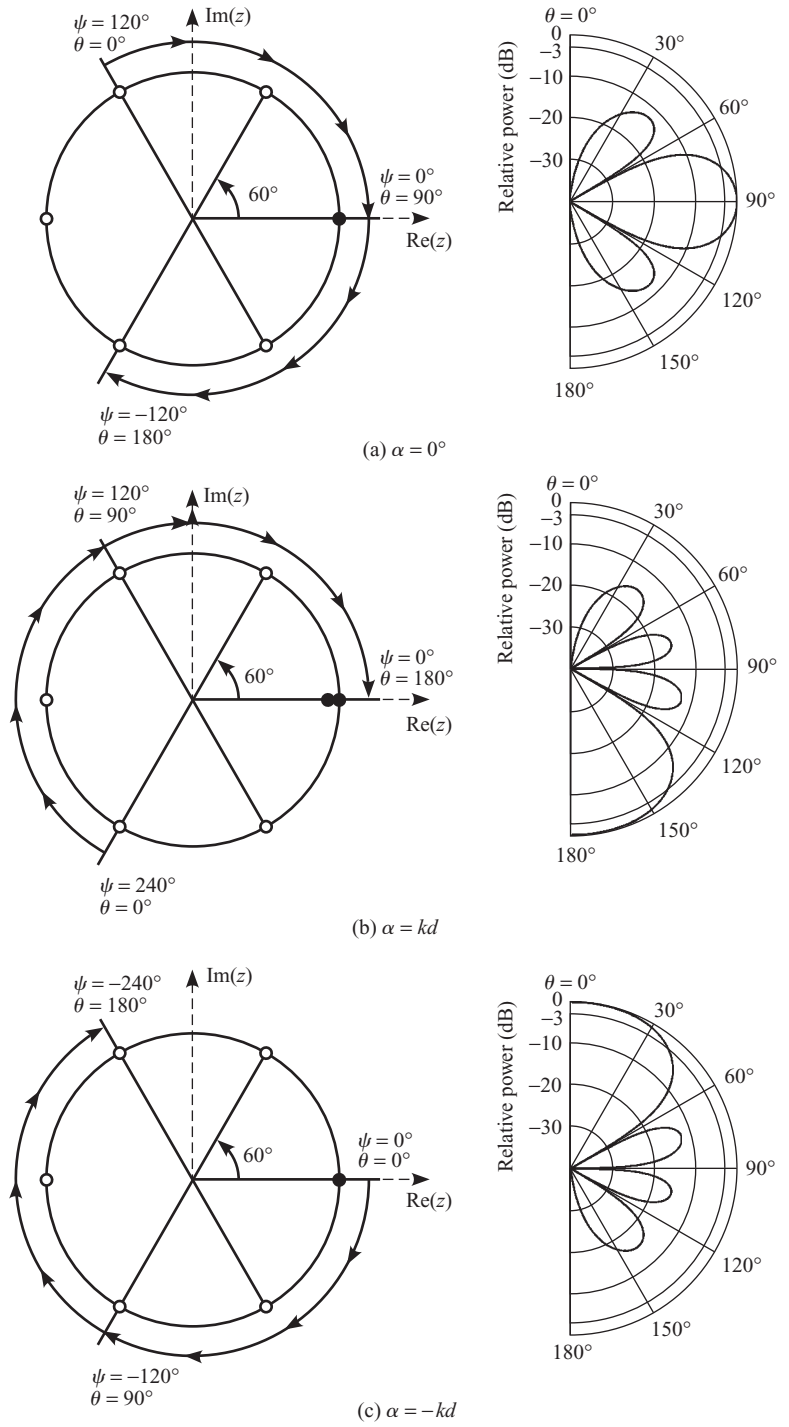

Fig. 5.18 Unit circle representation of a 6-element uniform array ($d = \lambda/3$)

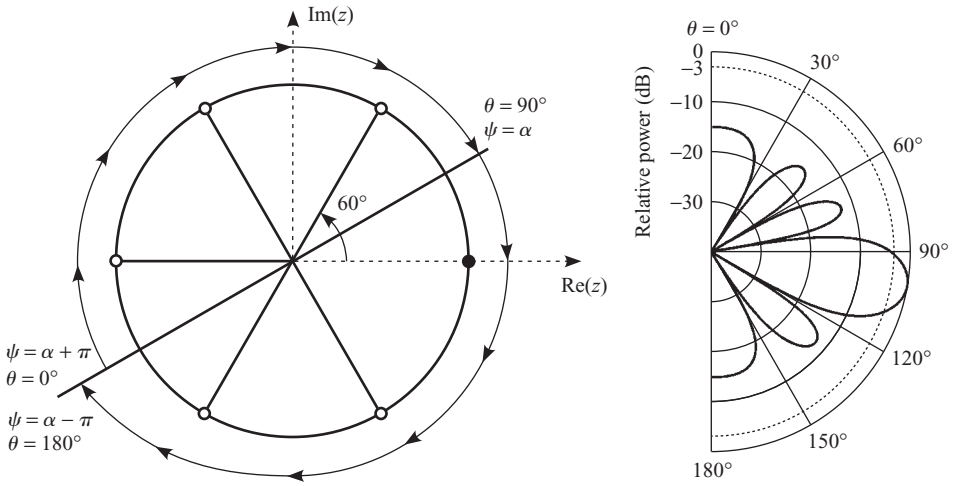

(a) $d = \lambda/2$; $\alpha = \pi/6$

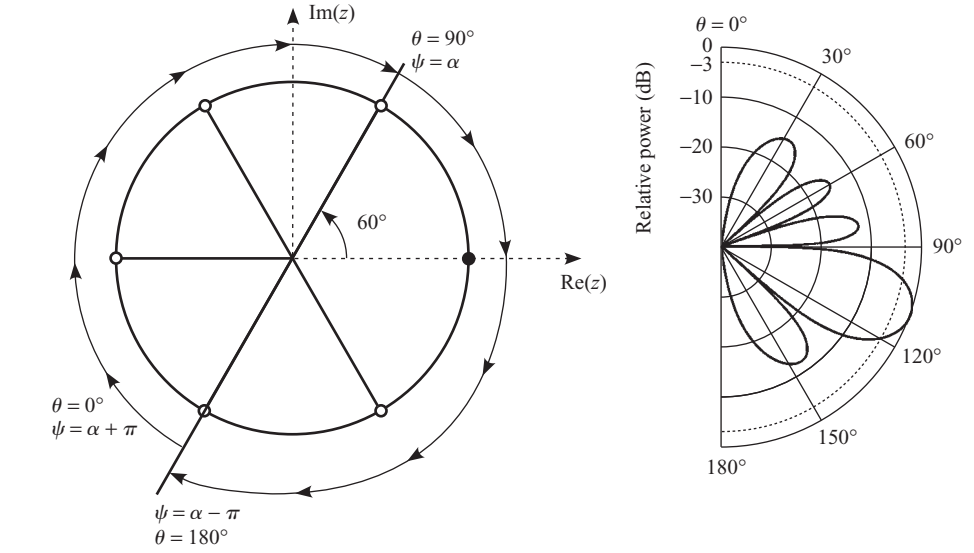

(b) $d = \lambda/2$; $\alpha = \pi/3$

Fig. 5.19 Unit circle representation of a 6-element uniform array and the effect of changing α on the extents of the visible region

As the inter-element spacing increases beyond $\lambda/2$, the span of ψ is greater than 2π and hence the path overlaps itself. For example, consider an endfire array with $d = 3\lambda/4$ and $\alpha = -kd$. The span of ψ representing the visible region is from 0 through $-kd$ to $-2kd$, which corresponds to ψ spanning 0 through -1.5π to -3π. The maximum is traversed twice, once when $\theta = 0°$

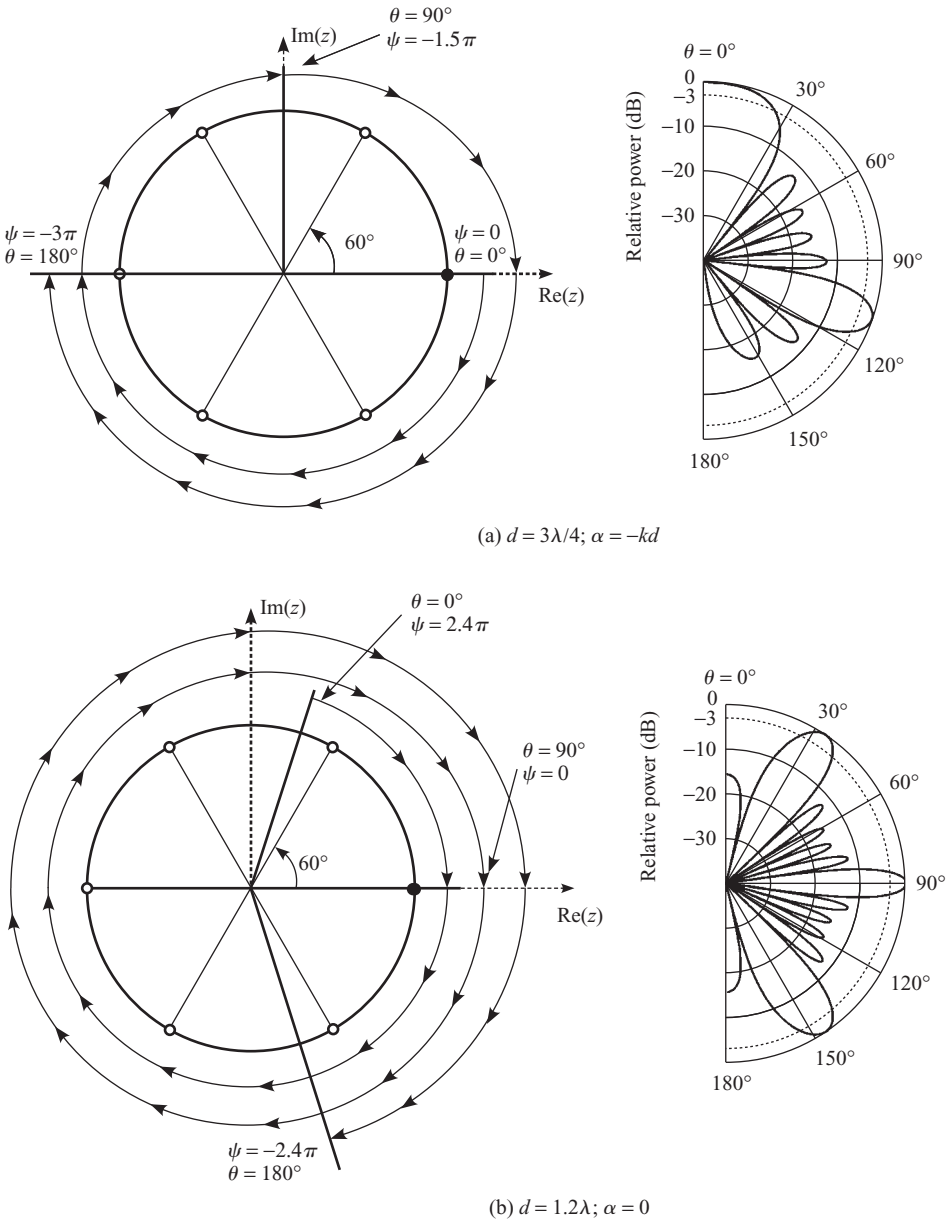

Fig. 5.20 Unit circle representation of a 6-element uniform array

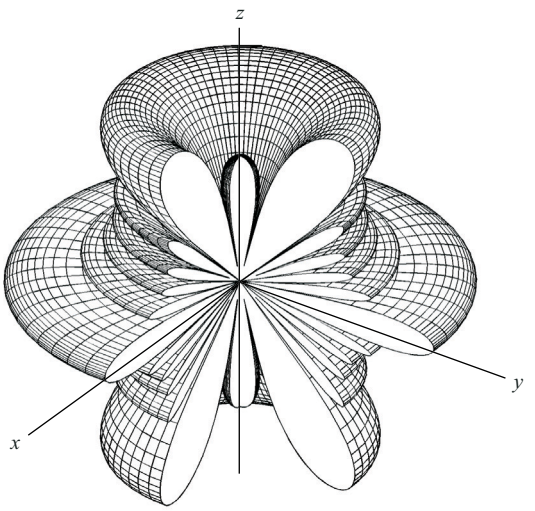

Fig. 5.21 Array factor of a 6-element uniform array with $d = 1.2\lambda$ and $\alpha = 0$

(corresponding to $\psi = 0$) and again at $\theta = 109.5°$, which corresponds to $\psi = -2\pi$, [Fig. 5.20(a)].

Further increase in the spacing brings more side lobes and gratings lobes into the visible region. For example, a broadside array ($\alpha = 0$) with $d = 1.2\lambda$ results in a span of ψ from $kd = 2.4\pi$ through 0 to $-kd = -2.4\pi$ [Fig. 5.20(b)]. There are three maxima in the visible region corresponding to $\psi = 2\pi$, 0, and -2π, ($\theta = 33.6°$, 90°, and 146.4°). A 3D representation of the pattern is shown in Fig. 5.21.

5.4 Array with Non-uniform Excitation

Some of the characteristics of the radiation pattern of an array of uniformly excited isotropic sources can be controlled by changing the number of elements, inter-element spacing, and the progressive phase shift. While spacing affects the extent of ψ, α controls the starting and ending values of ψ keeping the extent constant. However, the expression for the array factor in terms of ψ does not change; only the visible region is decided by d and α. The level of the first side lobe of a uniform array is always found to be greater than −13.5 dB from the main lobe peak. There are applications where it is required to suppress the side lobes to a much lower level. This can be achieved by changing the excitation amplitudes. In this section, we will consider two specific examples and show that it is possible to change the level of the side lobes by proper choice of amplitudes of the array excitation coefficients.

5.4.1 Binomial Array

Consider an array factor given by

$$\text{AF} = (z+1)^N \tag{5.66}$$

which has all the zeros at $z = -1$. Expanding this in a binomial series, we have

$$\text{AF} = 1 + {}^NC_1 z + {}^NC_2 z^2 + {}^NC_3 z^3 + \cdots + {}^NC_{N-1} z^{N-1} + Z^N \tag{5.67}$$

where

$${}^NC_r = \frac{N!}{(N-r)!\ r!} \tag{5.68}$$

are the binomial coefficients. For uniform spacing, z'_n in Eqn (5.11) can be replaced by $(n-1)d$. Now, substituting $z = e^{j\psi}$, where $\psi = (kd\cos\theta + \alpha)$, we can write the term inside the summation sign as $(I_n z^{n-1})$. Therefore, the array factor of an arbitrarily excited, uniformly spaced, $(N+1)$-element array can be written as

$$\text{AF} = I_1 + I_2 z + I_3 z^2 + \cdots + I_N z^{N-1} + I_{N+1} z^N \tag{5.69}$$

where $I_1, I_2, \ldots$, etc., are the excitation currents. Comparing this with the array factor given in Eqn (5.67), it can be seen that if the excitation coefficients correspond to binomial coefficients, we have an array factor with all the nulls at $z = -1$. This array is called a binomial array. For example, consider an array of 5 elements, the excitation currents of which are in the ratio given by the binomial coefficients $\{1 : {}^4C_1 : {}^4C_2 : {}^4C_3 : {}^4C_4\}$ or $\{1 : 4 : 6 : 4 : 1\}$. If the spacing and the progressive phase shift are selected such that the visible region on the unit circle is $\leq 2\pi$, we will have a pattern with only a main lobe and no side lobes.

In the text that follows it is demonstrated how the pattern of a binomial array can be built up using pattern multiplication theorem. Consider a 3-element binomial array with excitation coefficients in the ratio $\{1 : 2 : 1\}$, with a spacing d. This can be split into two arrays, each having two elements with equal excitation currents $\{1 : 1\}$. The array factor of each of these 2-element arrays is $(1 + z)$. Now, consider this 2-element array as an array element and construct an array of two such elements spaced d apart. The two inner elements will overlap or in other words, they add up to form a 3-element array with coefficients $\{1 : 2 : 1\}$ as shown in Fig. 5.22.

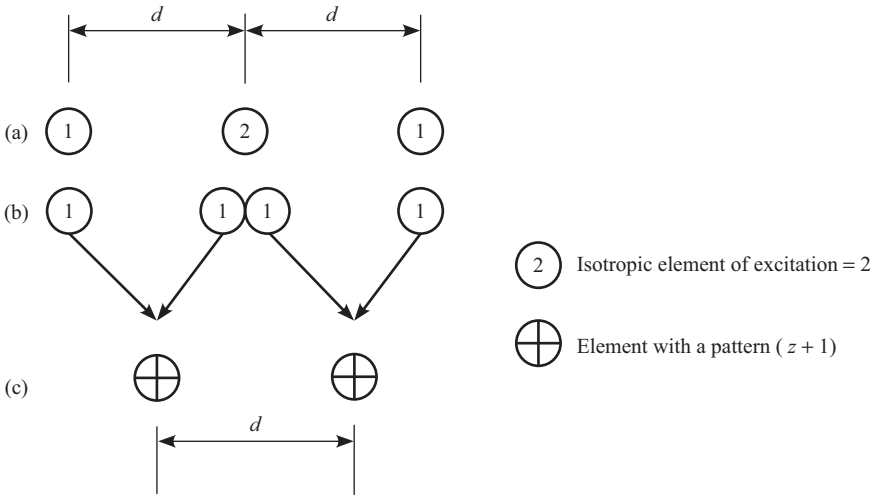

Fig. 5.22 Pattern multiplication to compute the array factor

The element pattern is $(1 + z)$ and so is the array factor. Thus, the array pattern, using pattern multiplication is

$$\mathrm{AF}_3 = (1 + z)^2 \tag{5.70}$$

for a 3-element binomial array. Now consider this 3-element binomial array as an element and construct a 2-element array out of these elements, with the same spacing d. Again the inner two elements will overlap to produce an array of 4 elements with excitation coefficients $\{1 : 3 : 3 : 1\}$ as shown in Fig. 5.23. The array factor of the 4-element binomial array can be obtained by pattern multiplication

$$\mathrm{AF}_4 = \mathrm{AF}_3(1 + z) = (1 + z)^3 \tag{5.71}$$

Thus, in general, we can look at an N-element binomial array as a 2-element array of an $(N - 1)$-element binomial array and build up the pattern function by applying the pattern multiplication theorem successively, starting from a 2-element array.

It may be noted that the binomial array has a non-uniform excitation, which results in no side lobes for an appropriate choice of α and d. It can also be inferred that by non-uniform excitation, we can influence the side lobe structure.

The binomial coefficients can be represented in terms of a triangle, called the Pascal's triangle. It is generated by starting with 1 (row 1). The second row is generated by simply repeating 1 twice. The first and the

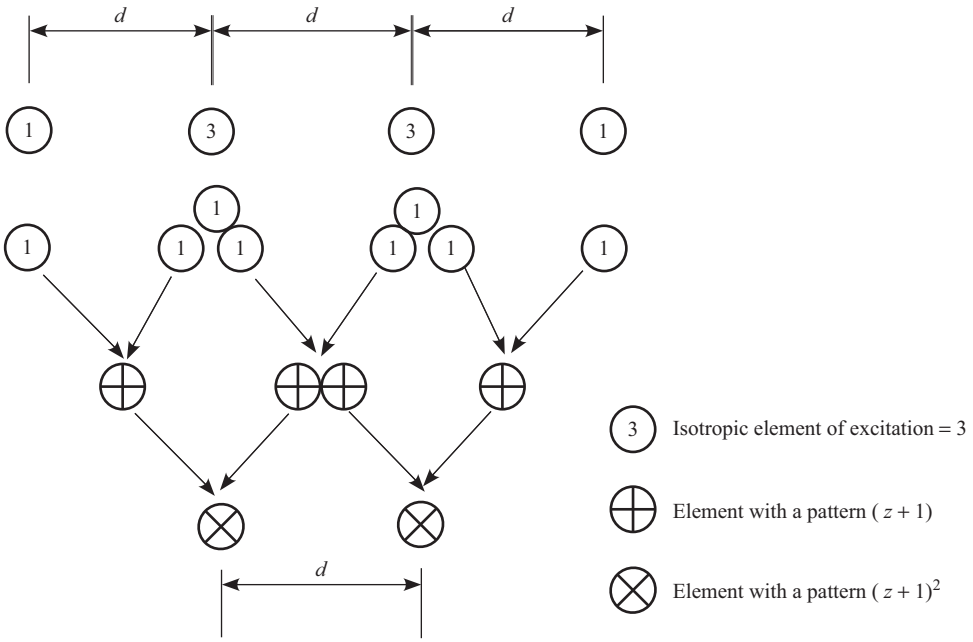

Fig. 5.23 Pattern multiplication to compute the array factor

last elements of the next row are equal to the respective elements of the previous row. The remaining elements are sum of the two adjacent elements of the previous row. For example, the second element of the third row is generated by adding the first and the second elements of the second row. Similarly, the third element of the fifth row is the sum of the second and the third elements of the fourth row. The Pascal's triangle and the technique to generate it are shown in Fig. 5.24.

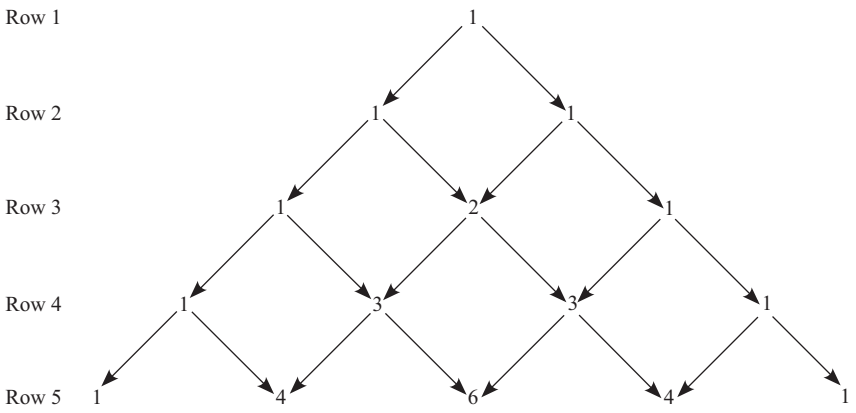

Fig. 5.24 Pascal's triangle and the generation of binomial coefficients

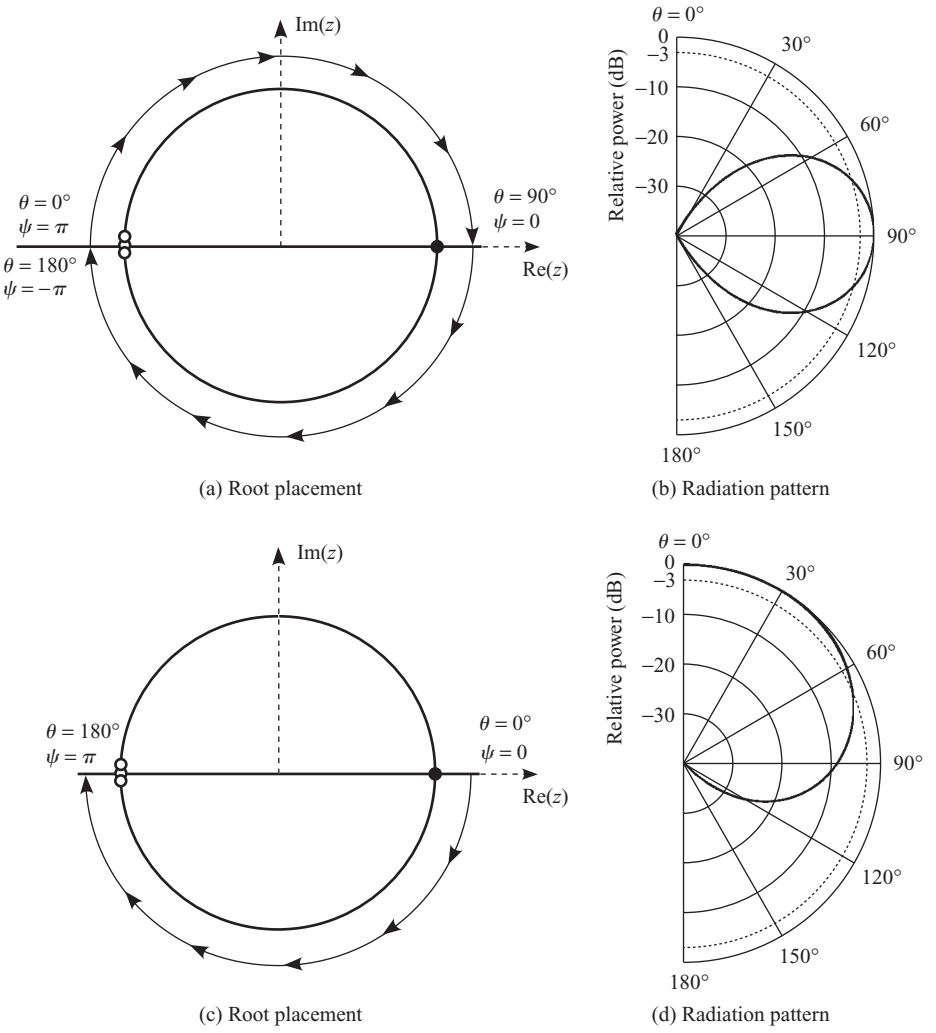

Fig. 5.25 Binomial array of 4 isotropic sources with $d = \lambda/2$ and $\alpha = 0$ [(a) and (b)] and with $d = \lambda/4$ and $\alpha = -kd$ [(c) and (d)]

The main feature of the binomial array is that all the zeros are located at $\psi = \pi$ as shown in Fig. 5.25(a). Therefore, a binomial broadside array will have no side lobes if the spacing $d \leq \lambda/2$. The extent of the visible region for $d = \lambda/2$ is shown in Fig. 5.25(a) and the corresponding radiation pattern in Fig. 5.25(b). The extent of the visible region for an endfire binomial array with $d \leq \lambda/4$ is shown in Fig. 5.25(c). The radiation pattern has no side lobes in the visible region [Fig. 5.25(d)]. If the spacing is increased beyond $\lambda/4$, the side lobes appear in the visible region of the array factor.

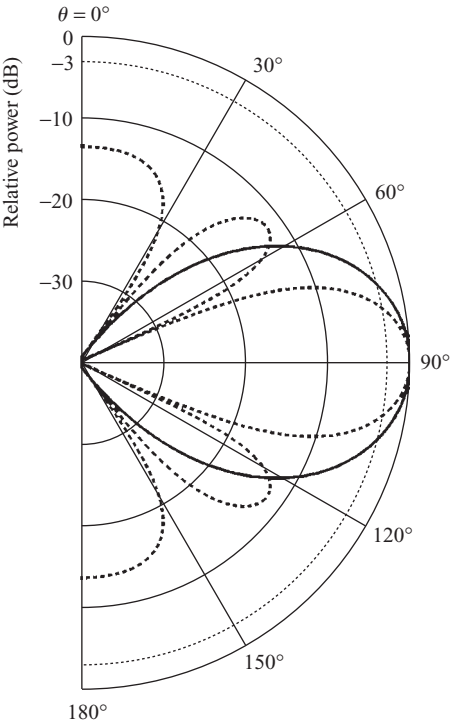

Fig. 5.26 Array factors of a 5-element broadside array with binomial (solid line) and uniform (dashed line) excitation

A comparison of the radiation patterns of a 5-element array with $d = \lambda/2$, radiating in the broadside direction and having (a) uniform excitation and (b) binomial excitation is shown in Fig. 5.26. The binomial array has no side lobes but has much wider 3 dB beamwidth compared to the uniform array.

5.4.2 Chebyshev Array Synthesis

So far we have examined the effect of element spacing, excitation coefficients and the progressive phase shift on the array factor of a uniformly spaced linear array. From the analysis presented so far, we can infer the following:

- The array factor of an N-element uniformly spaced linear array can be expressed as an $(N-1)$th degree polynomial

$$\text{AF} = \sum_{n=1}^{N-1} I_n z^n = I_1 + I_2 z + I_3 z^2 + \cdots + I_N z^{N-1} \tag{5.72}$$

which can be written in factored form as

$$\text{AF} = (z - z_1)(z - z_2)(z - z_3) \cdots (z - z_{N-1}) \tag{5.73}$$

In the factored form there are $(N-1)$ factors and $(z_1, z_2, z_3, \ldots, z_{N-1})$ are the roots of the polynomial, which form the zeros of the pattern function. $z = 1$ is always the main beam peak location.

- The roots of the array factor always fall on a unit circle in the complex z plane, with $z = 1$ being the peak of the array factor, which also is on the unit circle.
- For a given number of elements, there are a finite number of zeros available for manipulating the array factor.
- The array factor of any N-element uniformly spaced array is an $(N-1)$th degree polynomial, hence any $(N-1)$th degree polynomial can always be looked at as the array factor of an N-element array. We can make use of this to design or synthesize an array to give a desired pattern. Determining the array parameters starting from a desired pattern specifications is known as the array synthesis.

In this section we address the design of an array factor with all the side lobe peaks equal to a specified level. This type of array is known as a Chebyshev array, because the array coefficients are derived from the Chebyshev polynomials.

The array synthesis procedure follows the principle of matching a polynomial of appropriate degree and desired properties to the array factor of the array. The procedure is based on the simple observation that every polynomial of $(N-1)$th degree can be looked at as the array factor of an N-element array. Further, the array factor in the factored from gives the location of the roots and in the expanded form gives the excitation coefficients. Thus, from the knowledge of the roots of the polynomial we can write the factored from and by expanding it in power series form, we can get the excitation coefficients. The visible region and the main beam direction are determined using the variables d and α, as usual.

The array factor synthesized using a Chebyshev polynomial has an interesting property that it produces minimum beamwidth for a given side lobe level. Given below is the procedure for Chebyshev array synthesis.

The Chebyshev polynomial of mth degree is given by

$$T_m(x) = \begin{cases} \cos(m \cos^{-1} x) & -1 \leq x \leq 1 \\ \cosh(m \cosh^{-1} x) & |x| > 1 \end{cases} \tag{5.74}$$

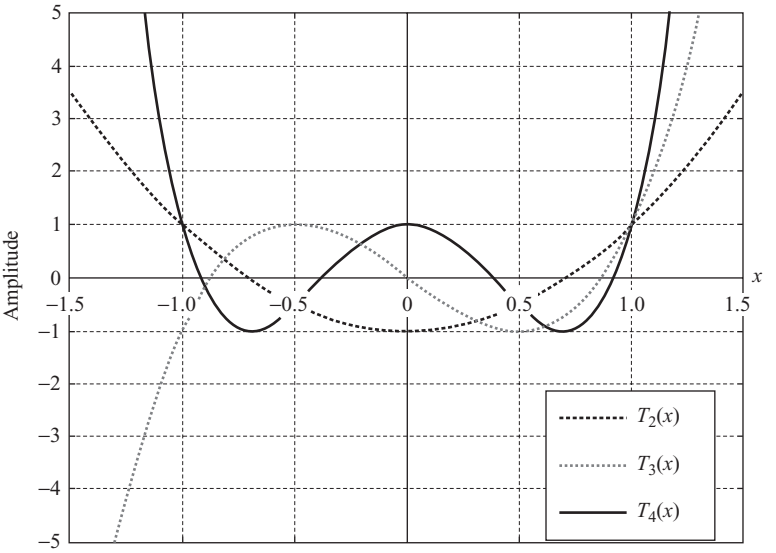

Fig. 5.27 Chebyshev polynomials (degrees 2, 3, and 4)

By inspection $T_0(x) = 1$ and $T_1(x) = x$. The recursive relation [Appendix C]

$$T_{m+1}(x) = 2T_m(x)T_1(x) - T_{m-1}(x) \tag{5.75}$$

can be used to compute the Chebyshev polynomials of higher degrees. For example, the Chebyshev polynomials for $m = 2$, 3, and 4 are

$$\begin{aligned} T_2(x) &= 2T_1(x)T_1(x) - T_0(x) = 2x^2 - 1 \\ T_3(x) &= 2T_2(x)T_1(x) - T_1(x) = 4x^3 - 3x \\ T_4(x) &= 2T_3(x)T_1(x) - T_2(x) = 8x^4 - 8x^2 + 1 \end{aligned}$$

and have been plotted in Fig. 5.27. It can be seen from the figure that $|T_m(x)| \leq 1$ for $|x| \leq 1$, and for $|x| > 1$ the modulus of the polynomial monotonically increases.

Let

$$x = x_0 \cos\left(\frac{\psi}{2}\right);\ x_0 > 1 \tag{5.76}$$

where x_0 is some known constant and $\psi = kd\cos\theta + \alpha$. Under this transformation, as θ goes from 0 to π, ψ goes from $kd + \alpha$ to 0 to $-kd + \alpha$, and x goes from $x_0 \cos[(kd + \alpha)/2]$ to x_0 to $x_0 \cos[(-kd + \alpha)/2]$ (Fig. 5.28). For example, if $d = \lambda/2$ and $\alpha = 0$, the visible region corresponds to $x = 0$ to x_0

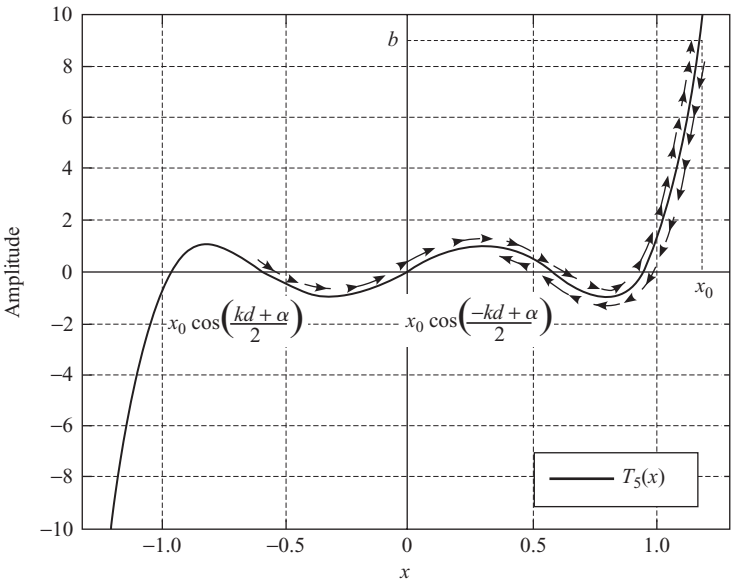

Fig. 5.28 Visible region in Chebyshev polynomial $T_5(x)$

and back to $x = 0$. If the Chebyshev polynomial represents the array factor, corresponding to $x = x_0$ it has a main lobe and several side lobes of equal amplitudes. If $T_m(x_0) = b$, where $b > 1$ (since $x_0 > 1$), the side lobe level will be equal to $1/b$. Expressed in decibel scale as

$$20 \log_{10}(b) = SLL_{\text{dB}} \tag{5.77}$$

With $\alpha = 0$ and $d = \lambda$, the visible region starts at $x = -x_0$, and extends all the way up to $x = x_0$ (corresponding to $\theta = \pi/2$) and then back to $x = -x_0$. The array factor has one main lobe, two grating lobes, and $2(m-1)$ side lobes in the visible region. As a third example, consider an array with $\alpha = kd$ and $d = \lambda/2$. For this array, the visible region extends from $-x_0$ to 0 to x_0, corresponding to $\theta = 0$ to $\pi/2$ to π. The array factor has a main lobe, a grating lobe, and $(m-1)$ side lobes in the visible region.

With the transformation given by Eqn (5.76), we are able to generate an array factor with equal side lobe peaks using Chebyshev polynomials. In order to compute the array factor, first we compute the zeros, x_i, of the Chebyshev polynomial $T_m(x_i) = 0$. The zeros of the Chebyshev polynomial of mth degree lie within $-1 < x_i < 1$, and are given by the solution of the following equation

$$\cos[m \cos^{-1}(x_i)] = 0 \tag{5.78}$$

Since the cosine function has a zero at every odd multiple of $\pi/2$

$$m\cos^{-1}(x_i) = (2i-1)\frac{\pi}{2};\ ki = 1, 2, \ldots, m \tag{5.79}$$

Therefore, the zeros of the Chebyshev polynomial of degree m are given by

$$x_i = \cos\frac{(2i-1)\pi}{2m};\ i = 1, 2, \ldots, m \tag{5.80}$$

The corresponding nulls in the ψ domain are given by Eqn (5.76) with $x = x_i$

$$\psi_i = 2\cos^{-1}\left(\frac{x_i}{x_0}\right);\ i = 1, 2, \ldots, m \tag{5.81}$$

An mth degree polynomial has m zeros and can be used to represent an array having $N = m + 1$ number of elements. With the knowledge of the locations of the m zeros in the ψ domain, the array factor can be written as

$$\text{AF} = \prod_{i=1}^{m}(z - e^{j\psi_i}) \tag{5.82}$$

where, $z = e^{j\psi} = e^{jkd\cos\theta+\alpha}$. Expanding this in series form we get the excitation coefficients.

A procedure to design an array of N elements having equal side lobe level of SLL_{dB} can now be written as follows:

1. Calculate the value of b from the SLL_{dB} using

$$b = 10^{SLL_{\text{dB}}/20} \tag{5.83}$$

2. Choose the order of the Chebyshev polynomial equal to one less than the number of elements

$$m = N - 1 \tag{5.84}$$

3. Calculate the value of x_0 by equating $T_m(x_0) = b$. Since $b > 1$, x_0 will also be greater than unity. Therefore, we use the second part of Eqn (5.74) and invert it to get

$$x_0 = \cosh\left(\frac{1}{m}\cosh^{-1} b\right) \tag{5.85}$$

4. Evaluate the zeros of the Chebyshev polynomial using Eqn (5.80)

$$x_i = \cos\frac{(2i-1)\pi}{2m};\ i = 1, 2, \ldots, m \tag{5.86}$$

5. Compute the location of the zeros using Eqn (5.81)

$$\psi_i = 2\cos^{-1}\left(\frac{x_i}{x_0}\right);\ i = 1, 2, \ldots, m \tag{5.87}$$

6. Form the array factor using Eqn (5.82)

$$\text{AF} = \prod_{i=1}^{m}(z - e^{j\psi_i}) \tag{5.88}$$

7. Multiply all the factors and arrange the terms in increasing powers of z. The coefficients of the series expansion are the excitation coefficients

$$\text{AF} = 1 + I_1 z + I_2 z^2 + \cdots + I_{N-1} z^{N-1} \tag{5.89}$$

EXAMPLE 5.6

Design a 4-element, broadside array of isotropic elements spaced $\lambda/2$ apart, that has an array factor with all the side lobes 25 dB below the main lobe.

Solution: Following the stepwise procedure given above:

1. Calculate the value of b from the $SLL_{\text{dB}} = 25\,\text{dB}$ using

$$b = 10^{25/20} = 17.7828$$

2. Choose the order of the Chebyshev polynomial equal to one less than the number of elements

$$m = N - 1 = 3$$

3. Calculate the value of x_0

$$x_0 = \cosh\left(\frac{1}{3}\cosh^{-1} 17.7828\right) = 1.7959$$

4. Evaluate the zeros of the Chebyshev polynomial using Eqn (5.80)

$$x_i = \cos\frac{(2i-1)\pi}{2\times 3};\ i = 1, 2, 3$$

The zeros are $x_1 = \sqrt{3}/2$, $x_2 = 0$, $x_3 = -\sqrt{3}/2$

5. Compute the location of the zeros using Eqn (5.81)

$$\psi_i = 2\cos^{-1}\left(\frac{x_i}{x_0}\right);\ i = 1, 2, \ldots, m$$

The location of the zeros in the ψ domain are $\psi_1 = 2.1352$ rad, $\psi_2 = \pi$ rad, $\psi_3 = 4.1478 = -2.1352$ rad.

6. Form the array factor using Eqn (5.82)

$$\text{AF} = (z - e^{j2.1352})(z - e^{j\pi})(z - e^{-j2.1352})$$

7. Expand the above product to get the excitation coefficients of the Chebyshev array. Multiplying the first and the last terms

$$\text{AF} = (z^2 + 1 - 2z\cos(2.1352))(z + 1) = z^3 + 2.0698z^2 + 2.0698z + 1$$

Therefore, the excitation coefficients are $\{1 : 2.0698 : 2.0698 : 1\}$.

EXAMPLE 5.7

Design an array of 7 elements with element spacing 0.75λ and side lobes 30 dB below the main lobe pointing along $\theta = 0°$.

Solution: Since all the side lobes are of equal amplitude, we choose Chebyshev pattern for the design of the array factor:

1. Given $SLL_{\text{dB}} = 30\,\text{dB}$, calculate the value of b as

$$b = 10^{30/20} = 31.62$$

2. Choose the order of the Chebyshev polynomial equal to one less than the number of elements

$$m = 7 - 1 = 6$$

3. x_0 is given by the solution of

$$x_0 = \cosh\left(\frac{1}{6}\cosh^{-1} 31.62\right) = 1.2485$$

which gives, $x_0 = 1.2485$.

4. Evaluate the zeros of the Chebyshev polynomial using Eqn (5.80)

$$x_i = \cos\frac{(2i-1)\pi}{2\times 6};\ i = 1, 2, \ldots, 6$$

The zeros in the x domain are 0.9659, 0.7071, 0.2588, −0.2588, −0.7071, −0.9659 and the corresponding zeros in the ψ domain are (using Eqn (5.81)), 1.3724, 1.9374, 2.724, −2.724, −1.9374, −1.3724.

5. Form the array factor using Eqn (5.82)

$$\begin{aligned}\text{AF} &= (z - e^{j1.3724})(z - e^{j1.9374})(z - e^{j2.724})(z - e^{-j2.724}) \\ &\quad \times (z - e^{-j1.9374})(z - e^{-j1.3724}) \\ &= (z^2 - 2z\cos(1.3724) + z)(z^2 - 2z\cos(1.9374) + z) \\ &\quad \times (z^2 - 2z\cos(2.724) + z) \\ &= z^6 + 2.1508z^5 + 3.3073z^4 + 3.785z^3 + 3.3073z^2 + 2.1508z + 1\end{aligned}$$

The excitation coefficients are in the ratio $\{1 : 2.1508 : 3.3073 : 3.785 : 3.3073 : 2.1508 : 1\}$.

The radiation pattern of the array is shown in Fig. 5.29.

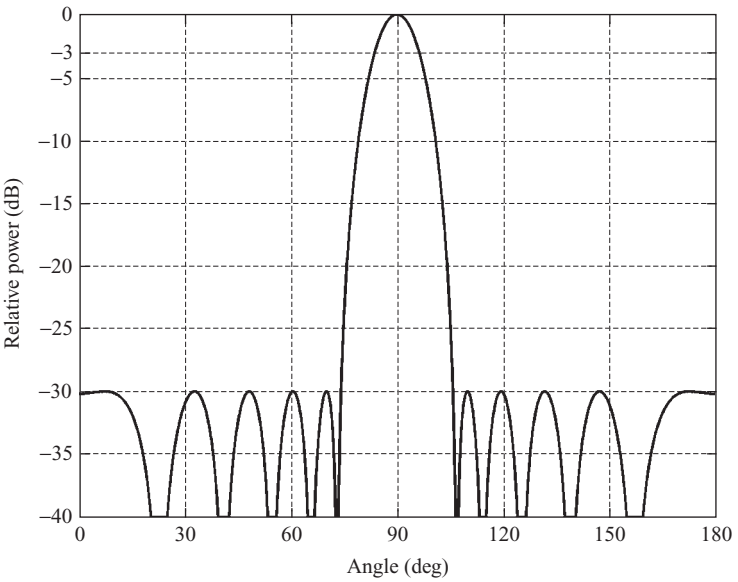

Fig. 5.29 Array factor of a 7-element Chebyshev array

Exercises

5.1 Show that the array factor of an N-element array of z-directed $\lambda/2$ dipoles kept along the z-axis at $z'_1, z'_2, \ldots, z'_N$ and carrying currents $I_1, I_2, \ldots, I_N$, respectively is given by

$$\sum_{n=1}^{N} I_n e^{jkz'_n} \cos\theta$$

5.2 Dipoles are used to construct linear arrays as shown in Fig. 5.30. Is it possible to apply the pattern multiplication principle to compute the antenna pattern of each of these arrays? Justify your answer.

5.3 An array antenna consists of two elements with uniform in-phase excitation and an element spacing of 2λ. Determine the number and the directions of maxima and nulls in the array factor.

Answer: 5 maxima; 0°, 60°, 90°, 120°, 180°. 4 nulls; 41.41°, 75.52°, 104.48°, 138.59°

5.4 Show that the array factor of a two-element array with the excitation having a progressive phase shift of $\alpha = kd$, where d is the element spacing, has two maxima and two nulls if $d = 0.75\lambda$. Determine the directions of these maxima and nulls.

Answer: maxima: 180°, 70.53° nulls: 0°, 109.47°

5.5 Determine the directions of maxima of the element pattern, array factor, and the array pattern shown in Fig. 5.8 for $d = 0.25\lambda$ and $d = 0.5\lambda$.

Answer: $\text{EP}_{\max}$: 90°; For $d = 0.25\lambda$: $\text{AF}_{\max}$ at 180°, $\text{AP}_{\max}$ at 111.5°. For $d = 0.5\lambda$: $\text{AF}_{\max}$ at 0° and 180°, $\text{AP}_{\max}$ at 51° and 129°

5.6 Calculate the exact value of ψ corresponding to the first side lobe peak of a 14-element uniform array with array axis along the z-axis. Compute the level of the first side lobe peak. If $\alpha = 0$ and $d = \lambda/2$, what is the direction of the first side lobe in θ coordinates?

Answer: 0.6429 rad, −13.11 dB, 78.19°

5.7 Calculate the extent of the visible region of a uniform array along the z-axis with

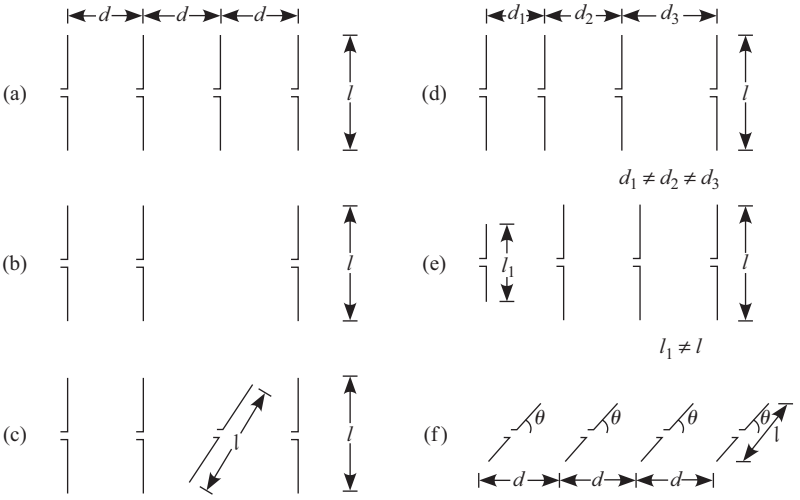

Fig. 5.30 Linear arrays of dipoles

$d = 2\lambda$ and $\alpha = \pi/4$. How many grating lobes are present in the visible region? What are the directions (in θ) of the main lobe and the grating lobes?

Answer: $\frac{-15\pi}{4}$ to $\frac{+17\pi}{4}$, 3, 93.58°, 20.36°, 64.06°, 124.23°

5.8 How many grating lobes are present in the visible region of the array factor of a uniform array having an inter-element spacing of 3λ and a uniform progressive phase shift $\alpha = -\pi/3$ in the excitation?

Answer: 5

5.9 Calculate the element spacing, d, and the progressive phase shift, α, of a 7-element uniform array so that the array factor has the maximum along $\theta = 90°$, nulls along $\theta = 0$ and 180°, and only one main lobe with minimum beamwidth in the visible region. Calculate the 3 dB beamwidth.

Answer: $\frac{6\lambda}{7}$, 0°, 8.54°

5.10 Repeat Problem 5.9 with the direction of the maximum along $\theta = 45°$.

Answer: 0.502λ, −127.79°, 21.08°

5.11 Indicate the nulls and the maximum of the array factor of a 7-element uniform array on a unit circle. Show that if $d = \lambda/2$ and $\alpha = 0$ the array factor does not have nulls along $\theta = 0$ and 180°.

5.12 Show the nulls of the array factor of the array designed in Problems 5.9 and 5.10 on a unit circle and indicate the visible region.

5.13 Calculate the 3 dB beamwidth of the main beam of the array factor of a 5-element broadside array with $d = \lambda/2$ having (a) uniform excitation and (b) binomial excitation.

Answer: (a) 20.76° (b) 27.1°

5.14 What is the maximum element spacing allowed in a binomial array so that no part of the grating lobe appears in the visible region if it is (a) a broadside array and (b) an endfire array?

Answer: (a) $\lambda/2$ (b) $\lambda/4$

5.15 Plot the location of the zeros of the array factor of the 4-element Chebyshev array designed in Example 5.6 on a unit circle and indicate the visible region.

5.16 Design a 7-element array with its array factor having all the side lobe peaks at 30 dB below the main beam peak, the main beam along $\theta = 45°$, narrowest possible main beam, and no part of the grating lobe appears in the visible region.

5.17 Redesign the array of Problem 5.16 if the grating lobe is allowed to appear in the visible region but its level is restricted to 30 dB below the main beam peak.

5.18 Calculate the 3 dB beamwidth of the Chebyshev array of Example 5.7 and compare it with that of a 7-element uniform broadside array with $d = 0.75\lambda$.

Answer: 12.56°, 9.76°

CHAPTER 6

Special Antennas

Introduction

In the previous chapters we studied the radiation characteristics of some generic antennas. By classifying the antennas into groups such as wire antennas, aperture antennas, array antennas, etc., we were able to identify analysis techniques that can be used to characterize antennas belonging to each of these classes. There are several antennas that cannot be easily classified into these categories. These antennas are explained in this chapter.

These antennas are special because of their construction or the principle of their operation. For example, a Yagi–Uda array is made up of an array of dipoles, but only one of the dipoles is directly excited and all other dipoles are excited parasitically. The length of the directly excited dipole is different from those of the parasitic elements. In the case of a log-periodic array, although the dipole elements are excited using a serial feed, their lengths are all different. Therefore, the pattern multiplication theorem cannot be applied to these structures. A turnstile antenna, on the other hand, is constructed using a pair of dipoles placed orthogonal to each other and fed by currents in phase quadrature. This produces a pattern that rotates in time. A spiral antenna shows frequency independent behaviour. Apart from these, this chapter also includes discussions on antennas that are used in practical systems, such as mobile phones, wireless local area networks, radio and television broadcasting, etc.

Besides discussing the radiation characteristics of special antennas, this chapter also presents procedures to design these antennas. In this chapter, too, the focus remains on the radiation characteristics. An antenna also needs to be matched to the transmitter or the receiver in order to minimize reflections. This is determined by the input impedance of the antenna. Therefore, for an antenna to work satisfactorily, it is not sufficient to determine the dimensions such that it meets the radiation pattern

requirements, it is also necessary to get the desired input impedance. In this book, we have not deliberately addressed the issue of input impedance. The computation of input impedance involves the solution of integral equations and is beyond the scope of this book (interested readers may refer to Balanis 2002, Elliott 1981, and Stutzmann & Thiele 1998).

6.1 Monopole and Dipole Antennas

In Chapter 3 we studied the radiation characterstics of dipole and monopole antennas. In this section, the attention is focussed on the adaptations of these antennas for different applications.

6.1.1 Monopole for MF and HF Applications

The medium frequency (MF) band extends from 300 kHz to 3000 kHz which corresponds to wavelengths of 1000 m to 100 m, and the high frequency (HF) band is from 3 MHz to 30 MHz (wavelengths from 100 m to 10 m). The antennas operating in these bands pose a unique set of challenges due to their size. For example, a quarter-wave monopole antenna with a ground plane, operating at 1.25 MHz has a height of 60 m. Generally, the antenna is constructed as a metallic tower held in place by a set of wire ropes, called guy wires, as shown in Fig. 6.1. The guy wires are isolated from the antenna with the help of insulators. The antenna is fed at its base and is isolated from the ground by placing it on an insulator.

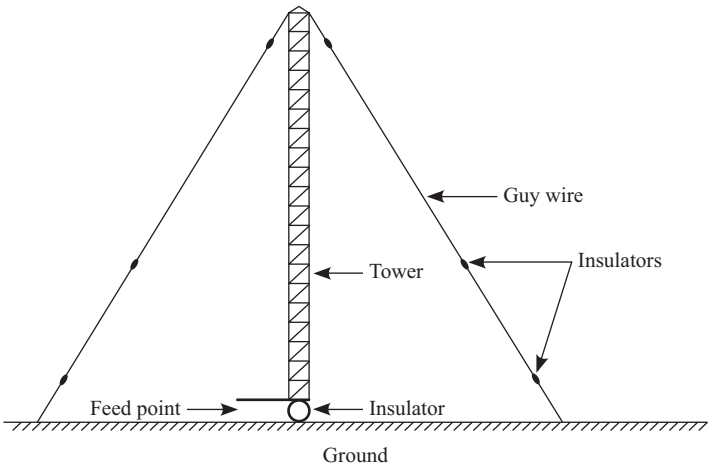

Fig. 6.1 Geometry of a monopole antenna above a ground plane held in place by guy wires

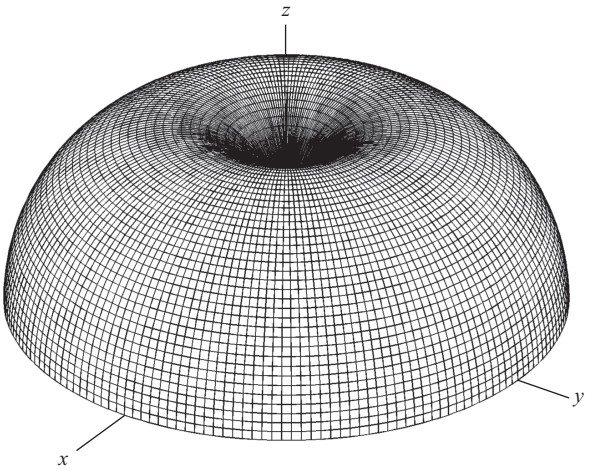

Fig. 6.2 Radiation pattern of a monopole above a ground plane

Let us go through some of the issues involved in the design and construction of this antenna with an example. Consider an antenna operating at 1250 kHz, which corresponds to a wavelength of 240 m. Therefore, a quarter-wave monopole is 60 m high. Assuming a perfectly conducting earth, we can use the image principle to compute the radiation pattern (Fig. 6.2) of a quarter-wave monopole above the ground. It is quite interesting to observe the effect of the guy wires on the performance of the antenna. The radiation pattern of a monopole with four guy wires, each 120 m long, is shown in Fig. 6.3. Since the guy wires are half a wavelength long, they become resonant structures and distort the radiation pattern of the monopole. Therefore, it is important to ensure that the support structure used in the construction of the monopole is not resonant at the frequency of operation of the antenna. The guy wires can be made non-resonant by introducing more insulators on each of the guy wires and the radiation pattern with this modification is very close to that of a free standing monopole.

The current on a quarter-wave monopole above a ground plane has a sinusoidal distribution. Making the antenna short, the current distribution becomes triangular and the radiation resistance of the antenna decreases. In Section 3.3 we showed that the radiation resistance of a monopole of length $l/2$ kept above a ground plane is equal to half the radiation resistance of a dipole of length l radiating into free space. The radiation resistance of a short dipole of length l, with triangular current distribution, radiating into

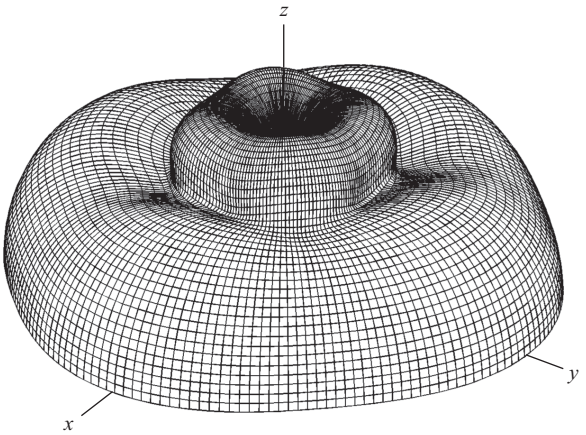

Fig. 6.3 Radiation pattern of a monopole above a ground plane with long guy wires

free space is given by Eqn (3.34) which is

$$R_{\text{rad}} = 20\pi^2 \left| \frac{l}{\lambda} \right|^2 \tag{6.1}$$

For a dipole of length $l = 0.2\lambda$, the radiation resistance is 7.9 Ω. Therefore, the radiation resistance of a monopole of length 0.1λ is half this value, i.e., 3.95 Ω. A low value of R_{rad} is difficult to match and the radiation efficiency is also low. One of the methods to increase the radiation resistance is to make the current distribution on the monopole near uniform. For a dipole of length l supporting uniform current distribution, the radiation resistance is given by Eqn (2.49)

$$R_{\text{rad}} = 80\pi^2 \left| \frac{l}{\lambda} \right|^2 \tag{6.2}$$

Therefore, the radiation resistance of the same length of dipole, i.e., $dl = 0.2\lambda$, supporting a uniform current distribution is 31.6 Ω and for a monopole of length $dl = 0.1\lambda$ kept above the ground plane it is 15.8 Ω. It is possible to make the current on the monopole more uniform by introducing a flat disk, radial mesh (Fig. 6.4) or a simple cross at the top of a short monopole. This is known as top loading of a monopole. This makes the current more uniform and hence the radiation resistance is increased. In practice, the current on the top loaded monopole has a slight taper, and hence, the radiation resistance will be less than that predicted by assumming a uniform current distribution.

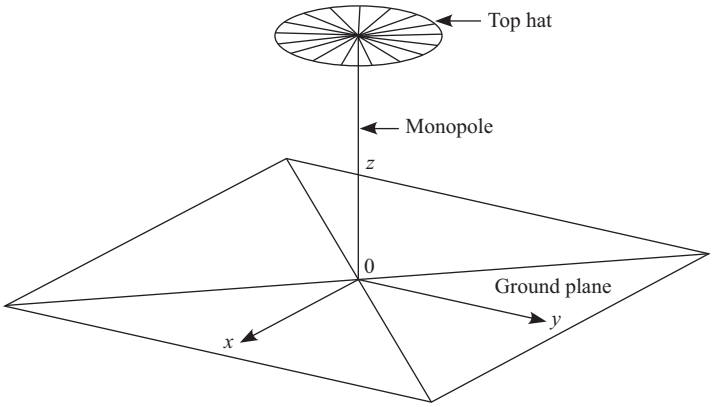

Fig. 6.4 A monopole above a ground plane with a top hat loading

In all the above cases, a perfect ground plane (infinitely large perfect electric conductor) has been assumed. However, the earth is usually used as a ground plane for monopoles operating in the MF and HF bands. It is observed that the conductivity of the earth is in the order of millisiemens (mS) and the relative permittivity is in the range of 3 to 12. Therefore, the earth does not meet the requirements of a good electric conductor. To increase the effective conductivity of the earth below the monopole, conducting wires are laid on the ground, running radially from the base of the monopole. These radial wires simulate a good conducting ground plane. For HF antennas, generally 120 radials at equal angular separation of 3°, each at least $\lambda/4$ long (perferably $\lambda/2$ long) are laid to realize a good ground. The performance of the monopole with the radials is slightly inferior compared to a monopole above a perfect electric conductor.

A variant of the top hat antenna is an inverted L-shaped antenna. This is more popular as a receiving antenna. The antenna is made in a shape of the English letter L and is fed at the base of the vertical arm (Fig. 6.5).

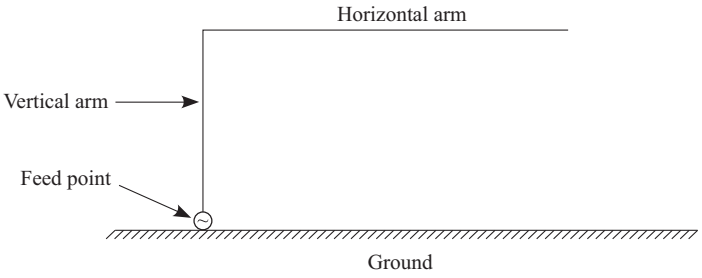

Fig. 6.5 Inverted L-shaped antenna above a ground plane

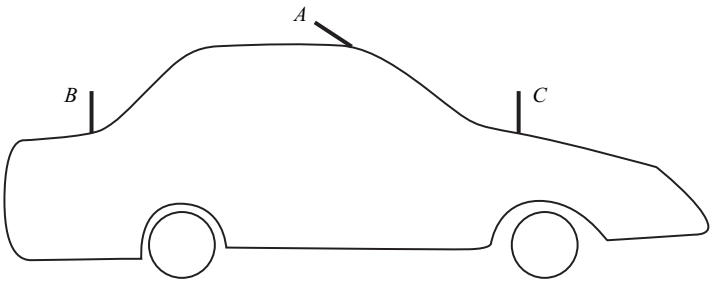

Fig. 6.6 Monopole on an automobile at three different places

For best performance, the total length of the wire needs to be equal to $\lambda/4$. However, in practice even shorter lengths have also been used for receiving applications.

6.1.2 Monopole at VHF

Let us suppose that the requirement is to design an antenna operating at 2 m wavelength which is to be mounted on an automobile. If the automobile body is used as a ground plane, the simplest choice would be a quarter-wave long monopole kept vertical above the ground plane. The height of the antenna would be 0.5 m and is shown in Fig. 6.6, marked as A. This antenna is simple to design, construct, and attach, but not a desirable one from the structural point of view. If possible, it is very much desirable to reduce its height, and locate it either at position B or C in the figure. From the aerodynamics point, it is preferable to tilt the structure.

In order to increase the gain of the monopole, a $5\lambda/8$ long monopole is used. It can be shown that a $5\lambda/8$ long monopole above an infinite ground plane has a directivity of 5.2 dB and its input impedance has a large capacitive reactance. Therefore, a matching section is required to efficiently transfer power from a 50 Ω transmission line into this antenna. By using an air core inductor near the base of the antenna, it is possible to tune out the capactive reactance and match the antenna to a coaxial transmission line having a characteristic impedance of 50 Ω (Fig. 6.7).

6.1.3 Antenna for Wireless Local Area Network Application

A wireless local area network (WLAN) consists of an access point (AP) and several client cards that communicate with the AP. The AP itself is usually stationary, while the client cards are attached to the laptop computers

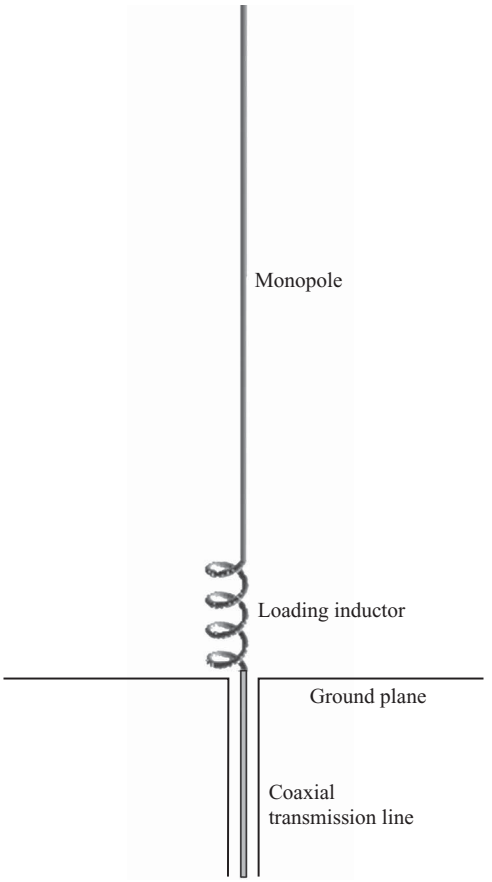

Fig. 6.7 A monopole with loading inductor

which can be taken from one place to another (mobile). Since the AP needs to communicate with the cards placed in any direction from it, the antenna connected to the AP usually has an omni-directional radiation pattern. A monopole above a ground plane is a good choice for this application. In the absence of a ground plane, a modified form of a dipole, known as a *sleeve dipole*, is one of the most popular antennas for an AP.

Sleeve dipole A sleeve dipole can easily be constructed using a coaxial cable. A certain length of the outer conductor of a coaxial cable is removed to expose the inner conductor [Fig. 6.8(a)]. This forms one arm of the dipole. The second arm of the dipole is formed by a metallic sleeve attached to the coaxial cable as shown in Fig. 6.8(b). The top end of the sleeve is electrically attached to the outer conductor of the coaxial cable. The lengths of the

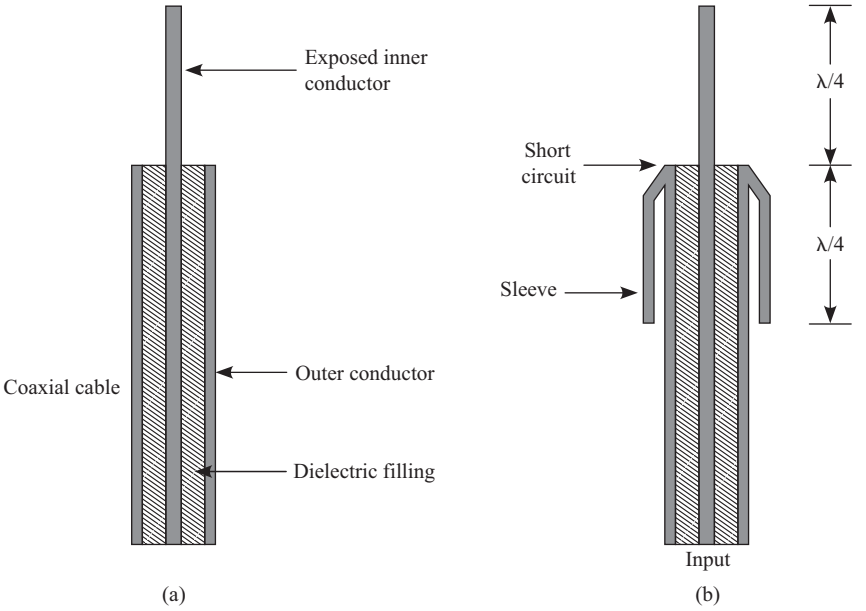

Fig. 6.8 (a) Coaxial cable with exposed inner conductor (b) Cross-section of a sleeve dipole

exposed inner conductor and the sleeve are both made approximately equal to $\lambda/4$ and together they form two arms of the dipole. The sleeve, apart from forming a radiating element, also performs the task of suppressing the currents from flowing on the outer surface of the coaxial cable.

Consider a coaxial cable with an exposed portion of the center conductor as shown in Fig. 6.8(a). The current flowing on the inner conductor of the coaxial cable establishes a return current both on the inner and the outer surfaces of the outer conductor. Therefore, the current on the outer surface of the outer conductor also radiates, which is not desirable. This is also known as cable radiation. Since the cable orientation and its environment is not under control, the performance of an antenna with cable radiation becomes unpredictable. Therefore, it is necessary to suppress the current flowing on the outer surface of the cable.

Consider a $\lambda/4$ long sleeve with one end attached to the outer conductor of the coaxial cable in a short-circuit and the other end left unterminated. Since the sleeve is quarter wavelength long, the short-circuit end creates an open-circuit impedance at the unterminated end and, hence, no current can flow on the inner surface of the sleeve or on the outer surface of the coaxial cable. Such an arrangement is known as a *balun* (short form for balance-to-unbalance).

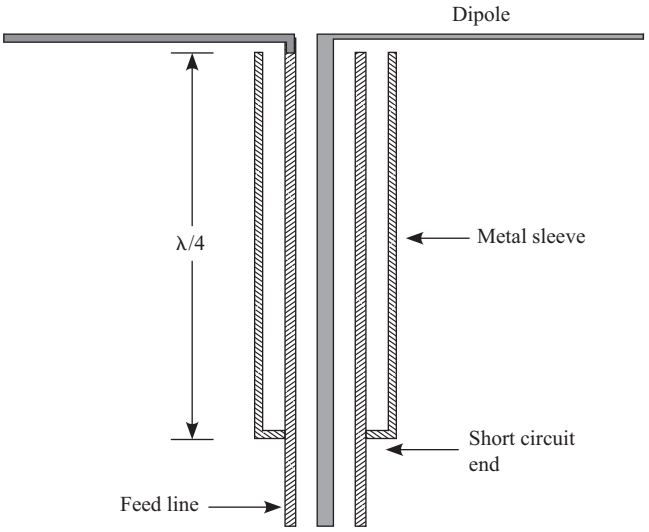

Fig. 6.9 Balun made of $\lambda/4$ long sleeve

A balun is used to connect an unbalanced line (e.g., coaxial cable) to a balanced antenna (e.g., dipole). A quarter wavelength long metal sleeve with its bottom end shorted to the outer of the coaxial feed acts as balun (Fig. 6.9). The sleeve along with the outer conductor of the feed line forms another coaxial line of length $\lambda/4$ that is shorted at one end. The input impedance looking into the other end of this transmission line is ideally infinity and hence no current is supported by this transmission line. The $\lambda/4$ sleeve is choking the current from flowing on the outer conductor of the feed line. Transmission-line-based baluns are useful for antennas operating in the UHF and microwave frequency bands. For applications in the HF and VHF band of frequencies, a transformer-based balun is more popular (Hall 1984).

Matching A balun is used to transform the balanced input of an antenna into an unbalanced impedance so that an unbalanced transmission line can be connected to it. Apart from a balun, a feed design must also take into consideration the impedance mismatch between the antenna and the feed line. If the antenna impedance, R_a, is purely real, a quarter-wave long transmission line of impedance $\sqrt{Z_0 R_a}$ (Z_0 is the characteristic impedance of the transmission line) can be used as an impedance transformer. If the antenna impedance is complex, a matching stub can be used to transform the complex antenna impedance into a real impedance equal to the characteristic impedance of the transmission line. This can be realized by either a single stub or multiple stubs (Pozar 2003).

6.2 Long Wire, V, and Rhombic Antennas

In Chapter 3 we studied the radiation characteristics of a centre-fed dipole that supports a sinusoidal current distribution. Let us now focus our attention on the radiation characteristics of a wire antenna fed near one end with the other end left open. For convenience, let us again assume that the antenna is oriented along the z-axis with the feed point in the region $0 < z' \leq \lambda/4$ (Fig. 6.10). Let L be the length of the wire and I_0 be the maximum amplitude of current on the dipole. The current at any point z' on the wire is assumed to be z-directed

$$\mathbf{I}(z') = \mathbf{a}_z I_z(z') \tag{6.3}$$

and $I_z(z')$ is given by

$$I_z(z') = I_0 \sin k(L - z') \quad 0 \leq z' \leq L \tag{6.4}$$

The current on a one wavelength long wire antenna is shown in Fig. 6.11.

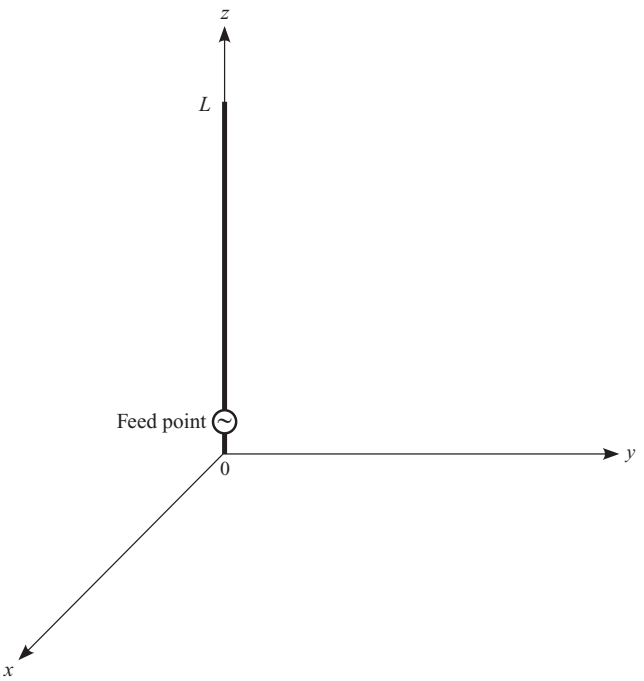

Fig. 6.10 Geometry of a z-directed long wire antenna

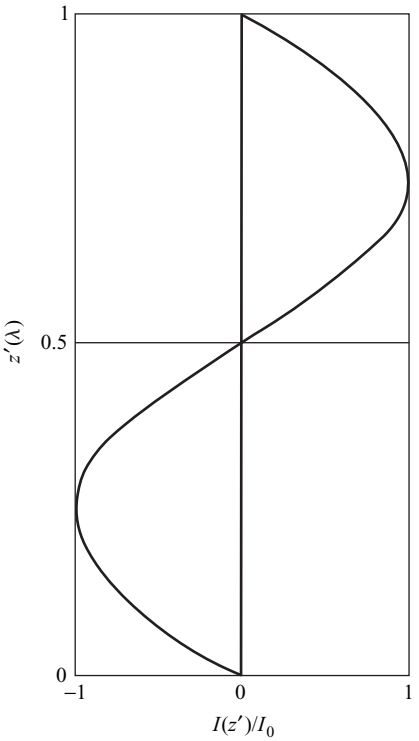

Fig. 6.11 Current distribution on a long wire antenna of length λ

Using the techniques described in Chapter 3, we can compute the far-field of the wire antenna by first computing the magnetic vector potential

$$A_z = \frac{\mu}{4\pi}\frac{e^{-jkr}}{r} I_0 \int_0^L \sin k(L - z') e^{jkz' \cos\theta} dz' \tag{6.5}$$

and then the electric field

$$\mathbf{E} = \mathbf{a}_\theta j\eta I_0 \frac{e^{-jkr}}{4\pi r} \frac{1}{\sin\theta} \left[e^{jkL\cos\theta} - j\cos\theta \sin(kL) - \cos(kL) \right] \tag{6.6}$$

For a long wire antenna whose length is equal to an integral multiple of a wavelength, i.e., $L = N\lambda$, where N is an integer, the magnitude of the electric field in the far-field region reduces to

$$|E_\theta| = \frac{\eta I_0}{2\pi r} \frac{1}{\sin\theta} \sin(N\pi\cos\theta) \tag{6.7}$$

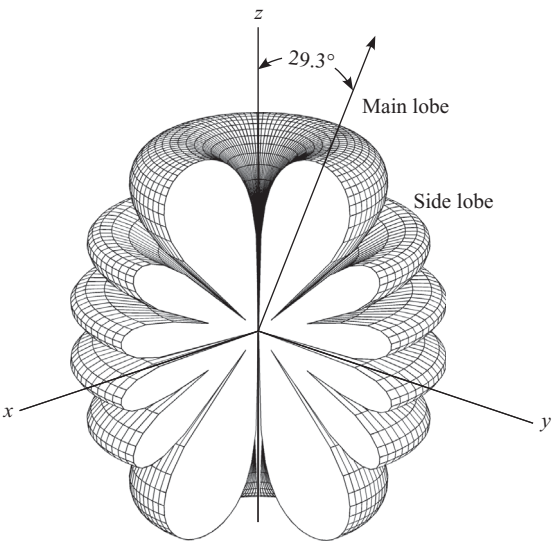

Fig. 6.12 Radiation pattern of a 3λ long wire antenna

The electric field is independent of ϕ and hence is symmetric in ϕ. The radiation pattern of a 3λ long wire is shown in Fig. 6.12. The pattern has two main lobes, one is symmetric about the positive z-axis and other with the negative z-axis. The surface passing through the direction of the maximum is a cone. The direction of the maximum is at 29.3° from the wire axis (z-axis). The pattern also has four side lobes. The radiation pattern of a longer wire has more number of side lobes.

For an $N\lambda$ long wire, the direction of the maximum, θ_m, is given by solving the following equation

$$(-N\pi)\frac{1-\cos^2\theta_m}{\cos\theta_m} = \tan\left(N\pi\cos\theta_m\right) \tag{6.8}$$

The location of the maximum as a function of the length of the wire antenna is shown in Fig. 6.13. The direction of the main beam gets closer to the axis of the wire (z-axis) as the length of the wire increases.

The direction of the nulls, θ_z, of the pattern are computed by equating the electric field given by Eqn (6.7) to zero and solving for θ_z

$$\frac{\sin\left(N\pi\cos\theta_z\right)}{\sin\theta_z} = 0 \tag{6.9}$$

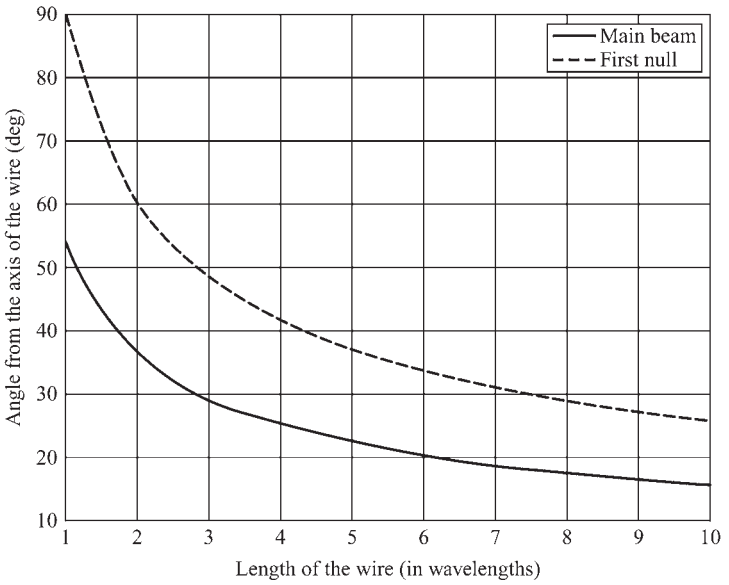

Fig. 6.13 Directions of the main beam and the first null of a long wire antenna

The above equation is satisfied if

$$N\pi \cos\theta_z = \pm n\pi \quad n = 0, 1, 2, \ldots, N \tag{6.10}$$

Therefore, the directions of the nulls are given by

$$\theta_z = \cos^{-1}\left(\pm\frac{n}{N}\right) \quad n = 0, 1, 2, \ldots, N \tag{6.11}$$

In the above equation, $n = 0$ corresponds to the null along $\theta_z = 90°$, and $n = N$ corresponds to the null along $\theta_z = 0$ and 180°. The direction of the next null closest to $\theta_z = 0$ is given by

$$\theta_z = \cos^{-1}\left(\frac{N-1}{N}\right) \tag{6.12}$$

The location of this null as a function of the length of the wire antenna is also shown in Fig. 6.13. For longer wires, the first null is closer to the axis of the wire and hence the beamwidth between the nulls gets narrower.

The current distribution and the radiation pattern of an end-fed wire antenna are quite different from that of a center-fed wire. For example, in Fig. 3.5, we observe that a 1λ long center fed dipole has an omni-directional

pattern with a maximum in the plane orthogonal to the axis of the wire. If the 1λ long wire is fed at one of its ends, the radiation pattern maxima are along 40° and 140° and the pattern has a null in the plane orthogonal to the axis of the wire.

EXAMPLE 6.1

Show that the directions of maxima of an $N\lambda$ long wire satisfy Eqn (6.8).

Solution: Along the direction of the main beam, the derivative of the electric field with respect to θ is zero

$$\frac{d}{d\theta}(E_\theta)|_{\theta=\theta_m} = \frac{d}{d\theta}\left\{\frac{\sin(N\pi\cos\theta)}{\sin\theta}\right\} = 0$$

Performing the indicated differentiation with respect to θ and equating the numerator to zero

$$-N\pi\sin^2\theta_m\cos(N\pi\cos\theta_m) - \cos\theta_m\sin(N\pi\cos\theta_m) = 0$$

This can be rearranged in the form

$$(-N\pi)\frac{1-\cos^2\theta_m}{\cos\theta_m} = \tan(N\pi\cos\theta_m)$$

6.2.1 V Antenna

Consider two thin wires arranged in the form of the English letter V, such that they make an angle χ with each other. Let the two wires be placed in the x-z plane symmetrically about the x-axis and a source be connected between the two wires at the common point as shown in Fig. 6.14. Since this structure resembles the English letter V, this antenna is popularaly known as a V *antenna*. The radiation characteristics of this antenna depends on both the length, L, of each of the two arms and the angle between them.

As the included angle χ is decreased, the two wires come closer to each other and hence the main lobes, too, come closer. Iteratively solving Eqn (6.8) with $L = 5\lambda$, we find that in the radiation pattern of the individual wire, the direction of the main lobe is oriented at an angle of 22.4° with respect to the axis of the wire. Therefore, by choosing $\chi = 2\theta_m = 44.8°$, it is possible to make the two maxima coincide with each other.

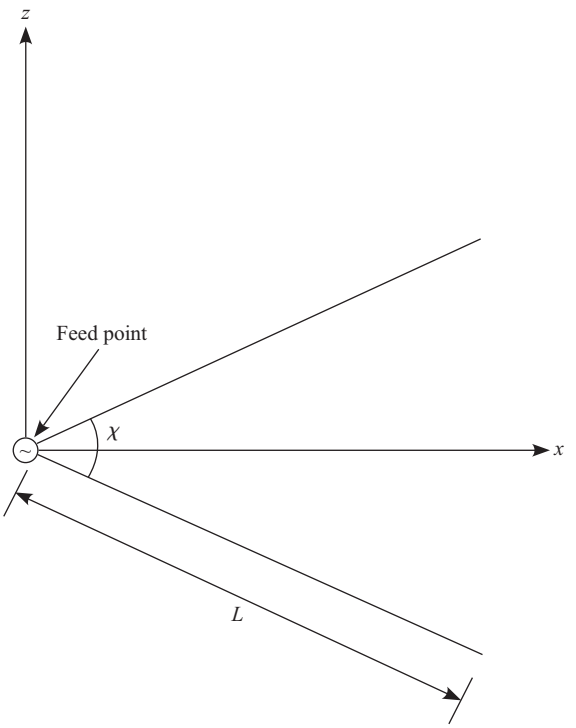

Fig. 6.14 Geometry of a V antenna

The radiation patterns of a V antenna with $\chi = 36^\circ$ is shown in Fig. 6.15, and it has one main lobe along the positive x-direction and another along the negative x-direction. If the two wires are brought closer, the two conical beams cross over each other and hence the final pattern has two maxima along the positive x-direction and two more along the negative x-direction. The radiation pattern for $\chi = 14^\circ$ is shown in Fig. 6.16.

In the wire antenna and the V antenna considered so far, one end of the wire was left open. The reflection at the open end sets up a standing wave current on the wire. Instead of leaving the far end open, if it is terminated in a load, a travelling wave is established on the wire. If the wire is long, most of the power gets radiated by the time the travelling wave reaches the load and hence very little power is lost in the load. Since a small amount of the power is absorbed by the load, the radiation efficiency of the antenna terminated with a load is lower than the unterminated counterpart. The main advantage of a wire supporting a travelling wave is that its radiation pattern has only one conical main beam in the direction of the current flow. The radiation pattern of a 6λ long wire supporting a travelling wave current is shown

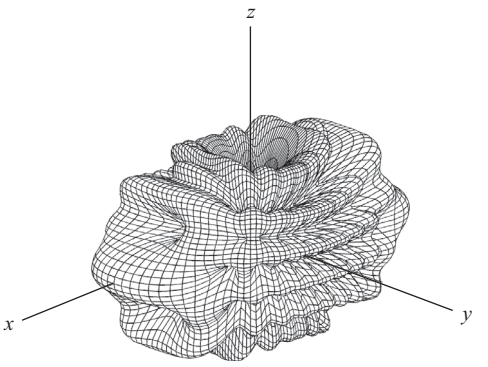

(a) 3D pattern

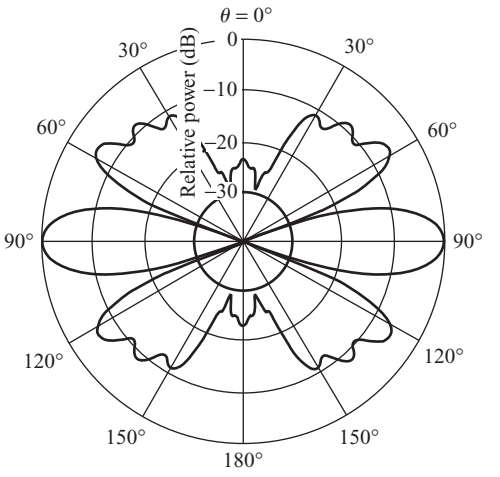

(b) Pattern in the $\phi = 0$ plane (x-z plane)

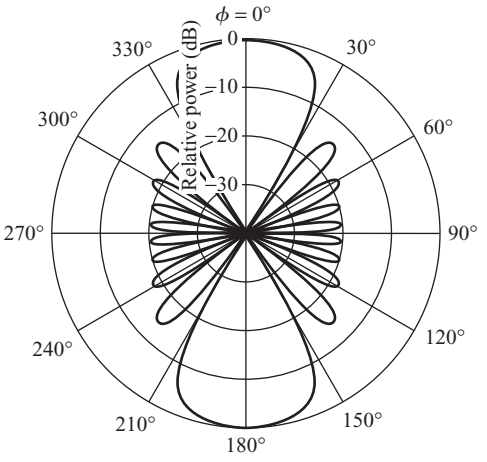

(c) Pattern in the $\theta = 90°$ plane (x-y plane)

Fig. 6.15 Radiation pattern of a V antenna with $\chi = 36°$ and $L = 5\lambda$

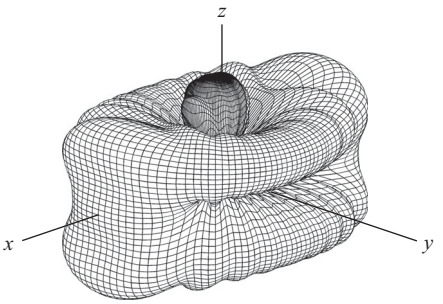

(a) 3D pattern

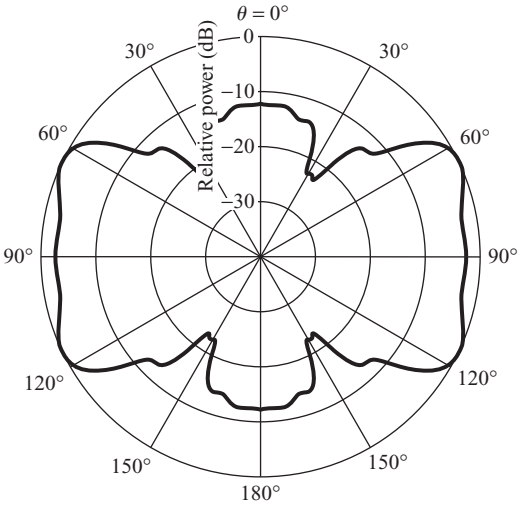

(b) Pattern in the $\phi = 0$ plane (x-z plane)

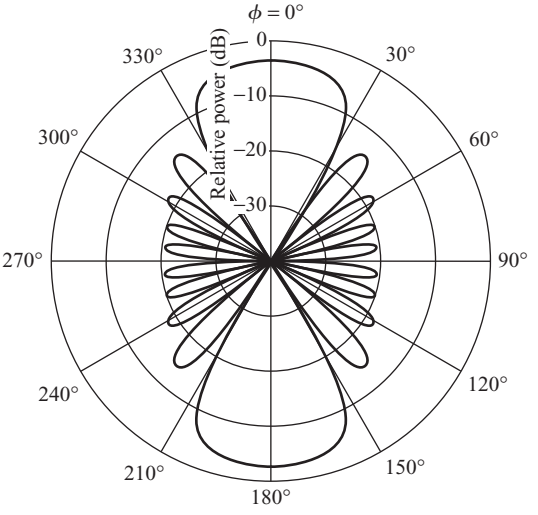

(c) Pattern in the $\theta = 90°$ plane (x-y plane)

Fig. 6.16 Radiation pattern of a V antenna with $\chi = 14°$ and $L = 5\lambda$

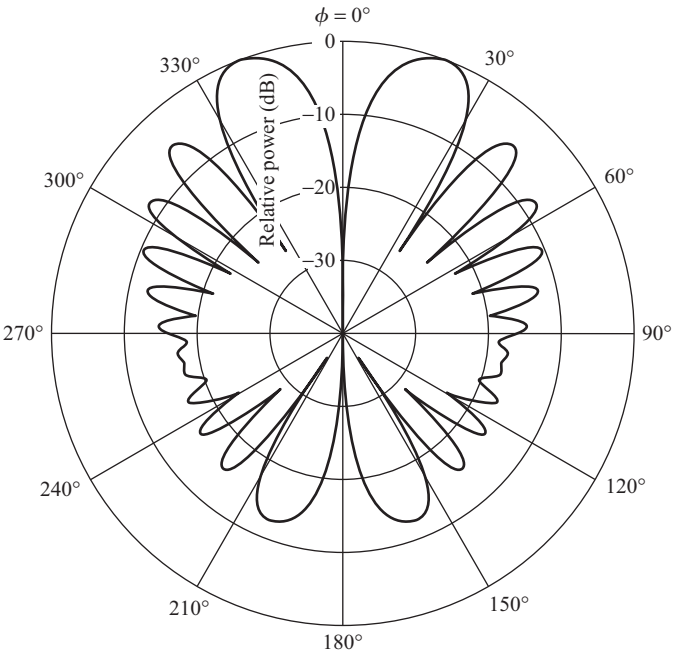

Fig. 6.17 Radiation pattern of a 6λ long wire antenna with a travelling wave current

in Fig. 6.17. The main beam makes an angle of 20.4° with the axis of the wire. The direction of the maximum approaches the axis of the wire as the length of the wire is increased. Once again, we can combine two wires in the form of a V to achieve a single main beam along the angle bisector of the two wires (Fig. 6.18). A horizontal cut of the pattern is shown in Fig. 6.19. The included angle, $\chi = 2 \times 20°$, is chosen such that the conical main beams of the two wires combine to form the main beam of the V antenna. Though we need a ground to terminate the wires, the radiation pattern of the V antenna shown in Fig. 6.19 does not take the effect of gound into account.

By combining two V antennas supporting travelling wave currents on them, a rhombic antenna is formed (Fig. 6.20). The rhombic antenna has maximum radiation along the x-axis, as shown in Fig. 6.21. Once again, we have not taken into account the influence of the ground on the radiation characteristics of the rhombic antenna.

The ground plane, if present, can be effectively used to simplify the construction of the rhombic antenna. One half of the rhombic antenna including the terminating resistor is placed vertically above the ground. The other half of the rhombus is realized by the image (Fig. 6.22). The radiation pattern of this structure is identical to that of a full rhombus radiating in free space, except that there is no radiation below the ground plane.

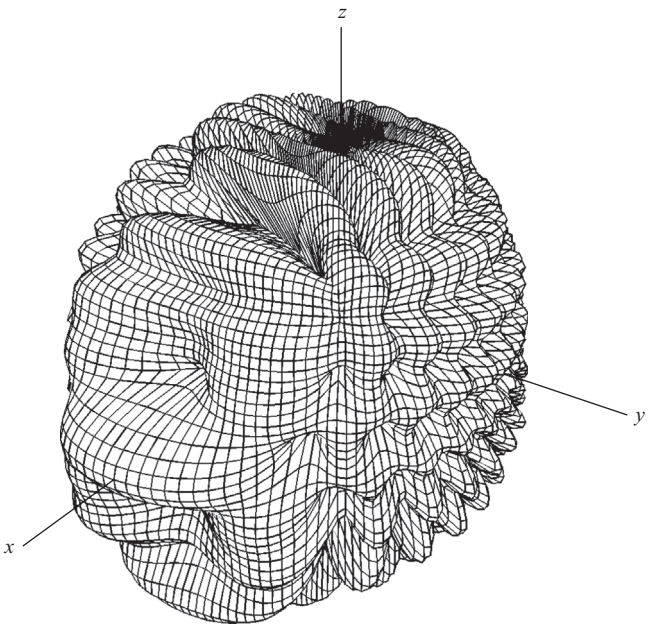

Fig. 6.18 Radiation pattern of a V antenna with travelling wave current (6λ long, $\chi = 40°$)

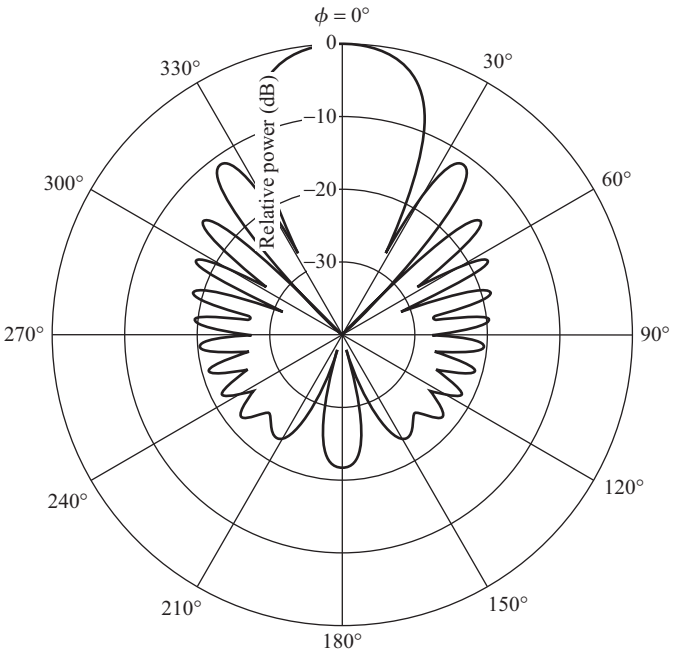

Fig. 6.19 Horizontal plane ($\theta = 90°$) pattern of a travelling wave V antenna (length $= 6\lambda$ and $\chi = 40°$)

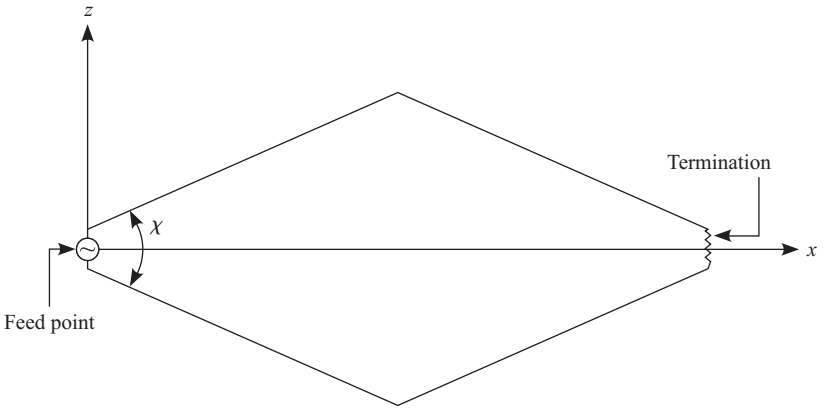

Fig. 6.20 Geometry of a rhombic antenna

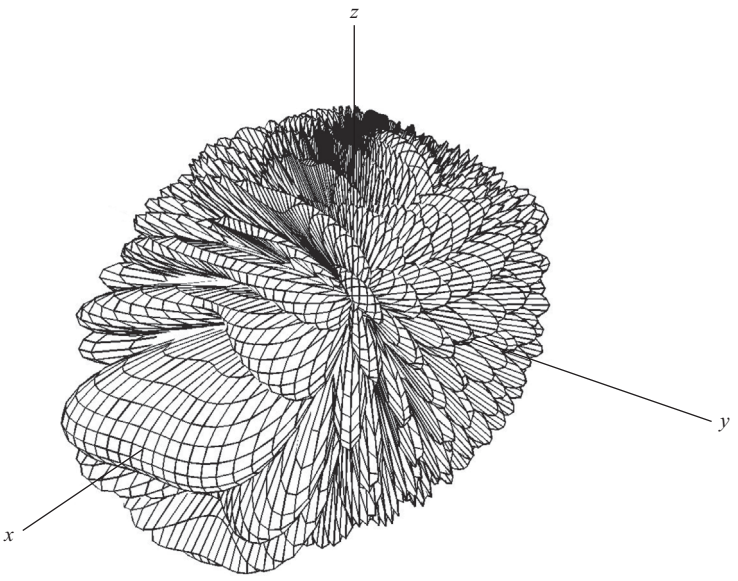

Fig. 6.21 Radiation pattern of a rhombic antenna

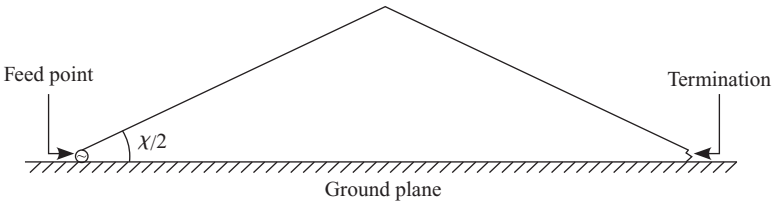

Fig. 6.22 Geometry of a rhombic antenna above a ground plane

6.3 Yagi–Uda array

An array antenna is used to realize pattern properties that are usually not achievable by a single antenna element. In Chapter 5, we considered a linear array of identical elements but with independent exciations. Here we consider a dipole array with only one excited dipole and all other dipoles parasitically coupled to it. One such antenna, named after its inventors, is known as a Yagi–Uda array. The induced currents in the parasitic elements and, hence, the radiation characteristics, depend on the length of the dipoles and the spacing between the dipoles. In this section, we study a parasitic array of dipoles and also give a procedure to design it.

Consider a dipole radiating in free space. If a second dipole, with its terminals short circuited, is brought near the driven dipole element and kept parallel to it, a current is established on the second dipole due to electromagnetic induction. Since the second dipole gets excited parasitically, it is called a parasitic element. The amplitude and phase of the induced current on the parastic element depends on the length and the radius of the element as well as the distance from the excited dipole. Let the driven element be kept at the origin and the parasitic dipole be placed at $z = -0.125\lambda$ and let both be oriented along the x-axis as shown in Fig. 6.23(a). Let the current on the driven element be 1 A, and the induced

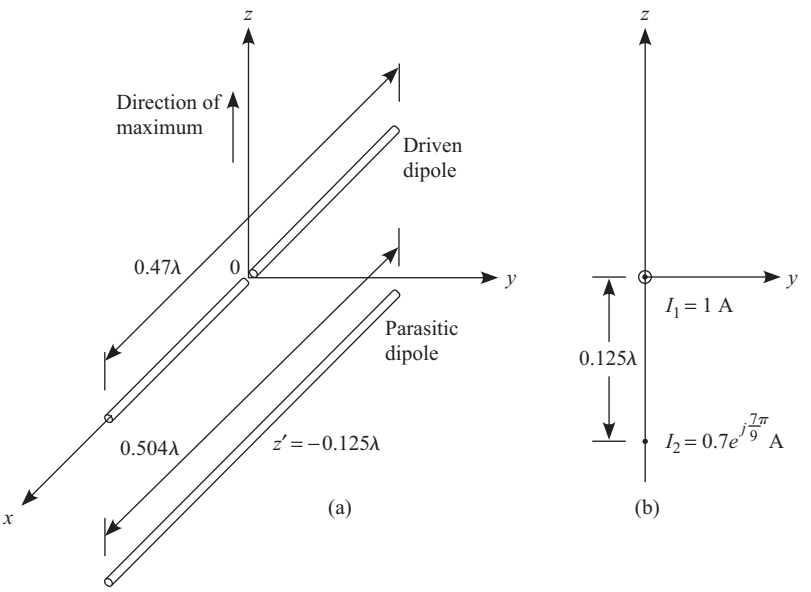

Fig. 6.23 A parasitic element in the presence of a driven element—(a) geometry and (b) currents for computing the array factor

current on the parasitic element be $0.7\angle 140°$ A [Fig. 6.23(b)]. The two dipole lengths may not be identical but are nearly same and we ignore the difference and treat it as a 2-element array and apply the array theory developed in Chapter 5. This is a 2-element array problem and hence we can compute the array factor of this array. Using Eqn (5.36)

$$\text{AF} = I_1 e^{jkz_1' \cos\theta} + I_2 e^{jkz_2' \cos\theta} \tag{6.13}$$

where $I_1 = 1$, $I_2 = 0.7\angle 140°$, $z_1' = 0$, $z_2' = -0.125\lambda$, and θ is the angle measured from the z-axis. Substituting these values in Eqn (6.13)

$$\text{AF} = 1 + 0.7e^{j\left(\frac{7\pi}{9} - \frac{\pi}{4}\right)\cos\theta} \tag{6.14}$$

The magnitude of the array factor along $\theta = 0°$ is $|\text{AF}| = |0.94 - j0.7| = 1.172$ and along $\theta = 180°$ is $|\text{AF}| = |0.303 - j0.06| = 0.309$. The antenna radiates more power along the $+z$-direction compared to the $-z$-direction. This can be looked at as the parasitic element reflecting the field incident on it. Therefore, such a parasitic element is called a reflector. The array factor as a function of θ is shown in Fig. 6.24. It is observed that if the driven dipole is 0.47λ long, and the parasitic dipole is chosen to be 0.504λ

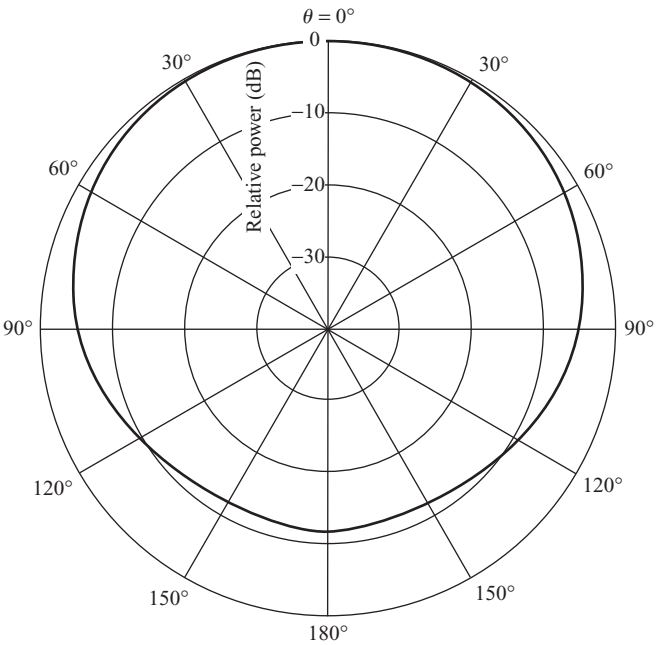

Fig. 6.24 Array factor of a 2-element array with the parasitic element acting as a reflector

long, the current on the parasitic element leads the current on the driven element and the parasitic element acts as a reflector.

Now consider again a 2-element parasitic array with $I_1 = 1$ A and $I_2 = 0.7\angle -140°$ A, i.e., the current in the parasitic element lags the current in the driven dipole. The array factor for this situation is given by

$$\text{AF} = 1 + 0.7e^{j\left(-\frac{7\pi}{9}-\frac{\pi}{4}\right)\cos\theta} \tag{6.15}$$

The magnitude of the array factor along $\theta = 0°$ is 0.309 and along $\theta = 180°$ is 1.172. Thus, the dipole field and that scattered from the parasitic element add along the direction of the parasitic element from the dipole, hence the parasitic element is called a director. The array factor of a driven element with a parasitic element acting as a director is shown in Fig. 6.25. It is observed that with a driven dipole of length 0.46λ, the current in the parasitic element of length 0.442λ lags that in the driven element and, hence, the parasitic element acts as a director. In general, a parasitic element shorter than the resonant length ($\sim \lambda/2$) acts as a director and one longer than the resonant length acts as a reflector.

Consider a 3-element array with one driven element and two parasitic elements on either side (Fig. 6.26), one longer and the other shorter than the driven element. In a Yagi–Uda array, the driven element is around 0.46λ

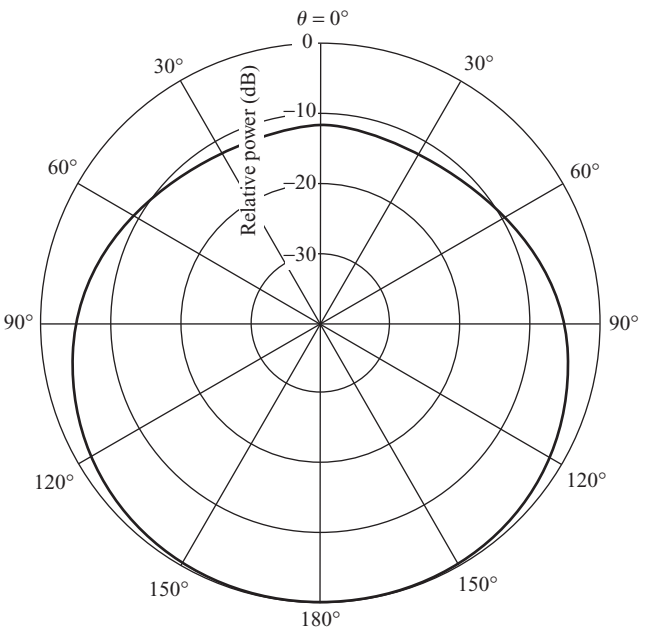

Fig. 6.25 Array factor of a 2-element array with the parasitic element acting as a director

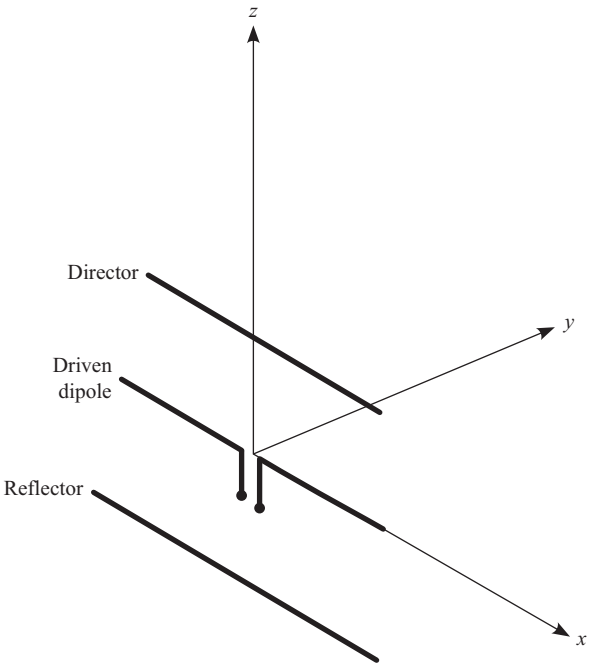

Fig. 6.26 Geometry of a 3-element Yagi–Uda array

to 0.47λ, the reflector is longer than the driven element, and the director is shorter. Typical dimensions of a 3-element Yagi–Uda antenna are:

Length of the driven element:	0.47λ
Length of the director:	0.442λ
Length of the reflector:	0.482λ

Optimum reflector-to-driven-element spacing (for maximum directivity) is between 0.15λ and 0.25λ and driven-element-to-director spacing is typically between 0.2λ and 0.35λ. The radiation patterns in the horizontal and vertical planes of the array with both the spacings set to 0.2λ are shown in Fig. 6.27.

The directivity of a Yagi–Uda array can be increased by adding more directors. These are generally added at approximately regular intervals of 0.18λ to 0.3λ spacing. The directivity of a Yagi–Uda array antenna is proportional to the overall length of the array in terms of wavelength. It is important to note that, in general, only one reflector is used in a Yagi–Uda antenna, because the field of the antenna just behind the reflector (in the negative z-direction) is small. Hence, a second parasitic element kept behind the reflector will not be effective, since very small current is induced on it.

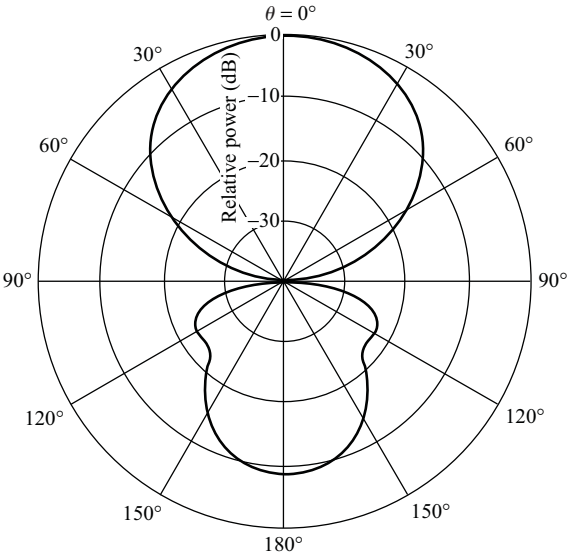

(a) **E**-plane pattern ($\phi = 0$ plane)

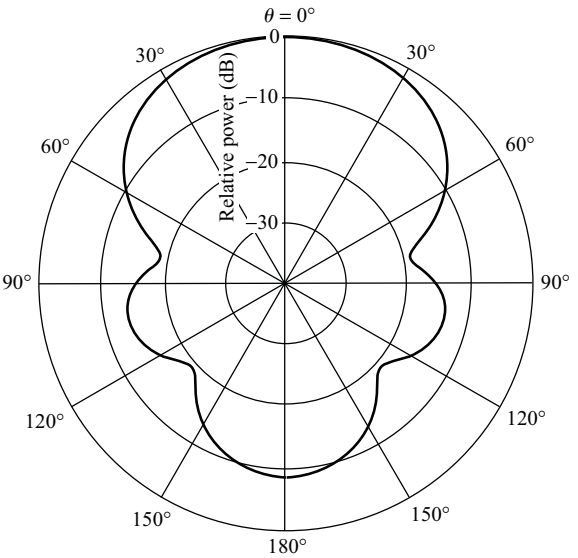

(b) **H**-plane pattern ($\phi = 90°$ plane)

Fig. 6.27 Radiation patterns of a 3-element Yagi–Uda array

The directivity of a Yagi–Uda array antenna as a function of number of directors is shown in Fig. 6.28. This plot is generated for a Yagi–Uda array, the parameters of which are shown in Table 6.1. Addition of the first few directors to a driven element and a reflector combination results in a

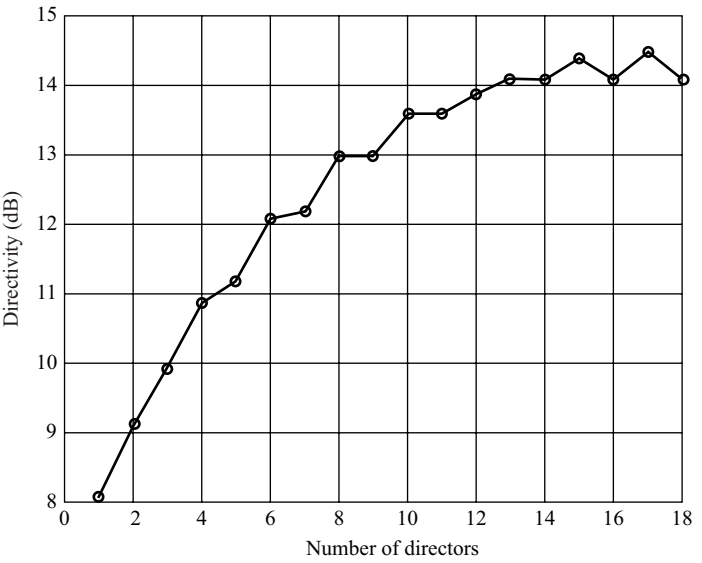

Fig. 6.28 Directivity versus the number of directors in a Yagi–Uda array (Array dimensions are as given in Table 6.1)

rapid increase in the directivity. The improvement in directivity for every additional director starts diminishing as the number of directors increases. As the number of directors increases, the length of the Yagi–Uda array also increases and so does the directivity.

Feed structure A balanced transmission line, such as a two-wire line, can be directly connected to the input terminals of the driven dipole, provided the input impedance of the antenna is equal to the characteristic impedance of the transmission line. An unbalanced line, e.g., a coaxial line, can be connected to the terminals of the driven dipole using a balun (a balanced-to-unbalanced transformer). If the input impedance of the antenna is purely

TABLE 6.1

Yagi–Uda array parameters

length of the reflector:	0.482λ
length of the driven element:	0.45λ
length of each of the directors:	0.40λ
spacing between the driven element and the reflector:	0.2λ
spacing between the driven element and the first director:	0.2λ
spacing between consecutive directors:	0.2λ

real but not equal to the characteristic impedance of the transmission line, a quarter-wave transformer can to be used to match the two impedances. It is also possible to integrate the impedance transformer into the balun itself.

The input impedance of a Yagi–Uda array is generally found to be complex. It is possible to adjust the lengths of the elements and the spacing between them such that the input impedance becomes purely resistive and equal to the characteristic impedance of the transmission line. This may result in a reduction in the gain of the antenna.

Another approach is to choose the dimensions of the array to maximize its gain. If the input impedance turns out to be complex, stub matching technique can be used to transform this impedance into a purely real quantity that is equal to the characteristic impedance of the transmission line.

Applications Yagi–Uda array is the most popular antenna for the reception of terrestrial television signals in the VHF band (30 MHz–300 MHz). The array for this application is constructed using aluminium pipes. The driven element is usually a folded dipole, which gives four times the impedance of a standard dipole. Thus, a two-wire balanced transmission line having a characteristic impedance of 300 Ω can be directly connected to the input terminals of the Yagi–Uda array.

Yagi–Uda arrays have been used in the HF, VHF, UHF, and microwave frequency bands. In the HF band, the array is usually constructed using wires and at VHF and UHF frequencies, hollow pipes are used for the construction of Yagi–Uda arrays. At microwave frequencies, the array is constructed using either printed circuit board (PCB) technology or machined out of a metal sheet.

EXAMPLE 6.2

Show that the input resistance of a $\lambda/2$ folded dipole is four times that of single half-wave dipole.

Solution: A folded dipole consists of two parallel $\lambda/2$ dipoles connected to each other at the ends as shown in Fig. 6.29. It is fed at the centre of one of the dipoles and the other dipole is shorted.

Let I_0 be the input current to the folded dipole and the current distribution over the dipole be sinusoidal. Because of the proximity ($d \ll \lambda$), the induced current distribution on the shorted dipole will also have a sinusoidal

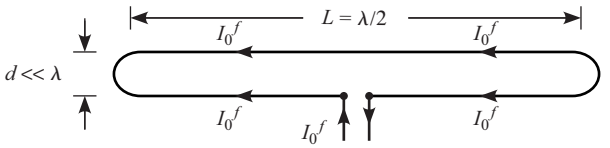

Fig. 6.29 Geometry of a folded dipole

distribution of the same amplitude. Thus, the field radiated by the folded dipole is equivalent to a single dipole carrying a sinusoidal current distribution with twice the amplitude. The field of a folded dipole is twice that of a single dipole and the power radiated is four times for the same input current I_0. Power radiated by the folded dipole is

$$P_{\text{rad}}^f = \frac{1}{2} I_0^2 R_{\text{rad}}^f$$

and the power radiated by the single dipole is

$$P_{\text{rad}}^d = \frac{1}{2} I_0^2 R_{\text{rad}}^d$$

where R_{rad}^f and R_{rad}^d are the radiation resistances of the folded and single dipoles, respectively. Since $P_{\text{rad}}^f = 4P_{\text{rad}}^d$

$$\frac{1}{2} I_0^2 R_{\text{rad}}^f = 4 \frac{1}{2} I_0^2 R_{\text{rad}}^d$$

which gives $R_{\text{rad}}^f = 4R_{\text{rad}}^d$. Therefore, the radiation resistance of a folded dipole is four times that of a single dipole.

EXAMPLE 6.3

Calculate the dimensions of a Yagi–Uda array that has a directivity of 12 dB at 145 MHz.

Solution: Referring to Fig. 6.28, at least six directors are required to achieve a directivity of 12 dB. At 145 MHz the wavelength is

$$\lambda = \frac{c}{f} = \frac{3 \times 10^8}{145 \times 10^6} = 2.069 \quad \text{m}$$

The dimensions of the elements and the spacings are given by

length of the reflector:	$0.482\lambda = 0.9973$ m
length of the driven element:	$0.45\lambda = 0.931$ m
length of each of the directors:	$0.40\lambda = 0.8276$ m
spacing between the driven element and the reflector:	$0.2\lambda = 0.4138$ m
spacing between the driven element and the first director:	$0.2\lambda = 0.4138$ m
spacing between consecutive directors:	$0.2\lambda = 0.4138$ m

The total length of the array is $7 \times 0.2\lambda = 2.9$ m.

6.4 Turnstile Antenna

Consider two $\lambda/2$ dipoles symmetrically placed about the origin with one dipole oriented along the x-axis and the other along the y-axis (Fig. 6.30). Let I_1 and I_2 be the currents at the centres of dipoles 1 and 2, respectively. Assuming a sinusoidal current distribution on the dipole, the electric field in the far field region of the dipole 1 is given by

$$\mathbf{E}_1 = -j\eta I_1 \frac{e^{-jkr}}{2\pi r} \frac{\cos\left(\frac{\pi}{2}\sin\theta\cos\phi\right)}{(1-\sin^2\theta\cos^2\phi)}[(\cos\theta\cos\phi)\mathbf{a}_\theta - (\sin\phi)\mathbf{a}_\phi] \quad (6.16)$$

and that due to dipole 2 is given by

$$\mathbf{E}_2 = -j\eta I_2 \frac{e^{-jkr}}{2\pi r} \frac{\cos\left(\frac{\pi}{2}\sin\theta\sin\phi\right)}{(1-\sin^2\theta\sin^2\phi)}[(\cos\theta\sin\phi)\mathbf{a}_\theta + (\cos\phi)\mathbf{a}_\phi] \quad (6.17)$$

Let us suppose that the magnitudes of I_1 and I_2 are equal but the two currents are in phase quadrature

$$I_1 = I_0 \quad (6.18)$$

$$I_2 = I_0 e^{-j\frac{\pi}{2}} \quad (6.19)$$

By superposition principle, the total electric field generated by the dipole pair is given by the sum of the two individual fields. Along the z-direction

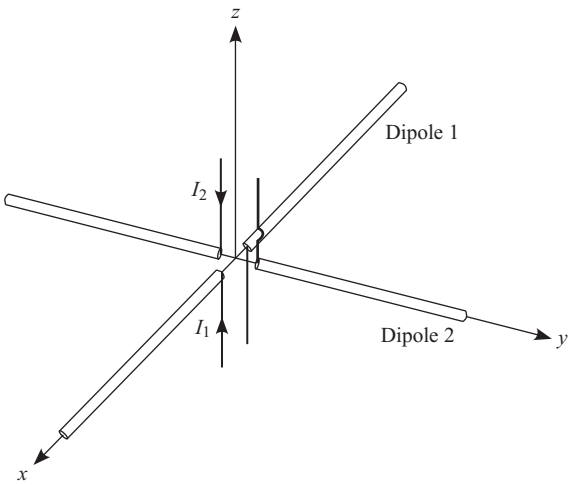

Fig. 6.30 Geometry of a turnstile antenna

($\theta = 0°$), the total field is given by

$$\mathbf{E} = -j\eta I_0 \frac{e^{-jkr}}{2\pi r}[(\cos\phi - j\sin\phi)\mathbf{a}_\theta + (-\sin\phi - j\cos\phi)\mathbf{a}_\phi] \tag{6.20}$$

Following the procedure explained in Section 2.4, we can show that this represents a right circularly polarized wave.

Now consider the fields radiated in the plane of the two dipoles ($\theta = 90°$)

$$\mathbf{E} = \mathbf{a}_\phi j\eta I_0 \frac{e^{-jkr}}{2\pi r}\left[\frac{\cos\left(\frac{\pi}{2}\cos\phi\right)}{\sin\phi} + j\frac{\cos\left(\frac{\pi}{2}\sin\phi\right)}{\cos\phi}\right] \tag{6.21}$$

The far-zone electric field in the plane of the dipoles has only a ϕ-component. We can express the above phasor as a function of time by multiplying Eqn (6.21) by $e^{j\omega t}$ and taking the real part of the product

$$\mathcal{E}_\phi(\phi, t) = \eta I_0 \frac{1}{2\pi r}\left[\frac{\cos\left(\frac{\pi}{2}\cos\phi\right)}{\sin\phi}\sin(\omega t) + \frac{\cos\left(\frac{\pi}{2}\sin\phi\right)}{\cos\phi}\cos(\omega t)\right] \tag{6.22}$$

A plot of this field as a function of ϕ is shown in Fig. 6.31 at three different time instants ($\omega t = 0$, $\pi/20$, and $\pi/10$). From these figures, we can conclude that the radiation pattern of the dipole pair rotates as a function of time. A plot of the maximum of the electric field pattern over one complete cycle ($\omega t = 0$ to 2π) as a function of ϕ is shown in the figure (labelled envelope),

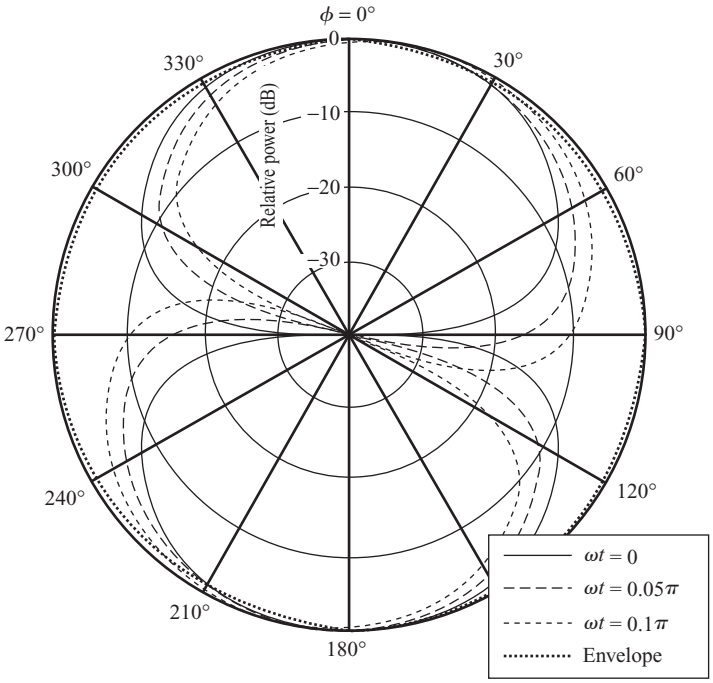

Fig. 6.31 Radiation pattern of a turnstile antenna in the plane of the antenna at three different time instants and the envelope over one complete cycle

which suggests that the radiation pattern is almost omni-directional in the plane containing the dipoles (x-y plane). An orthogonally oriented dipole pair excited in phase quadrature has a radiation pattern in the plane of the dipoles that is almost independent of direction. Such an antenna is known as a turnstile[1] antenna (Kraus 1988).

A turnstile antenna has a very broad beam in the vertical plane. We can stack turnstile antennas one above the other to form an array. Each element of the array is known as a *bay*. A 5-bay turnstile array is shown in Fig. 6.32. Such an antenna is used for transmitting television signals. The radiation pattern of the 5-bay turnstile array is found by multiplying the element pattern (pattern due to a single bay) by the array factor. The 5-bay turnstile array has an omni-directional pattern in the horizontal plane but the the pattern in the vertical plane is much narrower than that of a single bay. Thus, a higher gain is achieved along the direction of maximum radiation by stacking more than one bay vertically. A turnstile antenna array is an omni-directional antenna with horizontally polarized radiation.

[1] A turnstile is a mechanical gate consisting of revolving horizontal arms fixed to a vertical post, allowing only one person at a time to pass through it.

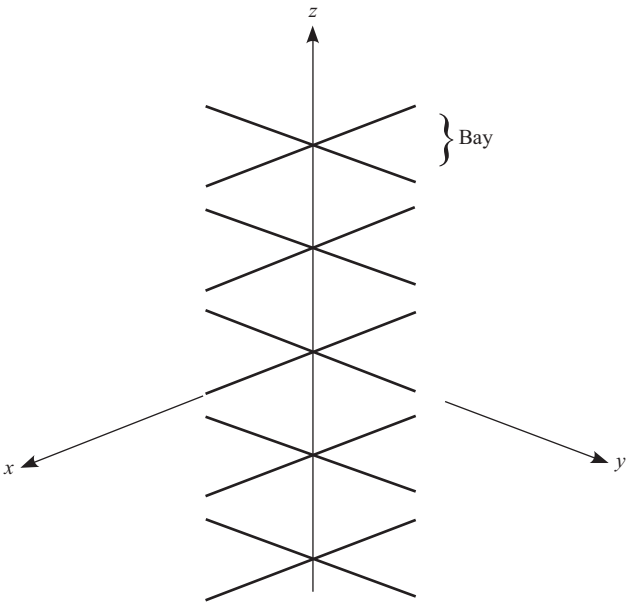

Fig. 6.32 Geometry of a 5-bay turnstile antenna array

6.4.1 Batwing and Super-turnstile Antennas

Consider a metal plate with a slot in the middle, as shown in Fig. 6.33(a). The two ends of the slot are shorted to the metal plates. This structure can

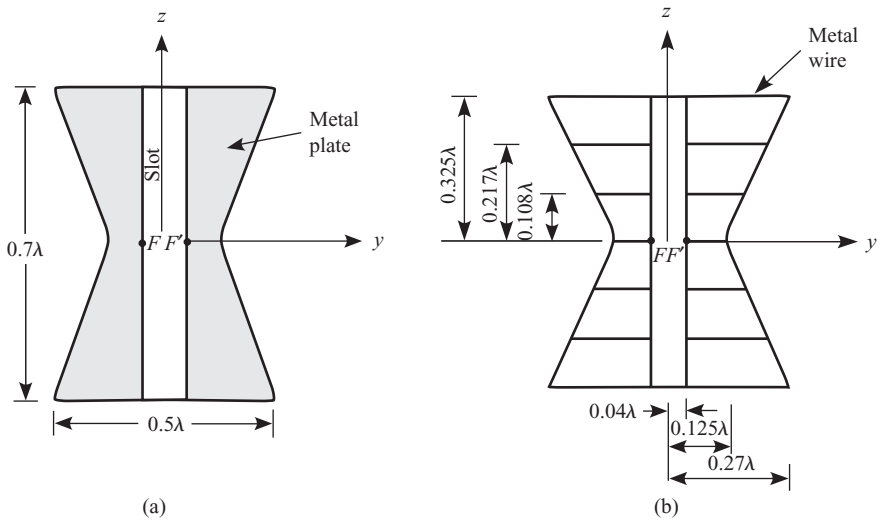

Fig. 6.33 Geometry of a batwing antenna—(a) metal plate design and (b) wire grid design

be fed by a balanced transmission line between the points FF' at the centre of the slot. This is popularly known as a *batwing* antenna.

A wire grid version of the batwing antenna can be constructed by forming a metal wire structure that follows the edges of the plate. The region within this structure is filled by a uniformly spaced wire grid [Fig. 6.33(b)]. The dimensions of the antenna are obtained using emperical data (Kraus 1988). The dimensions in terms of the operating wavelength, shown in Fig. 6.33(b), can be used to design a batwing antenna operating in the VHF and UHF bands (30 MHz–3 GHz).

The radiation from the batwing antennas shown in Fig. 6.33 is horizontally polarized. In the horizontal plane, the pattern has a maximum along the direction normal to the plane of the plate ($\phi = 0$ and 180°) and has a null along the plate or the y-axis (Fig. 6.34). In the vertical plane, the pattern has a maximum along $\theta = 90°$ and along the z-axis the radiated power is about 15 dB below the maximum (Fig. 6.35). The gain versus frequency curve of a batwing antenna designed to operate at 300 MHz and constructed using the wire grid structure is shown in Fig. 6.36. It is found that the gain of the antenna is more than 4 dB over a frequency range of

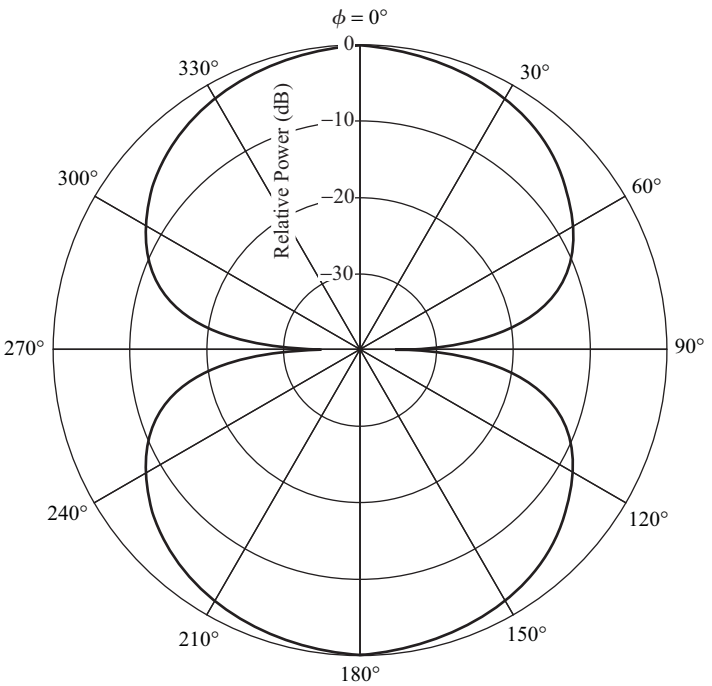

Fig. 6.34 Horizontal plane radiation pattern of a batwing antenna (wire grid design)

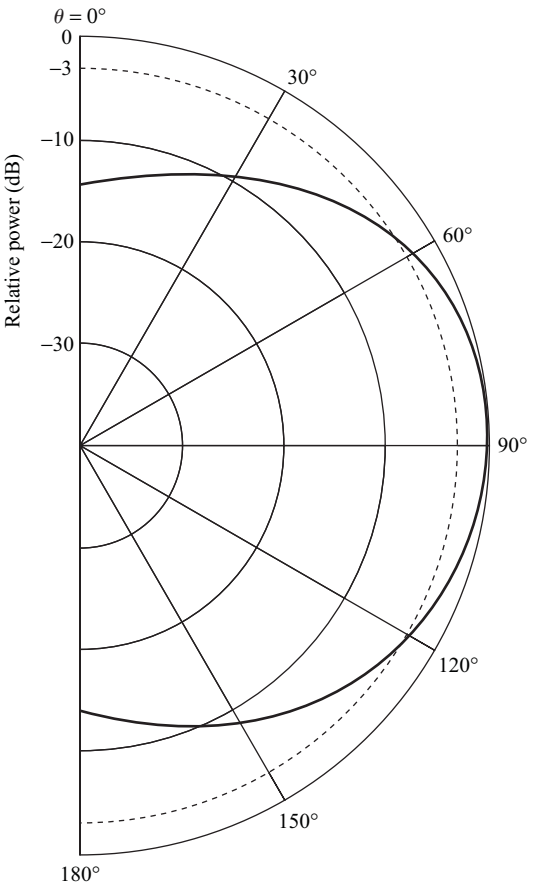

Fig. 6.35 Vertical plane radiation pattern of a batwing antenna (wire grid design)

200 MHz to 400 MHz (which gives 66% bandwidth). The input reflection coefficient of the batwing antenna as a function of frequency is plotted in Fig. 6.37. It is found that the over-the-frequency range of 200 MHz to 400 MHz the input reflection coefficient is less than −10 dB. Therefore, the 10 dB return-loss-bandwidth is also 66%.

Two such antennas placed orthogonal to each other (Fig. 6.38) and fed in phase quadrature produces an omni-directional pattern in the x-y plane with a higher gain than that generated by a turnstile antenna made of $\lambda/2$ dipoles. This antenna is also known as a *super-turnstile* antenna. Several super-turnstile antennas (each one is called a bay) can be stacked one above the other along the z-direction to produce a high-gain, omni-directional pattern with horizontal polarization.

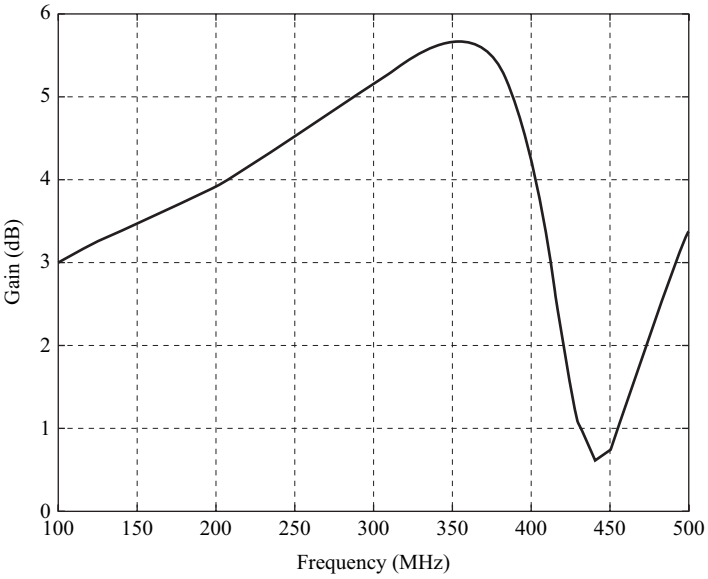

Fig. 6.36 Gain of a batwing antenna (wire grid design)

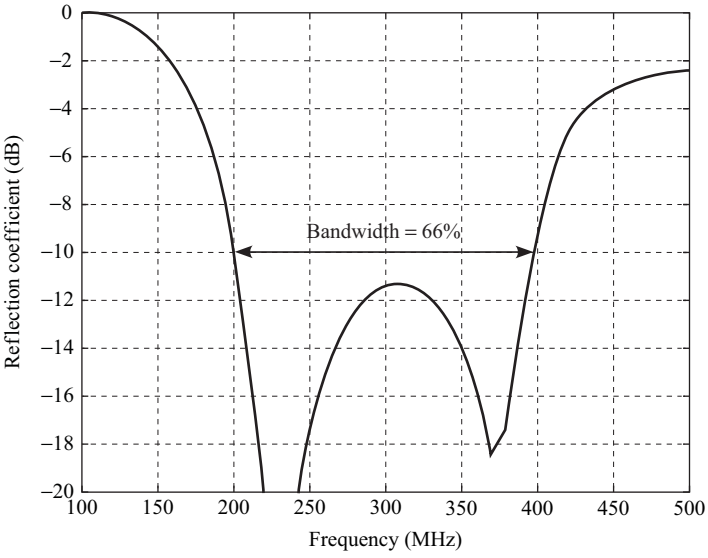

Fig. 6.37 Input reflection coefficient of a batwing antenna (wire grid design)

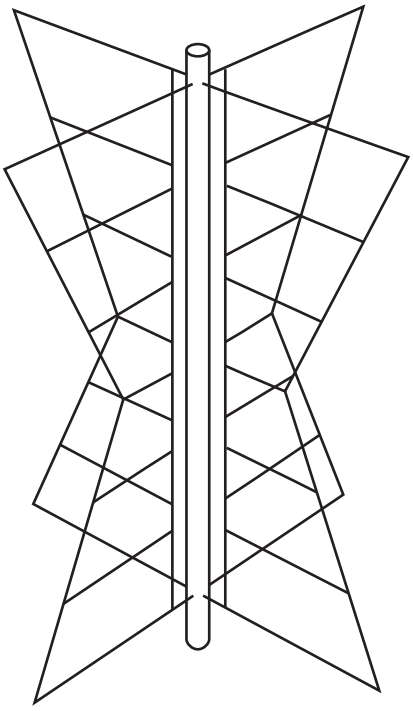

Fig. 6.38 Geometry of a super-turnstile antenna with an omni-directional pattern

6.5 Helical Antenna

One of the techniques to reduce the physical size of a wire antenna is to wind it over an imaginary cylinder as shown in Fig. 6.39. This structure is called a helix. In this figure a right-handed helix is shown. If the helix is wound in the opposite sense, it is known as a left-handed helix. Geometrically, a helix consists of N turns of diameter D with spacing S between each turn. Let $C = \pi D$ be the circumference of the cylindrical surface over which the helix is wound. The unwrapped length L, of one turn of the helix is given by $L = \sqrt{S^2 + C^2}$. Another important parameter of the helix is the pitch angle, α, which is the angle between the tangent to the helix and the plane perpendicular to the axis of the helix. The pitch angle can be related to S and C by the following relation

$$\tan \alpha = \frac{S}{C} = \frac{S}{\pi D} \tag{6.23}$$

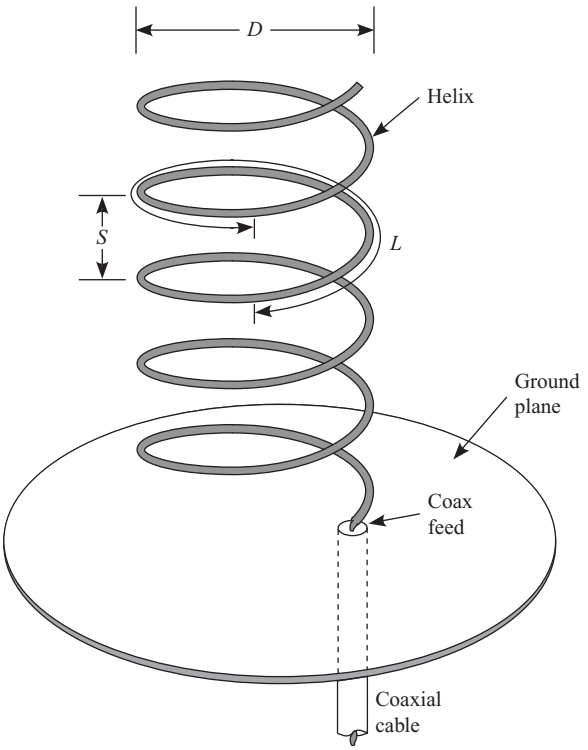

Fig. 6.39 A helical antenna with a ground plane fed by a coaxial cable

If $\alpha = 0°$, the helix reduces to a loop of N turns and for $\alpha = 90°$, the helix is the same as a straight wire of length NL.

A helical antenna generally consists of a wire wound in the form of a helix placed above a ground plane. The antenna is fed by a coaxial transmission line with the center conductor attached to the helical wire and the outer conductor to the ground plane. Typically the diameter of the ground plane is greater than $3\lambda/4$. A helical antenna has several modes of operation; two of the popular ones are—(a) the axial mode and (b) the normal mode.

6.5.1 Axial Mode Helix

In the axial mode of operation, a helical antenna radiates maximum energy along its axis. The radiation pattern has one major lobe and several minor lobes (Fig. 6.40). The axial mode of operation is achieved by choosing

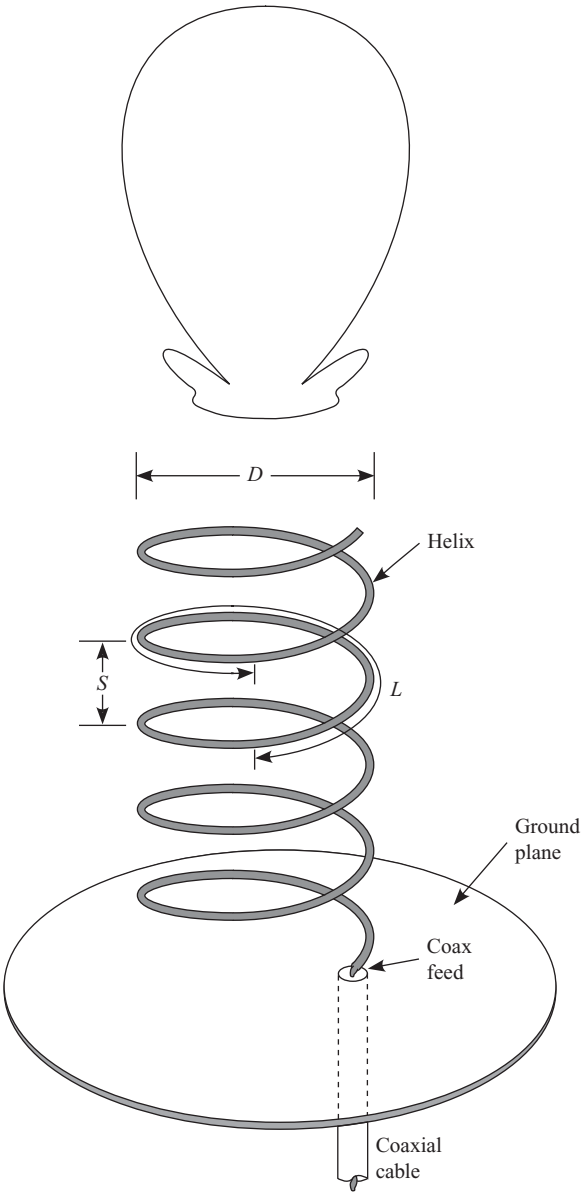

Fig. 6.40 Radiation pattern of a helical antenna operating in the axial mode ($C = \lambda$)

the circumference of the helix to be around a wavelength and the spacing between the turns $S = \lambda/4$. The pitch angle, α, of the helical antenna operating in the axial mode is usually between 12° and 15°. The following empirical formulae (Kraus 1988, Balanis 2002) are useful for the design of

a helical antenna operating in the axial mode

$$\text{Input Resistance } (\Omega) \simeq 140\frac{C}{\lambda} \tag{6.24}$$

$$\text{Half-power beamwidth (degrees)} = \frac{52\lambda^{1.5}}{C\sqrt{NS}} \tag{6.25}$$

$$\text{Beamwidth between nulls (degrees)} = \frac{115\lambda^{1.5}}{C\sqrt{NS}} \tag{6.26}$$

$$\text{Directivity} = 15N\frac{C^2S}{\lambda^3} \tag{6.27}$$

$$\text{Axial Radio} = \frac{2N+1}{2N} \tag{6.28}$$

The relations given by Eqn (6.24) to Eqn (6.28) are valid for $12^\circ < \alpha < 15^\circ$, $3/4 < C/\lambda < 4/3$, and $N > 3$.

Consider an 8-turn helical antenna with $S = 0.25\lambda$ and $C = 1\lambda$. Using Eqn (6.23) the pitch angle is found to be 14.04°. This represents a helical antenna operating in the axial mode. The directivity of the helical antenna can be computed from Eqn (6.27) as 30 or 14.77 dB.

The helical antenna operating in the axial mode produces circularly polarized waves along the axis of the helix. If the helix is a right-handed one (as shown in Fig. 6.39), it transmits as well as receives a right circularly polarized wave. A left-handed helix can be used to transmit as well as receive a left circularly polarized wave.

The input impedance of a helical antenna operating in the axial mode is around 140 Ω (Eqn (6.24) with $C = \lambda$). Therefore, a coaxial cable with a characteristic impedance of 50 Ω cannot be directly connected to the helix. A matching device is required to transform 140 Ω to 50 Ω. The matching device is formed by adjusting the launch angle of helical wire at the feed point. The characteristic impedance of a wire placed horizontally above a ground plane depends on the wire diameter and the spacing between the wire and the ground plane. A smaller spacing results in a larger capacitance between the wire and the ground plane and hence a lower characteristic impedance. The spacing between the wire and the ground plane is gradually increased so that the characteristic impedance of the line changes from 50 Ω to 140 Ω over about half a turn of the helix and then the helix takes off at angle α. It is also possible to make the cross-section of the wire flatter to increase the capacitance and, hence, achieve a lower characteristic impedance without going too close to the ground plane. For effective

impedance transformation without producing significant reflections, the length of the transition must be longer than about $\lambda/2$. An alternative is to incorporate a $\lambda/4$ transformer in coaxial form with a $Z_0 = \sqrt{140 \times 50} = 83.7\ \Omega$ and length equal to $\lambda_g/4$. λ_g is the wavelength in the coaxial transmission line. ($\lambda_g = \lambda/\sqrt{\epsilon_r}$; where λ is the free space wavelength and ϵ_r is the permittivity of the dielectric material of the coaxial transmission line.)

The radiated fields of an axial mode helical antenna are highly directional and circularly polarized. This antenna is a popular choice for satellite communication in the VHF and UHF bands. An array of axial mode helical antennas has also been used for satellite communication to realize the high gain required for this application.

EXAMPLE 6.4

Design a helical antenna operating in the axial mode that gives a directivity of 14 dB at 2.4 GHz. For this helical antenna, calculate the input impedance, half power beamwidth, beamwidth between the nulls, and the axial ratio.

Solution: The wavelength at 2.4 GHz is

$$\lambda = \frac{c}{f} = \frac{3 \times 10^8}{2.4 \times 10^9} = 0.125 \quad \text{m}$$

For axial mode of operation of the helical antenna, we can choose its circumference equal to one wavelength, i.e., $C = 1\lambda = 0.125$ m and the spacing between the two consecutive turns equal to $\lambda/4$, i.e., $S = \lambda/4 = 0.03125$ m. The directivity of the helical antenna is 14 dB, which is

$$D = 10^{\frac{14}{10}} = 25.12$$

Substituting the values of C, S, λ, and D into Eqn (6.27), we can compute the required number of turns of the helix as

$$N = \frac{D\lambda^3}{15C^2S} = \frac{25.12 \times 0.125^3}{15 \times 0.125^2 \times 0.03125} = 6.7$$

Rounding it off to the next higher integer, we get $N = 7$. This completes the design of the helical antenna.

Substituting the helix parameters into Eqns (6.24) to (6.28), we get

$$\text{Input Resistance} \simeq 140\frac{C}{\lambda} = 140 \quad \Omega$$

$$\text{Half-power beamwidth} = \frac{52\lambda^{1.5}}{C\sqrt{NS}} = \frac{52 \times 0.125^{1.5}}{0.125\sqrt{7 \times 0.03125}} = 39.3^\circ$$

$$\text{Beamwidth between nulls} = \frac{115\lambda^{1.5}}{C\sqrt{NS}} = \frac{115 \times 0.125^{1.5}}{0.125\sqrt{7 \times 0.03125}} = 86.9^\circ$$

$$\text{Directivity} = 15N\frac{C^2S}{\lambda^3} = 15 \times 7\frac{0.125^2 \times 0.03125}{0.125^3} = 26.25$$

(or 14.2 dB)

$$\text{Axial Ratio} = \frac{2N+1}{2N} = \frac{2 \times 7 + 1}{2 \times 7} = 1.07$$

Length of one turn of the helix is

$$L = \sqrt{S^2 + C^2} = \sqrt{0.03125^2 + 0.125^2} = 0.1288 \quad \text{m}$$

Since there are seven turns in the helix, the total length of the wire required to construct the helical antenna is $NL = 7 \times 0.1288 = 0.902$ m.

6.5.2 Normal Mode Helix

A helical antenna operates in the normal mode if its dimensions are small compared to the wavelength, that is $D \ll \lambda$ and $NL < \lambda$. The radiation of a helical antenna operating in the normal mode is minimum along the axis of the helix and is maximum in a plane normal to the axis (Fig. 6.41).

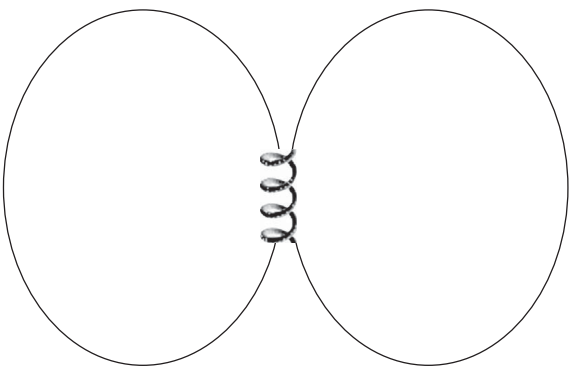

Fig. 6.41 Radiation pattern of a helical antenna operating in the normal mode ($D \ll \lambda$)

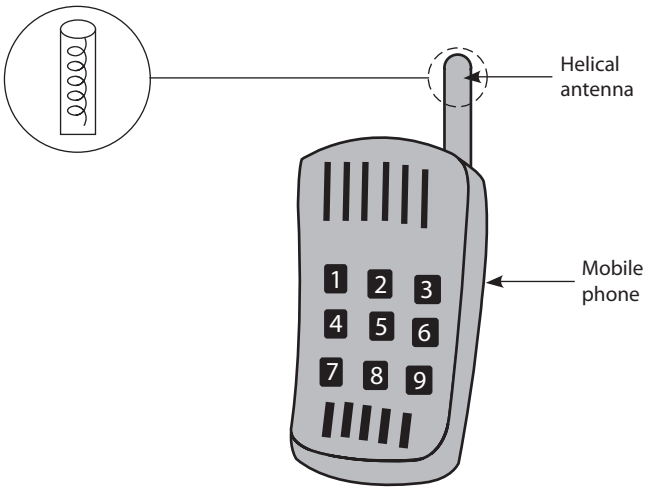

Fig. 6.42 A normal mode helical antenna on a mobile phone

The radiation pattern is a figure of eight rotated about the axis of the helix. The radiation pattern is very similar to that of a dipole of length $l < \lambda$ or a loop of radius $a \ll \lambda$. It is observed that if we choose $C = \sqrt{2S\lambda}$ or $\tan\alpha = [(\pi D)/(2\lambda)]$, the helical antenna radiates circularly polarized waves.

A normal mode helical antenna is compact and has an omni-directional radiation pattern and hence it is a popular antenna for mobile and wireless handset applications (Fig. 6.42).

6.6 Biconical Antenna

A biconical antenna (Fig. 6.43) consists of two infinitely large ($L \to \infty$) cones arranged such that their axes are in line and the vertices are an infinitesimal distance away from each other. The two cones are fed by a balanced transmission line connected to their vertices. It can be shown that the transmission line formed by the two infinite cones has a characteristic impedance which is only a function of the cone angle but independent of the radial distance from the feed point. By definition, the input impedance of an infinitely long transmission line is its characteristic impedance. Therefore, the input impedance of an infinitely long biconical antenna is independent of frequency. However, a biconical antenna of finite length is not frequency-independent but has a large bandwidth ($f_U : f_L = 2 : 1$). The lower band edge of operation usually corresponds to $L = \lambda/4$.

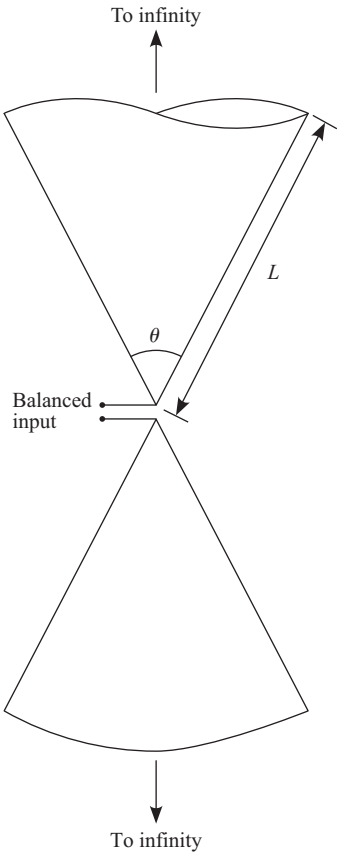

Fig. 6.43 Geometry of a biconical antenna fed by a balanced line

The biconical antenna is fed by a balanced transmission line. A single cone placed vertically above a large ground plane has radiation characteristics similar to those of a biconical antenna radiating into free space (image principle). This antenna can be fed by a coaxial line (an unbalanced transmission line) by connecting the outer conductor to the ground plane and the inner conductor to the cone. The input impedance is half that of a biconical antenna. A variant of the biconical antenna is known as a disc–cone or discone antenna, in which the upper cone is replaced by a finite, circular metal disc. This is fed by a coaxial line by connecting its inner conductor to the disc and the outer conductor to the cone, as shown in Fig. 6.44.

Both biconical and discone antennas have large bandwidths and omnidirectional radiation patterns. They are well suited for broadcast application.

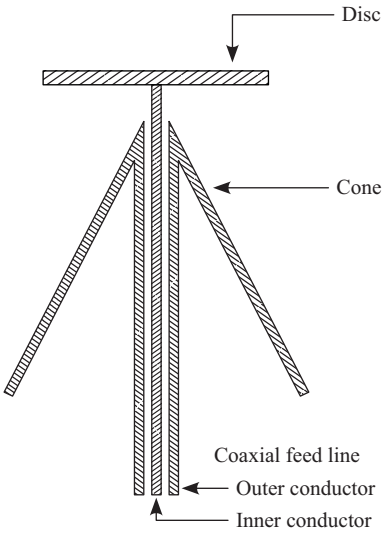

Fig. 6.44 Geometry of a discone antenna fed by a coaxial transmission line

6.7 Log-periodic Dipole Array

A log-periodic dipole array consists of dipoles of different lengths kept parallel to each other with different spacings. Unlike a Yagi–Uda array, all the dipoles in a log-periodic array are excited by a feed network. A log-periodic array can be designed to operate over a large bandwidth, sometimes as large as $f_U : f_L = 10 : 1$. It is not uncommon to design a log-periodic array operating over a bandwidth of 3 MHz to 30 MHz for HF communication purposes. Since the electrical characteristics of the antenna, namely, the input impedance, the gain, etc., vary periodically in the logarithm of the frequency domain, this antenna is known as a *log-periodic* array.

An N-element log-periodic dipole array is shown in Fig. 6.45. In this array, the nth dipole has a length l_n, diameter d_n, a feed gap g_n, and is kept at a distance R_n from the origin. The dimensions of the nth and the $(n+1)$th dipoles are related to each other by the following equation

$$\frac{R_n}{R_{n+1}} = \frac{g_n}{g_{n+1}} = \frac{l_n}{l_{n+1}} = \frac{d_n}{d_{n+1}} = \tau \tag{6.29}$$

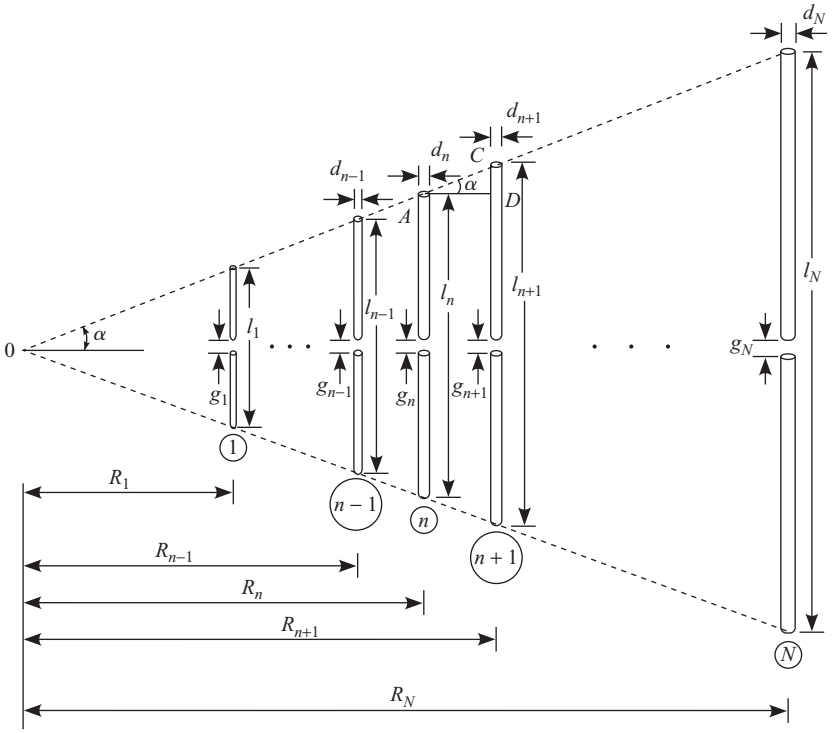

Fig. 6.45 Geometry of a log-periodic dipole array

where $\tau < 1$ and is known as the scale factor. Another parameter viz., the spacing factor, σ, of the array is defined by

$$\sigma = \frac{R_{n+1} - R_n}{2l_{n+1}} \tag{6.30}$$

The third parameter used to describe the array is the angle, 2α, subtended at the origin by the two imaginary lines that pass through the ends of the dipole (Fig. 6.45).

The three parameters τ, σ and α of a log-periodic dipole array are related to each other. Consider the nth and the $(n+1)$th dioples as shown in Fig. 6.45. From Eqn (6.29), the distance between these two dipoles is given by

$$\text{AD} = R_{n+1} - R_n = 2\sigma l_{n+1} \tag{6.31}$$

From the triangle ACD

$$\tan\alpha = \frac{\text{CD}}{\text{AD}} = \frac{\frac{l_{n+1}}{2} - \frac{l_n}{2}}{2\sigma l_{n+1}} = \frac{l_{n+1}}{2}\frac{\left[1 - \frac{l_n}{l_{n+1}}\right]}{2\sigma l_{n+1}} \tag{6.32}$$

Substituting $l_n/l_{n+1} = \tau$ [from Eqn (6.29)] we get the relationship between the three parameters as

$$\tan\alpha = \frac{(1-\tau)}{4\sigma} \tag{6.33}$$

Therefore, a log-periodic array is completely defined by any two of the three parameters.

Consider a log-periodic array consisting of an infinite number of elements. If all the dimensions of the array are multiplied by τ, the array scales on to itself with the $(n+1)$th element becoming the nth element. Therefore, the array has identical performance at frequencies that are related to each other by a factor of τ, i.e., at f_1, $f_2 = f_1\tau$, $f_3 = f_2\tau = f_1\tau^2$, and so on. Taking the logarithm

$$\ln(f_n) - \ln(f_{n+1}) = \ln\left(\frac{1}{\tau}\right);\ n = 1, 2, 3, \ldots \tag{6.34}$$

In other words, the performance of the array repeats or is periodic in the $\ln(f)$ domain and hence the name log-periodic array. If the variation in the electrical parameter is made sufficiently small so that the array has acceptable performance over one period, a broadband performance is ensured due to the log-periodic nature.

In order to maintain the self scaling property ideally, the log-periodic structure needs to be infinitely large. However, due to practical realization issues, the array is truncated at both ends. This limits the number of repetition cycles and hence the bandwidth. The periodicity is also not exactly maintained over the bandwidth.

It is found that for a given frequency, the elements with lengths close to half wavelength resonate. At the lowest frequency (f_L) of operation the longest dipole resonates and at the highest frequency (f_U) of operation the shortest dipole resonates. If l_1 is the length of the first (shortest) dipole and l_N is the length of the last (longest) dipole, using Eqn (6.29) successively

we can express the ratio of the lengths of the last and the first dipole as

$$\frac{l_N}{l_1} = \frac{l_N}{l_{N-1}} \cdot \frac{l_{N-1}}{l_{N-2}} \cdot \frac{l_{N-2}}{l_{N-3}} \cdots \frac{l_{n+1}}{l_n} \cdots \frac{l_3}{l_2} \cdot \frac{l_2}{l_1} \tag{6.35}$$

$$= \left(\frac{1}{\tau}\right)^{N-1} \tag{6.36}$$

The length, l_N, of the longest dipole is chosen to be equal to $\lambda/2$ at f_L.

$$l_N = \frac{1}{2}\frac{c}{f_L} \tag{6.37}$$

Similarly, the length of the first dipole is $\lambda/2$ at f_U

$$l_1 = \frac{1}{2}\frac{c}{f_U} \tag{6.38}$$

Substituting the expressions for l_N and l_1 from Eqn (6.37) and Eqn (6.38), respectively, into Eqn (6.36) and simplifying

$$\frac{f_U}{f_L} = \left(\frac{1}{\tau}\right)^{N-1} \tag{6.39}$$

A two-wire transmission line can be used to feed the log-periodic dipole array. The terminals of the shortest dipole form the input point of the array and the two-wire transmission line connects all other dipoles. At the terminals of the longest dipole, the transmission line can be either left unterminated or terminated in a load impedance. It has been observed that maximum radiation along the direction of the shortest dipole as well as a good input match is obtained if the feed line is criss-crossed between each of the dipoles [Fig. 6.46(a)]. Due to criss-crossing, the spacing between the two wires changes all along the length of the feed line and hence the characteristic impedance of the feed line does not remain constant.

Consider a transmission line formed by two wires placed one above the other at a constant spacing. The spacing is chosen to achieve the desired characteristic impedance. Let the right arm of dipole 1 be connected to the bottom wire and the left arm to the top wire [Fig. 6.46(b)]. The phase reversal at dipole 2 can be achieved by connecting the left arm of dipole 2 to the bottom wire and the right arm to the top wire of the feed line. Once again, by interchanging the connection of the two arms of the dipole to the feed line, it is possible to realize a phase reversal between two consecutive dipoles and hence achieve the same effect as obtained by criss-crossing the feed line.

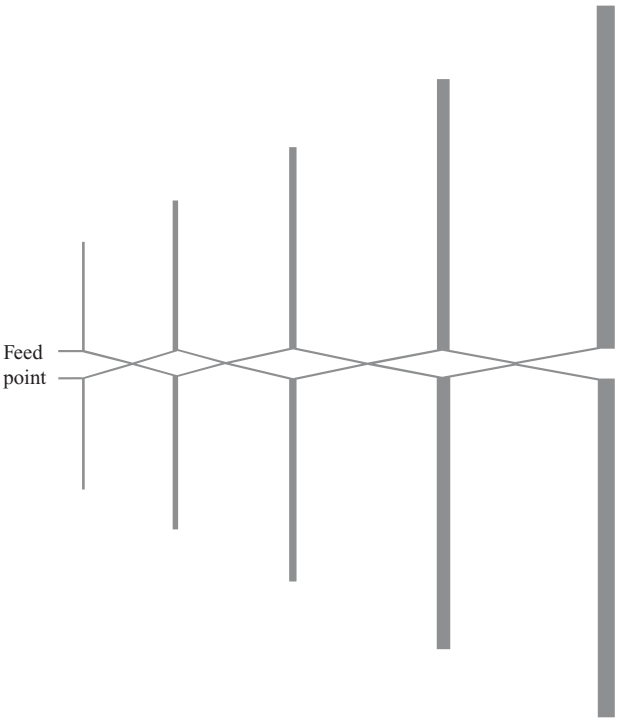

(a) Criss-crossed feed line

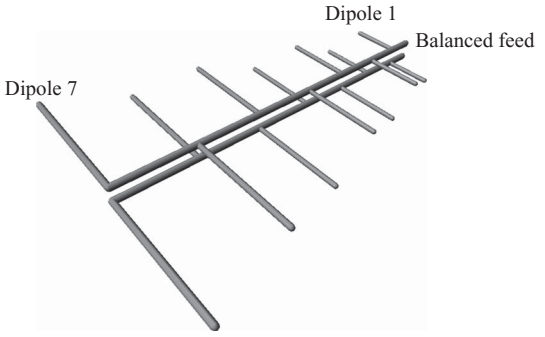

(b) Straight feed line

Fig. 6.46 Feed structures for a log-periodic dipole array

A qualitative reason for the formation of the radiation maximum of the array along the endfire direction towards the shortest dipole can be given by comparing the log-periodic antenna with the Yagi–Uda array. In the log-periodic array, at a given frequency of operation, the dipole with length closest to $\lambda/2$ becomes resonant. The longer dipole acts as a reflector and the shorter dipoles act as directors. A phase shift of 180° introduced by criss-crossing the transmission line, facilitates in setting up the correct phase of

the currents on the dipoles so that the maximum is along the direction of the smallest dipole, which is somewhat similar to how the reflector and directors function in a Yagi–Uda array.

6.7.1 Design Procedure

A procedure to compute the dimensions of a log-periodic array with a specified directivity and bandwidth is presented in this section. Before the exact procedure is presented, let us consider the performance graph (Fig. 6.47) of a log-periodic array. This is a plot of the maximum directivity and the corresponding σ, as a function of τ. This particular graph has been generated for a transmission line impedance of 100 Ω. From Fig. 6.47 we can conclude that a small value of τ results in an array with less number of elements separated by large distances and lower values of directivity. However, a larger value of τ results in an array with more number of closely spaced elements, a larger gain, and a smaller variation in the electrical characteristics as a function of frequency.

The goal of the design is to meet a given directivity specification with as few elements as possible. This is achieved by drawing a horizontal line corresponding to the given directivity value and noting the value of τ at the point of intersection of this line with the directivity curve in Fig. 6.47. Now, draw a vertical line passing through the calculated value of τ and make it intersect with the σ curve and read out the value of σ from the right

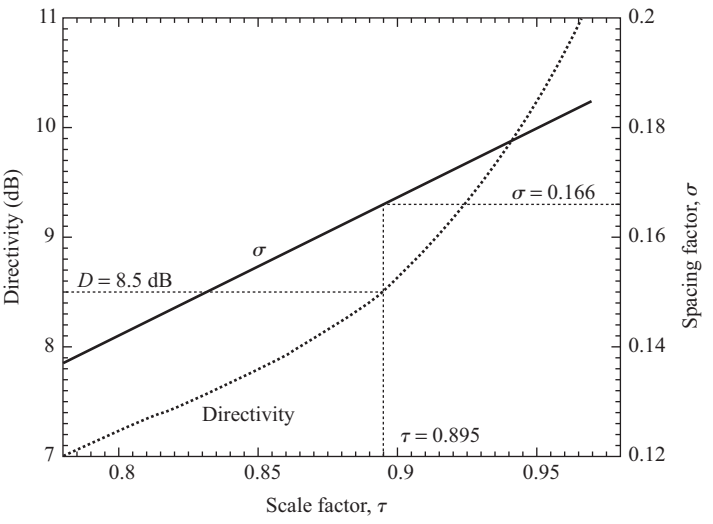

Fig. 6.47 Design curves for a log-periodic array

y-axis of the graph. For example, to achieve a directivity of 8.5 dB, the array parameters are $\tau = 0.895$ and $\sigma = 0.166$. With the knowledge of τ and σ, one can compute the value of α using Eqn (6.33).

The next step is to compute the number of elements in the array. Since the highest (f_U) and the lowest (f_L) frequencies of operation are specified and the value of τ has already been computed, the number of elements in the array is computed by solving Eqn (6.39). Taking the logarithm on both the sides of Eqn (6.39)

$$\log(f_U) - \log(f_L) = (N-1)\log\left(\frac{1}{\tau}\right) \tag{6.40}$$

which can be easily solved for N.

At the lowest frequency (f_L) of operation, the longest dipole is resonant and its length is given by Eqn (6.37). The lengths of the other dipoles can be computed using Eqn (6.29) recursively.

Similarly, the spacing between the dipoles can be obtained by starting from the Nth dipole and using Eqn (6.31) to get the spacing between the Nth and $(N-1)$th dipoles and then Eqn (6.29) is used recursively to calculate the other spacings. The diameters of the dipoles are also related to each other by a factor of τ. The diameter of one of the dipoles (either of the shortest or the longest) is assumed, and using Eqn (6.29) one can compute the diameters of the remaining dipoles.

The design procedure is explained in Example 6.5.

EXAMPLE 6.5

Design a log-periodic dipole array having a directivity of 8.5 dB over a frequency range of 10 MHz to 30 MHz.

Solution:

1. Calculate the value of τ and σ using the value of directivity in the design graph (Fig. 6.47)
   Corresponding to the directivity of 8.5 dB, we get $\tau = 0.895$ and $\sigma = 0.166$ from the graph.
2. Compute the value of α using Eqn (6.33)

$$\tan\alpha = \frac{(1-\tau)}{4\sigma} = \frac{(1-0.895)}{4\times 0.166} = 0.1581$$

   Therefore, $\alpha = 8.99°$.

3. Calculate the value of N using Eqn (6.40)
   Given that $f_U = 30$ MHz and $f_L = 10$ MHz

$$\log(30 \times 10^6) - \log(10 \times 10^6) = (N-1)\log\left(\frac{1}{0.895}\right)$$

   Solving for N, we get $N = 10.9$ and rounding it off to the next higher integer, the number of elements in the log-periodic array is $N = 11$.
4. Compute the lengths of the dipoles
   From Eqn (6.37), the length of the 11th dipole is

$$l_{11} = \frac{1}{2}\frac{3 \times 10^8}{10 \times 10^6} = 15 \quad \text{m}$$

   Using Eqn (6.29) recursively

$$\frac{l_n}{l_{n+1}} = \tau = 0.895$$

   we can calculate the lengths of the other dipoles as $l_{10} = 0.895 \times l_{11} = 13.425$ m, $l_9 = 0.895 \times l_{10} = 12.0154$ m, and so on, $l_8 = 10.7538$ m, $l_7 = 9.6246$ m, $l_6 = 8.614$ m, $l_5 = 7.7096$ m, $l_4 = 6.9$ m, $l_3 = 6.1755$ m, $l_2 = 5.5271$ m, and $l_1 = 4.9468$ m.
5. Calculate the location of the dipoles and hence the distance between them
   The length of the nth dipole and its location (R_n) are related by (refer to Fig. 6.45)

$$R_n = \frac{l_n}{2\tan(\alpha)}$$

   Therefore, $R_1 = l_1/(2\tan\alpha) = 4.9468/(2 \times 0.1582) = 15.6341$ m, $R_2 = 17.4681$ m, $R_3 = 19.5173$ m, $R_4 = 21.8073$ m, $R_5 = 24.3656$ m, $R_6 = 27.2242$ m, $R_7 = 30.4181$ m, $R_8 = 33.9867$ m, $R_9 = 37.9739$ m, $R_{10} = 42.429$ m, and $R_{11} = 47.4067$ m. The spacing between the nth and the $(n+1)$th element is obtained by taking the difference $(R_{n+1} - R_n)$.
6. Calculate the wire diameters
   Assume the diameter of the last dipole and using Eqn (6.29) compute the diameters of the other dipoles recursively. Let us suppose that $d_{11} = 10$ mm and we get, $d_{10} = 8.95$ mm, $d_9 = 8.0103$ mm, ... $d_2 = 3.6847$ mm, and $d_1 = 3.2978$ mm.

The current distribution on the elements of the log-periodic array operating at 10 MHz is shown in Fig. 6.48(a). The current distribution indicates

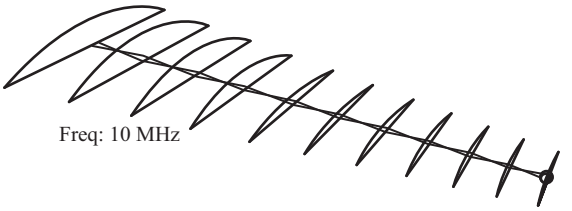

(a) Current distribution

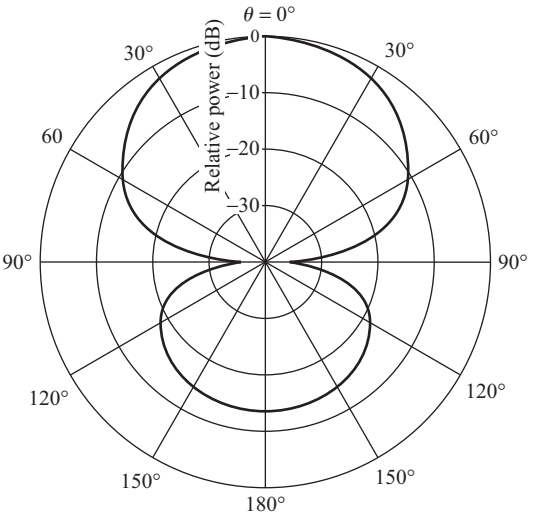

(b) **E**-plane pattern

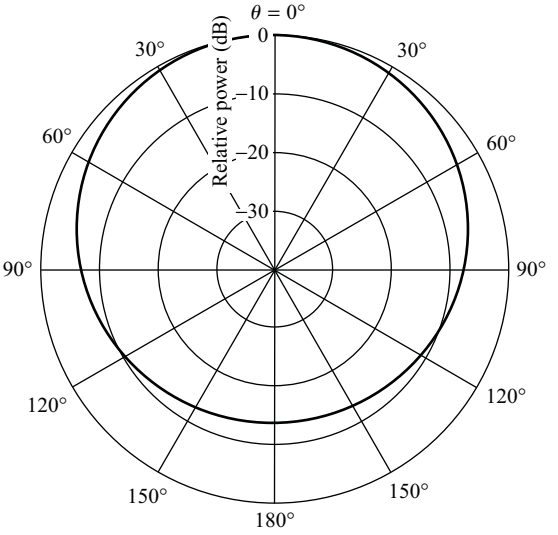

(c) **H**-plane pattern

Fig. 6.48 Current distribution and radiation patterns of the log-periodic antenna at 10 MHz

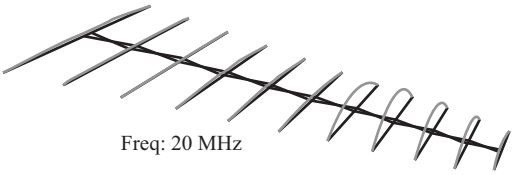

(a) Current distribution

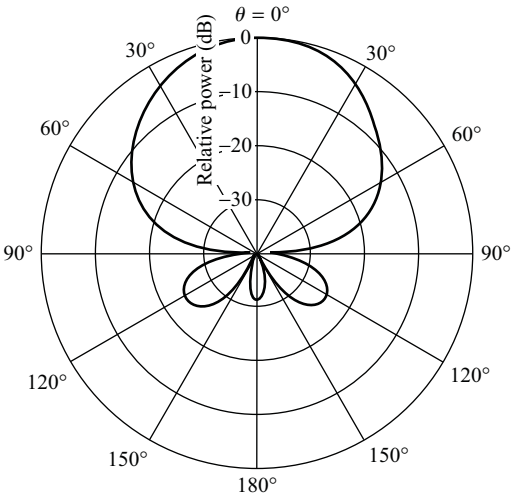

(b) **E**-plane pattern

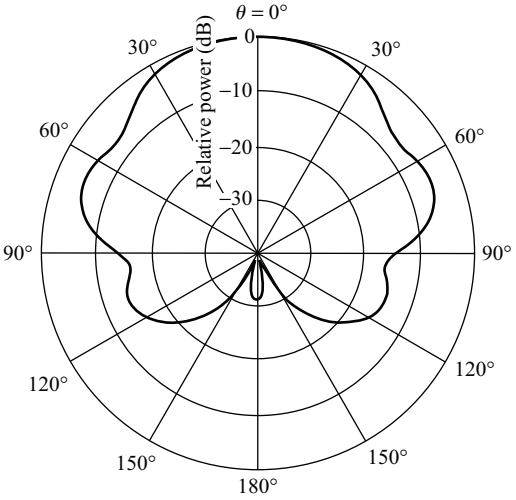

(c) **H**-plane pattern

Fig. 6.49 Current distribution and radiation patterns of the log-periodic antenna at 20 MHz

that the largest dipole is resonant at this frequency and the elements in front act as directors. However, there are no elements to act as directors, hence, the gain of the antenna is lower than the design value. The corresponding **E**-plane and **H**-plane radiation patterns are also shown in Figs 6.48(b) and 6.48(c), respectively. In Fig. 6.49 the pattern and the current distributions for the same antenna at the mid-band frequency, 20 MHz, are shown. At this frequency, the resonant dipole is in the middle of the array and there are elements on both sides to act as reflectors and directors. Thus, the gain corresponds to the design value, 8.6 dB. At the highest frequency, 30 MHz, the first dipole (the shortest one) is resonant, where again directors are not available in front of the resonant dipole. Thus, at both ends of the design frequency band, f_L and f_U, there is a reduction in the gain. Therefore, to maintain the gain over the entire band, we need to add more elements at both ends to act as reflectors and directors at the band edges. To achieve this, it is common practice to extend the band edges by 20–30% while designing the antenna.

6.8 Spiral Antenna

Spiral is a geometrical shape found in nature. A spiral can be geometrically described using polar coordinates. Let (r, θ) be a point in the polar coordinate system. The equation

$$r = r_0 e^{a\theta} \tag{6.41}$$

where, r_0 and a are positive constants, describes a curve known as a *logarithmic spiral* or an *equiangular spiral*. Figure 6.50 shows an equi-angular spiral for $r_0 = 1$ and $a = 0.4$. Taking natural logarithm on both sides of Eqn (6.41)

$$\ln r = \ln r_0 + a\theta \tag{6.42}$$

Differentiating with respect to θ

$$\frac{1}{r}\frac{dr}{d\theta} = a \tag{6.43}$$

From $\triangle ABC$ in Fig. 6.50

$$\tan\beta = \frac{BA}{BC} = \frac{r d\theta}{dr} = \frac{1}{a} \tag{6.44}$$

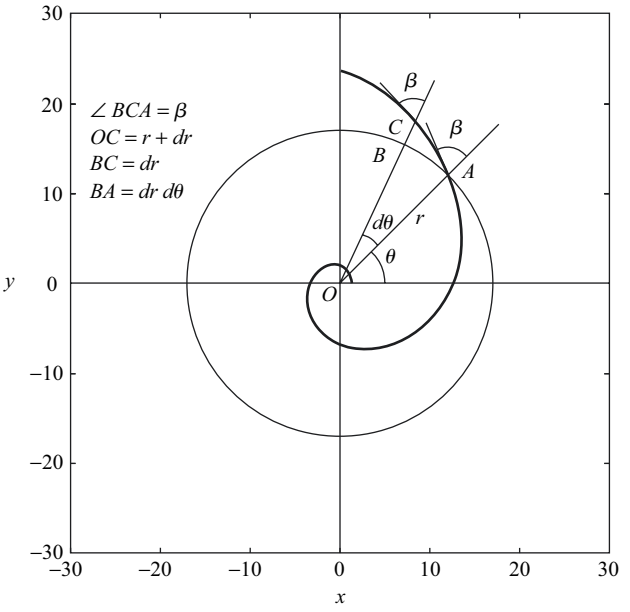

Fig. 6.50 Logarithmic spiral

Therefore, the angle between the tangent at any point on the sprial and the radial line from the origin to that point (designated as β) is the same for all points on the spiral (a is a constant). Hence, the spiral represented by Eqn (6.41) is also known as an equi-angular spiral.

Consider a spiral described by

$$r_1 = r_0 e^{a\theta} \tag{6.45}$$

Let the dimensions of an antenna designed to operate at a frequency, f_0, be defined in terms of Eqn (6.45). If we scale this antenna by a factor K, it would have the same radiation and input properties at a frequency f_0/K. Multiplying Eqn (6.45) by a factor K we have

$$r_2 = K r_0 e^{a\theta} \tag{6.46}$$

Expressing $K = e^{a\delta}$, we can reduce Eqn (6.46) to

$$r_2 = e^{a\delta} r_0 e^{a\theta} = r_0 e^{a(\theta+\delta)} \tag{6.47}$$

This shows that the scaled antenna is obtained by rotating the original antenna structure by an angle δ. The structure itself is unchanged. Hence, the radiation pattern alone rotates by an angle δ, keeping all the other

properties the same. Such an antenna is known as a *frequency-independent* antenna.

Frequency-independent antennas are governed by Rumsey's principle, which states that *the impedance and pattern properties of an antenna will be frequency independent if the antenna shape is specified only in terms of angles* (Kraus 1988). The antenna described by Eqn (6.45) satisfies this criterion provided the structure is infinite. For structures that are finite in size, the frequency invariance property is exhibited over a limited range of frequencies. The lower end of this band is decided by the largest dimension of the spiral and the upper end by the smallest dimension.

To construct an antenna using a spiral, consider a thin conducting strip of variable width with the edges defined by the following two equations

$$r_1 = r_0 e^{a\theta} \tag{6.48}$$

and

$$r_2 = r_0 e^{a(\theta-\delta)} \tag{6.49}$$

These two edges are shown in Fig. 6.51 for $0 \geq \theta \leq 2.25\pi$ and $\delta \geq \theta \leq (2.25\pi + \delta)$. A second conductor can be obtained by rotating the first spiral by 180°. The edges of the second spiral are given by

$$r_3 = r_0 e^{a(\theta+\pi)} \tag{6.50}$$

and

$$r_4 = r_0 e^{a(\theta+\pi-\delta)} \tag{6.51}$$

These edges, edge r_3 and edge r_4, are shown in Fig. 6.51 for $-\pi \geq \theta \leq 1.25\pi$ and $(-\pi + \delta) \geq \theta \leq (1.25\pi + \delta)$. These two conductors form a balanced structure with feed points FF'.

The parameters used to define this structure are

δ : determines the width of the arm

r_0 : determines the radius of the feed region

a : rate of growth of the spiral, and

$\theta_{\max}$: determines the maximum radius of the spiral.

The spiral antenna has a bidirectional main lobe perpendicular to the plane of the antenna. The radiated field is right circularly polarized on one

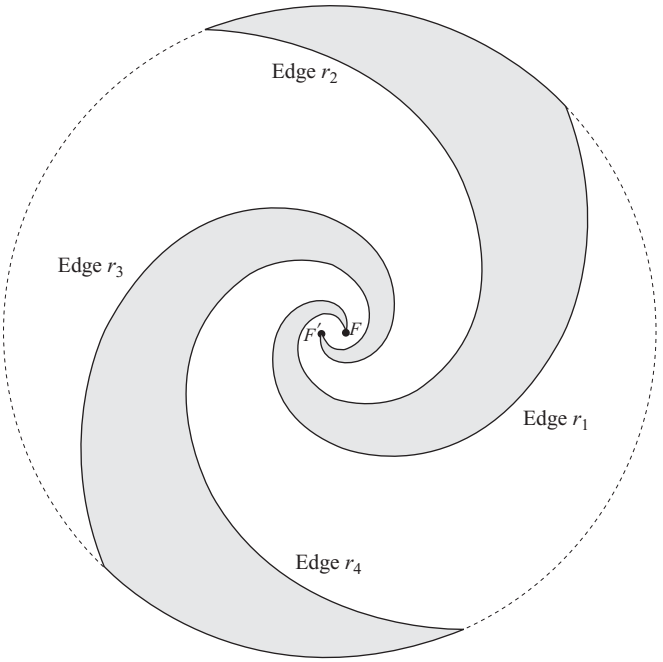

Fig. 6.51 An antenna based on a logarithmic spiral

side and is left circularly polarized on the other side of the spiral. The axial ratio is used as one of the convenient parameters to define the acceptable bandwidth of the antenna. Outside the band of operation of the antenna, the radiation is elliptically polarized.

6.9 Microstrip Patch Antenna

A microstrip patch antenna, shown in Fig. 6.52, consists of a thin (thickness very small compared to the free space wavelength) metallic patch above a large metallic ground plane. The patch is supported by a dielectric sheet, known as a substrate, the thickness of which is in the range of 0.005λ to 0.05λ. The patch is usually etched on the dielectric substrate using printed circuit board technology. Therefore, a microstrip patch antenna is also referred to as a printed antenna. The patch can be of any shape, e.g., square, circle, rectangle, triangle, etc. The performance of the patch depends on the its size and shape.

Consider a rectangular patch of length L and width W printed on a dielectric substrate of height h. The length of the patch is chosen to be around $\lambda_g/2$, where λ_g is the guide wavelength of the microstrip line of

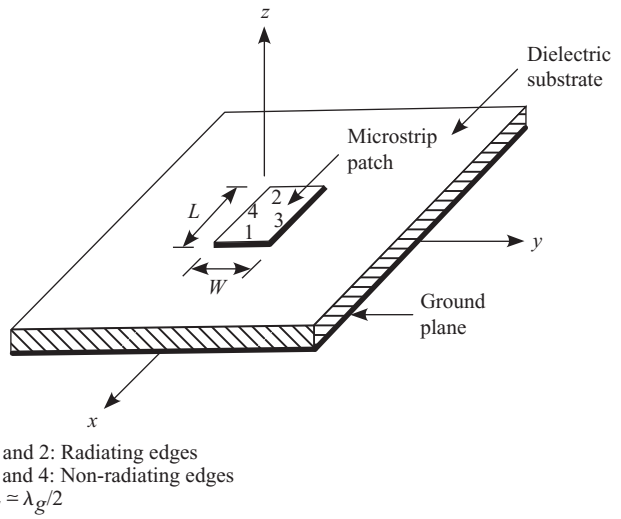

Fig. 6.52 Geometry of a rectangular microstrip patch antenna

width W printed on the same dielectric substrate. With this choice of the length, the electric field along x-direction undergoes a 180° phase reversal (Fig. 6.53) from one edge to the other. It can be shown that the fields near edges 1 and 2 constructively add up producing the radiation with a maximum along the z-direction. Hence, edges 1 and 2 are known as the radiating edges. Further, it has been shown that the fields near edges 3 and 4 do not contribute to the radiation (Balanis 2002). The rectangular microstrip patch shown in Fig. 6.52 radiates linearly polarized waves, with the electric field oriented along the x-direction when looking in the direction of maximum radiation. The radiation patterns in the two principal planes, viz., the **E**-plane (x-z plane) and the **H**-plane (y-z plane) are shown in Fig. 6.54. The pattern is very broad and has nulls along the y-direction.

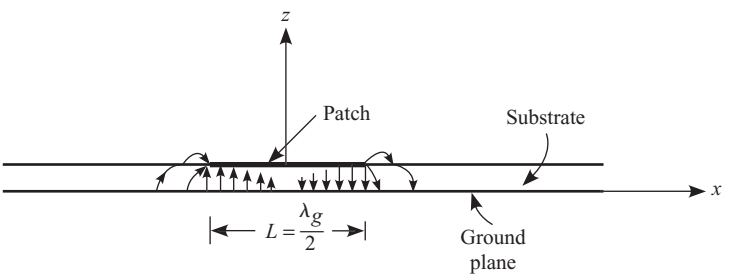

Fig. 6.53 Electric field distribution in a microstrip patch antenna

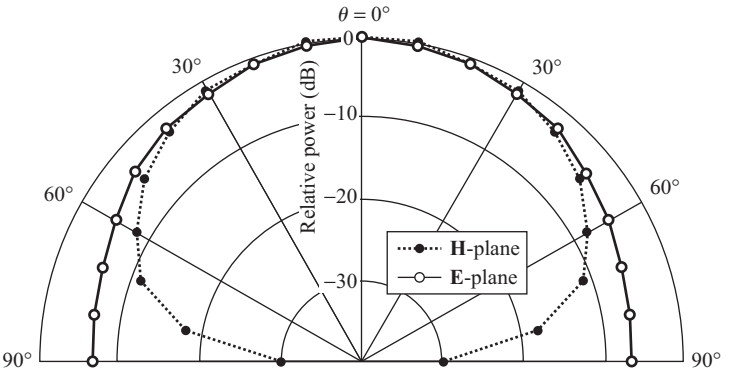

Fig. 6.54 Radiation patterns of a microstrip patch antenna

For efficient transfer of power from a transmission line to the patch antenna, we need to match the input impedance of the antenna to the characteristic impedance of the transmission line. It is observed that the impedance seen by a transmission line attached to the radiating edge is very high, and also the impedance (ratio of voltage to current) decreases as one moves towards the centre of the patch. Therefore, depending on the characteristic impedance of the transmission line, an appropriate point on the patch is chosen as the feed point.

A microstrip patch can be fed either by a microstrip transmission line [Fig. 6.55(a)] or by a coaxial transmission line [Fig. 6.55(b)]. The microstrip line can be etched along with the patch in a single process. In order to access the appropriate impedance point on the patch, a recess is created in the patch. The depth of the recess is adjusted to achieve the impedance matching. A coaxial transmission line is attached right below the patch, with the inner conductor soldered to the patch and the outer conductor of the coaxial line connected to the ground plane. A patch antenna fed by either a microstrip or a coaxial transmission line has about 2 to 4% input bandwidth.

Planar inverted* F *antenna From Fig. 6.53 it is seen that the electric field along the centre line of a rectangular half wavelength long microstrip patch antenna is zero. Therefore, we can introduce a perfect electric conductor along this line between the patch and the ground plane without disturbing the fields of the patch, resulting in a quarter wavelength long antenna. This structure is known as a planar inverted F antenna (PIFA) and is shown in Fig. 6.56(a). We can also realize an inverted F antenna by a wire structure above a ground plane which is shown in Fig. 6.56(b).

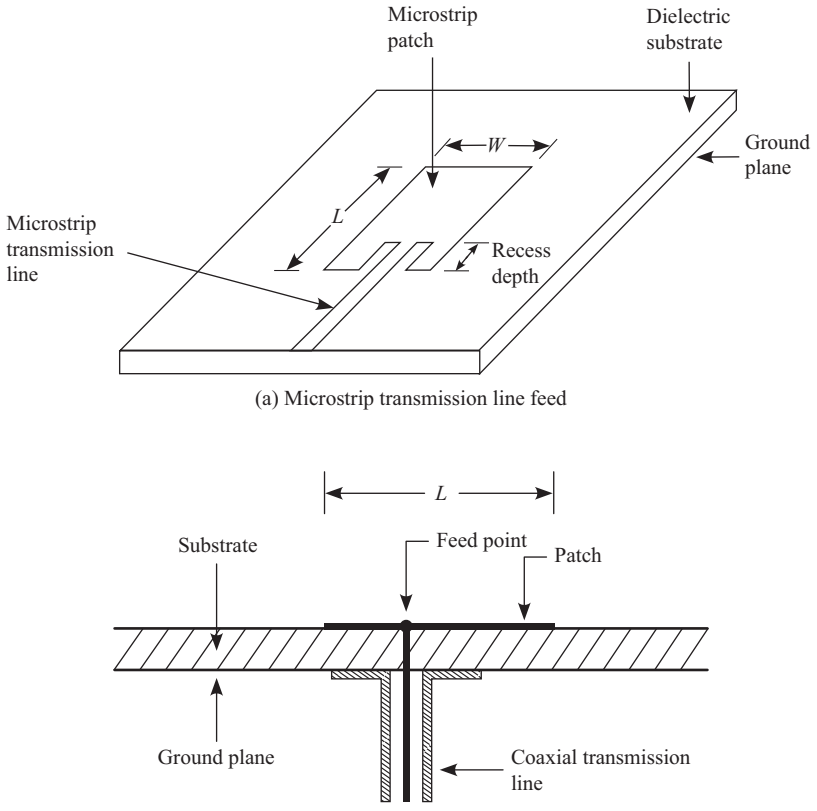

Fig. 6.55 Coupling power to a microstrip patch antenna

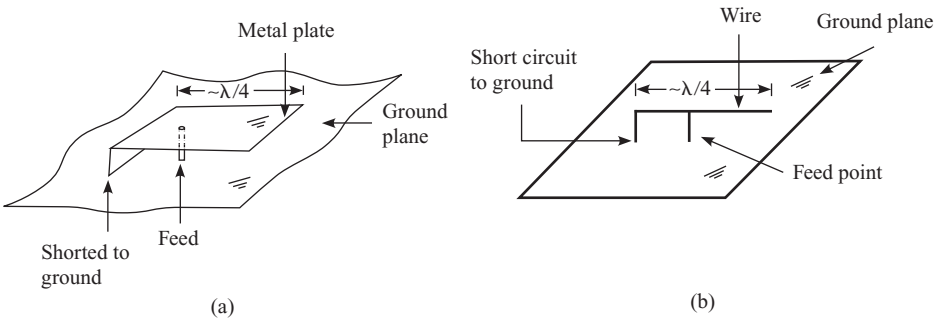

Fig. 6.56 Inverted F antenna—(a) in planar form (PIFA) and (b) using wires

Exercises

6.1 Calculate the dimensions of a 3-element Yagi–Uda antenna operating at 10 MHz.

6.2 The maximum received power at the terminals of an 8-turn helical antenna is −70 dBm. Calculate the received power (in dBm) if the number of turns of the helix is increased to 16 and all other parameters of the antenna remain unaltered. Ignore the losses in the structure.

Answer: −67 dBm

6.3 Design a helical antenna operating in the axial mode and having a maximum directivity of 10 dB at 5.2 GHz. Calculate the half-power beamwidth of the antenna and the length of the wire required to construct the antenna.

6.4 Design a log-periodic antenna that has a directivity of 10 dB over a frequency range of 10 MHz to 30 MHz.

6.5 Show that the electric field given by Eqn (6.21) represents the field of a right circularly polarized wave.

6.6 Calculate the dimensions of the turnstile antenna operating at 155 MHz.

Answer: dipole length 0.9675 m

6.7 Calculate the dimensions of a metallic wiregrid batwing antenna used for transmitting television signals at 155 MHz.

6.8 Show that Eqn (6.6) represents the electric field in the far-field region of the long wire antenna shown in Fig. 6.10 with a sinusoidal current distribution given by Eqn (6.4). If the length of the wire is an integral multiple of the wavelength, show that the electric field reduces to that given by Eqn (6.7).

6.9 A 4λ long wire antenna supports a sinusoidal current distribution. Calculate the direction (with respect to the axis of the wire) of the main beam.

Answer: 25.18°

6.10 Calculate the number of side lobes in the radiation pattern of a 6λ long wire antenna with a sinusoidal current distribution and radiating into free space.

Answer: 10

6.11 Show that the main lobe in the radiation pattern of a 20λ long wire antenna is oriented at an angle of 11.08° from the axis of the wire.

6.12 Show that after multiplying Eqn (6.21) by $e^{j\omega t}$ and taking the real part, it reduces to Eqn (6.22).

6.13 Calculate the maximum value of the electric field of the turnstile antenna shown in Fig. 6.30 when $\omega t = 0$, $\omega t = \pi/4$, and $\omega t = \pi/2$. Show that the envelope of the radiation pattern corresponding to $\omega t = \pi/4$ (Fig. 6.31) is 1.03 dB below that corresponding to $\omega t = 0$.

CHAPTER 7

Antenna Measurements

Introduction

So far we have discussed the analysis, working, and design of various types of antennas. Many assumptions have been made to simplify the analysis of antennas. The performance of an antenna is specified in terms of its input characteristics as well as its radiation characteristics and before an antenna can be used in a system, it is important to ensure that the required specifications have been met. This can only be done by actual measurement of these performance parameters.

Since an antenna is a device that couples power to and from the surrounding space, before measuring any antenna parameter, we first need to ensure that the environment does not influence the measurements. In other words, both input and radiation measurements must be carried out with the antenna kept in free space or a simulated free-space condition. Some of the important antenna parameters of interest are radiation patterns (field amplitude, phase, power, and polarization patterns), gain, directivity, radiation efficiency, antenna effective length, polarization, pattern bandwidth, input reflection coefficient, input frequency bandwidth, noise temperature, etc. While some of these parameters are calculated from the pattern, others are calculated from the input measurements. The two important measurements are the radiation pattern and the input reflection coefficient. This chapter addresses measurement issues connected with both pattern and input characteristics, measurement procedures, and measurement setups.

First we discuss methods of providing an appropriate environment for the antenna and then go on to the measurement procedure. The equipment required for the measurements is also discussed in some detail. In Chapter 2 we studied that the radiation and the receive patterns of an antenna are the same because of the reciprocity theorem satisfied by the antenna. Therefore, we can measure the pattern properties in the transmit or the receive mode

of operation. However, the input properties are generally measured in the transmit mode of the antenna.

7.1 Antenna Measurement Range

From the reciprocity theorem we know that the transmit and receive patterns are the same for any antenna. For convenience of measurement, it is common practice to measure the receive pattern rather than the transmit pattern. The receive pattern of an antenna is the plot of the received power as a function of the direction of arrival of the incident plane wave with a constant power density. Therefore, it is necessary to ensure that the antenna is receiving a plane wave and that there is only one plane wave incident on the antenna while measuring the received power. It is obvious that we require two antennas for pattern measurement, one transmitting and the other receiving. Unless indicated otherwise, in the rest of the discussion we assume that the receive antenna is the antenna under test and the transmit antenna is used for generating a plane wave at the location of the test antenna or the receive antenna.

In Chapter 3 it was discussed that at large distances from the antenna the spherical wave radiated by an antenna can be considered as a plane wave locally. We use this principle to generate a plane wave at the receive antenna location by keeping the transmit antenna at a large distance. Making the distance between the two antennas, R, large serves two purposes—(a) it ensures that the wave incident on the receive antenna is a plane wave and (b) the interaction between the two antennas is very small so that the characteristics of the receive antenna are not affected significantly by the presence of the transmit antenna.

It was shown in Section 3.1 that at a distance $R > 2D^2/\lambda$ from a transmit antenna, the far-field approximation is valid. D is the largest transverse dimension of the transmit antenna. A point source kept at a distance R radiating a spherical wave produces a maximum path difference of δR over a transverse dimension D, as shown in Fig. 7.1. In the figure, the point source is at S and D is the transverse dimension over which we are measuring the path difference with respect to the normal distance $SO = R$. The maximum phase error occurs at the edge which is $k\delta R$ and is equal to $\pi/8$ if $R = 2D^2/\lambda$.

Since two antennas are involved in the measurement setup, we have to select the larger of the two transverse dimensions as D to ensure that both antennas are in the far-field of each other. Generally, the transmit antenna is a horn antenna of small size and, hence, the transverse dimension of the receive antenna or the test antenna is taken as D and the distance R is always

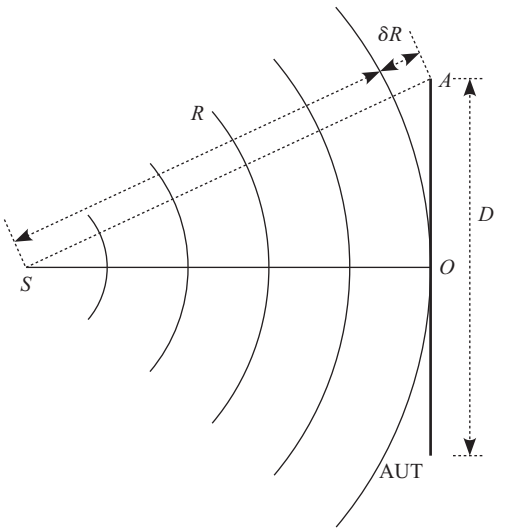

Fig. 7.1 Phase difference between the plane wavefront and spherical wavefront

selected greater than $2D^2/\lambda$. If the distance between the two antennas is made less than this limit, the measured pattern nulls and amplitudes can differ from the far-field pattern of the antenna.

EXAMPLE 7.1

Show that if a point source radiating a spherical wavefront and the antenna under test are separated by a distance equal to $2D^2/\lambda$, where D is the largest dimension of the antenna under test, the phase difference between the spherical wavefront and the plane wavefront at the edge of the antenna under test is equal to $\pi/8$.

Solution: From $\triangle SOA$ in Fig. 7.1

$$(R+\delta R)^2 = R^2 + \left(\frac{D}{2}\right)^2$$

$$\delta R = \sqrt{R^2 + \left(\frac{D}{2}\right)^2} - R$$

$$= R\left[\sqrt{1 + \left(\frac{D}{2R}\right)^2} - 1\right]$$

Using the first two terms of the binomial expansion, the path difference reduces to

$$\delta R \simeq R\left[1+\frac{1}{2}\left(\frac{D}{2R}\right)^2-1\right]$$
$$=\frac{D^2}{8R}$$

Since the two antennas are separated by $R = 2D^2/\lambda$, substituting in the above equation and simplifying

$$\delta R = \frac{\lambda}{16} \tag{7.1}$$

The phase difference between the waves following the path SO and SA is

$$\delta\phi = k\delta R = \frac{\pi}{8} \tag{7.2}$$

It is also equally important to make sure that there is only one plane wave at the antenna under test (AUT). Since the transmit antenna radiates in all directions, if there are any objects in the vicinity of the two antennas, a reflected wave may also be present at the AUT. This is generally not desirable. Therefore, the antenna range should be so designed that the reflected waves are either completely eliminated or are used constructively to produce a wave that has a uniform wavefront.

An antenna range can be constructed in open space. Such a range is known as an *outdoor range*. In an outdoor range, apart from ground reflections there may be reflections from other objects such as buildings, trees, moving vehicles, etc. The measurements in an outdoor range are usually prone to electromagnetic interference from other systems, such as local radio/TV broadcast, radar, mobile phones, etc. It is also possible to construct an antenna range in an enclosed building, which is known as an *indoor range*. To reduce the reflections from the walls, floor, and ceiling of the building, a special material called *absorber* is used to cover these surfaces. In this section we will study three types of outdoor ranges, namely, the elevated range, the reflection range, and the slant range. The indoor range and the compact range for measuring the far-field pattern are also discussed in some detail.

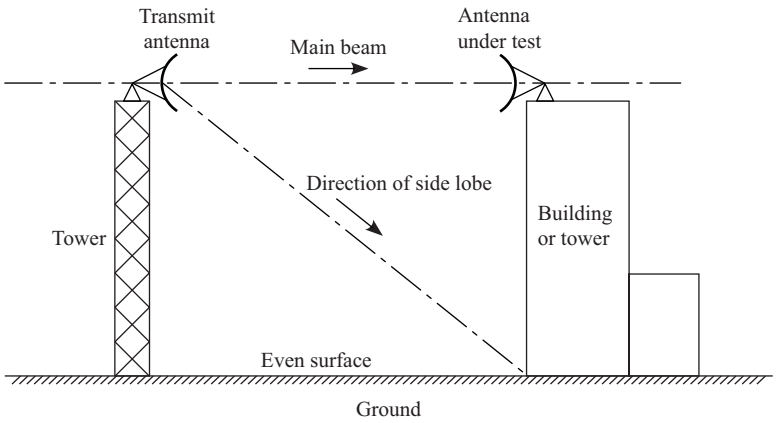

Fig. 7.2 Construction of an elevated range

Elevated range In an elevated range, both the transmit and the test antennas are situated above the ground at the same elevated height. The antennas are mounted on high towers or buildings. The ground beneath is maintained as smooth as possible. The height of the transmit antenna is chosen such that its main beam does not point towards the ground (Fig. 7.2). The side lobes of the transmit antenna can point towards the structure which is a source of reflection in an antenna range. The side lobes of the transmit antenna are kept very low so that practically no energy is reflected from these structures. The line-of-sight between the two antennas is always kept clear of any obstructions.

Let us now estimate the error in measurement due to reflection from the ground. Let E_D be the electric field at the test antenna due to the direct ray and E_R be the field due to the reflected ray. Both E_D and E_R are, in general, complex phasors and have arbitrary amplitude and phase. The total received signal at the AUT is given by the vector sum of the direct and reflected waves

$$E_T = E_D + E_R \tag{7.3}$$

Expressing the complex quantities in terms of their magnitudes and phases

$$|E_T|\angle E_T = |E_D|\angle E_D + |E_R|\angle E_R \tag{7.4}$$

The relative magnitude of the total field can be written as

$$\left|\frac{E_T}{E_D}\right| = \left|1 + \left|\frac{E_R}{E_D}\right|(\angle E_R - \angle E_D)\right| \tag{7.5}$$

If there is no reflected wave, $|E_R| = 0$ and the measured value is equal to that of the direct signal. If the reflected field strength is not zero, the relative measured value of the total field depends on the phase difference between the two signals. Two extreme situations are, when both E_R and E_D are in phase (i.e., $\angle E_R = \angle E_D$) and when they are out of phase (i.e., $\angle E_R - \angle E_D = \pi$). The relative measured levels corresponding to these two situations are given by

$$\left|\frac{E_T}{E_D}\right|_{\text{in-phase}} = \left|1 + \left|\frac{E_R}{E_D}\right|\right| \tag{7.6}$$

and

$$\left|\frac{E_T}{E_D}\right|_{\text{out-of-phase}} = \left|1 - \left|\frac{E_R}{E_D}\right|\right| \tag{7.7}$$

These two equations give the bounds for the error in measurement due to reflection and these are plotted as functions of $|E_R/E_D|$ in Fig. 7.3. The ratio of the electric field is converted to decibels using

$$\left|\frac{E_R}{E_D}\right|_{\text{dB}} = 20\log_{10}\left|\frac{E_R}{E_D}\right| \tag{7.8}$$

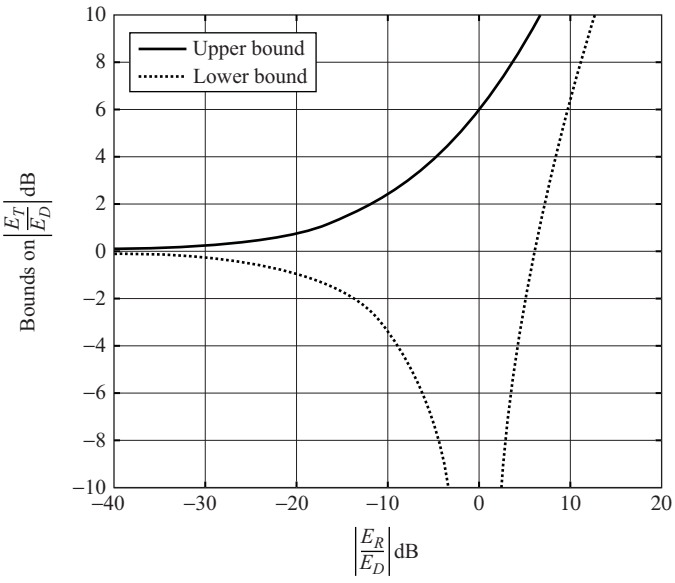

Fig. 7.3 Error bounds for the measured electric field

We can use this information to estimate the errors in the measurement system as well as design the measurement system to reduce the errors. Consider a transmit antenna with its main beam towards the AUT and a side lobe 25 dB below the main beam. Assume that the test antenna pattern also has a 25 dB side lobe level. Let us assume that when a wave is reflected off the ground, it gets attenuated by 10 dB.

Now we can estimate the error in the measurement when the two main beams are pointing at each other. The signal from the side lobe of the transmit antenna gets reflected by the ground and is picked up by a side lobe of the AUT. Ignoring the path loss for the direct and the reflected rays, the reflected wave signal will be $(25 + 25 + 10) = 60$ dB below the direct wave signal. The ratio of the reflected and direct fields will be 0.001 and the maximum and minimum values of the measured levels will be 1.001 and 0.999, which when expressed in decibels are 0.0087 dB and -0.0087 dB. Therefore, the measurement error is negligibly small when the two main beams are pointing at each other.

In order to measure the side lobe region of the elevation pattern, the test antenna has to be tilted in the θ-direction such that its side lobe points towards the transmit antenna [Fig. 7.4(a)]. In this configuration, the main beam intercepts the ground. The direct path signal is 25 dB below that in the previous case and the reflected signal is 25 dB higher. Therefore, $|E_R/E_D|_{\text{dB}} = -10$ dB and from Fig. 7.3 the error in the measured signal would be between -3.3 dB and $+2.4$ dB. Therefore, it is necessary to ensure that the main beam is not pointing towards to the ground when the side lobe part of the pattern is being measured [Fig. 7.4(b)]. This requires a facility

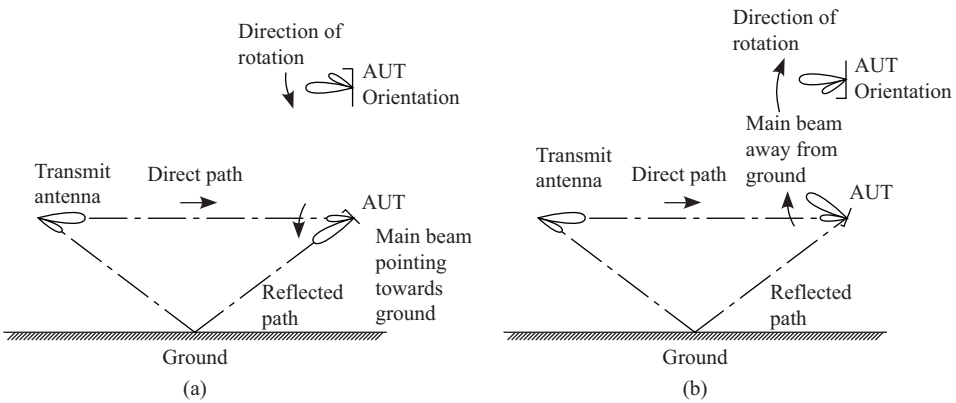

Fig. 7.4 Measurement of elevation pattern using an elevated range (a) main beam intercepting the ground (b) main beam pointing away from the ground

to rotate the test antenna about its axis by 180°, so that the main beam is pointing towards the sky and not towards the ground.

Reflection range In an elevated range, the goal is to minimize the reflected signal from the ground. In a reflection range, the signal reflected off the ground is used to create constructive interference and hence a uniform wavefront in the region of the antenna under test. This can be achieved by careful design of the reflecting surface. Hence the design of a reflection range is more complicated than that of an elevated range. Ground reflection ranges are very useful in the VHF band of frequencies for measuring moderately broad patterns (ANSI/IEEE Std 149-1979).

Slant range In a slant range, the transmit antenna is kept very close to the ground and the test antenna along with its positioner is mounted on a non-conducting tower, as shown in Fig. 7.5. The tower is usually made of fibreglass material. The transmit antenna is positioned and oriented such that its main beam points towards the test antenna and the side lobes point towards the reflection points on the ground. A slant range requires less space compared to an elevated range.

Indoor range It is not desirable to have reflecting surfaces in an antenna range. A closed chamber can be made reflection-free or echo-free by lining all the surfaces of the chamber with absorbing material. Such a chamber is known as an *anechoic chamber*. The indoor range is basically an anechoic chamber. The main advantages of an indoor range compared to an outdoor

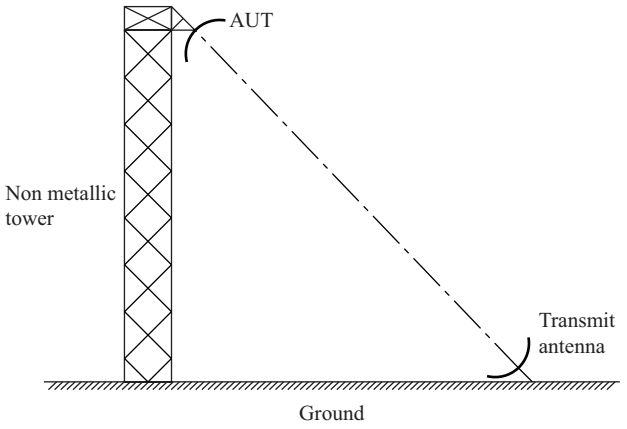

Fig. 7.5 Antenna arrangement in a slant range

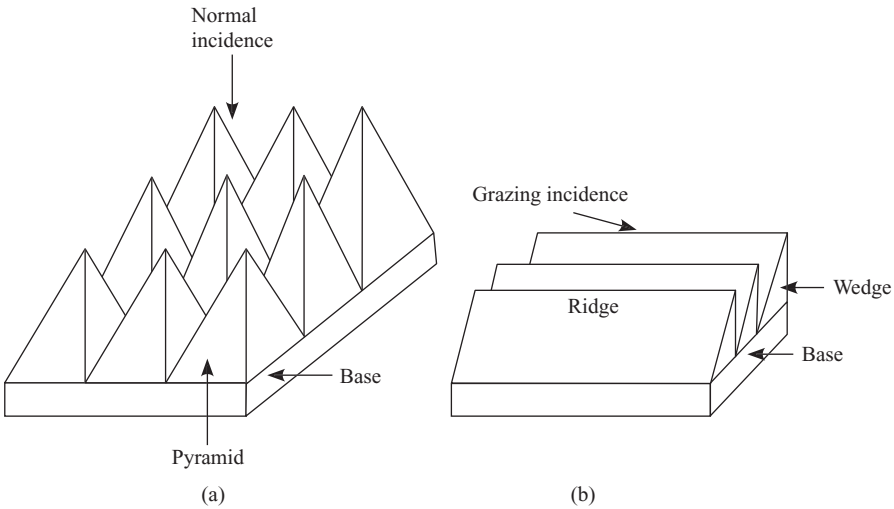

Fig. 7.6 Two types of absorbers—(a) pyramid shaped and (b) wedge shaped

range are protection of expensive equipment from environmental severities, security, all-weather operation, and absence of electromagnetic interference. An indoor range can be used to measure both far-field as well near-field patterns of an antenna. In this book we will consider the measurement of only the far-field pattern.

The main component of an anechoic chamber is the absorber. Absorbers are made in the form of pyramids or wedges [Fig. 7.6]. The pyramidal shaped absorbers have very low reflection coefficient over a wide frequency band for normal incidence. For example, it is possible to achieve a reflection coefficient of -30 dB from a one wavelength high pyramidal absorber. The wedge-shaped absorbers are best suited for the waves travelling nearly parallel to the ridges [see Fig. 7.6(b)].

A typical construction of an anechoic chamber is shown in Fig. 7.7. It is important to realize that depending on the requirements several variants of this arrangement are being used. A grounded metal shield is introduced between the absorber and the brickwork to achieve electromagnetic shielding. The choice of the absorber depends on the direction of the RF energy falling on it. For example, pyramidal absorbers are used on the back wall close to the AUT, because the energy from the transmit antenna is incident on this surface along the normal direction. In the region between the two antennas, wedge-type absorbers are best suited as the waves in this area have near grazing incidence on the absorber.

Absorbers are not perfect and they do reflect a small amount of energy. Superposition of waves radiated by the transmitter and the waves reflected

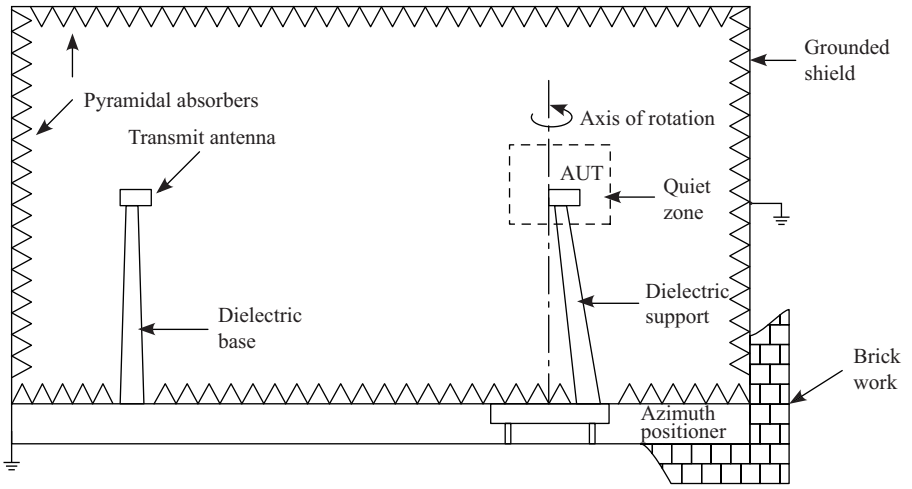

Fig. 7.7 Construction of an anechoic chamber

by the walls of the chamber results in a standing wave pattern. Close to the absorber surface, an unacceptable level of ripple in the wavefront is observed. However, farther away from the surface, the ripple levels become very small and the electromagnetic waves can be assumed to be plane. In an anechoic chamber, the plane-wave-like condition is created over a small volume near the test antenna and this region is known as the *quiet zone*. The ripple in the wavefront can be minimized by choosing good quality absorbers having low reflection coefficients and by making the size of the chamber large. A pictorial representation of how the ripples in the wavefront are generated in a rectangular anechoic chamber is shown in Fig. 7.8(a).

A tapered anechoic chamber is made in the form of a pyramidal horn. A longitudinal section of a tapered anechoic chamber is shown in Fig. 7.8(b). The transmit antenna is placed at the smaller end of the chamber and the antenna under test is placed at the larger end. At the lower end of the operating frequency band, the direct and the reflected rays add vectorially in such a manner that it produces a slowly varying spatial interference pattern and hence a relatively smooth illumination amplitude is obtained in the test region [Fig. 7.8(b)]. Since the field does not spread in the manner of a spherical wave, the tapered chamber cannot be used for a direct gain measurement based on Friis transmission formula (Kummer & Gillespie 1978).

Compact range One of the requirements of the far-field measurements is that the incident wave on the antenna under test should be a plane wave. In a compact range, this is achieved by using a reflector. For example, a

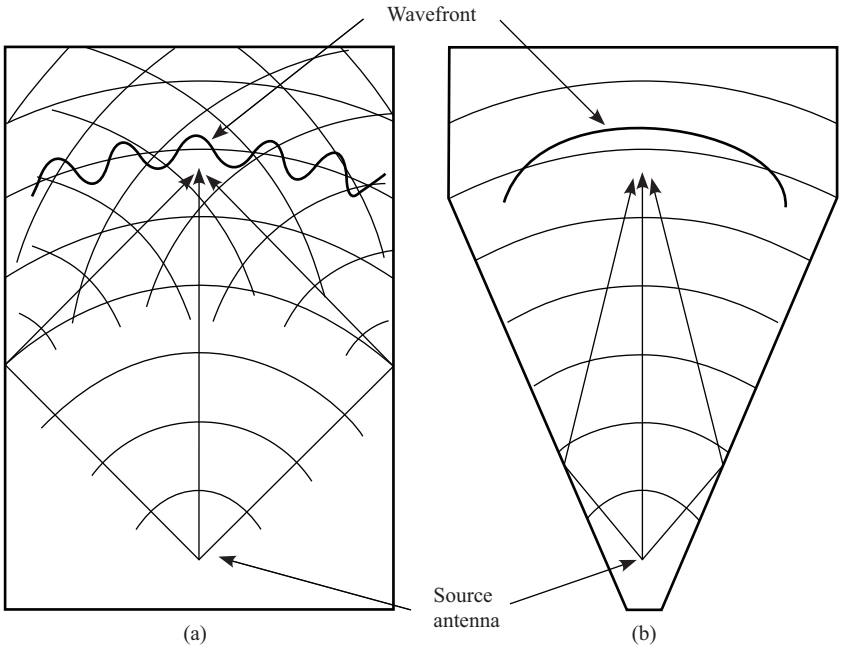

Fig. 7.8 Ripples in the wavefront due to reflections in a (a) rectangular anechoic chamber and (b) tapered anechoic chamber

paraboloid reflector can be used to collimate the energy from a feed located at its focal point (Fig. 7.9). An offset feed is generally used to reduce the aperture blockage. The size of the reflector needs to be at least three times the size of the AUT so that the illumination at the test antenna is

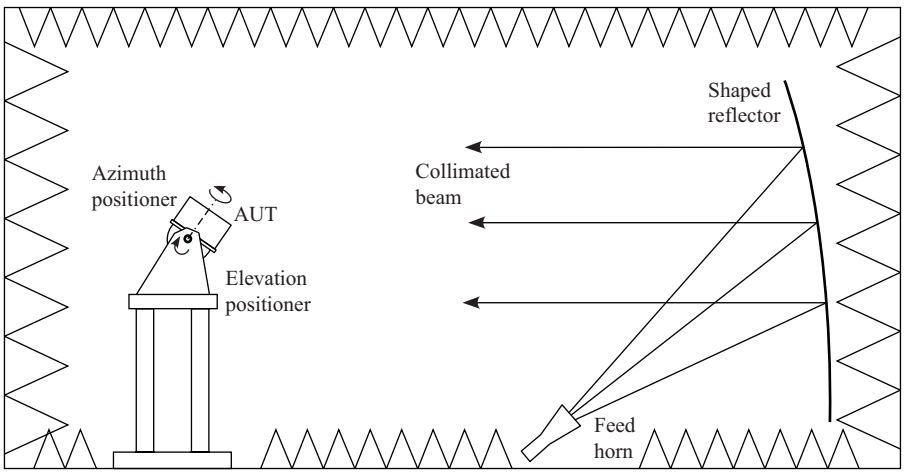

Fig. 7.9 Wave propagation in a compact range

approximately a plane wave. To reduce the edge diffraction, the edges of the reflector are serrated randomly. The scattered fields from these random serrations add up to nearly zero in most places.

This arrangement allows production of plane wave conditions or quiet zone with a much shorter distance between the transmit and the test antenna. The entire arrangement, including the test antenna positioner, is kept inside a rectangular anechoic chamber. This is an indoor range with much smaller dimensions than a conventional anechoic chamber. Hence it is called a compact range.

7.2 Radiation Pattern Measurement

As already indicated in the introduction to this chapter, the AUT is always used in the receive mode for pattern measurements. The receive pattern of an antenna is the power delivered to a matched load as a function of the direction of arrival of the incident plane wave of constant power density. Therefore, to measure the pattern of an antenna we need a second antenna kept at a distance $R > 2D^2/\lambda$ transmitting electromagnetic energy, so that it produces a plane wave at the location of the receive antenna. Now, to plot the received power as a function of the angle of incidence of the plane wave, we need to move the transmit antenna over the surface of a sphere of radius R with the test antenna placed at the center of the sphere. The transmit antenna orientation must be such that the centre of the sphere is always along the same direction with respect to the transmit antenna. This ensures that the power density of the plane wave incident from different directions is the same.

In practice, instead of moving the transmit antenna around a sphere, the receive antenna is rotated about the center of the sphere, keeping the position of the transmit antenna unaltered. In this arrangement the direction of arrival of the plane wave is kept the same but the receive antenna is rotated so that the plane wave orientation with respect to the receive antenna is changed. This exactly simulates the same condition as moving the transmit antenna around, provided the receive antenna environment does not change when rotated. If an antenna measurement range, either outdoor or indoor, is designed properly to have zero or negligible reflections in all directions simulating the free space conditions, then the environment of the receive antenna is independent of the rotation about its axis.

Thus, the antenna measurement range must have one fixed position for the transmit antenna and a rotatable mount for the receive antenna (which is the test antenna). In some of the antenna pattern measurements,

especially the polarization-dependent parameters, sometimes it becomes necessary to rotate the transmit antenna also. However, in most cases two discrete rotational positions, such as 0° or 90° are sufficient. Hence, the transmit antenna mount is generally provided with multiple discrete mounting positions but rarely with continuous rotation capability. The rotation capability is provided only on the receive antenna mount, which is known as the antenna positioner. With this arrangement and appropriate transmit and receive equipment, the pattern of an antenna can be measured. The filed pattern, phase pattern, polarization pattern, etc., are measured using the same arrangement but with different sensors to measure the corresponding parameters instead of the received power.

7.2.1 Antenna Positioner

An antenna pattern is most often represented by the principal plane cuts of the 3D pattern. Consider the coordinate system shown in Fig. 7.10 and let the test antenna be mounted at the origin. We take the direction of the transmit antenna as the z-axis for convenience and the y-axis as the vertical axis. Assume that the receive antenna, the pattern of which we are interested in measuring, is mounted with its main beam pointing along the z-axis. Further, assume that the transmit antenna is linearly polarized and is mounted with the **E** field along the y-axis (or vertically polarized).

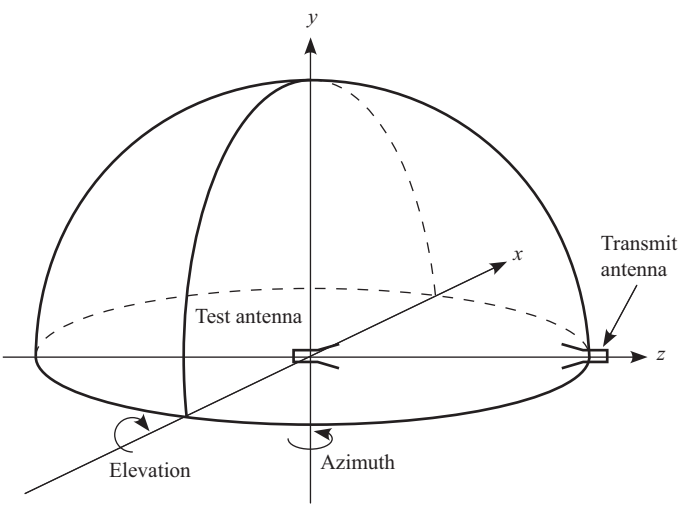

Fig. 7.10 Test antenna located at the origin of the spherical coordinate system

Now, if we have the flexibility to continuously rotate the receive antenna about the x, y, and z axes, we can measure the 3D pattern of the antenna or a pattern cut in any desired plane by simply rotating the antenna and recording the received power (or field, phase, polarization, etc.) as a function of angular position. The rotation about the y-axis (or the vertical axis) is generally known as the azimuth rotation and the rotation about the x-axis (or the horizontal axis) is known as the elevation rotation.

In Fig. 7.10, the antenna is mounted in the x-y plane with the main beam pointing towards the transmit antenna or the z-axis. If we record the received power as the antenna is rotated in azimuth, the received power versus the rotation angle produces a $\phi = 0^\circ$ cut of the pattern. If the antenna is rotated about the x-axis keeping the azimuth constant, we get a $\phi = 90^\circ$ cut or the y-z plane cut of the pattern. The rotation about the z-axis can be used to rotate the polarization of the antenna relative to the transmit antenna. This is useful for measuring the cross-polar pattern and the polarization properties of the antenna.

Generally, rotation about two axes, the azimuth and the elevation rotation, are sufficient for obtaining the principal pattern cuts. To measure the co- or the cross-polar patterns, either the transmit of the receive antenna are mounted with 90° rotation in the polarization.

Antenna positioners come in single-axis, two-axis, and, in most sophisticated ranges, three-axis mounts. Two of the most commonly used two-axis mounts are shown in Fig. 7.11. These are the elevation-over-azimuth and

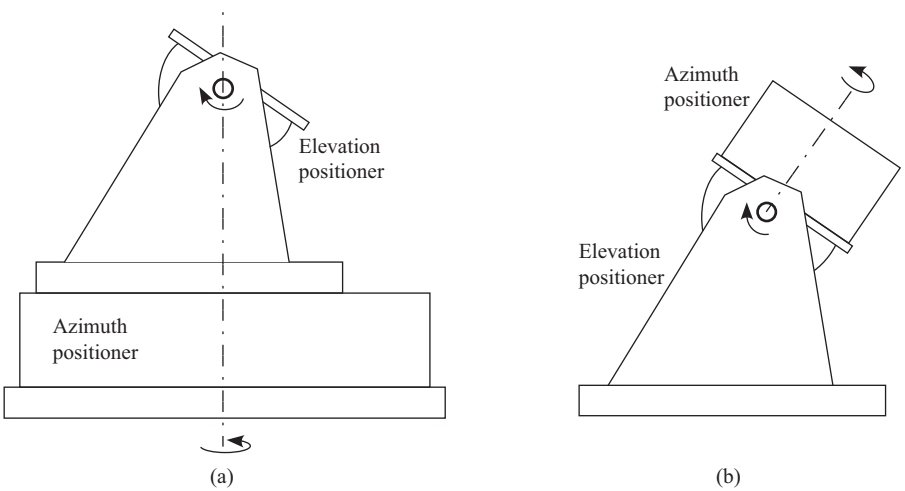

Fig. 7.11 Antenna positioners (a) elevation-over-azimuth positioner and (b) azimuth-over-elevation positioner

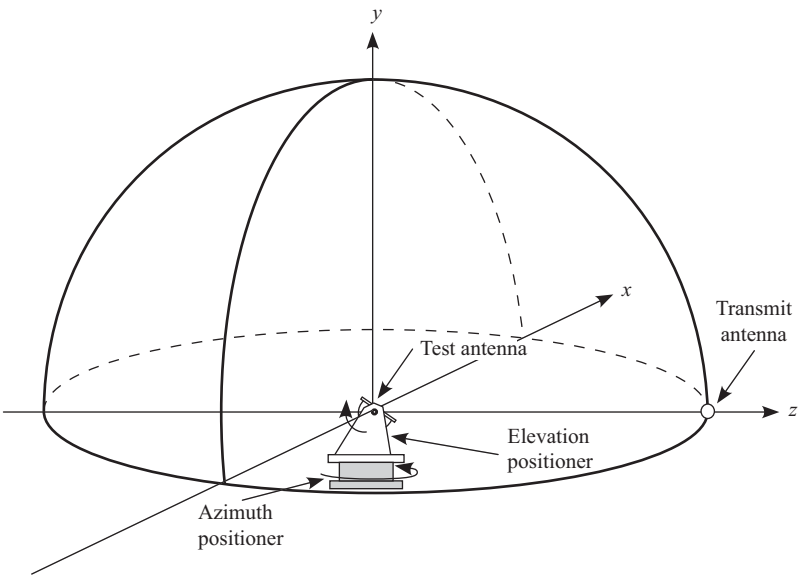

Fig. 7.12 Pattern measurement system using elevation-over-azimuth positioner

azimuth-over-elevation mounts. Several different arrangements are possible for measuring the radiation characteristics of an antenna. One of the arrangements shown in Fig. 7.12 uses elevation-over-azimuth positioner. The transmit antenna is mounted vertically above and along the z-axis. This arrangement can be used to plot different ϕ cuts of the pattern. The arrangement shown in Fig. 7.13 is a single-axis azimuth positioner.

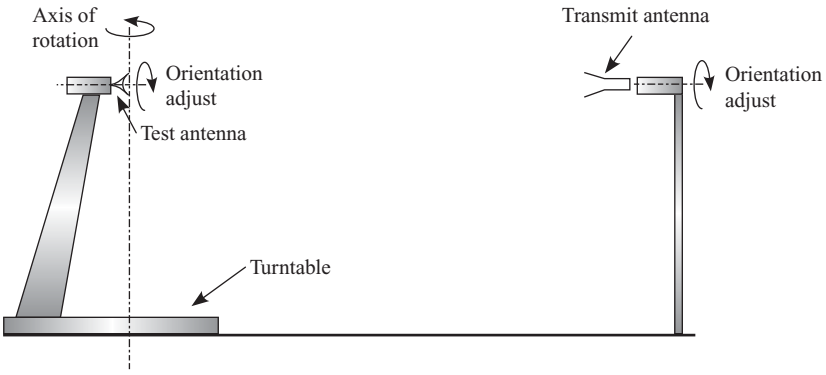

Fig. 7.13 Pattern measurement system using single-axis rotation (azimuth) mount

Although both these arrangements allow the antenna to be rotated to any (θ, ϕ) direction, only the principal plane cuts are measured. To measure the pattern in other cuts, one needs to have an additional axis of rotation to align the polarization. With a three-axis positioner, the 3D pattern can be measured.

7.2.2 Receiver Instrumentation

A schematic block diagram of a modern antenna positioner control system and the measurement system is shown in Fig. 7.14. The entire pattern measurement system is controlled by a computer. Present day automated pattern measurement systems are software driven and generates the pattern plot once the antenna is mounted properly. For the measurement of any pattern cut, the digital computer rotates the antenna in steps. At each angle the receiver output is digitized and stored in the computer. Pattern plots are generated from the stored data. Further processing of the recorded pattern data can also be carried out to extract other pattern properties, such as directivity, beamwidth, side lobe level, etc.

The receiver block is the main measurement unit. A measuring receiver or a network analyser type instrument can measure the received power, field amplitude, and phase. One can also use simpler and less expensive instruments for the pattern measurements. A power meter can be used to measure power with a reasonable dynamic range. A much simpler arrangement is to use the conventional voltage standing wave ratio (VSWR) meter and

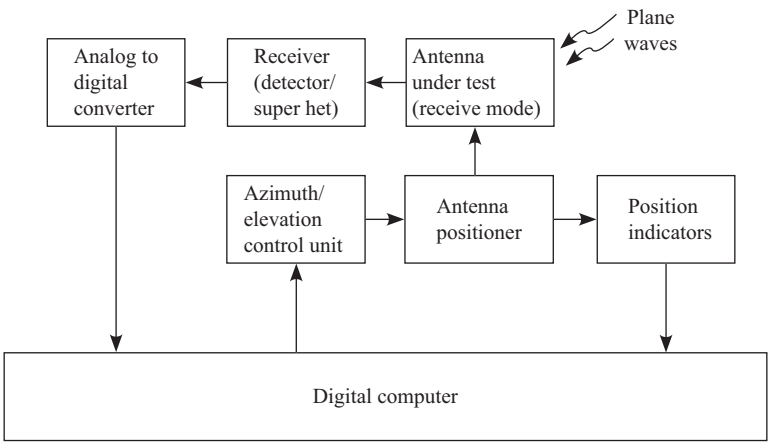

Fig. 7.14 A computer-based control of the positioner

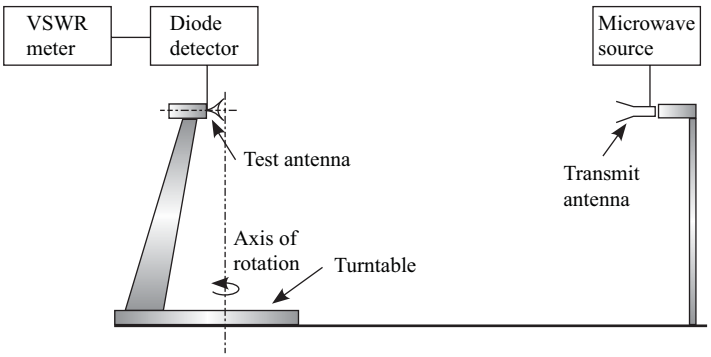

Fig. 7.15 Measurement of radiation pattern using a VSWR meter

a square law detector as a power measuring device (Fig. 7.15). The output voltage of a square law detector is proportional to the input power for low power inputs. Further, if the the transmitter is modulated by a 1 kHz square wave, a VSWR meter can be used to measure the output voltage over a 30 to 40 dB dynamic range. A VSWR meter is a narrow band (bandwidth: 50 to 100 Hz), 1 kHz tuned amplifier capable of measuring voltages as low as few micro volts. Because of the narrow bandwidth, the noise contribution of the amplifier is very low, and hence this system provides good sensitivity.

7.3 Gain and Directivity

Gain of an antenna in a specified direction (θ, ϕ) is given by

$$G(\theta, \phi) = 4\pi \frac{U(\theta, \phi)}{P_{\text{acc}}} \tag{7.9}$$

where $U(\theta, \phi)$ is the radiation intensity in the direction (θ, ϕ) and P_{acc} is the power accepted by the antenna. Gain does not take into account the input mismatch losses and polarization losses. Therefore, when measuring the gain of an antenna it is important to make sure that the antenna is both input-matched and polarization-matched.

The directivity of an antenna is given by

$$D(\theta, \phi) = 4\pi \frac{U(\theta, \phi)}{P_{\text{rad}}} \tag{7.10}$$

where P_{rad} is the total power radiated by the antenna. Directivity of an antenna differs from the gain as it does not include the dissipative losses

in the antenna. The gain and the directivity, along the same direction, are related to each other by the radiation efficiency of the antenna.

The gain and the directivity are usually measured in the direction of the pattern maximum. Their values in any other direction can be calculated from the radiation pattern. There are two techniques used for measuring the gain of an antenna—*absolute gain measurement* and *gain transfer measurement*. For the absolute gain measurement it is not necessary to have a prior knowledge of the gains of the antennas used in the measurement. The more commonly used gain transfer method, requires the use of a gain standard with which the gain of the antenna under test is compared.

7.3.1 Absolute Gain Measurement

Friis transmission formula (Section 2.7) forms the basis for absolute gain measurement. The Friis transmission formula expressed in decibels is

$$P_{r\mathrm{dBm}} = P_{t\mathrm{dBm}} + G_{t\mathrm{dB}} + G_{r\mathrm{dB}} + 20\log_{10}\left(\frac{\lambda}{4\pi R}\right) \tag{7.11}$$

where the symbols have the following meaning

$P_{r\mathrm{dBm}}$:	power received in dBm by the receive antenna into a matched load
$P_{t\mathrm{dBm}}$:	power transmitted in dBm by the transmit antenna into air
$G_{t\mathrm{dB}}$:	gain of the transmit antenna in dB
$G_{r\mathrm{dB}}$:	gain of the receive antenna in dB
R:	distance between the transmit and the receive antennas in m
λ:	wavelength in m

Consider two identical antennas placed in an elevated range or inside a rectangular anechoic chamber which are properly oriented and aligned such that (i) they are polarization matched and (ii) main beams of the two antennas are aligned with each other. With this arrangement, the gain in the direction of the maximum can be measured. The gain in any other direction can be computed from the radiation pattern.

Let R be the separation between the two antennas chosen such that the antennas operate in the far-field region. Let λ be the wavelength corresponding to the operating frequency. A calibrated coupling network and a matched receiver unit, as shown in Fig. 7.16, are used to measure the transmit and the receive powers $P_{t\mathrm{dBm}}$ and $P_{r\mathrm{dBm}}$ respectively. All the components are impedance matched using tuners.

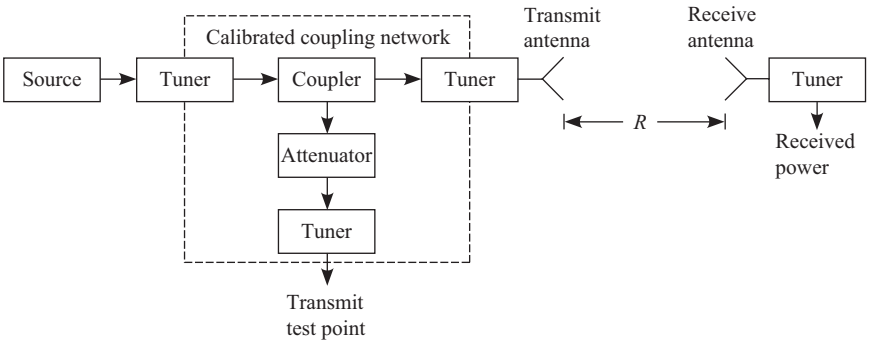

Fig. 7.16 Measurement of transmit and receive powers

If the two antennas are identical, their gains are identical and Eqn (7.11) can be written as

$$G_{t\mathrm{dB}} = G_{r\mathrm{dB}} = \frac{1}{2}\left[P_{r\mathrm{dBm}} - P_{t\mathrm{dBm}} - 20\log_{10}\left(\frac{\lambda}{4\pi R}\right)\right] \tag{7.12}$$

and hence the gain of the antennas can be calculated. Since this method uses two antennas, it is known as *two-antenna method* for gain measurement.

In the absence of two identical antennas, a third antenna is required to measure the gain. This is known as a *three-antenna method* of gain measurement. Let $G_{A\mathrm{dB}}$, $G_{B\mathrm{dB}}$, and $G_{C\mathrm{dB}}$ be the gains of the three antennas. Transmitted and received powers are recorded by taking two antennas at a time. Let $P^{AB}_{r\mathrm{dBm}}$, $P^{BC}_{r\mathrm{dBm}}$, and $P^{CA}_{r\mathrm{dBm}}$ be the received powers. The superscripts represent the antenna combinations used in the measurement. Similarly, let $P^{AB}_{t\mathrm{dBm}}$, $P^{BC}_{t\mathrm{dBm}}$, and $P^{CA}_{t\mathrm{dBm}}$ be the transmitted powers in each measurement. Now we have three linear equations corresponding to these three measurements

$$G_{A\mathrm{dB}} + G_{B\mathrm{dB}} = P^{AB}_{r\mathrm{dBm}} - P^{AB}_{t\mathrm{dBm}} - 20\log_{10}\left(\frac{\lambda}{4\pi R}\right) \tag{7.13}$$

$$G_{B\mathrm{dB}} + G_{C\mathrm{dB}} = P^{BC}_{r\mathrm{dBm}} - P^{BC}_{t\mathrm{dBm}} - 20\log_{10}\left(\frac{\lambda}{4\pi R}\right) \tag{7.14}$$

$$G_{C\mathrm{dB}} + G_{A\mathrm{dB}} = P^{CA}_{r\mathrm{dBm}} - P^{CA}_{t\mathrm{dBm}} - 20\log_{10}\left(\frac{\lambda}{4\pi R}\right) \tag{7.15}$$

which can be solved simultaneously to calculate the gains of each of the antennas.

EXAMPLE 7.2

In a three-antenna method of gain measurement, the measured receive powers taking two antennas at a time are 0.0297 mW, 0.0471 mW, and 0.0374 mW. Calculate the gains of the antennas, if the transmit power is 1 W, spacing between the antennas is 10 m and the frequency of operation is 980 MHz.

Solution: Expressing the powers in decibels

$$\begin{aligned} P_{r\mathrm{dBm}}^{AB} &= 10\log_{10}(0.0297) = -15.27 \text{ dBm} \\ P_{r\mathrm{dBm}}^{BC} &= 10\log_{10}(0.0471) = -13.27 \text{ dBm} \\ P_{r\mathrm{dBm}}^{CA} &= 10\log_{10}(0.0374) = -14.27 \text{ dBm} \\ P_{t\mathrm{dBm}} &= 10\log_{10}\left(\frac{1}{1\times 10^{-3}}\right) = 30 \text{ dBm} \\ &= P_{t\mathrm{dBm}}^{AB} = P_{t\mathrm{dBm}}^{BC} = P_{t\mathrm{dBm}}^{CA} \end{aligned}$$

The wavelength at 980 MHz is

$$\lambda = \frac{3\times 10^8}{f} = \frac{3\times 10^8}{980\times 10^6} = 0.306 \text{ m}$$

Substituting in Eqn (7.13) we get

$$\begin{aligned} G_{A\mathrm{dB}} + G_{B\mathrm{dB}} &= -15.27 - 30 - 20\log_{10}\left(\frac{0.306}{4\pi 10}\right) \\ &= 7 \text{ dB} \end{aligned}$$

Similarly from Eqn (7.14) and Eqn (7.15)

$$\begin{aligned} G_{B\mathrm{dB}} + G_{C\mathrm{dB}} &= 9 \text{ dB} \\ G_{C\mathrm{dB}} + G_{A\mathrm{dB}} &= 8 \text{ dB} \end{aligned}$$

Substituting $G_{A\mathrm{dB}} = 7 - G_{B\mathrm{dB}}$ into the above equations, and solving them simultaneously, we get

$$\begin{aligned} G_{A\mathrm{dB}} &= 3 \text{ dB} \\ G_{B\mathrm{dB}} &= 4 \text{ dB} \\ G_{C\mathrm{dB}} &= 5 \text{ dB} \end{aligned}$$

7.3.2 Gain Transfer Method

The gain of the test antenna is measured by comparing it with a standard gain antenna, of which the gain is known accurately. The test antenna is illuminated by a plane wave with its polarization matched to the test antenna. The received power into a matched load, $P^T_{r\mathrm{dBm}}$, is then measured. Let G^T_{dB} be the gain of the test antenna. From Friis formula

$$G_{t\mathrm{dB}} + G^T_{\mathrm{dB}} = P^T_{r\mathrm{dBm}} - P_{t\mathrm{dBm}} - 20\log_{10}\left(\frac{\lambda}{4\pi R}\right) \tag{7.16}$$

Now the test antenna is replaced by a standard gain antenna having a gain of G^S_{dB} and the received power $P^S_{r\mathrm{dBm}}$ is measured. Again from Friis transmission formula

$$G_{t\mathrm{dB}} + G^S_{\mathrm{dB}} = P^S_{r\mathrm{dBm}} - P_{t\mathrm{dBm}} - 20\log_{10}\left(\frac{\lambda}{4\pi R}\right) \tag{7.17}$$

Subtracting Eqn (7.17) from Eqn (7.16) we get

$$G^T_{\mathrm{dB}} = G^S_{\mathrm{dB}} + P^T_{r\mathrm{dBm}} - P^S_{r\mathrm{dBm}} \tag{7.18}$$

and hence the gain of the test antenna can be calculated. It is important to note that the polarization of the test antenna and the standard gain antenna need to be identical to each other and this should be matched with the polarization of the transmitter. Both antennas should be impedance matched to the receiver. This method is used to measure the gain of a linearly polarized antenna.

The gain of a circularly polarized antenna can also be measured using a linearly polarized standard gain antenna. Since a circularly polarized wave can be decomposed into two orthogonal linear components, we can use a linearly polarized antenna to measure the gains of each of these components and then the total gain is obtained by combining the two. For this, we take a linearly polarized transmit antenna and orient it so that it produces vertically polarized waves. Now, the power received by a standard gain antenna oriented to receive vertical polarization and the power received by the circularly polarized test antenna is measured. The gain of the test antenna for the vertically polarized wave is computed using Eqn (7.18). Let this gain be denoted by G^{TV}_{dB}. Now, rotate the transmit antenna by 90°, so that it radiates horizontally polarized waves. Measure the powers received by the test antenna and by the standard gain antenna oriented to receive horizontally polarized waves (rotating it by 90°). Once again, using Eqn (7.18) compute

the gain, G_{dB}^{TH}, of the test antenna for the horizontally polarized wave. The total gain of the test antenna is given by

$$G_{\text{dB}}^{T} = 10\log_{10}(G^{TV} + G^{TH}) \quad \text{dB} \tag{7.19}$$

In the above equation, G^{TV} and G^{TH} are the gains expressed as ratios and not in decibels.

7.3.3 Directivity

The total radiated power can be obtained by integrating the radiation pattern of an antenna over a closed sphere. Using Eqn (7.10), the directivity of the antenna can be computed. If the antenna has one main lobe and the side lobes are reasonably low, the maximum directivity can be computed from the half-power beamwidths in the two principal planes using Eqn (2.31).

If the losses of an antenna can be determined by any other method, its directivity can be estimated from the measured gain. Similarly, the gain can be calculated from the computed value of directivity.

7.4 Polarization

There are several methods for measuring the polarization of an antenna. In this section we present one of the simpler and popular methods to measure the polarization of an antenna. The polarization of an antenna refers to the polarization state of the transmitted wave along a given direction in the far-field region. The polarization state can be linear, circular, or elliptical. A simple method to measure the polarization of the incident wave is to use a linearly polarized antenna such as a dipole which intercepts only the **E** field component aligned with its arms and rejects the orthogonal component. For example, a vertically-oriented dipole receives only the vertical component of the **E** field of the incident wave. The horizontal component does not produce any voltage across its terminals. Therefore, the voltage at the antenna terminals, or the square root of the received power into a load, is proportional to the component of the incident **E** field along the dipole arms. In general, for arbitrary orientations of the dipole and the incident **E** field vector, the field coupled to the dipole is the projection of the **E** field vector onto the dipole. Here we have taken the dipole as an example, but this is applicable to any linearly polarized antenna. The voltage across the receiving antenna terminals is the dot product of the incident **E** field and the complex conjugate of the vector effective length of the antenna, as given in Eqn (2.109)

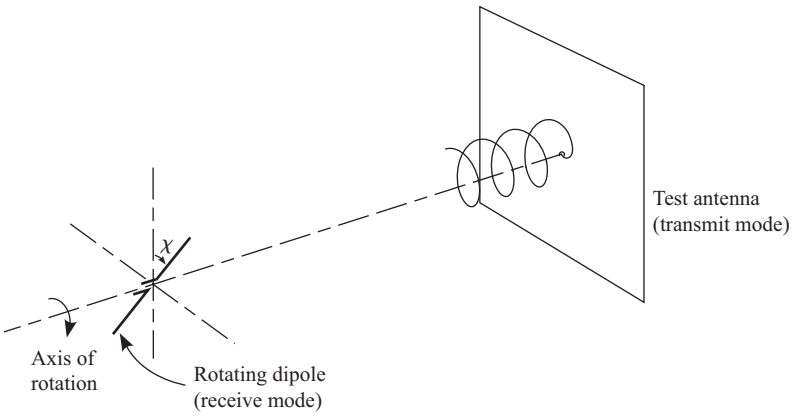

Fig. 7.17 Rotating linearly polarized receive antenna for polarization measurement

(see Section 2.6.5). If the relative angle between the incident **E** field and the receive antenna polarization is χ, the induced voltage across the antenna terminals is proportional to $\cos\chi$. Thus, by rotating the linearly polarized receiving antenna about its axis as shown in Fig. 7.17, the components of the incident **E** field in different directions can be sampled. This forms the basis of the measurement of the polarization of a wave or a transmit antenna.

Consider a measurement setup consisting of a linearly polarized receiving dipole antenna which can be slowly rotated about its axis as shown in Fig. 7.17, and the received voltage is recorded as a function of the rotation angle. The test antenna, the polarization of which is to be measured, is used in the transmit mode. A plot of the received voltage as a function of the orientation of the rotating receive antenna reveals the polarization state of the incident plane wave or that of the test antenna in the direction of the receive antenna. If the test antenna is linearly polarized in the vertical direction, the plot of the received voltage will be a figure of eight as shown in Fig. 7.18(a). It is essentially $\cos\chi$ shape, where χ is the angle between the orientation of the receive dipole and the vertical axis. The received voltage is maximum when the dipole orientation is vertical or $\chi = 0$ and it is zero for horizontal orientation. If the test antenna polarization is linear with the **E** field at ψ with respect to the vertical axis, the figure of eight plot will be rotated by ψ. The expression for the shape would be $\cos(\chi - \psi)$. The maximum occurs when $\chi = \psi$, which gives the direction of the polarization of the test antenna.

Now, consider the plot of the induced voltage using a circularly polarized test antenna. Since the incident wave is circularly polarized the received

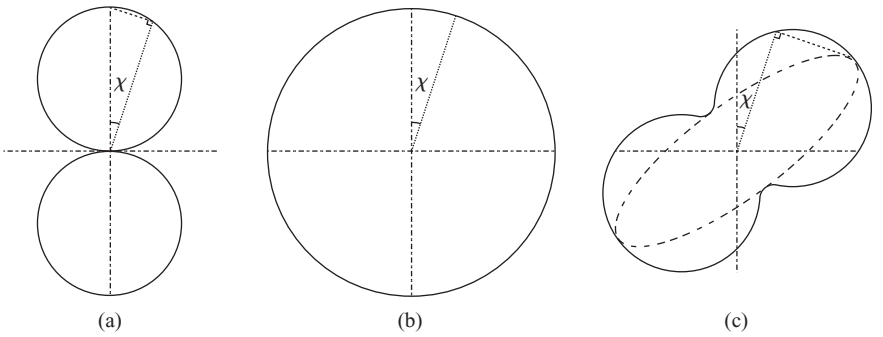

Fig. 7.18 Voltage received by a rotating linearly polarized antenna as a function of angle with (a) a vertically polarized, (b) a circularly polarized, and (c) an elliptically polarized test antenna in the transmit mode

voltage amplitude will be independent of the dipole orientation; only the phase of the received signal voltage will be a function of the rotation angle. The received voltage plot will be a circle as shown in Fig. 7.18(b). If the phase shift can be measured with respect to a reference, the sense of rotation of the circularly polarized wave can also be determined from the phase progression. But in most cases the phase measurement is not necessary because we can infer the sense of rotation (RCP or LCP) from the antenna structure. For example, the polarization of a helical antenna is the same as the sense in which the helix is wound. But the parameter of importance is the axis ratio which determines whether the polarization is really circular or elliptic. For a helical antenna we know that the polarization is circular only along the main beam axis and at the center frequency. For other directions and frequencies, the circularity may not be exact. It is common practice to measure the axis ratio to assess its circularity.

If the polarization of the test antenna in the direction of reception is right or left elliptic, then the trace of the received voltage will be as shown in Fig. 7.18(c). For an elliptically polarized wave, the incident **E** field orientation as well as amplitude are changing continuously at a rate of ω radians per second and the tip of the **E** field vector traces an ellipse. For any orientation of the linearly polarized receiving antenna, the received voltage is proportional to the projection of the polarization ellipse onto the dipole. Thus, when the dipole is oriented along the major axis, the received voltage is maximum and when the dipole is oriented along the minor axis, it is minimum. The shape will be like a dumb-bell and the polarization ellipse of the test antenna is the inscribed ellipse as shown in Fig. 7.18(c) (dashed lines). The ratio of the maximum voltage to the minimum voltage is the axis ratio (AR).

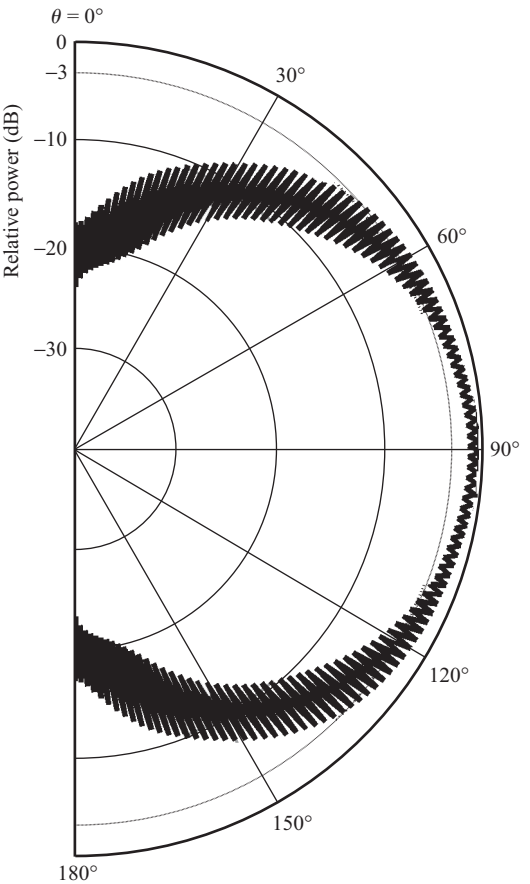

Fig. 7.19 Power received by a circularly polarized AUT as a function of direction

The antenna properties are the same in the transmit and receive modes because of the reciprocity theorem. Hence, the polarization state of the wave an antenna receives from a particular direction is the same as that it would transmit in that direction. In a polarization measurement setup, for convenience of measurement, it is common practice to use the test antenna as a receiver and the rotating linearly polarized antenna as a transmitter. The voltage received at the terminals of the test antenna are plotted as a function of the rotation angle of the transmit antenna. In this arrangement the incident wave is always a linearly polarized plane wave the **E** field vector of which is slowly rotated. The induced voltage at the test antenna terminals is proportional to the dot product between the vector effective lengths of the two antennas. Since one of the antenna is a linearly polarized

antenna, the shape of the received voltage plot gives the polarization state of the test antenna.

So far we have discussed the measurement of the polarization state of the test antenna in the direction in which the wave is received. The polarization state of the antenna as a function of the direction is the polarization pattern of the antenna. To measure the axis ratio of the polarization ellipse of the test antenna in different directions, the transmit antenna is rotated continuously about its axis and the received power is monitored for different orientations (θ, ϕ) of the test antenna. Consider an azimuth cut (ϕ = constant cut) and plot the power received as a function of θ. If the test antenna is circularly polarized, the received power does not change. Usually a circularly polarized antenna is circularly polarized only along the main beam and is elliptically polarized in other directions. A typical plot of the received voltage as a function of θ is shown in Fig. 7.19. The ratio of the maximum to minimum along any direction is the axial ratio of the polarization ellipse. For a linear polarized antenna, the minimum is always a zero or the AR is infinity.

7.5 Input Impedance and Input Reflection Coefficient

The input impedance of an antenna is measured at the specified terminals of the antenna. Since the antenna is a radiating system, the environment in which it is radiating affects the input impedance. Therefore, while making the input impedance measurement, it is important to create free space conditions. Generally a cable connected to the terminals (or port) of the antenna is used to carry power into the antenna. If Z_0 is the characteristic impedance of the cable and Z_a is the input impedance of the antenna, the complex reflection coefficient (Γ), which is the ratio of the reflected voltage to the incident voltage, is given by

$$\Gamma = \frac{Z_a - Z_0}{Z_a + Z_0} \tag{7.20}$$

Traditionally, input impedance of an antenna with a wave guide port is measured using a slotted line. However, with the availability of a swept frequency vector network analyser, it is possible to measure the complex reflection coefficient as a function of frequency and using the following formula one can compute the input impedance of the AUT.

$$Z_a = Z_0 \frac{1 + \Gamma}{1 - \Gamma} \tag{7.21}$$

Exercises

7.1 The separation between a point source radiating into free space and the receive antenna is $4D^2/\lambda$, where D is the largest dimension of the antenna and λ is the wavelength. Calculate the phase difference between the spherical wavefront and the plane wavefront at the edge of the receive antenna.

Answer: $\pi/16$

7.2 Two identical antennas operating at 2.4 GHz are used to measure their gains. With the transmit power set to 1 W, the power received by the receive antenna kept at a distance of 25 m is -8 dBm. Calculate the gain of the antennas.

Answer: 15 dB

7.3 An antenna with a gain, G dB, is transmitting 10 W power at 5 GHz and another antenna with a gain 3 dB higher than transmit antenna is used to receive the electromagnetic signal. The received power is 0.021 mW with the two antennas separated by a distance of 12 m. Calculate the gains of the two antennas.

Answer: 4.11 dB and 7.11 dB

7.4 The power received by a test antenna in free space conditions is 10 mW. If it is replaced by a standard gain antenna having a gain of 10 dB, the power received increases to 50 mW. Calculate the gain of the test antenna.

Answer: 3 dB

7.5 Two antennas, one linearly polarized and the other circularly polarized, having equal gains are used to establish a communication link which is operating at 1.8 GHz. If the transmit power is 60 W, received power is 30 μW, and the distance between the transmit and the receive antennas is 500 m, calculate the gain of the antennas.

Answer: 15.76 dB

7.6 Reflection coefficient of an antenna is measured to be $0.12\angle 120°$. If the characteristic impedance of the measurement system is 50 Ω, calculate the antenna impedance.

Answer: $(43.44 + j9.17)\ \Omega$

CHAPTER 8

Radio Wave Propagation

Introduction

In the exposition of antenna theory undertaken in the preceding chapters, the emphasis was on the computation of the fields due to a current distribution on the antenna. The environment was assumed to be infinite free space in all cases and the effects of the media and the discontinuities on the propagation of radio waves were ignored. However, this ideal situation is not met in practice.

There exist a number of factors which affect the propagation of radio waves in an actual environment. The most important of these are—(a) *Spherical shape of the earth:* Since the radio waves travel in a straight line path in free space, communication between any two points on the surface of the earth is limited by the distance to horizon. Therefore, for establishing a communication link beyond the horizon, the radio waves need to undergo a change in the direction of propagation. Several mechanisms can be made use of to effect the change. (b) *The atmosphere:* The earth's atmosphere extends all the way up to a height of about 600 km. The atmosphere is divided into several layers, viz., troposphere, stratosphere, mesosphere, and ionosphere. The propagation of the radio waves near the surface of the earth is affected mostly by the troposphere which extends up to a height of 8–15 km. Higher up in the atmosphere, it is the ionosphere which interacts with the radio waves. (c) *Interaction with the objects on the ground:* The radio waves travelling close to the surface of the earth encounter many obstacles such as buildings, trees, hills, valleys, water bodies, etc. The interaction of such objects or discontinuities with the radio waves is mostly manifested as the phenomena of reflection, refraction, diffraction, and scattering.

In this chapter we shall examine the aspects of radio wave propagation from the transmit antenna to the receive antenna, in the presence of media and boundaries. This can be looked at as an electromagnetic field problem.

A rigorous statement of the above electromagnetic field problem would be that the field distribution is set up such that Maxwell's equations are satisfied at every point in space and at every instant of time. A mathematical formulation of this statement and the solution of the resulting equations is extremely difficult except in some highly simplified situations. It is customary to simplify the field computation by separating the interaction of the electromagnetic fields with the environment into a few well-understood, idealized wave phenomena such as reflection, refraction, diffraction, scattering, etc. In a complex environment all these can co-exist. However, by identifying the different phenomena, we can treat each of these separately and use superposition of the fields to compute the overall effective field behaviour. It is evident that a significant amount of simplification, idealization, and modelling is involved in such an analysis. If sufficient care is taken in modelling the environment, a reasonably good prediction of the fields is possible for the purpose of establishing communication links.

In the analysis of radio wave propagation, the interaction of the fields with the medium and the discontinuities is mainly divided into four phenomena, viz., reflection, refraction, diffraction, and scattering. We are familiar with the *reflection* and *refraction* of a plane wave at a plane interface between two media with different electrical parameters. This situation is an idealization where the behaviour of the fields at the interface is described in terms of Snell's laws of reflection and refraction. This principle can be made use of in practical situations if the local radius of curvature of the interface as well as that of the wavefront is large compared to the wavelength of operation. The situation can be approximated to that of a plane wave interacting with a plane interface and geometrical ray techniques can be used to predict the ray paths and field strengths.

Whenever an edge, in an otherwise flat surface, is encountered by the electromagnetic fields, the induced currents can flow around the edge to the opposite side of the surface and produce fields in the shadow region. This phenomenon is known as *diffraction*. The computation of the fields in the diffraction zone requires a different mathematical formulation that is much more complex than Snell's laws.

The propagation constant in a medium is influenced by the electrical properties of the medium. If the medium is homogeneous and isotropic, the

propagation calculations are fairly straightforward as in a free-space environment, except for a change in the propagation constant. If the propagation constant is complex, then there is also some attenuation of the wave amplitude. However, in an inhomogeneous medium, the propagation paths are no longer straight lines. The bending of the ray path is known as the phenomenon of *refraction.*

There are situations in which the dimensions of the irregularities or the interacting discontinuities are small compared to the wavelength of operation. For example, a rain water drop of 1 mm diameter is illuminated by a plane electromagnetic wave of 10 cm wavelength, the induced currents on the drop produce secondary fields all around the drop. These fields are known as the scattered fields. The interaction of the fields with discontinuities or inhomogeneities which are small compared to the wavelength is generally known as *scattering.* In the atmosphere, scattering can take place due to inhomogeneities, turbulence, presence of rain drops, etc. While the fields due to a single scattering particle of regular shape illuminated by a plane wave can be rigorously formulated and solved, more complex situations involving distribution of particles or random irregularities and turbulence are analysed using statistical methods.

In order to establish a communication link between two points we need to study the intervening space between the transmit and receive antennas for its propagation characteristics. The presence of the earth and the atmosphere play a significant role in modifying the field distribution around the antenna and, hence, the communication-link parameters. In establishing a practical communication link between two points on the earth, the main constituents that influence the propagation are the troposphere; ground reflections; diffraction and scattering by obstacles such as buildings, trees, inhomogeneities, etc.; and the ionosphere. A study of the propagation of the electromagnetic waves including the interaction of the earth and troposphere is classified as ground wave propagation. The propagation through the ionosphere is treated separately as ionospheric propagation.

8.1 Ground Wave Propagation

The propagation of electromagnetic waves near the surface of the earth, including propagation in the troposphere is known as *ground wave propagation.* In a communication link between a transmit and a receive antenna situated on earth there can be multiple paths along which the transmitted wave can propagate to the receive antenna. If the antennas are in the line-of-sight of each other, a direct path will exist. The wave propagating

along this path is known as the *direct wave*. The electromagnetic energy can also reach the receive antenna via a ground-reflection path. Scattering and diffraction are the other two mechanisms by which the wave can travel to the receive antenna. The direct, reflected, diffracted, and scattered waves are collectively known as *space wave*. For example, in a cellular communication system, the electromagnetic waves travel in a complex environment consisting of several buildings, trees, streets, etc. The electromagnetic waves from the transmitter can reach the receiver by the direct path, as well as the reflected (from the ground or the building walls), scattered (by tree leaves or rain), or diffracted (by the edges of the buildings) paths.

Another mechanism of energy transfer is via surface waves. When an electromagnetic wave encounters an interface between two dissimilar media, apart from reflected and transmitted waves, a part of the energy can also flow along the interface which is known as a *surface wave*. At low and medium frequencies (LF and MF), this is the predominant mode of energy transfer for vertically polarized radiation.

In this section, different mechanisms of ground wave propagation and their characteristics are presented. This information is useful for establishing terrestrial communication links.

8.1.1 Free Space Propagation

Free space implies an infinite space without any medium or objects that can interact with the electromagnetic waves. When electromagnetic waves are radiated by an antenna kept in free space, at large distances from the antenna the radiated fields are in the form of spherical waves with angular power distribution given by the antenna pattern. The power received, P_r, at a distance R is given by the Friis formula

$$P_r = \frac{P_t G_t G_r \lambda^2}{(4\pi R)^2} \tag{8.1}$$

where P_t is the transmit power and G_t and G_r are the transmit and receive antenna gains, respectively. The transfer of electromagnetic energy from the transmit antenna to the receive antenna takes place in a straight-line path and, hence, such a communication link is called a line-of-sight (LOS) link.

The factor $[\lambda/(4\pi R)]^2$ is due to the propagation and is called the free-space path loss. It represents the attenuation of the signal due to the spreading of the power as a function of distance, R. In decibel units, the path loss

is expressed as

$$P_L = 10\log_{10}\left(\frac{4\pi R}{\lambda}\right)^2 \text{ dB} \tag{8.2}$$

EXAMPLE 8.1

A free-space LOS microwave link operating at 10 GHz consists of a transmit and a receive antenna each having a gain of 25 dB. The distance between the two antennas is 30 km and the power radiated by the transmit antenna is 10 W. Calculate the path loss of the link and the received power.

Solution: The wavelength at 10 GHz is

$$\lambda = \frac{3\times 10^8}{10\times 10^9} = 0.03 \text{ m}$$

The path loss of a free-space LOS link is given by Eqn (8.2)

$$P_L = 10\log_{10}\left(\frac{4\pi R}{\lambda}\right)^2 = 10\log_{10}\left(\frac{4\pi 30\times 10^3}{0.03}\right)^2 = 141.98 \text{ dB}$$

The received power can be calculated using the Friis formula

$$P_r = \frac{P_t G_t G_r \lambda^2}{(4\pi R)^2}$$

Expressing the gain of the antenna as a ratio, $G_t = G_r = 10^{25/10} = 316.23$. The received power is

$$P_r = \frac{10\times 316.23\times 316.23\times 0.03^2}{(4\pi\times 30\times 10^3)^2} = 6.3327\times 10^{-9} \text{ W}$$

In decibel units the received power is

$$P_r = 10\log_{10}\left(\frac{6.3327\times 10^{-9}}{1\times 10^{-3}}\right) = -51.98 \text{ dBm}$$

8.1.2 Ground Reflection

In the line-of-sight model, it is assumed that there is only one path for the propagation of electromagnetic waves from the transmit antenna to the receive antenna. This situation requires that the two antennas are kept in free space with no other objects intercepting the radiation from the transmit

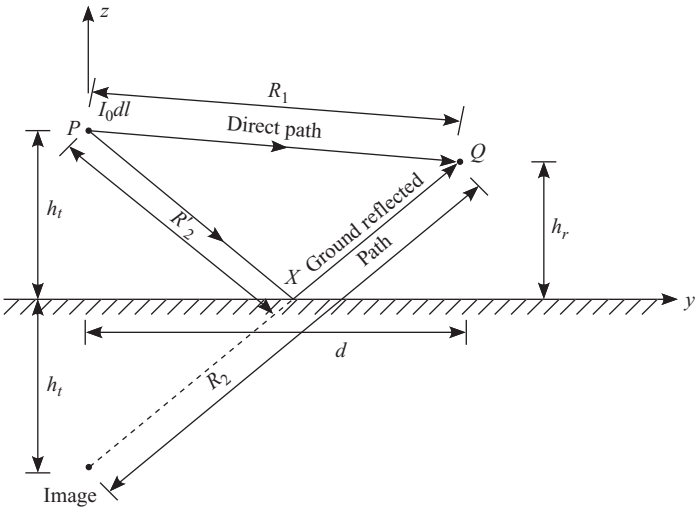

Fig. 8.1 Direct and ground-reflected paths of wave propagation

antenna. If the two antennas are situated close to the ground, due to the discontinuity in the electrical properties at the air–ground interface, any wave that falls on the ground is reflected. The amount of reflection depends on several factors such as angle of incidence, polarization of the wave, electrical properties (namely, conductivity and dielectric constant) of the ground, and the frequency of the propagating wave. Thus, the field at any point above the ground is a vector sum of the fields due to the direct and the reflected waves. In the text that follows we will derive a simple mathematical model to compute the fields of a transmit antenna above an imperfect ground, which can be used in the design of communication links, especially for selecting the locations of the transmit and receive antennas and their patterns.

Consider a transmit antenna located at point P at a height h_t and a receive antenna at point Q at a height h_r, from the surface of the ground (Fig. 8.1). Let the horizontal distance between the two antennas be d. The electromagnetic waves from the transmit antenna can reach the receive antenna by two possible paths—(a) the direct path and (b) the ground-reflected path. The total electric field at field point Q is given by the vector sum of the electric fields due to the direct and the ground-reflected waves. For convenience, let us assume that the transmit antenna and the field point are located in the y-z plane. Let us also assume that the transmit antenna is an infinitesimal dipole oriented along the x-axis. The electric field of an infinitesimal dipole oriented along the x-axis is given by (see Chapter 2, Exercise 2.17)

$$\mathbf{E} = -jk\eta \frac{I_0 dl}{4\pi} \frac{e^{-jkR}}{R} (\mathbf{a}_\theta \cos\theta \cos\phi - \mathbf{a}_\phi \sin\phi) \tag{8.3}$$

where R is the distance from the antenna to the field point. In the y-z plane, $\phi = 90°$. Since $\cos 90° = 0$, the θ-component of the electric field is zero. The ϕ-component of the electric field at Q due to the direct wave is given by

$$E_1 = jk\eta \frac{I_0 dl}{4\pi} \frac{e^{-jkR_1}}{R_1} \tag{8.4}$$

The field at Q also has a contribution from the wave that travels via the reflected path PXQ. The location of the point of reflection, X, depends on h_t, h_r, and d. At X the incident and the reflected rays satisfy Snell's law of reflection (i.e., the angle of incidence is equal to the angle of reflection). The incident ray PX, the reflected ray XQ, and the normal to the surface are all contained in the y-z plane. The y-z plane is also known as the plane of incidence. The incident field at X is given by

$$E_i = jk\eta \frac{I_0 dl}{4\pi} \frac{e^{-jkR_2'}}{R_2'} \tag{8.5}$$

where R_2' is the distance from the transmitter to X and the incident $\mathbf{E}$ field vector is perpendicular to the plane of incidence. At X, the reflection coefficient, $\Gamma_\perp$, which is the ratio of the reflected to the incident electric fields, is given by

$$\Gamma_\perp = \frac{E_r}{E_i} = \frac{\sin\psi - \sqrt{(\epsilon_r - j\chi) - \cos^2\psi}}{\sin\psi + \sqrt{(\epsilon_r - j\chi) - \cos^2\psi}} \tag{8.6}$$

The subscript $\perp$ indicates that the electric field is perpendicular to the plane of incidence (Fig. 8.2). The parameter χ is given by

$$\chi = \frac{\sigma}{\omega\epsilon_0} \tag{8.7}$$

where σ is the conductivity of the ground (in S/m), ω is the angular frequency (in rad/s), and ψ is the grazing angle of incidence. *Grazing angle*, ψ, is the angle of the incident wave with respect to the horizontal (Fig. 8.2).

The electric field at the receiver due the reflected wave is

$$E_2 = jk\eta\Gamma_\perp \frac{I_0 dl}{4\pi} \frac{e^{-jkR_2}}{R_2} \tag{8.8}$$

This is the field at Q due to an equivalent (image) dipole having a strength of $I_0 dl\Gamma_\perp$ located at $(0, 0, -h_t)$ (Fig. 8.1).

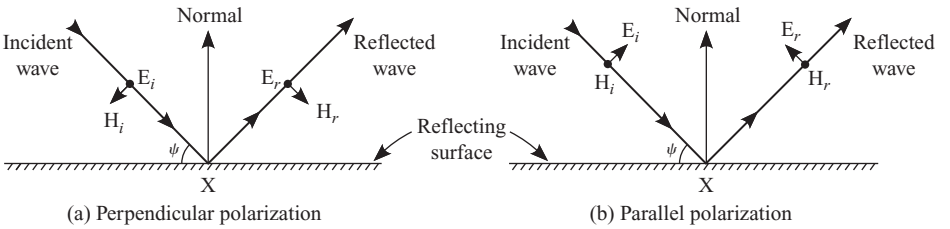

Fig. 8.2 Plane wave incident on a boundary

The total electric field at Q is given by

$$E = E_1 + E_2 = jk\eta \frac{I_0 dl}{4\pi} \left(\frac{e^{-jkR_1}}{R_1} + \Gamma_\perp \frac{e^{-jkR_2}}{R_2} \right) \tag{8.9}$$

If the field point Q is far away from the transmitter, we can use the approximation $R_2 \simeq R_1$ for R_1 and R_2 appearing in the denominator. Thus, the total electric field is given by

$$E = E_1 + E_2 = jk\eta \frac{I_0 dl}{4\pi} \frac{e^{-jkR_1}}{R_1} \left(1 + \Gamma_\perp e^{-jk(R_2 - R_1)} \right) \tag{8.10}$$

This can be thought of as a product of the free-space field and an environmental factor, $F_\perp$, given by

$$F_\perp = \left(1 + \Gamma_\perp e^{-jk(R_2 - R_1)} \right) \tag{8.11}$$

Let us now derive an expression for the total field at Q due to an infinitesimal dipole at $(0, 0, h_t)$ oriented along the z-direction. The electric field of a z-directed infinitesimal dipole is

$$\mathbf{E} = \mathbf{a}_\theta j\eta \frac{k I_0 dl \sin\theta}{4\pi} \frac{e^{-jkR_1}}{R_1} \tag{8.12}$$

where R_1 is the distance from the antenna to the field point. The electric field is parallel to the plane of incidence and the reflection coefficient, $\Gamma_\parallel$, at X is given by

$$\Gamma_\parallel = \frac{(\epsilon_r - j\chi)\sin\psi - \sqrt{(\epsilon_r - j\chi) - \cos^2\psi}}{(\epsilon_r - j\chi)\sin\psi + \sqrt{(\epsilon_r - j\chi) - \cos^2\psi}} \tag{8.13}$$

where χ is given by Eqn (8.7). The total field at point Q is given by

$$E = jk\eta \frac{I_0 dl}{4\pi} \frac{e^{-jkR_1}}{R_1} F_{\parallel} \tag{8.14}$$

where

$$F_{\parallel} = \left(1 + \Gamma_{\parallel} e^{-jk(R_2 - R_1)}\right) \tag{8.15}$$

From Fig. 8.1

$$R_1 = \sqrt{d^2 + (h_r - h_t)^2} = d\sqrt{1 + \left(\frac{h_r - h_t}{d}\right)^2} \tag{8.16}$$

For $d \gg h_r$ and $d \gg h_t$, using the first two significant terms in the binomial expansion of $\sqrt{1+x}$

$$\sqrt{(1+x)} \simeq 1 + \frac{x}{2} \quad \text{for } x \ll 1 \tag{8.17}$$

we can write

$$R_1 \simeq d\left[1 + \frac{1}{2}\left(\frac{h_r - h_t}{d}\right)^2\right] \tag{8.18}$$

Similarly, R_2 can be approximated to

$$R_2 \simeq d\left[1 + \frac{1}{2}\left(\frac{h_r + h_t}{d}\right)^2\right] \tag{8.19}$$

The path difference, $R_2 - R_1$, is given as

$$R_2 - R_1 = \frac{2h_r h_t}{d} \tag{8.20}$$

For $(h_t h_r / d) \ll \lambda$

$$\Delta\theta = k(R_2 - R_1) = \frac{4\pi h_r h_t}{d\lambda} \tag{8.21}$$

is small so that $\sin x \simeq x$ and $\cos x \simeq 1$, and we can write

$$e^{-jk(R_2 - R_1)} = \cos(\Delta\theta) - j\sin(\Delta\theta) \simeq 1 - j\frac{2kh_r h_t}{d} \tag{8.22}$$

For low angles of incidence, from Eqns (8.6) and (8.13)

$$\Gamma_{\perp} \simeq \Gamma_{\parallel} \simeq -1 \tag{8.23}$$

and hence we can set

$$F = F_{\perp} = F_{\parallel} \simeq j\frac{2kh_r h_t}{d} \tag{8.24}$$

Taking into account the ground reflection, the power received by the receive antenna can be written as

$$P_r = P_t G_t G_r \left(\frac{\lambda}{4\pi R_1}\right)^2 |F|^2 \tag{8.25}$$

For h_r and h_t small compared to d, from Eqn (8.18)

$$R_1 \simeq d \tag{8.26}$$

Therefore, the received power is approximately given by

$$P_r \simeq \frac{P_t G_t G_r (h_r h_t)^2}{d^4} \tag{8.27}$$

For large d, the received power decreases as d^4. This rate of change of power with distance is much faster than that observed in the free space propagation condition.

8.1.3 Surface Waves

The electric field due to a vertically-oriented dipole placed above the ground is given by Eqn (8.14). If both the dipole and the field points are on the surface of the earth but separated by the distance d, we have $R_2 = R_1 = d$ and $\psi = 0$. If the ground has finite conductivity (typically from 10^{-3} S/m to 30×10^{-3} S/m), we have from Eqn (8.13), $\Gamma_{\parallel} = -1$ and hence the electric fields due to the dipole and its image cancel with each other. The total electric field due to the direct and the ground-reflected waves, also known as the *space wave* is zero on the surface of the ground. In such a situation, the waves can propagate as *surface waves*. Surface waves constitute the primary mode of propagation for frequencies in the range of a few kilohertz to several megahertz. For example, in the AM broadcast application, a vertical monopole above the ground is used to radiate power in the MW frequency band. The receivers are generally placed very close to the surface of the earth

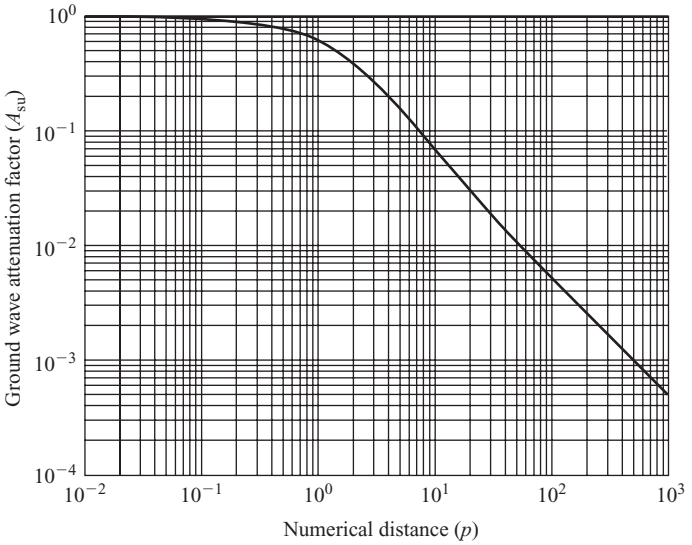

Fig. 8.3 Ground wave attenuation factor as a function of numerical distance

and hence they receive the broadcast signals via surface waves. Using the surface wave mode, it is possible to achieve useful propagation over several hundred kilometres (Collin 1985).

The attenuation factor of the surface wave depends on the distance between the transmitter and the receiver, the frequency and the electrical properties of the ground (relative permittivity, ϵ_r, and conductivity, σ) over which the wave is propagating. At the surface of the earth, the attenuation factor is also known as the *ground wave attenuation factor* and is designated by A_{su}. A plot of A_{su} as a function of the numerical distance, p, is shown in Fig. 8.3 for the power factor angle, $b = 0°$. The numerical distance, p, and the power factor angle, b, are given by

$$p = \frac{\pi R}{\lambda \chi} \cos b \tag{8.28}$$

$$b = \tan^{-1}\left(\frac{\epsilon_r + 1}{\chi}\right) \tag{8.29}$$

where R is the distance between the transmit and the receive antennas and χ is given as

$$\chi = \frac{\sigma}{\omega \epsilon_0} \tag{8.30}$$

For $\chi \gg \epsilon_r$, the power factor angle is nearly zero and the ground is mostly resistive. This is generally the case for the MW frequencies. For example, for a 1 MHz wave propagating over a ground surface with $\sigma = 12 \times 10^{-3}$ S/m and $\epsilon_r = 15$, the value of χ is 215.7 and is much greater than ϵ_r. The power factor angle is 4.24°. However, at a higher frequency, say 100 MHz, the value of χ is 2.157 and the power factor angle becomes 82.32°.

For large numerical distances, the attenuation factor decreases by a factor of 10 for every decade i.e., 20 dB/decade. Thus, the attenuation factor is inversely proportional to p. Since the numerical distance is proportional to R, the attenuation factor is also inversely proportional to R.

The electric field intensity due to the surface wave is proportional to the product of A_{su} and (e^{-jkR}/R). Thus the electric field intensity due to the surface wave at large distances from a vertically polarized antenna is inversely proportional to the square of the distance or the power is inversely proportional to R^4.

The electric field of a vertically polarized wave near the surface of the earth will have a forward tilt. The magnitude of the wave tilt depends on the conductivity and the permittivity of the earth. In general the horizontal component is much smaller than the vertical component and they are not in phase. Thus, the electric field is elliptically polarized very close to the surface of the earth.

8.1.4 Diffraction

The bending of the path of electromagnetic waves around sharp edges and corners of obstacles appearing in their path is known as *diffraction*. Diffraction allows the signals to propagate in regions that lie behind the obstructions. If the receiver is placed behind an obstruction such that the line-of-sight path is completely obstructed, the diffracted field may still have sufficient strength at the receiver location to establish a communication link. In the obstructed or the shadow region the strength of the received signal depends on the position of the receiver as well as the geometrical shape of the obstruction.

Calculating the strength of the diffracted field of a complex and irregular object is, mathematically, a difficult task. However, the calculation can be simplified by approximating the given terrain in terms of regular geometries. This procedure gives a fairly accurate prediction of the diffracted fields. For example, if the shadowing is caused by a single hill or a mountain, a knife-edge diffraction model is used to compute the diffracted field [Fig. 8.4(a)].

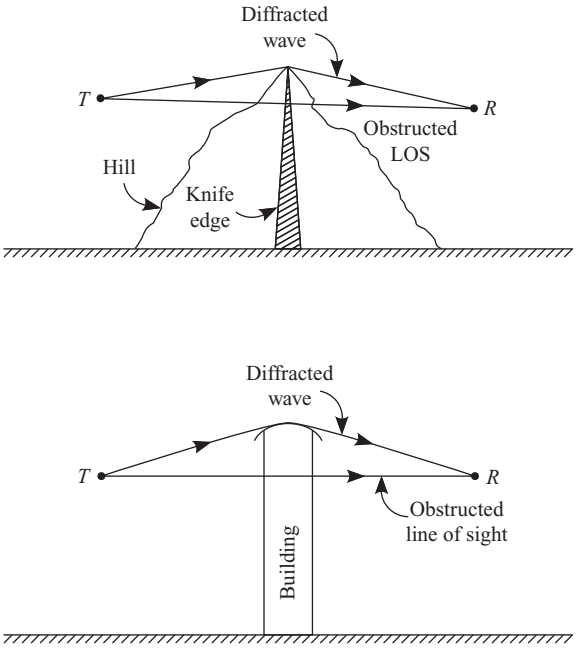

Fig. 8.4 (a) Knife-edge and (b) rounded-surface diffraction models

If the obstructing object is a building, a rounded-surface diffraction model is more appropriate [Fig. 8.4(b)].

In this section we will study some aspects of knife-edge diffraction without going into detailed derivations. Interested readers can refer to the published literature for the procedure (Jordan et al 2004).

Let a thin obstacle block the line-of-sight path between the transmitter T and the receiver R as shown in Fig. 8.5. For this analysis, it is assumed that the knife-edge obstacle extends to infinity into and out of the plane of the paper. The obstacle is placed at a distance d_1 from the transmitter and d_2 from the receiver. The tip of the obstacle is at a height h from the line-of-sight path. Let us also assume that $d_1 \gg h$ and $d_2 \gg h$.

It can be shown that the field strength at the receiver is given by

$$E = E_0\left(\frac{1+j}{2}\right)\int_{\nu_d}^{\infty} e^{-j\frac{\pi}{2}t^2}dt^2 \tag{8.31}$$

where E_0 is the free-space field strength in the absence of the knife edge and the ground (Jordan et al 2004). The parameter ν_d is known as the

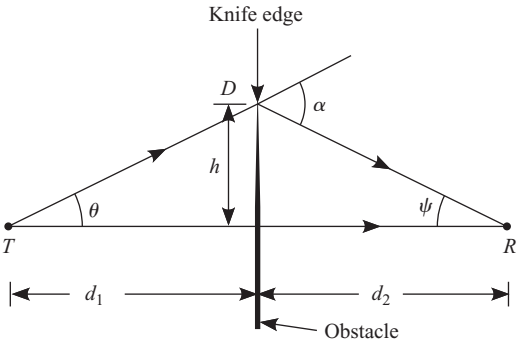

Fig. 8.5 Diffraction of electromagnetic waves by a knife edge

Fresnel–Kirchhoff diffraction parameter and is given by

$$\nu_d = h\sqrt{\frac{2(d_1 + d_2)}{d_1 d_2 \lambda}} \tag{8.32}$$

ν_d is directly proportional to height, h. The integral in Eqn (8.31) is known as the Fresnel integral and is usually evaluated using tables, graphs, or numerical methods for a given value of ν_d. The knife-edge diffraction gain is defined by

$$F_d = 20\log_{10}\left(\frac{E}{E_0}\right) \text{ dB} \tag{8.33}$$

The diffraction gain varies as a function of ν_d as shown in Fig. 8.6. For $\nu_d = 0$, which corresponds to $h = 0$, the tip of the knife edge touches the direct line-of-sight path between the transmitter and the receiver and the diffracted signal is 6 dB below that of the free-space signal. For $\nu_d > 0$, the knife edge blocks the line-of-sight path ($h > 0$) and the diffraction gain decreases monotonically. For $\nu_d < 0$, the signal at the receiver can be larger than the free space signal for certain values of ν_d. For example, the knife-edge diffraction gain is 1.37 dB for $\nu_d = -1.22$. As ν_d decreases further, the diffraction gain oscillates about 0 dB. Very small values of ν_d correspond to the situation where the knife edge is far away from the line-of-sight propagation path. Therefore, the knife-edge diffraction gain is 0 dB.

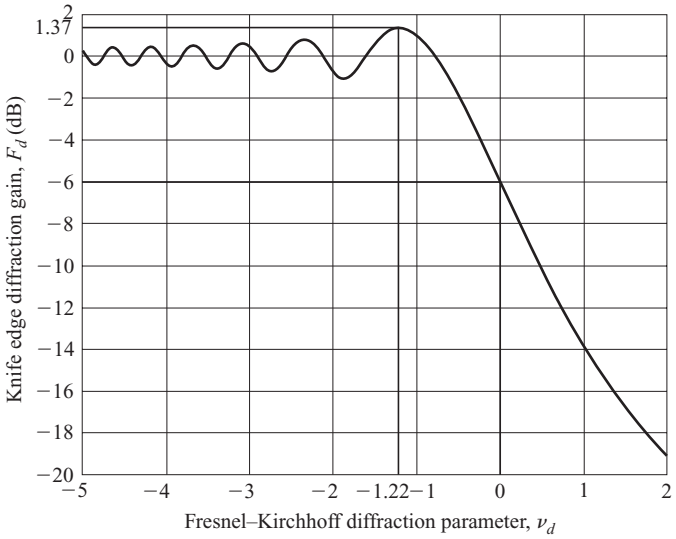

Fig. 8.6 Diffraction gain of a knife-edge obstacle

EXAMPLE 8.2

A transmit and a receive antenna are separated by a distance of 100λ. A knife-edge obstacle located exactly mid-way between the two antennas is obstructing the line-of-sight propagation path. What should be the distance between the tip of the obstacle and and the line-of-sight path so that the knife-edge diffraction gain is 1.37 dB.

Solution: Since the obstacle is located mid-way between the two antennas, $d_1 = d_2$ and Eqn (8.32) reduces to

$$\nu_d = h\sqrt{\frac{4}{d_1\lambda}} = \frac{h}{5\lambda} \tag{8.2.1}$$

for $d_1 = 100\lambda$. From Fig. 8.6, the knife-edge diffraction gain of 1.37 dB is obtained for $\nu_d = -1.22$. Substituting this into Eqn (8.2.1) and simplifying we get $h = -6.10\lambda$. Therefore, the tip of the obstacle is 6.10λ below the line-of-sight path.

8.1.5 Wave Propagation in Complex Environments

In a complex environment consisting of built-up structures, trees, lamp posts, vehicles, etc., the propagation of electromagnetic waves can take

place via the line-of-sight, reflected, diffracted, or scattered paths. Such a situation is generally encountered in mobile phone and wireless local area network applications. Computational tools such as the ray-tracing method (Rossi et al 1991, Schaubach et al 1992) and the finite-difference time domain method (Taflov 2000) have been used to predict the propagation of electromagnetic waves in a complex environment. These are specific tools that involve considerable computational effort to predict the propagation characteristics and need accurate electrical characteristics (conductivity and dielectric constant) and physical dimensions of the environment as inputs. Since it is generally difficult to obtain accurate electrical properties of the environment, the accuracy of the final prediction using these methods is limited.

Researchers have come up with empirical models to predict the propagation in complex environments. These models are based on extensive measurements carried out in the corresponding environments. These models are also known as *path-loss* models as they provide an estimate for the path loss between the transmitter and the receiver.

In free space, the path loss at a reference distance R_0 from the transmitter is [from Eqn (8.2)]

$$P_L(R_0) = 10\log_{10}\left[\left(\frac{4\pi R_0}{\lambda}\right)^2\right] \text{ dB} \tag{8.34}$$

The path loss at any other distance R can be expressed as

$$P_L(R) = 10\log_{10}\left[\left(\frac{4\pi R_0}{\lambda}\right)^2\left(\frac{R}{R_0}\right)^2\right] \text{ dB} \tag{8.35}$$

$$= P_L(R_0) + 10\log_{10}\left[\left(\frac{R}{R_0}\right)^2\right] \text{ dB} \tag{8.36}$$

Log-distance path loss model Equation (8.34) suggests that the path loss in free space conditions is proportional to the square of the distance between the transmitter and the receiver. However, for an arbitrary medium, the path loss can be expressed as the logarithm of the nth power of the distance between the transmitter and the receiver. This is known as the log–distance path loss model. If $P_{Ln}(R_0)$ is the path loss at a distance R_0 from the transmitter, the path loss at any distance R, $(R > R_0)$, can be

expressed as

$$P_{Ln}(R) = P_{Ln}(R_0) + 10\log_{10}\left(\frac{R}{R_0}\right)^n \quad \text{dB} \tag{8.37}$$

where n is known as the path loss exponent. This is obtained by replacing $P_L(R_0)$ by $P_{Ln}(R_0)$ and changing the power from 2 to n. The value of n depends on the environment. For example, at 900 MHz, n is in the range of 2.7 to 3.5 for an urban environment, and 4 to 6 in the case of obstructed buildings. These are typical values encountered in mobile phone network applications. In Section 8.1.2 we have seen that if the distance between the transmit and the receive antenna is very large compared to their heights, the path loss exponent is equal to 4 in the presence of ground-reflected waves.

The path loss, $P_{Ln}(R_0)$, is usually obtained by measurements. The reference distance, R_0, is chosen such that the receiver and the transmitter antennas are in the far-fields of each other.

EXAMPLE 8.3

A mobile base station antenna is radiating electromagnetic waves at 850 MHz in an urban environment which is characterized by a path loss exponent 3.5. The path loss is measured to be 85 dB at a distance of 500 m from the transmitter. Calculate the path loss at a distance 2 km in the same direction. If the base station antenna is radiating 100 W, calculate the distance at which the received power is −80 dBm. Assume the base station antenna gain to be 15 dB and the mobile phone antenna gain to be 1 dB.

Solution: Substituting $P_{Ln}(R_0) = 85$ dB, $n = 3.5$, $R_0 = 500$ m, and $R = 2000$ m in Eqn (8.37), we get the path loss at $R = 2$ km as

$$P_{Ln}(R) = 85 + 10\log_{10}\left(\frac{2000}{500}\right)^{3.5} = 106 \text{ dB}$$

The received power is given by

$$P_{r\text{dBm}} = P_{t\text{dBm}} + G_{t\text{dB}} + G_{r\text{dB}} - P_{Ln}(R)$$

Substituting, $P_r = -80$ dBm, $P_t = 100$ W $= 50$ dBm, $G_t = 15$ dB, and $G_r = 1$ dB, we get the path loss between the transmit and the receive antennas

as $P_{Ln}(R) = 146$ dB. Substituting these values in Eqn (8.37)

$$P_{Ln}(R) = P_{Ln}(R_0) + 10\log_{10}\left(\frac{R}{R_0}\right)^n \quad \text{dB}$$

$$146 = 85 + 10\log_{10}\left(\frac{R}{500}\right)^{3.5}$$

Solving for R, we get $R = 27.7$ km.

Okumura, Hata, and COST-231 models The log-distance path loss model is not accurate enough to predict the received power in urban areas. Based on extensive measurements, Okumura developed a set of curves for computing the attenuation relative to the free space attenuation in an urban environment (Rappaport 2002, Seybold 2005). These curves are based on the measurements carried out using a transmit antenna placed at a height of 200 m and the receive antenna at a height of 3 m from the surface. These are valid over a frequency range of 100–3000 MHz and for a distance between the transmit and the receive antenna ranging from 1 km to 100 km.

Based on the measured path loss data of Okumura, Hata published a formula for computing the path loss in an urban environment (Hata 1990)

$$\begin{aligned} P_{Lu} = {} & 69.55 + 26.16\log_{10} f - 13.82\log_{10} h_{te} - \alpha(h_{re}) \\ & + (44.9 - 6.55\log_{10} h_{te})\log_{10} d \quad \text{dB} \end{aligned} \tag{8.38}$$

where f is the frequency in MHz ranging from 150 MHz to 1500 MHz. h_{te} and h_{re} are the effective heights of the transmit and the receive antennas in metres. The effective height of the antenna indicates its vertical position from the mean ground level. The effective height of the transmit antenna can be in the range of 30–200 m and that of the receive antenna in the range of 1–10 m. The horizontal distance, d, between the transmitter and the receiver is in km. Equation (8.38) is valid for values of d between 1 km and 20 km. The parameter $\alpha(h_{re})$ represents the environmental correction factor for the effective height of the receive antenna. For a small- to medium-sized city, the correction factor is given by

$$\alpha(h_{re}) = (1.1\log_{10} f - 0.7)h_{re} - (1.56\log_{10} f - 0.8) \quad \text{dB} \tag{8.39}$$

and for a large city it is given by the following equations

$$\alpha(h_{re}) = 8.29[\log_{10}(1.54h_{re})]^2 - 1.1 \quad \text{dB} \quad \text{for } f \leq 300 \text{ MHz} \tag{8.40}$$

$$\alpha(h_{re}) = 3.2[\log_{10}(11.75h_{re})]^2 - 4.97 \quad \text{dB} \quad \text{for } f \geq 300 \text{ MHz} \tag{8.41}$$

The path loss in a suburban area can be computed by the following equation

$$P_{L\text{su}} = P_{L\text{u}} - 2[\log_{10}(f/28)]^2 - 5.4 \text{ dB} \tag{8.42}$$

and for the open rural areas, the path loss is given by

$$P_{L\text{ru}} = P_{L\text{u}} - 4.78(\log_{10} f)^2 + 18.33 \log_{10} f - 40.94 \text{ dB} \tag{8.43}$$

where $P_{L\text{u}}$ is the path loss for the urban environment given by Eqn (8.38).

The European Co-operative for Scientific and Technical Research (EURO-COST) formed a working committee called COST-231, which extended the Hata model to 2 GHz. The COST-231 model, which is valid between 1500 MHz and 2000 MHz, is given by

$$\begin{aligned} P_{Lu} = {} & 46.3 + 33.9 \log_{10} f - 13.82 \log_{10} h_{te} - \alpha(h_{re}) \\ & + [44.9 - 6.55 \log_{10} h_{te}] \log_{10} d + C_M \end{aligned} \tag{8.44}$$

The parameters h_{te}, h_{re}, f, and d, including the validity range, are as specified for the Hata model (Eqn 8.38). For a medium-sized city and suburban areas C_M is 0 dB and it is 3 dB for metropolitan areas.

8.1.6 Tropospheric Propagation

In all previous calculations, it was assumed that the relative dielectric constant of the air is equal to unity. It has been observed that in the troposphere, the relative dielectric constant is slightly higher than unity due to the presence of the atmosphere and, in particular, water vapour. The tropospheric region extends from the surface of the earth to a height of about 6 km at the poles and 18 km at the equator. The relative dielectric constant is a function of the temperature, pressure, and humidity (or water vapour pressure). The typical value of ϵ_r at the surface of the earth is found to be 1.000579 (Griffiths 1987). The value decreases as a function of height above the surface of the earth.

We know that the velocity of the electromagnetic wave in a medium depends on the dielectric constant of the medium.

$$v = \frac{c}{\sqrt{\epsilon_r}} = \frac{c}{n} \tag{8.45}$$

where c is the velocity in vacuum and $n = \sqrt{\epsilon_r}$ is the refractive index of the medium. At the surface of the earth (mean sea level), the refractive index of air is 1.000289. Therefore, it is common practice to work with a parameter known as the *refractivity*, N. The refractivity is related to refractive index by the following equation.

$$N = (n - 1) \times 10^6 \tag{8.46}$$

Thus, at the surface of the earth, the refractivity is equal to 289. For a standard atmosphere, the refractivity falls off linearly up to a height of 2 km above the surface of the earth and is expressed by the following equation

$$N = 289 - 39h \tag{8.47}$$

where h is the height in km. This is known as the *standard atmosphere* or *normal atmosphere*. The refractive index of the standard atmosphere is given by

$$n = 1 + (289 - 39h) \times 10^{-6} \tag{8.48}$$

Let us now derive an equation for the path of a wave propagating in a medium wherein the refractive index is a continuous function of height. For this derivation, let us assume that the earth is flat and the troposphere is made up of stratified layers parallel to the surface of the earth, i.e., the refractive index is a function of height only. Let the refractive index be a constant within each layer. Consider a layer that has a height dh with refractive index $(n + dn)$ (Fig. 8.7). A ray incident from the lower layer at point P is refracted through the layer dh and touches the upper layer at point Q. Let θ be the angle of incidence with the normal drawn to the plane at P and $(\theta + d\theta)$ be the angle of refraction at P. In order to calculate the radius of curvature, r, of the ray, draw angle bisectors at P and Q. Let them meet each other at O. From the inset in Fig. 8.7

$$\angle APQ = \pi - d\theta \tag{8.49}$$

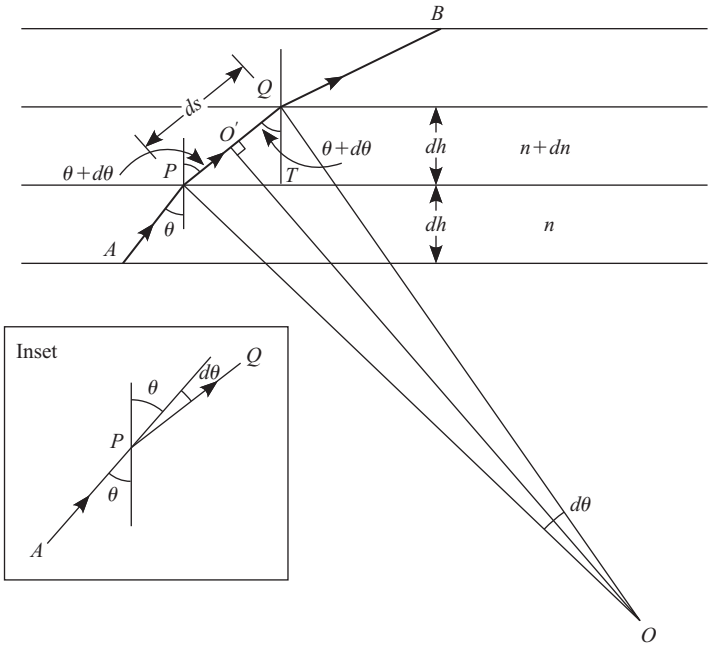

Fig. 8.7 Wave propagation in a stratified medium

Since OP bisects $\angle APQ$

$$\angle OPQ = \frac{1}{2}\angle APQ = \frac{\pi}{2} - \frac{d\theta}{2} \tag{8.50}$$

Draw OO' perpendicular to PQ. In $\triangle POO'$

$$\angle POO' = \frac{\pi}{2} - \angle OPQ = \frac{d\theta}{2} \tag{8.51}$$

The angle subtended by the segment ds at O is

$$\angle POQ = 2\angle POO' = d\theta \tag{8.52}$$

and hence the length ds is given by

$$ds = rd\theta \tag{8.53}$$

From $\triangle PQT$

$$ds = \frac{dh}{\cos(\theta + d\theta)} \simeq \frac{dh}{\cos\theta} \quad \text{for small } d\theta \tag{8.54}$$

Substituting the value of ds from Eqn (8.54) into Eqn (8.53)

$$r = \frac{ds}{d\theta} = \frac{dh}{\cos\theta d\theta} \tag{8.55}$$

The law of refraction can now be applied to the two points P and Q.

$$n\sin\theta = (n + dn)\sin(\theta + d\theta) \tag{8.56}$$

Expanding the right hand side

$$n\sin\theta = (n + dn)(\sin\theta\cos d\theta + \cos\theta\sin d\theta)$$

For small $d\theta$, $\cos d\theta \simeq 1$ and $\sin d\theta \simeq d\theta$. Introducing these approximations and expanding

$$n\sin\theta = n\sin\theta + n\cos\theta d\theta + dn\sin\theta + dn\cos\theta d\theta$$

Ignoring the last term on the right hand side as it is a product of two infinitesimals

$$n\sin\theta \simeq n\sin\theta + n\cos\theta d\theta + dn\sin\theta \tag{8.57}$$

which can be written as

$$\cos\theta d\theta = -\frac{\sin\theta dn}{n} \tag{8.58}$$

Substituting this in Eqn (8.55)

$$r = \frac{dh}{-\sin\theta\dfrac{dn}{n}} = \frac{n}{\sin\theta\left(-\dfrac{dn}{dh}\right)} \tag{8.59}$$

The radius of curvature can also be written in terms of the grazing angle, ϕ. This is the angle that the ray makes with the horizontal and is related to θ by the equation

$$\theta = \frac{\pi}{2} - \phi \tag{8.60}$$

The radius of curvature can be written in terms of ϕ as

$$r = \frac{n}{\cos\phi\left(-\dfrac{dn}{dh}\right)} \tag{8.61}$$

Consider a ray launched with a low grazing angle, ($\phi \simeq 0$), for which $\cos\phi \simeq 1$. Since the refractive index is also very close to unity, the radius of curvature reduces to

$$r = \frac{1}{-\dfrac{dn}{dh}} \tag{8.62}$$

We can express the radius of curvature in terms of the refractivity gradient, dN/dh, as

$$r = \frac{10^6}{-\dfrac{dN}{dh}} \tag{8.63}$$

If this ray is propagating in the standard atmosphere described by the refractivity profile given by Eqn (8.47), we have

$$\frac{dN}{dh} = -39 \text{ per km} \tag{8.64}$$

and the radius of curvature of the ray path is

$$r = \frac{1}{39 \times 10^{-6}} = 25641 \text{ km} \tag{8.65}$$

The ray droops towards the surface of the earth. If the refractivity does not change with the height, that is, $dN/dh = 0$, the radio wave does not undergo refraction hence it follows a straight line path.

Figure 8.8 depicts the propagation of a radio wave launched at low grazing angles for various values of refractivity gradients (dN/dh). If the refractivity gradient is between 39/km and 0, the refraction of the electromagnetic wave is lower than that in the standard atmosphere and is known as *sub-refraction*. If the refractivity slope is less than that of the standard atmosphere, i.e., $dN/dh < -39$/km, the wave is refracted more than that in a standard atmosphere and is known as *super refraction*. For $dN/dh = -157$/km, the

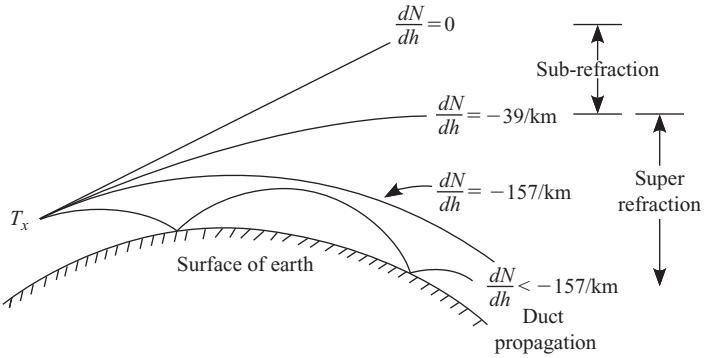

Fig. 8.8 Wave propagation through a stratified medium above the spherical earth

radius of curvature of the ray is

$$r = \frac{1}{157 \times 10^{-6}} \simeq 6370\,\text{km} \tag{8.66}$$

which is equal to the radius of the earth, and hence a horizontally incident wave travels parallel to the surface of the earth. If $dN/dh < -157$/km, the radius of curvature of the ray is smaller than the radius of the earth. The ray can, therefore, touch the surface of the earth and get reflected from the surface. This is known as *tropospheric duct propagation*. The regions corresponding to sub-refraction, super refraction, and duct propagation are shown in Fig. 8.9 on an N–h plot.

On a spherical earth, the maximum possible direct wave communication distance depends on the heights of the transmit and the receive antennas as well as the atmospheric conditions. For propagation calculations, a mean value of $r_0 = 6370$ km is chosen to be the radius of the earth. With $dN/dh = 0$, the radio waves travel along straight lines. Therefore, the maximum range is obtained when the straight line joining the two antennas grazes the surface of the earth (Fig. 8.10).

In $\triangle AOC$, the distance between the transmit antenna and the point of contact on the surface of the earth is given by

$$R_1^2 = (r_0 + h_t)^2 - r_0^2 = 2r_0h_t + h_t^2 \tag{8.67}$$

Since $r_0 \gg h_t$, R_1^2 is approximately given by

$$R_1^2 \simeq 2r_0h_t \tag{8.68}$$

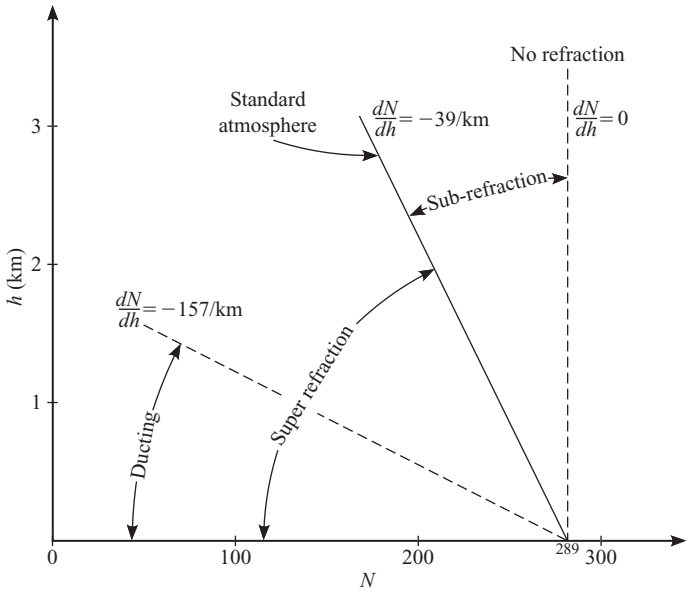

Fig. 8.9 Depiction of regions of super refraction, sub-refraction, and duct propagation on an N-h plot

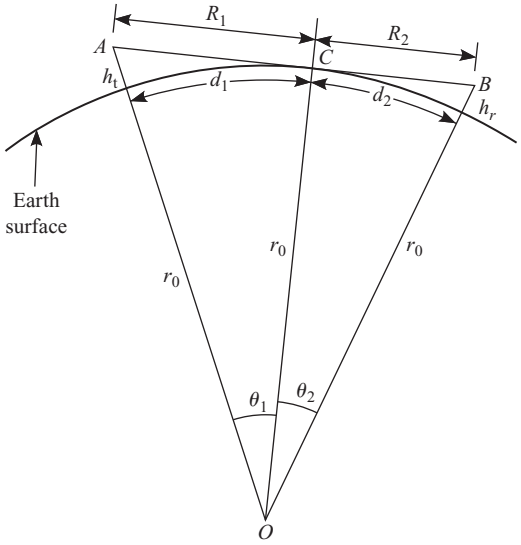

Fig. 8.10 Propagation path of radio waves over the surface of the earth with $dN/dh = 0$

Similarly from $\triangle BOC$, we get $R_2^2 \simeq 2r_0h_r$. Therefore, the line-of-sight distance between the transmit and the receive antennas is given by

$$R = R_1 + R_2 = \sqrt{2r_0}(\sqrt{h_t} + \sqrt{h_r}) \tag{8.69}$$

EXAMPLE 8.4

A line-of-sight 10 GHz microwave link is to be established on the surface of the earth (mean radius 6370 km). The straight line distance between the two antennas is 60 km and the height of the transmit antenna is 60 m. Calculate the minimum height of the receive antenna assuming that the propagation is taking place in the absence of atmosphere.

Solution: Substituting $R = 60 \times 10^3$ m, $r_0 = 6370 \times 10^3$ m, and $h_t = 60$ m in Eqn. (8.69)

$$R = \sqrt{2r_0}(\sqrt{h_t} + \sqrt{h_r})$$
$$60 \times 10^3 = \sqrt{2 \times 6370 \times 10^3}(\sqrt{60} + \sqrt{h_r})$$

we get the minimum height of the receiver as $h_r = 82.2$ m.

Let us now consider the propagation of radio waves under standard atmospheric conditions ($dN/dh = -39$/km). A horizontally launched ray from the surface of the earth follows a curved path with a radius of curvature r. If we subtract the curvature $(1/r)$ of the ray from the curvature of the earth $(1/r_0)$, we get the curvature of the equivalent ground, on which the wave can be considered to be travelling along a straight line path. If r_e is the equivalent radius of the earth, we can write

$$\frac{1}{r_e} = \frac{1}{r_0} - \frac{1}{r} \tag{8.70}$$

Multiplying both the sides by r_0 and rearranging

$$\frac{r_e}{r_0} = \frac{1}{1 - \dfrac{r_0}{r}} \tag{8.71}$$

Substituting $r_0 = 6370$ km and $r = 25641$ km [Eqn (8.65)], the equivalent radius is

$$r_e = \frac{4}{3}r_0 \tag{8.72}$$

The concept of equivalent radius of the earth simplifies the computation of the height of the propagating radio wave path as a function of distance. The ray path can now be taken as a straight line and the earth having a radius $(4/3)r_0$. For example, a horizontally launched ray in a standard atmosphere will have a height

$$h \simeq \frac{d^2}{2r_e} = \frac{3d^2}{8r_0} \tag{8.73}$$

at a distance, d, from the launch point on the earth's surface. The standard atmosphere is valid up to a height of 2 km from the surface of the earth.

Modified refractive index In the preceding text, it was shown that by choosing an equivalent radius for the earth, the ray path in the standard atmosphere can be considered to be a straight line. An alternative approach is to alter the curvature of the ray path so that the earth may be considered as flat. This is achieved by assuming that the electromagnetic wave is propagating in a medium with a modified refractive index, n^*, which is assumed to exist over a flat surface. The modified refractive index is related to the modified refractivity, M, by the following equation

$$M = (n^* - 1) \times 10^6 \tag{8.74}$$

Consider the troposphere shown in Fig. 8.11, consisting of an atmosphere with layers of height dh and refractive indices n_0, n_1, n_2, etc. An electromagnetic wave is radiated from point A on the surface of the earth, at a grazing angle of ψ_0. Let this wave propagate through the first layer having a refractive index of n_0 and reach the boundary between the first and the second layers at B. The angle of incidence at B is θ_{i0}, which is measured from the normal to the interface at B. The wave gets refracted at the interface and propagates into the medium with the refractive index of n_1. This ray path makes an angle of θ_{r1} with respect to the normal or ψ_1 with respect to the tangent to the interface at B. ψ_1 is related to θ_{r1} by the relation

$$\psi_1 = \frac{\pi}{2} - \theta_{r1} \tag{8.75}$$

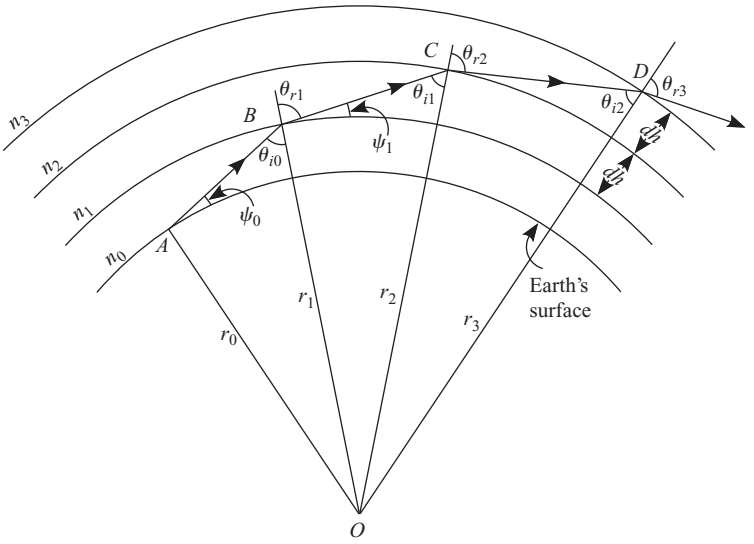

Fig. 8.11 Refraction by spherical troposphere

From $\triangle BOC$

$$\frac{\sin\theta_{i1}}{r_1} = \frac{\sin(\pi - \theta_{r1})}{r_2} \tag{8.76}$$

which can be written as

$$r_2 \sin\theta_{i1} = r_1 \sin\theta_{r1} \tag{8.77}$$

At point C, Snell's law gives

$$n_1 \sin\theta_{i1} = n_2 \sin\theta_{r2} \tag{8.78}$$

Substituting the value of $\sin\theta_{i1}$ from Eqn (8.78) into Eqn (8.77)

$$r_1 n_1 \sin\theta_{r1} = r_2 n_2 \sin\theta_{r2} \tag{8.79}$$

Similarly applying Snell's law at point D, we can show that

$$r_2 n_2 \sin\theta_{r2} = r_3 n_3 \sin\theta_{r3} \tag{8.80}$$

where r_3, n_3, and θ_{r3} are as shown in Fig. 8.11. Combining the previous two equations

$$r_1 n_1 \sin\theta_{r1} = r_2 n_2 \sin\theta_{r2} = r_3 n_3 \sin\theta_{r3} = \text{const} \tag{8.81}$$

which can be written in terms of the grazing angle ψ as

$$r_1 n_1 \cos\psi_1 = r_2 n_2 \cos\psi_2 = \text{const} \tag{8.82}$$

This represents Snell's law for a spherically stratified medium.

Equation (8.82) indicates that this law can be applied to any two arbitrary points. Consider an arbitrary point at a height h from the surface of the earth. Let n be the refractive index and ψ be grazing angle at this point. Applying Snell's law [Eqn (8.82)] between point A and the chosen arbitrary point, we get

$$r_0 n_0 \cos\psi_0 = (r_0 + h) n \cos\psi \tag{8.83}$$

This can be simplified to

$$n_0 \cos\psi_0 = \left\{ n\left(1 + \frac{h}{r_0}\right) \right\} \cos\psi = n^* \cos\psi \tag{8.84}$$

This represents the Snell's law for a plane stratified medium if the medium has an equivalent refractive index of n^* given by

$$n^* = n\left(1 + \frac{h}{r_0}\right) \tag{8.85}$$

Since n is very close to unity

$$n^* \simeq n + \frac{h}{r_0} \tag{8.86}$$

For the standard atmosphere the refractive index profile is given by Eqn (8.48). Substituting the value of n in Eqn (8.86), n^* is given by

$$n^* = 1 + (289 + 118h) \times 10^{-6} \tag{8.87}$$

and the modified refractivity can be expressed in terms of h as

$$M = 289 + 118h \tag{8.88}$$

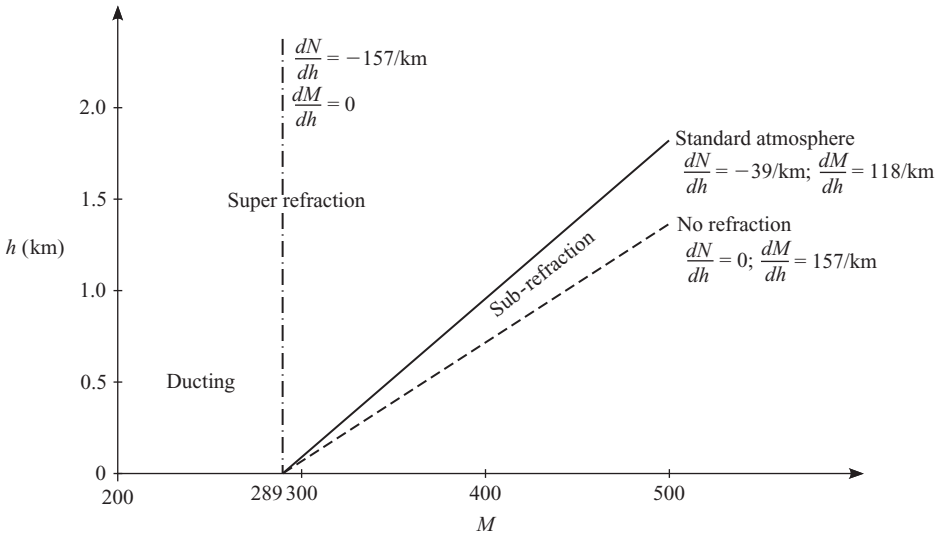

Fig. 8.12 Depiction of regions of super refraction, sub-refraction, and duct propagation on an M–h plot

where the height h from the surface of the earth is measured in kilometers. The variation of the modified refractivity with height is shown in Fig. 8.12 by the solid line.

In an environment with $dN/dh = 0$, we have $N = 289$ or $n = 1 + 289 \times 10^{-6}$. Thus, the modified refractive index is given by

$$n^* = 1 + (289 + 157h) \times 10^{-6} \tag{8.89}$$

and the modified refractivity reduces to

$$M = 289 + 157h \tag{8.90}$$

This corresponds to a straight line of slope 157/km and is shown by the dashed line in Fig. 8.12. The region between these two lines corresponds to sub-refraction. If the slope of the modified refractivity is less than 118/km, the modified refractivity line will be to the left of the line corresponding to the standard atmosphere and in such an environment, the wave undergoes super refraction. For the atmosphere with $dN/dh = -157$/km, the gradient of the modified refractivity $dM/dh = 0$ and the modified refractivity curve is a vertical line. Duct propagation is observed if the gradient of the modified refractivity is less than zero.

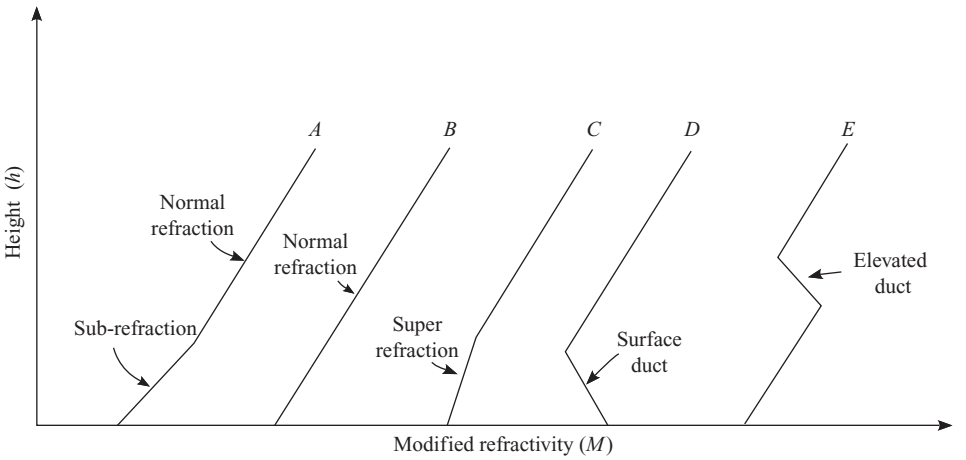

Fig. 8.13 Several possible refractivity profiles

The gradient of the modified refractivity can change with height. This can result in different modes of propagation in the troposphere. Several possibilities are shown in Fig. 8.13. In the troposphere having the profile A, electromagnetic waves undergo sub-refraction near the surface of the earth and normal refraction at greater heights. Profile B corresponds to a normal atmosphere and, hence, normal refraction is observed. In profile C, the gradient of M is less than 118/km near the surface of the earth and it corresponds to super refraction. Profile D indicates that the gradient of M near the surface of the earth is negative and, hence, duct propagation is observed. This is known as a surface duct. It is also possible to have an elevated duct (profile E). The ducts in the atmosphere are observed up to a height of 1500 m (Collin 1985). The thickness of the duct may range from a few metres to several hundred metres. If a wave is launched into the elevated duct at low grazing angles, an antenna located at the height of the duct will be able to receive considerably strong signals. If the receive antenna is placed either below or above the duct, the received signals will be substantially lower.

8.1.7 Tropospheric Scatter

The curvature of the earth limits the maximum LOS distance between the transmit and the receive antennas in a communication link. As shown in Fig. 8.14, if h_t is the height of the transmit antenna and h_r is the height of the receive antenna above the surface of the earth, the straight line AB is the LOS path between the two antennas. The optical horizon is the maximum distance between the two antennas along the surface of the earth for which

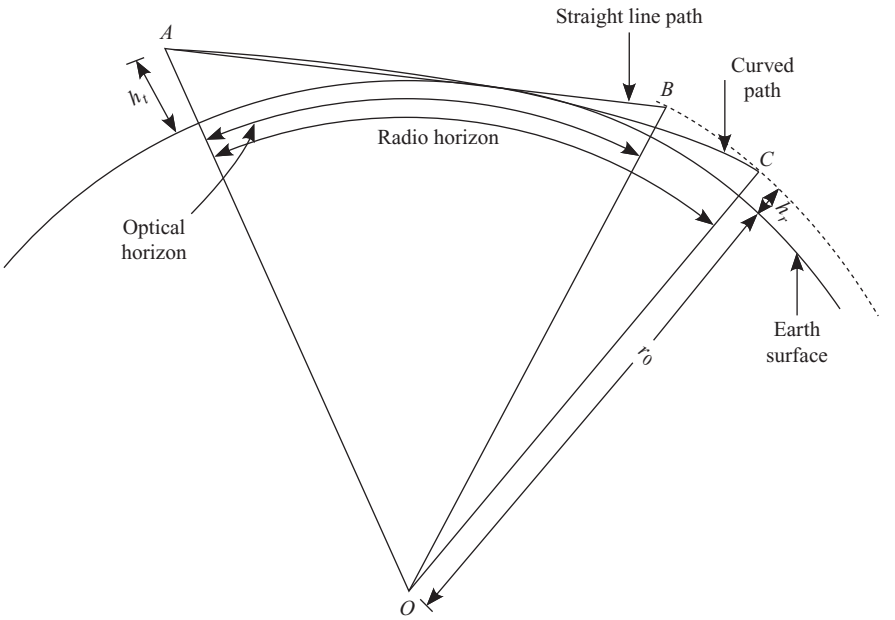

Fig. 8.14 Optical and radio horizons

the line AB just touches the surface of the earth. Referring to Fig. 8.10, the optical horizon, d, is

$$d = d_1 + d_2 = r_0(\theta_1 + \theta_2) \tag{8.91}$$

where r_0 is the radius of the earth and

$$\theta_1 = \tan^{-1}\left(\frac{R_1}{r_0}\right) \tag{8.92}$$

$$\theta_2 = \tan^{-1}\left(\frac{R_2}{r_0}\right) \tag{8.93}$$

The straight-line path lengths, R_1 and R_2, are given by

$$R_1 = \sqrt{(r_0 + h_t)^2 - r_0^2} \tag{8.94}$$

$$R_2 = \sqrt{(r_0 + h_r)^2 - r_0^2} \tag{8.95}$$

The radio waves take a curved propagation path through the atmosphere and, hence, can reach a longer distance before being intercepted by the earth. The curved line AC shown in Fig. 8.14 corresponds to the radio horizon.

A radio horizon is the maximum distance over which a direct radio wave link can be established.

We have already seen that the bending of the radio wave propagation path can be taken into account by using a 4/3 earth's radius model and a straight line propagation path. Eqns (8.91) to (8.95) can be used to compute the radio horizon by replacing r_0 with $(4/3)r_0$.

The tropospheric scattering phenomenon can be used to establish a communication link over a distance much beyond the radio horizon. The troposphere can scatter electromagnetic waves due to its inhomogenous nature. The tropospheric scattering has been attributed to the *blobs* of refractive index changes and turbulence. These could be due to sudden changes in the temperature or humidity or the presence of dust particles.

The troposcatter link consists of a transmit and a receive antenna, the main beams of which make very low angles with the horizontal ($< 4°$). The scattering volume is the common volume shared by the two beams and is just a few kilometers from the surface of the earth (Fig. 8.15).

Due to the random nature of scattering, the received signal strength also shows random fluctuations. Consider a scattering volume consisting of several regions of irregularities. These irregularities have different shapes,

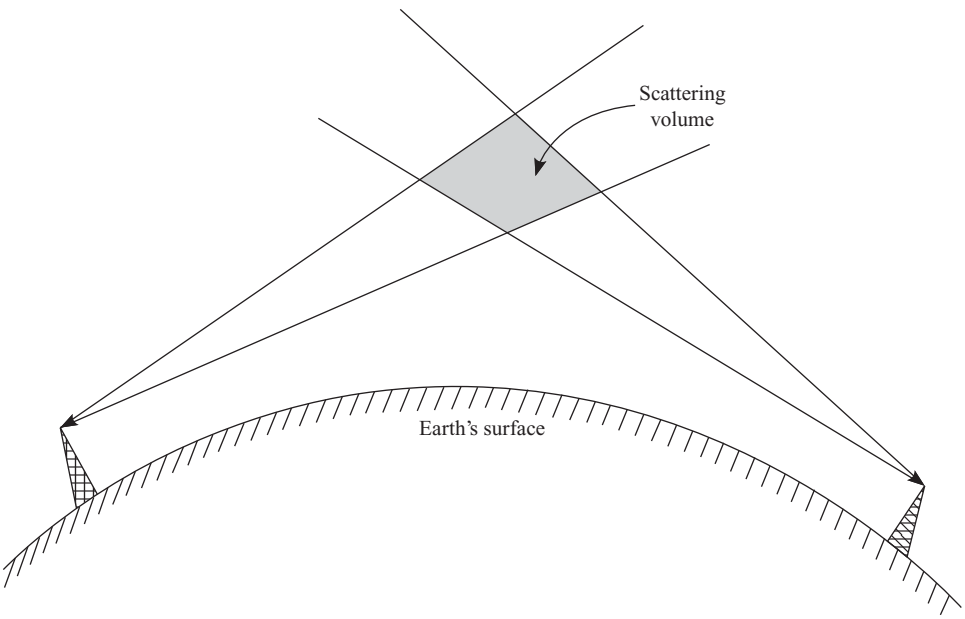

Fig. 8.15 Illustration of a troposcatter link

sizes, and positions which are changing randomly with time. The received signal which is the superposition of the scattered signals from these irregularities, sees a multipath environment. That is, there exists more than one path through which the signals from the transmitter can reach the receiver. A signal in a multipath environment typically undergoes fading (received signal strength changes as a function of time). Thus, the signals received by the troposcatter link also show fading.

Troposcatter can be used to establish communication links in the UHF and microwave frequency bands. These links typically have a range of up to a thousand kilometres and can have bandwidths of a few megahertz. Troposcatter links can be used in multi-channel telephony and television applications.

EXAMPLE 8.5

An antenna located at the surface of the earth is used to receive the signals transmitted by another antenna located at a height of 80 m from the spherical surface of the earth (mean radius = 6370 km). Calculate the optical and radio horizons if $dN/dh = -39$/km.

Solution: From Fig. 8.10

$$R_1 = \sqrt{(r_0 + h_t)^2 - r_0^2} = \sqrt{h_t^2 + 2r_0 h_t}$$
$$= \sqrt{80^2 + 2 \times 6370 \times 10^3 \times 80} = 31.93 \text{ km}$$

The ground distance, d_1, from the transmitter to the point where the ray becomes tangent to the surface of the earth is given by

$$d_1 = r_0 \theta_1 = r_0 \tan^{-1}\left(\frac{R_1}{r_0}\right) = 6370 \times \tan^{-1}\left(\frac{31.93}{6370}\right) = 31.93 \text{ km}$$

In the 4/3 earth radius model, the propagation path is a straight line. Therefore, the radio horizon, d_{e1}, is given by

$$d_{e1} = r_e \theta_1 = r_e \tan^{-1}\left(\frac{R_{e1}}{r_e}\right)$$

where $r_e = r_0 \times 4/3 = 8493$ km and

$$R_{e1} = \sqrt{h_t^2 + 2r_e h_t} = \sqrt{80^2 + 2 \times 8493 \times 10^3 \times 80} = 36.86 \text{ km}$$

Therefore

$$d_{e1} = 8493 \tan^{-1}\left(\frac{36.86}{8493}\right) = 36.86 \text{ km}$$

8.2 Ionospheric Propagation

The radiation from the space, in particular that from the sun, ionizes the gas molecules present in the atmosphere. The ionized layer that extends from about 90 km above the surface of the earth to several thousand kilometers is known as the ionosphere. At great heights from the surface of the earth the intensity of the ionizing radiation is very high, but there are very few molecules to be ionized. Therefore, in this region the ionization density (number of electrons or ions per unit volume) is low. As the height is decreased, atmospheric pressure increases, which implies that more molecules are present in the atmosphere. Therefore, the ionization density increases closer to the surface of the earth. With further reduction in height, though the number of molecules keeps increasing, the ionization density reduces because the energy in the ionizing radiation has been used up or absorbed to create ions. Therefore, the ionization density has a maximum that exists neither at the surface of the earth nor at the outer periphery of the ionosphere, but somewhere in the middle.

If a gas with molecules having an ionization energy of W J is exposed to a radiation of frequency f Hz, the ionization will occur if

$$hf > W \tag{8.96}$$

where h is the Planck's constant ($h = 6.626068 \times 10^{-34}$ Js); i.e., the energy contained in the radiation should be higher than that of the ionization energy of the molecule. Usually the ionization energy of a gas is expressed in electron volts. If W_i is the ionization energy of a gas in electron volts by dividing W by e, where e is the electronic charge in coulomb ($e = 1.602 \times 10^{-19}$ C), for ionization

$$W_i < \frac{hf}{e} \quad \text{eV} \tag{8.97}$$

where, e is the electronic charge in coulombs.

For example, to ionize oxygen having an ionization energy of 12.5 eV, the wavelength of the radiation should be less than 99 nm. Since the wavelength of the visible light falls in the range of 400–800 nm, it cannot ionize oxygen molecules.

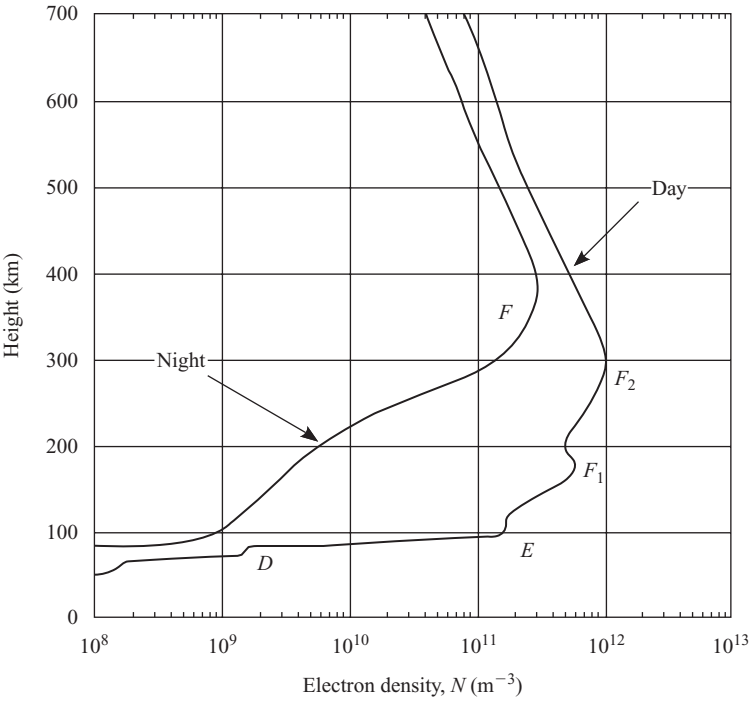

Fig. 8.16 Electron density profiles of ionosphere

It has been observed that the electron density profile (electron density versus height), has regions of maxima as well as regions of constant density (Fig. 8.16). These regions are known as layers of the ionosphere. There are mainly three layers in the ionosphere designated by the letters D, E, and F. The F layer splits into separate layers F_1 and F_2 during day time. The E and F layers, which are present during both day and night times, make long distance communication possible by reflecting radio waves in the frequency range of 3–30 MHz. Radio waves above 30 MHz pass through the ionosphere. The D layer, which is present only during the day time, does not reflect high frequency electromagnetic waves (3–30 MHz), but attenuates the waves passing through it. Even though the D layer reflects lower frequency waves (< 1 MHz), due to the high absorption of the electromagnetic energy by the D layer, the utility of the reflected waves is limited.

The electron density profile shown in Fig. 8.16 is a long-term average plot. The actual profile depends on several variables such as time of the day, season, latitude, and the sunspot number. The ionosphere undergoes both regular and irregular variations. The regular variation depends on the periodic phenomena such as, the time of the day, season, sunspot number, etc.

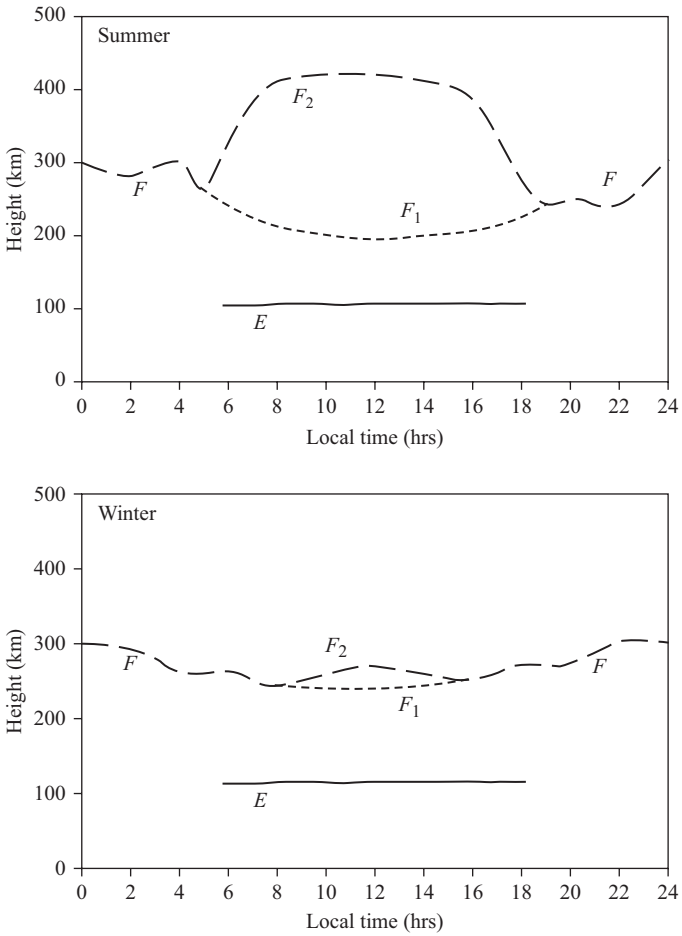

Fig. 8.17 Diurnal variation of heights of the ionospheric layers during the summer and winter seasons

Typical plots of heights of E and F layers during summer and winter seasons are shown in Fig. 8.17. During the day time the F layer splits into two layers namely, F_1 and F_2. The height of the F_2 layer is lower during winter as compared to that during summer. The sunspot number also undergoes a periodic change. It is observed that the sunspot number has a 11-year cycle (Fig. 8.18). A strong correlation is observed between the sunspot number and the radiation flux output of the sun. Therefore, the variations in the ionospheric condition also shows a strong correlation with the sunspot number.

In addition to the periodic, regular or normal variations of the ionosphere, there are irregular and unpredictable variations of the ionosphere that have

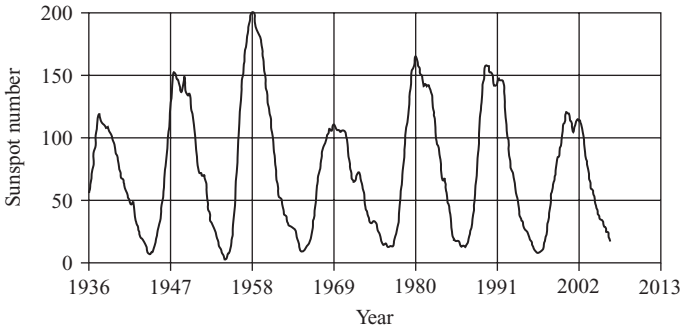

Fig. 8.18 Average sunspot number showing a 11-year cycle

a marked influence on the propagation characteristics. Sudden erruptions on the sun generate a large amount of radiation reaching the D layer. This increases the electron density of the D layer, and hence makes it more absorptive. Therefore, the waves propagating through the D layer undergo higher attenuation and the communication system experiences *fading* of signals. The fading may last for a few minutes or for several hours. This is known as the *sudden ionospheric disturbance* (SID) or the *Dellinger effect*. However, the intensity of the low frequency waves that are normally reflected by the D layer increases under SID. SID is never observed at night.

Another irregular variation is known as an *ionospheric storm*. In this irregularity, the ionosphere becomes turbulent and loses its stratified structure. Under this condition, electromagnetic wave propagation becomes erratic. It is observed that the ionospheric storm tends to recur at 27-day intervals. The cause of the storms has been attributed to the emission of burst of electrified particles from the sun.

8.2.1 Electrical Properties of the Ionosphere

Consider the motion of an electron in an electric field of strength E V/m. The force on the electron is $-eE$ N. In the event of a collision between the electron and a gas molecule, energy is lost in the form of heat. The frictional or retarding force due to the collision is mv/τ or $mv\nu$, where τ is the mean time between collision, ν is the frequency of collision and m is the mass of the electron. Therefore, net force on the electron is

$$F = (-eE - \nu mv) \text{ N} \tag{8.98}$$

Since the electron is moving with a velocity v, the force on the electron is equal to the rate of change of the momentum

$$F = -eE - \nu m v = m\frac{dv}{dt} \tag{8.99}$$

For a sinusoidal field having a time variation of $e^{j\omega t}$, this equation reduces to

$$j\omega m\mathbf{v} = -e\mathbf{E} - \nu m\mathbf{v} \tag{8.100}$$

or

$$\mathbf{v} = \frac{-e\mathbf{E}}{(j\omega m + \nu m)} \tag{8.101}$$

Since the moving charge is the current, the induced current density in an ionized gas containing N electrons per unit volume is

$$\mathbf{J} = -eN\mathbf{v} \quad \text{A/m}^2 \tag{8.102}$$

Substituting the value of $\mathbf{v}$ from Eqn (8.101)

$$\mathbf{J} = \frac{Ne^2\mathbf{E}}{m(\nu + j\omega)} \quad \text{A/m}^2 \tag{8.103}$$

An expression for the complex dielectric constant of the ionized air can be derived by introducing Eqn (8.103) for $\mathbf{J}$ into Maxwell's Curl equation [Eqn (1.7)]

$$\nabla \times \mathbf{H} = j\omega\epsilon_0\mathbf{E} + \mathbf{J} \tag{8.104}$$

$$= j\omega\epsilon_0\left[1 - \left(\frac{Ne^2}{m\epsilon_0}\right)\frac{1}{\omega(\omega - \nu)}\right]\mathbf{E} \tag{8.105}$$

$$= j\omega\epsilon_0\left[1 - \frac{\omega_p^2}{\omega(\omega - j\nu)}\right]\mathbf{E} \tag{8.106}$$

where

$$\omega_p = \sqrt{\frac{Ne^2}{m\epsilon_0}} \tag{8.107}$$

is known as the plasma frequency of the ionized medium. The term within the square brackets in Eqn (8.106) represents the complex relative dielectric constant, $\tilde{\epsilon}_r$, of the medium and is given by

$$\tilde{\epsilon}_r = 1 - \frac{\omega_p^2}{\omega(\omega - j\nu)} \tag{8.108}$$

Multiplying and dividing by the complex conjugate of the denominator and expanding

$$\tilde{\epsilon}_r = \left(1 - \frac{\omega_p^2}{\omega^2 + \nu^2}\right) - j\left(\omega_p^2 \frac{\frac{\nu}{\omega}}{\omega^2 + \nu^2}\right) \tag{8.109}$$

For a lossy medium, the complex relative dielectric constant can be expressed as

$$\tilde{\epsilon}_r = \epsilon_r - j\frac{\sigma}{\omega\epsilon_0} \tag{8.110}$$

where ϵ_r and σ are the relative permittivity and the conductivity of the medium, respectively. Comparing Eqns (8.109) and (8.110), we can write

$$\epsilon_r = 1 - \frac{\omega_p^2}{\omega^2 + \nu^2} \tag{8.111}$$

$$\sigma = \frac{\epsilon_0 \omega_p^2}{\omega} \frac{\frac{\nu}{\omega}}{1 + \frac{\nu^2}{\omega^2}} \tag{8.112}$$

In the ionosphere, the approximate values of ν are 10^6 Hz at 90 km from the surface of the earth and 10^3 Hz at 300 km (Jordan et al 2004). For a given angular frequency, ω, if $\nu \ll \omega$, the conductivity of the ionosphere is small, but the effective dielectric constant is

$$\epsilon_r \simeq 1 - \frac{Ne^2}{m\epsilon_0(\omega^2)} = 1 - \frac{\omega_p^2}{\omega^2} = 1 - \frac{81N}{f^2} \tag{8.113}$$

where the last part of the equation is obtained by substituting the value of $\epsilon_0 = 8.854 \times 10^{-12}$ F/m, $e = 1.602 \times 10^{-19}$ C for electronic charge, and $m = 9.1096 \times 10^{-31}$ kg for electronic mass. In this equation f represents the frequency in Hz and is related to ω by $\omega = 2\pi f$.

Ignoring the conductivity of the ionosphere, the propagation constant of the wave in it can be written as

$$k = \omega\sqrt{\mu_0\epsilon_0\epsilon_r} = k_0\sqrt{\epsilon_r} \text{ rad/m} \tag{8.114}$$

where, k_0 is the propagation constant in vacuum. From Eqn (8.113) we can conclude that the relative dielectric constant of the ionosphere depends on the ratio of the plasma frequency, ω_p, and the wave frequency ω. For $\omega < \omega_p$, ϵ_r is negative, hence the propagation constant is purely imaginary. Under this condition, the plane wave becomes purely evanescent. When $\omega = \omega_p$, the permittivity $\epsilon_r = 0$. For $\omega > \omega_p$, the relative dielectric constant is less than unity.

Let us assume that the ionosphere is lossless, has a relative permeability of unity and can be modelled as plane stratified media (Fig. 8.19). The wave path can be predicted using Snell's law

$$\sqrt{\epsilon_{r0}}\sin\theta_0 = \sqrt{\epsilon_{r1}}\sin\theta_1 = \cdots = \sqrt{\epsilon_{rn}}\sin\theta_n \tag{8.115}$$

where θ_0 is the angle of incidence with respect to the normal and θ_1 is the angle of refraction at the lower edge of the ionosphere. At the next interface between layers having dielectric constants ϵ_{r1} and ϵ_{r2}, the angle of incidence is θ_1 and the angle of refraction is θ_2. At the lower edge of the ionosphere the electron density is zero and hence $\epsilon_{r0} = 1$. Therefore, the equation representing Snell's law reduces to

$$\sin\theta_0 = \sqrt{\epsilon_{rn}}\sin\theta_n \tag{8.116}$$

The relative dielectric constant is a function of the electron density N. As the electromagnetic wave propagates deeper into the ionosphere, it passes through a region of higher N into a region of lower N. Since higher values of N correspond to lower ϵ_r (for $\omega > \omega_p$), the wave travels from a region of higher ϵ_r into a region with lower relative permittivity.

For a given angle of incidence $\theta_0 = \theta_i$, if N increases to a level such that the angle of refraction, $\theta = 90°$, the wave becomes horizontal. Under this condition Eqn (8.116) reduces to

$$\sin\theta_i = \sqrt{\epsilon_{rn}} \tag{8.117}$$

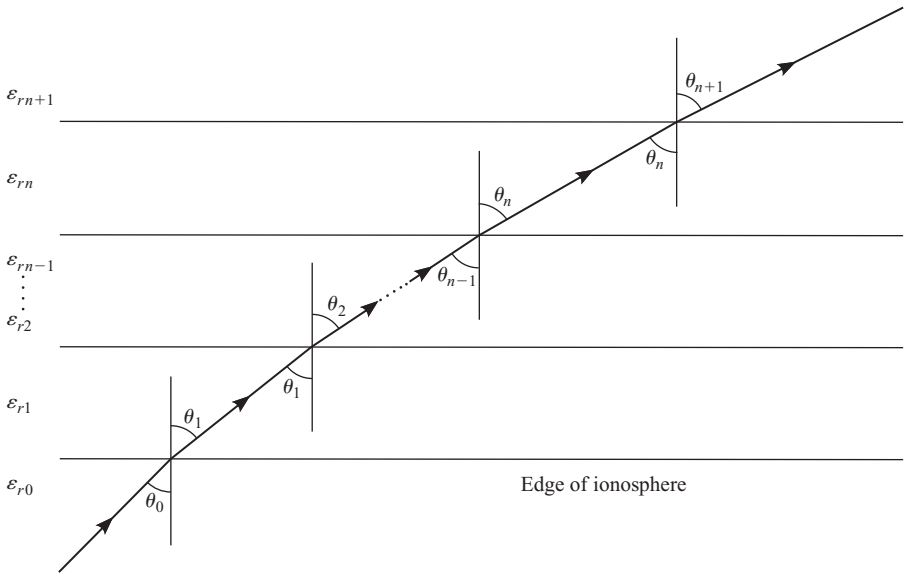

Fig. 8.19 Ray path through a plane stratified ionosphere

Let the dielectric constant of the nth layer be $\epsilon_{rn} = \epsilon_r$. Substituting the value of ϵ_r from Eqn (8.113)

$$\sin\theta_i = \sqrt{1 - \frac{81N}{f^2}} \tag{8.118}$$

If the incidence angle is greater than θ_i, the wave returns to the earth.

For a given angle of incidence, higher frequency electromagnetic waves are reflected from the region having a higher value of N. For example, a 5 MHz electromagnetic wave incident at 45° gets reflected by the ionospheric layer having $N = 1.54 \times 10^{11}\, m^{-3}$, which is at a height of about 100 km from the surface of the earth (see Fig. 8.16). A 10 MHz wave (incident at the same angle) is reflected by the ionospheric layer having an electron density of $6.17 \times 10^{11}\, m^{-3}$. This layer is found further away at about 170 km from the surface of the earth. Therefore, higher the frequency, the wave has to travel deeper into the ionosphere before it can be reflected.

Consider an electromagnetic wave launched vertically into the ionosphere having a maximum electron density N. Substituting $\theta_i = 0$ in Eqn (8.118), the highest frequency that gets reflected is given by

$$f_{\text{cr}} = \sqrt{81N} \tag{8.119}$$

which is also known as the *critical frequency*. The critical frequency is the highest frequency of the vertically launched electromagnetic wave that can be reflected from the ionosphere having a certain maximum electron density. For example, if the highest electron density in the ionosphere is $10^{12}/\text{m}^3$, the critical frequency is 9 MHz.

For any other angle of incidence, the highest frequency that can be reflected from the ionosphere will be greater than the critical frequency. The highest frequency that gets reflected by the ionosphere for a given value of angle of incidence (say θ_m) is known as the maximum usable frequency, f_{MUF}. Substituting $\theta_i = \theta_m$ and $f = f_{\text{MUF}}$ in Eqn (8.118)

$$\sin\theta_m = \sqrt{1 - \frac{81N}{f_{\text{MUF}}^2}} \tag{8.120}$$

From Eqn (8.119), we have $81N = f_{\text{cr}}^2$. Substituting this in Eqn (8.120) we get

$$\sin\theta_m = \sqrt{1 - \frac{f_{\text{cr}}^2}{f_{\text{MUF}}^2}} \tag{8.121}$$

which can be written as

$$1 - \sin^2\theta_m = \frac{f_{\text{cr}}^2}{f_{\text{MUF}}^2} \tag{8.122}$$

The left hand side of the above equation can be further simplified to get

$$\cos^2\theta_m = \frac{f_{\text{cr}}^2}{f_{\text{MUF}}^2} \tag{8.123}$$

Taking the square root, we can write an expression that relates the critical frequency and the angle of incidence to the maximum usable frequency

$$f_{\text{MUF}} = f_{\text{cr}} \sec\theta_m \tag{8.124}$$

For example, if the critical frequency is 9 MHz, the maximum usable frequency corresponding to an angle of incidence of 45° is 12.73 MHz.

Virtual height Consider an electromagnetic wave from a transmitter reaching the receiver after being reflected by the ionosphere as shown in Fig. 8.20. Let the wave enter the ionosphere at A, and take a curved path ABC before it emerges out of the ionosphere. If the incident and the reflected rays are extended, they meet at point D as shown in Fig. 8.20. The vertical height

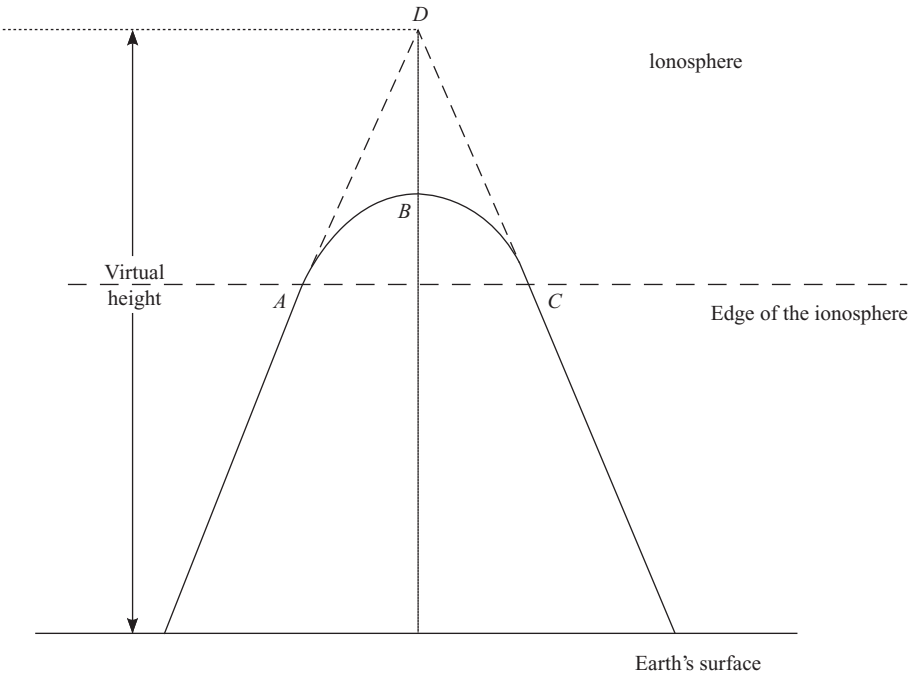

Fig. 8.20 Propagation path in the ionosphere and the depiction of virtual height

from the ground to the point D is known as the *virtual height* which is higher than the lower edge of the ionosphere.

An *ionosonde* is the instrument used to measure the virtual height of the ionosphere. This instrument transmits an RF pulse vertically into the ionosphere from the ground. This pulse is reflected from the ionosphere and is received by the ionosonde. The time delay between the transmit and the receive pulse is measured and plotted as a function frequency of the electromagnetic wave. The time delay is a measure of the virtual height of the ionosphere. A plot of the virtual height as a function of frequency is known as an *ionogram*.

A typical ionogram for daytime is shown in Fig. 8.21. As the frequency of the electromagnetic wave increases, the virtual height also increases slightly, indicating that the waves of higher frequencies are returned from higher levels within the layer. As the frequency approaches the critical frequency (5 MHz for the F_1 layer), the virtual height steeply increases. Once the critical frequency is crossed, the virtual height drops back to a steady value (350 km for 5.5 MHz) which is higher than that for a lower frequency (200 km for 4 MHz). This sudden increase in the virtual height near the critical frequency is attributed to the increased group delay of the waves.

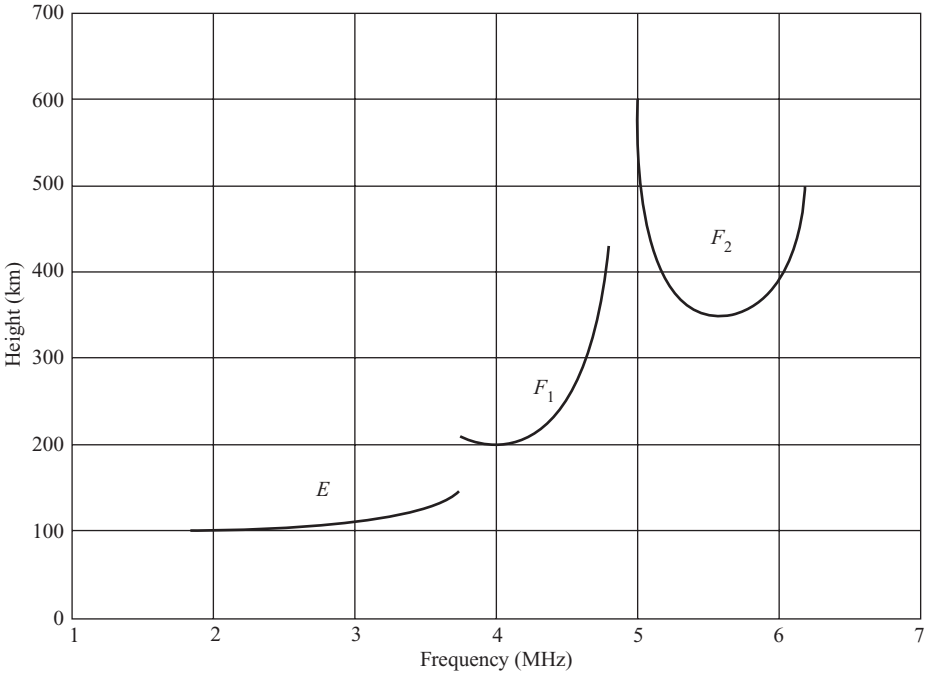

Fig. 8.21 A typical ionogram recorded during daytime

Skip distance Assume that the ionosphere can be modelled as a flat reflecting surface at a height h (virtual height) from the surface of the flat earth. Let θ_m be the angle of incidence of a wave of frequency f_{MUF} which gets reflected from the ionosphere. If the angle of incidence is greater than θ_m, the wave is reflected back by the ionosphere. For $\theta_i > \theta_m$, Eqn (8.118) is satisfied for a lower value of N, which occurs at a height less than h. For launch angles $\theta_i < \theta_m$ the ionosphere cannot reflect the waves back (Fig. 8.22). Let the wave launched at $\theta_i = \theta_m$ reach the surface of the earth at R, at a distance of D_{skip} from the transmitter. The distance D_{skip} is known as the *skip distance*. In the region of radius less than D_{skip}, it is not possible to establish a communication link by the waves reflected from the ionosphere.

We can derive an expression for the skip distance in terms of the critical frequency and the maximum usable frequency by considering the ΔDOT in Fig. 8.22. From ΔDOT, we can write

$$\cos^2 \theta_m = \left(\frac{DO}{DT}\right)^2 = \left[\frac{h}{\sqrt{h^2 + \left(\frac{D_{\text{skip}}}{2}\right)^2}}\right]^2 = \frac{1}{1 + \left(\frac{D_{\text{skip}}}{2h}\right)^2} \qquad (8.125)$$

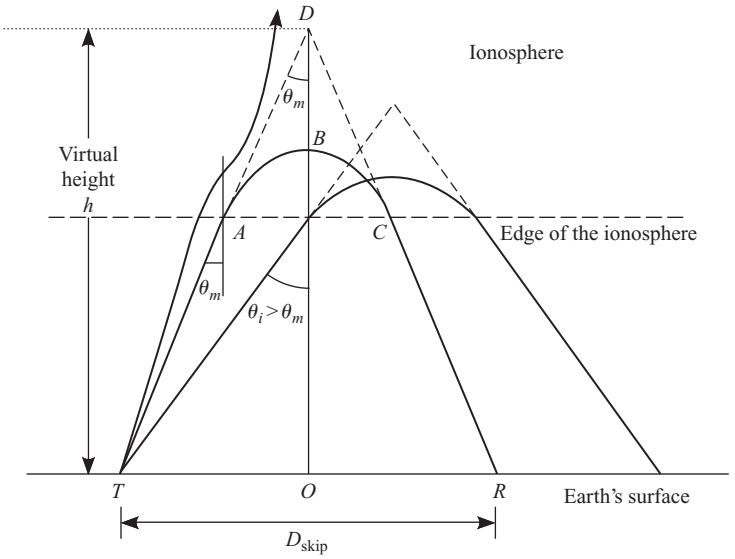

Fig. 8.22 Ray paths for different angles of incidence, illustrating skip distance

From Eqn (8.123) and Eqn (8.125) we get

$$D_{\text{skip}} = 2h\sqrt{\left(\frac{f_{\text{MUF}}}{f_{\text{cr}}}\right)^2 - 1} \tag{8.126}$$

Sky waves over spherical earth Let us now consider the transmit and receive antennas located on the surface of the spherical earth. The ionosphere is modelled as a spherical reflecting surface at a virtual height h from the surface of the earth [Fig. 8.23(a)]. A wave launched at a grazing angle ψ from point A gets reflected by the ionosphere (provided $\theta_i > \theta_m$) and reaches the surface of the earth at C. If the earth is a good reflector, the wave can undergo multi-hops and thus can establish communication between the points A and E in addition to that between A and C.

The single-hop distance AC is a function of the grazing angle, ψ. The maximum value of the single hop distance occurs for $\psi = 0$ or horizontal launch as shown in Fig. 8.23(b). The incidence angle at P is given by

$$\theta = \sin^{-1}\left(\frac{r_0}{r_0 + h}\right) \tag{8.127}$$

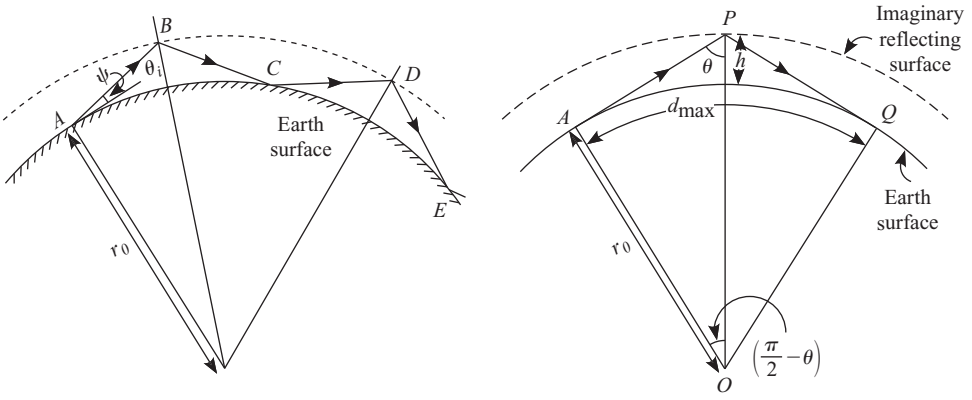

(a) Multi-hop propagation (b) Maximum single hop distance

Fig. 8.23 Propagation of sky waves above the spherical earth

Therefore the maximum single hop distance is

$$d_{\max} = 2r_0\left(\frac{\pi}{2} - \theta\right) \tag{8.128}$$

For example, the reflection from the E layer with $h = 100$ km, the angle of incidence is

$$\theta = \sin^{-1}\left(\frac{6370}{6470}\right) = 79.91^\circ = 1.395 \text{ rad} \tag{8.129}$$

The maximum single-hop distance is

$$d_{\max} = 2 \times 6370 \times \left(\frac{\pi}{2} - 1.395\right) = 2240 \text{ km} \tag{8.130}$$

Similarly, for the F layer, with a virtual height of 300 km, the maximum angle of incidence is 72.75° and the maximum single-hop distance is 3836 km.

EXAMPLE 8.6

An electromagnetic wave at frequency f is propagating through a lossy dielectric medium having conductivity σ, permittivity $\epsilon = \epsilon_0\epsilon_r$, and permeability $\mu = \mu_0$. Derive an expression for the attenuation per unit length of the medium. If $\sigma/(\omega\epsilon) \ll 1$, show that the attenuation is given by $60\pi\sigma/\sqrt{\epsilon_r}$.

Solution: For a lossy dielectric medium, the propagation constant is given by

$$\gamma^2 = (\sigma + j\omega\epsilon)(j\omega\mu) = (\alpha + j\beta)^2$$

where α and β are the attenuation and the phase constants. Expanding and equating the real and the imaginary parts

$$\alpha^2 - \beta^2 = -\omega^2\mu\epsilon \tag{8.6.1}$$

$$2\alpha\beta = \omega\mu\sigma \tag{8.6.2}$$

Substituting the expression for β from Eqn (8.6.2) into Eqn (8.6.1) above we get

$$\alpha^2 - \left(\frac{\omega\mu\sigma}{2\alpha}\right)^2 = -\omega^2\mu\epsilon$$

This can be written as

$$\alpha^4 + \omega^2\mu\epsilon\alpha^2 - \left(\frac{\omega\mu\sigma}{2}\right)^2 = 0$$

Solving for α^2 and taking the square root

$$\alpha = \omega\sqrt{\frac{\mu\epsilon}{2}\left\{\sqrt{1 + \left(\frac{\sigma}{\omega\epsilon}\right)^2} - 1\right\}}$$

For $\sigma/(\omega\epsilon) \ll 1$, using binomial expansion we can write

$$\sqrt{1 + \left(\frac{\sigma}{\omega\epsilon}\right)^2} \simeq 1 + \frac{1}{2}\left(\frac{\sigma}{\omega\epsilon}\right)^2$$

and hence the attenuation constant reduces to

$$\alpha = \frac{\sigma}{2}\sqrt{\frac{\mu}{\epsilon}}$$

Substituting $\epsilon_0 = 8.854 \times 10^{-12}$ F/m and $\mu_0 = 4\pi \times 10^{-7}$ H/m we get

$$\alpha = \frac{60\pi\sigma}{\sqrt{\epsilon_r}}$$

8.2.2 Effect of Earth's Magnetic Field

In the previous sections we studied the propagation of the electromagnetic waves in an ionized medium. Because of the presence of free charges in the ionosphere, there is an exchange of energy between the field and the electrons. The effect is reflected as a complex permittivity in a gross sense (the medium is modelled to have a bulk complex premittivity). The propagation constant, therefore, has a real and an imaginary part.

In the analysis so far, we have ignored the presence of the earth's magnetic field. In the presence of magnetic field, $\mathbf{B}_0$, the free electrons moving with a velocity, $\mathbf{v}$, perpendicular to the direction of $\mathbf{B}_0$, move in a circular path because of the force, $\mathbf{F}$, exerted by the magnetic field, $\mathbf{F} = \mathbf{v} \times \mathbf{B}_0$. The sense of rotation of the electron is given by the force equation. Now, consider a circularly polarized electromagnetic wave propagating along the direction of the earth's magnetic field. The interaction of the electromagnetic wave with the electron depends on the relative sense of rotation of the electric field vector and the electron. This results in different effective permittivities for the left and right circularly polarized waves and, hence, different propagation constants.

If the electromagnetic wave is propagating perpendicular to the earth's magnetic field, with the electric field vector along $\mathbf{B}_0$, the magnetic field does not affect the propagation characteristics of the wave. In other words, the propagation constant of the wave is same as that in the absence of the earth's magnetic field. This wave is known as the *ordinary wave*.

If the electromagnetic wave is propagating perpendicular to $\mathbf{B}_0$ with its electric field also perpendicular to $\mathbf{B}_0$, the resulting wave is no longer linearly polarized, nor can be considered as a plane wave. This interaction generates a component of the electric field in the direction of propagation making the tip of the electric field vector trace an ellipse in a plane parallel to the direction of propagation. This wave is known as the *extraordinary wave*.

Faraday rotation Consider a linearly polarized plane wave

$$\mathbf{E} = E_0 \mathbf{a}_x e^{-jk_0 z} \tag{8.131}$$

propagating along the z-direction. This can be split into two circularly polarized waves.

$$\mathbf{E} = \frac{E_0}{2}(\mathbf{a}_x + j\mathbf{a}_y)e^{-jk_0 z} + \frac{E_0}{2}(\mathbf{a}_x - j\mathbf{a}_y)e^{-jk_0 z} \tag{8.132}$$

Let this wave enter the ionosphere at $z = 0$ having a thickness of l m. The two circularly polarized components travel with different phase velocities (Jordan et al 2004). In other words, they travel with two different propagation constants k_1 and k_2. The electric field at $z = l$ is given by

$$\mathbf{E} = \frac{E_0}{2}(\mathbf{a}_x - j\mathbf{a}_y)e^{-jk_1 l} + \frac{E_0}{2}(\mathbf{a}_x + j\mathbf{a}_y)e^{-jk_2 l} \tag{8.133}$$

Rewriting this expression

$$\begin{aligned}\mathbf{E} &= \frac{E_0}{2}e^{-jk_1\frac{l}{2}}e^{-jk_2\frac{l}{2}}\Big[(\mathbf{a}_x - j\mathbf{a}_y)e^{-jk_1\frac{l}{2}+jk_2\frac{l}{2}} \\ &\quad + (\mathbf{a}_x + j\mathbf{a}_y)e^{-jk_2\frac{l}{2}+jk_1\frac{l}{2}}\Big] \qquad (8.134)\\ &= \frac{E_0}{2}e^{-j(k_1+k_2)\frac{l}{2}}\Big[\mathbf{a}_x(e^{j(k_2-k_1)\frac{l}{2}} + e^{-j(k_2-k_1)\frac{l}{2}}) \\ &\quad - j\mathbf{a}_y(e^{j(k_2-k_1)\frac{l}{2}} - e^{-j(k_2-k_1)\frac{l}{2}})\Big] \qquad (8.135)\\ &= E_0 e^{-j(k_1+k_2)\frac{l}{2}}\left[\mathbf{a}_x\cos(k_2-k_1)\frac{l}{2} + \mathbf{a}_y\sin(k_2-k_1)\frac{l}{2}\right] \qquad (8.136)\end{aligned}$$

Equation (8.136) represents a linearly polarized wave with the electric field tilted by an angle τ with respect to the x-axis, and the angle τ is given by

$$\tau = \tan^{-1}\frac{E_y}{E_x} = \tan^{-1}\left[\frac{\sin(k_2-k_1)\frac{l}{2}}{\cos(k_2-k_1)\frac{l}{2}}\right] = (k_2-k_1)\frac{l}{2} \tag{8.137}$$

The rotation of the plane of polarization of a plane wave when it passes through the ionosphere is known as the *Faraday rotation.*

Whistlers Lightning flashes occurring in the troposphere generate pulses of electromagnetic radiation, the frequencies of which fall in the audible frequency range. These waves propagate along the lines of the earth's magnetic field and can be heard by sensitive audio amplifiers (Jordan et al 2004). The group velocity of these waves is frequency-dependent. The high frequency part travels faster than the lower frequency component. As a result of this, at the output of the receiver, there appears a whistling tone of a steadily falling pitch, known as *whistlers.* It is observed that the frequency of the whistler decreases as a function of time. Depending on their duration, whistlers are classified as *long whistlers* and *short whistlers.*

Exercises

8.1 A free space line-of-sight link at 2.4 GHz is established between two antennas separated by a distance of 10 km and aligned to receive maximum power. The transmit antenna has a gain of 20 dB and radiates 20 dBm power. If the power received by the receive antenna is −70 dBm, calculate its gain.

Answer: 10 dB

8.2 Calculate the received power in a communication link having a path loss of 160 dB, transmit antenna gain of 20 dB, receive antenna gain of 25 dB, and a transmit power of 100 mW. If the minimum received power required to establish a reliable communication link is −80 dBm, what should be the transmit power?

Answer: −95 dBm, 3.16 W

8.3 A horizontal dipole antenna situated at a height of 9 m from the ground is radiating electromagnetic waves at 900 MHz. A polarization-matched receive antenna is kept at a height of 1.5 m above the ground. Calculate and plot the path loss if the horizontal distance between the two antennas changes from 50 m to 250 m. Assume that the reflection coefficient of the ground is −1. On the same graph, plot the path loss factor obtained from Eqn. (8.27).

8.4 An electromagnetic wave is incident on an interface of air and a medium with a relative permittivity ϵ_r and conductivity $\sigma = 0$. If ψ is the grazing angle of incidence, show that $\Gamma_\perp = 0$ is possible only if $\epsilon_r = 1$, irrespective of the value of ψ.

Derive an expression that relates the grazing angle ψ and ϵ_r so that $\Gamma_\parallel = 0$.

8.5 A mobile telephone system is operating at 900 MHz in a large city. The effective height of the transmit antenna is 30 m and that of the receive antenna is 1 m. The horizontal distance between the antennas is 2 km. (a) Calculate the path loss using the LOS propagation model ignoring the effect of the ground and the environment. (b) Calculate the path loss using log-distance path loss model with a path loss exponent of 2.7. (c) Calculate the path loss using the Hata model.

Answer: (a) 97.6 dB (b) 131.5 dB (c) 135.1 dB

8.6 A mobile telephone system at 1800 MHz needs to be established in a medium-sized city. The receive antenna has a gain of 1.2 dB and the transmit antenna has a gain of 7 dB. The two antennas are located 80 m and 1.5 m above the ground, respectively. What should be the transmit power so that the received power at a horizontal distance of 3 km from the transmitter is −80 dBm?

Answer: 575 W

8.7 An LOS link at 2.4 GHz needs to be established between two antennas located on the surface of the earth (mean radius 6370 km). One of the antennas is at a height of 20 m and the other, 10 m from the surface of the earth. Calculate the maximum possible straight-line distance between the two antennas if the propagation is taking place in the absence of the atmosphere. Repeat the calculation if the propagation is taking place in a standard atmosphere.

Answer: 27.25 km, 31.46 km

8.8 Electromagnetic waves are propagating in an atmosphere that has $dN/dh = -100$/km over the earth (mean radius 6370 km). Calculate the equivalent radius

of the earth so that the propagation path becomes a straight line.

Answer: 9347 km

8.9 A troposcatter link is established between two antennas that are separated by a ground distance of 300 km. The two antennas are located at a height of 6 m from the surface of the earth and are launching electromagnetic waves horizontally into space. Calculate the height of the scatter volume situated mid-way between the two antennas which can be used to establish the troposcatter link.

Answer: 1336.6 m

8.10 Calculate the wavelength of the radiation required to ionize nitrogen and carbon dioxide having the ionization energies of 15.8 eV and 13.8 eV, respectively.

Answer: 78.5 nm and 89.9 nm

8.11 An ionospheric communication link is to be established between two points on the surface of the earth that are separated by 3000 km. The ionosphere is modelled as a perfectly reflecting sphere which is concentric with the earth. The height of the ionosphere from the surface of the earth is 180.8 km. Calculate the launch angle, measured from the tangent to the earth's surface at the transmitter, required to establish a communication link. (Earth radius = 6370 km).

Answer: 0°

8.12 A transmit antenna with a beamwidth of 30° is used in an ionospheric communication link. The ionosphere is modelled as a perfectly reflecting spherical surface which is concentric with the earth. The height of the ionosphere is 150 km from the surface of the earth. If the antenna is oriented such that one of the main beam edges is along the horizontal, calculate the minimum and maximum distances from antenna over which the signals from the main beam are received on the surface of the earth.

Answer: 491.4 km, 2737.8 km

8.13 Repeat Problem 8.12 if the antenna is oriented such that the main beam points vertically upwards.

Answer: 0 km, 77.84 km

8.14 If the height of the ionosphere is 200 km, calculate the launch angle (measured from the tangent to the surface of the earth at the transmitter) required to establish the link with the receiver located on the surface of the earth at a ground distance of 2500 km.

Answer: 3.29°

8.15 Calculate the conductivity, relative permittivity, and attenuation rate of the D layer having $N = 10^9/\text{m}^3$ and $\nu = 10^6/\text{s}$, for a radio wave at 1 MHz. Repeat the calculation at 10 MHz. ($\epsilon_0 = 8.854 \times 10^{-12}$ F/m, $e = 1.602 \times 10^{-19}$ C, m $= 9.1096 \times 10^{-31}$ kg)

Answer: 6.96×10^{-7} S/m, 0.92, 1.368×10^{-4} Np/m, 7.134×10^{-9} S/m, 0.9992, 1.3453×10^{-6} Np/m

List of Symbols

Vectors, matrices, and phasors	:	Bold face symbols (e.g. $\mathbf{E}$)
Scalar quantities	:	Italic characters (e.g. t)
Instantaneous scalar	:	Script characters (e.g. $\mathcal{E}$)
Instantaneous vector	:	Script characters with an over-bar (e.g. $\bar{\mathcal{E}}$)

a	:	radius (m)
$\mathbf{A}$	:	magnetic vector potential (Wb/m)
A_c	:	effective collecting aperture (m^2)
A_e	:	effective aperture (m^2)
A_{su}	:	ground wave attenuation factor (ratio)
$a \times b$	:	aperture dimensions
$a_w \times b_w$	:	waveguide dimensions
AF	:	array factor
b	:	power factor angle (rad)
$\mathbf{B}$	:	magnetic flux density (Wb/m^2 or T)
B, BW	:	bandwidth (Hz)
c	:	velocity of light in vaccum (m/s) $\simeq 3 \times 10^8$ m/s
$\mathbf{D}$	:	electric flux density (C/m^2)
D	:	directivity (ratio)
D_{skip}	:	skip distance (m)
e	:	electron charge (C) $= 1.602 \times 190^{-19}$ C
$\mathbf{E}$	:	electric field intensity (V/m)
$\hat{e}^i$	:	unit vector along the electric field intensity $\mathbf{E}^i$
f	:	frequency (Hz or cycles/s), focal length of the parabola (m)
$\mathbf{F}$	:	electric vector potential (C/m)

F	:	environmental factor (dimensionless)
f_{cr}	:	critical frequency (Hz)
f_{MUF}	:	maximum usable frequency (Hz)
F_d	:	knife edge diffraction gain (ratio)
G	:	gain (ratio), scalar spherical wave function $\frac{e^{-jkr}}{4\pi r}$
HPBW	:	half-power beamwidth
$\mathbf{J}_s$	:	electric surface current density (A/m)
h	:	Planck's constnat (J s) $= 6.626068 \times 10^{-34}$ J s
$\mathbf{H}$	:	magnetic field intensity (A/m)
I	:	current (A)
$\mathbf{J}$	:	electric current density (A/m^2)
k	:	propagation constant (rad/m), Boltzmann's constnat (J/K) $= 1.38 \times 10^{-23}$ J/K
l	:	length (m)
$\mathbf{l}_{\mathrm{eff}}$	:	vector effective length (m)
$\hat{l}^*_{\mathrm{eff}}$	:	unit vector along $\mathbf{l}^*_{\mathrm{eff}}$ (dimensionless)
L	:	horn length (m)
m	:	rest mass of electron (kg) $= 9.107 \times 10^{-31}$ kg
M	:	modified refractivity
$\mathbf{M}$	:	magnetic current density (V/m^2)
$\mathbf{M}_s$	:	magnetic surface current density (V/m)
$\mathbf{n}$	:	unit normal
n	:	path loss exponent, refractive index
n^*	:	modified refractive index
N	:	refractivity, electron density (m^{-3})
p	:	numerical distance
P	:	power (W)
P_L	:	power dissipated in the load impedance (W), path loss (dB)
q	:	charge (C)
r	:	distance (m)
$\mathbf{r}$	:	position vector of a point (x, y, z), (ρ, ϕ, z), or (r, θ, ϕ)
$\mathbf{r}'$	:	position vector of a point (x', y', z'), (ρ', ϕ', z'), or (r', θ', ϕ')
R	:	distance (m), Resistance (Ω)
$\mathbf{R}$	:	vector from source point to the field point
r_0	:	radius of earth (m) $= 7370$ km
r_e	:	equivalent radius of the earth (m) $= \frac{4}{3} r_0$
r_{ox}	:	radius of curvature of the phase front in the $x-z$ plane
r_{oy}	:	radius of curvature of the phase front in the $y-z$ plane
$\mathbf{S}$	:	power density vector (W/m^2)

T	:	temperature (K)
T_a	:	antenna temperature (K)
T_b	:	brightness temperature (K)
U	:	radiation intensity (W/sr)
v	:	velocity (m/s)
$\mathbf{v}$	:	velocity vector (m)
V	:	electric scalar potential (V), potential difference (V)
W	:	energy (J)
W_i	:	ionization energy (eV)
X	:	reactance (Ω)
z	:	$e^{j\psi}$
Z	:	impedance (Ω)
$Z_{11} \ldots Z_{22}$	:	Z parameters of the network
α	:	attenuation constant of cable (Np/m), progressive phase shift (rad)
Γ	:	reflection coefficient (ratio)
ϵ	:	permittivity (F/m)
ϵ_0	:	permittivity of free space (F/m) $= 8.854 \times 10^{-12}$ F/m
ϵ_{r}	:	relative permittivity (dimensionless)
$\tilde{\epsilon_r}$	:	complex relative dielectric constant (dimensionless)
η	:	impedance of the medium (Ω) (for free space $\eta = 376.73\ \Omega$)
$\Theta_{1\mathrm{HP}}, \Theta_{2\mathrm{HP}}$	:	half-power beamwidths in the two principal planes (rad)
θ_z	:	direction of the null
κ	:	efficiency (ratio)
λ	:	wavelength (m)
μ	:	permeability (H/m)
μ_0	:	permeability of free space (H/m) $= 4\pi 10^{-7}$ H/m
μ_{r}	:	relative permeability (dimensionless)
ν	:	collision frequency (Hz)
ν_d	:	Fresnel–Kirchhoff diffraction parameter (ratio)
ρ	:	electric charge density (C/m^3)
ρ_m	:	magnetic charge density (Wb/m^3)
ψ	:	angle between the vectors $\mathbf{r}$ and $\mathbf{R}$ (rad), $(kd\cos\theta + \alpha)$
Ψ_e	:	flare angle in the **E**-plane
Ψ_h	:	flare angle in the **H**-plane
σ	:	conductivity (S/m)
χ	:	angle between $\mathbf{E}^i$ and $\mathbf{l}^*_{\mathrm{eff}}$ (rad), $\sigma/(\omega\epsilon_0)$
ψ	:	grazing angle (rad, deg)
Ψ	:	brightness (W m^{-2} sr^{-2} Hz^{-1})

ω	:	angular frequency (rad/s)
Ω	:	solid angle (sr)
ω_p	:	plasma frequency (Hz)
Ω_A	:	beam solid angle (sr)
$\mathbf{a}_x, \mathbf{a}_y, \mathbf{a}_z$	:	unit vectors along x, y, and z directions, respectively
$\mathbf{a}_\rho, \mathbf{a}_\phi, \mathbf{a}_z$	:	unit vectors along ρ, ϕ, and z directions, respectively
$\mathbf{a}_r, \mathbf{a}_\theta, \mathbf{a}_\phi$	:	unit vectors along r, θ, and ϕ directions, respectively
A_x, A_y, A_z	:	components of the vector $\mathbf{A}$ along x, y, and z directions, respectively
A_ρ, A_ϕ, A_z	:	components of the vector $\mathbf{A}$ along ρ, ϕ, and z directions, respectively
A_r, A_θ, A_ϕ	:	components of the vector $\mathbf{A}$ along r, θ, and ϕ directions, respectively

References

Balanis, C.A. 2002, *Antenna Theory*, John Wiley & Sons (ASIA), Singapore.

Boithias, L. 1987, *Radio Wave Propagation*, North Oxford Academic Publishers, London.

Cheng, D.K. 2002, *Field and Wave Electromagnetics*, Pearson Education, Delhi.

Collin, R.E. 1985, *Antennas and Radiowave Propagation*, McGraw–Hill, New York.

Davies, K. 1990, *Ionospheric Radio*, Peter Peregrinus, London.

Dolukhanov, M. 1971, *Propagation of Radio Waves*, Mir Publishers, Moscow.

Elliott, R.S. 1981, *Antenna Theory and Design*, Prentice–Hall, New Jersey.

Griffiths, J. 1987, *Radio Wave Propagation and Antennas*, Prentice–Hall International, London.

Hall, G.L. 1984, *The ARRL Antenna Book*, The American Radio Relay League, USA.

Harrington, R.F. 1961, *Time-harmonic Electromagnetic Fields*, McGraw–Hill, New York.

Hayt, W.H., Jr. and J.A. Buck 2001, *Engineering Electromagnetics*, Tata McGraw–Hill, New Delhi.

"IEEE Standard Definitions of Terms for Antennas" November 1983, *IEEE Transactions on Antennas and Propagation*, AP-31, no. 6, part II.

"IEEE Standard Definitions of Terms for Antennas" 1990, *IEEE Standard 145–1990*, IEEE, USA.

"IEEE Standard Test Procedures for Antennas" 1979, *ANSI/IEEE Std 149–1979*, IEEE, USA.

Jordan, E.C. and K.G. Balmain 2004, *Electromagnetic Waves and Radiating Systems*, Prentice–Hall of India, New Delhi.

Kraus, J.D. 1966, *Radio Astronomy*, McGraw–Hill, New York.

Kraus, J.D. 1988, *Antennas*, McGraw–Hill, Singapore.

Kreyszig, E. 1999, *Advanced Engineering Mathematics*, John Wiley & Sons, USA.

Kummer, W.H. and E.S. Gillespie 1978, "Antenna measurements", *Proceedings of the IEEE*, vol. 66, no. 4.

Lo, Y.T. and S.W. Lee 1988, *Antenna Handbook*, Van Nostrand Reinhold, New York.

Pozar, D.M. 2001, *Microwave and RF Wireless Systems*, John Wiley & Sons, New Jersey.

Pozar, D.M. 2003, *Microwave Engineering*, John Wiley & Sons, Singapore.

Ramo, S., J.R. Whinnery, and T. Van Duzer 2004, *Fields and Waves in Communication Electronics*, John Wiley & Sons, Singapore.

Rappaport, T.S. 2002, *Wireless Communications*, Prentice–Hall, New Jersey.

Rossi, J.P., J.C. Bic, A.J. Levy, Y. Gabillet, and M. Rosen 1991, "A ray launching method for radio-mobile propagation in urban area", *IEEE Antenna Propagation Symposium, London, Ontario, Canada*, p. 1540–1543.

Schaubach, K.R., N.J. Davis, and T.S. Rappaport 1992, "A ray tracing method for predicting path loss and delay spread in microcellular environments," *42nd IEEE Vehicular Technology Conference, Denver*, p. 932–935.

Seybold, J.S. 2005, *Introduction to RF Propagation*, John Wiley & Sons, New Jersey.

Stutzman, W.L. and G.A. Thiele 1998, *Antenna Theory and Design*, John Wiley & Sons, New Jersey.

Taflov, A. and S.C. Hagness 2000, *Computational Electrodynamics*, Artech House, Boston.

Thomas, G.B. and R.L. Finney 1996, *Calculus and Analytic Geometry*, Pearson Education, Delhi.

APPENDIX A

Trigonometric Formulae

$$\sin^2\theta + \cos^2\theta = 1 \tag{A.1}$$

$$\sec^2\theta = 1 + \tan^2\theta \tag{A.2}$$

$$\mathrm{cosec}^2\theta = 1 + \cot^2\theta \tag{A.3}$$

$$\sin 2\theta = 2\sin\theta\cos\theta \tag{A.4}$$

$$\cos 2\theta = \cos^2\theta - \sin^2\theta \tag{A.5}$$

$$\sin(A \pm B) = \sin A\cos B \pm \cos A\sin B \tag{A.6}$$

$$\cos(A \pm B) = \cos A\cos B \mp \sin A\sin B \tag{A.7}$$

$$\tan(A \pm B) = \frac{\tan A \pm \tan B}{1 \mp \tan A\tan B} \tag{A.8}$$

$$\sin A + \sin B = 2\sin\left(\frac{A+B}{2}\right)\cos\left(\frac{A-B}{2}\right) \tag{A.9}$$

$$\sin A - \sin B = 2\cos\left(\frac{A+B}{2}\right)\sin\left(\frac{A-B}{2}\right) \tag{A.10}$$

$$\cos A + \cos B = 2\cos\left(\frac{A+B}{2}\right)\cos\left(\frac{A-B}{2}\right) \tag{A.11}$$

$$\cos A - \cos B = -2\sin\left(\frac{A+B}{2}\right)\sin\left(\frac{A-B}{2}\right) \tag{A.12}$$

$$e^{jx} = \cos x + j \sin x \tag{A.13}$$

$$\cos x = \frac{e^{jx} + e^{-jx}}{2} \tag{A.14}$$

$$\sin x = \frac{e^{jx} - e^{-jx}}{2j} \tag{A.15}$$

INDEX

G

S